
Citation:

Nadir, H. (2024) Development of Sustainable Materials for Greener Infrastructure Construction and Hydromodifications/ Water Channel Stabilisation [Online]. Leeds Beckett University. Available from: <https://figshare.leedsbeckett.ac.uk/articles/thesis/Development_of_Sustainable_Materials_for_Greener_Infrastructure_Construction_and_Hydromodifications_Water_Channel_Stabilisation/27123327/2> [Accessed 25 November 2024]. - [Link](#)

Link to Leeds Beckett University Research Data and Thesis Repository record:

[10.25448/lbu.27123327.v2](#)

Item Type:

Thesis

Licence:

CC BY-NC 4.0

The aim of the Leeds Beckett University Research Data and Thesis Repository is to provide open access to the outputs and data from our research, as required by funder policies and permitted by publishers and copyright law.

The Leeds Beckett University Research Data and Thesis Repository holds a wide range of outputs and data, each of which has been checked for copyright, licenses and any relevant embargo periods have been applied by the Research Services team.

We operate on a standard take-down policy. If you are the author or publisher of an output and you would like it removed from the repository or believe there to be any issues with copyright please [contact us](#) and we will investigate on a case-by-case basis.



Faculty of Built Environment and Engineering

**DEVELOPMENT OF SUSTAINABLE MATERIALS FOR
GREENER INFRASTRUCTURE CONSTRUCTION AND
HYDROMODIFICATIONS/ WATER CHANNEL
STABILISATION**

Hafiz Muhammad Nadir

Student No. 77224513

A Dissertation Submitted in Partial Fulfilment of the
Requirements of Leeds Beckett University for the Degree of
Doctor of Philosophy

2024

Abstract

Anthropogenic activities in river catchments and hydromodification in the channel's morphology impact the ecology/ climate, resulting in catastrophic flooding. Structural measures using cement concrete are employed without efficient flood risk assessment, resulting in additional environmental damages as cement concrete is considered the third biggest emitter of CO₂ globally (7-10%) after power generation and aviation/ transportation industries. The researchers always endeavoured to dispose of substantial waste exhibiting pozzolanic properties from diverse industrial/ agricultural fields and the construction industry to formulate greener supplementary cementitious composites (SCMs). The incorporation of fibres obtained from the waste materials had been envisaged as an inexpensive solution to overcome the weak tensile/ flexural strength of binders for lesser reinforcement stipulations for mitigation against rupture before the initiation of plastic deformation. As a solution, non-cement alternative, lime-based fibre-reinforced pozzolanic, innovative composites (**NALFRIC**) (low - medium strength requirements of 10-30 MPa), fibre-reinforced partial cement-based SCMs (medium - high-strength SCMs 50-70 MPa), and novel, alternative fibre reinforced iron-based composites (**NAFRIC**) (high-strength SCMs 50-70 MPa) were developed in this research project as sustainable, eco-friendly greener materials. NAFRIC contains iron powder, pozzolans, limestone and fibres, which was anticipated to attain a lower CO₂ equilibrium as it absorbs CO₂ from the environment to produce ferrous carbonate (FeCO₃), yielding a rock-like sustainable performance to drying/ setting. The durability study using concentrated sulphate solution of 2.5% Na₂SO₄ + 2.5% MgSO₄ and chemical-mechanical synthesis/ micro-structural studies using advanced XRD/ SEM/ TEM/ EDX testing supported the findings about the developed composites as sustainable/ eco-friendly. These materials demonstrated up to 50% lower embodied CO₂ with up to 25% lower cost and are considered suitable for all types of applications/ strength stipulations in the construction industry, especially in megaprojects, marine environments, and water channel stabilisation/ hydromodifications.

Declaration

It is certified that the work is that of the author alone, except where due acknowledgement was made by giving references. The work has not been submitted previously, in whole or in part, to qualify for any other academic award except the published research papers. The content of the thesis is the output of genuine research conducted by the author as per the planned research programme within the university timeline, ethics, procedures, and guidelines. The portion of the dissertation was published in the form of review/ research journal papers during the research period, and these were made part of the dissertation with proper referencing/ disclosure after permission from DoS to avoid any self-plagiarism (all the research papers are attached in appendices I-XIV).

I understand that to use the work and ideas of others, including generative AI output, without full acknowledgement, is academic unfair practice.

I confirm that this coursework submission is all my own, original work and that all sources, summaries, paraphrases and quotations are fully referenced as required by the LBU Academic Regulations.

DECLARATION OF GENERATIVE AI USE

I DID NOT use Generative AI technology in developing, writing, or editing this thesis, except using MS Editor/ Grammarly for spelling mistakes.

Hafiz Muhammad Nadir

Research Papers Declaration Form
Referencing the Doctoral Candidate's Own Published Works in This
Dissertation

I declare that a significant portion of my dissertation has already been published in the following peer-reviewed international journals papers under Creative Commons licences (CC licences) during my research period with me as the first/ main and my DoS, Dr Ash Ahmed as co-author, and vice versa. DoS has granted necessary permission for full/ part incorporation of these papers in my dissertation (Appendix I-XVI).

- Nadir, HM. (2024). A Comparative Evaluation of Embodied Environmental Impacts of Channel Stabilisation Using Concrete Lining and Alternative Pozzolanic Materials, *Advances in Earth and Environmental Science* (ISSN 2766-2624) (u/pub).
- Nadir, HM. (2024). A Projected Hydrological Study and Catchment-Level Hydrograph Modelling for Channel Stabilisation. *Journal of Earth and Environmental Science Research*. SRC/JEESR-299. DOI: [https://doi.org/10.47363/JEESR/2024\(6\)227](https://doi.org/10.47363/JEESR/2024(6)227).
- Nadir, H. M., et al., (2024). Strategic Integration of Catchment Level Natural and Structural Methods of Sustainable Flood Management: A Case Study of River Wharfe Catchment Area. *Adv Earth & Env Sci*; 5(2):1-11. DOI: <https://doi.org/10.47485/2766-2624.1043>.
- Nadir, H. M., Ahmed, A. and Moshi, I. (2024). Elucidation of Novel Eco-Friendly Iron-Based Fibre Reinforced Pozzolanic Supplementary Cementitious Materials (under publication).
- Ahmed, A., Nadir, H. M., (2023c). A Comparative Study Investigating the Feasibility and Potential of Utilising Polymer, Demolition, and Glass Waste as a Partial Replacement for Fine and Coarse Aggregate in Concrete. *Journal of Material Sciences & Manufacturing Research*. SRC/JMSMR-194. DOI: doi:[10.47363/JMSMR/2023\(4\)162](https://doi.org/10.47363/JMSMR/2023(4)162).
- Nadir, H. M., Ahmed, A. (2023b). The Critical Review of the Efficacy of the Environmental Impact Assessment (EIA) Process as a Tool Intended to Protect the Environment from Construction Development's Hazards. *Journal of Civil Engineering Research & Technology*, 5(2), 1-7. doi:[10.47363/JCERT/2023\(5\)143](https://doi.org/10.47363/JCERT/2023(5)143).
- Nadir, H. M., Ahmed, A and West, J., (2023a). Experimental Investigation of Engineering Properties of Iron-Based Binary and Ternary Pozzolanic Supplementary Cementitious Materials. *Journal of Materials and Polymer Science*, 3(1), 1-13. DOI: doi.org/10.47485/2832-9384.1024
- Nadir, H. M., & Ahmed, A. (2022c). Elucidating Chemical-Mechanical Synthesis and Microstructural Study on the Performance of Partial Cement-Based Concrete Composites Against Sulphate Attack – A Review. *Research &*

- Development in Material Science*, 18(2), 2065-2078.
doi:[10.31031/RDMS.2022.18.000935](https://doi.org/10.31031/RDMS.2022.18.000935).
- Nadir, H. M., & Ahmed, A. (2022b). The Mechanisms of Sulphate Attack in Concrete – A Review. *Modern Approaches on Material Science*, 5(2), 658-670. doi:[10.32474/MAMS.2022.05.000206](https://doi.org/10.32474/MAMS.2022.05.000206).
- Nadir, H. M., & Ahmed, A. (2022a). Hydrological Analysis and Statistical Modelling of Swat River Basin for Flood Risk Assessment. *Advances in Earth & Environmental Science*, 3(4), 1-13.
- Nadir, H., Ahmed, A., Paul, P., and Mitchell, M. (2022a). Potential of Utilizing Coir, Straw, and Recycled PET Fibres as Sustainable & Economical Alternative in Fibre Reinforced Concrete. *Research and Developments in Materials Science*, 16(5), 1885-1897. doi:[10.31031/RDMS.2022.16.000899](https://doi.org/10.31031/RDMS.2022.16.000899).
- Ahmed, A, Nadir, H, Cunliffe, J, Yates, C, Yates, L, Abdelwahab, O, Aljahed, A, Limbu, N and Patel, N (2021) Potential Sustainable Cement Free Limecrete Based on GGBS & Hydrated Lime as an Alternative for Standardised Prescribed Concrete Applications. *Research & Development in Material Science*, 15 (5). pp. 1753-1763. ISSN 2576-8840 DOI: <https://doi.org/10.31031/RDMS.2021.15.000874>.
- Nadir, H. M., & Ahmed, A. (2021b). Comparative Evaluation of Potential Impacts of Agricultural and Industrial Waste Pozzolanic Binders on Strengths of Concrete. *Journal of Material Sciences & Manufacturing Research*.
- Ahmed, A., Nadir, H. M., Yates, C., and Yates, L. (2020). Use of Coconut COIR in fibre-reinforced Concrete, Soil and Lime. *Modern Approaches on Material Science*. doi:[10.32474/MAMS.2020.03.000166](https://doi.org/10.32474/MAMS.2020.03.000166).

Hafiz Muhammad Nadir
(PhD Candidate)
Dr Ash Ahmed
DoS

Acknowledgements

First, I would like to convey my heartiest gratitude to my director of studies and supervisor "Dr Ash Ahmed" of the School of Built Environment and Engineering at Leeds Beckett University, who remained the beacon of light throughout my PhD research journey. It was his emboldening support and unflinching guidance throughout the planning, designing and execution of my research activities, including enormous laboratory testing, data collection, review/ research, dissertation writing up and, above all, guiding me to the rewarding track of research publication even before the completion of PhD and enabling me to publish more than twenty review/ research papers in international journals under his candid supervision. I attribute all my success to his sole professional guidance and excellent supervision, which has made my solo research flight successful.

I am grateful to the material science laboratory manager, Mr Keven Smith and Mr Andy Brannan, who have always been exceptional technical/ physical support. I am thankful to all the members/ staff of the library and graduate school for always helping in the hour of need. My special thanks to my fellow students/ colleagues/ friends for helping me with laboratory testing in my research journey. I thankfully acknowledge Pakistan Army, Leeds Beckett University, University of Leeds, UK Analytistics, Conserve Lime, and other material suppliers for the provision/ supply of required support / construction materials. I thank my parents and teachers, whose teachings and support will remain the hallmark of my life from the cradle to the grave.

"Behind every successful man, there is a woman behind," so I dedicate all my success to my wife "Muntaha Nadir" who has always been a source of inspiration with her undaunting support at every step of my life. I have no words to reciprocate her relentless support, our firm maternal bond, and her unwavering cooperation in sparing me for my studies when I was required to share the family responsibilities. I thank her and my children, Muhammad Usman Nadir, Muhammad bin Nadir and Iman Muntaha Nadir, for being my proponent supporters in adjudicating all my responsibilities and studies.

Table of Contents

List of Abbreviations	i
List of Figures	v
List of Tables	xvi
List of Equations	xix
1 Chapter 1: Introduction	1
1.1 Background	1
1.2 Outline of Dissertation	4
1.3 Problem Statement.....	5
1.4 Research Questions.....	6
1.5 Research Aim and Objectives	6
1.5.1 Aim	6
1.5.2 Objectives.....	6
1.6 Contribution to Knowledge	7
1.7 Research Methodology	8
1.7.1 In-depth Study of Existing Literature/ Research.....	8
1.7.2 Laboratory Testing/ Quantitative Analysis	8
1.8 Ethical Considerations/ Risk Assessment	10
1.9 Summary.....	11
2 Chapter 2: Literature Review	12
2.1 Water Resource Management and Hydrological Studies in Flood Prevention.....	12
2.1.1 Historical Flood Events	14
2.1.2 Rainfall/ Discharge Forecasting Techniques.....	15

2.1.3	Use of Log Pearson 3 Equations to Ascertain the Probability of Storm/ Discharge Events with Return Periods.	16
2.1.4	Significance of Hydrology Studies and Flood Forecasting.	18
2.2	Strategic Integration of Catchment Level Natural and Structural Methods of Sustainable Flood Management (Nadir et al., 2024).	19
2.2.1	Natural Flood Management (NFM) Techniques.	20
2.2.2	Afforestation and Riparian Woodlands	21
2.2.3	Flood Management with Hard Engineering Structures	22
2.2.4	Case Study: Sustainable Flood Management in Wharfe River Basin 25	
2.2.5	The Efficiency of NFM Techniques and Integrations of Engineering Materials and Hydraulic Structures for Sustainable Flood Management ...	32
2.2.6	Considerations for Environmentally Friendly Materials and Methods of Construction	34
2.3	Review of the Traditional/ Innovative Construction Materials	35
2.3.1	Lime.....	35
2.3.2	Broad Spectrum Applications of Hydrated Lime (CL-90)	40
2.3.3	<i>Review of Hydrated Lime Applications in the Construction Industry</i> 44	
2.3.4	Ordinary Portland Cement (OPC).....	48
2.3.5	The Cement Hydration Process.....	51
2.3.6	<i>Cement Concrete</i>	55
2.3.7	Carbon Footprint of Construction Industry / Materials.....	56
2.3.8	Efficacy of the Environmental Impact Assessment Reports Against Construction/ Development Hazards.....	60
2.3.9	Impact of Hydromodifications on River Ecology and Environment – Case Study of Mississippi River, USA (Nadir and Ahmed, 2023b Appendix XIII) 66	

2.3.10	Global Waste from Agricultural/ Industrial Fields	70
2.3.11	Review of the Cement Alternatives/ Pozzolan Materials and Their Global Use	73
2.3.12	Review of Fine and Coarse Aggregates Alternate Materials	89
2.3.13	Review of Fibres Selection for Fibre Reinforced Cement/ Lime Concrete	97
2.3.14	Review of Properties/ Use of Cement, Water, Plasticiser and Aggregates.....	104
2.4	Durability Testing of Composites Against Sulphate Attack.....	105
2.4.1	The Synthesis of External/ Internal Sulphate Attacks	107
2.4.2	Types/ Causes of Sulphate Attacks	109
2.4.3	Sources of Sulphate Attack.....	110
2.4.4	Factors and Prevention of Sulphate Attack.....	110
2.4.5	Use of High Sulphate Resistance Cement.....	111
2.4.6	Chemical Synthesis of Use of Pozzolans as Partial SCMs in Cement Concrete	112
2.4.7	Microstructural Analysis of OPC-Based Pozzolan Composites	113
2.5	Summary.....	130
3	Chapter 3: Methodology	131
3.1	Introduction	131
3.2	Research Methodology	131
3.3	Selection/ Formulation of Materials	132
3.4	Selection of Materials and Formulation of Sustainable Composites..	136
3.4.1	OPC-Based Supplementary Cementitious Materials (SCMs)	136
3.4.2	Cement-free hydrated Lime (CL90) Based Pozzolan Composites with GGBS, PFA, SF and MK.....	143

3.4.3	Iron-Based Binary/ Ternary Pozzolanic Composites (Fe-Composites)	147
3.4.4	Novel, Alternative Fibre-Reinforced Iron-Based Composites (NAFRIC)	149
3.5	Types/ Procedures/ Testing Equipment/ Materials/ Moulds Preparation 150	
3.5.1	Density.....	152
3.5.2	Slump Test.....	152
3.5.3	Sieve Analysis and Particle Size Gradation Curve	153
3.5.4	Compressive Strength	154
3.5.5	Tensile Strength.....	157
3.5.6	Flexural Strength	158
3.5.7	Carbonation Testing	159
3.6	Durability Testing for Sulphate Attack	160
3.7	Microstructural Analysis using XRF/ XRD/ SEM/ EDS	163
3.8	Data Management/ Synthesis/ Analysis	167
3.9	Risk/ Hazard Assessment	167
3.10	Summary.....	168
4	Chapter 4: Results and Discussion	169
4.1	Hydrological Assessments for Channel Lining Requirements	170
4.1.1	Case Study of Swale River	170
4.1.2	Hydrograph Analysis for Assumed/ Predicted 200 Years Return Period 176	
4.1.3	Storm Hydrograph Calculations Using The Unit Hydrograph.....	179
4.1.4	Channel Lining Designing Parameters	180

4.1.5	Material Calculations and CO ₂ Emissions by Concrete Channel Lining	183
4.2	Density, Workability and Particle Size Distribution	184
4.2.1	Density	184
4.2.2	Workability	185
4.2.3	Particle Size Distribution/ Gradation Curve / Sieve Analysis	186
4.3	Evaluation of OPC-Based Pozzolanic SCMs (PCR Composites)	189
4.4	Fibre Reinforced Cement Concrete (FRC)	195
4.5	Investigation of OPC-Based Composites with Partial Replacement of Fine/ Coarse Aggregates	199
4.6	Elucidation of Cement-Free Hydrated Lime-Based Pozzolanic Composites	205
4.6.1	Control Mixes	207
4.6.2	Hydrated Lime (CL90)-Based Composites with 10-90% GGBS/ Slag (SL)	208
4.6.3	Hydrated Lime (CL90)-Based Composites with 10 -90% Fly Ash (FA), Silica Fume (SF) and Metakaolin (MK)	213
4.7	Evaluation of Non-Cement, Alternative, Lime-Based Fibre-Reinforced Innovative Pozzolanic Composites (NALFRIC)	216
4.8	Investigation of Iron-Based Binary/ Ternary Pozzolanic Composites	224
4.9	Elucidation of Novel, Alternative, Fibre-Reinforced Iron-Based Binary/ Ternary Pozzolanic Composites (NAFRIC)	234
4.9.1	Compressive Strength of NAFRIC Composites	237
4.9.2	Flexural Strength of NAFRIC Composites	243
4.10	Analysis of Post-Crack Ductility of Fibre-Reinforced Composites	244
4.10.1	Post-Crack Ductility of OPC-Based FRC	246
4.10.2	Post-Crack Ductility of Hydrated Lime-Based Pozzolanic FRC NALFRIC	253

4.10.3	Post-Crack Ductility of Iron-Based Binary/ Ternay Pozzolanic FRC NAFRIC	256
4.11	Carbonation Testing.....	260
4.12	Chemical-Mechanical Synthesis and Durability Testing Against Sulphate Attack.....	263
4.12.1	OPC-Based FRC Composites	266
4.12.2	NALFRIC Composites	273
4.12.3	NAFRIC Composites	282
4.13	Microstructural Analysis Using XRD/ XRF and SEM/ EDM.....	288
4.13.1	Microstructural Analysis Using XRD/ XRF.....	288
4.13.2	Microstructural Analysis Using Energy Dispersive X-ray Spectroscopy (EDS).....	293
4.13.3	Microstructural Analysis Using Energy Dispersive Analysis with X-ray Spectroscopy (EDAX) and Transmission Electron Microscopy (TEM) with TEAM Software.....	298
4.13.4	Microstructural Analysis Using Scanning Electron Microscopy (SEM)	299
4.14	Significance of PhD Research and the Developed Composites.....	303
4.15	Calculation of Embodied CO ₂ and Cost-Benefits Analysis of Developed Composites.....	305
4.16	Applications of NALFRIC and NAFRIC in Channel Stabilisation, Hydromodifications and Infrastructure Construction.	318
4.16.1	Channel Stabilisation with Lining	318
4.16.2	Use of NALFRIC and NAFRIC in Infrastructure/ Building Construction	322
4.16.3	Preservation/ Reducing the Depletion of Natural Resources and Waste Recycling	325
4.17	Summary.....	326
5	Chapter 5: Conclusions and Recommendations.....	328

5.1	Conclusions.....	328
5.1.1	Impacts of Technical Advancement, Urbanisation, Anthropogenic Activities and Hydromodifications.....	328
5.1.2	Global Impacts of Waste Materials and CO ₂ Emissions	329
5.1.3	Selection of Waste Materials as SCMs/ PCRs.....	329
5.1.4	PCC and Partial Cement Replacement (PCRs) / Supplementary Cementitious Materials (SCMs).....	330
5.1.5	Fine/ Coarse Aggregate Replacement Composites.....	331
5.1.6	NALFRIC Materials.....	331
5.1.7	NAFRIC Materials.....	333
5.2	Recommendations for Future Research.....	335
6	References.....	338
7	Appendices.....	428

List of Abbreviations

°C: - Degrees

Celsius

3CaO.Al₂O₃.3CaSO₄.12H₂O - Monosulphate aluminate hydrate (3C4ASH18)

3CaO.Al₂O₃.3CaSO₄.32H₂O (C₆AS₃H₃₂) - Ettringite

3CaO.Al₂O₃.CaSO₄ – Monosulfate hydrate

AC – Air Cured

ACI – American Concrete Institute

ASTM – American society for testing and materials

Al₂O₃ – Aluminium oxide

Al₂SiO₅(OH)₄ or Al₂O₃.2SiO₂.2H₂O - Hydrated aluminium disilicate (Kaolinite)

BSI - British Standards Institution

BS/EN Standards - British/ European engineering standards

Brucite/ Epsom - Mg(OH)₂

C₂S (2CaO.SiO₂) – Belite

C₃A (3CaO.Al₂O₃) – Aluminate

C₃ACS_xHy: – Calcium sulfoaluminate hydrates

C₃S (3CaO.SiO₂) – Allite

C₄AF (4CaO.Al₂O₃Fe₂O₃) – Ferrite (Tetracalcium alumina ferrite)

C₄AS₃H₁₂₋₁₈ – Monosulfate

Ca(OH)₂ – Calcium hydroxide

CaO: – Calcium oxide

CaSiO₃.CaCO₃.CaSO₄.15H₂O: - Thaumasite

CaSO₄.2H₂O: – Ground hydrated gypsum

CaSO₄: – Anhydrate gypsum

CG – Crushed Glass

CO₂: – Carbon dioxide

Coir/ COF - Coir Fibre

COP28 – Conference of Parties (on climate change) number 28

CR – Crumb Rubber

C-S-H - ($3\text{CaO} \cdot 2\text{SiO}_2 \cdot 3\text{H}_2\text{O}$) - Calcium Silicate Hydrate

CT- Crushed/ shredded tyres

CxAHy ($4\text{CaO} \cdot \text{Al}_2\text{O}_3 \cdot 13\text{H}_2\text{O}$) – Calcium aluminate hydrates

EDAX/ EDS – Energy Dispersive X-Ray Spectroscopy/ Energy Dispersive Spectroscopy

EIA - Environmental Impact Assessment

Embodied CO₂ – Embodied Carbon Dioxide

f_{ck}, - Characteristic strength derived from cubes

f_{cm} – Mean compressive strength

Fe₂O₃ – Iron oxide

Fe/ F – Iron powder

FeCO₃ – Ferrous carbonate/ siderite/ iron carbonate

FRC – Fibre reinforced concrete

g - Grams

GGBS/ Slag/ SL – Ground Granulated Blast Furnace Slag

GHG – Greenhouse gas emission

gypsum – CaSO₄

H₂O: – Water

K₂O: – Potassium oxide

KAL₃(SO₄)₂ - K-alunite

kg – Kilogram

kg/m³ – Kilograms per cubic meter

KgCO_{2e} - kilogram carbon dioxide equivalent

Km - kilometre

LOI – Loss on ignition

Mg(OH)₂: – Brucite

MgO – Magnesium oxide

MgSO₄ – Magnesium Sulfate

MK – Metakaolin

mm - millimetre

MPa – Mega Pascal

M-S-H - Magnesium Silicate Hydrate

N/mm² – Newton per square millimetres

Na₂O – Sodium oxide

Na₂SO₄ – Sodium Sulfate

NaCl – Sodium Chloride

NAFRIC – Novel alternative fibre-reinforced iron-based binary/ ternary pozzolanic composites

NALFRIC – Non-cement alternative lime-based fibre-reinforced innovative composites

N-S-H - Sodium Silicate Hydrate

OPC – Ordinary Portland Cement

PA – Palm Ash

PCC – Plain cement concrete

PCR – Partial cement replacement

PET/ PET Fibre – Polyethene terephthalate fibres

PFA – Pulverised fly ash

PPF – Polypropylene fibres

RCA - Recycled Concrete Aggregate

RCC - Reinforced Cement Concrete

RHA – Rice Husk Ash

RPB – Recycled plastic bottles

SCMs – Supplementary Cementitious Materials

SDF – Strength Deterioration Factor

SEM - Scanning Electron Microscopy

SF – Silica Fume

SiO₂ – Silicone dioxide / Cristobalite

SO₃ – Sulphur trioxide (sulfite)
SO₄ – Sulfate
ST – Steel fibres
STF – Steel Fibres ST fibres
TCR – Total cement replacement
TEM – Transmission Electron Microscopy
Thaumasite - (3CaO.2SiO₂.CaCO₃.CaSO₄.15H₂O)
TiO₂ – Rulite / Titanium oxide
UK: – United Kingdom
UN: – United Nations
US\$: – US Dollar
W/B – Water binder ratio
W/C – Water Cement Ratio
WC – Water Cured
WS/ WSF – Wheat straw fibre
XRD – X-Ray Diffraction
XRF – X-Ray Refractrometry
µm: – Micrometer

List of Figures

Figure 2.1: Woody Debris Blocked by a Bridge (McDonald et al., 2004)	22
Figure 2.2: Water Cycle (Cunningham et al., 2015)	22
Figure 2.3: Natural Flood Management Techniques (JBA Consulting, 2018)...	23
Figure 2.4: Flood Protection Concrete Wall (Admin, 2012)	23
Figure 2.5: Flood Protection Bunds and Gabions (www.pixshark.com, 2023) ..	23
Figure 2.6: Pyramid Breakwater Stones with Raised Berms/ Walls and Edges (www.geograph.org.uk, 2023)	24
Figure 2.7: River Wharfe Weir at Tadcaster (Glazzard, 2007).....	24
Figure 2.8: Sheet Pile in Yorkshire (www.northernsheetpiles.co.uk, 2021)	24
Figure 2.9: Sheet Piled Wall in Tadcaster (Aeyates, 2018)	24
Figure 2.10: Flood Protection Dykes (Alamy Limited, (2019).)	24
Figure 2.11: Flood Protection Dam (www.blog.weatherflow.com, 2016)	24
Figure 2.12: Flood Retarding Structures (www.geography.org.uk, 2021)	25
Figure 2.13: Storage Pond Belford UK (The Flow Partnership, 2021)	25
Figure 2.14: Sponge Cities in China, Structural Flood Management (Clean Technica, 2018).....	25
Figure 2.15: River Wharf Catchment Overview (Rowland et al., 2015)	26
Figure 2.16: Wharf River Flood Risk Areas (Environmental Agency, 2010; North Yorkshire County Council, 2017.	26
Figure 2.17: Ecology Status in the River Wharfe Catchment Area (Environment Agency, 2018a)	28
Figure 2.18: Buffer Strip Growth Over Three Years on a Reach in the River Wharfe (Yorkshire River Dales Trust, 2014).....	28
Figure 2.19: Leaky Dams on the River Wharfe During Low/ High Floods (Yorkshire Dales River Trust, 2018)	29

Figure 2.20: Earth Bunds Retaining Storm Runoff on the River Wharfe Floodplain (Yorkshire Dales River Trust, 2017)	29
Figure 2.21: Offline Pond in the River Wharfe Floodplain (Yorkshire Dales River Trust, 2017)	29
Figure 2.22: Blackstone Bank Revetment to avoid Erosion due to Gravel Deposition (Environment Agency, 1999)	29
Figure 2.23: Afforestation to Prevent Flash Flooding and Sediment Transport (Environment Agency, 2018b)	29
Figure 2.24: Flood Protection Plan in Wharf River Basin using Structural Measures (different segments) (www.geographypod.com, 2018; Nadir et al., 2024)	31
Figure 2.25: Lime Quarry Norway (Oates,1998; Ahmed et al., 2020 Appendix IX).....	36
Figure 2.26: Lime Cycle for High Calcium Lime (Peter,2013; Ahmed et al., 2020 Appendix IX).....	37
Figure 2.27: Dry Density/ Water Contents of Soil with 0%-2% Coir and 5% Lime (Anggraini et al., 2014).	38
Figure 2.28: Liquid Limit/ Plastic Limit of Soil with 0%-2% Coir and 5% Lime (Anggraini et al., 2014).	38
Figure 2.29: Shrinkage limit/ linear shrinkage limit of soil with 0%-2% coir and 5% lime (Anggraini et al., 2014)	39
Figure 2.30: Compressive strengths of soil with 0%-2% coir and 5% lime (Anggraini et al., 2014)	39
Figure 2.31: Worldwide lime use by different sectors (Nadir et al., 2022b Appendix XII)	42
Figure 2.32: Raw Materials For OPC Manufacturing (<i>Bogues Compounds</i> , 2022)	50
Figure 2.33: Chemical composition of cement clinker (Show, 2020)	51
Figure 2.34: The chemical composition of cement clinker (Prodyogi, 2018)	51

Figure 2.35: Composition of Hydrated Cement Paste in Concrete Containing 100% Cement (www.engr.psu.edu, 2023)	55
Figure 2.36: Global Energy Consumption and CO ₂ Emissions Data (UNEP, 2020)	57
Figure 2.37: Percentage of Life Cycle CO ₂ Emissions of a Building (ICE Energy Briefing Sheet, 2011).....	58
Figure 2.38: Steps in the EIA Process (Scottish Gov, 2016)	62
Figure 2.39: Issues of Orange Train Project in Lahore, Pakistan (TheNews.com, 2018).	64
Figure 2.40: Mississippi River Flood Protection Infrastructure (MFDP,2004). ..	68
Figure 2.41: River Mississippi Channelisation (Tenenbaum, 2010).....	69
Figure 2.42: Old and New River Mississippi Landscape (USACE,2016).	69
Figure 2.43: Floods in Mississippi River 1993 (FEMA, 1993; NASA,1993; EPA, 2006).	70
Figure 2.44: Waste Generation by the Countries - Income-Wise Economies (Hoorweg and Bhadha, 2012)	72
Figure 2.45: Waste Composition by the Countries - Income-Wise Economies (a-d) (Hoorweg and Bhadha, 2012)	72
Figure 2.46: Global annual availability of cement, lime (filler)and SCMs (Scrivener, 2018; Sentucq and Clayton, 2021).....	75
Figure 2.47: Global Annual Substitution of OPC by SCMs (Scrivener, 2018) ..	76
Figure 2.48: Expansion of GGBS prisms in Na ₂ SO ₄ solution after one year (Higgins, 2003).	79
Figure 2.49: Expansion of prisms in Na ₂ SO ₄ solution after three years (Higgins, 2003).	80
Figure 2.50: Compressive Strength of Low/High PFA-Based Concrete (Troii et al., 1995).	82
Figure 2.51: Expansion of Low/High PFA-Based Concrete Samples in Na ₂ SO ₄ Solution (Troii et al., 1995).	82

Figure 2.52: Percentage of Global Aggregate Market Share By Usage/ Application (www.grandviewresearch.com, 2020; Ahmed and Nadir, 2023c) ..	93
Figure 2.53: Different Uses of Waste Glass in Concrete (Mansour et al., 2023; Ahmed and Nadir, 2023c).....	93
Figure 2.54: Use of crumb rubber/ shredded/ crushed tyres as fine/ coarse aggregate in concrete composites (Islam et al., 2022; Ahmed and Nadir, 2023c).	95
Figure 2.55: Straight, Crippled and Hooked Steel Fibres (Tariq et al., 2017) ...	99
Figure 2.56: Polypropylene Fibres (Macro/Microfibres) (Synthetic Fibres, 2020; Nadir et al., 2022a)	100
Figure 2.57: Coconut Coir Fibre (Ahmed et al., 2020)	101
Figure 2.58: Coir Mesh Used in Erosion Control Measures (Sutton and Rayan, 2020; Ahmed et al., 2020)	102
Figure 2.59: Wheat Straw (Tufail et al., 2021; Nadir et al., 2022a Appendix X)	103
Figure 2.60: Compressive strength of 15% and 35% lime-based concrete cubes immersed in the sulphate solution (Sotiriadis, Nikolopoulou and Tsivilis, 2012)	114
Figure 2.61: Surface deterioration of 15% lime-based concrete cubes immersed in the water and sulphate solution (Sotiriadis, Nikolopoulou and Tsivilis, 2012)	115
Figure 2.62: Surface deterioration of 35% lime-based concrete cubes immersed in the water and sulphate solution (Sotiriadis, Nikolopoulou and Tsivilis, 2012).	115
Figure 2.63: XRD study of 15% lime samples in $MgSO_4$ and $NaCl+MgSO_4$ solutions after 18 months	116
Figure 2.64: XRD study of 15% 35% lime samples in water $MgSO_4$ and $NaCl+MgSO_4$ solutions after nine months (Sotiriadis, Nikolopoulou and Tsivilis, 2012)	116
Figure 2.65: Qualitative Analysis of OPC cubes in 0.5% and 5% Na_2SO_4 solution after 900 days (Liu et al., 2015).....	118

Figure 2.66: Reduction in compressive strength of OPC cubes in sulphate solution (Liu et al., 2015)	118
Figure 2.67: Reduction in the mass of OPC cubes in sulphate solution (Liu et al., 2015)	118
Figure 2.68: Microstructural Analysis of OPC cubes by SEM in 5% Na ₂ SO ₄ solution after 600 and 900 days (Liu et al., 2015).....	119
Figure 2.69: Percentage elongation of mixes with max replacement @ 30% PFA, 30% GGBS and 30% PFA+GGBS (Kamau and Ahmed, 2017).....	121
Figure 2.70: Compressive strength loss after sulphate attack of 224 and 700 days (Ahmed et al., 2008).	122
Figure 2.71: Reduction in compressive strength after 15 weeks of immersion in 5% MgSO ₄ solution (Kavitha et al., 2016).	122
Figure 2.72: SEM images showing improvement in pore structure due to MK10% (b) filler capability (Kavitha et al., 2016).	123
Figure 2.73: Compressive/ split tensile strength of 0-20% RHA (Divya et al., 2015).	124
Figure 2.74: Microstructural analysis of RHA mixes by SEM (a) 0% RHA, (b) 10% RHA, (c) 15% RHA, (d) 20% RHA. The densest formation of C-S-H gel was observed with 15% RHA (c) (Divya et al., 2015).	125
Figure 2.75: SDF of 0% and 7.5% CCA blended cement composites immersed in 5% Na ₂ SO ₄ , 5% MgSO ₄ and 2.5% Na ₂ SO ₄ +2.5% MgSO ₄ solutions after nine months (Ahmed and Kamau, 2016).....	125
Figure 2.76: Weight changes in 0%, 15%, and 30% zeolite mixes after immersion in H ₂ SO ₄ for 300 days (Najimi et al., 2012)	127
Figure 2.77: Comparison of Surface Degradation in 0% (a), 15% (b), and 30% (c) Zeolite Mixes (Najimi et al., 2012).	127
Figure 2.78: Manufacturing of Geopolymer Concrete (Skariah et al., 2022)...	128
Figure 2.79: Compressive strength (MPa) 7 and 28 days (Jawahar et al., 2016).	129
Figure 3.1: Cement Replacement Materials/ Pozzolans.....	138

Figure 3.2: Established and New Fibres.....	138
Figure 3.3: Partial Fine Aggregate Replacement Materials	141
Figure 3.4: Partial Coarse Aggregate Replacement Materials.....	142
Figure 3.5: Slump Testing Stepwise Procedure (BS EN 12350-2:2019).	153
Figure 3.6: Sieve Analysis for Fine/ Coarse Aggregates	154
Figure 3.7: Mixing of Materials	156
Figure 3.8: Compaction on a vibration machine	156
Figure 3.9: Cubes and prism moulds.....	156
Figure 3.10: Curing of cubes in the water tank.	157
Figure 3.11: Compressive testing machine for testing of 100 mm cubes	157
<i>Figure 3.12: Cylinder testing for split tensile strength of concrete</i>	<i>159</i>
<i>Figure 3.13: Three-point flexural strength testing of prism</i>	<i>159</i>
Figure 3.14: Philips Minipal 4 EDXRF Machine for XRD/ XRF	166
Figure 3.15: SEM Machine (Carleton.edu, 2023)	167
Figure 4.1: Empirical correlation between stream discharge and stage gauge reading	174
Figure 4.2: Analysis/ correlation of rainfall versus discharge data - River Swale	174
Figure 4.3: Comparison of Monthly rainfall versus total runoff (in mm) in the Swale River catchment area to ascertain a storm event and resultant discharge	175
Figure 4.4: Duration flow curve to assess the probability of maximum base flow in River Swale	175
Figure 4.5: A: Hydrographs Analysis for 200 Years Predicted Storm Event - Swale River, B: Hydrographs of storms of different rainfall intensity/ intervals.	178

Figure 4.6: Proposed Channel Cross-Section for Swale River Channalisation.	182
Figure 4.7: (A) and (B) Particle Size Gradation Curves - Virgin Coarse/ Fine Aggregates and Replacement Materials.....	188
Figure 4.8: Comparison of Compressive Strength (MPa) - Pozzolanic-Based PCR Composites.	191
Figure 4.9: Comparison of Split Tensile Strength (MPa) - Pozzolanic-Based PCR Composites.	194
Figure 4.10: Comparison of Compressive Strength of FRC Composites.....	197
Figure 4.11: Split Tensile Strength of FRC Composites at 90 Days	198
Figure 4.12: Flexural Strength of FRC Composites at 90 Days.....	199
Figure 4.13: Comparison of Compressive Strengths of Fine Aggregate Replacement Composites	203
Figure 4.14: Comparison of Compressive Strength of Coarse Aggregate Replacement Composites	204
Figure 4.15: Comparison of Split Tensile Strength of Fine/ Coarse Aggregate Replacement Composites.	204
Figure 4.16: Compressive Strength of Cement Free Lime-Based Control Mixes.	208
Figure 4.17: Compressive Strength of CL90-Based Composites With GGBS (SL) 10-90%.	210
Figure 4.18: Compressive Strength of CL90-Based Composites With GGBS (SL) 10-90% 1:1:2 Job Mix Ratio.....	210
Figure 4.19: Compressive Strength of CL90-Based Composites With GGBS (SL) 10-90% 1:1:3 Job Mix Ratio.....	211
Figure 4.20: Compressive Strength of CL90-Based Composites With GGBS (SL) 10-90% 1:2:3 Job Mix Ratio.....	211
Figure 4.21: Compressive Strength of CL90-Based Composites With GGBS (SL) 10-90% 2:1 Job Mix Ratio.....	212

Figure 4.22: Flexural Strength - CL90-Based SL 10-90% Composites	212
Figure 4.23: Compressive Strength of CL90-Based Composites with 10,30,50,70 and 90% MK.	214
Figure 4.24: Compressive Strength of CL90-Based Composites with PFA 10- 90%	215
Figure 4.25: Compressive Strength of CL90-Based Composites with 10,30,50,70 and 90% SF	215
Figure 4.26: Comparison of Compressive Strengths of Best Performing CL90- Based Pozzolanic Composites	216
Figure 4.27: Compressive Strength of CL-90/ SL80-Based NALFRIC	219
Figure 4.28: Flexural Strength of CL-90/ SL80-Based NALFRIC	219
Figure 4.29: Compressive Strength of CL90 MK50-Based NALFRIC	223
Figure 4.30: Flexural Strength of CL-90/ MK50-Based NALFRIC	223
Figure 4.31: Compressive Strength - Set 1 - 5, 10-50% Replacement of OPC with Conventional/ Modified Fe-composites.	228
Figure 4.32: Compressive Strength - Set 1 20% PFA.	231
Figure 4.33: Compressive Strength - Set 2 20% GGBS	231
Figure 4.34: Compressive Strength - Set 3 20% PA.	232
Figure 4.35: Compressive Strength - Set 4 10%PFA+GGBS.....	232
Figure 4.36: Compressive Strength - Set 5 10%PFA+10%SF.	233
Figure 4.37: Flexural Strength - Set 1 - 5, 10-50% Replacement of OPC with Conventional/Modified Fe-composites.	233
Figure 4.38: Comparison of Compressive Strength - NAFRIC Mixes.....	237
Figure 4.39: Comparison of Compressive Strength of NAFRIC Mixes With STF 10% and STF 17%.	238
Figure 4.40: Comparison of Compressive Strength of NAFRIC Mixes With 1% & 2% PP Fibres.	239

Figure 4.41: Comparison of Compressive Strength of NAFRIC Mixes With 1% & 2% PET Fibres.	241
Figure 4.42: Comparison of Compressive Strength of NAFRIC Mixes With 1% & 2% WS Fibres.	242
Figure 4.43: Flexural Strength of Fe-Based Composites with Different Fibres.	244
Figure 4.44: Mechanism of Post-Crack Ductility in Fibre-Reinforced Prisms During Flexural Strength Testing.....	247
Figure 4.45: Post-Crack Ductility of Various Prisms.	248
Figure 4.46: Prism Flexural Strength Versus Displacement Graph – FRC Control.....	249
Figure 4.47: Post Crack Ductility - FRC 1:2:3 with ST17%.....	249
Figure 4.48: Post Crack Ductility - FRC 1:2:3 with PPF 2%.	250
Figure 4.49: Post Crack Ductility - FRC 1:2:3 with Coir 2%.....	250
Figure 4.50: Post Crack Ductility - FRC 1:2:3 with PET 2%.	251
Figure 4.51: Post Crack Ductility - FRC 1:2:3 with WSF 2%.	252
Figure 4.52: Comparison of Flexural Strength - FRC and NALFRIC Composites.	253
Figure 4.53: Post Crack Ductility - SL80 1:1:2 with PET 2%	254
Figure 4.54: Post Crack Ductility - SL80 1:1:2 with ST17%.....	255
Figure 4.55: Post Crack Ductility - SL80 1:1:2 with PPF1.5%.	255
Figure 4.56: Post Crack Ductility of F/PFA 20% with ST17%.....	257
Figure 4.57: Post Crack Ductility of F/PA PET2%	257
Figure 4.58: Post Crack Ductility of F/GGBS with WSF2%	258
Figure 4.59: Post Crack Ductility of P/PFA/SF with WSF 1%.	258

Figure 4.60: Carbonation Testing Using Phenolphthalein and Assessing Presence/ Absorption of CO ₂ (Pink colour- CO ₂ present, light pink or no colour – no or less CO ₂ present)	262
Figure 4.61: Decolouration, mild pitting, exposure of aggregates and corner damages in FRC Composites after Sulphate Attack.	269
Figure 4.62: Comparison of Percentage Elongation at 270 Days of Sulphate Attack - FRC 1:2:3	272
Figure 4.63: Comparison of Compressive Strengths after 270 Days of Water Curing and Sulphate Exposure.....	273
Figure 4.64: Decolouration, mild pitting, mild corner damages in SL80-based NALFRIC Composites after Sulphate Attack.	275
Figure 4.65: Total/partial damage, pitting, and Corner damages in MK50-Based NALFRIC Composites after sulphate attack.	275
Figure 4.66: Compressive Strength of SL80-Based NALFRIC Composites after 270 Days of Water Curing and Sulphate Exposure.	281
Figure 4.67: Compressive Strength of MK50-Based NALFRIC Composites after 270 Days of Water Curing and Sulphate Exposure.	281
Figure 4.68: Qualitative Analysis and Physical Deterioration in NAFRIC Composites after 270 Days of Sulphate Attack.	284
Figure 4.69: XRD Spectrometry - Compound Composition, Phases/ Peaks of SL80 COF1%.	291
Figure 4.70: XRD Spectrometry - Compound Composition, Phases/ Peaks of SL80 PET0.5%.	291
Figure 4.71: XRD Spectrometry - Compound Composition, Phases/ Peaks of F/PFA/SF PET1%.	292
Figure 4.72: XRD Spectrometry - Compound Composition, Phases/ Peaks of F/PA PET1%.	292
Figure 4.73: Combined Spectrum of NALFRIC/ NAFRIC Composites after Sulphate Attack Using EDS.....	294
Figure 4.74: Spectrum of NALFRIC SL80 COF1% Composites after Sulphate Attack Using EDS.....	296

Figure 4.75: Spectrum of NALFRIC SL80 PET0.5% Composites after Sulphate Attack Using EDS.....	296
Figure 4.76: Spectrum of NAFRIC F/PFA/SF PET1% Composites after Sulphate Attack Using EDS.....	297
Figure 4.77: Spectrum of NAFRIC F/FA PET1% Composites after Sulphate Attack Using EDS.....	297
Figure 4.78: Elemental Mapping Using EDAX-TEM for SL80 COF1%.....	298
Figure 4.79: Elemental Mapping Using EDAX-TEM for SL80 PET 0.5%	298
Figure 4.80: Elemental Mapping Using EDAX-TEM for F/PFA/SF PET1%	298
Figure 4.81: Elemental Mapping Using EDAX-TEM for F/PA PET1%.....	298
Figure 4.82: SEM Image- SL8- COF1%	300
Figure 4.83: SEM Image SL80 PET0.5%.	300
Figure 4.84: SEM Image - F/PFA/SF PET1%.....	301
Figure 4.85: SEM Image F/PA PET1%.	301
Figure 4.86: GHG Emissions Phases of Cement Concrete Manufacturing (Spencer et al., 2023).....	307
Figure 4.87: Lifecycle Stages of GHG Emissions of a Project - Cradle to Grave (Victor, 2023).....	307
Figure 4.88: %age Contributing Sectors to Achieve Net Zero CO ₂ Emissions (GCCA, 2021).....	310
Figure 4.89: Recommended uses of NALFRIC and NAFRIC as Alternative Materials.....	320
Figure 4.90: Recommended uses of NALFRIC and NAFRIC as Alternative Erosion Control Materials.	321
Figure 4.91: Use STF-Based SCMs in Tunnel Lining (Kim and Lee, 2021). ..	322
Figure 4.92: Recommended Uses of NALFRIC and NAFRIC Composites.....	323
Figure 4.93: Recommended Uses of NAFRIC Composites.....	324

List of Tables

Table 2.1: Reaction of $\text{Ca}(\text{OH})_2$ and CaCO_3 lime with soil (Anderson et al., 2013)	44
Table 2.2: Comparison Of Cement-Lime Mortars to GGBS-Lime-Based Mortars (BS EN 5627; Ahmed et al., 2022a,2022b)	48
Table 2.3: Bogues Compounds (Bogues Compounds, 2022)	50
Table 2.4: Concrete Strength Grades (Base Concrete, 2018; Sir, 2021)	56
Table 2.5: Embodied CO_2 of Different Construction Materials (ICE Energy Briefing Sheet, 2011; Obinna, 2023).	59
Table 2.6: Efficacy of EIA reports on emission control and their environmental effects (Reproduced from Bruhn & Eklund, 2002).	65
Table 2.7: Elemental/ ingredient composition analysis by X-ray fluorescence (XRF) of different materials	77
Table 2.8: Compressive strength of GGBS composites in water and sulphate solutions (Higgins, 2003).	78
Table 2.9: Compressive strength of 0,5,7.5,10,15,20,25 and 30% CCA blended cement composites (Ahmed and Kamau, 2016).....	126
Table 2.10: Comparison of loss in weight and compressive strength of geopolymer concrete composites after the acid attack (Jawahar et al., 2016)	129
Table 3.1: Selected Construction Materials/ Unit Price in Leed, UK, in 2023.	135
Table 3.2: Classification of Characteristic Compressive Strength of Concrete (BS 196-1, 2016; Eurocode Applied, 2017).	136
Table 3.3: Partial Replacement of Cement with Pozzolanic Materials.....	139
Table 3.4: Incorporation of Various Fibres for Preparation of FRC Composites	141
Table 3.5: Partial Replacement of Fine Aggregate with Crushed Glass (CG), Crumb Rubber (CR), and Recycled Shredded PET Bottles (RPB).....	142
Table 3.6: Partial Replacement of Coarse Aggregate with Recycled Concrete Aggregate (RCA) and Crushed/ shredded Tyres (CT)	143

Table 3.7: Cement-Free Hydrated Lime-Based Limecrete Mixes.....	145
Table 3.8: Fibre-Reinforced Cement-Free Limecrete Mixes with SL80.	146
Table 3.9: Fibre-reinforced cement-free Limecrete Mixes with MK50.	146
Table 3.10: Composition of Conventional/ Modified Fe-Composites-Based Binary/ Ternary Pozzolanic SCMs with 10-50% replacement sets 1-5.....	148
Table 3.11: Composition of 10% Fe-Composites-Based SCMs with Binary and Ternary Pozzolans and Fibres (FRC 123).....	149
Table 3.12: Slump Classification (BS EN 206-1: 2000; BS, 12390-2:2019) ...	153
Table 4.1: River Swale Monthly Rainfall Data 2019-2022, Discharge, V_{DRH} and Catchment Efficiency.....	173
Table 4.2: A : Quantities of discharge and precipitation duration for a 200-year predicted hydrograph analysis and B : hydrographs for different storms.	177
Table 4.3: Density Ranges - Composites Developed in the Research	185
Table 4.4: A and B: Sieve Analysis/ Particle Size Gradation.	187
Table 4.5: Compressive/ Flexural Strength of CL-90/ SL80-Based NALFRIC	220
Table 4.6: Compressive/ Flexural Strength of CL90 + MK50-Based NALFRIC	222
Table 4.7: Engineering Properties of Iron-Based Binary/ Ternary Pozzolanic Composites.	227
Table 4.8: Compressive and Flexural Strength of NAFRIC Composites.	236
Table 4.9: Qualitative/ Quantitative Analysis - Post-Crack Ductility - FRC 1:2:3.	252
Table 4.10: Qualitative Analysis - Post-Crack Ductility of NALFRIC Composites (SL80 1:1:2 and MK50 1:1:2).	256
Table 4.11: Qualitative/ Quantitative Analysis - Post-Crack Ductility of NAFRIC Composites.	259

Table 4.12: Physical Deterioration at 270 Days of Sulphate Attack - FRC 1:2:3.	270
Table 4.13: Percentage Elongation after 270 Days Sulphate Attack – FRC 1:2:3.	270
Table 4.14: Compressive Strength and Strength Deterioration Index SDI (%) after 270 Days of Water Curing and Sulphate Exposure - FRC 1:2:3	272
Table 4.15: Physical Deterioration after Sulphate Attack – NALFRIC (SL80).	276
Table 4.16: Physical Deterioration at 270 Days of Sulphate Attack – NALFRIC (MK50).....	277
Table 4.17: Percentage Elongation at 270 Days of Sulphate Attack - NALFRIC Composites.	279
Table 4.18: Compressive Strength and Strength Deterioration Index of NALFRIC Composites after 270 Days of Water Curing and Sulphate Exposure.	282
Table 4.19: Deterioration at 270 Days of Sulphate Attack - NAFRIC	285
Table 4.20: Percentage Elongation at 270 Days of Sulphate Attack - NAFRIC Composites.	286
Table 4.21: Best-Performing Composites Selected for Microstructural Analysis.	287
Table 4.22: Comparison of Compressive Strength and Strength Deterioration Index (SDI%) - NAFRIC Composites after 270 days of Sulphate Attack.	288
Table 4.23: Elemental Composition of Composites Using X-RAY Spectrometry.	290
Table 4.24: Elemental Compound Composition of Composites Using X-RAY Spectrometry/ Eva Software.....	293
Table 4.25: Embodied CO ₂ (kgCO _{2e} /kg) of Cement, aggregate and SCMs...	313
Table 4.26: Embodied CO ₂ and Cost-Benefits of PCRs/ SCMs Composites.	314
Table 4.27: Embodied CO ₂ and Cost-Benefits of NALFRIC Composites.	316
Table 4.28: Embodied CO ₂ and Cost-Benefits of NAFRIC Composites.	317

List of Equations

Equation 1: $R_i = \text{Log}(R)$	16
Equation 2: $R_m = 1/n \sum R_i$	16
Equation 3: $S_d = (\sum (\text{Log}(R) - \text{Avg}(\text{Log } R))^2 / (n-1))^{1/2}$	16
Equation 4: $\text{Skewness} = (\text{Log}(R) - \text{Avg}(\text{Log } R))^3$	17
Equation 5: $\text{Skewness coefficient } G = n * (\sum (\text{Log}(R) - \text{Avg}(\text{Log } R))^3 / ((n-1) * (n-2) * S_d)$	17
Equation 6: $\text{Return Period } (T_r) = 2n / (2m-1)$	17
Equation 7: $\text{Exceedance probability } R_m = 1/T_r$	17
Equation 8: $R_t = R_m + K_t * S_d$	17
Equation 9: $R_p = \text{Anti Log } R_t = (10)^{(R_t)}$	17
Equation 10: $Q_t = Q_m + K_t * S_d$	17
Equation 11: $Q_p = \text{Anti Log } Q_t = (10)^{(Q_t)}$	17
Equation 12: $\text{CaCO}_3 = \text{CaO} + \text{CO}_2$	36
Equation 13: $\text{CaO} + \text{H}_2\text{O} = \text{Ca(OH)}_2 + \text{heat}$	36
Equation 14: $\text{Ca(OH)}_2 + \text{CO}_2 = \text{CaCO}_3 + \text{H}_2\text{O}$	36
Equation 15: $2\text{SiO}_2 + 3\text{Ca(OH)}_2 = 3\text{CaO} \cdot 2\text{SiO}_2 \cdot 3\text{H}_2\text{O}$	47
Equation 16: $2(3\text{CaO} \cdot \text{SiO}_2) + 6\text{H}_2\text{O} = 3\text{CaO} \cdot 2\text{SiO}_2 \cdot 3\text{H}_2\text{O} + 3\text{Ca(OH)}_2 + \text{Heat}$	52
Equation 17: $2(2\text{CaO} \cdot \text{SiO}_2) + 4\text{H}_2\text{O} = 3\text{CaO} \cdot 2\text{SiO}_2 \cdot 3\text{H}_2\text{O} + \text{Ca(OH)}_2 + \text{Heat}$	52
Equation 18: $3\text{CaO} \cdot \text{Al}_2\text{O}_3 + 3\text{CaSO}_4 + 32\text{H}_2\text{O} = 3\text{CaO} \cdot \text{Al}_2\text{O}_3 \cdot 3\text{CaSO}_4 \cdot 32\text{H}_2\text{O}$	53
Equation 19: $3\text{CaO} \cdot \text{Al}_2\text{O}_3 + 3\text{CaO} \cdot \text{Al}_2\text{O}_3 \cdot 3\text{CaSO}_4 \cdot 32\text{H}_2\text{O} + 22\text{H}_2\text{O} = 3(3\text{CaO} \cdot \text{Al}_2\text{O}_3 \cdot 3\text{CaSO}_4 \cdot 12\text{H}_2\text{O})$	53
Equation 20: $\text{Ca(OH)}_2 + \text{CO}_2 = \text{CaCO}_3 + \text{H}_2\text{O}$	54

Equation 21: $3\text{CaO} \cdot \text{Al}_2\text{O}_3 \cdot 3\text{CaSO}_4 \cdot 32\text{H}_2\text{O} + 3\text{CO}_2 = 3\text{CaCO}_3 + 3\text{CaSO}_4 + \text{Al}_2\text{O}_3 + \text{H}_2\text{O}$	54
Equation 22: $\text{C}_4\text{AF} + \text{Gypsum} + \text{water} = \text{Ettringite} + \text{Ferric aluminium hydrate} + \text{Lime}$	54
Equation 23: $\text{C}_4\text{AF} + \text{Ettringite} + \text{Lime} + \text{Water} = 3\text{C}_4\text{AF} \cdot \text{CaSO}_4 \cdot 18\text{H}_2\text{O} + \text{Ferric aluminium hydrate}$	54
Equation 24: $\text{KgCO}_2\text{e} = \text{Weight of CO}_2 \times \text{GWP}$	58
Equation 25: $\text{Fe} + \text{CO}_2 + \text{H}_2\text{O} = \text{FeCO}_3 + \text{H}_2$	87
Equation 26: $\text{SiO}_2 + 2\text{Ca}(\text{OH})_2 = \text{Si}(\text{OH})_4 \cdot 2\text{CaO}$ (Nadir and Ahmed, 2022b)	94
Equation 27: $\text{Ca}(\text{OH})_2 + \text{MgSO}_4 + 2\text{H}_2\text{O} = \text{CaSO}_4 \cdot 2\text{H}_2\text{O} + \text{Mg}(\text{OH})_2$	108
Equation 28: $\text{Ca}(\text{OH})_2 + \text{Na}_2\text{SO}_4 + 2\text{H}_2\text{O} = \text{CaSO}_4 \cdot 2\text{H}_2\text{O} + 2\text{NaOH}$	108
Equation 29: $\text{CaSO}_4 \cdot 2\text{H}_2\text{O} + 3\text{C}_4\text{ASH}18 + \text{water} = 3\text{CaO} \cdot \text{Al}_2\text{O}_3 \cdot \text{CaSO}_4 \cdot 32\text{H}_2\text{O}$	108
Equation 30: $3\text{CaO} \cdot 2\text{SiO}_2 \cdot 3\text{H}_2\text{O} + 3\text{MgSO}_4 + 2\text{H}_2\text{O} = 3\text{MgO} \cdot 2\text{SiO}_2 \cdot 3\text{H}_2\text{O} + 3\text{CaSO}_4 \cdot 2\text{H}_2\text{O}$	108
Equation 31: $\text{SiO}_2 + 2\text{H}_2\text{O} = \text{Si}(\text{OH})_4$	113
Equation 32: $\text{Si}(\text{OH})_4 + 2\text{Ca}(\text{OH})_2 = \text{Si}(\text{OH})_4 \cdot 2\text{CaO} + 2\text{H}_2\text{O}$	113
Equation 33: $\text{SiO}_2 (\text{Solid}) = \text{SiO}_2 (\text{Aqueous}) = \text{SiO}_2 (\text{Solution}) = \text{SiO}_2 (\text{gel Swelling})$	113
Equation 34: $3\text{CaO} \cdot 2\text{SiO}_2 \cdot 3\text{H}_2\text{O} + 2\text{CaCO}_3 + \text{MgSO}_4 + 13\text{H}_2\text{O} = 3\text{CaO} \cdot \text{SiO}_2 \cdot \text{CaCO}_3 \cdot \text{CaSO}_4 \cdot 15\text{H}_2\text{O} + \text{Mg}(\text{OH})_2 + \text{CO}_2$	114
Equation 35: Density “D” = $[\text{M}_d / (\text{M}_d - \text{M}_w)] \times 1000$	152
Equation 36: $F_{ck} = f_{cm} - 1.64 \times S_d$	155
Equation 37: Compressive Strength $f_c = P/A$	156
Equation 38: Tensile Strength = $f_t = (2 \cdot P) / (\pi \cdot d \cdot h)$	158
Equation 39: Flexural Strength = $f_f = (3 \cdot P \cdot l) / (2 \cdot b \cdot d^2)$	159

Equation 40: Length variation index (%) $\Delta L = [(L_s - L_i)/L_o] \times 100$	162
Equation 41: Strength deterioration index (%) $SDI = [(f_w - f_s)/f_w] \times 100$...	162
Equation 42: $Q = a(h)^b$ and $Q = AV$	170
Equation 43: $V_{DRH} VDRH = t_0 QDRH \int dt \cong i QDRH \Delta$	171
Equation 44: Manning Equation $Q = 1.49 A R^{2/3} S^{1/2} = 1.49 P A^{5/3} S^{1/2}$...	181
Equation 45: Rational method equation $Q = 1.48 C i A$	181
Equation 46: Lag time $t_c = 0.01947 L^{0.77} / S^{0.385}$	182

1 Chapter 1: Introduction

1.1 Background

The development of megacities along river channels, anthropogenic activities to nature and the environment, heavily modified water structures and climatic changes are causing devastation as uncontrolled cloud bursts and floods. Huge dams, barrages, channels, break walls/ retaining structures and other engineering infrastructures of cement concrete/ stones were erected to overcome these calamities, thus adding environmental disturbance in the form of greenhouse gas (GHG) emissions due to human-inflicted climatic disturbances/ global warming (Rehan and Nehdi, 2005; MPA, 2007; Nadir and Ahmed, 2022a Appendix II). Cement concrete is considered the second most widely used material on earth after water, with its intrinsic characteristics as a significant global annual CO₂ emitter (7-10%, estimated to be around 4000 million tons, with an emission rate of one ton per ton of cement) classified as third largest CO₂ emitter following the power generation (15000 million tons) at first place, and aviation/ transportation industry at second place (8000 million tons) (Brander and Davis, 2012; Gagg, 2014; Ahmed et al., 2019; Chatham, 2021; Cunliffe et al., 2021 Appendix III, Nadir, West and Ahmed, 2023 Appendix IV; Tiseo, 2023a). Therefore, the solution to minimise the environmental impacts lies in the minimum anthropogenic activities/ lesser modification to water bodies/adequate hydrological studies and the development of carbon-neutral materials, cement-free lime-based composites and supplementary cementitious composites (SCMs) with lesser cement usage. The chemistry and microstructural effects of the physical and mechanical properties of various construction materials/ composites are not widely understood within the construction/ civil engineering fields, e.g., the molecular configuration effects on the transition from classical binders to supplementary cementitious composites and exchange of cations/ anions during hydration process/sulphate attack. The post-crack ductility effect on the transition from rigid to plastic behaviour in structural components on

embedding various organic and inorganic fibrous materials in binary/ ternary pozzolanic composites, primarily focusing on low-embodied CO₂, strength and sustainability need elaboration. A knowledge gap was observed, encouraging further research, especially around the understanding of the kinetics associated with organic/ inorganic chemistry in both covalent and ionic bonded materials, e.g., chemical synthesis based on the exothermic cement hydration reactions of trisilicate and disilicate to produce calcium silicate hydrate gel (C-S-H) $2\text{Ca}_3\text{SiO}_5 + 7\text{H}_2\text{O} \rightarrow 3\text{CaO} \cdot 2\text{SiO}_2 \cdot 4\text{H}_2\text{O} + 3\text{Ca}(\text{OH})_2$ & $2\text{Ca}_2\text{SiO}_4 + 5\text{H}_2\text{O} \rightarrow 3\text{CaO} \cdot 2\text{SiO}_2 \cdot 4\text{H}_2\text{O} + \text{Ca}(\text{OH})_2$ (Nadir and Ahmed 2022b, 2022c Appendix V and VI). Furthermore, the capacity to impart post-crack ductile behaviour due to embedded fibres also needed elucidation by mixing various secondary sources (agricultural/ industrial waste materials as fibres) within the primary $\text{CaO} \cdot \text{SiO}_2 \cdot \text{H}_2\text{O}$ (C-S-H) matrix. The mitigation against rupture before the initiation of plastic deformation with the primary objective of imparting gross plastic deformation should be evaluated.

This project involved the formulation of job mix ratios, laboratory synthesis of more than 320 sustainable combinations, and elucidation of physical/ mechanical properties of around 3000 cubes/ prisms/ cylinders. Furthermore, the durability study on the material's resistance to chemical degradation was assessed by immersion in SO_4^{2-} concentrated solution for nine months. The kinetics associated with the long-term durability of the sustainable composites was elaborated, involving the chemical/ mechanical synthesis of sulphate attack and chemical reactions in the formation of ettringite ($\text{CaO} \cdot \text{Al}_2\text{O}_3 \cdot 3\text{CaSO}_4 \cdot \text{H}_2\text{O}$); $\text{Na}_2\text{SO}_4 + \text{Ca}(\text{OH})_2 + 2\text{H}_2\text{O} = \text{CaSO}_4 \cdot 2\text{H}_2\text{O} + 2\text{NaOH}$, $\text{MgSO}_4 + \text{Ca}(\text{OH})_2 + 2\text{H}_2\text{O} = \text{CaSO}_4 \cdot 2\text{H}_2\text{O} + \text{Mg}(\text{OH})_2$, $3\text{CaO} \cdot \text{Al}_2\text{O}_3 + 3\text{CaSO}_4 + 32\text{H}_2\text{O} = 3\text{CaO} \cdot \text{Al}_2\text{O}_3 \cdot 3\text{CaSO}_4 \cdot 32\text{H}_2\text{O}$. The $\text{Mg}^{++}/ \text{Na}^+$ and Ca^{++} cations exchange with anions SO_4^{2-} and OH^- . The ion SO_4^{2-} from epsom salt (MgSO_4)/ sulphate soda/ thenardite (Na_2SO_4) transferred inwards to form gypsum (CaSO_4), whereas the OH^- ion from Portlandite ($\text{Ca}(\text{OH})_2$) exchanged outward to form brucite ($\text{Mg}(\text{OH})_2$) or caustic soda (NaOH) the dynamic shift from the primary strength producing

CaO.SiO₂.H₂O (Calcium-Silicate-Hydrates C-S-H gel) matrix to secondary weaker 3MgO.2SiO₂.3H₂O (Magnesium-Silicate-Hydrates M-S-H gel) / 3Na₂O.2SiO₂.3H₂O (Sodium-Silicate-Hydrates N-S-H gel) matrix dictated the durability implications/ decrease in strength with the reaction; $3\text{CaO}.2\text{SiO}_2.3\text{H}_2\text{O} + 3\text{MgSO}_4 + 2\text{H}_2\text{O} = 3\text{MgO}.2\text{SiO}_2.3\text{H}_2\text{O} + 3\text{CaSO}_4.2\text{H}_2\text{O}$ (Nadir and Ahmed 2022b, 2022c Appendix V and VI). Chemical/ mechanical synthesis based on established British/ European engineering standards (BS/EN) and American ASTM standards was fundamental to comprehending the long-term durability of structures that minimise flood risks, particularly in concentrated marine/ sulphate environments. This necessitated studying hydrology and water resource engineering/ management with material science as a research subject for developing sustainable infrastructure/ hydromodifications by incorporating durable, greener/ low CO₂-embedded materials.

The researchers pioneered the substantial disposal of waste materials exhibiting pozzolanic properties from diverse industrial/ agricultural fields to the construction industry to formulate greener supplementary cementitious composites (SCMs). These SCMs generate additional calcium silicate hydrate gel, inducing extra strength to the concrete by contributing silica during the cement hydration (Nadir and Ahmed, 2021b Appendix VII). The formulation of low-medium strength cement-free materials as concrete alternatives endeavoured to reduce the carbon footprints of the construction industry by mixing 10-90% hydrated lime (CL90) with 10-90% GGBS, MK, SF and PFA. The formulation of materials demonstrating comparable performance with cement concrete with negligible/ negative CO₂ balance has always been the aspiration of innovative construction. As a solution, iron-based pozzolanic composites (Fe-composites) were formulated using iron powder (Fe), metakaolin (MK), pulverised fly ash (PFA) and limestone, which was anticipated to accomplish a negative CO₂ equilibrium as it absorbed CO₂ spawned during the hydration process or from the environment to produce siderite (ferrous carbonate FeCO₃) yielding a rock like sustainable performance on drying/ setting (Nadir, Ahmed and James, 2023a Appendix IV,

Nadir, Ahmed and Moshi, 2024 Appendix VIII). The incorporation of fibres obtained from the shredding of scrap/ waste materials like steel fibre (STF), polypropylene (PPF), polyethene terephthalate (PETF), high-density polyethene (HDPE), wheat straw (WSF), and coconut coir fibres (COF) had been envisaged as a rewarding/ historically inexpensive solution to overcome the weak tensile/ flexural strength of binders for lower strength stipulations (Ahmed et al., 2020 Appendix IX; Nadir et al., 2022 Appendix X). The durability of sustainable materials was assessed by studying selected mixes under concentrated exposure in 2.5% Na₂SO₄ + MgSO₄ solution for 270 days, followed by chemical-mechanical synthesis using advanced testing methods of SEM/ EDM/ XRD/ XRF.

1.2 Outline of Dissertation

The dissertation mainly consists of five chapters encompassing all the activities/ research/ publications conducted during the currency of the project. Chapter One briefly introduces the project background, problem statement, research questions and significance of the research. Chapter two covers the review of existing literature on hydrological studies, flood forecasting techniques, natural/ structural flood management, environmental impact assessment process for construction projects, impacts of hydromodifications on streams ecology/ climate, CO₂ emissions and lifecycle GHG emissions of construction materials, review of construction materials including cement, concrete lime, hydrated lime, pozzolans, waste industrial/ agricultural materials including ashes and fibres, chemical-mechanical synthesis of cement hydration and sulphate attack and microstructural studies using advance testing of SEM/ EDM / XRD. Chapter three explains the methodology of formulation of multiple mixes and ratios, testing standards, procedures, types of equipment, and methods of obtaining results/ measurements. Chapter four discusses the results and analyses these results in light of established materials, approved standards, and existing literature/ research for comparison with the results of innovative materials. Chapter five encompasses the recommendations from the study, outlining the significance of

the research and concluding the project's outcome, followed by the references and appendices.

1.3 Problem Statement

The world is now more apprehensive about environmental impacts whenever an endeavour is planned to construct a megastructure, or a natural watercourse is modified using structural methods disturbing the natural outlook/ habitation. Any treatment using artificial materials would likely disturb a stream basin's natural course/ habitat. However, sometimes it becomes essential to modify nature with artificial means to overcome the damages caused by previous anthropogenic activities, negligent execution of prior projects, especially when dealing with water streams, or harnessing uncontrolled natural calamities. Sometimes, constructing a megaproject is considered more rewarding/ beneficial for humankind than its inherent environmental impacts due to its potential benefits. Using recycled, greener materials is then considered a better option for minimal ecological consequences, which needs to be considered to suggest sustainable materials. The uncontrolled waste production at an enormous scale, especially non-biodegrade polymers and agricultural/ industrial waste, and the colossal efforts required for their disposal, entails the adoption of efficient waste recycling. Therefore, focused studies must be conducted on how to absorb/ recycle waste materials to produce innovative, valuable materials. This project elucidated the formulation of sustainable composites using organic waste (rice husk ash, palm ash, wheat straw, coconut fibres, PET/ HDPEF, PPF) and inorganic materials (GGBS, PFA, MK, SF, lime, iron powder, steel fibres and OPC) in specific ratios for the preparation of sustainable materials. Comprehensive classical/ advanced laboratory testing was required to validate sustainability/ strength for the intended purpose as an alternative to cement concrete in infrastructure construction in general and to use it as an eco-friendly stabilisation material in hydro-structures in particular.

1.4 Research Questions

- How could agricultural/ industrial waste impact the environment, and how could it be recycled into other useful construction materials to minimise environmental impacts?
- Can agricultural/ industrial waste be recycled into the formulation of low, medium and high-strength fibre-reinforced SCMs, low-carbon iron-based binary/ tertiary pozzolanic composites and cement-free fibre-reinforced limecrete to minimise environmental impacts by the construction industry?
- How do these materials compare their environmental impact to traditional materials like cement concrete?
- What would the chemical-mechanical properties of such sustainable materials be, and how much would their durability be in the marine environment/ sulphate attack?
- What are these sustainable materials' beneficial/ significant applications in infrastructure construction/ channel stabilisation?

1.5 Research Aim and Objectives

1.5.1 Aim

This project aimed to "develop/ elucidate the sustainable materials for greener infrastructure construction and hydromodifications/ water channel stabilisation."

1.5.2 Objectives

The following were the main objectives of this study:

- Formulating, preparing and validating the low, medium and high-strength SCMs/ FRC, low-carbon iron-based binary/ tertiary pozzolanic composites and cement-free fibre-reinforced limecrete for greener infrastructure construction and water channel stabilisation.

- Investigating the durability/ sustainability of the developed sustainable materials against sulphate attack and elucidating chemical-mechanical synthesis using SEM/ XRD/ XRF advance testing.
- Recommending the applications of these materials for channel stabilisation and infrastructure construction with lower embodied CO₂ emissions.

1.6 Contribution to Knowledge

Due to climatic variations and anthropogenic activities, the world faces frequent natural disasters and wastage of natural resources due to a lack of strategic river basin management and preventive planning/ non-availability of requisite infrastructure. A slight slackness was observed when considering catchment-level water resource management and statistical forecasting/ hydrological studies. The environmental implications were observed as under-determined, and suitable materials selection was found to be missing before undertaking the megaprojects. Instead, firefighting efforts are made piecemeal in a localised domain, which might disturb the overall environment. Moreover, waste materials from industrial/ agricultural fields need to be recycled/ disposed of properly, which otherwise might result in accelerated waste production/ atmospheric degradation.

The sustainable material suggested by this study would help mitigate erosion of channel structures, beds, banks, and embankments by their use in manufacturing durable but comparatively cheaper breakwater blocks/ walls or shotcrete on soil surfaces and mixing sustainable materials in soil for stabilisation. An effort was made to measure the research/ practical gap by formulating/ recycling low-cost sustainable waste material/ fibres to protect the environment and water structures. The sustainable composites developed as greener SCMs by this study incorporating waste material with cement/ lime/ iron powder/ pozzolans/fibres would likely reduce global waste production and minimise CO₂ emissions by the construction industry. This study recommended methods of using sustainable materials that were least disturbing to ecology/aqua life/ habitat

if employed in channel lining, break walls, and embankment treatment. The recommended channel stabilisation methods would help minimise water wastage due to unnecessary subsoil inflow and prevent flood disasters by amicably securing the structures with the required strength/ materials.

Lime with pozzolanic binders was also used as limecrete, a substitute for OPC, which had a lower cost and minimum environmental impact. The enhanced use of lime with pozzolans developed in this study as cement-free limecrete would likely accelerate/ flourish the lime industry. The high-strength/ high-performance cement-based SCMs and modified iron-based binary/ ternary pozzolanic composites with fibres extracted from industrial/ agricultural waste would likely reduce cement utilisation. They would increase waste absorption with befitting recycling, thus reducing construction costs and minimising the construction industry's carbon footprints.

1.7 Research Methodology

1.7.1 In-depth Study of Existing Literature/ Research

A literature review of the physical/ chemical properties of various organic/ inorganic materials was conducted to formulate a sustainable job mix formula using waste materials like rice husk, coconut fibre, fly ash, and plastic waste from PET/ HDPE bottles, OPC, and lime. The research on using sustainable material was explored to draw lessons for this study. The sustainable materials were studied to suggest their use as greener materials in the construction industry, particularly for different stabilisation/ protective options for channels/ structures like lining, breakwater walls/ blocks, and gabion blocks.

1.7.2 Laboratory Testing/ Quantitative Analysis

The quantitative analysis technique evaluated SCMs containing sustainable materials as per the BS and ASTM's specified global testing standards. Laboratory testing for different job mix formulas and materials was conducted in

concrete laboratories using BS and ASTM relevant standards for testing/ materials like BS 8500:2019 and BS EN 206, BS 1881, BS EN 14889-2:2006, Cement BS EN 12:1971, aggregates BS 882:1975, ASTM C39/ ASTM C192 and ASTM D1102-1112 to determine the sustainable physical/ chemical properties like compressive strength (BS 12390-4:2000), flexural/ tensile strength and measurement of post ductility cracks using BS EN 14651:2005, absorption, density, bulk density, thickness, swelling, hydration/ hydraulic behaviours, diffraction. In this project, an endeavour was made to develop low, medium and high-strength cement-free/cement-based SCMs, which could help achieve low carbon footprints in the construction industry and could be used in the construction of greener infrastructure and waterfront structures in channels/ flood defences exhibiting sustainability/ durability against sulphate attack. The dissertation elaborated on working on three categories of materials (SCMs demonstrating a strength range of 10 - 80 MPa) for better comparison of established versus sustainable low, medium and high-strength materials:

Cat 1: High-strength cement-based composites incorporated the binders/ pozzolans (2.5-30%), 0.5-2% fibres and alternative fine/ coarse aggregates (10-30% glass, shredded PET, rubber tyres and RCA). In the initial experimental stage, the engineering properties of plain/ FRC/ SCMs were studied. They were formulated using established binders/ pozzolanic materials like OPC, GGBS, PFA, SF and MK with fibres like steel (STF) and PPF to compare with FRC-based SCMs containing agricultural waste materials like RHA, PA, and fibres extracted from PET/ HDPE bottles, wheat straw (WSF) and coconut coir.

Cat 2: Low/ medium strength sustainable cement-free hydrated lime-based pozzolanic composites were formulated using 10-90% GGBS, PFA, SF and MK, and the best strength-achieving materials (GGBS 80%+ CL90 20% and MK 50%+ CL90 50%) were used to evaluate the engineering properties of fibre-based composites using 1-2% SF, PPF, PET and WSF.

Cat 3: High-strength iron-based pozzolanic composites (10-50% Fe-composites +10-50 % OPC) with/ without fibres were formulated as innovative carbon-negative, waste-absorbent, eco-friendly, greener materials. The best-performing iron-based composites were used to develop FRC composites containing 10% modified Fe-composites with binary/ tertiary pozzolans (PFA/SF/MK/GGBS/PA) and 1-2% SF, PPF, PETF and WSF.

The durability of best-performing sustainable cement-free and iron-based FRC composites was elucidated as per ASTM C1012/C1012M:2019 by immersion of cubes for 270 days in a sulphate solution of 2.5% Na_2SO_4 + 2.5% MgSO_4 concentrated environment to depict an accelerated field sulphate attack of 10-20 years in laboratory conditions. The chemical-mechanical/ microstructural synthesis was investigated using SEM/ EDM and XRD/ XRF advanced testing to evaluate the durability of sustainable materials by analysing strength, morphology, elemental composition, degree of degradation, elongation/ deterioration and development of ettringite in the sustainable materials.

1.8 Ethical Considerations/ Risk Assessment

A risk assessment was conducted, and ethical approval was obtained from the concerned university authority/ director of studies (attached in Appendix I). The confidentiality of participating departments/ people/ data was considered at all levels, and no data/ knowledge was used without consent and proper referencing. All kinds of ethical practices required to be considered in a research project were observed along with the university rules and regulations. Adequate referencing was given where needed to acknowledge the work of others included in this project for literature review/ comparison, with no plagiarism. The dissertation's research/ literature review was published as international journal papers (attached as Appendices II -XIV). Confidentiality of persons/ departments was preserved as required, and the work was conducted/modified as per approval of the director of studies and university norms.

1.9 Summary

This chapter explored why there is a need for a research project which could elaborate on the collaboration of water resource engineering with material sciences. The various requirements of strength/ materials for greener infrastructure/ water bodies for channel stabilisation/ flood defences could lead to the development of sustainable, innovative low cement-based/cement-free lime-based and iron-based pozzolanic SCMs. Adequate analysis/ forecasting of rainfall/ channel flow discharge using historical data to ascertain the flood risk/ mitigation would help devise the engineering solutions to avert the disasters. The chemical-mechanical synthesis and advanced testing for formulation and testing of engineering properties/ durability of the sustainable materials were outlined. The aim/ objectives of the project, research questions to focus on, and expected significance of developing environmentally friendly innovative materials recommended for low, medium, and high-strength construction were introduced conclusively.

2 Chapter 2: Literature Review

Chapter 2 comprises the literature review portion of the dissertation. It discusses the hydrology studies, flood/ rain forecasting, flood management techniques, cement, lime, concrete, alternative materials, environmental impact assessment of construction hazards, internal/ external sulphate attack mechanism, global wastage and its beneficial disposal and the review of the contemporary research on the formulation of cement alternative SCMs broadly.

2.1 Water Resource Management and Hydrological Studies in Flood Prevention

The climatic variations and anthropogenic activities in the river catchments worldwide are causing severe weather events and flooding. The construction of bridges, roads and built-up areas across water drainage paths disturb the natural flow pattern and give rise to inundation and flood disasters in low-lying areas. Hydrological studies, flood modelling, and statistical flood frequency analysis are imperative for assessing the hazards/ risks of flooding and their mitigation measures. Estimating predicted storms/ floods for different return periods could give a reasonable idea about the frequency of occurrence of storm events (Nadir and Ahmed, 2022a). Water has a crucial place in the advent of humankind and the flourishing of mega population centres, and it is an essential source of food, water transportation, and irrigation. The anthropogenic activities in taming the natural water streams to the optimum benefit of human beings disturb natural flood plains, ecology and habitat. The channelisation of streams and hydromodifications in dams, barrages, or reservoirs results in local/regional climatic variations and impacts transborder stream flow. The reclamation of land for agricultural purposes, deforestation, peatland modification, the convergence of vast flood plains to narrow streams, heavy structural modifications obstructing surface runoff, micro/ macro-pore soil capabilities, disturbed water cycle, lesser sub-soil absorption and increased velocity of drainage in the river basins are the major anthropogenic activities in river basins. The cloud bursts due to global

warming/ climatic variations cause heavy precipitation in short intervals, thus decreasing the lag time between a storm event and a peak discharge, resulting in flash flooding/ disasters. Researchers endeavoured to restore the floodplains to their natural conditions. Still, huge hydromodifications and the development of megacities right in the flood plains or adjacent to the streams have resulted in irreversible disturbances to the natural lay of ground/ landscape (Nadir and Ahmed, 2022a). Therefore, to avoid flooding disasters, further structural interventions are undertaken to augment the natural flood prevention methods using advanced materials like cement concrete, steel, and polymers rather than increasing the emissions of greenhouse gases. Considering the strategic necessity of engineering structures as an integrated catchment level solution to augment the natural methods, the researchers/ engineers are now focussing on the use of sustainable, eco-friendly materials and demountable/ hydraulic structures to minimise the carbon footprints of hydromodifications and to decrease the obstruction to the natural flow of streams by using the flood prevention structures/ gates/ walls/ reservoirs only in case of disastrous flooding and otherwise keeping them unemployed during normal stream discharges.

The characteristic global warming potential of ordinary Portland cement (OPC) makes it a huge challenge for researchers to weigh its enormous use with potentially feasible engineering properties versus the environmental impacts. The formulation of sustainable, economical, and greener supplementary cementitious materials (SCMs) is an ongoing phenomenon, attracting the large-scale attention of industry/ academia. The formulation of Fe-composites by David Stone (2010) with low embodied energy, lower consumption of natural resources and minimal global warming potential has paved the way for the use of sustainable material comprising iron powder, pozzolans (pulverised fly ash (PFA) and metakaolin (MK) and lime exhibiting at par performance with OPC. However, a gap was identified in its formulation, raising a further research question on how it would perform if PFA and MK were replaced by ground granulated blast furnace slag (GGBS) or other pozzolans like silica fume (SF) with different mix ratios.

Therefore, an endeavour was made in this study to identify the engineering properties with sustainable use of fibre-reinforced low OPC-based SCMs, cement-free hydrated lime-based pozzolanic composites and iron-based modified binary and ternary pozzolans/ GGBS/ OPC composites (Nadir, Ahmed and West, 2023a).

2.1.1 Historical Flood Events

Water has a special place in the life of human beings as a basic necessity (Shirleyana and Anindya,2012), and all civilisations developed along the waterfront which resulted in ecological modifications/ pollution, glaciers melting, extraordinary precipitation events, flooding and damage to aqua life and wildlife (WWF,2012). The disturbance in supply in the stream's catchments was causing many battles to occupy land/ water resources (Herve et al.,2003). In the South Asian sub-continent, Kashmir is the originating point of many significant rivers of Pakistan and India, and both countries have fought three wars in Kashmir. It is still considered a nuclear war flash point (Roy,2019). Yangtze River in China has a history of devastating floods periodically, especially the floods in 1911, 1935 and 1954, which were the worst floods which resulted in the deaths of millions of people and the swapping of properties/ land in 6300 km stretch, Yellow River in China, Indus in Pakistan, Ganges, Jumna and Brahma Putra in India and Bangladesh are the major flood causing rivers mainly arising from climatic changes and urbanisation/ modifications along natural rivers stretches (Kumar,2017). The flood in 2011 in the Mississippi River was the worst of its kind, impacting 31 states, including hundreds of casualties and destruction/evacuation of millions of populations (USACE,2008; Schleifstein,2011; NMRM,2018 & WIKI2,2019). Europe had numerous casualties and property losses in the last few decades because of heavy rain/ flood events due to climatic changes and human modifications/ pollution (Prevention Web, 2008). Elbe flooding in 2002 in central Europe, the UK flooding in 2007 (Flood site, 2009) and the Copenhagen, Denmark flooding in 2011(Shandana,2012) caused horrific impacts of Billions of dollars on the economy/ routine life (Nadir and Ahmed, 2022a).

2.1.2 Rainfall/ Discharge Forecasting Techniques.

Conducting storm/flood frequency analysis is imperative to statistically predict their future occurrence for hazard assessment and risk mitigation (Benameur et al.,2017; Renard et al.,2013). It is generally a widespread practice in the hydrology and construction industry to statistically evaluate the probability of flood events and the impacts of the construction of hydraulic structures (Saleh,2011; Helsel & Hirsch, 2010; Stewart et al., 1999). The accuracy of such studies based on the selection of the best probability distribution function with the best ranking of Goodness of fit (Saghafian et al.,2014), suitability of long-term past data (Kamal et al.,2016) and adoption of suitable estimation parameters (Millington et al.,2011). Researchers like Rahman et al. (2013) and Millington et al. (2011), in their studies about discharge in the River Thames, described Log Pearson 3 (LP3), Generalized Extreme Value (GEV) and Gumbel Maximum (Gum Max) as better fitting probabilistic approaches with better Goodness of Fit ranking on Kolmogorov Smirnov, Anderson Darling and Chi-Squared methods (Rahman et al .,2013; Millington, Das and Simonovic, 2011). The EasyFit software provided by Mathwave.com could be used to statistically analyse the existing rainfall/ discharge data sets. The EasyFit software uses the given data on the horizontal axis as "x." It provides the probability distribution function, cumulative distribution and hazard function on the vertical axis as a function of x $f(x)$ (Mathwave EasyFit 5.6 Pro, 2019). In this study, Log Pearson 3 (LP 3), Generalized Extreme Value (GEV), and Gumbel Maximum (Gumb Max) were recommended for statistical analysis of rainfall/ discharge data using EasyFit software. These are considered the top best-fit probability distribution functions (PDF) (Millington, Das and Simonovic, 2011) and were used by several researchers. Log Pearson 3, GEV and Gumbel max are preferred as they fit the data well to predict storm/ flood frequency return periods with a better ranking of the Goodness of the fit test (Singho et al., 2013; Bezek, Brilly and Sraj, 2014; Liu et al., 2015; Deng, Reng and Feng, 2016; Rulfova et al., 2016; Kamal et al., 2018). These methods used estimation parameters based on the technique of methods of moments (MOM)

or method of L (long dataset) movements as per the length of the given data set (less than 50 entries or more than 50 entries) (Rowinski, Strupczewski and Singh, 2002). The Goodness of Fit of these probability functions could be evaluated using Anderson Darling, Kolmogorov Smirnov and Chi-Squared using EasyFit inbuilt programming to statistically forecast the precipitation and discharge in a river (full paper is attached as an Appendix II). (Cunnane, 1981; Cunnane, 2010; Millington, Das and Simonovic, 2011; Nadir and Ahmed, 2022a Appendix II).

2.1.3 Use of Log Pearson 3 Equations to Ascertain the Probability of Storm/ Discharge Events with Return Periods.

Oke and Aiyelokun (2014) and Nadir and Ahmed (2022a Appendix II) observed in their hydrology studies that the Log Pearson 3 performed at the top with the best Goodness of fit test ranking for all kinds of data; therefore, they chose it for further calculation using its equations for the determination of return periods. The given annual 24-hour max rainfall "R" and annual peak discharge "Q" data is converted into Logarithm values using equation 1 (use R for rainfall and Q for discharge data in these equations):

Equation 1: $R_i = \text{Log}(R)$

Calculation of Mean, Standard deviation, Skewness coefficient and Return Periods for storm/ flood frequency analysis (Oke and Aiyelokun, 2014)

The mean " R_m " of R_i is calculated by equation 2, summing all rainfall values and dividing by the total number of readings/ years.

Equation 2: $R_m = 1/n \sum R_i$

Standard deviation is calculated using the equation 3:

Equation 3: $S_d = (\sum (\text{Log}(R) - \text{Avg}(\text{Log } R))^2 / (n-1))^{1/2}$

Skewness is calculated by equation 4:

Equation 4: Skewness = (Log(R)-Avg (Log R))³

Skewness coefficient G is calculated using equation 5 to determine the value of a frequency factor constant "K" from the Table in Hann's book (Hann,1977).

Equation 5: Skewness coefficient G = $n \cdot (\sum (\text{Log}(R) - \text{Avg} (\text{Log R}))^3 / ((n-1) \cdot (n-2) \cdot S_d)$

The return period is calculated using equation 6 by putting the rank of the value of rainfall/ discharge in the data set "m" and the total number of entries/ years in the data "n":

Equation 6: Return Period (T_r) = $2n/(2m-1)$

Where m=Rank, n=No of years

Exceedance probability is the reverse of the return period and is calculated by using equation 7:

Equation 7: Exceedance probability $R_m = 1/T_r$

All the above equations are used to do the discharge calculations by substituting "Q" in place of "R." Now predicted/ designed rainfall " R_p " or discharge " Q_p " is calculated for 2, 5, 10, 25, 50, 100 and 200 years, taking the value of K_t from Table 7.7 of Hann's study (Hann, 1977) for each period and then taking anti Logarithm of the results obtained from the following equations:

Equation 8: $R_t = R_m + K_t \cdot S_d$

Equation 9: $R_p = \text{Anti Log } R_t = (10)^{(R_t)}$

Equation 10: $Q_t = Q_m + K_t \cdot S_d$

Equation 11: $Q_p = \text{Anti Log } Q_t = (10)^{(Q_t)}$

Equations 9 and 11 give the predicted designed rainfall R_p / discharge Q_p as per the Log Pearson 3 method of probability distribution function (Oke and Aiyelokun, 2014; Nadir and Ahmed, 2022a Appendix II).

2.1.4 Significance of Hydrology Studies and Flood Forecasting.

Hydrological studies, flood modelling, and statistical flood frequency analysis are imperative for assessing the hazards/ risks of flooding and their mitigation measures. Estimating predicted storms/ floods for different return periods could give a reasonable idea about the frequency of storm events. Flood frequency and statistical analysis using Log Pearson 3 (LP3), Generalized Extreme Value (GEV), and Gumbel Maximum (Gumb. Max) on EasyFit software and Log Pearson 3 equations could predict weather instability in a river basin with the prediction of super rain/ flood events. Construction of hydraulic structures or roads/ embankments along the rivers or cross-drainage structures would disturb the natural drainage pattern and likely result in inundation in flood plains due to the inadequate capacity of cross-drainage structures to withstand spontaneous flash flooding. The probability density and hazard functions showed a probability of any mega hazard; therefore, cross drainage structures and crisscrossing channels in the river catchments should be planned on a minimum 100-year return period as an economic/ reasonable safe limit or to a 200-year return period plus safety factor for climate control if resources are available. Still, additional structural/ non-structural measures (natural flood management techniques) should be employed to augment the engineering structures for efficient flood-fighting. These include plantation, afforestation, buffer strips, leaky dams, maintenance of flood plains, and maintenance of drainage structures. The construction of small dams/ weirs, barrages, sluice gates, and offline ponds/ reservoirs were good options for swift water management in flash floods. Placing rescue/ relief resources at accessible points based on flood zoning/ population centres is essential after the flood events. The forecasted rainfall and discharge assessed by the hydrology study could elucidate the types of structures with discharge capacity and the strength of materials required for undertaking the

structural flood defences/ channel stabilisation arrangements. Instead of using normal earthen flood levees and cement-based concrete, it was found imperative to use environmentally friendly materials in channel enhancement methods/ shapes, which could lower the carbon footprints, preserve the ecology/ habitat of the water bodies, minimise the CO₂ emissions and incorporate the waste agricultural/ industrial waste materials to formulate sustainable materials. These suggested requirements gave impetus to continue further studies to develop cement-free lime-based, lower cement-containing alternative materials/ binders cement concrete and iron-based binary/ ternary pozzolanic SCMs for utilising in a variety of low, medium and high strength materials requirements (Nadir and Ahmed, 2022a).

2.2 Strategic Integration of Catchment Level Natural and Structural Methods of Sustainable Flood Management (Nadir et al., 2024).

Flood management is about managing flood risk to minimise loss of life, damage to property and economic disruption (Solin and Skubincan, 2013). Flood management measures could have unintended adverse social or environmental impacts downstream, e.g., on river ecology (Keep, 2017). Sustainable flood management aims to provide maximum physical, social and economic resilience to flooding and its impacts (Werrity, 2006). It is susceptible to various interpretations according to the causes/ effects of flooding, intended objectives, and the quantum/ capacity of flood protection management (Kundzewicz, 2002). Sustainability depends on local context, drivers of flooding and flood risk (Qi and Altinaker, 2011) and incorporates the requisite balancing of environmental goals by amicably addressing the social and economic consequences of any anthropogenic activities/ hydromodifications (Emery and Hannah, 2014). It includes natural flood management and resilience measures employed using structural solutions (Qi and Altinaker, 2011). Sustainable flood management includes several techniques which could be employed alone or as a combination based on required protection, the geology of the area, resources available, the

importance of infrastructure/ land to be protected, the extent of flood protection and environmental goals/ repercussions (Nadir et al., 2024).

2.2.1 Natural Flood Management (NFM) Techniques.

Natural flood management involves working with biological processes to primarily reduce the flooding risk by employing natural methods to intercept the stream flow, slow down the water velocity and store water throughout the catchment area in small reservoirs to avoid converting surface runoff into flash flooding by getting swiftly into the water body (Environment Agency, 2018b). NFM is employed to replace or complement the traditional complex engineering flood defences. NFM is considered to exhibit its inherent economic benefits of low-cost flood defence measures, environmental benefits of maintaining natural habitats, improved water quality and resilient catchments with minimum impacts on climate. The NFM's social benefits include improved ecological quality, enhanced human health, and well-being in all living organisms in the surrounding localities. However, NFM has various limitations, primarily because it could cater to small streams with a limited extent of flood protection mechanism, which is restricted to around 10 Km² (Environment Agency, 2018b). NFM measures become less effective as flood magnitude increases so they could be employed for smaller streams/ channels. Woody debris/ grass/ plantation used as NFM could get dislodged and block the subsequent structures (bridges, culverts), resulting in bursting/ flooding (Figure 2.1). Re-connecting the river with the floodplain and making small reservoirs/ ponds/ flood buffer zones and land management with reforestation/ extensive plantation may increase the groundwater levels and decrease agricultural productivity as it disturbs the water cycle of precipitation/ infiltration/ evaporation/ evapotranspiration due to standing water and increased number of trees as depicted in Figure 2.2 (Cunningham et al., 2015; Environment Agency, 2018b). A few NFM techniques like leaky dams, cross-slope woodlands, drainage slope management, catchment/ runoff pathway management using a plantation, forestation, creation of offline reservoirs, ponds, flood buffer zones, river channel restoration by extracting gravels/ desilting, farmland management,

salt marsh, mudflats and dune management at the estuary points employed throughout the river catchment were illustrated in Figure 2.3 (JBA Consulting, 2018; Nadir et al., 2024).

2.2.2 Afforestation and Riparian Woodlands

Riparian is extracted from the Latin word “Rippa”, meaning on the river bank, so riparian woodlands are the forests created along the rivers/ water streams primarily to absorb the extensive flood water by inundation and to decrease the Mannings “n” of the adjacent land to decrease the water velocity to avoid a flash flood by creating hindrance to flow and creation of macropores in the soil for swift absorption of water beyond natural absorption limit of soil (Zhang et al., 2001; Forest Research, 2018). Hydraulic roughness - Mannings “n” values are affected by spacing and layout of trees, smoothness of trunks, presence of lower branches, abundance and nature of undergrowth, and amount of dead wood (Dadson et al., 2017). Coniferous trees have higher water uptake but do not have the biodiversity and ecological richness levels compared to deciduous trees (Forest Research, 2018). Various native tree species are favoured for adaptability to climate, and a wide variety of species are beneficial for disease resistance options (Lane et al., 2007). Willow and poplar are preferred for their increased water uptake. The creation of riparian woodlands in the river catchment as an NFM technique is considered beneficial due to the cost-effectiveness, design of ecologically rich habitats (Forest Research, 2018), reconnection of fragmented habitats (EA, 2014), binding and strengthening of stream banks, reducing erosion and bank collapsing, entrapment/ binding of stream structure, reduced sediment delivery from land to streams by up to 85% per year (Lane et al., 2007) and performs as a safety barrier to the ingress of fertilisers/ pesticides into the streams (EA, 2010). However, over-application could adversely affect catchment yield, and too much water is being removed to the detriment of the catchment system's ecological and human requirements (Europe Economics, 2017). An overabundance of tree canopy could dramatically reduce water temperature, resulting in the slow growth of fish (Forest Research, 2018). It takes a long time

for woodlands to mature sufficiently to be effective (EA, 2018a). The inherent difficulty in modelling the quantitative benefit of woodland implementation is experienced by many variables like topography, soil characteristics, land hydraulic factors, and other flood prevention measures (Thorne and Warburton, 2010; Nadir et al., 2024).

2.2.3 Flood Management with Hard Engineering Structures

Therefore, engineering structures are erected/ employed as reliable, sustainable and cost-effective measures (based on cost-benefit analysis) to avoid flash flooding and disaster damages (Plate, 2000; Plate, 2002; WWF Scotland, 2010). Some structural/ engineered flood management techniques are stone-pitched flood bunds, gabions, stone-lined banks, storage ponds/ tanks, dams and dykes. Concrete/ stones/ masonry walls, raised and permeable pavements, raised bumps, sponge cities, storage parks, car parks and wash lands, raised berms and edges, flood channels and canals, pumping stations, sheet piles, land use zoning, the extension of bridges, the raising of banks, dredging and widening (Figures 2.4 - 2.14) (Nadir et al., 2024).



Figure 2.1: Woody Debris Blocked by a Bridge (McDonald et al., 2004)

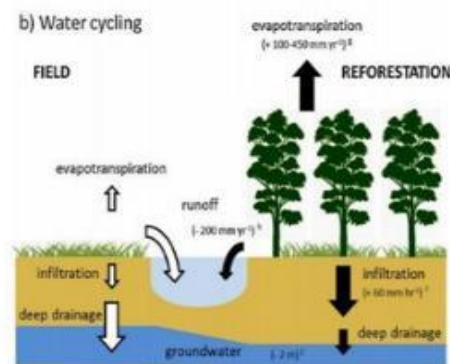


Figure 2.2: Water Cycle (Cunningham et al., 2015)

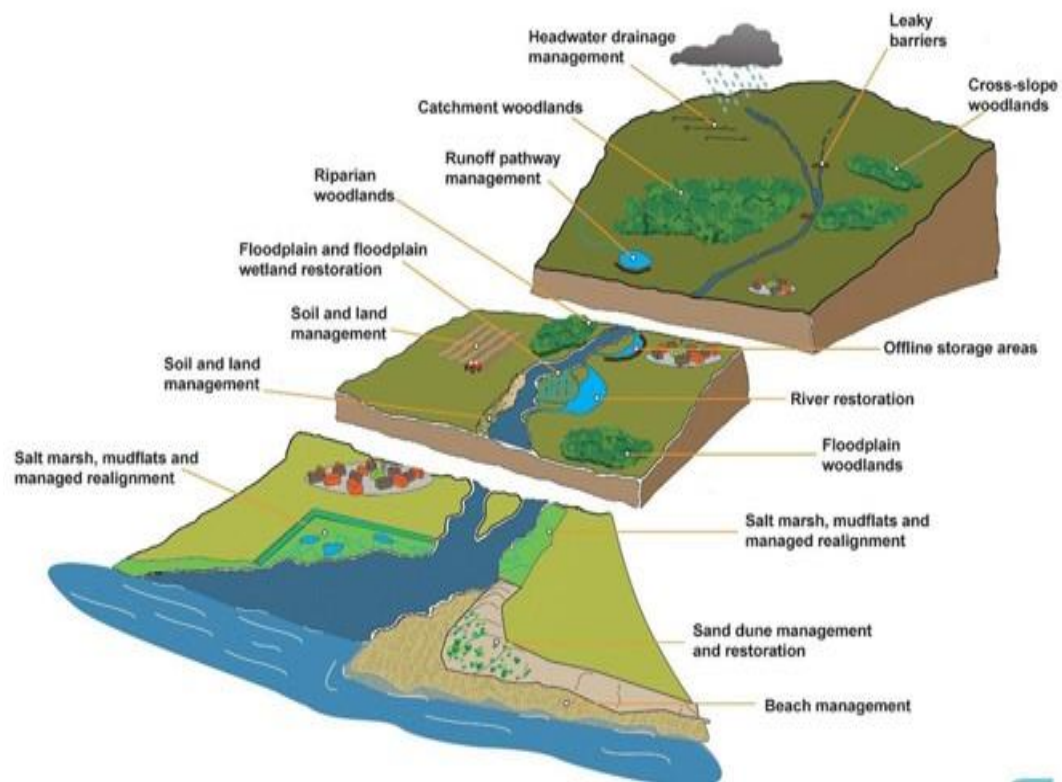


Figure 2.3: Natural Flood Management Techniques (JBA Consulting, 2018)



Figure 2.4: Flood Protection Concrete Wall (Admin, 2012)



Figure 2.5: Flood Protection Bunds and Gabions (www.pixshark.com, 2023)



Figure 2.6: Pyramid Breakwater Stones with Raised Berms/ Walls and Edges (www.geograph.org.uk, 2023)



Figure 2.7: River Wharfe Weir at Tadcaster (Glazzard, 2007)



Figure 2.8: Sheet Pile in Yorkshire (www.northernsheetpiles.co.uk, 2021)



Figure 2.9: Sheet Piled Wall in Tadcaster (Aeyates, 2018)



Figure 2.10: Flood Protection Dykes (Alamy Limited, (2019).)



Figure 2.11: Flood Protection Dam (www.blog.weatherflow.com, 2016)



Figure 2.12: Flood Retarding Structures (www.geography.org.uk, 2021) Figure 2.13: Storage Pond Belford UK (The Flow Partnership, 2021)



Figure 2.14: Sponge Cities in China, Structural Flood Management (Clean Technica, 2018)

2.2.4 Case Study: Sustainable Flood Management in Wharfe River Basin

The Wharfe upper catchment receives around 2000 mm of precipitation annually (JBA, 2013). Characterised by a ‘flashy’ flow regime due to catchment geomorphology, aggravated by historic upland drainage (JBA, 2013) and low permeability soil conditions/ geology. It is considered a flash flooding small river with the fastest formulation of storm-to-flood event stream in the UK. Therefore, it was selected as a case study to explore flood management techniques. (Dales to Vale Rivers Network, 2018).

2.2.4.1 River Wharfe Catchment Overview (Figure 2.15)

River Wharfe originates near Buckden in Yorkshire Dales (North Yorkshire County Council, 2017), runs through glacially formed valleys (McDonald et al.

2004), joins River Ouse at Cawood and flows out into the Humber estuary below Tadcaster (North Yorkshire County Council, 2017). It comprises rural, agricultural and sparsely populated catchment with a few towns and small villages (Environment Agency, 2014; Nadir et al., 2024).

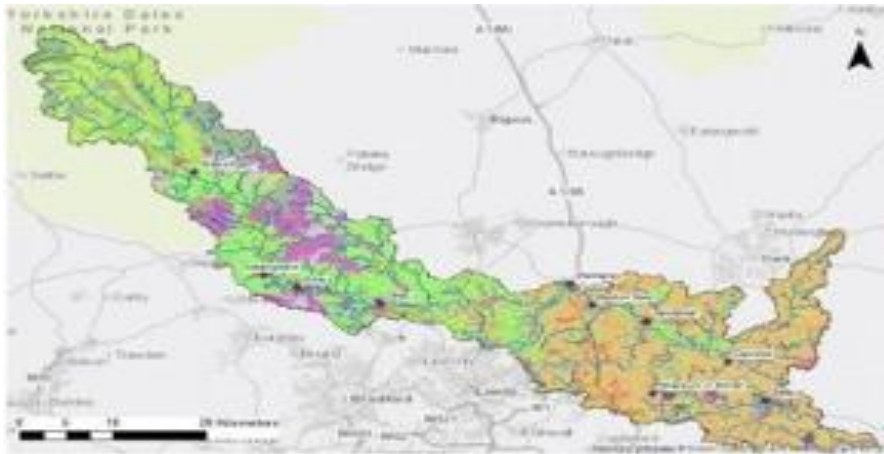


Figure 2.15: River Wharf Catchment Overview (Rowland et al., 2015)

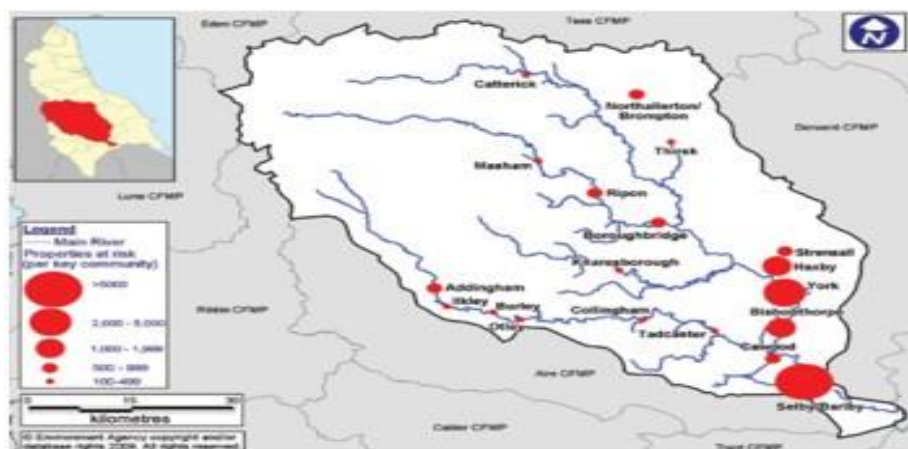


Figure 2.16: Wharf River Flood Risk Areas (Environmental Agency, 2010; North Yorkshire County Council, 2017).

2.2.4.2 Flood Risk Overview - River Wharf Catchment

River Wharfe frequently floods towns and villages in the catchment, which is generally adjacent to the river stream and is a crucial receptor for fluvial flooding

(Leeds City Council, 2015; Dales to Vale Rivers Network, 2018). Otley, Collingham, Wetherby, Thorpe Arch and Boston Spa are the settlements severely affected by flooding, especially the famous “Boxing Day” flooding in 2015 (Environment Agency, 2010; Leeds City Council, 2015), as shown in Figure 2.16 (Environment Agency, 2010; Nadir et al., 2024).

2.2.4.3 Wharfe Catchment Flood Drivers Overview

Flooding is further exacerbated by a high coarse sediment supply into the stream with surface runoff, reducing channel capacity and increasing flood frequency (Reid et al., 2005). Raven et al. (2009, 2010) found that the sedimentation reduced channel capacity in the upper River Wharfe by 21.9% in 4 years, increasing annual flood frequency by 2.6 times on average. Therefore, the sediment transport/ silting control in the upper catchment is vital in preventing bank overflowing/ flooding, especially in peak flow discharge events (Lane, 2007; Nadir et al., 2024).

2.2.4.4 NFM Techniques Employed in Wharf River Basin

NFM was predominantly used in the Upper Wharfe catchment area (Dales to Vale Rivers Network, 2018). NFM was adequate for small communities in the Upper Wharfe, where flood risk might not justify the higher cost of structural flood defence measures. NFM is effective where complex engineering may damage river ecology. In 2015, 9 out of 14 water bodies in the Upper Wharfe were classified as having ‘good ecological status’ (Figure 2.17) (Environment Agency, 2018a). Buffer Strips are the buffer zones adjacent to the riverbanks adjoining the nearby agricultural land. It increases catchment roughness and intercepts the direct movement of sediment/nutrients-laden water into the river channel. It is an NFM technique that rehabilitates riverbanks with grass/ vegetation using the silt/ soil from the bed/ adjacent lands. It takes considerable time to mature with appropriate strength to serve the intended purpose of bank overflowing and preventing the ingress of sediments and polluted debris in the stream, as shown in Figure 2.18. Leaky dams are made from woody debris and are installed across

the river channel to help slow the flow of water (Figure 2.19). Earth bunds are constructed as physical barriers using adjacent soil, restricting overflowing water to the floodplains (Figure 2.20). Offline ponds are created as permanent water storage on the floodplain to store overflowing water as reservoirs. They could be used for drinking water, irrigation, or replenishing stream water in drought (Figure 2.21) (Nadir et al., 2024).

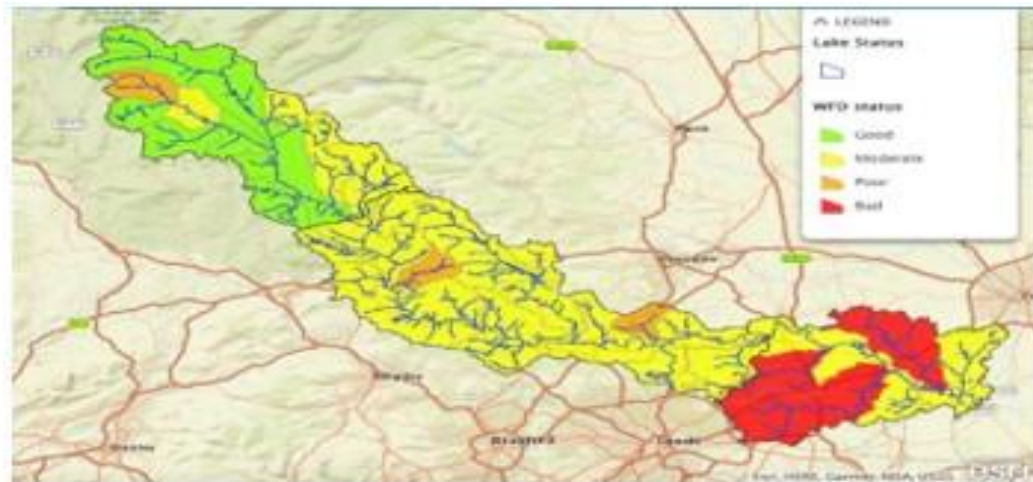


Figure 2.17: Ecology Status in the River Wharfe Catchment Area (Environment Agency, 2018a)



Before 2011

After 2014

Figure 2.18: Buffer Strip Growth Over Three Years on a Reach in the River Wharfe (Yorkshire River Dales Trust, 2014)



Figure 2.19: Leaky Dams on the River Wharfe During Low/ High Floods (Yorkshire Dales River Trust, 2018)



Figure 2.20: Earth Bunds Retaining Storm Runoff on the River Wharfe Floodplain (Yorkshire Dales River Trust, 2017)



Figure 2.21: Offline Pond in the River Wharfe Floodplain (Yorkshire Dales River Trust, 2017)



Figure 2.22: Blackstone Bank Revetment to avoid Erosion due to Gravel Deposition (Environment Agency, 1999)



Figure 2.23: Afforestation to Prevent Flash Flooding and Sediment Transport (Environment Agency, 2018b)

2.2.4.5 River Channel Restoration Techniques - Working with Natural Processes

Working towards restoring the river to a more natural form and function is the removal of silt/ gravel deposits on the riverbed and banks (JBA, 2013). Gravel deposition is a significant driver of flooding in the Wharfe catchment (Lane et al., 2007). The accumulated sediment/gravel results in bank erosion, while the river stream maintains its capacity/ flow (Raven et al., 2009). Thus, rivers such as the Wharfe, with high sediment supply, often overflow across the floodplain as it floods the Buckden area more than 30 times a year because of gravel deposition issues (Environment Agency, 1999). The prevention measures included block-stone revetments to prevent bank erosion (Figure 2.22) (Environment Agency, 1999); however, it proved to be a temporary measure for Wharf River upper catchment stretches, where it failed after 14 years and became full of gravel deposits necessitating reclamation again in 2002 and 2018 (Reid et al., 2007; Waterhouse, 2008; JBA, 2013; EA, 2018a). Peatland restoration with vegetation and natural streams also proved to work towards NFM techniques. The geology of the upper/ middle Wharfe catchment consists primarily of carboniferous limestone overlain with shallow, loamy, free-draining upland soils. Therefore, afforestation and the creation of riparian woodlands helped increase macropores in reforested land, supporting increased infiltration (Figure 2.23) (EA, 2018b). Evapotranspiration through the trees could account for 30 - 40% of annual rainfall (Zhang et al., 2001). The higher water uptake by root action means less water enters deep drainage, lowering the water table. The higher soil moisture level on agricultural land due to the lack of root uptake raises the water table (Europe Economics, 2017), necessitating more tree plantation/ afforestation in a river basin to prevent flooding. Therefore, upper and middle Wharfedale were vital areas considered feasible for reforestation of riparian woodland (EA, 2018a). Implementing these woodlands in uplands where rainfall is highest would significantly impact downstream flow levels (Thorne and Warburton, 2010). However, the riparian woodland cover in upper/ middle Wharfe was relatively low,

with riverbanks characterised by single trees (JBA, 2013). The nascent nature of studies in the catchment showed that the results of the efficacy of NFM were still largely unknown, and widespread implementation was partially applicable (EA, 2014). A survey of afforestation revealed that reforested land resulted in less runoff than grazed land by around 50% in smaller streams (Thorne and Warburton, 2010; Europe Economics, 2017; Dadson et al., 2017; Nadir et al., 2024).

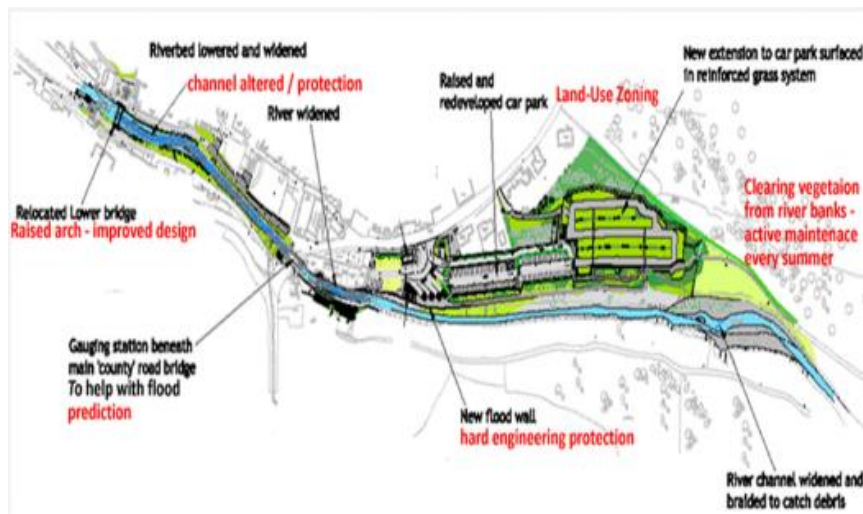


Figure 2.24: Flood Protection Plan in Wharf River Basin using Structural Measures (different segments) (www.geographypod.com, 2018; Nadir et al., 2024)

2.2.4.6 Wharf River Flood Management with Structures (Different Segments)

2.2.4.6.1 Wharfe Foothills

The portion includes Cock Beck, Oak Beck and the town of Harrogate. Flood risk is low, as around 200 properties and some parts of A61 road could be at risk (Figure 2.16 & Figure 2.24) (Environmental Agency, 2010; Flood Protection Plan, 2010; North Yorkshire County Council, 2017). The surface runoff could cause urban flooding in heavy rain. Some small earthen defences already exist. Stone-lined flood protection bunds or concrete walls along the riverbank near the

properties are required. Modifying old bridges as these may obstruct their extension, spurs and wing walls along bridges to channel the stream water, widening of bed, dredging or raising of banks are suggested as suitable structural measures for flood prevention (Nadir et al., 2024).

2.2.4.6.2 Wharfe Rural Towns

This stretch includes the rural towns of Addingham, Ilkley, Burley and Otley, Kirkby, Tadcaster, and Cawood. Runoff from Ilkley and Denton Moors could cause surface water flooding. More than 1,500 properties and A65 are at risk in this stretch. Controlled wash lands, some storage ponds (some are already in place), raised car parking spaces with concrete walls, widening of beds, dredging or raising of banks and raising bunds on sides towards the properties could be reasonable solutions (Figure 2.16 & Figure 2.24) (Environmental Agency, 2010; Flood Protection Plan, 2010; North Yorkshire County Council, 2017; Nadir et al., 2024).

2.2.4.6.3 Ouse and Wharfe in Selby to Goole Town (Combined effect)

This area is affected by the combined tidal/ fluvial flow of Wharfe/ Ouse and surface runoff. Thousands of properties are at risk in this stretch, which could be reduced by earthen flood protection bunds, Controlled wash lands, and some storage ponds like Selby Dam and Bishop's Dyke could mitigate flood. Stoned lined bunds, widening of beds, dredging or raising of banks or raised berms could be suitable structural measures (Figure 2.16 & Figure 2.24) (Environmental Agency, 2010; Flood Protection Plan, 2010; North Yorkshire County Council, 2017; Nadir et al., 2024).

2.2.5 The Efficiency of NFM Techniques and Integrations of Engineering Materials and Hydraulic Structures for Sustainable Flood Management

NFM, having its intrinsic benefits/ limitations, was suggested to achieve partial success if used alone for the prevention/ stoppage of flood events. The cost/

benefit analysis suggested NFM to be time/ cost/ resource constraints, causing methodology that cannot be used to exceed water loads on broader extents of catchments. It could provide a delayed surface runoff lag from storm event to peak discharge event due to slowing down of water velocity; however, considering the climatic variations and cloud bursting mechanisms, these NFM techniques not only failed to stop the flooding but instead resulted in accumulated peak discharge events as experienced in Pakistan, India and Bangladesh, Derna in Libya, USA, Canada, Greece, Turkey, Italy and the Netherlands in recent years causing a loss of more than 30000 lives and 310 billion USD (AON, 2023). Therefore, the researchers/ engineers considered it essential to augment the NFM by using sustainable materials and hydraulic structures engineered to cater for a 100 - 200-year return period of precipitation/ discharge. The provision of hydraulic structures duly augmented with advanced engineering materials/ reinforcement is required essentially to provide a wholistic sustainable flood management system exhibiting reliability, resilience, resistance to dynamic water loading/ storm events, flexibility to withstand peak discharge, capability to regulate needs-based storage/ discharge by employing highest safety standards to absorb varying nature of flood probabilities and consequences (Sebastiaan et al., 2018; Tian et al., 2023). The hydraulic structures are categorised as fixed, demountable and temporary structures, having inbuilt safety standards to protect against abrupt failure, including dams, barrages, weirs, notches, dykes, embankments, the lining of channels, sheet piles, groynes, jetties, pumping stations, buffer zones, flood levees, berms, sluice gates, hydraulic barriers, flood walls, breakwater walls and breakwater stones, (Weller, 2023). The structural techniques of flood prevention were in practice for centuries, as found in the form of earthen flood levees in the Yellow River basin in China, dating back to 2900 BC (Li, Li and Zhang, 2020), raised flood bunds and embankments in London and Rome during the Romans empire in 50 AD and construction NFM and flood buns in England during the rule of Henery VIII during the 1600s (English Heritage, 2011; Nadir et al., 2024).

2.2.6 Considerations for Environmentally Friendly Materials and Methods of Construction

The cost and resources are the main constraints for constructing hydraulic structures in floodplains/ rivers/ coasts (Harman, Bramly and Funnel, 2002). However, their consequential disturbances to climate, water streams, ecology, and the environment raised concerns about the construction of infrastructure/ hydromodifications and the use/ types of construction materials (Koks and Jongman, 2015; Bramly and Bowker, 2002). With the advent of science and technology, the design/ methods and materials used for hydromodifications also evolved from soil, lime, stones and rocks to state-of-the-art OPC-based concrete with reinforcement combining steel and heavy equipment (Chik, 2018). The primary aim was to give protection against flooding/ erosion by breaking the wave energy/ quantum of discharge with/ without using fancy materials/ equipment. These flood control items sometimes remain on the riverbanks/ shores for decades without even facing the designed/ full flood impact. The design requirements and cost/ benefit analysis often do not merit the provision of high-strength OPC-based steel-reinforced concrete, e.g., concrete lining on small distributaries/ channels or protection of land without considerable men/ material assets. The engineers then suggested using alternative materials that could give appropriate strength and serve the intended purpose of structural/ engineering flood protection/ channel stabilisation methods.

Moreover, alternative eco-friendly fibre-based SCMs incorporated waste materials from other industries to perform beneficially as waste absorbent and flood protection materials simultaneously. Therefore, using sustainable materials like combinations of soil, lime and pozzolans, SCMs with fibres/ ashes derived from waste agricultural/ industrial materials or iron-based binary/ ternary pozzolanic composites in meticulously designed strength/ types could reduce disturbances to natural habitat, ecology, environment, the quantum of stone/ gravel quarrying, rock blasting, earth moving. These sustainable materials would help to reduce embodied CO₂ emissions and vulnerability to sulphate attack in

marine/ water exposures while giving appropriate strength to structures (Vrijling, 1989; Weller, 2023; Wilkinson, Quinn and Hewett, 2013; Ahmed et al., 2020 Appendix IX; Ahmed et al., 2021 Appendix III; Nadir and Ahmed, 2021b Appendix VII; Nadir and Ahmed, 2022a Appendix X; Nadir, Ahmed and, West 2023 Appendix IV; Nadir et al., 2024). Sustainable flood management is possible in a river catchment by an integrated catchment level wholistic strategy based on minimum hydromodifications, accepting the reality that flood is a natural hazard, so we must live with it by mitigation employing natural flood management techniques duly augmented by advanced engineered methods and environmentally friendly construction materials. Urban areas that have more men/ material assets should be prioritised. However, modification of old structures, provision/ raising of flood bunds and walls, having more washlands flood storage areas, and revision of riverbeds/ banks might be good options for preventing damaging flood events. The researchers and engineers should endeavour to use alternative greener SCMs/ limecrete in place of cement concrete and soil with lime or pozzolans to construct sustainable but environmentally friendly methods/ materials for a catchment level strategic flood management, including embankment strengthening, channel stabilisation, hydromodifications and flood protection hydraulic structures.

2.3 Review of the Traditional/ Innovative Construction Materials

2.3.1 Lime

The quicklime CaO and slaked lime Ca(OH)_2 are considered among the oldest construction materials, which were used for thousands of years since the inception of great civilisations like the Romans, Greeks, and Egyptians. The naturally occurring calcareous rocks (limestone) containing CaCO_3 are quarried and burnt to produce pure lime, called the calcination process, and are responsible for the construction industry's primary direct CO_2 gas emissions (Ahmed et al., 2020 Appendix IX). The lime is then used as hydrated lime Ca(OH)_2 by slaking the CaO (quicklime CL90 Q) with water as internal/ external

masonry, mortar, and faced work paints. (Ty-Mawr Lime, 2019). The natural hydraulic lime is manufactured under BS EN 459-1:2015 (BS EN 459-1:2015) and is available in the industry as NHL2, NHL3.5 and NHL5 for use as lime mortars, plasters, and renders with 2-5 MPa strength. Non-hydraulic lime, or soft/slow-setting lime putty, is the third type of industrial lime used in construction (Ty-Mawr Lime, 2019; Oates,1998). When used as construction material, the hydrated slaked lime Ca(OH)_2 absorbs CO_2 and slowly sets to create hardened CaCO_3 , thus completing a lime cycle as illustrated in equations 12-14 and Figure 2.25 (Peter,2013; Oates,1998; Akca, 2015; Ty-Mawr Lime, 2019; Ahmed et al., 2020 Appendix IX; Nadir et al., 2022b, 2022c Appendix V, VI).

Equation 12: $\text{CaCO}_3 = \text{CaO} + \text{CO}_2$

Equation 13: $\text{CaO} + \text{H}_2\text{O} = \text{Ca(OH)}_2 + \text{heat}$

Equation 14: $\text{Ca(OH)}_2 + \text{CO}_2 = \text{CaCO}_3 + \text{H}_2\text{O}$

Lime mortars are especially recommended in underwater construction, along coastal lines, flood leaves, break walls/ blocks in the sea and enhancement of marine clay soil strength due to their moisture absorption capability and strength-gaining characteristic in water (Ahmed et al., 2020 Appendix IX).



Figure 2.25: Lime Quarry Norway (Oates,1998; Ahmed et al., 2020 Appendix IX).

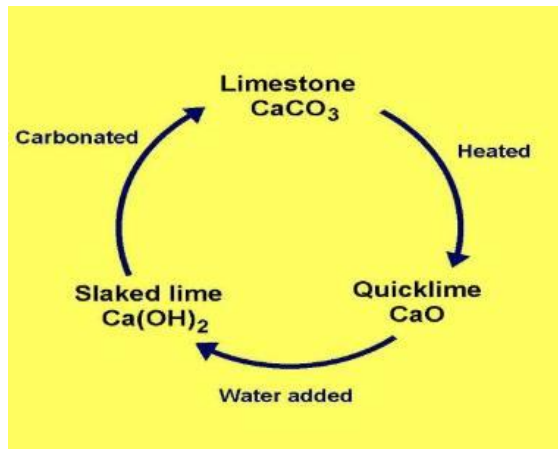


Figure 2.26: Lime Cycle for High Calcium Lime (Peter,2013; Ahmed et al., 2020 Appendix IX)

2.3.1.1 Use of Lime in Soil

The lime is considered a consolidating/ stabilising agent in treating expansive soils, especially in marine environments or on the waterfront (Ahmed et al., 2020 Appendix IX). Soil has diverse types based on composition, water absorption, grain size, porosity, shrinkage, swelling, liquid limit, plastic limit, bearing capacity, and compressive strength. Soils like marine clay, which has a lesser bearing capacity and more swelling or expansion on water absorption, are considered weaker soil and must be treated to improve geotechnical properties to function as suitable bearing structures (Rosenbalm and Zapata, 2018). Any infrastructure constructed on expansive/ swelling marine soil experiences heavy cracking/ failure if untreated (Inkoom et al., 2019). The most economical and eco-friendly solution is to treat the soil with naturally occurring materials, bio-degradable organic fibres, and industrial waste materials (Agopyan, 1998; Thirumalai et al., 2017). The researchers have worked out the use of lime and coir fibre as suitable mixing materials to enhance soil properties. Lime mixed with 1-2% coir fibre has better strength properties, especially in swelling soils. Lime and coir were considered suitable for reducing the liquid limit of marine soils, which contain more water than their liquid limit (Rao et al., 2009).

2.3.1.2 Use of Lime with Coir for Soil Stabilisation

Anggraini et al. (2014) conducted a study using 5% lime with 0.5% to 2% coir fibre in marine clay. They observed that the dry density of this soil mixture decreased due to the lesser weight/ density of the lime and coir composite. In contrast, it improved the water absorption capability, and water contents increased up to 13% using 5% lime and 2% coir, as illustrated in Figure 2.27 (Anggraini, Afhin and Haslinda, 2014; Ahmed et al., 2020 Appendix IX).

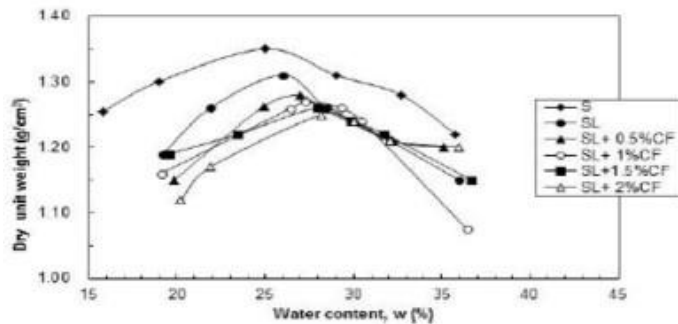


Figure 2.27: Dry Density/ Water Contents of Soil with 0%-2% Coir and 5% Lime (Anggraini et al., 2014).

They observed that the optimum plastic limit was found at 5% lime with 2% coir, whereas the minimum liquid limit was observed with this composite, as shown in graph Figure 2.28 (Anggraini et al., 2014).

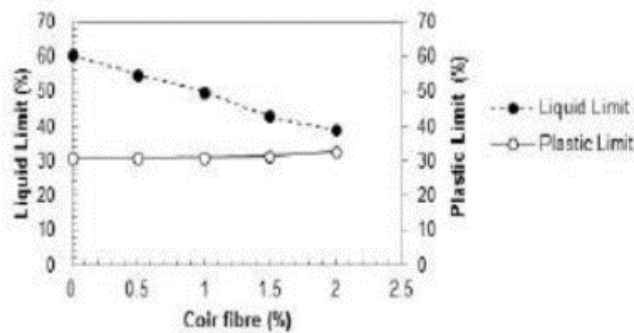


Figure 2.28: Liquid Limit/ Plastic Limit of Soil with 0%-2% Coir and 5% Lime (Anggraini et al., 2014).

The shrinkage limit and Linear shrinkage limit were reduced using lime and coir. They showed minimum values at a maximum of 2% use of coir with 5% lime stabilisation in the soil, as shown in graph Figure 2.29 (Anggraini, Afhin and Haslinda, 2014; Ahmed et al., 2020 Appendix IX).

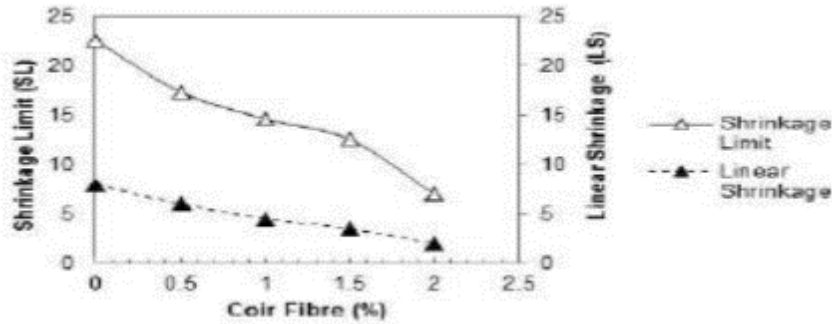


Figure 2.29: Shrinkage limit/ linear shrinkage limit of soil with 0%-2% coir and 5% lime (Anggraini et al., 2014)

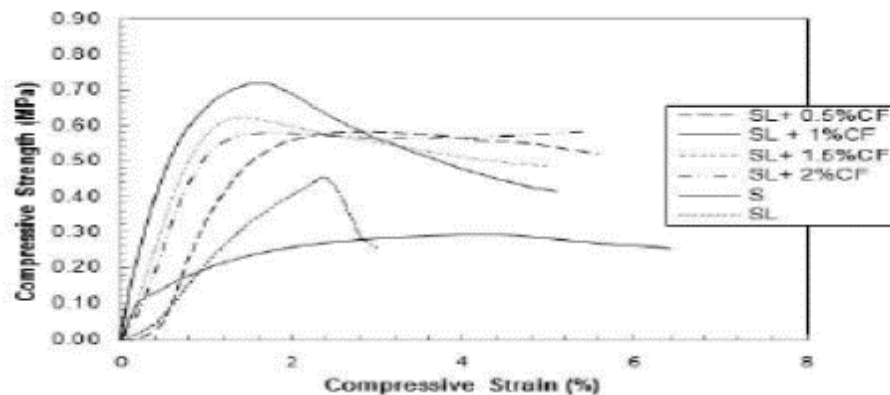


Figure 2.30: Compressive strengths of soil with 0%-2% coir and 5% lime (Anggraini et al., 2014)

The compressive strength of lime-coir composite soil was observed at its optimum level with 5% lime and 1% coir, and it increased by 1.5 times the untreated soil from 0.3 MPa to 0.75 MPa. However, compressive strength was decreased if the coir quantity was increased by more than 1%, as shown in Figure 2.30 (Anggraini, Afhin and Haslinda, 2014; Ahmed et al., 2020). The reduction in

compressive strength of lime-coir treated soil with more than 1% coir could be attributed to the coir fibre structure having cavities in the fibres, which produced lumps and decreased contact with soil particles, giving rise to more voids and lesser compactness and lesser absorption of lime contents to soil due to more coir fibres (Prabakar and Sridhar, 2002; Cai et al., 2006; Sivakumar, Vasudevan and Sayida, 2008). The presence of Silicate crystals, lignin, pith and cellulose in coir fibre also reduced compressive strength if more quantities were used. The presence of fibre increased the soil composite's adhesion, compactness and shear resistance till 1% use of coir fibre. However, more than 1% of the use of coir demonstrated a decrease in the density of soil, compactness, and increased creation of clay lumps around coir fibres, resulting in voids and unevenness in the structure of soil due to the non-uniform spread of coir fibres. Therefore, it could be inferred that using the optimum level of 1-2% coir fibre is suitable for expansive soils like clay marine soil. The coir fibres are biodegradable and have a life of 3-4 years; therefore, coating of non-hazardous, environmentally friendly natural coating materials may enhance the coir fibre life to around 20 years (Gaw and Zamora, 2010).

2.3.2 Broad Spectrum Applications of Hydrated Lime (CL-90)

Lime (CL-90) is one of the widely used materials in several industries, with an estimated production of 430 million tons worldwide, with the iron, steel and metal industries as the leader, using 250 million tons, followed by the construction industry, employing around 75 million tons and the chemical industry with 55 million tons usage per annum worldwide. The globally used types of lime are quick lime CaO (CL90 Q) and hydrated lime Ca(OH)_2 (CL90 S). The primary purpose of hydrated lime is to induce alkalinity and use it as filler material to control porosity. Hydrated lime does not exhibit much-cementing properties when mixed with water. Therefore, it requires blending with suitable binders like cement, pozzolans, and bitumen to acquire better binding characteristics. Hydrated lime is widely used in the iron and steel industry as a cheap, sustainable material for converting iron into pig iron and steel and improving the durability of

refractories in the blast furnace. The agriculture and food industry also relies heavily on hydrated lime as a purifying, flocculating, and coagulating agent, especially in the sugar industry. The hydrated lime is used as an alkali activator, deodorising, and anti-bacterial chemical to treat wastewater/ sludge, agricultural fields, and environmental protection. Hydrated lime treats wet, marine, cohesive, and clayey soils, absorbing moisture and improving engineering properties like compressibility, strength, plasticity, bearing capacity, consistency, and sheer strength shrinkage. It is used very frequently in cement-based mortars as a plasticiser. The hydrated lime could be recommended for use in diverse industries for multi-purpose roles (Nadir et al., 2022b Appendix XII). It is well known that hydrated lime is produced by carefully mixing quick lime CaO with water to make Ca(OH)_2 , which contains 25% water and 75% lime (www.graymont.com, 2022). Quick and hydrated lime is used most in construction, manufacturing, agriculture and food industries. Worldwide use of lime is estimated to be 430 million tons per year (www.usgs.gov, 2023). The construction industry had been a significant lime user in ancient times. Still, with the advancement of chemical and manufacturing industries after the industrial revolutions in the 1900s, these industries have become prominent users of lime (www.usgs.gov, 2023; Carmeuse, 2020). The iron and steel industry was observed as the leading user of lime (51%), followed by the construction industry, chemical industry and environmental protection/ waste disposal and treatments, as shown in Figure 2.31 (Piringer, 2017; Carmeuse, 2020; Nadir et al., 2022b Appendix XII).

2.3.2.1 Iron, Steel and other Metals Industry

Lime is a significant component used in the iron and steel industry to convert iron ore into pig iron, which is then used to produce steel. Lime is used as a fluxing agent to remove impurities like sulphur, silica and phosphorus in electric arc or oxygen furnaces to form a slag as a waste product, which is used as ground granulated blast furnace slag (GGBS) as a supplementary cementitious material SCM in concrete. Dolomite (lime with MgO) enhances the refractory life furnace

as it prevents slag from depleting furnaces by absorbing MgO from the refractory walls. Lime is a floatation agent for purification in sulphur, nickel, gold, silver, lead, copper, zinc, and ore mining and concentrated extraction of desired metals. High calcium-hydrated lime has exhibited the best flocculation, absorption, neutralising and stabilising capabilities in the purification of metals from ores, making it the top-used material in the mineralogy and manufacturing of pure metals and steel worldwide (www.graymont.com, 2022; Nadir et al., 2022b Appendix XII).

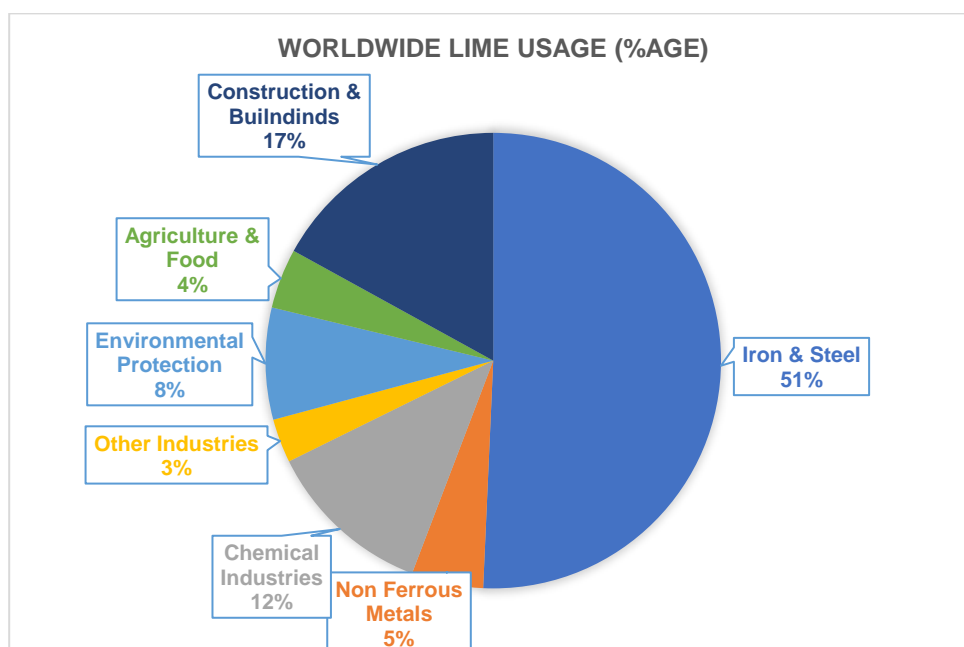


Figure 2.31: Worldwide lime use by different sectors (Nadir et al., 2022b Appendix XII)

2.3.2.2 Chemical Industry

As shown in Figure 2.31, the chemical industry is the third leading sector, using around 12% of the world's lime production (www.usgs.gov, 2023). Hydrated lime is primarily used as an alkali activator and a purifier/ fluxing agent in the chemical industry (Piringer, 2017). It is also a low-cost protective material against chemical hazards and the emission of dangerous gases to the environment. It is a commonly used purifier in the sugar industry, sulphide manufacturing, soda ash,

paper and pulp, water-based emulsions, and mining industry as an anti-leaching and protective agent against the release of cyanide into the environment. It is used in the paper and pulp industry to reform caustic soda reactions with Na_2CO_3 and $\text{Ca}(\text{OH})_2$ (www.graymont.com, 2022; Nadir et al., 2022b Appendix XII).

2.3.2.3 Environmental Protection and Waste Disposal/ Sewerage Treatment

Hydrated lime is widely used to treat black water/ sludge as a cost-effective and easy-to-use option. The OH-rich hydrated lime induces an alkaline environment in sludge treatment to prevent further reproducing pathogens, germs and bacteria. It acts as a coagulant and flocculant anti-bacterial agent. The hydrated lime is injected into the sludge tanks in the mixing phase, segregating effluent and solid sludge in 24-72 hours. It is then pumped out separately as liquid and solid for further disposal. Lime removes hazardous minerals containing phosphorus, sulphur, nitrogen, sulphide, nitrates, phosphates, and CO_2 (Farzadkia and Bazrafshan, 2014; Blitzitzco, 2022; www.emersan-compendium.org, 2023). Production of hydrogen sulphide from sewerage disposal, landfilling sites, and disposal of crops, vegetables, and other organic matter is another environmental hazard which causes acid rains and deterioration of concrete structures due to external sulphate attack caused by hydration/ ingress of hydrogen sulphide. Hydrated and quick lime is used to treat sewerage disposal and landfilling/ waste disposal sites. Hwidi et al. (2018) found that an increased percentage of hydrated lime for treating organic waste disposal decreases the emission of hydrogen sulphide (HS). They used 1%, 3%, 5% and 8% hydrated lime with the same samples of 40% vegetables, 30% meat and 30% rice products in Malaysia. They compared hydrogen sulphide production in ppm with a 0% lime-containing standard sample for 9, 12 and 15 days. They found out that the sample containing 8% hydrated lime best controlled the emission of HS and could be used as an economic waste disposal agent.

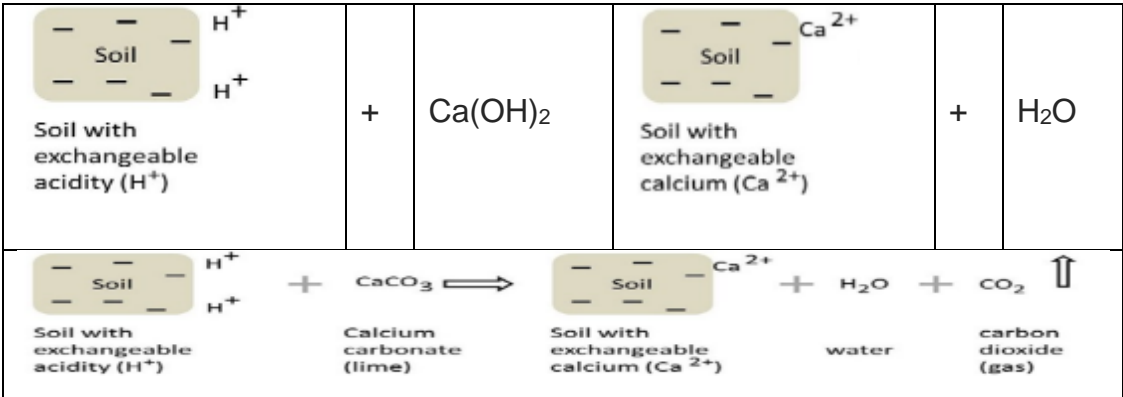
Similarly, hydrated lime is used as a deodorising agent and water purification chemical in water treatment plants. Mixing lime in water ponds prevents the

uncontrolled growth of weeds and algae and reduces stagnation. Lime is also used in coal power plants and incinerators to treat their harmful sulphur emissions to save the environment and trees (Sagastume et al., 2012; Nadir et al., 2022b Appendix XII).

2.3.2.4 Agricultural Industry

The use of fertilisers and manure by the farmers in the agriculture fields causes a reduction in the pH value of soil, resulting in acidic behaviour, which is hazardous for crop production. The hydrated lime is used to mix with soil to improve (increase) the pH value to induce alkalinity, aeration, and better soil structure and fertility (Anderson et al., 2013; Goulding,2016; Anderson and Bell, 2019). The exchange of cations and anions of hydrated lime with acidic soil transforms the soil into hydrated and calcium-rich matter by reducing H⁺ ions attached to the soil particles. Using CaCO₃ instead of Ca(OH)₂ increases the alkalinity similarly but increases the CO₂ emissions, as tabulated in the reaction in Table 2.1 (Anderson et al., 2013; Nadir et al., 2022b Appendix XII).

Table 2.1: Reaction of Ca(OH)₂ and CaCO₃ lime with soil (Anderson et al., 2013)



2.3.3 Review of Hydrated Lime Applications in the Construction Industry

The construction industry has been the primary user of lime since ancient times, as all masterpieces of construction by Romans, Egyptians, Chinese and

Babylonians used lime as the essential material for rendering, masonry, plastering, cementing and facade work. It was used primarily in the construction sector for buildings, soil stabilisation, road construction and all cementing works till the 1860s when Portland cement was manufactured and replaced lime as a large-scale construction material. The researchers used hydrated lime and natural/ industrial/ agricultural pozzolanic materials to make composites of SCMs as environmentally friendly, economical, sustainable concrete replacements. The hydrated lime (CL90) conforms to BS EN 197-1 and is considered a suitable building material (Nadir and Ahmed, 2020; Britannica, 2022; Rehan and Nehdi, 2020; Worrell et al., 2001; Rajkumar, 2017; Nadir and Ahmed, 2021b Appendix VII; Akca, Cakir and Pek, 2015; Yildirim, Sahmaran and Ahmed, 2015; Ahmed et al., 2020 Appendix IX). Lime is still the essential ingredient in cement manufacturing as it constitutes around 62% of limestone, 27% of silica and up to 11% of gypsum, magnesia, and sulphur soda (MIT, 2009; History of Concrete, 2012; EPA, 2015; Nadir et al., 2022b Appendix XII).

2.3.3.1 Use of Lime in Cement and Concrete

Cement contains around 62% lime with other ingredients (MIT, 2009). Hydrated lime has less cementing capability than hydraulic lime, which becomes a cementitious material when mixed with water. Therefore, adding hydrated lime directly to cement concrete reduces the strength of the cement-lime composite. Hydrated and quick lime with aluminium powder and concrete produce lightweight and honeycombed autoclave aerated concrete blocks that give excellent thermal and sound insulation but pose severe durability issues (Didier et al., 2011). The hydrated lime could partially replace cement with different pozzolans to produce SCMs (Nadir et al., 2022b Appendix XII).

2.3.3.2 Lime in Stabilization of Hydraulic Structures

Destabilising hydraulic structures and embankments made of expansive soils is a widespread problem in civil engineering structures along water streams, rivers and channels. The researchers were exploring using hydrated lime with soil for

its long-term stability and improvement of soil properties. Akula et al. (2020), in their study on the long-term effects of lime on hydraulic structures, explored the case study of the Friant Kern Canal in California, where lime was used for channel stabilisation in the 1980s. They found that mixed lime soil remained stable after 40 years, with a tenfold strength improvement and a fourfold reduction in plasticity index. Therefore, using quick or hydrated lime in soil for improvement of soil structure and stability along with other mechanical properties like plastic limit, liquid limit, moisture contents, moisture containing capability, and prevention against expansion on moisture absorption, is a recommended and feasible option (Akula et al. (2020; Nadir et al., 2022b Appendix XII).

2.3.3.3 Application of Hydrated Lime in Road Construction and Asphalt

Hydrated lime is a primary additive used with subgrade soil and hot mixed asphalt as an anti-slipping neutralising agent to prevent the ingress of moisture loaded with hazardous chemicals from underground or overground sources (UK Essays, 2018). Mixing hydrated lime with clayey soils for subgrade preparation is an economical option compared to transforming cement-treated soil into friable soil. Mixing quick lime with wet soils results in moisture absorption and converts it into stable, impervious, better load-bearing soil (Blitzco, 2022). Hot mixed asphalt uses stone dust, cement, or hydrated lime as a binder/ filler with fine aggregate to create a smooth and flexible binding layer of asphalt carpeting in road construction (UK Essays, 2018). Abdullah and Salih (2020) investigated using hydrated lime to improve the strength of the subgrade soil by mixing 0%, 2.5%, 5%, 7.5%, and 10% hydrated lime with the soil samples. They found that hydrated lime increased the unconfined compressive strength of subgrade soil (Abdullah and Salih, 2020; Nadir et al., 2022b Appendix XII).

2.3.3.4 Use of Hydrated Lime with Pozzolans as Supplementary Cementitious Materials SCMs

Contemporary research for the last few decades has focused on developing environmentally friendly, greener materials, especially to substitute cement.

Pozzolans and lime have historically been recognised as excellent supplementary cementitious materials. Several pozzolans from industrial (pulverised fly ash, ground granulated blast furnace slag, silica fume), agricultural (rice husk ash, palm ash) and natural (metakaolin, zeolite) sources were explored to mix with hydrated lime as better SCMs (Sotiriadis, Nikolopoulou and Tsvilis, 2012; Divya, Rafat and Kunal, 2015; Kamau et al., 2016; Kavitha et al., 2016; Ahmed and Kamau, 2017; Sinngu and Ekoru, 2022). The pozzolans provide silicates, and hydrated lime provides portlandite Ca(OH)_2 to create calcium silicate hydrates C-S-H gel, which has excellent binding properties like cement concrete, as shown in equation 15 (Nadir and Ahmed, 2021b Appendix VII). Moreover, using hydrated lime and pozzolans with cement concrete acts as a good filler material to reduce porosity and permeability and prevent external attacks by chemicals like sulphates, thus increasing the sustainability of structures (Nadir et al., 2022b).



2.3.3.5 Application of Hydrated Lime as Partial/ Full Replacement of Cement-Based Mortar

A well-known application of lime is its use as a brick/ stone masonry mortar since ancient times. Cement-based mortars have taken over the use of lime mortars due to their swift setting time. However, the emission of CO_2 from manufacturing/ use of cement is returning the industry to use lime mortars again due to their economic/ environmental benefits. Lime could be partially or fully replaced after mixing with pozzolans or cement replacement materials. The typical lime-based cement mortar ratios with their designated classification and range of compressive strength are shown in Table 2.2 (BS EN 5627). Ahmed et al. (2022a; 2022b), in their experimental studies on pozzolan-based lime putty mortar, elucidated that 2% -20% pozzolan-based lime mortar exhibited at par or better strength than the typically designated i-iv lime-cement-based mortars (Ahmed et al., 2022a; 2022b). The main disadvantage of lime mortars is the slow setting

time. Still, their environmental/ economic benefits could rule out this weakness in engineering applications where quick setting time is optional (Ahmed et al., 2022a; 2022b). The hydrated lime (CL90 S) conforms to BS EN 197-1 as a good building material. It could broadly be used as a basic mortaring, rendering, plastering, and lime-washing material in civil engineering applications. It is used as water stripping, anti-slipping, flocculating, and coagulating filler binding material in soil stabilisation, subgrade preparation, channel stabilisation, pozzolans-based SCMs, and wastewater treatment, waste disposal and filler in hot mixed asphalt carpeting of road surfacing. It reduces porosity/ permeability, shrinkage/ expansion of soils, increases moisture absorption in wet soils, and improves mechanical properties of soil, concrete and SCMs. It helps prevent external sulphate attacks, cracking, rutting, and leaching of blended materials (Sotiriadis, Nikolopoulou and Tsivilis, 2012; Divya, Rafat and Kunal, 2015; Kamau et al., 2016; Kavitha et al., 2016; Ahmed and Kamau, 2017; Nadir et al., 2022b Appendix XII).

Table 2.2: Comparison Of Cement-Lime Mortars to GGBS-Lime-Based Mortars (BS EN 5627; Ahmed et al., 2022a,2022b)

Mortar Designation	Cement: Lime Ratio	Sand Ratio	Known as	Mortar Class	Compressive Strength Range(MPa)
(i)	1:0.25	3	1:3	M12	9 - 12
(ii)	1:0.5	4	1:1/2:4	M6	5 - 8
(iii)	1:1	6	1:1:6	M4	3 - 5
(iv)	1:2	8/9	1:2:9	M2	1.5 - 2.5

2.3.4 Ordinary Portland Cement (OPC)

The calcareous rock (lime) is an essential ingredient of cement manufacturing (around 62%), where it is mixed with argillaceous minerals containing clay/ aluminosilicates (about 27%) in the kiln over 1600 C° to produce clinker, which is then ground to less than 2 µm fine particles. Magnesia (about 2%), alkalis like

soda and potash (around 1%), gypsum (about 4%) and iron oxide (about 3%) are also found in ordinary Portland cement (Conserve, 2020; Brehm, 2009; US EPA, 2015; History of Concrete, 2012). Egyptians invented cement, which has since been used in different forms/ compositions by other nations/civilisations, including Babylonians, Assyrians, Romans, Greeks, Gothics, Chinese, Russians, Europeans and Americans. However, OPC was first produced in its present form in England using Portland claystone from the Isle of Portland by Joseph Aspdin in 1822, which was further refined by his son William Aspdin in 1840 as calcium silicates and further improved by Isaac Charles Johnson in the 1850s. Present-day cement is primarily divided into non-hydraulic and hydraulic cement, e.g., OPC (History of Concrete, 2012; Johannes, 2021; Nadir and Ahmed, 2021b Appendix VII). R.H. Bogue first identified the broadly occurring chemical reaction in 1960 by identifying four main components in cement, which are known as Bogue's compounds, which include alite (C_3S tricalcium silicate $3CaO.SiO_2$), belite (C_2A dicalcium silicate $2CaO.SiO_2$), celite (C_3A tricalcium aluminate $3CaO.Al_2O_3$) and felite (C_4AF tetracalcium alumina ferrite $4CaO.Al_2O_3.Fe_2O_3$). Alite exhibits medium setting time, is highly exothermic, and gives early strength in the first hydration phase. Belite demonstrates low setting time, is less exothermic, gives ultimate strength in the second hydration phase, and provides defence against chemical attacks. Celite causes flash setting, is less exothermic, does not contribute to strength, and induces vulnerability to internal/ external sulphate attacks. Felite exhibits slow setting time, is less exothermic, does not contribute to strength, and helps prevent sulphate attacks (Bogues Compounds, 2022; Construction How, 2020; Prodyogi, 2018; Show, 2020; Nadir and Ahmed, 2022b; Nadir and Ahmed, 2022c Appendix V, VI). Bogue's compound composition in cement is shown in Figures 2.32 - 2.34 and Table 2.3.

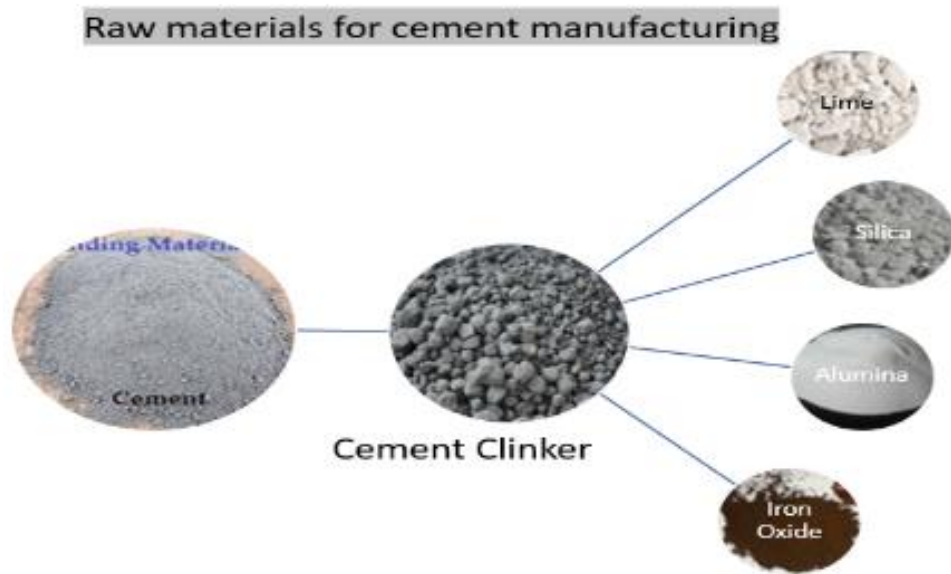


Figure 2.32: Raw Materials For OPC Manufacturing (*Bogues Compounds, 2022*)

Table 2.3: Bogues Compounds (*Bogues Compounds, 2022*)

Bogue's compound Name	Chemical Formula	Abbreviated Symbol	Generic/Torne Bohm Name	Colour	%age
Tricalcium silicate	$3\text{CaO} \cdot \text{SiO}_2$	C_3S	Alite	White	30-50
Dicalcium silicate	$2\text{CaO} \cdot \text{SiO}_2$	C_2S	Belite	White	20-45
Tricalcium aluminate	$3\text{CaO} \cdot \text{Al}_2\text{O}_3$	C_3A	Celite	White/ grey	8-12
Tetracalcium alumina ferrite	$4\text{CaO} \cdot \text{Al}_2\text{O}_3 \cdot \text{Fe}_2\text{O}_3$	C_4AF	Felite	Black	6-10

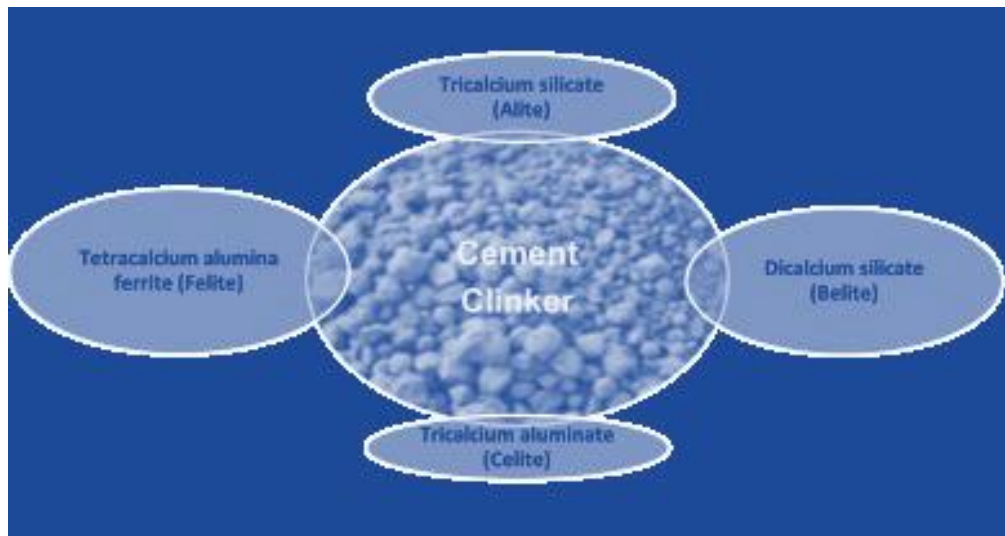


Figure 2.33: Chemical composition of cement clinker (Show, 2020)

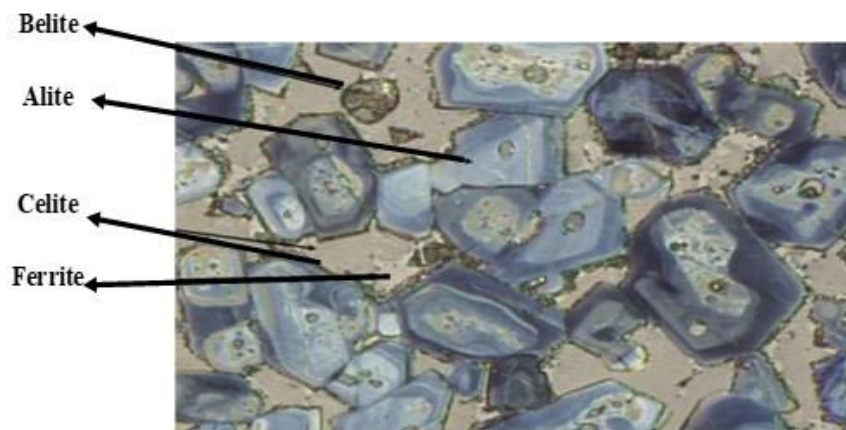


Figure 2.34: The chemical composition of cement clinker (Prodyogi, 2018)

2.3.5 The Cement Hydration Process

The dry hydraulic cement OPC does not constitute any strength. It needs water for hydration and initiating chemical reactions, leading to its setting/ hardening and gaining strength over 28 days. The hydration process is exothermic and starts quickly by mixing with water. Lime and silica are responsible for the early setting of cement concrete and for producing strength (Civil Giant,2022). Alite (C_3S tricalcium silicate $3CaO.SiO_2$) is the compound which reacts at first instance with water and produces calcium silicate hydrate, also known as C-S-H gel

($3\text{CaO} \cdot 2\text{SiO}_2 \cdot 3\text{H}_2\text{O}$) responsible for the strength of concrete. The excess quantity of portlandite or calcium hydroxide $\text{Ca}(\text{OH})_2$ is responsible for the reduction in the strength of concrete and long-term adverse effects due to its reaction with sulphates to form gypsum. C_3S produces 61% C-S-H gel and 39% $\text{Ca}(\text{OH})_2$, giving 60% of overall concrete strength and releasing 500 Joules/gram of heat of hydration (equation 16) (Shweta and Devender, 2020; Civil Giant, 2022; Johannes, 2021; Nadir and Ahmed 2021b Appendix VII; Nadir and Ahmed 2022b Appendix V; Nadir and Ahmed 2022c Appendix VI).

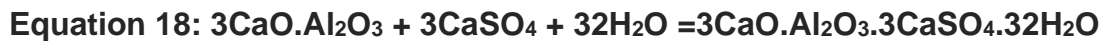
Equation 16: $2(3\text{CaO} \cdot \text{SiO}_2) + 6\text{H}_2\text{O} = 3\text{CaO} \cdot 2\text{SiO}_2 \cdot 3\text{H}_2\text{O} + 3\text{Ca}(\text{OH})_2 + \text{Heat}$

Belite (C_2S dicalcium silicate $2\text{CaO} \cdot \text{SiO}_2$) produces 82% C-S-H gel and 18% $\text{Ca}(\text{OH})_2$ in the second phase of hydration and is generally responsible for prolonged development of strength in later curing time, measuring up to 30% of overall concrete strength, releasing 260 Joules/gram of heat of hydration (equation 17) (Nadir and Ahmed 2021b Appendix VII; Nadir and Ahmed 2022b Appendix V; Nadir and Ahmed 2022c Appendix VI).

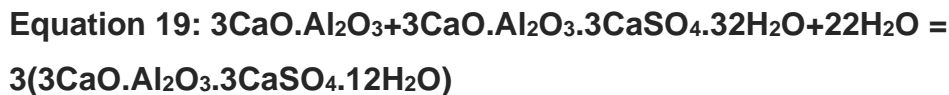
Equation 17: $2(2\text{CaO} \cdot \text{SiO}_2) + 4\text{H}_2\text{O} = 3\text{CaO} \cdot 2\text{SiO}_2 \cdot 3\text{H}_2\text{O} + \text{Ca}(\text{OH})_2 + \text{Heat}$

Considering the quantity of formation of C-S-H gel and $\text{Ca}(\text{OH})_2$ by C_3S and C_2S , it could be inferred that C_3S produces more strength but more vulnerability in contrast to C_2S , which contributes lesser strength and lesser vulnerability due to the reduced percentage formation of $\text{Ca}(\text{OH})_2$, respectively. Therefore, the percentage of C_3S and C_2S components in cement is critical and generally comprises 70-80% of the overall hydration process. Increasing C_3S will increase setting time and strength but decrease defence against chemical attacks. Increased C_2S will increase delayed strength, delay setting time, and improve vulnerability to sulphate attacks. Celite (C_3A tricalcium aluminate $3\text{CaO} \cdot \text{Al}_2\text{O}_3$) does not contribute much to gaining strength and is responsible for the flash setting of cement during hydration. Therefore, gypsum is added to cement to avoid flash setting. Still, celite reacts with gypsum and forms long rod-type

crystals of ettringite ($3\text{CaO} \cdot \text{Al}_2\text{O}_3 \cdot \text{CaSO}_4 \cdot 32\text{H}_2\text{O}$), responsible for internal sulphate attack/ cracking in concrete (equation 18) (www.engr.psu.edu, 2023; Sidney and Francis, 1981; Steve and William, 1988; Michael and Zohn, 1999; Scribd, 2018).

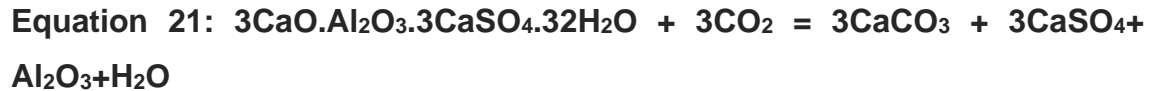
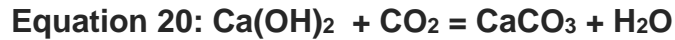


When gypsum is wholly depleted, ettringite, in reaction with C_3A and water, converts into monosulphate aluminate hydrate ($3\text{C}_4\text{ASH18}$), which is 2.5 times smaller than ettringite and forms a membrane around C_3A to prevent the further flash setting and reformation of ettringite (equation 19) (Eldidamony et al., 2012; www.engr.psu.edu, 2023). The $3\text{C}_4\text{ASH18}$ could sustain only in sulphate deficient solution and reconverts into ettringite on the absorption of sulphate solution from the atmosphere, which is called an external sulphate attack and causes cracking in concrete mass (Eldidamony et al., 2012; Nadir and Ahmed 2022b Appendix V; Nadir and Ahmed 2022c Appendix VI).



The presence of $\text{Ca}(\text{OH})_2$ gives rise to an excess quantity of aqueous portlandite in concrete pores in the form of hexagonal crystals in water. On the attack of sulphates (MgSO_4), an exchange of cations occurs between $\text{Ca}(\text{OH})_2$ and sulphates and $\text{Mg}(\text{OH})_2$ (brucite) is formed (Claudia, 2017; Civil Giant, 2022). The excess $\text{Ca}(\text{OH})_2$ quantity is generally considered unsuitable for concrete. Still, it produces alkaline solutions and keeps the 'pH value high to avoid acid attacks and corrosion in concrete or steel (Civil Giant, 2022). Meanwhile, $\text{Ca}(\text{OH})_2$ and ettringite carbonation form CaCO_3 and monocarbonate calcium aluminate hydrates ($\text{C}_3\text{A} \cdot \text{CaCO}_3 \cdot 11\text{H}_2\text{O}$), as shown in equations 20 and 21. Carbonation initially adds to the strength, pore refinement, and hardening of cement/ lime composite. It reduces permeability, but an increased quantity of CaCO_3 reduces strength and increases the chances of corrosion of reinforcement on the

absorption of CO₂ from the environment by reduced alkalinity (decreased Ca(OH)₂ and increased carbonic acid) of hardened concrete (Neville, 2004; Lei et al., 2013). Equations 20 and 21 show the carbonation reactions (Lei et al., 2013; Nadir and Ahmed 2022b Appendix V; Nadir and Ahmed 2022c Appendix VI).



Felite or ferrite (C₄AF tetracalcium alumina ferrite 4CaO·Al₂O₃·Fe₂O₃) on hydration produces garnets (monosulphate ferric aluminium hydrates), which work as filler material for refined pore structure and does not contribute to strength (www.engr.psu.edu, 2023). Its reaction is completed in two phases. In the first phase, it reacts with gypsum and water to produce ettringite, ferric aluminium hydrates, and portlandite (equation 22). In the second phase, felite reacts with ettringite, water and portlandite to form garnets and ferric aluminium hydrates (equation 23) (Scribd, 2018; Civil Giant, 2022; www.engr.psu.edu, 2023). After complete hydration of Bogue's compounds, the cement paste contains 50-60% C-S-H gel, 5-15% ettringite, 20-25% portlandite and 5-6% voids/entrapped air, as shown in Figure 2.35 (www.engr.psu.edu, 2023; Nadir and Ahmed 2022b).



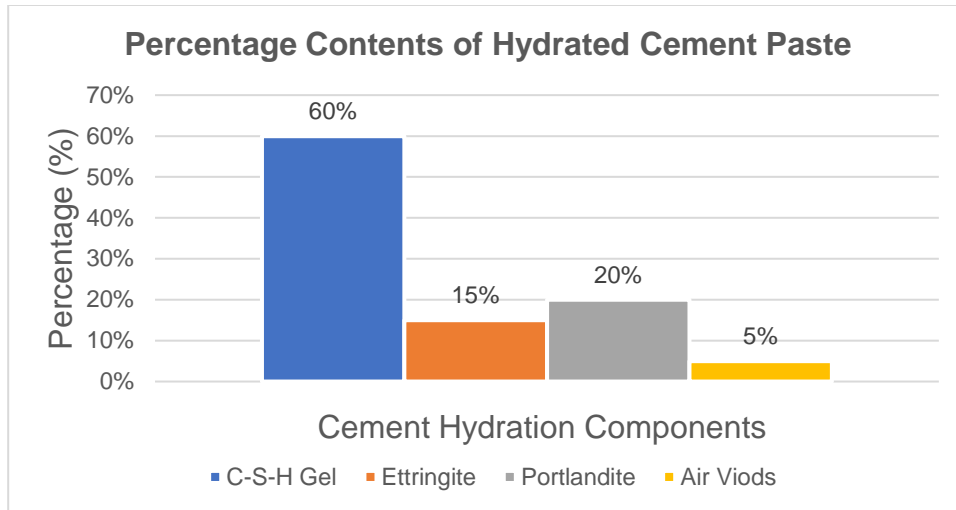


Figure 2.35: Composition of Hydrated Cement Paste in Concrete Containing 100% Cement (www.engr.psu.edu, 2023)

2.3.6 Cement Concrete

concrete has become the most widely used construction material (Britannica, 2020). The shift from naturally occurring lime and pozzolanic binders as construction material in ancient times to the present use of cement concrete has successfully enabled the construction of mega infrastructure on marvellous scales (Nadir and Ahmed, 2021b Appendix VII). Classical cement concrete is a volumetric combination of around 13% OPC as the binder and 67% binding material/ aggregate, including fine (sand) and coarse aggregates (gravels/ crushed rocks) mixed with up to 20% water contents to a certain water-cement ratio (generally less than 0.55 and keeping consistent w/c ratio as per Abrams's law) (Jain, 2020). The concrete is categorised based on strength and design combinations/ job mix formulas written as cement: sand: aggregate. The concrete is generally divided into the normal grade/ low strength 5-20 MPa, M5 - M20 (sub-grade, flooring, foundations, hollow blocks and single-story buildings), standard grade/ medium strength concrete 25-45 MPa (for all civil engineering applications including normal triple story building construction), high strength concrete grade 50-70 MPa and high-performance concrete grade having strength

more than 80 MPa as shown in Table 2.4 (Base Concrete, 2018; BS 8500, 2019; Mahajan, 2021; concrete.org.uk, 2020; Sir, 2021).

Table 2.4: Concrete Strength Grades (Base Concrete, 2018; Sir, 2021)

Concrete Grade	Strength Grade	Mix Ratio	Compressive Strength	
Normal Grade/ Low strength	Symbol	(cement: sand: aggregates)	MPa	Psi
	M5	1:5:10	5	725
	M7.5	1:4:8	7.5	1087
	M10	1:3:6	10	1450
	M15	1:2:4	15	2175
	M20	1:0.5:3	20	2900
Standard Grade/ Medium Strength	M25	1:1:2	25	3625
	M30	Design Mix	30	4350
	M35	Design Mix	35	5075
	M40	Design Mix	40	5800
	M45	Design Mix	45	6525
High Grade/ High Strength	M50	Design Mix	50	7250
	M55	Design Mix	55	7975
	M60	Design Mix	60	8700
	M65	Design Mix	65	9425
	M70	Design Mix	70	10150
≥80 MPa is considered high-strength, high-performance concrete (Base Concrete, 2018; Sir, 2021)				

2.3.7 Carbon Footprint of Construction Industry / Materials

Using cement concrete and mining/ transportation of raw materials makes the construction industry the second biggest emitter of CO₂ gas, with 4 billion tons annually. The waste materials from different industries/ agriculture contribute to 90% of waste disposal/ recycling efforts worldwide. Increased use of OPC and concrete poses a severe environmental sustainability threat because of its large-scale contribution to greenhouse gas emissions. The cement industry is considered one of the biggest CO₂ emitters (10% of global emissions), estimated to be three times more than the aviation industry (3%). The mining of raw materials, transportation, cement production, delivery, concrete preparation, and

fuel usage by the industry all are considered hazardous to the environment and raising serious questions on sustainability and environment protection (Vashisht and Paliwal, 2020; Nadir and Ahmed, 2021b). The demolition/reconstruction of old buildings/infrastructure is adding further to the waste contribution by the construction industry. Sand and aggregate are the other main components of the production of concrete. The total quantum of fine/ coarse aggregate is estimated to be around 20 billion tons, contributing around a billion tons of CO₂. The quarrying, transportation and crushing/ extraction of approximately 20 billion tons of sand, gravel and aggregates for the construction industry emit one billion tons of additional CO₂ emission per year (Brander and Davis, 2012; Gagg, 2014; www.grandviewresearch.com, 2020; Nadir and Ahmed, 2021a; Garside, 2022a; Garside, 2022b; MPA, 2007; Nadir et al., 2022b Appendix XII). Reinforced cement concrete using steel bars/ wires as reinforcement is a step forward in modern construction and is considered the basis for all engineering masterpieces by providing increased tensile/ flexural strength to plain cement concrete but is responsible for double the embodied carbon/ GHG emissions. The construction industry emits around 10-11% of GHG and consumes 6% of direct and 30% of indirect energy from global resources, as shown in Figure 2.36 (Purnell, 2013; UNEP, 2020; Lupien, 2020; Obinna, 2023).

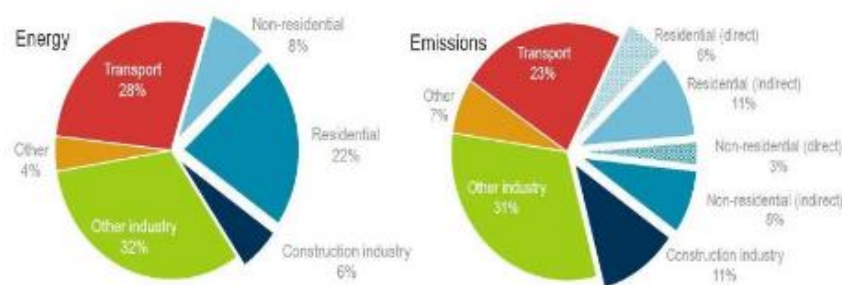


Figure 2.36: Global Energy Consumption and CO₂ Emissions Data (UNEP, 2020)

The global greenhouse gas emissions/ embodied CO₂ is the sum of all the emissions by all the elements, members, equipment, materials, machinery and living things in that particular structure. It is calculated on a statistical scale of

KgCO₂e, which is calculated by multiplication of CO₂ emitted in Kg and its global warming potential (GWP) using equation 24:

Equation 24: $\text{KgCO}_2\text{e} = \text{Weight of CO}_2 \times \text{GWP}$

The total carbon footprint/ CO₂ emission or KgCO₂e requires estimating and summing all the emissions by all the materials used in a structure. There are generally tens of materials used in constructing a structure that contributes simultaneously towards the GHG of the structure. The estimated embodied CO₂ of some materials are shown in Table 2.5. The researchers have given an approach of cradle to site and cradle to grave for calculation of the total carbon footprints of any infrastructure, starting from the planning to execution, materials manufacturing/ transport, construction, completion, maintenance/ operation and finally, the demolition to be included in the estimation of total GHG emissions as every step involves production of CO₂/ environmental impact. Mining raw materials, transportation, cement production, delivery, concrete preparation, and fuel usage by the industry are all considered hazardous to the environment and raise serious questions on sustainability and environmental protection [2]. (DEFRA, 2008; DEFRA, 2010; ICE Energy Briefing Sheet, 2011; Densley and Davison, 2011; Carre, 2011; Hasik et al., 2019; Hemsath, 2021; Nadir and Ahmed, 2021b Appendix VII; Obinna, 2023).

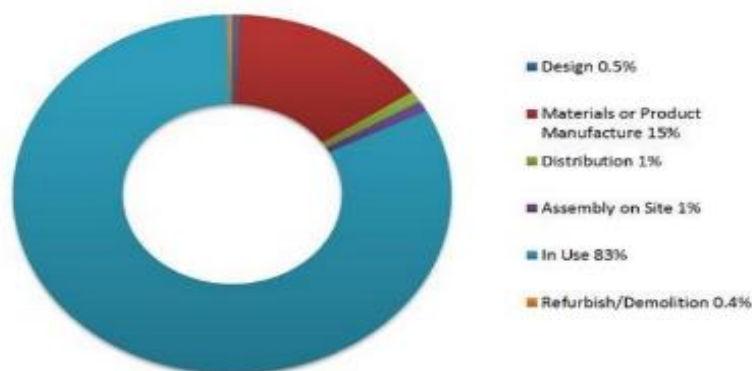


Figure 2.37: Percentage of Life Cycle CO₂ Emissions of a Building (ICE Energy Briefing Sheet, 2011).

Table 2.5: Embodied CO₂ of Different Construction Materials (ICE Energy Briefing Sheet, 2011; Obinna, 2023).

Construction Material	Embodied Carbon (kgCO ₂ e/kg)
Gravel or crushed rock	0.0052
Average CEM I (Portland cement 94% clinker)	0.74
Sand	0.0051
Mortar 1:3 (Cement:Sand mix)	0.221
Mortar 1:4 (Cement:Sand mix)	0.182
Mortar 1:5 (Cement:Sand mix)	0.156
Mortar 1:6 (Cement:Sand mix)	0.136
Steel (average recycled content)	1.46
Steel (virgin)	2.89
Steel (recycled)	0.44
Concrete C16/20	0.1
Concrete C20/25	0.107
Concrete C25/30	0.113
Concrete C28/35	0.120
Concrete C32/40	0.132
Concrete C40/45	0.151
Reinforced concrete 25/30 (with 110 kg/m ² of steel)	0.198
Rammed soil	0.024
Expanded polystyrene	3.29

Table 2.5 and Figure 2.37 infer the assessment of an infrastructure's total life cycle CO₂ emissions considering all the materials and activities. Li and Chen (2017) estimated that infrastructure contributes 13-15% of its lifecycle CO₂ during the construction/ materials manufacturing phase, 83% during its operational lifecycle and 2% during demolition (Li and Chen, 2017). It is, therefore, a paramount step in considering the careful selection of materials and operations of each infrastructure, considering the cradle-to-grave approach to estimate the real impact of GHG emissions on the environment. The use of steel, cement concrete, RCC, glass, metals, wood and polymers/ plastic is a common practice in almost every civil engineering project without giving much acknowledgement to the fact that the most GHG is contributed by polymers/ plastic, followed by steel, RCC and cement as shown in Table 2.5 (ICE Energy Briefing Sheet, 2011; Rossi et al., 2012; Thiel et al., 2013; Skullestad et al., 2016; Hoxha et al., 2017). Moreover, due consideration should be given to the study of potential

environmental hazards and pollution impacts caused by any construction project or hydromodifications on a water stream by adequately employing the environmental impact assessment procedure and implementation of its entire recommendations to achieve optimum efficacy of such studies against damages to environment (Nadir and Ahmed, 2023).

2.3.8 Efficacy of the Environmental Impact Assessment Reports Against Construction/ Development Hazards.

The developed countries were doing extraordinary scientific, technological, and construction marvels, aiming to tame nature coherently. This domination desire has negatively/ irreversibly impacted the environment. However, after generating enormous challenges to nature through uncontrolled developments, the developed countries started endeavouring to save the environment from the devastating impacts of construction projects at the end of the 20th century by incorporating the environmental impact assessment (EIA). EIA identifies, evaluates, and mitigates development projects' damaging environmental and social effects. In the last 25 years, EIA has developed into a mature system and is an effective tool for assessing, minimising, and mitigating severe impacts of development projects on the environment. EIA is only an assessment tool to ascertain the damaging effects of projects on the environment and alternative proposals for their mitigation; however, the final decision rests with political authorities who may consider the EIA report or turn it down in the name of better interests of society/country. Unfortunately, EIA has not proved to be a fully effective process as the developed countries are still undertaking unobstructed/ unopposed mega development projects best conforming to their better interests, and developing countries are still far behind in the apprehension of the necessity of EIA. However, with the UN, USA, and EU efforts, more than 120 countries have pledged to exercise EIA to assess development projects before their commencement (Nadir and Ahmed, 2023b Appendix XIII). EIA aims to inform local/ political authorities on the ecological consequences for their decision-making to endorse secure and environmentally friendly development using

suitable alternatives and mitigation processes (Nadir and Ahmed, 2023b Appendix XIII).

2.3.8.1 Constraints for Meeting EIA Objectives

EIA is a new process developed in the last 25 years and has a false sense of being an anti-development tool. Being an assessment tool only for the decision maker to decide the importance of projects versus the environmental aspects, EIA has several constraints in its implementation, which could mainly be attributed to the lack of understanding of EIA, lack of public participation, inadequate and uncertain data, knowledge gaps for prediction of future impacts, cost of EIA process (who will bear it and how it will be paid), doubtful effectiveness of EIA process to satisfy stakeholders, lack of influence of EIA on trans-border issues (like construction of dams on a trans-border river), complicated and time-consuming procedures in EIA especially the preparation of the technical report, and lack of adequacy in mitigation methods and weakness in litigation procedures (Abbas et al., 1998).

2.3.8.2 EIA Process

The EIA process comprises screening the projects as the first step to determine whether or not EIA is required, then scoping as step 2 to anticipate all issues to be considered for EIA, and a draft EIA report is prepared in step 3, which is then floated for public participation/ technical consultation in step 4. After concocting a detailed assessment of issues, different mitigation options are considered to formulate a final EIA statement or report. The political authority then uses this report to decide in favour or against the commencement of a project. When a decision is constituted, an appropriate monitoring and auditing mechanism is implemented to ensure the contrivance to the EIA report in letter and spirit during the execution phase. The flow chart of the EIA process as per the Scottish government (2016) is illustrated in Figure 2.38 (Scottish Gov, 2016) (Nadir and Ahmed, 2023b Appendix XIII).

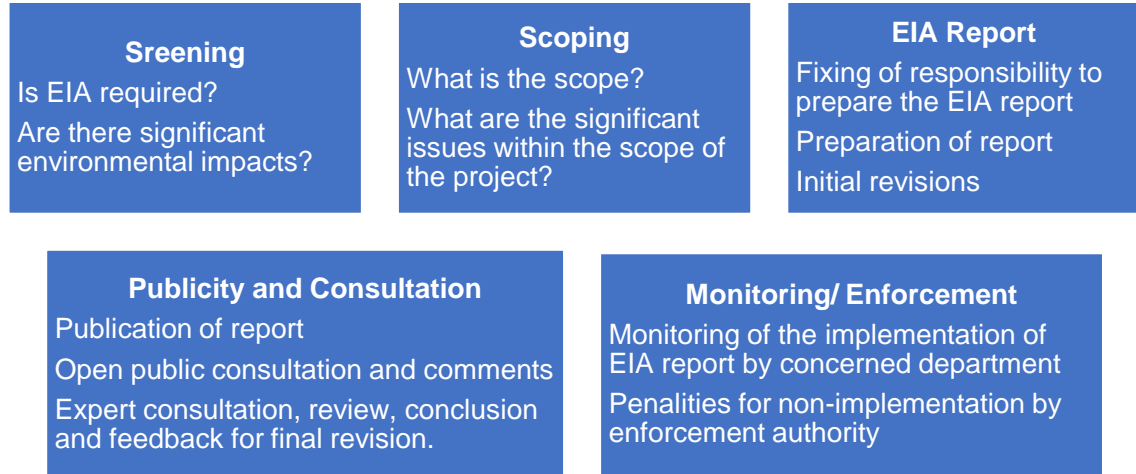


Figure 2.38: Steps in the EIA Process (Scottish Gov, 2016)

An EIA report has three parts: the planning application, the environmental statement, and the technical report (FOE, 2014). According to the latest directive on EIA in 2017, which is the continuation of the 2014 directive, conducting analyses for at least two alternatives for a project is now mandatory. The EIA process includes validating climatic impacts due to carbon emissions and adapting the proposed project to the changing climate (Jiricka et al., 2015). The resilience of any proposed project against any accident-causing environmental damage is ascertained (Tajima et al., 2014). The requirement of emergency services related to projects should be assessed (Swain & Therival, 2014). EIA directive requires the project to be evaluated on heritage aspect, archaeological disturbances, impacts on landscape, any disturbance to the reserved forest/ national parks sites and ecological health of sea/ water bodies, habitat, species and air pollution along with voluntary validation from the institute of environmental management & assessment (IEMA) (Fischer & Fothergill, 2015; IEMA, 2017) (Nadir and Ahmed, 2023b Appendix XIII).

2.3.8.3 Case Studies - Effectiveness of EIA as a Tool for the Protection of the Environment from Hazards of Uncontrolled Construction

The EIA process requires a legal authority endorsed by all member countries of the International Association of Impact Assessment (IAIA) to conduct an assessment before undertaking any major project. Over time, it has gained significant importance, especially in developed countries. However, the effectiveness of EIA in comprehensively tackling the environmental issues arising from substantial development remains controversial. Thauker and Fischer (2016), while analysing 25 years of EIA in the UK, have assessed that slight improvements in internal factors of strength and weaknesses of EIA through the incorporation of IT tools were achieved with increased linkage to external factors of opportunities in EIA since 1999 (Thauker & Fischer, 2016). Glasson and Cozens (2011) have elaborated that the influence of environmental pressure groups in implementing EIA has reduced, but consideration of socioeconomic impacts has increased (Glasson & Cozens, 2011). Fischer and Jha-Thakur (2013) have assessed that there are a lot of gaps/ inadequacies in the interpretation/ implementation of EIA regulations in the UK, which give rise to the ineffectiveness of EIA (Fischer & Jha-Thakur, 2013). EIA is still struggling to become a successful result-oriented/ impacts-preventing tool against the hazards inflicted by mega projects like motorways, heavily modified water bodies, and modified land use, especially where the political interests of the UK or any other country are involved (Fisher et al., 2015; Bond et al., 2017; Nadir and Ahmed, 2023b Appendix XIII).

2.3.8.3.1 Orange Line Metro Train Project in Lahore, Pakistan – Partial Efficacy of EIA as a Tool for Sustainable Construction Project

Lahore is the Second largest urban city in Pakistan and the provincial capital of Punjab Province, with a population of around 10 million (Megacity - Wikipedia 2023). To cater to the transportation requirements of the people of Lahore, the government decided to introduce a metro train with a 27 km route to benefit more than 200,000 commuters. The cost of the project is around \$1.2 billion. According

to “The Blue Register Pakistan” (2018), this project was started due to the vested interests of the ex-government in Pakistan without any necessity to benefit only 200000 commuters by affecting more than 3 Million people, the environment, archaeological assets, the landscape of the historical city, air pollution, contamination of ground water (shown in Figure 2.39) (The Blue Register 2018 and The News,2018). EIA report was prepared under the “Environmental Protection Department Punjab,” but it could only encompass some of these issues due to political pressures (Bangash,2018). Ultimately, the case went into litigation, and the Lahore High Court suspended the work on the problems of pollution, environmental impacts, and damage to historical buildings (Tanveer, 2016). However, on the instructions of the Supreme Court of Pakistan, archaeological sites were preserved by making the route underground, adopting alternative options, proper disposal of waste/ rubbles and sprinkling water to prevent air pollution (Haseeb,2017). Enormous pollution and diseases were reported in the affected area. However, the EIA report was biased and could not propose suitable mitigation alternatives until the intervention/ modifications by the Supreme Court of Pakistan exhibited merely a partial efficacy of EIA in preventing this mega project’s environmental hazards (The Blue Register 2018) (Nadir and Ahmed, 2023b Appendix XIII).



Figure 2.39: Issues of Orange Train Project in Lahore, Pakistan (TheNews.com, 2018).

Table 2.6: Efficacy of EIA reports on emission control and their environmental effects (Reproduced from Bruhn & Eklund, 2002).

Reviewed issues	Number of EISs, including the issue		
	Adequate	Inadequate	No Information
Description of the current project's air and water emissions	44	4	7
Description of the planned project's air and water emissions	48	2	5
Assessment of the direct effects on the natural environment	23	10	22
Assessment of the indirect effects on the natural environment	9	2	44
Assessment of the direct effects on the cultural environment	1	5	49
Assessment of the indirect effects on the cultural environment	–	–	55
Assessment of the direct effects on the public health	7	17	31
Assessment of the indirect effects on public health	6	–	49

2.3.8.3.2 A Case Study of Biofuel Energy Plants in Sweden - Partial Efficacy of EIA as a Tool for Sustainable Power Plants

Bruhn and Eklund (2002) conducted a study on EIA reports of 55 biofuel power plants in Sweden to assess the effectiveness of EIA as an effective tool for sustainable development without adverse effects on the environment. Their study focused on evaluating local and global impacts, the use of resources, and public participation. Their analysis showed that the environmental aspects of sustainable development on a local level were partly met, but global effects and management of natural resources were not assessed. They assessed that EIA in Sweden could only partially deliver the intended purpose. Many adverse effects were noticed, especially in using natural resources to preserve them for future generations. The EIA reports lacked information on public health, cultural heritage, natural environment, water emissions and use of current resources,

which are creating destructive impacts on the global climate due to biofuel power plants in Sweden, as shown in Table 2.6 (Bruhn & Eklund, 2002) (Nadir and Ahmed, 2023b Appendix XIII). EIA is an essential tool for giving a fair assessment to decision-makers and evolving mitigation proposals to prevent the impacts of projects on the environment. It has increased public awareness about the hazardous effects of developments. EIA has raised the sense that the protection/preservation of the environment is the legal responsibility of all stakeholders. However, EIA, being only a tool for decision-makers, could not portray itself as an effective regulatory process for sustainable development and presents significant flaws in preparing relevant reports. The lack of consideration of EIA reports by the political authorities and knowledge gaps were the significant causes of the partial success of EIA. There is a need for enhanced use of IT, realistic technical data, global consideration of impacts, especially for the projects influencing the trans-border environment, award of legal implementation power to regulators and reduced influence of political authority on accepting/ rejecting an EIA. The future of EIA is expected to be more fruitful, realistic, and influential in preserving the global environment by incorporating sustainable development (Nadir and Ahmed, 2023b Appendix XIII).

2.3.9 Impact of Hydromodifications on River Ecology and Environment – Case Study of Mississippi River, USA (Nadir and Ahmed, 2023b Appendix XIII)

Engineers endeavoured to channel rivers worldwide to control the flow and prevent flood, sediment transport, efficient drainage, and perennial navigation without gross consideration of the regions' hazardous impacts on the environment, ecology, and biodiversity (Brookes, 1983). Harnessing the streams through channelisation often results in a decreased water Table in adjacent segments but induces an increased water Table downstream. The heavily modified water bodies disturb hydraulic repercussions, hydrological regimes, and fluvial processes across spatial/ temporal scales (Hoerbinger et al., 2020). The sediment transport impacts the morphology (erosion/ deposition pattern) and

biodiversity in the water streams, being the source of nutrients (Landwehr and Rhoads, 2003). The EIA process could be considered a tool to anticipate such damages while planning the channelisation of the rivers; however, historically, its efficacy could be better by not collaborating the overall impacts, especially trans-border rivers and long-term environmental impacts. Mississippi is the biggest river in the USA, with a length of 3700 km and an annual flow of 16000 m³/sec, starting from Lake Itasca and falling in the Gulf of Mexico (Galloway, 2004). It was under substantial human modification for centuries, especially by the US Corps of Engineers. Eight thousand dams/ dykes, 2000 levees, bank channels and barraging structures were constructed even in modern times after the incorporation of EIA in the USA to convert the naturally meandering river into a beautiful channel, as shown in Figures 2.40 – 2.42 (MFDP, 2004; Tenenbaum, 2010; USACE, 2016). The five deep-water ports on the lower Mississippi River generate billions of dollars annually (Price, 2018). The straightening of the river has reduced its length by 240 km, thus increasing the flood speed (Parrett, 1993; Perri, 1998). Land infertility, deforestation and water Table lowering are caused by confining water from large flood planes to small channels (Robert, 2008; Wang et al., 2014). Climate changes due to modified morphology/ hydrology resulted in increased weather extremes in the US states, especially the neighbouring Mississippi River (Zhang et al., 2016). The weather changes, a combination of rare atmospheric events accumulated and caused storms to become 'trapped', which resulted in prolonged periods of torrential rainfall and heavy flooding in the whole catchment of River Mississippi and caused disastrous super floods in 1993 (Figure 2.43) (FEMA, 1993; NASA, 1993; EPA, 2006). Sediment movements and accumulation issues caused a 10 – 13% loss of sediments/ water quality/ fertility of flood plains (Smith and Bentley, 2015). Fish species and invertebrate biodiversity decreased due to concrete-lined channels/ structures (Buisson et al., 2008). They have affected the ecosystem badly by reducing the population of Algy, grazers, predators, and fish due to reduced nutrient recycling, decomposition, biomass conversion and reproduction (Woodward et al., 2010).

A large number of EIA studies were conducted; still, all the EIA studies have partially prevented the USA from the damaging impacts of heavy modifications/ channelisation of the Mississippi River. All mitigation measures were less effective in reducing the effects of taming of the Mississippi River on the environment in surrounding states and the Gulf of Mexico (Dudgeon et al., 2006; DiStasio, 2015; Dams and Locks on Mississippi River, 2015; NMRM, 2018; Nadir and Ahmed, 2023b Appendix XIII).

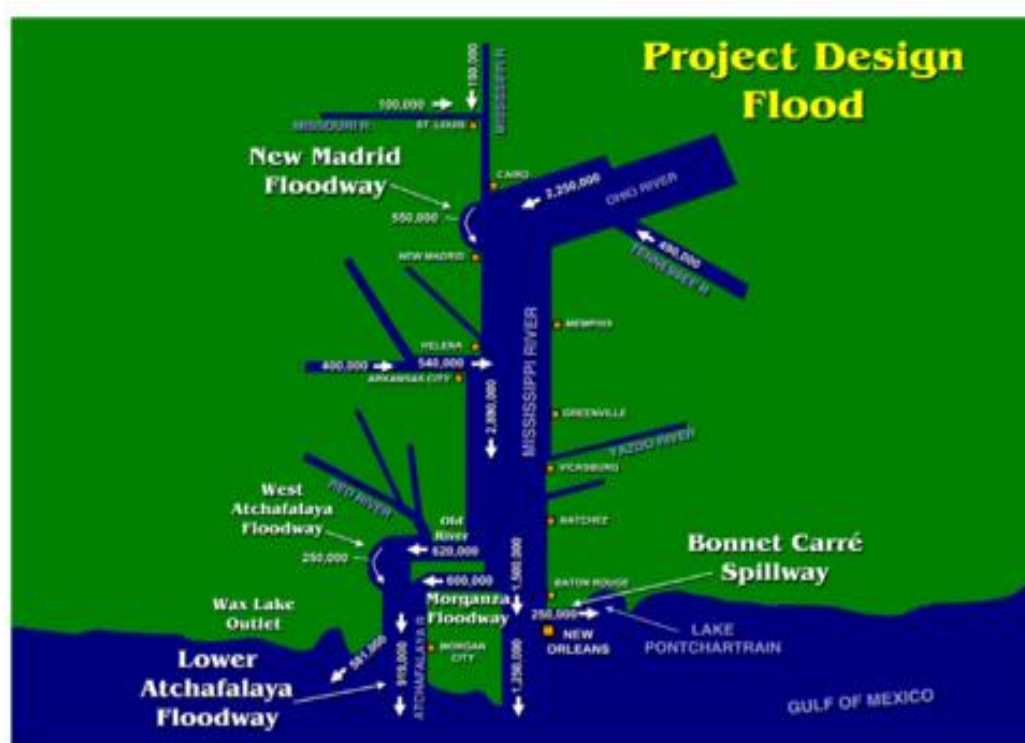


Figure 2.40: Mississippi River Flood Protection Infrastructure (MFDP,2004).



Figure 2.41: River Mississippi Channelisation (Tenenbaum, 2010).



Figure 2.42: Old and New River Mississippi Landscape (USACE,2016).

FLOODS

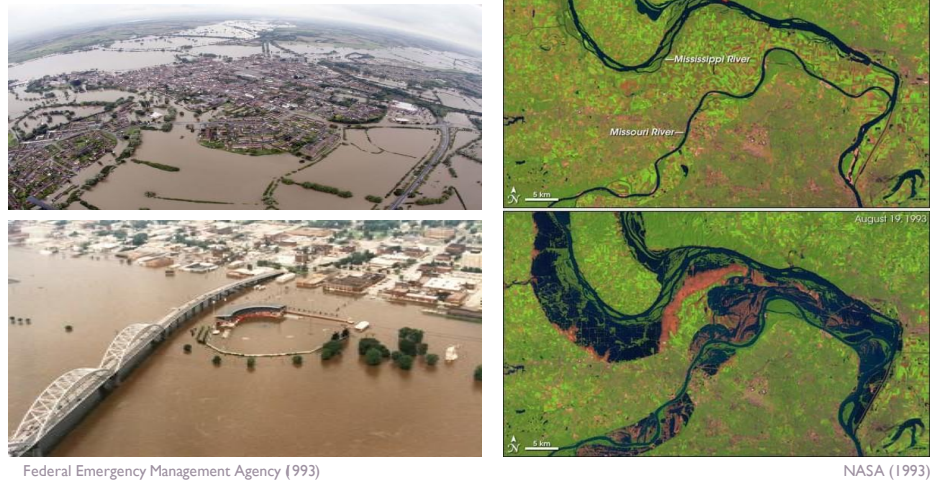


Figure 2.43: Floods in Mississippi River 1993 (FEMA, 1993; NASA, 1993; EPA, 2006).

2.3.10 Global Waste from Agricultural/ Industrial Fields

The waste materials from different industries/ agriculture contribute to 90% of waste disposal/ recycling efforts worldwide (Nadir and Ahmed, 2021b Appendix VII). Faster growth, urbanisation, increased population, and technological advancements have resulted in the invention of new materials/ resources and more waste production. Waste production is significantly pronounced in high-income developed countries due to industrialisation but less in low-income countries. The agricultural/ organic waste is more pronounced in low-income countries as these economies rely heavily on agrarian productions (Figure 2.38, 2.39) (Hoornweg and Bhadha, 2012; Nadir et al., 2022a Appendix X). As per a study conducted by Hoornweg and Bhada (2012), the world is now facing disposal issue of ten times more waste than in the last century; waste production has doubled in the last decade, and low/middle-income countries would double their waste production by 2025 from 1.3 billion tons to 2.5 billion tons. Global waste comprises around 50% organic waste, including crops/ plants, and approximately 40% industrial waste, including paper, steel, glass, metal, and

plastic. The world is projected to produce 12 million tons of waste per day by the end of this century, which requires millions of incinerators to dispose of this waste apart from dumping it into landfills or sea disposal (Hoornweg and Bhadha, 2012). The best environmental strategy is to produce net-zero waste for disposal, recycling, and reusing in other industries (Guerrero, Maas and Hogland, 2013). One of the options is to use recycled waste in the form of fibres in concrete to improve its mechanical properties in line with the reduced use of RCC with steel (Brandt, 2009; Al-Salem, 2009). Therefore, the researchers were working to formulate FRC composites by incorporating different fibres ranging from natural waste like coir, wheat straw, rice straw, horsehair and animal wool to industrial waste like steel fibres, glass, polypropylene, other polymer fibres like polystyrene, pet plastic bottles fibre, carpet fibres and synthetic wood fibres. (Akca, Kaker and Pek, 2020; Yildirim et al., 2015). Another option to absorb this enormous waste is to recycle the industrial waste materials/ ashes having pozzolanic characteristics/ cumulative quantity of metal oxides, including SiO_2 more than 70% like silica fume (SF), pulverised fly ash (PFA), metakaolin (MK), ground granulated blast furnace slag (GGBS), rice husk ash (RHA), palm ash (PA) as an alternative pozzolanic binder for cement replacement, glass, plastic, crushed tyres, rubber, steel fibres, coconut coir, shredded plastic fibres, polymer fibres, carpet fibres, horsehair and sheep wool as replacement of fine/ coarse aggregate and enhancer of engineering properties of concrete. These efforts achieved impressive success, though with certain limitations on the use of type/ quantity/ quality of composite/ replacement materials (Onuaguluchi and Panisar, 2014; Akca, Kaker and Pek, 2015; Qadir et al., 2015; Yildirim et al., 2015; ASTM C 125/ ASTM C 618/ C125, 2019; Abbasi et al., 2020; Girts et al., 2020; Shahbazpanahi and Faraj, 2020; Shahbazpanahi et al., 2021; Nadir et al., 2021b).

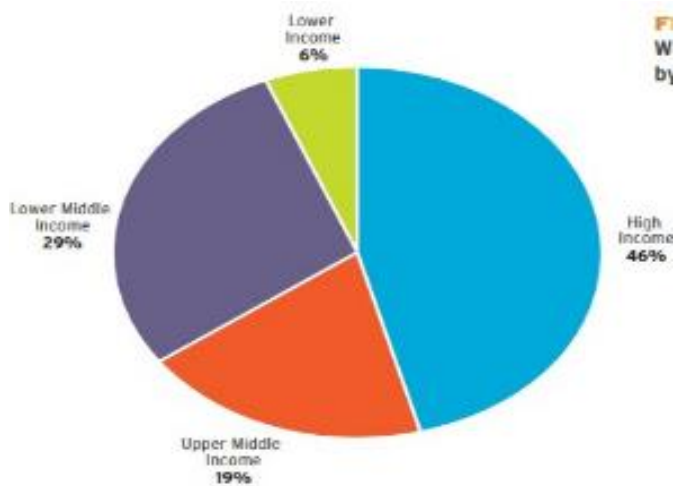


Figure 2.44: Waste Generation by the Countries - Income-Wise Economies (Hoornweg and Bhadha, 2012)

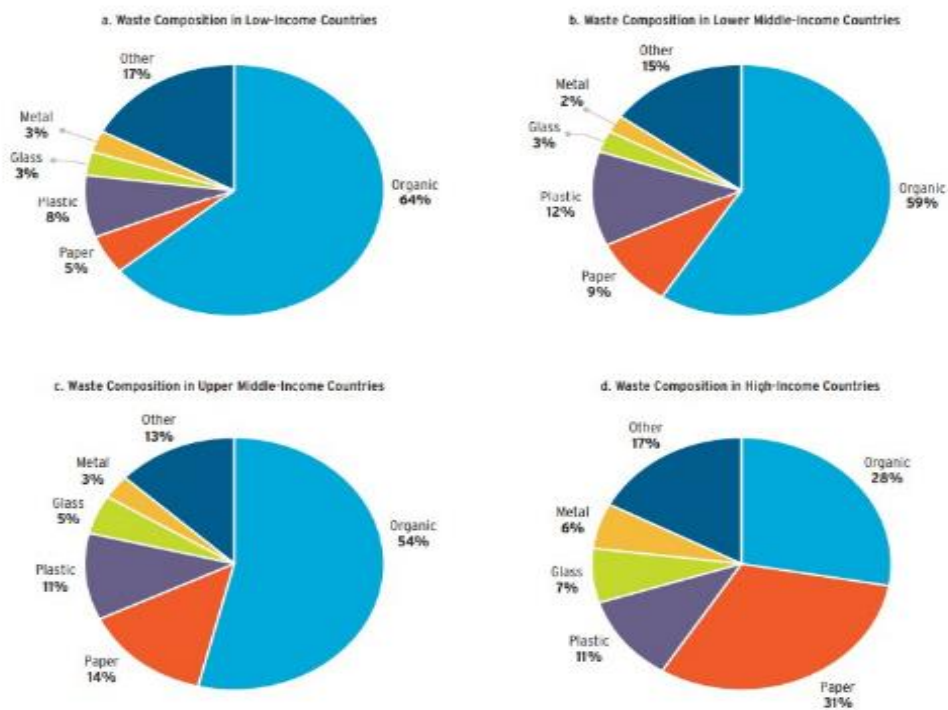


Figure 2.45: Waste Composition by the Countries - Income-Wise Economies (a-d) (Hoornweg and Bhadha, 2012)

2.3.11 Review of the Cement Alternatives/ Pozzolanic Materials and Their Global Use

Concrete is one of the most widely used construction materials, accounting for around 10% of global GHG emissions. Using cement concrete and mining/ transportation of raw materials makes the construction industry increase any construction project's carbon footprint. The waste materials from different industries/ agriculture contribute to 90% of waste disposal/ recycling efforts worldwide. The researchers endeavoured to use these waste materials as supplementary cementitious materials (SCM) to prevent the emission of CO₂, as recycling/ absorption of waste from other industries to the construction industry could result in increased sustainability. As per ASTM C 125-19 and C 618, the materials having a combined value of silicate, alumina, ferrous oxide and oxides of metals more than 70% are considered a good pozzolanic material suitable for cement replacement as the materials shown in Table 2.7, (Siddique, 2004; Akeem and Mitui, 2017; Scrivener, 2018; ASTM C 125, 2019; Selvapriya, 2019; Girts et al., 2020; Nadir and Ahmed, 2021b Appendix VII). It was an imperative research objective of contemporary research and this project to study existing cement alternatives and compare/ develop with new sustainable materials which could absorb waste from other industries (lime, calcined clay, cement alternatives like GGBS/ pozzolanic cement, pozzolanic materials such as binders, crushed/ recycled glass, rubber, tyres, plastic as aggregates, various fibres as alternative to RCC). These materials contribute to reduced emissions during their entire life cycle and minimal emissions during their manufacturing process as these are either recycled or waste materials from other processes/ fields. Rather, they sometimes absorb the CO₂ from the environment or generate a net zero CO₂ balance (like iron-based binary/ ternary pozzolanic composites). These materials were expected to perform sustainably and fulfil the concrete grades/ strength requirements and durability parameters like sustainability against sulphate attack for various low, medium, and high strength utilisations in construction. However, the quantity and cost impact were the major issues in the broad spectrum

selection of these alternative pozzolanic materials/ waste recycling. OPC is produced in abundance to fulfil the demands of the construction industry to the tune of 4800 million tons/ year globally due to the availability of its abundant raw materials in nature, like clinker and lime. On the contrary, only lime and calcined clay are available in abundance (infinite quantities) as limestone and China clay or kaolinite to produce a variety of limes and metakaolin; the rest of the SCMs are available in limited quantity. The alternative SCMs are generally extracted from industrial/ agricultural waste/by-products and heavily depend on the production/ output of that particular industry; the estimated availability of GGBS quantity from the steel industry is around 600 million tons/ year and likely to reduce as alternative materials are being introduced to substitute steel due to its inherent environmental impacts. PFA is extracted from coal power plants with an estimated quantity of 850 million tons/ year. It is expected to reduce shortly as coal/ fuel power plants are on the verge of closing soon due to their extreme GHG emissions. Natural pozzolans like zeolite and magma are available in less than 500 million tons annually. The vegetable ashes from the agriculture fields are available at around 400 million tons/ year. Their major use as fodder for animals and natural manure in the farmlands would likely reduce their availability for utilisation as pozzolanic materials in the construction industry. Waste glass is available in the amount of around 200 million tons/per year. Still, its large-scale recycling in the glass industry and its inherent alkali silica reaction in cement concrete make it less suitable for construction. One hundred million tons/ year of silica fume is available as the waste product from the reaction of quartz with coal in an arc furnace to manufacture silicon or ferrosilicon alloys. It is expected to increase slightly with increased use of the silicon industry, but it is not likely to be available in abundance. The optimum quantity of all kinds of cement alternatives/ pozzolans is almost half of the manufactured quantity of OPC, which is otherwise unavailable to use as supplementary cementitious materials due to their supply/ transportation/ availability issues for the construction industry. Generally, lime and GGBS make up 7% and 5% of worldwide cement replacement, respectively,

whereas only 4% fly ash and 2-3% agricultural/ natural pozzolans are used as cement alternatives. Therefore, it was suggested that neither the cement alternatives were available in abundance to fulfil the cement demand nor the available quantities of these SCMS were being used to the optimum levels due to inherent industry-wise reluctance to use these as cement alternatives/ SCMs, thus hardly creating around 10% control on GHG emissions by the construction industry (Figure 2.46 and 2.47) (Scrivener, 2018). Therefore, diverse, innovative cement alternatives should be explored/ formulated in various types/ quantities rather than relying on existing/ established materials. It gave impetus to this research to elaborate/ elucidate the use of various agricultural/ industrial waste materials that required pozzolanic characteristics to introduce as novel sustainable materials for the construction industry and hydromodifications.

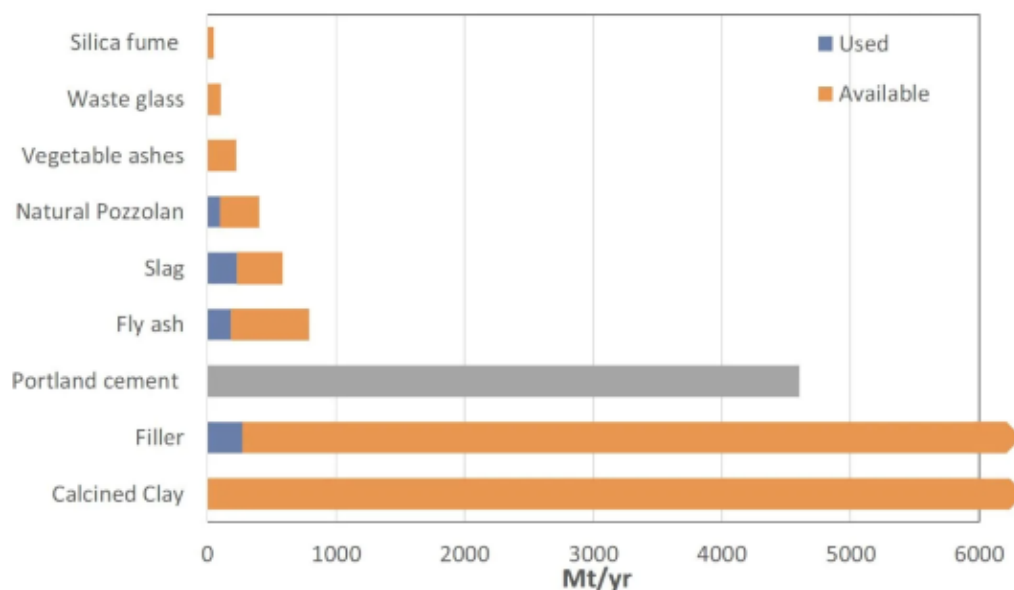


Figure 2.46: Global annual availability of cement, lime (filler) and SCMs (Scrivener, 2018; Sentucq and Clayton, 2021).

Evolution of Clinker substitution



Clinker substitution most successful strategy to reduce CO₂

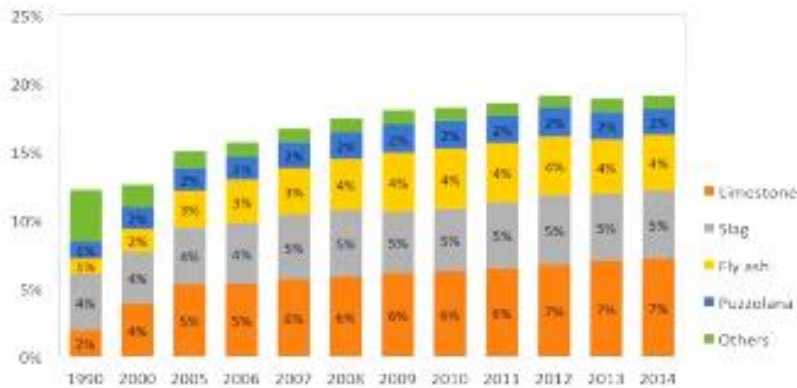


Figure 2.47: Global Annual Substitution of OPC by SCMs (Scrivener, 2018)

2.3.11.1 Ground Granulated Blast Furnace Slag (GGBS)

GGBS is obtained from iron industries as a waste product of blast furnace slag containing almost similar quantities of CaO (44.7%), SiO₂ (39.4%) and Al₂O₃ (11.1%) (Table 2.7) at par with the ingredients of OPC. It is a steel industry waste and is considered a direct cement replacement and a main ingredient in the production of geopolymers in the construction industry. Its OPC/ lime-based composites with up to 70% to 80% replacement have exhibited excellent strength performance/ durability against sulphate attack and demonstrated enhanced engineering properties, making it an established cement alternative (Hewlett, 2004; Oner and Akyuz, 2007; Neville, 2011; Sakai, Nakamura, and Kishi, 2013; Samad and Shah, 2017; Prasanna, Srinivasu and Murthy, 2019; Cunliffe et al., 2021 Appendix III). It is available in off-white colour powder with a specific gravity of 2.9, vibrated bulk density of 1100-1300 kg/m³, and fineness of 350 m²/g (CSMA, 2023) (Nadir and Ahmed, 2021b Appendix VII; Nadir, Ahmed and West, 2023b Appendix IV)

Table 2.7: Elemental/ ingredient composition analysis by X-ray fluorescence (XRF) of different materials

(Hewlett, 2004; Neville, 2011; Premalatha et al., 2016; Jonida et al., 2018; Darweesh and Abo El-Suoud, 2019; Nadir and Ahmed, 2021b Appendix VII; Nadir, Ahmed and West, 2023b Appendix IV; UKA, 2023)

Ingredients	CEM1 52.5 (%)	GGBS (%)	SF (%)	MK (%)	PFA (%)	RHA (%)	PA (%)	Fe Powder (%)
Fe₂O₃	0.32	0.31	0.43	0.45	8.88	1.66	4.7	93.4 Fe
SiO₂	25.2	39.4	99.1	52.1	56.2	97.6	43.6	
TiO₂	0.18	0.47	<0.1	0.88	0.83	<0.1	0.12	
CaO	67.1	44.7	<0.1	0.31	3.46	<0.1	8.44	
K₂O	0.3	0.43	<0.1	0.17	0.66	0.21	22.2	
Al₂O₃	3.18	11.1	<0.1	45.1	23.7	<0.1	11.4	
MgO	1.33	1.46	<0.1	0.2	3.28	<0.1	4.8	
Na₂O	<0.1	0.11	<0.1	0.25	1.93	<0.1	1.94	
P₂O₅	<0.11	<0.1	<0.1	<0.1	<0.31	<0.1	<0.1	
Cl	<0.23	<0.1	<0.1	<0.1	<0.1	<0.1	<0.1	
SO₃	<1.57	<1.49	<0.1	<0.1	0.25	<0.1	<2.8	

Higgins (2003) conducted a detailed experimental study on the improved sulphate resistance of GGBS blended cement concrete. He blended 60% and 70% GGBS with 40% and 30% OPC along with 2% and 3% CaSO₄ and 3% CaCO₃ and immersed cubes and prisms in Na₂SO₄ and MgSO₄ solutions for six years to observe expansion and reduction in compressive strength. The tests were conducted after 3,7,28 days, and 1,2 and 6 years. The study revealed that 60% GGBS-cement composite with 3% lime and 3% CaSO₄ performed the best in all the compressive strength and expansion parameters testing, as shown in Table 2.8 (Higgins, 2003). The consistent efficacy of GGBS-based cement composite exhibited beneficial impacts against external sulphate attack of concentrated Na₂SO₄ and MgSO₄. The presence of lime and CaSO₄ provided the Ca⁺⁺ and SO₃⁻ cations and anions in a chemical reaction which prevented annihilation/ de-

calcination of C-S-H gel during the formation of ettringite and gypsum on external sulphate attack by concentrated sulphate solutions. The study shows a beneficial use of GGBS as SCM with lime and CaSO_4 for the long-term durability of concrete (Higgins, 2003). OPC cubes were almost wholly disintegrated after five years; 60% of GGBS cubes also impacted Na_2SO_4 more than MgSO_4 . 70% GGBS composite performed the best in both solutions, especially with higher percentages of lime and CaSO_4 , elucidating that the increased quantity of GGBS performs better in a sulphate environment (Higgins, 2003) (Nadir and Ahmed, 2021b Appendix VII; Nadir, Ahmed and West, 2023b Appendix IV).

Table 2.8: Compressive strength of GGBS composites in water and sulphate solutions (Higgins, 2003).

	3-day	7-day	28-day	1-year	2-year	6-year	1-year	2-year	6-year	1-year	2-year	6-year
Portland cement	34	41	53	66	68	69	97	87	0	85	74	28
60% GGBS	17	31	48	65	69	73	106	97	62	95	75	18
70% GGBS	13	28	49	63	66	71	105	89	90	94	77	28
60% GGBS + LS	15	28	45	67	69	76	99	97	84	96	83	41
60% GGBS 2% SO_3	19	29	47	68	67	72	97	99	33	94	81	19
60% GGBS 3% SO_3	18	32	50	62	69	75	102	99	80	94	88	50

Higgins (2003) evaluated prisms for sustainability/ expansion in Na_2SO_4 and MgSO_4 solutions. The prisms were prepared using composites of OPC with 60% and 70% GGBS with 2% and 3% CaSO_4 and 3% CaCO_3 . Prisms were emersed in Na_2SO_4 solution for 1 and 3 years, whereas the duration of emersion was extended to 6 years in MgSO_4 solution. The promising results exhibited an increased quantity of GGBS up to 70% with higher quantities of CaSO_4 and CaCO_3 performed better by showing negligible expansion/ surface erosions, followed by 60% GGBS composites as the second-best performer in the sulphate environment. At the same time, control mix prisms comprising only OPC performed the worst by showing considerable surface wear and tear with up to 0.1% expansion in the first nine months of emersion in sulphate solutions

(Figures 2.48, 2.49) (Higgins, 2003). The results reassured that GGBS composites perform better in sulphate attacks by lesser production of ettringite and increased output of C-S-H gel during the hydration process due to pozzolanic reactions, as depicted in Table 2.8 (Higgins, 2003). Suresh and Nagaraju (2015), Shumuye et al. (2018) and Desta and Jun (2018), in their studies on the evaluation of the performance of GGBS-based concrete, found that 50-60% of GGBS-cement composites performed better in resistance against sulphate and chloride attacks in the aggressive environment. Jawahar et al. (2016) elucidated that 100%, 50%GGBS+50%PFA, and 50% PFA-based geopolymers performed excellent engineering properties, especially 100% GGBS-based geopolymer exhibited performance at par OPC. They immersed these pozzolans-based geopolymer/ cement concrete cubes in a 5% H_2SO_4 solution for 90 days. They assessed that a weight loss of 3% was observed in pozzolans-based geopolymers composites compared to an 11% weight loss in OPC concrete, supporting a beneficial use of pozzolanic geopolymers/ SCMs over cement concrete (Jawahar et al., 2016) (Nadir and Ahmed, 2021b Appendix VII; Nadir, Ahmed and West, 2023b Appendix IV).

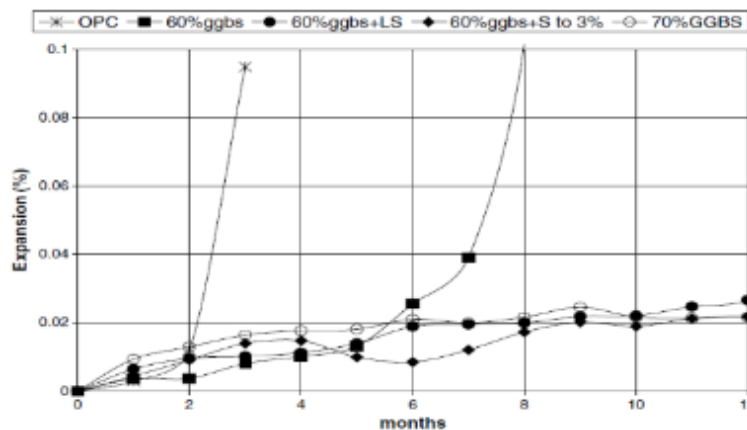


Figure 2.48: Expansion of GGBS prisms in Na_2SO_4 solution after one year (Higgins, 2003).

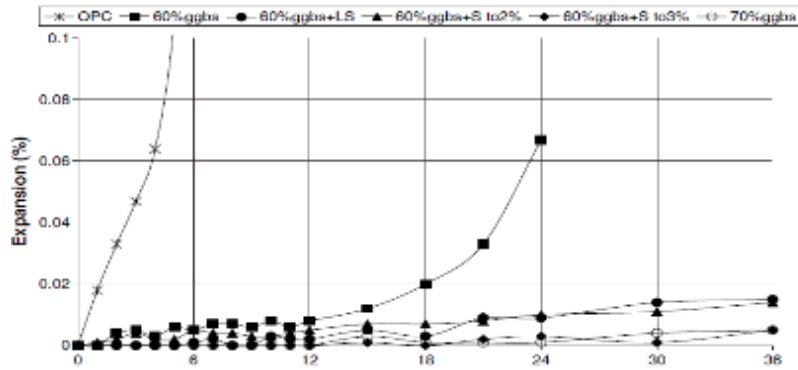


Figure 2.49: Expansion of prisms in Na_2SO_4 solution after three years (Higgins, 2003).

2.3.11.2 Pulverised Fly Ash (PFA)

Fly ash is a waste product of coal-burnt power plants. It is considered one of the significant pozzolanic materials used as SCM in cement concrete to impart economic/ environmental/ strength benefits due to containing a high quantity of SiO_2 (56.2%), Al_2O_3 (23.7%) and Fe_2O_3 (8.88%) as shown in Table 2.7. Class F fly ash is rich in silica and widely used in the construction industry, followed by class C, which has a comparatively lower percentage of silica. Their particles are spherical in shape and range in size from 0.5 to 300 μm . PFA converts to suspended solids on moisture absorption and hardens like concrete after the pozzolanic reaction. Therefore, its use in high-performance concrete or partial cement replacement is a fact in conformance to ASTM C 618/ C125-19 that a pozzolanic material giving the combined sum of silica, alumina and other metals oxide of more than 60% is considered an excellent pozzolanic material and could be used as cement alternative (ASTM C 618/ C125, 2019). All the pozzolans contain SiO_2 , which reacts with $\text{Ca}(\text{OH})_2$ during cement hydration and produce additional C-S-H gel, increasing strength to pozzolan-based SCMs, as shown in equation 15. However, if the quantity of pozzolan is increased to a specific limit, they start to produce $\text{Si}(\text{OH})_4$ gel with swelling properties and decrease the strength of composites (Hemnet, 2011; Nadir and Ahmed, 2021b Appendix VII; Nadir and Ahmed, 2022b Appendix V; Nadir, Ahmed and West, 2023b Appendix

IV). PFA is an established pozzolanic industrial waste material considered to improve the mechanical properties and durability of concrete/ composites when used in appropriate percentages. Ahmed and Kamau conducted studies on the use of PFA and GGBS to prepare better-performing pozzolans-based concrete composites, especially in sulphate environments, and they suggested the feasible use of 30% GGBS and 15% PFA for better compressive strengths and durability against sodium/ magnesium sulphate solutions (Ahmed and Kamau, 2017). Shannag and Shaia (2003), Thomas (2007), and Chi and Hang (2014) found it beneficial to use 15-25% PFA for better resistance/ durability of concrete in an aggressive environment against sulphate and chloride penetration (Nadir and Ahmed, 2021b Appendix VII; Nadir and Ahmed, 2022b Appendix V; Nadir, Ahmed and West, 2023b Appendix IV). Troii et al. (1995) studied the mixing of 30% and 50% low and high pulverised fly ash with OPC to produce cubes and prisms of composite mortar and cylinders of composite concrete containing 300 kg/m³ and 400 kg/m³ binders. The samples were immersed in 5% Na₂SO₄ solutions for 24 months, and tests were conducted to check compressive strength, expansion and relative dynamic elasticity after 6,12,18 and 24 months. The study found that the samples with only OPC performed the worst and collapsed after ten months. Samples with 30% low fly ash with 400 kg/m³ binder performed well in all testing, followed by 30% high fly ash with 300 kg/m³. The samples with fly ash generally remained stable after six months in sulphate solutions. They did not show much deterioration or expansion after the six months, elucidating that fly ash-based mortar/ concrete composites perform better under sulphate attack due to their tendency to absorb Ca(OH)₂, form more C-S-H gel and prevent the formation of ettringite. However, increased use of fly ash resulted in the extensive formation of Si(OH)₄, which has swelling properties and results in weakness of composites (Figures 2.50, 2.51) (Troii et al., 1995; Nadir and Ahmed, 2021b Appendix VII; Nadir and Ahmed, 2022b Appendix V; Nadir, Ahmed and West, 2023b Appendix IV).

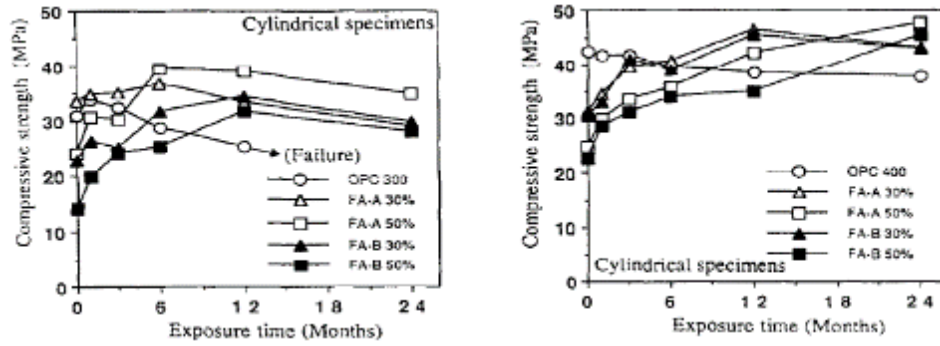


Figure 2.50: Compressive Strength of Low/High PFA-Based Concrete (Troii et al., 1995).

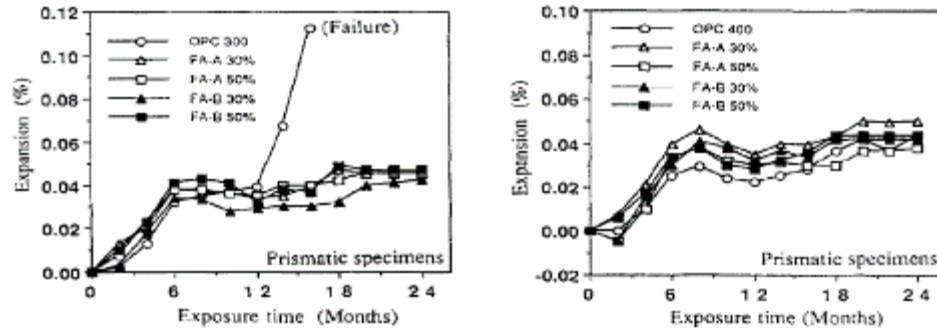


Figure 2.51: Expansion of Low/High PFA-Based Concrete Samples in Na_2SO_4 Solution (Troii et al., 1995).

2.3.11.3 Silica fume (SF)

SF is an amorphous crystalline industrial waste material produced during the reaction of quartz with coal in an arc furnace to manufacture silicon or ferrosilicon alloys. The elemental composition of SF was determined by x-ray spectrometry in UK Analytical Limited's laboratory (UKA), and it was found to contain 99.1% SiO_2 and 0.9% oxides of other metals, as shown in Table 2.7. The bulk quantity of silicate available in SF makes it an excellent partial cement replacement material if mixed in specific percentages of cement weight. The excess silicate in SF reacts with excess $\text{Ca}(\text{OH})_2$ to increase the C-S-H gel in concrete. However, an extra quantity of SF used as cement replacement reduced the concrete strength due to the extensive availability of silicate from SF and reduced reaction/

consumption of silicate from cement. Based on particle size, SF is categorised as micro (greater than $0.5\mu\text{m}$) and nano SF ($0.1 - 0.2 \mu\text{m}$). The surface area of $0.1\text{-}0.2\text{-micron}$ SF is $30,000 \text{ m}^2/\text{kg}$, and the density is $150\text{-}700 \text{ kg/m}^3$ (Selvapriya, 2019; Nadir et al., 2022a Appendix X). There are varying results of strength improvement using different percentages of SF as cement replacement based on cement/ concrete grade, W/C ratio and other concrete formulation conditions. The maximum quantity of SF for partial cement replacement was suggested to be 20%, as the excess of silica makes it a good pozzolanic SCM. Still, its excess quantity of more than 5% could cause swelling and cracks due to the production of Si(OH)_4 gel during the hydration process (Vikas et al., 2012; Ajileye, 2012; Pradhan and Dutta, 2013; Girts et al., 2020). 10% use of SF increased the compressive strength of M30 grade concrete, but 15% SF reduced the strength (Ajileye, 2012). Roy (2012) also supported a 10% optimum quantity of SF for better strength improvement. SF quantity of 7.5% cement replacement was suggested as optimum for high-grade 60MPa concrete (Shanmugapriya and Uma, 2013). Jain and Pawada (2015) assessed SF mixed concrete composite at 5,10,15,20,25% for durability testing under sulphate, nitrate and chloride environment versus a control mix of 0% SF. They suggested that 15 SF is the best-performing mix ratio for better durability (Jain and Pawada, 2015). Kumar and Dhaka (2016) conducted a study with 0,3,6,9,12, and 15% SF cement composites for M35-grade concrete. They suggested that compressive, tensile and flexural strength on 7, 14 and 28 days were improved compared to the control mix (Kumar and Dhaka, 2016). Ghutke and Bhandari (2014) found that increased percentages of SF decrease the workability; however, the optimum quantity of SF with high-grade concrete is 10-15% (Ghutke and Bhandari, 2014). Contemporary research established SF as a suitable cement replacement for enhancing the mechanical properties of concrete composite and absorption of industrial waste from the silicon industry to the construction industry to reduce environmental impact for both industries (Nadir et al., 2022a Appendix X).

2.3.11.4 Metakaolin (MK)

Metakaolin is obtained by calcinating naturally occurring Kaolinite clay mineral under 450-650 C°. It is dehydroxylated aluminium silicate ($\text{Al}_2\text{O}_3 \cdot 2\text{SiO}_2 \cdot 2\text{H}_2\text{O}$) which is formed by a weaker/ more reactive structure after losing hydrate ion OH^- during calcination (Aiswarya, Prince and Dilip, 2013; Nadir et al., 2022a Appendix X). The elemental composition of SF was determined by x-ray spectrometry, and it was found to contain 52% Si_2O and 45% aluminium oxide, as shown in Table 2.7. It contains more than 90% combined quantity of pozzolanic elements so is considered suitable pozzolanic material as per ASTM C 618/ C125-19 (ASTM C 618/ C125, 2019). It is an amorphous crystalline material and tends to react with the excess $\text{Ca}(\text{OH})_2$ molecules in cement hydration reactions to form an additional quantity of C-S-H gel, thus enhancing the mechanical properties of concrete composites. However, if more than a specified quantity is used, it would weaken the cement concrete hydration process by increasing the supply of silicate molecules in cement paste. Using MK in cement concrete improves the pore structure, reducing porosity and permeability (Sabir, Wild and Bai, 2001). Sinngu and Ekolu et al. (2023) observed that up to 15% MK as cement replacement incorporated enhanced compressive strength refined pore structure, greater flowability, increased durability against sulphate attack and alkali-silica reaction (ASR) and lowered the drying shrinkage for CEMI and CEMII as use of class N pozzolanic cement blend as per ASTM C618 and SANS EN 50197-1 (Sinngu et al., 2023). Eva et al. (2010), Erhan (2012), and Vikas (2012) studied the use of Mk. They found improved mechanical properties, shrinkage and durability under a chloride environment with 10% Mk as the optimum quantity. MK use with cement results in a decreased workability of concrete and requires a suitable quantity of plasticiser to maintain consistency and control the water-cement ratio. A composite of Mk with fly ash and iron oxide in cement concrete gave a considerable increase of up to 20% in compressive and tensile strength of the composite (Hemnet, 2011; Dojkov, 2013; Nadir et al., 2022a Appendix X).

2.3.11.5 *Rice Husk Ash*

Rice is considered the second biggest edible crop as the primary food ingredient in the world, and its production is estimated to be around 700 million tons per year. The rice plant absorbs silicon from the soil and stores it in the husk, forming a cover around the rice seed to protect it. During rice milling, the husk is removed from the seed and used as a burning material in other industries (Edodzigi, 2001; Oyetola and Abdulahi, 2006; FAO, 2013; FAO, 2014). The milled rice husk is estimated to be around 100 million tons annually. The husk is converted into ash after burning, having more than 97% silica and 3% oxides of other metals, as shown in Table 2.7. It is considered suitable pozzolanic material as per ASTM C 618/ C125-19 (ASTM C 618/ C125, 2019). 15% RHA mixed with OPC was considered the optimum quantity for better strength, fineness, consistency and durability (Akeem and Mutiu, 2017). The engineering properties improved at 28 and 90 days with 15% RHA mixing with OPC (Ephraim, Akeke, and Ukpata, 2012). The workability of concrete composite is reduced, and permeability is improved with increased RHA (Ganesan and Rajagopal, 2008). The durability of RHA composite with OPC increases by 5-25%; however, a decrease in strength of more than 10% was observed with RHA. Overall, the RHA could be considered the best cement replacement material partially due to the abundance of silica available in the ash, which could react well with loose calcium hydroxide to form consistent C-S-H gel during cement hydration (Rashid, Ali and Ahmed, 2010; Nadir et al., 2022a)

2.3.11.6 *Palm Ash (PA)*

Palm trees are found worldwide and have different kinds of fruits. The palm leaves and branches are considered solid waste and create much environmental nuisance when disposed of as a landfill or rubbish. The palm leaves and branches are used to construct mats and roofs as packing material and as burning fuel. Palm burning at 700C° produces ash containing oxides of metals, providing pozzolanic quality during cement hydration. It has a particle size of around 300µm

surface area of $3400 \text{ cm}^2/\text{g}$ (Hewlett, 2004; Neville, 2011; Jonida et al., 2018; Darweesh and Abo El-Suoud, 2019). The palm ash sample was evaluated through x-ray spectrometry and was found to be rich in potassium and oxides of other metals. Out of the understudy's four materials, PA has the least alumina/silicate compared to MK, SF, RHA and PFA composition (Table 2.7), so its use as cement replacement is a good research question. PA has around 55% $\text{SiO}_2 + \text{Al}_2\text{O}_3$ and 23% K_2O , making it a suitable alternative pozzolanic material to impart increased strength with the formation of additional C-S-H gel during the pozzolanic reaction phase of hydration. Although its optimum dosage is not yet determined and researchers use it carefully due to the increased presence of K_2O , which is considered a crack-inducing material (Hewlett, 2004; Neville, 2011; Premalatha et al., 2016; Jonida et al., 2018; Darweesh and Abo El-Suoud, 2019; ASTM C 618/ C125, 2019). The compressive strength was found to be optimum at 2.5% palm oil ash, and it started to decrease with more use of palm ash after 5% (Hewlett, 2004; Neville, 2011). The fineness, porosity, and compressive strength were found to improve, and workability, hydration, and setting time decreased with increasing quantities of PA from 0-10%, and after 10%, all parameters were found to decrease (Neville, 2011). The disposal of/ recycling of PA in concrete would likely reduce its direct environmental impact, as landfills and rubbish burning directly threaten the open environment (Nadir et al., 2022a Appendix X).

2.3.11.7 Iron Powder (Fe)

Iron powder is the waste product from steel mills obtained during scrap steel processing from other industries through shot blasting. It is a finely-grained powder having a particle size ranging from $19\text{-}45 \mu\text{m}$, having a specific density of 2.8 g/cm^3 , and containing Fe metallic particles to the extent of 93% (Table 2.7). Iron powder/ dust is hazardous and harmful to the environment. It could cause an explosion and is generally disposed of in landfilling, costing huge disposal costs to steel mills; however, its use as an alternative to cement could give some environmental benefits, making it slightly costly compared to OPC

(Karuppasamy, Dinesh and Janardhan, 2011; Garcia et al., 2017; Iron Powder, 2023). The large-scale environmental impact of OPC has encouraged researchers to continuously explore the complete/ partial replacement materials as enhanced supplementary cementitious materials (Nadir and Ahmed, 2022b, 2022c). The researchers have endeavoured to use naturally occurring pozzolanic materials like metakaolin (MK) or zeolite or waste materials derived from industrial/agricultural fields having good aluminous and siliceous constituents demonstrating OPC-like properties, e.g., ferrous carbonate (FeCO_3), ground granulated blast furnace slag (GGBS, an established OPC replacement material), pozzolans like silica fume (SF), pulverised fly ash (PFA), palm ash (PA) and rice husk ash (RHA). These materials are considered to enhance the engineering properties of concrete, increasing its durability. The materials containing “Fe” produce considerably fewer CO_2 emissions, resulting in a negative CO_2 balance by absorbing the CO_2 from the environment to make FeCO_3 (Vijayan et al., 2019; Nadir et al., 2022a). David Stone (2010) conducted a failed test during the material formulation based on “Fe” and threw the discarded mix in the bin. While discarding the rubbish, he observed that the discarded material gained strength after the initial setting, like cement concrete. Then, he used this material as a concrete alternative, naming it ‘iron shell’ and later ‘ferrock,’ a greener SCM containing 60% Fe, 20% PFA, 12% MK and 8% CaCO_3 . The atomic absorption spectroscopy analysis concluded that this material absorbs 8-11% of environment CO_2 during curing while converting “Fe” into FeCO_3 , making it a better eco-friendly material than cement concrete which emits 8-10% CO_2 during manufacturing/curing, as explained by chemical equation 25 (Stone, 2010; Das, Souliman and Stone, 2014; USGS, 2014; Vijayan et al., 2019; Nadir, Ahmed and West, 2023 Appendix IV; Nadir, Ahmed and Moshi, 2024 Appendix VII).

Equation 25: $\text{Fe} + \text{CO}_2 + \text{H}_2\text{O} = \text{FeCO}_3 + \text{H}_2$

The Fe-composites could be used as a partial SCM and could result in plausibly better, greener, more robust material if an ideal environment of 100% CO_2 curing

is provided, which is not feasible. Therefore, contemporary researchers have used it partially with OPC to formulate better-performing eco-friendly material at par OPC. It could be used in the marine environment where corrosion due to saltish sea water accelerates the formation of FeCO_3 by providing more Fe^{++} for the chemical reaction with CO_2 , increasing the production of Fe-composites and adding more strength to the structure and preventing further corrosion. Fe-composites-based concrete could be identified by its characteristic iron brownish colour used in pavement tiles and facade work. Oxalic acid could also be used as an accelerator catalyst and a de-scaler/ cleaning agent to minimise the colouring/ scaling effect and to accelerate the ionisation of Fe^{++} to convert insoluble iron to soluble iron carbonate (Stone, 2010; Das, Souliman and Stone, 2014; USGS, 2014; Vijayan et al., 2019; Nadir, Ahmed and West, 2023). Vijayan et al. (2019), in an evaluation study on Fe-composites-based concrete as a greener material, elucidated the engineering properties of the composites by mixing 4%, 8% and 12% Fe-composites with OPC and compared the compressive and split tensile strength with 0% control mix. It was observed that the iron-based concrete composite with 8% exhibited the best performance in comparison to the control mix and other composites (Vijayan et al., 2019). In a study on eco-friendly Fe-based cement mortar, cubes of 5, 10, 15, 20% Fe-cement composites were cast and assessed for compressive/ flexural strength on 7-, 14- and 28-days strength, and 10% Fe-mix/ cement mortar composite exhibited the best performance in all mechanical properties' indicators. The cubes were immersed in a 5% Na_2SO_4 concentrated solution for 90 days, and again, the 10% composite was found to perform better in durability studies against sulphate attack (Karthika, Leema and Priyadarshini, 2021). A study was conducted on Fe-cement composites with variation in the quantity of oxalic acid to elucidate the strength performance and setting time with 4, 6, 8, 10, and 12 moles of oxalic acid and 10 moles of oxalic acid performed the best but increased the cost of composite considerably thus determining that 2% oxalic acid use with Fe-cement composite is the most feasible combination basing on cost-benefit analysis

(Prashanth, Gokul, and Shanmugasundaram, 2019). The literature review revealed that negligible work had been conducted on further study of iron-based composites with different varieties of pozzolanic materials in different mix ratios, and no work could be found on the performance of fibre-reinforced iron-based pozzolanic composites, identifying a research gap which influenced this research project to explore various innovative iron-based fibre-reinforced composites further.

2.3.11.8 Limestone (CaCO_3)

Limestone powder is the ground form of calcite containing 96.8% CaCO_3 , with a particle size of $4\mu\text{m}$ and bulk density of 900 kg/m^3 (loose) to 1100 kg/m^3 (vibrated). On hydration, it is converted into hydrated/ slaked lime Ca(OH)_2 . It provides Ca^{++} ions to form C-S-H gel after reacting with silica from pozzolanic material in the aqueous solution (Oates, 2010). It was used to produce iron-based binary/ ternary pozzolanic composites in this project (Nadir, Ahmed and West, 2023 Appendix IV; Nadir, Ahmed and Moshi, 2024 Appendix VII).

2.3.11.9 Oxalic Acid

Oxalic acid is a weak organic alpha,omega-dicarboxylic acid having formula $\text{C}_2\text{H}_2\text{O}_4$ or $(\text{COOH})_2$. It is broadly used as a cleaning agent, like weak acid, e.g., vinegar, to remove stains from different surfaces. Its use in Fe-based concrete as a catalyst accelerates the reaction for the increased formation of FeCO_3 . The research has elucidated the use of oxalic acid in the range of 10 moles/ m^3 of concrete. However, cost-benefit analysis versus strength achievement suggests using oxalic acid in the 2% binder quantity (National Centre for Biotechnology Information, 2023; Nadir, Ahmed and West, 2023 Appendix IV; Nadir, Ahmed and Moshi, 2024 Appendix VIII).

2.3.12 Review of Fine and Coarse Aggregates Alternate Materials

The construction industry is a crucial CO_2 contributor. Contemporary research focuses on formulating cement replacement composites; however, less attention

is paid to formulating fine/coarse aggregate composites. The waste from different fields contributes enormously to adverse environmental effects, thus necessitating reuse/recycling. The demolition/ reconstruction of old buildings/ infrastructure is adding further to the waste contribution by the construction industry. The total quantum of fine/ coarse aggregate is estimated to be around 20 billion tons, contributing around a billion tons of CO₂. Therefore, even partial replacement of virgin sand/coarse aggregates with various waste materials like glass, rubber, plastic, tyres, recycled concrete and others would likely economise the cost of manufacturing the concrete with reduced CO₂ footprints as eco-friendly materials. The quarrying, transportation and crushing/ extraction of around 20 billion tons of sand, gravel and aggregates for the formulation of cement concrete/ road construction produce one billion tons of additional CO₂ emission per year (Brander and Davis, 2012; Gagg, 2014; Garside, 2022a; Garside, 2022b; MPA, 2007; Nadir et al., 2022a Appendix X; Nadir and Ahmed, 2021b Appendix VII; www.grandviewresearch.com, 2020). The global aggregate market size is estimated at around 500 billion USD. The leading share is approximately 70% taken by concrete manufacturing, 18% by highways/ airfield construction and 12% by all other industries/ uses, as illustrated in Figure 2.52 (www.grandviewresearch.com, 2020). The USA, Canada and Mexico in North America, Brazil in South America, Germany and the UK in Europe, Gulf countries in the Middle East, and China and India in Pacific Asia are the primary consumers of the aggregates due to ongoing significant construction/development work (www.grandviewresearch.com, 2020). The mining, excavation, and crushing industry, which produces fine and coarse aggregates, is experiencing a surge in demand and financial benefits. However, this trend has led to illegal and uncontrolled production (Leal Filho et al., 2021), resulting in a faster depletion of natural resources (Pitchaiah, 2017), non-conservation of these resources for future generations (Koehnken and Rintoul, 2018), and damaging impacts on the environment (Adu-Gymfi, 2016; Dugan et al., 2010). The ecology and biodiversity of natural habitats are also disturbed (Freedman et al., 2013), and fauna and flora

are adversely affected due to the loss of vegetation and reduced water levels after excavation (Haghnazar and Saneie, 2019). Furthermore, this industry impacts the coastal and marine landscapes (Boers, 2005), induces variations in geographical and morphological patterns (Kondolf, 1994), and causes degradation of stream beds' longitudinal and transverse gradients (Jia et al., 2007). It also adversely affects beds and channel stability (Jordan et al., 2019), resulting in erosion and stream flow variations (Lousiagustin and Kusratmoko, 2016; Nadir and Ahmed, 2023c). Moreover, the construction industry is also a substantial contributor to construction waste in the form of demolished buildings and road resurfacing/ reconstruction, which could be used as recycled concrete aggregates for the preparation of fresh concrete with added cost/ environmental benefits though with reduced strengths benefits (Ohemeng and Ekolu, 2020). Other sectors also produce significant waste, such as glass, rubber, tyres, and polyethene terephthalate (PET) plastic bottles (Nadir and Ahmed, 2021). The researchers were endeavouring to formulate supplementary cementitious materials (SCMs) using different industrial/ agricultural waste materials/ ashes having pozzolanic qualities/ silica (SiO_2) as partial/ full cement replacement, objectively to reduce the cement consumption, formulation of environmentally friendly materials by lowering greenhouse gases footprints of the construction industry and to absorb the enormously produced industrial/ agricultural waste by incorporating into the cement concrete composites in the form of ashes/ fibres (Guerrero et al., 2013; Hoornweg and Bhada-Tata, 2021; Nadir et al., 2022b Appendix X; Thomas and Gupta, 2013; Shahbaz and Faraj, 2020). However, considering the vast market share/ quantum of aggregates and their CO_2 footprints, conducting concerted endeavours to evaluate the replacement of the fine/ coarse aggregate partially/ entirely with different industrial waste materials is essential. Contemporary researchers have conducted experimental studies to partially replace the aggregate with a dual-purpose option of absorbing a portion of around 2 billion tons/ year of solid waste going into sea/ landfill and to economically formulate eco-friendly concrete composites targeting improved

mechanical properties by employing specific mixing ratios. The researchers were using different percentages of cement replacement/ enhancement materials like pulverised fly ash (Arioze et al., 2013; Yildirim et al., 2015), metakaolin (Zhan et al., 2020), ground granulated blast furnace slag (Fan et al., 2021; Ismaeel and Hashimi, 2008), palm ash (Al-saleem et al., 2009; Sheikh Khalid et al., 2018), rice husk ash (Endale et al., 2022; Mohammadi et al., 2009), the fibres like glass fibres (Mohammed et al., 2021), wheat straw (Nadir et al., 2022b Appendix X), polypropylene fibres (Akca et al., 2015), steel fibres (Qadir et al., 2020), and fine/ coarse aggregate replacements like crushed/ shredded glass (Mohammed et al., 2021), crumb rubber (Onuaguluchi and Panesar, 2014), crushed/ shredded PET bottles (Brandit, 2008; Saikia, 2012), crushed tyres (Rowhani and Rainey, 2016) and recycled concrete aggregates (Shahbaz and Tajara, 2021) as economic/ eco-friendly considerations (Nadir and Ahmed, 2023c). This research also focussed on the formulation and experimental/ comparative investigation of the performance of cement concrete by partially replacing fine aggregate with 10%, 20%, and 30% crushed glass (CG) crumb rubber (CR). It shredded recycled PET bottles (RPB) and partially replaced coarse aggregate with 10%, 20%, and 30% recycled concrete aggregate (RCA), 5%, 7.5%, and 10% crushed/ shredded tyres (CT). The mechanical properties of all the composite mixes were compared with the control mix and mutually with other composites to ascertain the best-performing composites/ mixes, replacement materials and optimum mixing ratios (Nadir and Ahmed, 2023c Appendix XIV).

2.3.12.1 *Fine Aggregates Replacement*

2.3.12.1.1 *Crushed Glass*

The industry is estimated to produce more than one hundred million tons of glass annually, with only a 21% recycling rate of around 27 million tons (Tiseo, 2023). The balance quantity of more than 70 million tons goes into the sea/ landfill without serving any beneficial use but adding to the world's solid waste (Tiseo, 2023). The glass generally contains around 70% SiO₂, 11% CaO, 10-12% Na₂O,

BaO, PbO and 8-9% other elemental minerals/compounds. The crushed/ shredded/ fine glass has a density of 2380 kg/m^3 , a specific gravity of 1.7, a hardness of 6-7 on the Mosh scale, and a pH of less than 11 in water. The chemical composition/ physical properties make it a suitable material for replacement as cement (glass powder), fine aggregate (fine glass passing 4.75 mm sieve), coarse aggregate (crushed/ shredded glass passing 20 mm sieve) and glass fibres as shown in Figure 2.53 (Mansour et al., 2023) for improvement

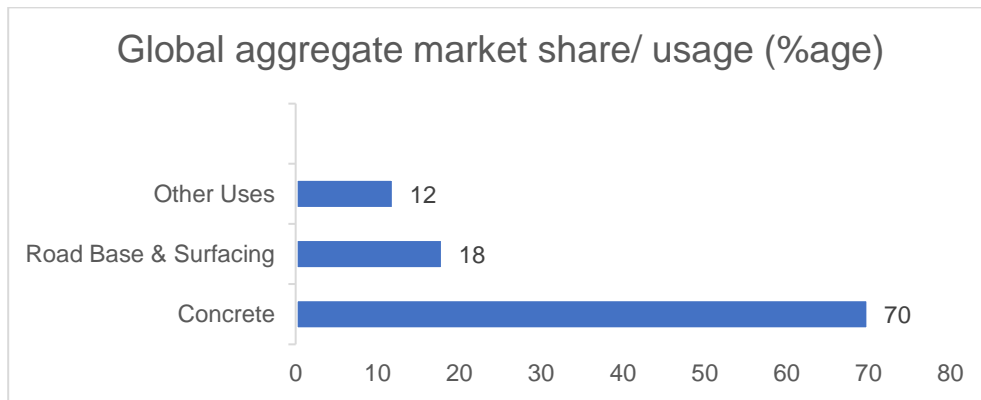


Figure 2.52: Percentage of Global Aggregate Market Share By Usage/ Application (www.grandviewresearch.com, 2020; Ahmed and Nadir, 2023c)

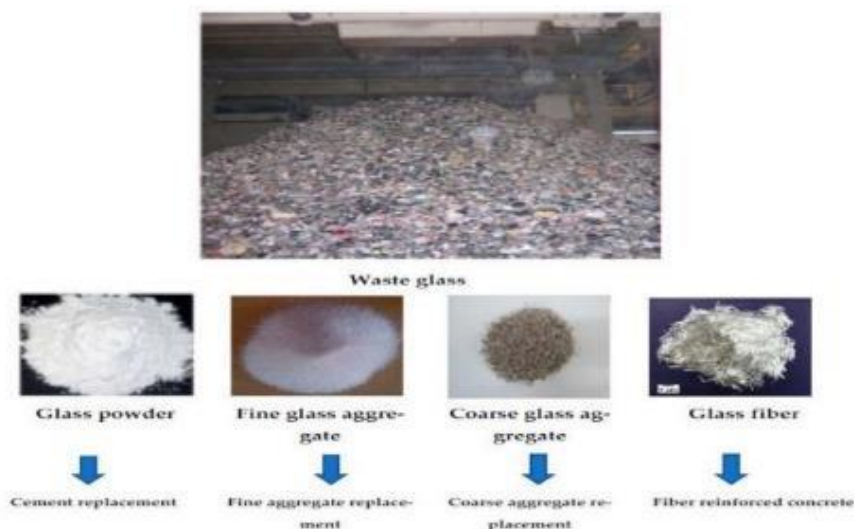


Figure 2.53: Different Uses of Waste Glass in Concrete (Mansour et al., 2023; Ahmed and Nadir, 2023c).

of mechanical properties of concrete, as an SCM and as replacement material/ eco-friendly waste disposal in conformance with BS EN 12620-2009, and 8500-2 (BS 12620, 2009; BS 8500-2; 2013; Mansour et al., 2023; Tiseo, 2023; www.concrete.org.uk, 2020). Using more than 20% fine glass powder (smaller than 75µm) as SCM in concrete induces an alkali-silica reaction (ASR) due to excess silica in the glass powder imparted during the OPC hydration process. Crushed/ shredded glass remained cement replacement in 1980-1990, but its use was discontinued/ reduced due to pronounced ASR impacts. It could result in the production of swollen Si(OH)_4 . CaO gel creates cracks and weakens the concrete, as shown by the chemical equation 26 (Nadir and Ahmed, 2022b). The use of crushed glass as a fine aggregate replacement with lower dosages, along with the GGBS mixing, was observed as a beneficial option with reduced ASR impacts on the composites (Mansour et al., 2019). Moreover, using crushed/ shredded glass as a partial replacement of fine and coarse aggregates has exhibited promising/ improved chemical-mechanical properties of concrete by reaching the strength threshold of high-strength concrete (Natarajan et al., 2020; Pierce et al., 2021; Zeybek et al., 2022; Nadir and Ahmed, 2023c).

Equation 26: $\text{SiO}_2 + 2\text{Ca(OH)}_2 = \text{Si(OH)}_4.2\text{CaO}$ (Nadir and Ahmed, 2022b)

2.3.12.1.2 *Crumb Rubber (CR)*

Rubber is a widely used natural/ synthetic material in numerous domestic/ commercial products/ packaging/ tyres. The tyre industry alone is estimated to produce around 1.5 trillion tyres annually, making it a significant recycling/ disposal issue globally (Williams, 2017). The tyres are estimated to comprise approximately 20-34% natural rubber, 11-25% synthetic polymers, 24-26% fillers/ antioxidants, and 12-25% steel wires (Ren et al., 2022). The tyres are generally crushed/ shredded/ grounded into rubber particles of different fine/ coarse grain sizes (0.5-20 mm) using a cracker, granular, or micro milling process (Rohit et al., 2021). Islam et al. (2022) conducted a study illustrated in Figure 2.54, elaborated on how the tyres from vehicles generate waste which goes into

landfills or burnt, causing pollution/ global warming/ reduction of valuable land; so if these tyres are converted into fine/ coarse recycled aggregates and are then used as composites with partial/ total replacement as normal/ lightweight concrete in domestic/ commercial construction could exhibit economic/ eco-friendly benefits along with improving the physio-chemical composition of OPC based composites resulting in enhanced strength and sustainability (Islam et al., 2022; Nadir and Ahmed, 2023c Appendix XIV). Therefore, special care should be exercised for formulating fine aggregate composites with crumb rubber up to 10-30% due to crumb rubber particles' lightweight/ hydrophobic properties.

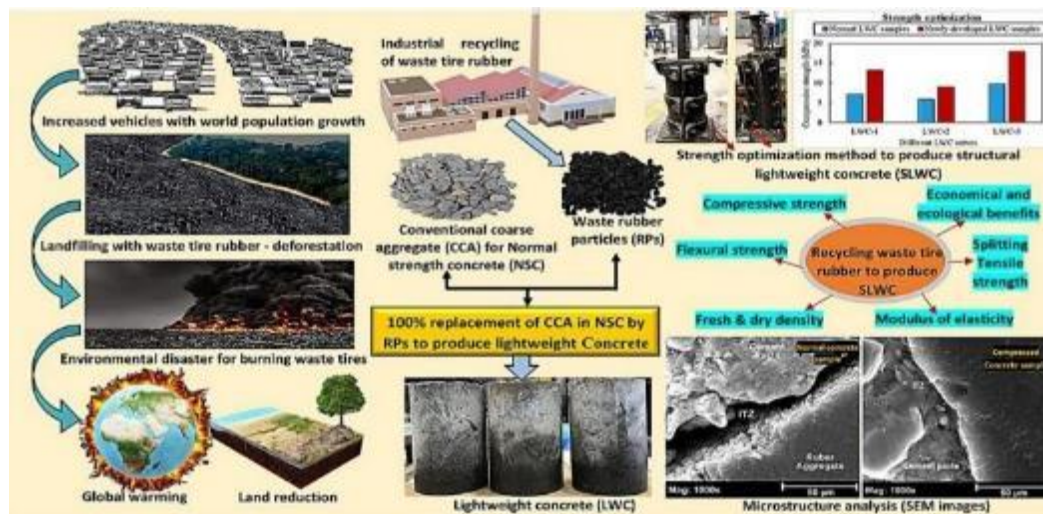


Figure 2.54: Use of crumb rubber/ shredded/ crushed tyres as fine/ coarse aggregate in concrete composites (Islam et al., 2022; Ahmed and Nadir, 2023c).

2.3.12.1.3 Crushed Recycled PET Bottles (RPB)

Scientific inventions in organic chemistry introduced humankind to new materials based on polymers named plastic. Historically, around 10 billion tons of plastic have been manufactured, and the trend suggests the quantity will reach approximately 15 billion tons by 2050. Plastic recycling is estimated to be around 9%, disposal by incineration is about 12%, and the rest, 79%, is going into landfills/ sea/ environment around us with a remote possibility of biodegradation/ termination (Almeshal et al., 2020; Geyer et al., 2017; Gu and Ozbakkaloglu,

2016; Sharma and Bansal, 2106; UNEP, 2018;). The world produces around 15% polyethylene terephthalate (PET) plastic as plastic bottles and packing material annually, and around 20000 PET bottles are manufactured per second. The shredded plastic with a 1-5 mm grain size could be an excellent fine aggregate replacement due to its inherent elastic/ non-water absorbent properties. The shredded/ crushed/ shredded PET fine aggregates exhibit an elasticity of around 2-3 GPa, a specific gravity of 1.1, and a 1.4 g/cm³ density. However, the lightweight/ low-density grains could reduce the density of the composite and uneven distribution/ morphology could decrease the intra-cement-aggregates bonding compared to the natural aggregate's bonding, leading to weaker zones/ failure points (Galvao et al., 2011; Guerrero et al., 2013; Hoornweg et al., 2012; Laville, 2021; Nkomo et al., 2022; Nadir and Ahmed, 2023c).

2.3.12.2 Coarse Aggregate Replacement

2.3.12.2.1 Recycled Concrete Aggregate (RCA)

OPC-based concrete has revolutionised the construction mechanics of modern infrastructure. Still, it also has a specific life restriction, necessitating the demolition/ reconstruction of structures after the expiry of their life. This reconstruction/ demolition has created an enormous waste disposal issue in the construction industry. It is already under intense criticism due to its coherent CO₂ footprints (responsible for 40% of CO₂ emissions and 35% of global waste) (Miller, 2021). An estimated 300 million tons of recycled concrete/pavement waste is produced annually in Europe alone, with India producing around 200 million tons and China and the USA about 500-600 million tons annually (Panda et al., 2020). The researchers have endeavoured to absorb this gigantic waste into the formulation of new concrete composites and resurfacing/ paving materials using the old concrete as recycled aggregates with up to 40% in concrete and up to 75% in the road surfaces/ pavements, especially in 1990-2000 but were limited to low-strength utilisations due to inherent characteristic limitations of RCA (Adnan et al., 2010; Marinkovi et al., 2014; Soares et al., 2014;

Wen et al., 2014; Wen et al., 2015). The morphology of old concrete aggregates, higher water absorption, toughness index, marshal stability, sustainability against chemical attacks and decreased flexural strength are the issues which necessitate the careful formulation of concrete composites using recycled aggregates (Nadir and Ahmed, 2023c Appendix XIV).

2.3.12.2.2 Crushed/ Shredded Tyres (CT)

The crushed/ shredded/ ground tyres contain around 55% rubber polymers, 25-40% carbon black, 5% ash, and about 15% other chemicals/ fillers/ acetones exhibiting a density of around 480 kg/m³, the specific gravity of 1.15, elasticity of 4-15 MPa and water absorption of up to 10% (Ren et al., 2022). The hydrophobic, porous, low-density and elastic crumb rubber/ crushed/ shredded tyres could result in consumption of water during the hydration process, air entrapment, low-density lightweight concrete, uneven distribution on mixing with natural aggregates, weak load-bearing zones in the concrete structure leading to the creation of abrupt failure initiation points when subjected to compressive loading. However, the characteristic elasticity might increase the tensile/ flexural strength of the composites (Najim et al., 2012; Ren et al., 2022; Rohit et al., 2021; Sukontasukkul and Tiamlom, 2012; Thomas et al., 2014; Williams, 2017; Yousuf et al., 2017; Zhu et al., 2018). These phenomena were pronounced especially when replacing virgin coarse aggregates with shredded tyre particles passing a 20mm sieve in various uses, as shown in Figure 2.54. Therefore, special care should be exercised for formulating fine aggregate composites with crumb rubber up to 30% and coarse aggregate composites up to 5-10%, as considered in this study (Ahmed and Nadir, 2023c).

2.3.13 Review of Fibres Selection for Fibre Reinforced Cement/ Lime Concrete

Generally, up to a maximum of 1-2% fibres have shown around 20% compressive strength improvement, and up to 5% fibres show around 25% tensile/ flexural strength enhancement with ductile behaviour but with decreased compressive

strength. However, conflicting results and restricted usability were found in different research. This fact has paved the way for this study to evaluate the suitability of different types of natural/ industrial fibres with varying quantities to determine the best possible concrete composites with enhanced properties. A focus was given on the use of two established suitable fibres, polypropylene fibre (PPF) and steel fibre (STF), two natural fibres from agricultural waste, coconut coir fibre (COF) and wheat straw fibre (WSF) and an industrial waste material, polyethylene terephthalate/high-density polyethylene (PET/ HDPE) bottles' shredded fibres (Ismail and Hashmi, 2008; Mohammadi et al., 2009; Saikia and Brito, 2012; Akca, Kaker and Pek, 2015; Yildirim et al., 2015; Qadir et al., 2015; Rajkumar, 2017; Mohammed et al., 2021; Hemm et al., 2021; Nadir et al., 2022a). Incorporating fibres in concrete has significantly improved compressive/ tensile/ flexural strengths, post-ductility behaviour and micro surface crack propagation control. However, researchers have shown certain limitations also on types, optimum quantity, segregation, distribution, length/ diameter/ aspect ratio, durability, sustainability, decay resistance and flexibility of fibres (Qadir et al., 2015; Mohammed et al., 2021). It reflects that the use of fibres in concrete does not develop a linear relationship versus different mechanical properties; instead, it varies significantly based on the type of material, quality and quantity of fibres (Mohammadi et al., 2009; Saikia and Brito, 2012; Nadir et al., 2022a).

2.3.13.1 *Steel Fibres (ST Fibres/ STF)*

Steel fibres are internationally recognised concrete reinforcement materials derived from mill-cut steel sheets, recycled tyres and shredding of steel objects. It is ductile, elastic, and heat/ crack resistant but is liable to corrosion material, considerably enhancing the concrete's tensile and flexural strength (Barros, 2011). Steel fibres broadly used in fibre reinforcement concrete are categorised as straight, crippled or hooked fibres, as shown in Figure 2.55. Steel fibres of 0.2 mm diameter and 10-60 mm length exhibit 7800 kg/m³ density, 200 GPa modulus of elasticity and 1200-2600 MPa tensile strength. The established/ Suitable use

of STF is designated at a rate of 10-17 % fibres to the cement weight (Tariq et al., 2017; www.becaert.com/dosingdramix, 2024; Nadir et al., 2022a).

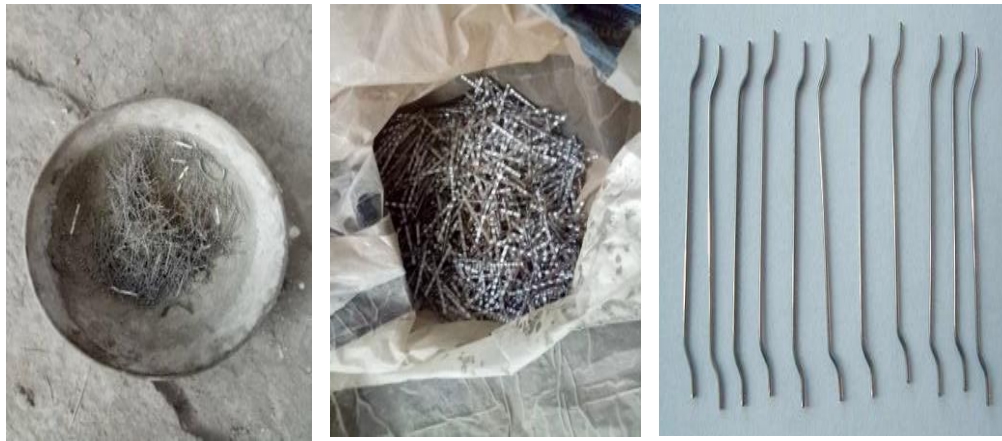


Figure 2.55: Straight, Crippled and Hooked Steel Fibres (Tariq et al., 2017)

2.3.13.2 Polypropylene Fibre (PPF)

Polypropylene is a stereognosis thermoplastic fibre transformed from 85% propylene (Synthetic Fibres, 2020). It has good properties and could be used as a concrete flexural/ tensile strength improvement material. Three different polypropylene fibres are used: monofilament, microfilament and fibrillated fibres, as shown in Figure 2.56 (Synthetic Fibres, 2020). It is a lighter material having a density of 0.9 g/cm^3 and exhibits near zero water absorption, 30-100% elongation, 0.2- 0.5 mm diameter, 10-50 mm length, 3.5-10 GPa modulus of elasticity and 330-750 MPa tensile strength. Zero water absorption, super elongation capacity, low density and excellent tensile strength make it an internationally recognised/ established fibre to use as an enhancer of mechanical properties of concrete at a rate of 1-2% (Singh, 2016; Nadir et al., 2022a).



Figure 2.56: Polypropylene Fibres (Macro/Microfibres) (Synthetic Fibres, 2020; Nadir et al., 2022a)

2.3.13.3 Coconut Coir Fibre

One of the most used natural fibres in different sectors is coconut coir, which belongs to the palm family (Rajkumar, 2017). Coir is a stiff, renewable, and biodegradable fibre produced by the extraction of fibre from waste coconut husk by the retting process, mainly in coastal areas of Africa, Asia, and America (Figure 2.57). Coir is then soaked in water and NaOH solution for around a month to separate dirt, silica crystals, moisture, and pith to get a clean, fibrous product (www.madehow.com, 2019). The coir production in the world is estimated to be around 800,000 metric tons annually. India and Sri Lanka alone contribute more than 80% of coir, which is used in different categories of products, including upholstery, ropes, meshes, sacks, the construction industry and horticulture (Ministry of MSME India, 2017). The coir is also used in making anti-corrosion mesh nets for embankments, slope stabilisation, and strengthening flood bunds and road subgrade. Bitumen-treated coir sheets are often used on road surfaces, rail embankments, and waterproofing on wet surfaces (www.madehow.com, 2019). The mature coir fibre retted in saline water is generally short in length up to a maximum of 0.15m to 0.3m long with 0.1 mm to 0.5 mm diameter, comprising mainly of cellulose and water having various cavities along the cross-section, which increase their stickiness/ bonding property. The main composition by

weight of coir is 40-45% cellulose/ hemicellulose, up to 10-25% moisture, 40-45% Lignin/ pith/ pectin and traces of Ash up to 2.5%; its density is 1.4 g/cm³, elongation is up to 30% of the length and could swell up to 5% with an average life of 3 - 20 years (Alam, 2014). The Lime, Silica and saline-treated coir have shown much-improved life if used with cement or lime in a composite. Its physical/ chemical properties and cheap availability in abundance suggest its numerous uses in the construction industry, especially in bituminous mats, marine clay soils, embankment stabilisation and cement/ lime concrete/ mortars for improved life and compressive/ flexural/ torsional strengths (Alam, 2017; Ahmed et al., 2020). The hardness and good elongation characteristics of coir make it an excellent material to use in fibre-reinforced concrete, especially for the enhancement of tensile/ flexural strength and ductile behaviour of concrete. Some of the uses of coir in the construction industry as erosion control measures are illustrated in Figure 2.58 (Sutton and Rayan, 2020; Ahmed et al., 2020).



Figure 2.57: Coconut Coir Fibre (Ahmed et al., 2020)



Figure 2.58: Coir Mesh Used in Erosion Control Measures (Sutton and Rayan, 2020; Ahmed et al., 2020)

2.3.13.4 *Wheat Straw Fibre*

Wheat straw is the byproduct of wheat crops produced after harvesting wheat plants, as shown in Figure 2.59. The worldwide production of wheat straw is estimated to be more than five hundred million tons per year. Around 50% of wheat straw is reused in soil fertilisation after harvesting, and the balance is used broadly for animal fodder, some industrial uses and mushroom growth (Tufail et al., 2021). It contains 28-40% cellulose/ hemicellulose, 20-23% moisture and 15-25% lignin/ pith/pectin with traces of ash (Hector et al., 2011). The wheat straw has four basic parameters for its categorisation for strength: maturity stage, internode levels, stem diameter, and presence of moisture. A mature wheat straw of three to four-level internode, 2-3 mm diameter with more than 20% moisture

exhibits 20-30 MPa tensile strength, 5-7 MPa shear strength, young modulus of 4.75-6.5 GPa and rigidity modulus of 260-550 MPa (Dougherty et al., 1995). These characteristics of wheat straw make it a suitable material for fibre-reinforced concrete, especially for the enhancement of tensile and flexural properties of concrete (Nadir et al., 2022a Appendix X).



Figure 2.59: Wheat Straw (Tufail et al., 2021; Nadir et al., 2022a Appendix X)

2.3.13.5 *Shredded fibres of PET*

Polyethene terephthalate (PET) bottles are widely used in domestic and industrial packing of an enormous range of products. They are found as a prominent waste in abundance, which needs recycling on a colossal scale. As per a study conducted by Hoornweg and Bhada (2012), 0.5-1-million-ton plastic waste is added daily, and 20,000 PET bottles are wasted every second in the world (Hoornweg and Bhada, 2012; Nadir et al., 2022a). Plastic, a very slowly degradable material, is always considered better to be recycled or reused instead of disposed of in landfills, sea or incinerators. The shredding of PET bottles through a suitable shredder could produce plastic fibres with appropriate dimensions (shown in Figure 2.60), which could be used in concrete as a substitute for industrially produced costly polymer fibres. The PET shredded fibres of 1-5 mm dia, 50-200 mm long, exhibit an extension capacity of 39%, a tensile strength of 190-260 MPa, a density of 1.39 g/cm³, Young's modulus of 2-2.7 GPa and modulus of elasticity of 2-4 GPa (Laville, 2019). All these mechanical

properties make it a good reinforcement material to overcome concrete's tensile/ flexural weakness (Nadir et al., 2022a).



Figure 2.60: PET Bottle Fibres Shredded Using a Paper Shredder (Nadir et al., 2022a)

2.3.14 Review of Properties/ Use of Cement, Water, Plasticiser and Aggregates

In this project, OPC white cement CEM1 52.5 was used in conformance to BS EN 197-1 (BS 197-1, 2011), composing CaO (67.1%), SiO₂ (25.2%) and Al₂O₃ (3.18%) as shown in Table 2.7. Cement is an anhydrous material requiring a sufficient quantity of water for the hydration reaction to produce calcium-silicate-hydrates (C-S-H gel) responsible for the strength of cement concrete, as shown in the equations 16 and 17 (Nadir and Ahmed, 2022a). Regular tap water in the UK could be used for cement hydration in conformance with BS EN 1008:2002, with a consistent water/ cement ratio (BS 1008, 2002) as per Abrams's law (Jain, 2020). A suitable quantity of carboxylate polymer-based plasticiser could be used to obtain the workable consistency of the composites with a target slump S1 (10-40mm) (Oscrite Alphaflow, 2014). The angular/ crushed/ shredded stone coarse aggregate passing a 20 mm sieve and fine aggregate (river sand) passing a 4.75 mm sieve could be used as suitable virgin aggregates in conformance with BS EN 12620/2013 (BS 12620, 2013; Nadir and Ahmed, 2022a).

2.4 Durability Testing of Composites Against Sulphate Attack

The exposure of engineering structures to complex chemical hazards in omnifarious geographical/ environmental locations and emission of greenhouse gases from manufacturing and usage of cement have encouraged researchers to explore the chemical synthesis taking place in the blending of different raw materials, formation of complex compounds, hydration of cement concrete and reactions taking place during internal/ external sulphate attacks. This study has carried out an in-depth elucidation of the contemporary research to understand better the raw material composition of cement-like calcareous and argillaceous minerals, the hydration process, the reaction of complex compounds to create cement paste, kinetics associated with the formation of ettringite, monosulphate aluminate ferrate hydrates, exchange of cations and anions between reactive metals hydroxide, hydrates, sulphates and their impacts on long term sustainability properties of concrete. An endeavour was made to explore using lime and pozzolans derived from industrial, agricultural, and natural resources. The microstructural studies were examined, which augmented the research findings that the development of cracks/ failure in concrete is attributed to the formation of ettringite, gypsum, brucite, magnesium silicate hydrate (M-S-H) gel, thaumasite, portlandite, expansive silica hydroxide gel and carbonation of metal hydroxides due to internal/ external sulphate attacks on samples having more water-cement ratio and exposed to more concentrated magnesium/ sodium sulphate solutions (Nadir and Ahmed 2022b; 2022c Appendix V, VI). The human's desire to conquer oceans, rivers, plains, mountains and deserts has led to the construction of diverse infrastructure in different environments, thus giving rise not only to disturbance to the natural environment but equally causing hazards to infrastructure from the environment too in the form of deterioration/ depletion due to ageing, spalling, thawing, corrosion, erosion, temperature variation, chemicals attacks, ingress of moisture/ acidic/ alkaline solutions and different atmospheric conditions (Nadir and Ahmed, 2020). Historically, building materials like stone, clay, lime, pozzolanic binders, and modern-day cement-

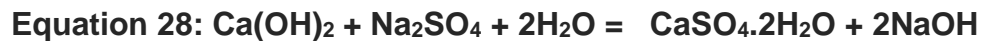
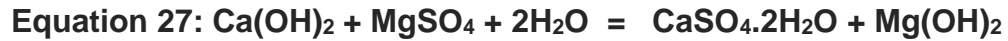
based ingredients were in inventory for various construction requirements. One of the most widely used materials in modern construction is concrete, which is preferred due to its mechanical properties and ease of use (Rehan and Nehdi, 2005; Britannica, 2020). The variation in the composition/ performance of cement concrete in different climatic conditions is its vulnerability against external/ internal chemical attacks, especially sulphate attacks, over an extended exposure period with an increased presence of sulphate to aluminosilicate molar ratio in concrete more than 0.8 making it more susceptible to deterioration within a few years (Worrell et al., 2001; Rehan and Nehdi, 2005; Mulongo and Eklou, 2013a and 2013b; Rajkumar, 2017; Timperley, 2018; Britannica, 2020; Vashisht and Paliwal, 2020; Ahmed et al., 2020). These phenomenal concrete vulnerabilities have encouraged researchers to study chemical synthesis igniting the sulphate attack and formulate composite sustainable materials (Akca, Kakar and Pek, 2015; Nadir and Ahmed, 2021b). This research reviews contemporary research conducted on cement composition, chemical reactions, hydration process, chemical-mechanical kinetics and microstructural synthesis during sulphate attack (Nadir and Ahmed 2022b; 2022c). The well-known weakness of cement concrete against external/internal sulphate attack and an estimated 10% global greenhouse gas emission by the construction industry (contributed by cement manufacturing/ supply/ hydration) have encouraged researchers to elucidate the chemical synthesis taking place in the preparation and hydration of cement concrete along with the factors affecting the sustainability of hardened concrete. In this study, an endeavour was made to explore the use of supplementary cementitious materials (SCMs) of different hydrocarbon compositions, including organic/ inorganic compounds like pozzolans derived from natural (zeolite/ metakaolin derived from kaolinite), agricultural (rice husk ash, corn cob ash) and industrial fields pulverised fly ash (PFA), silica fume (SF) and a renowned cement replacement material, i.e., ground granulated blast furnace slag (GGBS). The partial replacement of 0-30% pozzolans with cement as a binder was reviewed objectively to achieve economic/ environmental

benefits by enhancing strength and durability against dangerous sulphate attacks. The research elucidates an improvement in strength to optimum ratios of up to 10-60% for different SCMs. However, the strength was observed to reduce beyond the optimum ratio of different SCMs' blending due to the formation of expansive alkaline silica hydroxide gel, which causes cracking/ weakness of structure. The construction industry is considered a major emitter of CO₂; therefore, the supportive optimum use of SCMs could effectively reduce CO₂ emissions. Microstructural studies using scanning electron microscopy (SEM) and X-ray diffraction (XRD) have also been explored. These microstructural studies have further clarified the development of ettringite in concrete after sulphate attack and the beneficial use of pozzolans to a certain optimum extent to prevent the formation/ propagation of ettringite-specific cracks in the micro/ nano-pores of concrete structures (Nadir and Ahmed 2022b; 2022c).

2.4.1 The Synthesis of External/ Internal Sulphate Attacks

The synthesis of cement composition and hydration process in earlier sections explains that the formation of ettringite inside the cement paste by gypsum mixed with clinker causes internal sulphate attack due to its rod-type long crystals that form cracks and propagate a weaker plane throughout the length of damage over an extended period (Cefis and Claudia, 2017). However, the formation of monosulphate aluminate hydrates prevents more ettringite formation and internal cracking. Later, cement concrete is exposed to sodium or magnesium sulphate (Na₂SO₄/ MgSO₄) by introducing a sulphate solution through the concrete surface (Lei et al., 2013). This monosulphate aluminium hydrate reacts with sulphate ions, and an exchange of cations occurs. It forms ettringite again and exchanges cations and anions to produce CaSO₄ (gypsum), brucite Mg(OH)₂ and NaOH (Neville, 2004; Cefis and Claudia, 2017). A sodium sulphate attack is an expansive reaction that expands the outer surface, resulting in cracks and swelling (Collepardi, 2003; Neville, 2004,40). However, the attack of magnesium sulphate is described as a strength-reducing attack due to internal crack formation by ettringite crystals (Neville, 2004; Civil Giant, 2022b). The cations

Mg⁺⁺/ Na⁺ and Ca⁺⁺ exchange, and the anions SO₄⁻ and OH⁻ exchange. The sulphate ion SO₄⁻ from magnesium/ sodium sulphate transfers inwards to form gypsum CaSO₄, whereas the OH⁻ ion from Ca(OH)₂ exchanges outward to form brucite Mg(OH)₂ or NaOH (equation 27,28) (Marchand, Older and Skalny, 2003; Tixier and Mobasher, 2003; Idiart, Lopez and Carol, 2011; Ahmed and Kamau, 2017; Nadir and Ahmed, 2022b Appendix V).



The gypsum and brucite produced during external MgSO₄ attacks initially make a membrane around concrete ingredients to save from sulphate attacks (Stutzman, Bullard and Feng 2016). However, later, the presence of gypsum initiates the formation of ettringite by reacting with monosulphate aluminium hydrate, which causes peeling off this membrane and propagates inwards, cracking inside the concrete mass (equation 29) (www.engr.psu.edu, 2023; Eldidamony et al., 2012).



The diffusion/ exchange of Mg⁺⁺ cation with Ca⁺⁺ of calcium silicate hydrates (C-S-H gel) forms magnesium silicate hydrates (M-S-H gel) (Stutzman, Bullard and Feng 2016). M-S-H gel does not possess any strength or binding properties. It causes a reduction in the compressive strength of concrete by reducing intra-ingredient binding (equation 30) (Zhang, Vandeperre and Cheeseman, 2014).



The decrease in intra-ingredients binding and formation/ propagation of cracks by ettringite long needles like crystals let the sulphate diffuse deep inside and slowly/ gradually spread this sulphate attack in all dimensions of concrete mass,

failing/ collapsing the total concrete structure (www.engr.psu.edu, 2023). The increased presence of Ca^{++} highly influences the typical internal sulphate attack $(\text{OH})_2$ (Show, 2020), tricalcium aluminates C_3A (celite) (Eldidamony, 2012), monosulphate aluminate hydrate ($3\text{C}_4\text{ASH}_{18}$) (Zhang, Vandeperre and Cheeseman, 2014), which contains a single molar SO_3 (Civil Giant, 2020), and converts readily to ettringite on the formation of gypsum during sulphate attack (Nadir and Ahmed 2022b; 2022c Appendix V, VI).

2.4.2 Types/ Causes of Sulphate Attacks

The sulphate attack on cement concrete comprises two main internal and external sulphate attack categories. The internal attack is due to the formation of ettringite by the reaction of gypsum used in cement manufacturing to prevent premature/ flash setting due to C_3A (www.engr.psu.edu, 2023). However, the ettringite produced is converted into lightweight monosulphate aluminate hydrate after reaction with C_3A . This sulphate-deficient molecule is 2.5 times smaller (Civil Giant, 2020b). It gives protection against any damage and further chemical attack till the ingress of sulphate solution in hardened concrete in the form of an external sulphate attack from any external source (Eldidamony et al., 2012). After that, it swells 2.5 times on gaining sulphate exposure by converting into ettringite crystals, resulting in cracking/ expansion (Bhi, 2016; Civil Giant, 2020b). The external sulphate attack transforms monosulphate aluminate hydrate into long ettringite, needle-like crystals, creating cracking inside hardened concrete [50]. In contrast, the formation of micro-ettringite crystals in voids causes structures to expand (Yuan et al., 2021). The magnesium sulphate attack produces gypsum and crumbly fibrous magnesium-silicate-hydrates gel, which has no strength and generates the final collapse of the structure (www.engr.psu.edu, 2023; Panesar, 2016; Civil Giant, 2020b; Yuan et al., 2021; (Nadir and Ahmed 2022b; 2022c Appendix V, VI).

2.4.3 Sources of Sulphate Attack

The external source could be soil containing calcium/ magnesium/ sodium/ potassium/ ammonium sulphates (Civil Giant, 2022b). However, solid sulphates cannot harm hardened concrete (www.engr.psu.edu, 2023). When these minerals are mixed with rain/ drainage water and pass through the soil as groundwater, they dissolve minerals and contain aqueous sulphate. This water attacks the surface and could ingress into the hardened concrete/ mortar structure through osmosis using voids (Technology, 2010). The bacterial action to decay organic matter in shallow lakes and marshes produces H_2S , which is converted into H_2SO_4 and causes an acid/ sulphate attack (Estokov, 2012). Agricultural soil fertilisers give rise to ammonium sulphate, which could be transported with surface drainage into sub-soil groundwater (Beddoe and Dorner, 2005). Sea water also contains sulphate minerals and chlorides and could badly result in sulphate/ chloride attacks (Breysse, 2010; Santhanam and Oteino, 2016; Dezhampanah et al., 2020). The water from cooling towers, sewers, acid rains, and poor chemical waste disposal could result in aqueous sulphates in soil and groundwater (Nadir and Ahmed 2022b; 2022c Appendix V, VI).

2.4.4 Factors and Prevention of Sulphate Attack

The severity of sulphate attack depends upon the quality/ ingredients of cement (www.engr.psu.edu, 2023), water/ cement ratio (Stutzman, Bullard and Feng 2016), permeability/ voids (Civil Giant, 2022b), the concentration/ replenishment of sulphate solution (Breysse, 2010), alternate wetting/ drying (Santhanam and Oteino, 2016), period of exposure (Civil Giant, 2022b) compaction (Santhanam and Oteino, 2016), air entrainment (Civil Giant, 2022b). The presence of more C_3S and less C_3A causes vulnerability to sulphate attack. Therefore, reduced C_3S and increased C_3A with rich cement ratios are recommended in sulphate-resistant cement [60]. Air entrainment in concrete could improve workability and reduce segregation, an excellent preventive measure for sulphate attacks (Civil Giant, 2022b). However, lowering C_3S could decrease strength as it is

responsible for a 60% gain of early strength, and an increase in C_3A could result in the flash setting of cement (www.engr.psu.edu, 2023). Similarly, more than 5-6% of air entrainment could cause permeable/ previous structures with lower strength due to the induction of more voids (Civil Giant, 2022b). Therefore, the total percentage of C_3S/C_2S should not be less than 50%, C_3A and C_4AF should not be increased by more than 20%, and air entrainment agents should not be used more than 1% to prevent the formation of more than 6% voids (Civil Giant, 2021). High/ super sulphate resistance cement containing more C_3A is highly recommended in a rich sulphate environment (The Constructor, 2016). A water-cement ratio (w/c) lower than 0.45 is recommended, and no sulphate attacks were observed on a w/c ratio lower than/ equal to 0.35 (Stutzman, Bullard and Feng 2016; Civil Giant, 2022b). Therefore w/c ratio should be kept at 0.35-0.45. Continuous wetting/ drying mechanisms should be avoided. Still, suppose it is unavoidable, like structures in the sea/ rivers. In that case, the coating of bituminous materials (Singh, Singh and Siddique, 2022), chlorinated rubber (Tixier and Mobashar, 2003), epoxy or polyurethane (Civil Giant, 2022b), use of polyethylene or polychloroprene lining or acrylic coating are recommended, or the use of super sulphate resistance cement is recommended (The Constructor, 2016; Creasey and Ekolu et al., 2017). The efforts should either reduce or stop the increase in the concentration of sulphate solution or its replenishment by terminating the source of sulphate ingress (Sara et al., 2020; Nadir and Ahmed 2022b; 2022c Appendix V, VI).

2.4.5 Use of High Sulphate Resistance Cement

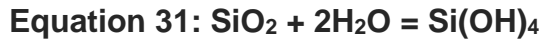
High sulphate resistance cement is recommended if construction is undertaken in a rich sulphate environment like bridges/ piers in sea/ rivers/ coastal areas where alternate wetting/ drying is a pronounced phenomenon (Civil Giant, 2022b; Stutzman, Bullard and Feng 2016). The high sulphate resistance cement is type 1 cement as per ASTM 150-C:22 and is manufactured under BS 4027-1980 and BS 12-1996, IS 12330-1988 and EN 197-1/2000 (SRC, 2022). It contains C_3S 40-50%, C_2S 20-25%, C_3A 5-6% and C_4AF 10-15%. Sulphate

contents are limited to 3%, MgO to 4%, CaO around 60%, Al_2O_3 5%, Si_2O_3 around 20% and lime saturation factor should be 0.6-1% (SRC, 2022). It produces low heat of hydration and decreases the vulnerability of concrete structures against sulphate attacks in coastal, underwater, underground, sewerage, petrochemical, marshal areas, canal lining, prone to sulphate-rich alkaline environments not suitable against chloride attack and not very feasible being a costly option (www.engr.psu.edu, 2023; Ideker and Thomas, 2015; ASTM 150-C, 2022; Civil Giant, 2022b; SRC, 2022; Nadir and Ahmed 2022b; 2022c Appendix V, VI).

2.4.6 Chemical Synthesis of Use of Pozzolans as Partial SCMs in Cement Concrete

Research has focussed on devising composites containing cement, lime (Sotiriadis, Nikolopoulou and Tsivilis, 2012), and SCMs like industrial/ agricultural pozzolanic materials like pulverised fly ash (PFA), ground granulated blast furnace slag (GGBS) (Ahmed and Kamau, 2017), rice husk ash (RHA), palm ash (PA), corn cob ash (CCA) (Kamau et al., 2016), metakaolin (MK) (Kavitha et al., 2016), zeolite (Najimi et al., 2012) and silica fume (SF) (Divya, Rafat and Kunal, 2015). These materials react with $\text{Ca}(\text{OH})_2$ to produce more C-S-H gel and lesser gypsum during sulphate reaction by absorbing portlandite due to the high presence of silicates in their composition (equation 26) (Nadir and Ahmed, 2021b Appendix VII; Nadir and Ahmed 2022b; 2022c Appendix V, VI). However, excess use of pozzolans results in alkaline silica gel $\text{CaO} \cdot \text{Si}(\text{OH})_4$ formation (calcium-silica-hydroxide gel) in the reaction between excess silicate ions SiO^- from SiO_2 (a significant component of pozzolanic materials) and OH^- from portlandite along with the formation of C-S-H gel. The researchers have suggested different optimum quantities of mixing pozzolans and cement replacement materials, e.g., up to 70% GGBS (Ahmed and Kamau, 2017), 20% MK (Kavitha et al., 2016), 40% PFA (Ahmed and Kamau, 2017) and 15% SF (Kavitha et al., 2016). Pozzolans with OPC are considered economically viable and environmentally friendly materials (Nadir and Ahmed, 2021b). The alkaline silica gel does not

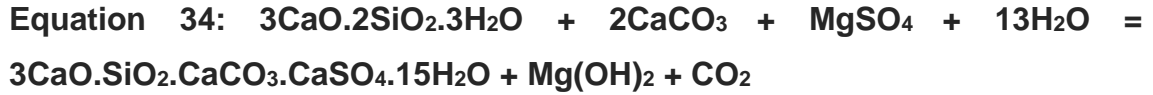
contribute to strength but somewhat weakens hardened concrete by creating cracks on swelling (equation 26. Excess SiO_2 also reacts with water to convert to silica hydroxide but remains in the pores as an aqueous solution till it further reacts with portlandite (equation 31,32). This alkaline silica gel is formed in four steps: SiO_2 (solid), SiO_2 (aqueous), SiO_2 (solution), and swelling SiO_2 (gel), as shown in equation 33 (Powers and Steinour, 1995; Ideker and Thomas, 2015). Therefore, pozzolanic materials contribute to the strength of SCMs to a specific mixing ratio, beyond which they would likely start to weaken the hardened concrete (Nadir and Ahmed 2022b; 2022c Appendix V, VI).



2.4.7 Microstructural Analysis of OPC-Based Pozzolanic Composites

2.4.7.1 Microstructural Analysis of OPC and OPC- Lime Composites

Sotiriadis et al. (2012) studied using an additional 15% and 35% lime with cement clinker to determine the performance of lime-based concrete against sulphate attack. Lime is the main ingredient in cement manufacturing (62%) and is responsible for supplying CaO and Ca(OH)_2 in cement hydration to form C-S-H gel (Sotiriadis, Nikolopoulou and Tsivilis, 2012). However, increased mixing of lime in OPC produces an additional quantity of Ca(OH)_2 and thaumasite ($3\text{CaO}.2\text{SiO}_2.\text{CaCO}_3.\text{CaSO}_4.15\text{H}_2\text{O}$) during sulphate attack at low temperatures ($\leq 5^\circ\text{C}$). Ca(OH)_2 creates an alkaline environment and readily converts to crumbling gypsum on cationic exchange with MgSO_4 , as shown in equations 27 and 28. Thaumasite is produced by the reaction of C-S-H gel with lime under sulphate attack at low temperatures, as shown in equation 34 (Wang, Cai and Wu, 2018; Nadir and Ahmed, 2022b; 2022c).



Thaumasite is a complex combination of C-S-H gel with carbonates and sulphate ions bonded with calcium obtained either from additional lime or calcareous sand in concrete at low temperature after the formation of ettringite when presumably aluminates were consumed by an initial/ internal sulphate attack. Thaumasite has no strength value and rapidly converts concrete into fragile mush and is badly augmented by the formation of magnesium silicate hydrate (M-S-H) gel, brucite and gypsum (Sotiriadis, Nikolopoulou and Tsivilis, 2012; SRC, 2022; Nadir and Ahmed 2022b; 2022c). Sotiriadis et al. (2012) conducted a study on mixing additional lime with OPC with a w/b ratio of 0.52, making 15% mix (LC1) and 35% mix (LC2). A considerable decrease was observed in compressive strength with increased lime contents (Figure 2.61). They observed a greater degree of surface deterioration in 15% and 35% lime composite over 24 months of immersion in water, 2.5% NaCl+, 2.5% MgSO₄ Solution and 5% MgSO₄ solutions. The concentrated sulphate solution caused extensive surface damage to cubes of 35% lime, as shown in Figures 2.62 and 2.63, compared to the chloride-sulphate solution because the chloride solution dissolves ettringite three times faster. Thus, less C₃A could react with sulphates (Sotiriadis, Nikolopoulou and Tsivilis, 2012; Nadir and Ahmed 2022b; 2022c Appendix V, VI).

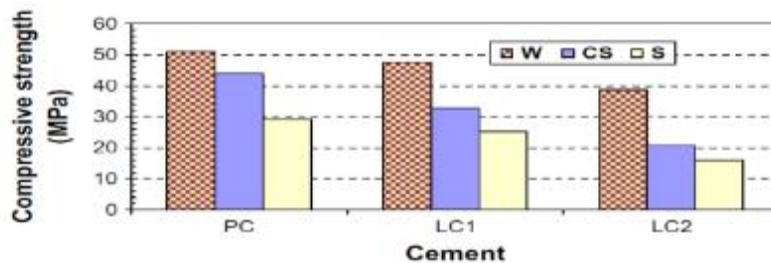


Figure 2.60: Compressive strength of 15% and 35% lime-based concrete cubes immersed in the sulphate solution (Sotiriadis, Nikolopoulou and Tsivilis, 2012)

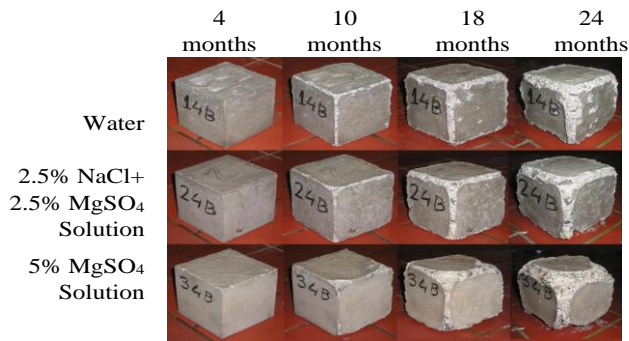


Figure 2.61: Surface deterioration of 15% lime-based concrete cubes immersed in the water and sulphate solution (Sotiriadis, Nikolopoulou and Tsivilis, 2012)

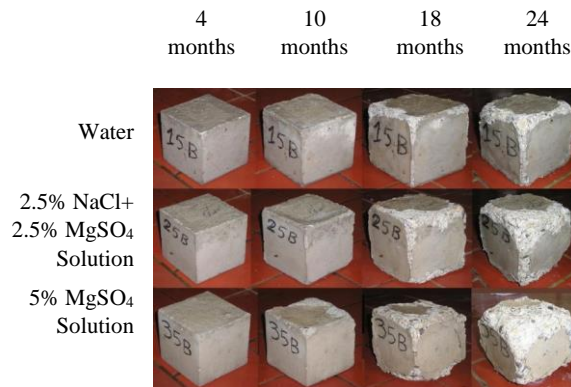


Figure 2.62: Surface deterioration of 35% lime-based concrete cubes immersed in the water and sulphate solution (Sotiriadis, Nikolopoulou and Tsivilis, 2012).

The microstructural studies using XRD showed that the cement concrete containing 35% lime produced more thaumasite, secondary ettringite, gypsum and brucite in sulphate solution at 5°C, followed by samples with 15%, and no thaumasite was observed in OPC samples at nine months and 18 months. As a result, concrete deterioration was observed more in samples with more lime contents, and sulphate attack by MgSO_4 solution was more severe than $\text{NaCl}+\text{MgSO}_4$ solution, as shown in Figures 2.64 and 2.65 (Sotiriadis, Nikolopoulou and Tsivilis, 2012; (Nadir and Ahmed 2022b; 2022c).

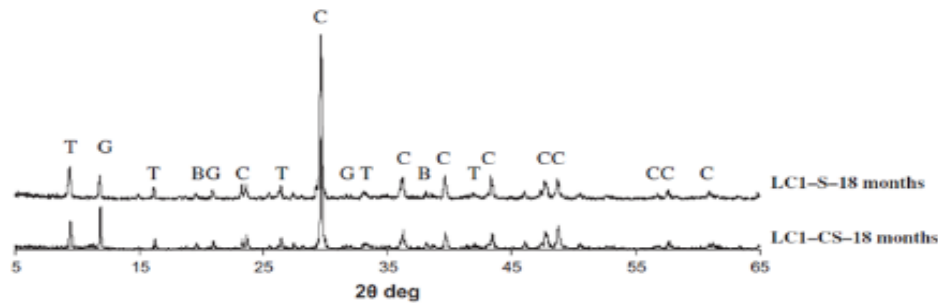


Figure 2.63: XRD study of 15% lime samples in MgSO_4 and $\text{NaCl}+\text{MgSO}_4$ solutions after 18 months

(T: thaumasite, c: calcite, BG: brucite gypsum, CC: calcium chloride, B: brucite, G: gypsum) (Sotiriadis, Nikolopoulou and Tsivilis, 2012)

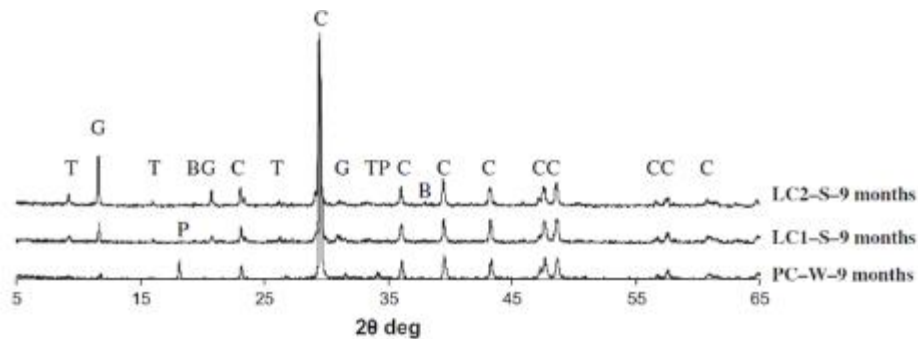


Figure 2.64: XRD study of 15% 35% lime samples in water MgSO_4 and $\text{NaCl}+\text{MgSO}_4$ solutions after nine months (Sotiriadis, Nikolopoulou and Tsivilis, 2012)

Liu et al. (2015) conducted a microstructural and qualitative analysis of OPC paste cubes of 20 mm by placing them in water (reference readings) 0.03 mole/l (0.5% by weight) and 0.35 mole/l (5% by weight) Na_2SO_4 solution for up to 900 days. They studied the cubes for surface deterioration and crack propagation on 90, 180, 300, 600 and 900 days. The lightly concentrated 0.5% Na_2SO_4 inflicted slight cracking on edges after 180 days and slight spalling of cubes was observed after 900 days. However, the cubes placed in 5% Na_2SO_4 solution started to crack considerably on the edges after 90 days, which was found to spread to the

surface of the cubes after 180 days. The ingress of Na_2SO_4 solution into the inner body of cubes started after 300 days, and considerable peeling and spalling were observed in the cubes due to the formation of gypsum in the veins. After 600 days, significant spalling and peeling of the outer layer were observed due to expansion caused by the development of long ettringite needle crystals inside the outer and inner cores of cubes and the decalcification of C-S-H gel. After 900 days, the complete outer layer was peeling; cubes started bulging due to expansion/ spalling and loss in mass was observed, showing a significant impact of sulphate attack on cement paste cubes as shown in Figure 2.66 (Liu et al., 2015). A reduction of 64% compressive strength (from 70 MPa to 25 MPa) and 3% mass loss were observed in 5% Na_2SO_4 after 900 days, as shown in Figures 2.67 and 2.68 (Liu et al., 2015; Nadir and Ahmed 2022c Appendix VI). Liu et al. (2015) conducted a microstructural analysis on these cubes to assess the ingress of sulphate solution, propagation of cracks, development of gypsum and ettringite crystals in the cubes and peeling off surface/ loss of mass due to sulphate attack after 900 days. Scanning electron microscopy (SEM) was done after 600 and 900 days on the surface (Figure 2.69 a) and 1 mm under the surface (Figure 2.69 b). The sulphate attack was described as impacting the cubes in four stages. In the first stage, sulphate ions penetrate the surface, react with Ca^{++} and OH^- ions, and form monosulphate. In the second stage, decalcification of C-S-H gel starts, and CaSO_4 is produced in the veins/ cracks. In the third stage, cracks propagate, and gypsum is depleted by converting C-S-H gel into ettringite. In the fourth stage, the sulphate ions keep consuming the Ca^{++} from C-S-H gel and convert it into mushy Na-S-H gel with no strength, ultimately resulting in spalling, peeling, loss of mass and reduction in strength. The concentration of sulphate solution, permeability, exposure period, and cement composition influence the degree of sulphate attack/ deterioration (Liu et al., 2015; Nadir and Ahmed, 2022c Appendix VI).



Figure 2.65: Qualitative Analysis of OPC cubes in 0.5% and 5% Na_2SO_4 solution after 900 days (Liu et al., 2015).

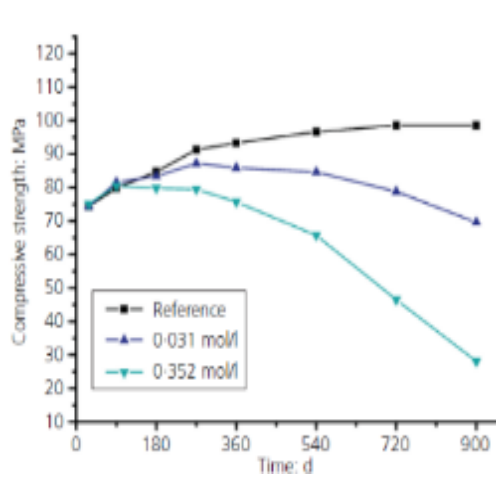


Figure 2.66: Reduction in compressive strength of OPC cubes in sulphate solution (Liu et al., 2015)

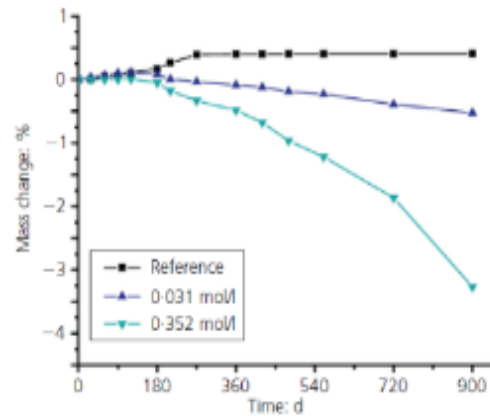
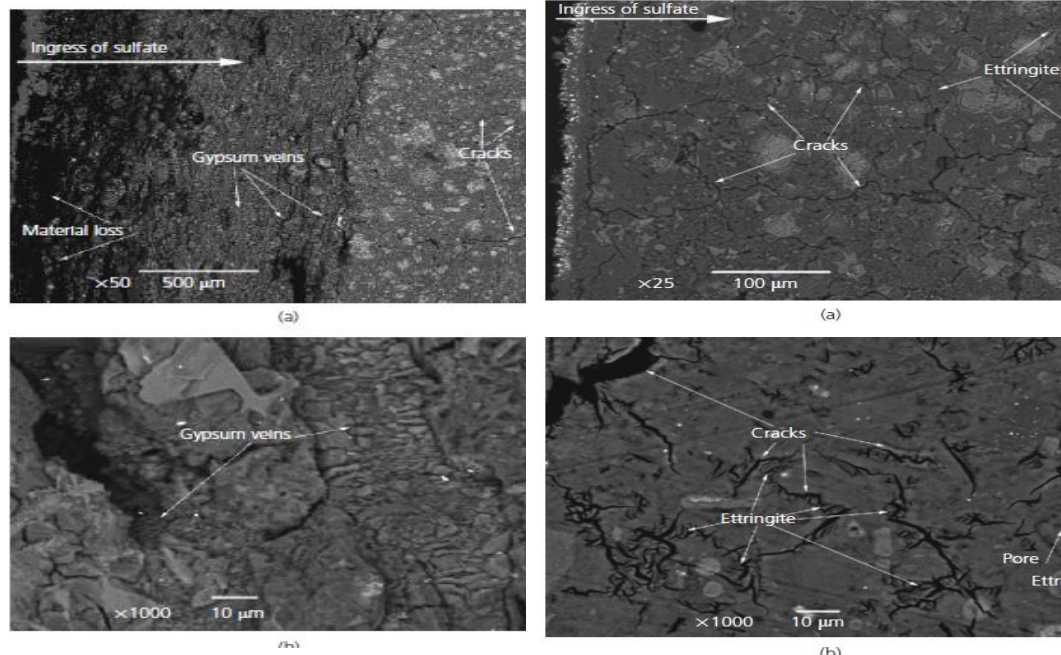


Figure 2.67: Reduction in the mass of OPC cubes in sulphate solution (Liu et



Microstructural Analysis of OPC cubes in 5% Na_2SO_4 solution after 600

Microstructural Analysis of OPC cubes in 5% Na_2SO_4 solution after 900 days

Figure 2.68: Microstructural Analysis of OPC cubes by SEM in 5% Na_2SO_4 solution after 600 and 900 days (Liu et al., 2015).

2.4.7.2 Use of Pozzolans as Partial SCMs in Cement Concrete for Prevention of Sulphate Attack

Kamau and Ahmed (2017), in their studies on the assessment of the impact of sulphate attack on binary concrete and ternary concrete using PFA, GGBS, and PFA/GGBS mixes as SCMs with OPC in 5% sodium sulphate, 5% magnesium sulphate and 2.5% sodium/ 2.5% magnesium sulphate solution for 270 days immersion, observed that ternary concrete mixes with up to 30% PFA+GGBS exhibited good performance as compared to individual/ binary composites of OPC with PFA and GGBS (Kamau and Ahmed, 2017). They observed that maximum compressive strength was achieved with 5% PFA, 15 % GGBS binary blends, and 3.75% PFA+3.75% GGBS ternary blend. However, the complete replacement of 30 % SCMs also gave some advantages, e.g., good resistance

against sulphate attack, less permeability and water absorption compared to the control mix. Still, the disadvantage is a reduction in compressive strength. Visual observations showed the worst degradation with 30% PFA followed by 30% GGBS, whereas the ternary blend of 30% PFA/GGBS showed minimum degradation. The maximum degradation was infused with a mixed solution of 2.5% sodium/ 2.5% magnesium sulphate, followed by 5% magnesium sulphate and 5% sodium sulphate. The sulphate attack by sodium sulphate is characterised by elongation, whereas loss of strength is pronounced more in MgSO_4 and $\text{Na}_2\text{SO}_4 + \text{MgSO}_4$ (Kamau and Ahmed, 2017). The binary PFA and GGBS mixes with maximum compressive strength exhibited the lowest elongation, whereas the ternary blend showed maximum extension. However, the ternary mixture exhibited higher performance against sulphate attack in 5% magnesium sulphate, 2.5% sodium and 2.5% magnesium sulphate solution (Figure 2.70). The reduced elongation in SCM mixes is due to the pozzolans' pore-filling capability, which prevents the formation of secondary ettringite and deep propagation of cracks/ expansion. Mixing SCMs up to 30% reduced alite and celite, resulting in reduced production of portlandite, ettringite and monosulphate aluminates with SO_3 , thus reducing the vulnerability of concrete composites against sulphate attacks (Kamau and Ahmed, 2017; Nadir and Ahmed 2022c Appendix VI). Ahmed et al. (2008) used 0 % (control mix), 10%, 15% and 25% SF with class I and class V cement (350 kg/m^3 and 450 kg/m^3) with 0.4 and 0.5 w/c ratios. They elucidated that 10% SF used with OPC 450 kg/m^3 and 0.4 w/c ratios exhibited the best performance when subjected to a concentrated sulphate attack of 5% MgSO_4 for 224 and 700 days, as shown in Figure 2.71 (Ahmed et al., 2008). The research on existing literature supports the use of pozzolans in cement concrete and geopolymer concrete for enhancement of mechanical properties and resistance of composites against sulphate attack due to absorption of portlandite, production of more C-S-H gel and filling of voids to prevent the propagation of cracks and formation of ettringite (Nadir and Ahmed 2022c).

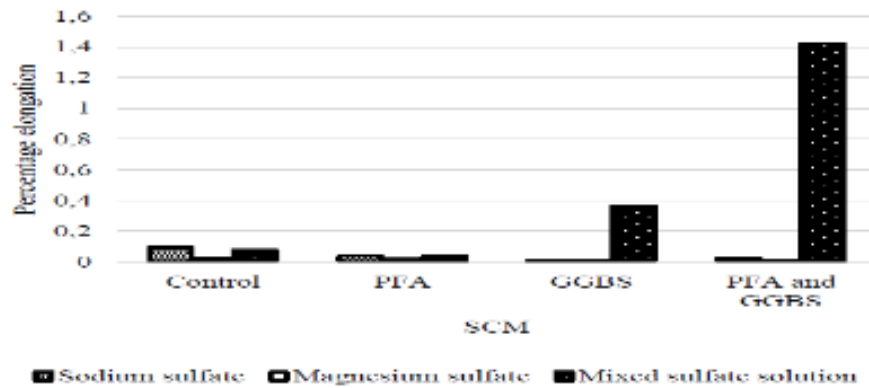
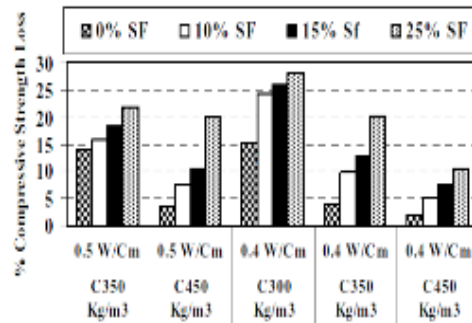
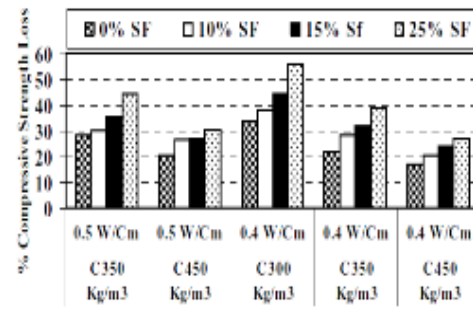


Figure 2.69: Percentage elongation of mixes with max replacement @ 30% PFA, 30% GGBS and 30% PFA+GGBS (Kamau and Ahmed, 2017).

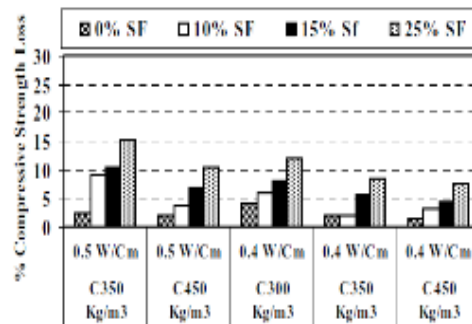
Kavitha et al. (2016) used metakaolin (MK) as pozzolan in cement concrete composite. They observed that an optimum value of 10% MK in OPC exhibited higher resistance against sulphate and chloride attacks. The use of 10-15% MK exhibited up to 15% reduction in the emission of CO₂ (Cassagnabère et al., 2010), and 5% MK improved compressive strength by 10%. The compressive strength was reduced with increased use of metakaolin up to 10% and 15% MK; water absorption was observed maximum in the control mix with 0% MK and minimum in MK10%. The durability testing after 15 weeks of immersion in 5% MgSO₄ solution exhibited a maximum reduction in compressive strength in control samples (MK 0%), whereas 10% MK performed the best with minimum reduction in strength and minimum water absorption in sulphate solution (Figure 2.72). The microstructural investigation using SEM (Figure 2.73) supported the findings by showing improvement in the pore structure due to pozzolanic filler capability and reduction in the formation of ettringite, thaumasite, gypsum and brucite (resultant products due to sulphate attack) in MK10% mix as compared to MK 0% (Kavitha et al., 2016; Nadir and Ahmed 2022c Appendix VI).



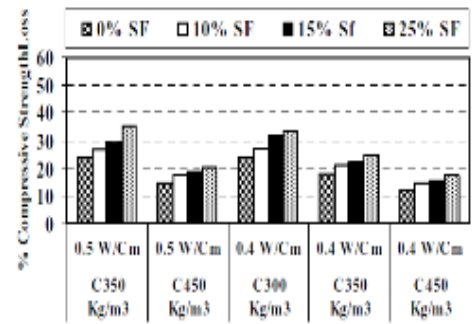
2-a Compressive strength after 224 days, Type I Cement



2-b Compressive strength after 700 days, Type I cement



2-c Compressive strength after 224 days, Type V Cement



2-d Compressive strength after 700 days, Type V Cement

Figure 2.70: Compressive strength loss after sulphate attack of 224 and 700 days (Ahmed et al., 2008).

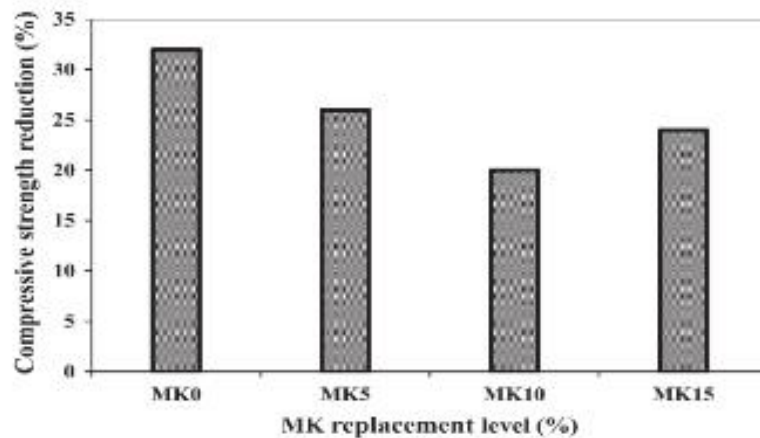


Figure 2.71: Reduction in compressive strength after 15 weeks of immersion in 5% MgSO₄ solution (Kavitha et al., 2016).

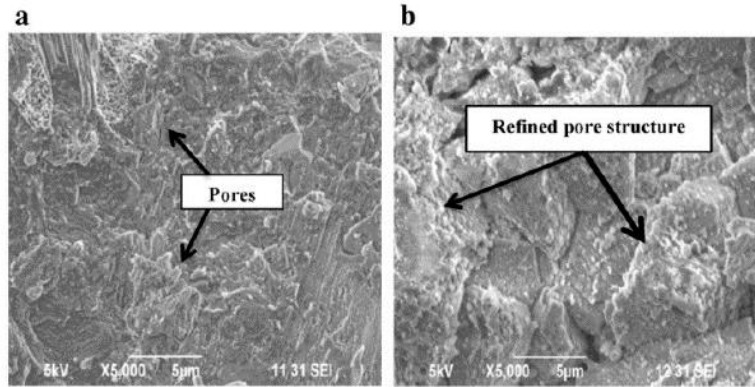


Figure 2.72: SEM images showing improvement in pore structure due to MK10% (b) filler capability (Kavitha et al., 2016).

2.4.7.3 Applications of Agriculture-Based Pozzolans like RHA and CCA

Divya et al. (2015), in their study on rice husk ash (RHA), blended 0-20% RHA with OPC as SCM and observed an increase of 25-36% in compressive strength and split tensile strength with 15% RHA at 7, 28 and 56 days of curing (Figure 2.74) (Divya et al., 2015). RHA was found to be a feasible alternative pozzolan and filled the pores befittingly to reduce permeability. They performed rapid chloride permeability tests and observed that RHA reduces porosity, thus exhibiting reduced chloride permeability. The increase in strength was attributed to more formation of C-S-H gel due to pozzolanic reaction in cement concrete composites (Divya et al., 2015). They conducted the microstructural analysis of RHA mixes by SEM and observed the formation of dense C-S-H gel and improvement in void filling with the use of up to 15% RHA in concrete composites; however, due to the formation of Si(OH)_4 (because of excess SiO_2 and its hydration with portlandite in aqueous solution in pozzolanic material). C-S-H gel was observed to reduce/thin out beyond 15% use of RHA, as is evident by lower strength and decreased permeability observed with 20% use of RHA (Figure 2.75) (Divya et al., 2015; Nadir and Ahmed 2022c Appendix VI).

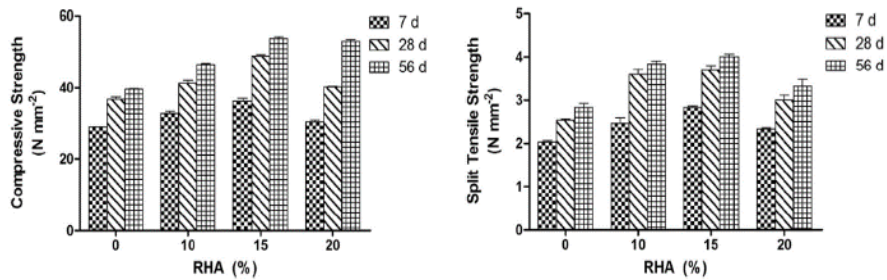


Figure 2.73: Compressive/ split tensile strength of 0-20% RHA (Divya et al., 2015).

Ahmed and Kamau (2016) used corn cob ash (CCA) as SCM in cement concrete using 0-30% replacement and suggested 7.5% as an optimum value for better compressive strength (Table 2.9). The cubes from the control mix (0% CCA) and 7.5% were immersed in 5% Na_2SO_4 , 5% MgSO_4 and 2.5% Na_2SO_4 +2.5% MgSO_4 solutions for 270 days. It was observed that the use of CCA exhibited good performance versus the control mix against all sulphate attacks in all three solutions because of the pozzolanic reaction of CCA in concrete hydration by reacting with excess $\text{Ca}(\text{OH})_2$ and forming more C-S-H gel, reduction of secondary ettringite and behaving as filler material to reduce the porosity of CCA blended concrete composite (Ahmed and Kamau, 2016). The 7.5% CCA blended mix exhibited reduced elongation in 5% Na_2SO_4 and 2.5% Na_2SO_4 +2.5% MgSO_4 solutions compared to the control mix. However, the control mix performed better in the MgSO_4 solution than the 7.5% CCA mix. It exhibited lesser elongation because the control has more compressive strength than CCA mixes. The strength deterioration factors were calculated for these samples using the formulae $\text{SDF} = ((\text{fcw}' - \text{fcs}')/\text{fcw}') \times 100$ (where fcw' is the compressive strength of control specimen cubes and fcs' is the compressive strength of sulphate immersed specimen cubes.). The control was observed to be the least impacted by sodium sulphate due to its higher compressive strength, but 7.5% CCA blended composite performed better in 5% MgSO_4 and 2.5% Na_2SO_4 +2.5% MgSO_4 , concluding that the use of CCA up to 7.5% is a feasible option against

sulphate attacks as shown in Figure 2.76 (Ahmed and Kamau, 2016; Nadir and Ahmed 2022c Appendix VI).

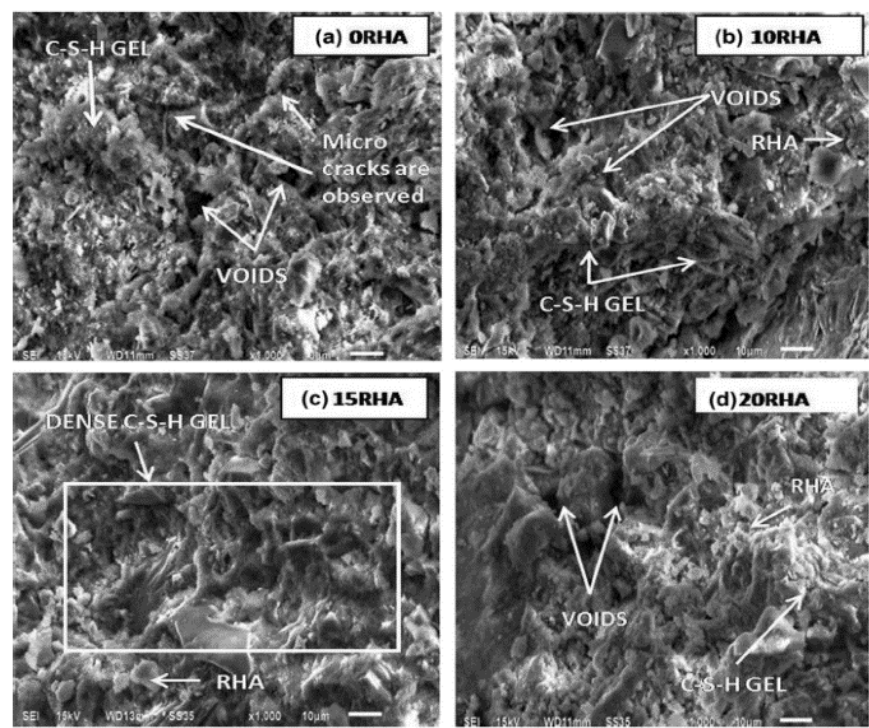


Figure 2.74: Microstructural analysis of RHA mixes by SEM (a) 0% RHA, (b) 10% RHA, (c) 15% RHA, (d) 20% RHA. The densest formation of C-S-H gel was observed with 15% RHA (c) (Divya et al., 2015).

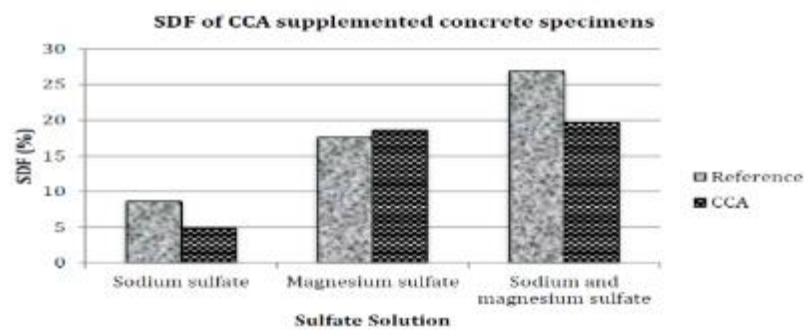


Figure 2.75: SDF of 0% and 7.5% CCA blended cement composites immersed in 5% Na₂SO₄, 5% MgSO₄ and 2.5% Na₂SO₄+2.5% MgSO₄ solutions after nine months (Ahmed and Kamau, 2016).

Table 2.9: Compressive strength of 0,5,7.5,10,15,20,25 and 30% CCA blended cement composites (Ahmed and Kamau, 2016).

Curing age (days)	Compressive strength at percentage replacement (N/mm ²)							
	Control	5%	7.50%	10%	15%	20%	25%	30%
7	56.2	42.0	42.3	32.1	28.1	19.2	16.2	15.3
28	61.6	49.0	51.3	37.9	34.3	23.5	18.9	19.3
56	67.6	51.8	54.4	43.1	38.3	25.9	23.0	22.0
90	71.3	55.9	63.5	47.8	41.5	29.8	24.0	23.5

2.4.7.4 Use of Natural Pozzolan like Zeolite

Zeolite is used effectively in the cement industry to reduce CO₂ gas emissions in developed countries. Zeolite is found naturally in volcanic and sedimentary rocks and contains hydrated aluminosilicates of alkali/ alkaline metal cations. These cations react swiftly with portlandite to form dense C-S-H gel. The three-dimensional molecular structure of zeolite makes it a suitable filler to decrease porosity and create a defence against sulphate/ chloride attack (Najimi et al., 2012). An experimental study was conducted on the durability properties of concrete containing 0, 15% and 30% zeolites as SCM with OPC. It was found that zeolite improves the mechanical and micro-structural properties of concrete. Although the compressive strength remained lower than the control mix, later curing ages showed a reduced gap in strength achievement due to a slow pozzolanic reaction. The increased quantity of zeolite improved water absorption, porosity, dry shrinkage and corrosion rate. However, enhanced resistance against sulphate attack was observed with increased zeolite use versus the control mix (Figure 2.77, 2.78) (Najimi et al., 2012). Using up to 30% of zeolite could decrease CO₂ emissions by 30% while giving compatible structural outputs at par with OPC. However, a 15% replacement ratio produces the optimum blended composite. Considering its environmental benefits and the improvements in mechanical properties of the zeolite-cement composite, it could

be recommended as a suitable pozzolanic SCM (Najimi et al., 2012; Nadir and Ahmed, 2022c).

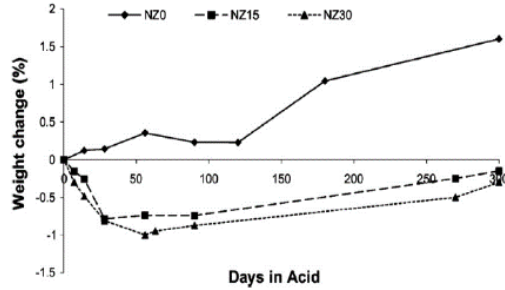


Figure 2.76: Weight changes in 0%, 15%, and 30% zeolite mixes after immersion in H_2SO_4 for 300 days (Najimi et al., 2012)

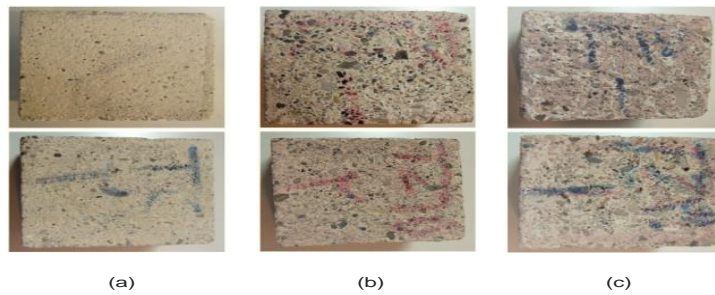


Figure 2.77: Comparison of Surface Degradation in 0% (a), 15% (b), and 30% (c) Zeolite Mixes (Najimi et al., 2012).

2.4.7.5 Application of SF, PFA and GGBS in Geopolymer-Based Concrete for Better Sulphate Resistance

The use of SF, PFA and GGBS in manufacturing geopolymer-based concrete is already in practice due to their enhanced environmental benefits. Their use as total cement replacement to produce geopolymer concrete is explained in Figure 2.79 (Skariah et al., 2022), where industrial/ agricultural/ natural pozzolans are mixed with an alkali activator with normal sand and aggregates to produce geopolymer concrete (Skariah et al., 2022).

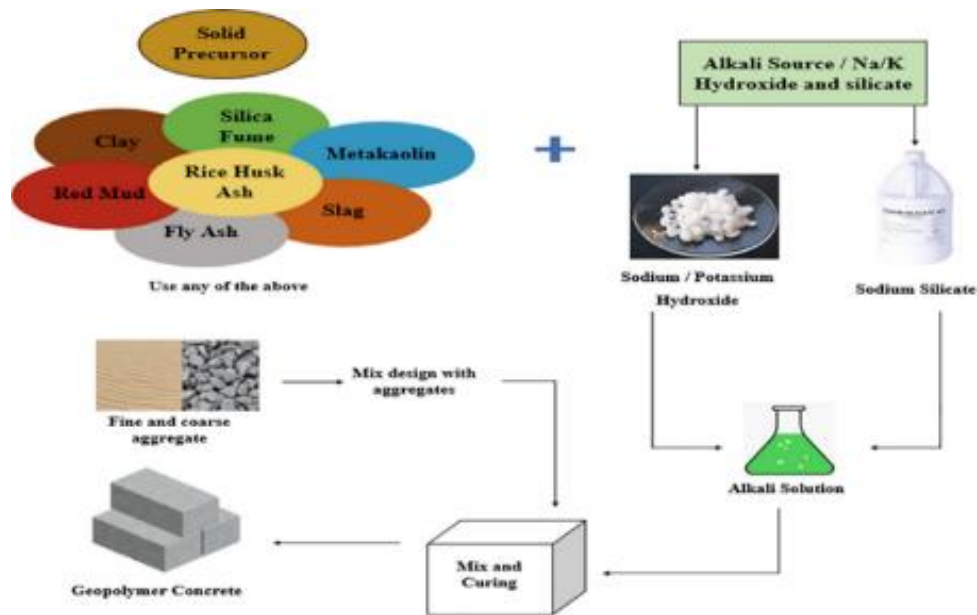


Figure 2.78: Manufacturing of Geopolymer Concrete (Skariah et al., 2022).

Jawahar et al. (2016) studied geopolymer concrete containing 100% PFA, 50% PFA+50% GGBS and 100% GGBS. They found that 100% of the GGBS geopolymer concrete was on par with the OPC concrete. They exhibited 57.6 MPa compressive strength on 28 days, followed by 50% PFA+50% GGBS composite achieving 52.5 MPa strength, and 100% PFA geopolymer provided the least compressive strength of 11 MPa as shown in Figure 2.80 (Jawahar et al., 2016). The sulphate resistance studies were conducted by immersing geopolymer concrete cubes in 3% H_2SO_4 for 28 days. The maximum loss in weight and compressive strength post-acid attack was observed in 100% PFA composite by 5.6% and 33.6%, respectively. Meanwhile, 100% GGBS geopolymer composite performed the best, with the least weight and compressive strength reduction of 1.5% and 11%, respectively, as shown in Table 2.10. The GGBS-based geopolymers exhibited a par performance with OPC concrete because GGBS is considered a suitable/complete cement replacement (Jawahar et al., 2016; Nadir and Ahmed, 2022c). Ekolu et al. (2017 and 2022) have studied the formulation of geopolymers effectively using GGBS, PFA, MK and waste pozzolanic materials using various concentrations of alkali

activators and have observed these as eco-friendly durable materials. However, an increased quantity of activators increases the ASR reaction and cracking along the cement paste/ aggregate, causing expansion/ weakness of geopolymers, emphasising careful selection of pozzolanic material and use of potassium or sodium hydroxide (KOH/ NaOH) as alkali activators (Tchadjie and Ekolu, 2017; Naghizadeh, and Ekolu, 2017; Ekolu, Tchadjie and Naghizadeh, 2022)

Table 2.10: Comparison of loss in weight and compressive strength of geopolymer concrete composites after the acid attack (Jawahar et al., 2016)

Properties		Geopolymer Composite Types		
Composites		FA100%	FA50%- GGBS50%	GGBS100%
Weight (kg)	Initial	7.3	7.73	8.09
	After acid attack	6.89	7.55	7.97
Loss of weight (%)		5.62	2.33	1.48
Compressive strength (MPa)	Initial	11.08	52.5	57.6
	After acid attack	7.35	44.61	51.24
Loss of compressive strength (%)		33.66	15.03	11.04

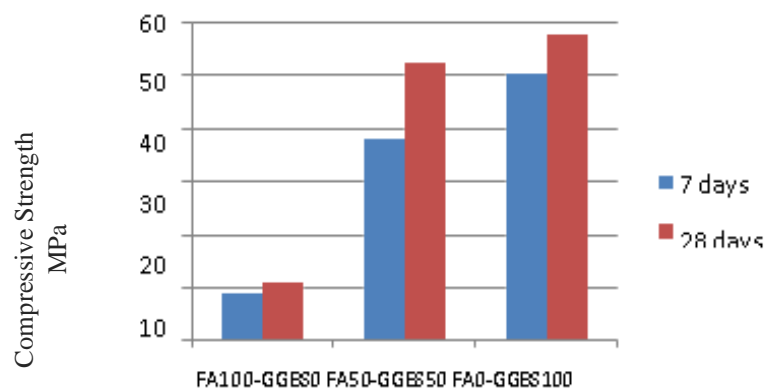


Figure 2.79: Compressive strength (MPa) 7 and 28 days (Jawahar et al., 2016).

2.5 Summary

The flood risks assessment, natural/ structural flood protection techniques, and forecasting tools were reviewed to assess the predicted rainfall/ discharge. It was observed that predicting a 10-200 years return period for rainfall/ discharge in a region/ river using Log Pearson 3 equations and statistical software like Easyfit could help in planning/ designing the channels/ drainage/ storage structures to avoid flooding. However, to avert disturbances to ecology/ environment, suitable, sustainable, greener materials should be used to merge with the natural discourse of channels for mitigating erosion/ damages by flooding. A detailed literature review on cement/ concrete elucidated its chemical synthesis and microstructural studies, especially in the case of sulphate attack. It was inferred that cement, despite its intrinsic characteristics of early setting time, ease of use and strength stipulations, is among the highest CO₂ emission materials and gets degraded/weakened on chemical attacks. This conclusion led to the study of alternative materials for total/ partial replacement with industrial/ agricultural waste materials having pozzolanic qualities to simultaneously reduce the carbon footprints of the construction industry and absorb the ever-increasing global waste as useful SCMs. A deliberate effort was made to review the established/ innovative sustainable composites like cement with lime, GGBS (a cement alternative), pozzolanic materials (PFA, SF, MK, Palm ash, rice husk ash), hydrated lime, iron powder and fibres (steel, polypropylene PPF, polyethylene terephthalate plastic PET, coconut coir, wheat straw). The embodied CO₂, carbon footprints of OPC/ various materials, chemical-mechanical synthesis of sulphate attack and use of advanced XRD/ XRF/ SEM testing in understanding the morphology/ microstructural study of materials by different researchers were explored. It was established that fibre-based pozzolan, hydrated lime, iron powder and certain waste materials could be used to formulate sustainable eco-friendly SCMs with improved engineering properties of concrete for low, Medium and high strength requirements/ hydromodifications gave impetus to conduct further PhD research.

3 Chapter 3: Methodology

3.1 Introduction

Chapter 3 briefly introduces the research methodology adopted for this research project. The details of experimental procedures, materials selection, quantities/ ratios and formulation were elaborated. Testing types, equipment, and procedures employed in this project were discussed along with the ethical approval, risk, health, and safety assessment conducted to work in the construction material laboratory, which is attached in Appendix I.

3.2 Research Methodology

The research questions framed in chapter one if agricultural/ industrial waste could be recycled into the formulation of low, medium and high-strength fibre-reinforced SCMs, carbon-neutral iron-based binary/ tertiary pozzolanic composites and cement-free limecrete to minimise environmental impacts by the construction industry, required adequate experimental work for explanation/ investigation. Therefore, to answer all the framed research questions in Chapter One, a quantitative research method was adopted to conduct a multivariate experimental study based on physical laboratory testing/ observations. Concerted efforts were made to keep the research clear, concise, logical, controllable, accurate, credible, dependable, replicable, valid, accurate, and systematic based on the characteristics reviewed in the literature review. Quantitative research is considered a broad-based, multivariate, logical observational study incorporating the “What? And What if? Synopsis,” e.g., what materials could be used? What if these materials are combined/ replaced/ substituted by other materials? The quantitative research then collaborates experimental synthesis into the observational statistics/ results, combining the sizeable number of variables and describing, explaining and predicting the path to achieve the objectives. The generalised findings/ outcome of the research

could then be applied to multi-spectrum stipulations with real-time correlation and comparison (Kothari, 2004; Apuke, 2017; Johnson and Christensen, 2020).

3.3 Selection/ Formulation of Materials

In the detailed literature review on established and innovative materials in **Section 2.3.11 of Chapter 2**, several natural/ agricultural / commercially manufactured industrial or waste materials were identified to be employed in formulating greener sustainable materials in this research project, as shown in Table 3.1. **Section 2.3.11 and Table 2.7 in Chapter 2 covered the detailed characteristics of all these materials.** The rationale/ analogy for selecting these materials was to concentrate on the formulation of greener infrastructure materials to reduce the embodied CO₂ of composites and the construction industry's carbon footprint. Cement-based concrete and steel reinforcement are the primary construction materials responsible for gross GHG emissions from construction (Rughooputh and Rana, 2014; Kamau et al., 2016; Hamada et al., 2018; Ahmed et al., 2019). Therefore, efforts were concentrated on the formulation of sustainable concrete based on low cement dosages, incorporation of partial/total cement replacement by waste pozzolanic materials (PFA, SF, MK, RHA, PA, cement alternatives like hydrated lime, GGBS and iron powder **as discussed in sections 2.3.11, 2.3.11.1, 2.3.11.1 to 2.3.11.9 and Table 2.7**), fine aggregate replacement materials (CG, CR, RPB **as discussed in sections 2.3.12, 2.3.12.1, 2.3.12.1.1 to 2.3.12.1.3**) and coarse aggregate replacement materials (RCA, CT **as discussed in sections 2.3.12, 2.3.12.2, 2.3.12.2.1 to 2.3.12.2.2**). The study focussed on the investigation of increased benefits achieved by the incorporation of waste-established/ innovative fibres (STF, PPF, PETF, COF, WSF **as discussed in sections 2.3.13, 2.3.13.1 to 2.3.13.5**) mainly to increase the tensile/ flexural behaviour of plain concrete and as a substitute for traditional reinforcement for low strength stipulations. The fibre reinforcement was suggested to enhance the mechanical properties of concrete to certain specifications/ limits (PPF/ waste fibres up to 1-2% of binder weight and steel

fibres for 10% and 17% of binder weight), but it is not assumed as the equivalent to the total replacement of steel reinforcement requirements.

A total of 402 combinations of different materials/ ratios were formulated to prepare 2752 cubes of 100 x 100 x 100 mm dimension for compressive strength testing according to BS EN 12390-3:2019 (BS 12390-3, 2019), 321 prisms and 117 cylinders [cylinders of 150mm dia x 300 mm length for tensile strength testing according to BS EN 12390-6:2019/ BS 1881-117 (BS 12390-6, 2019), and prisms/ beams of 500 x 100 x 100 mm dimensions for flexural strength testing as per BS EN 12350-1:2019 (BS 12350-1, 2019)], cured in air/ water/ sulphate solution (for durability testing). The testing was conducted mainly on 7, 28, 90 and 270 days of curing. Well-graded angular/ crushed coarse aggregate passing through a 20 mm sieve and fine aggregate extracted from river sand passing a 4.75 mm sieve were used for this study, conforming to BS EN 12620/2013 (BS 12620, 2013). CEM 1 52.5, white cement conforming to BS EN 197-1/2011 (BS 197-1, 2011), **as discussed in section 2.3.14**, was used for this study to formulate SCMs, and hydrated lime CL-90 was used to formulate limecrete (BS 8500-1, 2015). CEM1 achieves a target characteristic compressive strength of 52.5 MPa at 28 days of curing (BS 934-2A1, 2012). The target characteristic strength of all the SCM mixes formulated in this study was kept as C16/18 (18 MPa) for low strength, C32/40 (40 MPa) for normal/ medium strength, and C55/60 (60 MPa) for high strength utilisations as shown in Table 2.4 and Table 3.2 (BS 196-1, 2016; Base Concrete, 2018; Sir, 2021). The water/ cement or water/ binder ratio is the relative amount of water used in relation to the quantity of cement or binder materials for preparing concrete or limecrete. W/c or w/b ratio controls concrete's strength, workability, porosity and durability, necessitating careful selection of the proper ratio. Less than 0.35 is considered least workable, and more than 0.60 is considered weak in concrete's strength/ durability properties (Mahajan, 2020; 2021). The mixes were prepared using a water-cement ratio (w/c) of 0.35 for OPC-based SCMS/ PCR and 0.55 for lime-based composites (as a percentage of the total weight of the cement/ binder). A

carboxylate polymer-based plasticiser was used from 0.2-0.25% of the binder's total weight to maintain the consistency of self-compacting concrete as per BS EN 934-2:2009+A1:2012 (BS 934-2A1, 2012) **as discussed in section 2.3.14.** The materials exhibiting/ containing pozzolanic performance/ ingredients conforming to ASTM C 618/ C125-19 were used in this study (Sotiriadis, Nikolopoulou and Tsivilis, 2012; ASTM C 618/ C125, 2019; Nadir and Ahmed 2022b; 2022c Appendix V, VI). The study aimed at the formulation of established materials' composites (cement-based pozzolanic SCMs, fine/ coarse aggregate replacement SCMs and fibre-reinforced concrete FRC) for investigation of their engineering properties and then comparing the results with the engineering properties of innovative materials (cement-free lime-based composites and iron-based binary/ ternary pozzolanic SCMs with/ without fibres). An effort was made to formulate various composites with 1:1:3 and 1:2:3 ratios to investigate the strength of different mixes and, in turn, their embodied CO₂ based on the constituent materials. The SCMs in partial cement-based composites were replaced as per the percentage of the weight of cement, whereas, in lime-based cement-free composites, pozzolans were used as per the weight-to-volume ratio of cement as standard, and their quantities were calculated considering the densities of the binders/ materials in comparison to OPC as standard. The optimum-performing materials were selected for durability testing and chemical-mechanical synthesis/ microstructural studies due to time/resource constraints. The comparison of engineering properties, durability studies on sulphate attack, assessment of embodied CO₂ and morphology/ micro-structural studies facilitated the identification of suitable greener sustainable materials to cut down carbon footprints of the construction industry and befitting utilisation in marine environment/ water channels with the least ecological disturbance.

Table 3.1: Selected Construction Materials/ Unit Price in Leed, UK, in 2023.

Material	Est Price (GBP/ unit)	Est Price (GBP/ kg)
White cement CEM1 52.5	16/ 25 kg bag	0.64
Plasticiser	1/ litre	1.00
Fine aggregate (sand)	53/ 850 kg	0.06
Coarse aggregate	55/ 850 kg	0.06
Hydrated lime CL90	10/ 25 kg bag	0.40
Hydraulic lime NH2, NH3.5, NH5	11/ 25 kg bag	0.44
Lime putty	7/ 10 kg tub	0.70
Limestone CaCO ₃	8/ 25 kg bag	0.32
Crushed glass	27.60/ ton	0.03
Crumb rubber	12/ 25 kg bag	0.48
Recycled PET bottles (crushed)	60/ ton	0.06
Recycled concrete aggregate	38/ 850 kg	0.04
Crushed tyres	277.20/ 500 kg	0.55
PFA	9/ 25 kg bag	0.36
Rice husk ash RHA	9/ 25 kg bag	0.36
Palm ash (PA)	10.00/ 25 kg bag	0.40
Metakaolin	10/ 20 kg bag	0.50
SF	16/ 20 kg bag	0.80
GGBS	12/ 25 kg bag	0.48
Iron powder	90/ 25 kg tub	3.60
Oxalic acid	38/ 5 kg	7.60
Steel fibres	12/ 25 kg bag	0.48
PP fibres (micro/ macro)	10/ 25 kg bag	0.40
Coconut coir	100/ ton	0.10
Wheat straw	80/ ton	0.08

Table 3.2: Classification of Characteristic Compressive Strength of Concrete (BS 196-1, 2016; Eurocode Applied, 2017).

Compressive strength Classification	Characteristic cylinder strength	Characteristic cube strength
f_{ck} cylinder/ f_{ck} cube (MPa)	f_{ck} cylinder (MPa)	f_{ck} cube (MPa)
C12/15	12	15
C16/20	16	20
C20/25	20	25
C25/30	25	30
C30/37	30	37
C35/45	35	45
C40/50	40	50
C45/55	45	55
C50/60	50	60
C55/67	55	67
C60/75	60	75
C70/85	70	85
C80/95	80	95
C90/105	90	105

3.4 Selection of Materials and Formulation of Sustainable Composites

3.4.1 OPC-Based Supplementary Cementitious Materials (SCMs)

3.4.1.1 Cement -Based Pozzolanic SCMs

In this study, partial cement replacement with pozzolanic materials was endeavoured to formulate lower cement-based SCMs. A design mix ratio of 1:1:3 was used to prepare high-strength cement-based pozzolanic SCMs with a target strength of 45-60 MPa characteristic compressive strength. Three industrial wastes, pozzolanic materials, pulverised fly ash (PFA), silica fume (SF) and metakaolin (Mk), one industrial waste cement alternative ground granulated blast furnace slag (GGBS) and two agricultural wastes, rice husk ash (RHA) and palm

ash (PA), to investigate/ compare their use as pozzolanic cement replacement materials. All the materials had more than 75% silicate/ alumina or other oxides of metals, **as discussed in sections 2.3.11, 2.3.11.1, 2.3.11.1 to 2.3.11.9 and Table 2.7 in Chapter 2**, to accelerate the reaction with OH^- ions released from cement hydration to help form the calcium silica hydrate (C-S-H) gel ideally (Equation 15). The control design mix contains 100% cement CEM1 52.5 as binder with fine river sand and crushed coarse aggregate in a 1:1:3 ratio. GGBS was replaced as 30%, 45% and 60% of the cement weight (kg) as it is considered as direct cement replacement due to at par contents of SiO_2 and CaO to OPC, with a feasible optimum dosage of 40-80% of the binder (Nadir and Ahmed, 2021b, 2022a). PFA was replaced as 10, 20 and 40% of the OPC weight (kg) as the optimum dosage is up to 40% (Nadir and Ahmed, 2021b, 2022a). SF contains around 99% SiO_2 (Table 2.7) and is considered to react readily with $\text{Ca}(\text{OH})_2$ to form C-S-H gel, but an extensive quantity of SiO_2 could cause the production of $\text{Si}(\text{OH})_4$ gel, which has swelling properties (Equations 31-33). Therefore, researchers suggest the optimum dosage of SF is up to 10%, so 2.5%, 5% and 10% SF were used to formulate the cement-based SF composites (Nadir and Ahmed, 2021b, 2022a). MK is the naturally occurring pozzolanic material derived from calcined kaolinite and contains SiO_2 and Al_2O_3 in abundance, making it less/slow-strength-inducing pozzolan. Studies are still underway to suggest the optimum dosages; therefore, 5, 10 and 20% of binder weight were replaced with MK to ascertain cement-based MK composites' engineering properties/ benefits (Nadir and Ahmed, 2021b, 2022a). RHA and PA are agricultural waste-based ashes. RHA contains around 97% SiO_2 (Table 2.7), making it an excellent pozzolanic replacement material to produce sufficient C-S-H gel in reaction with $\text{Ca}(\text{OH})_2$. Still, the extensive presence of SiO_2 could produce swelling $\text{Si}(\text{OH})_4$ gel. PA has lower density and contains comparatively lesser SiO_2 , Al_2O_3 , and CaO (43%, 8% and 11%) but contains 23% K_2O (Table 2.7), which could result in the weakening of the composites due to K_2O -specific cracking, alkali-silica reaction and production of ettringite on internal sulphate attack. Therefore, their

testing dosages for the formulation of SCMs were kept at 2.5, 5 %, and 10% (Nadir and Ahmed, 2021b, 2022a), as shown in Figure 3.1 and Table 3.3.

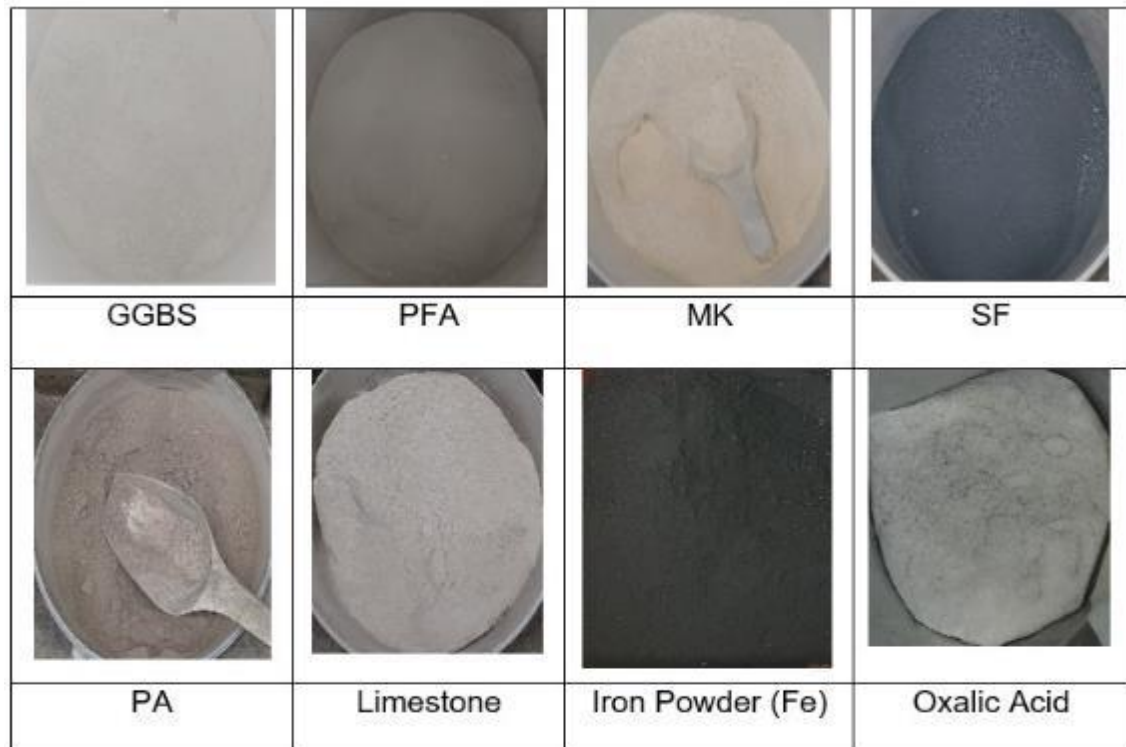


Figure 3.1: Cement Replacement Materials/ Pozzolans

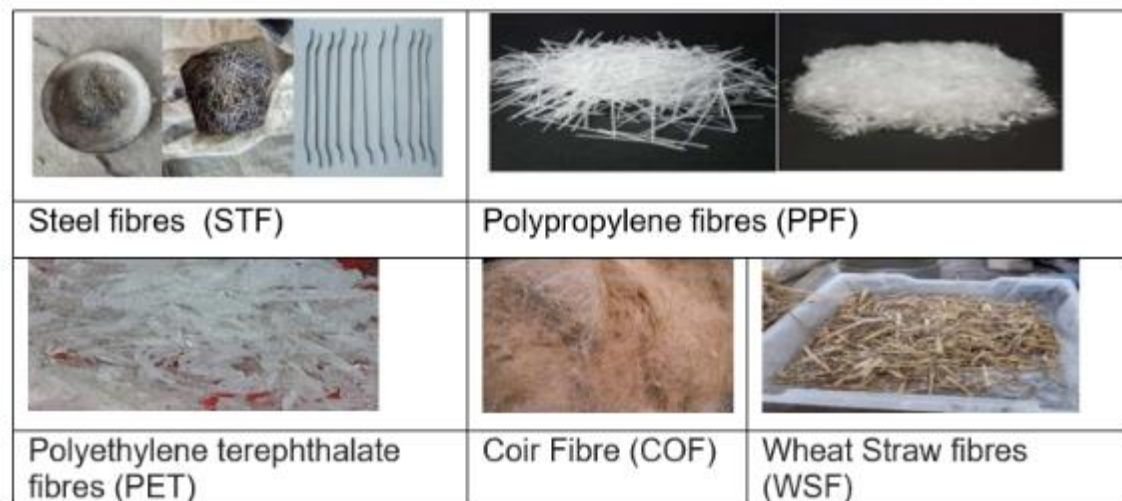


Figure 3.2: Established and New Fibres.

Table 3.3: Partial Replacement of Cement with Pozzolanic Materials

Mix Material	Replacement Material (Kg)	Cement (kg)	Sand (kg)	Coarse Aggregate (kg)	Water (l) @ 0.35 W/C Ratio	Slump
Control	0	6.2	6.2	18.6	2.2	S1
GGBS 30%	1.9	4.3	6.2	18.6	2.2	S1
GGBS 45%	2.8	3.4	6.2	18.6	2.2	S1
GGBS 60%	3.7	2.5	6.2	18.6	2.2	S1
PFA 10%	0.62	5.58	6.2	18.6	2.2	S1
PFA 20%	1.24	4.96	6.2	18.6	2.2	S1
PFA 40%	2.48	3.72	6.2	18.6	2.2	S1
SF 2.5%	0.16	6.04	6.2	18.6	2.2	S1
SF 5%	0.32	5.88	6.2	18.6	2.2	S1
SF 10%	0.62	5.58	6.2	18.6	2.2	S1
MK5%	0.31	5.89	6.2	18.6	2.2	S1
MK 10%	0.62	5.58	6.2	18.6	2.2	S1
MK 20%	1.24	4.96	6.2	18.6	2.2	S1
RHA 2.5%	0.16	6.04	6.2	18.6	2.2	S1
RHA 5%	0.32	5.88	6.2	18.6	2.2	S1
RHA 10%	0.62	5.58	6.2	18.6	2.2	S1
PA 2.5%	0.16	6.04	6.2	18.6	2.2	S1
PA 5%	0.32	5.88	6.2	18.6	2.2	S1
PA 10%	0.62	5.58	6.2	18.6	2.2	S1

3.4.1.2 Fibre Reinforced Concrete (FRC)

In the subsequent experimental stage of the research, fibre-reinforced cement-based composites were formulated using a 1:2:3 ratio to investigate the engineering properties of the FRC composites. Steel (ST) fibres (ST/ STF) and polypropylene (PPF) are established fibres. They are used in various civil engineering applications like tunnels/channel lining, especially for improving surface finishing, enhancing ductility, and providing resistance to crack propagation, impact, and spalling (Dramix, 2023). Contemporary researchers and industry have established using steel fibres as 10% to 17% of the binder with a dosage of 40-60 kg/m³ (Dramix, 2023). Therefore, steel fibres equal to 10%

and 17% of cement weight were considered for this experimental study. The established dosages of PPF of 1% - 2% of the binder were incorporated for this research (Nadir and Ahmed, 2021b, 2022a). Coconut coir fibres (COF), wheat straw fibres (WSF) and polyethylene terephthalate bottle fibres (PET fibres) are considered under-study fibres extracted from agricultural/ industrial waste. Their optimum dosage is still being researched; therefore, for a better comparison, their dosage was set at par PPF as 1% and 2% of the cement weight, i.e., 60g and 120g. Hooked steel fibres, a combination of micro PPF (25%) and macro PPF (75%), 2-3 cm long, and up to 4-5 mm wide coir, wheat and PET fibres were used (Nadir and Ahmed, 2021b, 2022a) **as discussed in sections 2.3.13, 2.3.13.1 to 2.3.13.5** and shown in Figures 2.57-2.60, Figure 3.2 and Table 3.4.

3.4.1.3 SCMs with Waste Replacement Fine/ Coarse Aggregate

In investigating the strength of greener composites, attention was focused on partially replacing fine and coarse aggregate. **As discussed in section 2.3.12**, it was inferred that quarrying/ mining/ transportation/ crushing of virgin fine/ coarse aggregates involves 20 billion tons of materials and emissions of around a billion tons of CO₂. As a step towards the formulation of greener concrete to minimise the carbon footprints of the construction industry, the absorption of global waste from other industries, and to preserve natural resources from depletion due to extensive mining/ crushing of sand/ rock reserves, an endeavour was made to explore the extent of replacing fine/ coarse aggregate with materials extracted from industrial waste. In this part of the study, cement-based concrete composites with a 1:1:3 ratio were formulated by incorporating 10-30% crushed glass (CG), 10-30% crumb rubber (CR) and 10-30% recycled shredded PET bottles (RPB) as partial replacement of virgin river sand by weight **as discussed in sections 2.3.12, 2.3.12.1, 2.3.12.1.1 to 2.3.12.1.3** and shown in Figure 3.3 and Table 3.5. 10-30% recycled concrete aggregate and 2.5 - 7.5% crushed tyres were used to replace the virgin coarse aggregate. The density of crushed/ shredded tyres (CT) is almost 25% of the virgin coarse aggregate; therefore, a reduced quantity of its replacement was considered to avoid extensive

weakening of composite as coarse aggregate is responsible for higher strength of concrete with cement, **as discussed in sections 2.3.12, 2.3.12.2, 2.3.12.2.1 to 2.3.12.2.2** and shown in Figure 3.4 and Table 3.6.

Table 3.4: Incorporation of Various Fibres for Preparation of FRC Composites

Cement-Based FRC Composites with Established/ Waste Fibres							
Mix	Fibre Type	CEM I (kg)	Sand (kg)	Gravel (kg)	Fibres (g)	Water (l)	Slump
Control	-	6	12	18	-	2.2	S1
ST10%	Steel	6	12	18	680	2.2	S1
ST17%	Steel	6	12	18	1020	2.2	S1
PPF 1%	PP	6	12	18	60	2.2	S1
PPF 2%	PP	6	12	18	120	2.2	S1
COF1 1%	Coco	6	12	18	60	2.2	S1
COF2 2%	Coco	6	12	18	120	2.2	S1
PET 1%	PET	6	12	18	60	2.2	S1
PET 2%	PET	6	12	18	120	2.2	S1
WSF1 1%	Straw	6	12	18	60	2.2	S1
WSF2 2%	Straw	6	12	18	120	2.2	S1



Crushed Glass (CG)



Crumb Rubber (CR)



Recycled Shredded PET Bottles (RPB)

Figure 3.3: Partial Fine Aggregate Replacement Materials



Recycled Concrete Aggregate
(RCA)

Crushed tyres (CT)

Figure 3.4: Partial Coarse Aggregate Replacement Materials

Table 3.5: Partial Replacement of Fine Aggregate with Crushed Glass (CG), Crumb Rubber (CR), and Recycled Shredded PET Bottles (RPB).

Partial Replacement of Fine Aggregate with Glass, CR, RPB

Mix Material	Replacement Material (kg)	Cement (kg)	Fine Aggregate Sand (kg)	Coarse aggregate (kg)	Slump (mm)
Control	0	6.2	6.2	18.6	S1
CG 10%	0.6	6.2	5.6	18.6	S1
CG 20%	1.2	6.2	5	18.6	S1
CG 30%	1.8	6.2	4.4	18.6	S1
CR 10%	0.6	6.2	5.6	18.6	S1
CR 20%	1.2	6.2	5	18.6	S1
CR 30%	1.8	6.2	4.4	18.6	S1
RPB 10%	0.6	6.2	5.6	18.6	S1
RPB 20%	1.2	6.2	5	18.6	S1
RPB 30%	1.8	6.2	4.4	18.6	S1

Table 3.6: Partial Replacement of Coarse Aggregate with Recycled Concrete Aggregate (RCA) and Crushed/ shredded Tyres (CT)

Partial Replacement of Coarse Aggregate with RCA and ST

Mix Material	Replacement Material (kg)	Cement (kg)	Fine Aggregate Sand (kg)	Coarse aggregate (kg)	Slump (mm)
Control	0	6.2	6.2	18.6	S1
RCA 10%	1.8	6.2	6.2	16.8	S1
RCA 20%	3.6	6.2	6.2	15	S1
RCA 30%	5.4	6.2	6.2	13.2	S1
CT 5%	0.9	6.2	6.2	17.7	S1
CT 7.5%	1.4	6.2	6.2	17.2	S1
CT 10%	1.9	6.2	6.2	16.7	S1

3.4.2 Cement-free hydrated Lime (CL90) Based Pozzolanic Composites with GGBS, PFA, SF and MK.

The primary focus of this research is to formulate sustainable, greener infrastructure materials without using cement as a binder. In this research phase, extensive experimental work was conducted to formulate suitable cement-free hydrated lime-based composites. Lime in raw forms, such as limestone CaCO_3 , quick lime CaO , and natural hydraulic lime, was used as construction materials. However, owing to its intrinsic lower strength, the use of slaked/ hydrated lime (CL90) Ca(OH)_2 in the construction industry as a binder is less pronounced as compared to its large-scale utilisation in other industries, agriculture, gardening and soil stabilisation (Nadir et al., 2022b). Therefore, a research gap was identified, encouraging the use of hydrated lime with pozzolanic materials to formulate cement-free composites for low-medium strength utilisation in the construction industry. OPC comprises 67% CaO and 25% SiO_2 (Table 2.7), which react during the hydration process to produce C-S-H gel responsible for the

strength of concrete. An endeavour was exercised to combine hydrated lime containing $\text{Ca}(\text{OH})_2$ with pozzolans having an extensive quantity of SiO_2 to form C-S-H gel to demonstrate the OPC type of configuration (Nadir and Ahmed, 2021b, 2022a; Nadir et al., 2022b).

3.4.2.1 Cement-free Hydrated Lime-Based Plain Composites with GGBS, PFA, SF and MK

A considerable effort was undertaken to formulate cement-free hydrated-lime-based pozzolanic composites, which involved investigating mixes with job mix ratios of 1:1:2, 1:1:3, 1:2:3 and 2:1 (two parts of total aggregate and one part of binder). Control mixes were formulated with hydrated lime as 50% of the OPC binder because the density of CL90 is equal to 50% of cement, as shown in Table 3.6. GGBS density was taken at par OPC; SF density was considered equal to CL90 or 50% of OPC, whereas the density of PFA/ MK is equal to 50% of CL90 or 25% of OPC. Therefore, in the traditional cement/ sand/ aggregate ratios, the binder was replaced by CL90 (for control mixes) and was taken in half the cement quantity. In contrast, sand and coarse aggregate were taken as the multiple of CL90 quantity as per the traditional ratios, as shown in Table 3.7. The pozzolanic lime-based composites comprised 90-10% hydrated lime (50% of cement equivalent) and 10-90 pozzolans (GGBS, PFA, SF, MK) as combined binder weight (substituted by volume). Sand and fine aggregated were taken as the multiple of traditional ratios/ job mix formulas, as shown in Table 3.7. The use of plasticiser for hydrated lime base concrete was not recommended in the literature; therefore, to achieve a self-compacting workable mixture of minimum S1 target slump, a water binder ratio of 0.55 was used, making a standard water quantity of 3.3 litres. The cubes were tested on 7, 28 days and 90 days of air curing and testing of two cubes on 90 days of water curing for assessment of characteristic compressive strength and testing of air cured prism after 90 days to determine the flexural strength of the limecrete composites.

Table 3.7: Cement-Free Hydrated Lime-Based Limecrete Mixes.

Cement-Free Hydrated Lime-Based Limecrete								
Mix	Mix Ratio	Mix %age	Hydrated Lime (HL)	Pozzolan %	Fine Aggregate (kg)	Coarse Aggregate (kg)	Water (l)	Slump
Control (HL)	1:02:03		2.5	0	10	15	3.3	S1
Control (HL)	1:01:02		3.75	0	7.5	15	3.3	S1
Control (HL)	1:01:03		3	0	6	18	3.3	S1
Control (HL)	2:01		2	0	13.3	6.7	3.3	S1
SL (GGBS)	1:02:03	10, 20, 30, 40, 50, 60, 70, 80, 90	90, 80, 70, 60, 50, 40, 30, 20, 10	10, 20, 30, 40, 50, 60, 70, 80, 90	10	15	3.3	S1
SL	1:01:02				7.5	15	3.3	S1
SL	1:01:03				6	18	3.3	S1
SL	2:01				13.3	6.7	3.3	S1
PFA	1:02:03				10	15	3.3	S1
PFA	1:01:02				7.5	15	3.3	S1
PFA	1:01:03				6	18	3.3	S1
PFA	2:01				13.3	6.7	3.3	S1
SF	1:02:03				10	15	3.3	S1
SF	1:01:02				7.5	15	3.3	S1
SF	1:01:03				6	18	3.3	S1
SF	2:01				13.3	6.7	3.3	S1
MK	1:02:03				10	15	3.3	S1
MK	1:01:02				7.5	15	3.3	S1
MK	1:01:03				6	18	3.3	S1
MK	2:01				13.3	6.7	3.3	S1

3.4.2.2 Non-Cement Alternative Lime-Based Fibre-Reinforced Innovative Pozzolan Composites (NALFRIC)

This study was further elaborated after finding the best strength demonstrating lime-based pozzolan composites with the incorporation of fibres as fibre-reinforced cement-free lime-based pozzolan composites. The hydrated lime-based composites were formulated using a 1:1:2 ratio with 80% slag (GGBS) + 20% CL90 (SL80), and 50% MK + 50% CL90 (MK50) demonstrated the best results among their respective composites/ combinations as medium and low

strength materials, respectively (as shown in the results section). SL80 and MK 50 were selected for further simplified experimentation to formulate fibre-reinforced cement-free limecrete. Steel fibres were used as 5% and 10% of the binder with optimum/ best performing established industrial dosage of 40 - 60 kg/m³. PPF, PET and COF were used as 1 and 2% in line with FRC, as no established dosage was found with CL90-based pozzolanic composites developed in this PhD research, as shown in Tables 3.8 and 3.9.

Table 3.8: Fibre-Reinforced Cement-Free Limecrete Mixes with SL80.

Fibre-reinforced cement-free Limecrete Mixes with SL80 1-1-2

Mix (FA %)	Lime (CL-90) (kg)	GGBS (kg)	Sand (kg)	Gravel (kg)	Fibres (grams)	Water (l)	Slump (mm)
HL SL 80 (Control)	0.75	6	7.5	15		3.3	S1
HL SL80 ST10%	0.75	6	7.5	15	337.5	3.3	S1
HL SL80 ST17%	0.75	6	7.5	15	675	3.3	S1
HL SL80 PP1%	0.75	6	7.5	15	67.5	3.3	S1
HL SL80 PP2%	0.75	6	7.5	15	135	3.3	S1
HL SL80 PET1%	0.75	6	7.5	15	67.5	3.3	S1
HL SL80 PET2%	0.75	6	7.5	15	135	3.3	S1
HL SL80 COF1%	0.75	6	7.5	15	67.5	3.3	S1
HL SL80 COF2%	0.75	6	7.5	15	135	3.3	S1

Table 3.9: Fibre-reinforced cement-free Limecrete Mixes with MK50.

Fibre-reinforced cement-free Limecrete Mixes with MK50 1-1-2

Mix (FA %)	Lime (CL-90) (kg)	MK (kg)	Sand (kg)	Gravel (kg)	Fibres (grams)	Water (l)	Slump (mm)
HL MK 50 (Control)	2.3	1.1	9	18		3.3	S1
HL MK 50 ST10%	2.3	1.1	9	18	170	3.3	S1
HL MK 50 ST17%	2.3	1.1	9	18	340	3.3	S1
HL MK 50 PP1%	2.3	1.1	9	18	34	3.3	S1
HL MK 50 PP2%	2.3	1.1	9	18	68	3.3	S1
HL MK 50 PET1%	2.3	1.1	9	18	34	3.3	S1
HL MK 50 PET2%	2.3	1.1	9	18	68	3.3	S1
HL MK 50 COF1%	2.3	1.1	9	18	34	3.3	S1
HL MK 50 COF2%	2.3	1.1	9	18	68	3.3	S1

3.4.3 Iron-Based Binary/ Ternary Pozzolanitic Composites (Fe-Composites)

The second primary objective of this PhD research is to formulate/develop the materials/ SCMs containing lower cement dosages and the materials which could absorb the CO₂ emitted during the hydration process, making it a carbon-neutral composite or even absorb CO₂ from the environment targeting to become a low-carbon material. David Stone (2016) accidentally discovered that iron powder (Fe) in combination with limestone and PFA/ MK results in cement concrete-like hardened material. Further investigations revealed that iron reacts with CO₂ absorbed from the environment to form ferrous carbonate FeCO₃, having sedimentary rock-like properties (siderite), achieving more strength than cement concrete and stopping the ingress of moisture-containing sulphates from avoiding external sulphate attack, thus increasing the strength and durability of the iron-based composites. This study intended to use the same analogy but endeavoured to incorporate various pozzolanitic/ cement alternatives as binary/ ternary pozzolanitic combinations with 10-50% use of modified Fe-composites. In the first formulation phase, iron-based binary/ ternary pozzolanitic composites plain SCMs (without fibres) were developed using a 1:2:3 mix ratio. The control mixes with 100% OPC using 1:2:3 cement, sand, and the aggregate ratio was incorporated as per the prescribed British standards for materials/ mixing concrete as mentioned in the preceding sections targeting C32/ 40 or M40 concrete (Table 2.4, Table 3.2). The conventional Fe-composites constituted 60% iron powder, 20% PFA, 8% MK, 10% CaCO₃, and 2% oxalic acid, were used to mix in a 1:2:3 ratio by partially replacing Fe-composites as 10,20,30,40 and 50% of OPC as a binder, as shown in set 1 in Table 3.10. The modified Fe-composites-based binary pozzolanitic SCMs were formulated using a 1:2:3 ratio by complete replacement of 20% PFA with 20% GGBS (set 2, Table 3.10) and 20% PA (set 3, Table 3.10) along with 60% iron powder, 8% MK, 10% CaCO₃

and 2% oxalic acid. These modified Fe-composites-based binary pozzolanic composites/ mixtures have partially replaced the OPC by 10,20,30,40, and 50% as a binder. The ternary iron-based pozzolanic composites constitute 10%PFA+10%GGBS (set 4, Table 3.10) and 10%PFA+10%SF (set 5, Table 3.10) as replacement of 20% PFA in conventional Fe-composites. However, the exact quantities of 60% iron powder, 8% MK, 10% CaCO₃ and 2% oxalic acid were combined in binary pozzolanic composites. 10-20 ml plasticiser quantity of 0.2 - 0.25% of binder was used with the mixes to get a compactable consistency/ workability. The water-cement ratio of 0.35 and the concrete ratio of 1:2:3 were used to mix the ingredients to cast 100 mm cubes to assess on 7, 28 and 90 days of curing for compressive strength as per BS EN 12390-3:2019 on the compressive testing machine (BS, 12390-3:2019). The prisms of 500 x 100 x 100 mm for testing of flexural strength on 90 days of curing were cast in conformance with BS EN 12350-1 and were assessed on a flexural testing machine with gradual hydraulic three-point loading (BS, 12350-1:2019). The consistency was ascertained using slump testing using standard cone and rod apparatus with target S1 slump as per BS EN 8500 and BS EN, 12390-2:2019 (BS, 12390-2:2019).

Table 3.10: Composition of Conventional/ Modified Fe-Composites-Based Binary/ Ternary Pozzolanic SCMs with 10-50% replacement sets 1-5.

Material	Set1: Fe-composites with 20% PFA (%)	Set2: Fe-composites with 20% GGBS (%)	Set3: Fe-composites with 20% PA (%)	Set4: Fe-composites with 10% PFA+10%GGB S (%)	Set5: Fe-composites with 10% PFA+10%SF (%)
Iron powder	60	60	60	60	60
PFA	20	-	-	10	10
GGBS	-	20	-	10	-
PA	-	-	20	-	-
SF	-	-	-	-	10
MK	8	8	8	8	8
Limestone	10	10	10	10	10
Oxalic Acid	2	2	2	2	2

Table 3.11: Composition of 10% Fe-Composites-Based SCMs with Binary and Ternary Pozzolans and Fibres (FRC 123).

10% NAFRIC SCMs with Binary Pozzolans (20% PFA/20% GGBS/ 20% PA											
1). 10% Fe Mixes with 20% PFA/ 20% GGBS/ 20% PA & Fibers FRC 1 2 3											
Fibers Type	Fibers (g)	Fe-Composite Replacement 10%, kg	Iron Powder (g)	Fly Ash or GGBS or PA (g)	Limestone (g)	MK (g)	Oxalic Acid (g)	Cement (kg)	Fine Aggregate (kg)	Coarse Aggregate (kg)	Water (l) @W/C= 0.35
Control (PCC)								6	12	18	2.1
Fe/Con (PFA/GGBS/ PA)	0	0.6	356	119	59	48	12	5.4	12	18	2.1
STF10%	680	0.6	356	119	59	48	12	5.4	12	18	2.1
STF17%	1020	0.6	356	119	59	48	12	5.4	12	18	2.1
PPF1%	60	0.6	356	119	59	48	12	5.4	12	18	2.1
PPF2%	120	0.6	356	119	59	48	12	5.4	12	18	2.1
PET1%	60	0.6	356	119	59	48	12	5.4	12	18	2.1
PET2%	120	0.6	356	119	59	48	12	5.4	12	18	2.1
WSF1%	60	0.6	356	119	59	48	12	5.4	12	18	2.1
WSF2%	120	0.6	356	119	59	48	12	5.4	12	18	2.1
10% NAFRIC SCMs with TernaryPozzolans (10% PFA+10% GGBS or 10% PFA+10% SF)											
2). 10% Fe Mixes with 10% PFA+10% GGBS or 10% PFA+10% SF & Fibers FRC 1 2 3											
Fibers Types	Fibers (g)	Fe-Composite Replacement 10%, kg	Iron Powder (kg)	PFA + (GGBS or SF) (g)	Limestone (g)	MK (g)	Oxalic Acid (g)	Cement (kg)	Fine Aggregate (kg)	Coarse Aggregate (kg)	Water (l) @W/C= 0.35
Fe/Con (PFA+GGBS or PFA+ SF)		0.6	356	71+48	59	48	12	5.4	12	18	2.1
STF10%	680	0.6	356	71+48	59	48	12	5.4	12	18	2.1
STF17%	1020	0.6	356	71+48	59	48	12	5.4	12	18	2.1
PPF1%	60	0.6	356	71+48	59	48	12	5.4	12	18	2.1
PPF2%	120	0.6	356	71+48	59	48	12	5.4	12	18	2.1
PET1%	60	0.6	356	71+48	59	48	12	5.4	12	18	2.1
PET2%	120	0.6	356	71+48	59	48	12	5.4	12	18	2.1
WSF1%	60	0.6	356	71+48	59	48	12	5.4	12	18	2.1
WSF2%	120	0.6	356	71+48	59	48	12	5.4	12	18	2.1

3.4.4 Novel, Alternative Fibre-Reinforced Iron-Based Composites (NAFRIC)

The previous experimental work suggested 10-50% feasible usage of iron-based pozzolanic composites with the best strength achieved by 10% partial replacement and the best environmental impacts obtained by increased dosage of iron powder to absorb more CO₂. However, the cost of iron powder and its broad-spectrum availability restrict its use from 10-30% of partial cement replacement. This further study was conducted to elucidate the impacts of mixing established fibres like 10% and 17% STF, 1% and 2% PPF, and 1% and 2%

innovative fibres like PET and WSF with the best performing 10% conventional/ modified Fe-composites-based SCMs containing the binary pozzolans/ ternary pozzolans as shown in Table 3.11. Set 1-3 contain Fe-composites with binary pozzolans, i.e., 8% MK with 20% PFA (set 1), 8% MK with 20% GGBS (set 2) and 8% MK with 20% PA (set 3), respectively. Set 4 and 5 contain modified Fe-composites with ternary pozzolans, i.e., 8% MK with 10%PFA+10%GGBS (set 4) and 8% MK with 10%PFA+10%SF (set 5), respectively, as shown in Table 3.10. The control mixes containing only cement concrete without Fe-composites/ fibres and the 10% iron-based SCMs without fibres were prepared for comparison/investigation. The “Novel, Alternative Fibre-Reinforced Iron-based Composites (NAFRIC)” mixes were formulated using CEM1 52.5 with virgin coarse/ fine aggregates and 10% iron-based pozzolans, 90% OPC and 1-2% fibres mixing as FRC with a 1:2:3 mix ratio in conformance with BS EN 12620/2013 (BS, 2013). The 100 mm cubes were prepared/ investigated for compressive strength at 28, 90 and 270 days in conformance with BS EN 12390-3:2019 (BS, 2019). The 500 x 100 x 100 mm prisms/ beams were prepared/ assessed for flexural strengths at 90 days, per BS EN 12350-1:2019 (BS, 2019). The standard cone and rod apparatus was used to measure the slump to ascertain workability with the target S1 slump as per BS EN 8500 and BS EN, 12390-2:2019 (BS, 12390-2:2019) (BS, 2019) using a consistent 0.35 w/c ratio as per Abram's law (Jain, 2020) and 10-25 ml plasticiser (0.2-0.25% of the binder) for a self-compacting workable mixture. The target characteristic compressive strength of C32/40 or M40 concrete was set to be achieved by the mixes of this study (Table 2.4, Table 3.2).

3.5 Types/ Procedures/ Testing Equipment/ Materials/ Moulds Preparation

All the mixed materials were prepared in a controlled environment in the material science laboratory using, storing, preparing and curing the materials at 20 ± 5 Celsius temperature (BS EN 12390-2:2019). The binding materials (Snowcrete CEM1 52.5 (BS EN 197-1), lime (BS EN 459-1:2015), pozzolans, GGBS, iron

powder (BS EN 450, 15167, 13263; ASTM C 618/ C125-19), fibres (STF, PPF, PET, COF, WSF) (BS EN 14889-1:2006) were mixed with fine aggregate (virgin river sand or replacement materials), coarse aggregate (virgin crushed rocks or replacement materials) (BS EN 12620/ 2013) after proper measurement as per the design mix ratio/ required number of testing specimens (cubes, cylinders, prisms) in a material mixing machine using tap water and plasticisers (where applicable) as per related BS EN/ ASTM standards (BS EN 1008:2002; BS EN 13670:2009; BS EN 934-2:2009+A1:2012; ASTM C 618/ C125-19; BS EN 12390-1:2019; BS EN 12390-2:2019; BS EN 12390-3:2019). The wet mixed materials were poured into the moulds of 100mm cubes, 150mm dia x 300mm length cylinders and 500x100x100mm prisms and were well compacted on a mould vibration machine. The moulds were demoulded after 24 hours for OPC/ PCR/ SCMs concrete and after seven days for lime-based composites. The OPC/ PCR/ SCMs cubes specimens were water cured in water for 7, 14, 28, 90 and 270 days, maintaining a temperature of $20 \pm 5^{\circ}\text{C}$ and pH of 7 (BS, 2009; USGSWSS, 2016). The long duration of curing ensures the completion of the second phase of the hydration process to produce the total amount of C-S-H gel and attain neat to 100% strength, especially the pozzolanic composites react slowly to produce C-S-H gel requiring longer curing durations (BS, 2000; Kosmatka et al., 2002; Atis and Bilim, 2007; Ganesan et al., 2008; Bapat, 2012; Hannesson et al., 2012; Reddy et al., 2013). The OPC/ PCR/ SCMs cylinder/ prisms and lime-based cubes/ cylinder/ prisms specimens were air-cured before testing. Some lime-based cubes were also water-cured for 90 days and 270 days to compare strengths between water-cured and air-cured specimens and assess their behaviour on utilisation in the water channels and subject to the marine environment. Specimens from selected materials were placed in a concentrated 2.5%MgSO₄+2.5%Na₂SO₄ sulphate solution for 270 days to depict hydraulic modelling of 10-20 years of field exposure and then testing for the compressive strength to compare with the strength of cubes cured in water for 270 days.

3.5.1 Density

BS EN 12390-7:2019 provides guidelines to ascertain the density of concrete and classify it into three categories: light (800-2000 kg/m³), regular (2000-2600 kg/m³) and heavy density concrete (>2600kg/m³) (BS, 12390-7:2019). The density of all the materials under study was calculated using dry mass M_d of 100 mm cubes in the air on digital balance and then weighing the same cube in water M_w . The density was calculated using the formula:

Equation 35: Density “D” = $[M_d / (M_d - M_w)] \times 1000$

3.5.2 Slump Test

The consistency of all the mixes/ specimens was ascertained using slump testing using standard cone and rod apparatus with target S1 slump (Figure 3.5 and Table 3.12) as per BS EN 8500 and BS EN, 12390-2:2019 (BS, 12390-2:2019; Tuan et al., 2021). A true slump of 10-40 mm was targeted during the whole study while keeping the w/c ratio to 0.35 for cement concrete, partial cement concrete (PCR), pozzolanic SCMs and iron-based pozzolanic SCMs with the use of 10-25ml plasticiser and using 0.55 water/ cement ratio (w/c) for hydrated lime-based composites without any plasticiser. The stepwise procedure (Figure 3.5) of pouring/ shovelling/ heaping/ mixing the material on the tray (steps 1-4), filling the cone with three layers with rod temping at every layer (step 5), levelling/ removing any residual material from the top of the cone (step 6,7), carefully raising the cone in 5-10 seconds (step 8) and finally placing the cone with upside-down along the slump and then measure the drop of the slump in comparison to the height of cone would give the slump of the material.

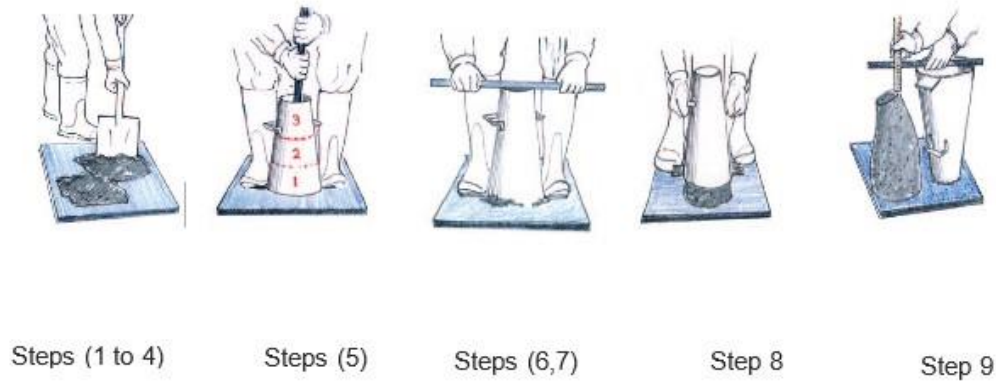


Figure 3.5: Slump Testing Stepwise Procedure (BS EN 12350-2:2019).

Table 3.12: Slump Classification (BS EN 206-1: 2000; BS, 12390-2:2019)

Slump Classification	
Class	Slump Range (mm)
S1	10-40
S2	50-90
S3	100-150
S4	160-210

3.5.3 Sieve Analysis and Particle Size Gradation Curve

The sieve analysis aims to obtain various particle gradation/ size distributions in a given soil/ fine/ coarse aggregate sample. Generally, the aggregates are categorised as well-graded, uniformly graded or gap-graded materials. Well-graded materials contain a variety of small/ large particles so that the small-sized particles appropriately fill the voids/ gaps between large-sized particles to make a homogeneous/ dense composition of mass. Uniformly graded materials comprise the same-sized particles and cannot fill the voids. The gap-graded materials have a variety of sizes available in the composition, but some grading sizes are missing again, resulting in lesser homogeneity/ density of the material (Alam and Ahmad, 2020). In classical terms, fine aggregates are particle-size materials that could pass through the ASTM sieve number 4 or 4.75 mm opening sieve, whereas coarse aggregates are materials of particle size retained on

ASTM sieve number 4 or 4.75 mm sieve. The particles passing through 200 microns or sieve number 200 are called clays (BS 812-2, 1995; Vashisth, 2018; ASTM C136/C136M, 2019; Alam and Ahmad, 2020). The oven-dried samples of virgin coarse (4000 g) aggregates/ replacement coarse aggregate materials RCA (4200 g) and CT (1150 g) were taken for particle size distribution analysis. The sieves of 28 mm, 20 mm, 14 mm, 10 mm, 4.75 mm, 2.36 mm and the pan were stacked with the largest size at the top and the pan at the bottom as per BS 812-2, 1995. For fine aggregate gradation analysis, oven-dried samples of 250 – 1000 g virgin sand, CG, RPB and CR were taken based on the density/ volume of the materials. The sieves of sizes 4.75 mm, 2.36 mm, 1.18 mm, 0.6 mm, 0.3 mm, 0.15 mm and 0.075 mm were stacked with the largest size at the top and the pan at the bottom as per BS 812-2, 1995. The stacked sieves were placed on an electronic shaker and shaken for 10 minutes (Figure 3.6). Then, the materials retained/ passing from each sieve were measured, and percentages retained/passing were determined. The percentage passing was drawn on the vertical axis with sieve sizes on the semi-logarithmic horizontal axis to obtain the particle size gradation curve, as discussed in section 4.2.3.



Figure 3.6: Sieve Analysis for Fine/ Coarse Aggregates

3.5.4 Compressive Strength

Compressive strength is one of the significant engineering properties of concrete, as it is considered vital in compression and weak in tensile strength (Arya, 2009; Yoo and Banthia, 2019; Civil Concept, 2020; Vu et al., 2020; Ahmed et al., 2021).

Generally, tensile strength is around 10% of the compressive strength of the concrete. Therefore, the characteristics of the compressive strength of the concrete are generally taken as the strength of the concrete when discussing its strength. The characteristic compressive strength is defined as the strength of the concrete attained by 95% of specimens of the same mixture at 28 days of curing when evaluated using a 150 mm cube and is calculated statistically using equation 36.

Equation 36: $F_{ck} = f_{cm} - 1.64 \times S_d$

$F_{ck} = f_{cm} - 1.64 \times S_d$ or $F_{ck} = 0.8 \times f_{\text{average}}$ Where, $f_{cm} = n \times f_{ci} / n$ and $f_{cm} = f_{ck} + 8$

Where f_{ck} is the characteristic compressive strength of the concrete mix, f_{cm} is the mean compressive strength of all the cubes of the same concrete mix, and S_d is the standard deviation between the 5% specimens giving less strength than the mean value of compressive strength f_{cm} . and could be calculated using the following formula:

$$S_d = \left[\frac{\sum_i^n (f_{ci} - f_{cm})^2}{n - 1} \right]^{\frac{1}{2}}$$

S_d is the standard deviation, f_{ci} is the compressive strength of the i^{th} specimen, and f_{cm} is the mean compressive strength of “n” total numbers of specimens.

In this study, the target characteristic strength of all the SCM mixes was kept as C16/18 (18 MPa) for low strength, C32/40 (40 MPa) for regular/ medium strength, and C55/60 (60 MPa) for high strength utilisations and more than 80MPa for high-performance concrete as shown in Table 2.4 and Table 3.2 (BS, 2016; Base Concrete, 2018; Sir, 2021). Moreover, only two cubes were evaluated for each specimen at a specified age of curing, not making reasonable data for statistical analysis; therefore, target compressive strength was taken as the characteristic compressive strength for which no more than 5% of specimens fail to achieve lesser than that target strength. f_{cm} was calculated, adding 8 to the target compressive strength. After thoroughly mixing the materials as per the designed ratios/ job mix formula (Figure 3.7), the prepared concrete was poured into pre-

oiled moulds of 100 mm cubes and placed on vibration stations to remove the air voids to achieve good compactness (Figure 3.8, 3.9). Any residual material was removed, and moulds were opened after 24 hours for OPC/ PCR specimens and after three days for pozzolanic-based limecrete. The OPC/ PCR cubes were placed in a water tank (Figure 3.10) for 7, 14, 28, 90 or 270 days as per the required age of curing, maintaining a temperature of $20 \pm 5^\circ\text{C}$ and pH of 7 (BS, 2009; USGSWSS, 2016), and pozzolanic-based limecrete were air-cured for required age of curing. After attaining the curing age, the cubes were taken out of the water, cleaned/ dried and placed in a compressive testing machine (Figure 3.11) on the smooth faces as per BS EN 12390-3:2019 (BS, 2019). A uniform hydraulic load of $0.6 \text{ KN} \pm 0.2$ per second was applied until the occurrence of the failure of the cube. The maximum load “P” was noted in “Newtons N” from the machine to calculate the compressive strength f_c using equation 37. Mean compressive strength was then calculated using the mean of the strengths of identical cubes.

Equation 37: Compressive Strength $f_c = P/A$

$f_c = P/A$ where f_c is the compressive strength in N/mm^2 or MPa , “P” is the load in “N”, and “A” is the area of the cube ($100 \times 100 \text{ mm}^2$).



Figure 3.7: Mixing of Materials



Figure 3.8: Compaction on a vibration machine



Figure 3.9: Cubes and prism moulds



Figure 3.10: Curing of cubes in the water tank.



Figure 3.11: Compressive testing machine for testing of 100 mm cubes

3.5.5 Tensile Strength

The tensile strength of a material is another significant engineering property which demonstrates the flexibility of materials subject to a pulling load to withstand rupture/ failure, although it is not considered a dependable leading property for concrete usage. Concrete demonstrates a tensile force equal to around 10% of compressive strength. It is only relied upon for reasonable tensile strength solutions with the incorporation of steel reinforcement in the construction industry (Malesev et al., 2010; Behbahani et al., 2011; Grzymiski et al., 2019; Pachideh and Gholhaki, 2019; Sowmya, 2020; Vu et al., 2020; Li et al., 2020; Ahmed et al., 2021; Lopez et al., 2022; Nadir and Ahmed, 2021b, 2022a). However, plain concrete also undergoes tensile loading during thawing/ spalling and shrinkage, therefore necessitating the study of the behaviour of concrete under tensile loading. This study evaluated some specimens for tensile strength, whereas most specimens were studied for flexural strength. The split tensile strength of concrete was determined by testing 150 mm dia (d) and 300 mm high (l) cylinders. The prepared concrete mix was poured into the pre-oiled cylinder moulds and placed on the vibratory station to remove air/ voids as per BS EN 12390-2 (BS 12390-2, 2019). The cylinders were opened after 1-3 days and were cured for all the mixes. After the required curing age, the cylinder was subject to

a uniform hydraulic loading of $0.6 \text{ kN} \pm 0.2$ per second on the longitudinal axis until it split/cracked on a longer axis, as shown in Figure 3.12. The load “P” in kN was noted from the machine, and the tensile strength was then calculated using Equation 38.

Equation 38: $Tensile\ Strength = f_t = (2*P)/(\pi*d*h)$

Tensile Strength = f_t in N/mm^2 or MPa, P = load in “N”, d = dia of cylinder (150 mm), h = height of the cylinder (300 mm)

3.5.6 Flexural Strength

The flexural strength of concrete is a significant engineering property that assesses the ability of the material to withstand the bending load against rupture. It is generally considered equal to 7-10% of the compressive strength of concrete. (Malesev et al., 2010; Behbahani et al., 2011; Grzymiski et al., 2019; Pachideh and Gholhaki, 2019; Sowmya, 2020; Vu et al., 2020; Li et al., 2020; Ahmed et al., 2021; Lopez et al., 2022). When an element is subject to a bending load, its upper portion experiences compression and the lower portion experiences a tensile force that tries to pull it out while bent on the loading point. A universal three-point loading machine was used to assess prisms of 500 mm long (l), 100 mm wide (b) and 100 mm deep (d) while supporting on two edges as supported beam and exerting the uniform hydraulic loading at the centre of the beam with $0.6 \text{ kN} \pm 0.2$ per second as shown in Figure 3.13. Prisms were cast using design mix concrete pouring in pre-oiled moulds of 500 x 100 x 100 mm and placed on a vibration station to remove air/ voids. The moulds were opened after 1-7 days for OPC/ PCR and lime-based pozzolanic composites. An attached laptop measured the load with the three-point universal loading machine in kN, and displacement/ crack width was measured in mm to assess the post-rupture ductility of fibre-reinforced composites. Equation 39 was then used to determine the flexural strength transverse modulus of rupture to determine the ductility of the material to withstand the rupture on bending forces caused by direct forces, spalling/

thawing, warping or angular application of loading on different elements of construction.

Equation 39: Flexural Strength = $f_f = (3*P*l)/(2*b*d^2)$

Where Flexural Strength = f_f in N/mm² or MPa, P = load in “N” Newtons

b = width of prism (100 mm) and d = depth of prism (100 mm)



Figure 3.12: Cylinder testing for split tensile strength of concrete



Figure 3.13: Three-point flexural strength testing of prism

3.5.7 Carbonation Testing

The carbonation of the concrete is the primary cause of corrosion (ISO 1920-12:2015; www.aeis.com, 2023). The test measures the presence of CO₂ in the specimen and the depth to which it was absorbed and penetrated from the environment. The CO₂ cannot penetrate directly into the materials; it requires moisture to convert into a weak carbonic acid, which reacts with portlandite Ca(OH)₂ to convert it into CaCO₃. The 100mm cubes were cut at a depth of 1 cm after 28, 90 and 270 days of curing, and the test was conducted at 18-25°C temperature, 60-75% relative humidity and under an average of 0.04% atmospheric CO₂ concentration to depict normal field carbonation process. Due to a lack of resources in the University laboratory, additional CO₂ exposure to the specimen using CO₂ tanks and the measurement of CO₂ absorption quantity were not included in the testing methodology. However, the results obtained by

microstructural analysis (section 4.13.1) exhibiting decreased Ca(OH)_2 and increased formation of C-S-H gel and FeCO_3 could predict the absorption of CO_2 , thus decreasing the CO_2 emissions/ embodied CO_2 potential of composites. A phenolphthalein solution is used to determine the presence of CO_2 / carbonation in the specimen by identifying the colour after its spray. If the colour after the spray of phenolphthalein turns into light pink or remains colourless, it means the pH is more than nine, and low CO_2 is available. If it turns bright pink, it means pH is less than nine, carbonation has occurred/ high CO_2 concentration and the alkalinity of the concrete specimen has decreased. In this study, a carbonation test was conducted to determine the absorption of CO_2 during the hydration process to convert iron powder to FeCO_3 in iron-based binary/ ternary pozzolanic composites. If the phenolphthalein spray turns light pink or remains colourless, then it means that iron powder has absorbed the CO_2 emitted during the hydration process or from the atmosphere and has even reacted with limestone CaCO_3 to convert itself into rock-like FeCO_3 , giving enhanced strength to the materials and fully converting Ca(OH)_2 , CaO and SiO_2 into C-S-H gel. This phenomenon was supported by using “Fe” powder with pozzolans and CaCO_3 to produce high-strength SCMs with low-carbon, greener construction materials for better environmental impacts and to reduce the carbon footprints of the construction industry.

3.6 Durability Testing for Sulphate Attack

The details of the internal/ external sulphate attack are covered in section 2.4, which elaborates on how the chemical attack occurs and the preventive/ curative measures. It is, however, of immense importance to investigate the durability of sustainable, greener composites against any sulphate attack. Cement concrete with higher sulphate contents, higher w/c ratio of more than 0.45, increased permeability due to porous structure because of aeration/ voids, extensive moisture, contact with the marine environment, and saltish soils are some of the significant causes of sulphate attack. Pozzolans, low C_3A contents cement and

other preventive measures could reduce the chances of attack (Arya, 2013; ASTM C1012, 2015; Kamau and Ahmed, 2017; Teng et al., 2018; Yi et al., 2020; Ahmed et al., 2021; Nadir and Ahmed 2022b; 2022c Appendix V, VI). The greener OPC/ iron/ lime-based composites formulated in this study are assumed to perform better against sulphate attack due to the presence of pozzolans and iron, which are considered to improve the pore structures, enhanced protection against ingress of chemicals-laden moisture and production of ettringite. American Society for Testing and Materials C1012/C1012M–15:2018 specifies the testing procedure for assessment of durability/ resistance of concrete against sulphate attack, and BS EN 206:2013+A2:2021 specifies the required performance of composites and concrete (ASTM C1012, 2015; ASTM C1012M, 2018; BS 206:2013+A2, 2021). The cubes or tiny prisms are kept in a 5% sulphate concentrated solution (50 g/l of Na_2SO_4 or MgSO_4 or H_2SO_4) after attaining 20 MPa strength for a prolonged period to replicate the field attack of 10-20 years in controlled conditions of the laboratory. Sulphate attack by Na_2SO_4 solution is characterised by causing elongation in the concrete specimens. In contrast, sulphate attack by MgSO_4 is considered an internal attack by producing needles like ettringite crystals, which cause cracking and failure of the structure. In the field, the process of sulphate ingress is prolonged. It could be sourced from any chemical substance broadly depending upon the surrounding soil strata/ water conditions, production of cracks, permeability, air voids, w/c ratio and temporal variations (Bapat, 2012; Abdelalim et al., 2015; ASTM C1012, 2015; Kamau et al., 2016; ASTM C1012M, 2018; Babu et al., 2018; Nadir and Ahmed, 2021). Due to time/ resource constraints in this study, only the best performing fibre-reinforced OPC, lime and iron-based materials' cubes were selected and placed in a covered curing tank containing a combined, concentrated solution of 2.5% MgSO_4 +2.5% Na_2SO_4 after attaining more than 20 MPa strength (except low strength MK and lime-based specimens) for 270 days maintaining a temperature of $20 \pm 5^\circ\text{C}$. The objective of this durability test is to assess the sustainability/ behaviour of developed PCR/ SCMs/ lime and iron-based fibre-

reinforced composites after 270 days of exposure to the combined effect of elongation (by Na_2SO_4) and ettringite formation (by MgSO_4). The cubes were taken out of the tank every three months. They were subject to a low temperature of 5 degrees Celsius to replicate the effect of temporal variations in the field and replace the fresh, concentrated 2.5% MgSO_4 +2.5% Na_2SO_4 solution to maintain pH levels of 6-8. Cubes of the identical specimens were also placed in a water tank for 270 days, maintaining a pH of 7 and a temperature of $20 \pm 5^\circ\text{C}$. After completion of 270 days of exposure in the concentrated sulphate solutions, the dimensions of the cubes were measured on pre-marked/ pre-measured surfaces to check for any elongation and a physical examination was conducted to notice the surface deterioration/ pitting/ salt deposition for qualitative analysis. The compressive strength testing for all the cubes exposed in a concentrated sulphate solution tank and water tank was conducted to determine the strength variation/ durability of materials by comparing them with each other and with other specimens in sulphate solution/ water. The change in length/ elongation was determined by using Equation 40, and the strength deterioration index (SDI) was calculated using Equation 41 (Moon, Lee and Kim, 2003; ASTM C1012M, 2015).

Equation 40: Length variation index (%) $\Delta L = [(L_s - L_i)/L_o] \times 100$

Where ΔL is the length variation index in %age

L_i is the initial length of the cube face on immersion.

L_s is the length of the same cube surface after 270 days of immersion in a sulphate solution.

L_o is the inner dimension of the original mould.

A negative index shows reduction and a positive index shows elongation in length.

Equation 41: Strength deterioration index (%) $\text{SDI} = [(f_w - f_s)/f_w] \times 100$

Where f_w is the compressive strength of water-cured cubes,

f_s is the compressive strength of cubes' surface after 270 days of immersion in a sulphate solution. **A negative strength variation index shows improved strength, and a positive index shows strength reduction.**

3.7 Microstructural Analysis using XRF/ XRD/ SEM/ EDS

The chemical-mechanical synthesis of the composites is determined by analysing the chemical actions between the constituent ingredients to produce the end products and conducting physical/ laboratory testing to assess the engineering properties of the specimens. These results could then be verified/ augmented by conducting advanced testing of x-ray diffraction/ spectrometry (XRD/ XRF) and scanning electron microscopy/ energy dispersive x-ray spectrometry SEM/ EDS. All these tests use the analogy of extracting the electrons from the atom's orbitals of the elements/ compounds contained by a specific material using X-ray (XRD/ XRF) or electrons (SEM/ EDS) for image processing/ segmentation for morphological identification of materials (Ogbonna et al., 2020). These electrons from the target materials' atoms require a characteristic amount of energy specified to each type of material to diffract it to a certain angle. The energy is measured in "keV," and the angle is measured in 1θ , 2θ , and 3θ , respectively. Each element/ compound is then identified using this information by matching it to the AMCSD database (AMCSD, 2023) of this energy versus angle for all the known materials. XRD spectrum is used to determine the crystalline structure of elements, elemental composition, and quantitative/ qualitative analysis using separate phases of diffractions and energy levels. XRD is used to identify the presence of different minerals/ elements/ compounds in a material, given the percentage of each material by giving a series of peaks. Elements having a lesser atomic number than Na could also be identified by XRD. The XRD spectrum's peaks could precisely tell the mineralogy, phase, and percentage presence. The electrons are diffracted from different orbitals like innermost orbit K, outer orbit L (L1, L2, L3) and outermost M orbit (M1, M2, M3, M4, M5). The diffraction of electrons merge, making diffraction beams of different wavelengths and could be calculated using the Bragg formula $2d\sin\theta = n\lambda$. (Mineral Processing &

Metallurgy, 2015; Gravina et al., 2016; www.drawellanalytical.com, 2024; Adithya and Magudeswaran, 2017; Nanoscience Instruments, 2018; AMCSD, 2023; Susan, 2023). XRF and XRD use X-rays to extract the orbital electrons, but XRD could identify compounds, whereas XRF could only identify elements of elemental composition. Therefore, XRD and XRF could be employed to better analyse material composition. Due to time/ resource constraints, only a few selected composites were considered for advanced testing in the local modern materials testing laboratory. The samples from crushed cubes of selected innovative fibre-reinforced lime-based cement-free and iron-based binary/ ternary pozzolanic composites (NALFRIC/ NAFRIC) were sent to the laboratory where these samples were ground to particles size less than 150µm using a ball mill, heated up to 975°C, tested for loss on ignition (LOI) and then analysed for several elements using a Philips Minipal 4 EDXRF machine (Figure 3.14) to assess the elemental configuration through XRF as oxides of metals. The powder grinding and heating of the specimen to 975°C caused a sample to lose some of its hydrated ingredients, but it helped to identify any pre-hydration/ damage to materials due to moisture absorption. This LOI testing on heating to 975°C is specially incorporated for cement-related studies in the construction industry to identify the storage conditions and resulting damages by wrong storage/ moisture absorption, which may result in an increased loss on ignition of specimen more than 30% before and a reduction in strength of material. The powder grinding and 975°C heating of the specimen provided the material with a near-perfect form of crystalline morphology and agitated/vibrated the electrons in the shells to diffract sharply after colliding with x-rays to produce peculiar/ identifiable materials peaks, wavelength and diffraction distance shifting for the clear recognition of phases/ and types of ingredients using CRF/ XRD spectrums in line with AMCSD databank (Hu, Liu and Liu, 2011; Swider, 2017; Fakouri, 2017; Dutrow and Clark, 2019; Wikipedia Contributors, 2019; Krygier et al., 2022; AMCSD, 2023; University of Alberta, 2023; www.drawellanalytical.com, 2024). Moreover, the pre-heating is useful in XRD analysis and identification of the presence of

compounds; these samples were ground to particle size less than 150 μ m using a ball mill, heated up to 975°C, assessed for loss of ignition and then analysed for compounds using powder diffractometry techniques employing a Bruker D500 XRD machine. The traces were identified for crystalline compounds using EVA software to create a spectrum showing different peaks/ phases of the compound. The SEM, on the other hand, is a modern technology for analysing the morphology, chemical composition, crystalline formation and orientation of compounds on the surface of the specimen slices and identifying the composition using electron beams originating from cathode ray tubes. SEM produces outstanding two-dimensional images of 20 - 30000 times magnification with 50-100 μ m resolution, showing spatial variation in the sample size from 5 microns to 1 cm. EDS is employed to determine the chemical composition of the crystalline structure/ orientation and perform the SEM. The electron beams from cathode ray tubes extract the electrons from the atoms of under investigation specimen; these extracted electrons create further extraction of electrons from lower orbitals as secondary beams, and some extracted electrons are backscattered, creating other beams with specified photon energy and further creating x-rays which in turn are used for energy dispersive x-ray spectrometry (EDS). In this study, a section from each of the specimen's slices was mounted, coated and examined by SEM and EDS under various magnifications using an SEM machine (Figure 3.15) and getting microfabric/ crystallographic results in the attached visual display monitor as images and EDS spectrum (Carleton.edu, 2023; JEOL Ltd., 2023). The images and EDS spectrum could be used to analyse the crystalline morphology of the specimen with up to 25000 times magnification, showing the presence of different compounds which could be identified by matching these to an AMCSD-like database by SEM experts, augmented by EDS-spectrum quantifying the exact percentage presence of various compounds in the given specimen. The results obtained by XRD/ XRF are then compared/ supported by SEM/ EDS findings to analyse the configuration/ composition of the composites. In this study, these tests were used to identify the formation of C-S-H gel and

FeCO_3 for required strength attainment and production of ettringite/ sulphur compounds to identify the durability properties of the composites after the sulphate attack.



Figure 3.14: Philips Minipal 4 EDXRF Machine for XRD/ XRF



Figure 3.15: SEM Machine (Carleton.edu, 2023)

3.8 Data Management/ Synthesis/ Analysis

An enormous amount of data was obtained from formulating 321 materials composites and testing more than 3000 specimens in the laboratory. This raw data was transformed into Microsoft Excel spreadsheets and then analysed compared to standard values, with a set of mixes and graphical representations to demonstrate the correlation between various dependent/ independent variables. The analysis and outcome were discussed in Chapter 4 to focus on achieving the objectives set for this study.

3.9 Risk/ Hazard Assessment

The project involved the physical laboratory work comprising the use of different construction materials, chemicals, moulds, specimens and testing machines, warranting a detailed risk assessment before conducting the study as per United

Kingdom health and safety regulations and the university policy/ guidelines as per the prescribed templates duly endorsed by the laboratory manager and director of studies (attached as Appendix I). The risk assessment involves the identification of working hazards, victims of these risks/ hazards, explaining the prevention for the identified hazards, recording and reviewing the hazards incidents and curative measures (health and safety/ risk assessment evaluation is attached as Appendix I) (Leedsbeckett.ac.uk., 2021; Health and safety executive, 2022).

3.10 Summary

This chapter elaborated on the logical selection of fundamental multivariate quantitative analysis. It attempted to provide requisite details about types/ methods of testing, selection of materials and their various combinations, data collection, collation, correlation, comparison, analysis techniques and referencing of the standard guidelines followed from the instructions of a variety of British Standards (BS) and American society of testing and materials (ASTM). This chapter outlined the methodology of formulation/ testing of various OPC/ PCR/SCMs-based composites, cement-free hydrated lime-based composites and iron-based binary/ ternary pozzolanic composites (with/ without fibres) to target the achievement of the aim of this study to “develop/ elucidate the sustainable materials for greener infrastructure construction and hydromodifications/ water channel stabilisation” by fulfilling the objectives after addressing all the research questions outlined in chapter one of the dissertation by the detailed methodology to evaluate the engineering properties/ sustainability/ durability of the developed materials.

4 Chapter 4: Results and Discussion

Chapter 4 presents the laboratory testing results envisaged for formulation/ development/ elucidation of traditional and innovative composites to logically answer the questions set in Chapter 1 if the waste materials from agricultural/ industrial fields could be used to produce composites with PCR/ SCMs. The results obtained from all these chemical-mechanical syntheses and micro-structural analyses were analysed to determine the effectiveness/ usefulness of this study to achieve the aims and objectives targeted by this research to develop/ elucidate the sustainable materials for greener infrastructure construction and hydromodifications/ water channel stabilisation. The chapter analysed the test results to determine the comparative suitability/ durability/ sustainability and eco-friendliness of the developed composites, especially the **NALFRIC** (Non-Cement, Alternative Lime-Based Fibre-Reinforced Innovative Pozzolanic Composites) and **NAFRIC** (Novel, Alternative Fibre-Reinforced Iron-Based Composites) (NALFRIC and NAFRIC are not legal trademarks but were used to identify the materials formulated in this study).

The results helped investigate/ analyse the suitability of these materials in line with the existing research employing the materials/ methods elaborated in chapters 2 and 3 to determine which pozzolanic materials (GGBS, PFA, SF, MK, RHA, PA) could be used with binders as PCR/ FCR/ SCMs (OPC, lime, iron powder) to formulate in variety of mix ratios by partial replacement of virgin fine/ coarse aggregate (by CG, CR, RPB, RCA, CT) with/ without incorporation of industrial/ agricultural waste fibres (STF, PPF, COF, PETF, WSF). The durability of these developed materials was analysed by comparing the mechanical properties of the composites with the control mixes after 270 days of accelerated exposure in the concentrated sulphate environment and then was investigated for micro-structural analysis using XRD/ SEM to verify the investigation of results obtained by comparison of mechanical properties. The envisaged study on embodied CO₂ and cost/ benefit analysis of the composites demonstrated the eco-friendliness of the developed materials as greener/ sustainable construction

materials as intended substitutes for the traditional OPC-based concrete in multifarious construction stipulations.

4.1 Hydrological Assessments for Channel Lining Requirements

4.1.1 Case Study of Swale River

The research incorporated the hydrological assessments of water channels on a catchment scale to determine the quantum of rainfall/ discharge in a stream and to calculate the strength requirements of greener materials for channel stabilisation/ hydromodifications. Forecasting the predicted precipitation in a stream's catchment and discharge due to a storm event was essential before designing the parameters of channel stabilisation/ lining/ hydromodifications. The Log Pearson 3 Equations 1-11, discussed in section 2.13, could ascertain the exceedance/ probability of storm/ discharge events with the 10 to 200 years return periods. The results obtained could be verified with statistical analysis using Easyfit software to determine the probability distribution factors (Oke and Aiyelokun, 2014; Nadir and Ahmed, 2022a Appendix II, Appendix XIX). The capacity of the structures is then designed based on 100-200 years of predicted storm/ discharge events with a safety and cost-benefit analysis. The discharge in a stream could also be calculated using the correlation between the stage gauge reading placed inside a stream and discharge as shown in Equation 42 and Figure 4.1 (showing a correlation of River Swale four years data for known values of stage gauge reading and discharge to empirically deduce the relationship for future discharge using the stage readings) (NRFA, 2015):

Equation 42: $Q = a(h)^b$ and $Q = AV$

Where Q = discharge; a = coefficient of correlation, h = height of water level/ stage gauge reading and b = exponent of the correlation matrix.

River Swale UK's four-year daily rainfall data (Appendix XIX) and monthly rainfall data (Table 4.1) were used to calculate the hydrological parameters for assessing

materials' strength requirements. Figure 4.1 shows an empirical equation $y = 3.5(x)^{1.412}$ by using an X-Y plotter to identify the values of “a” (3.5) and “b” (1.412) where y is “discharge (Q)” and X is stage gauge reading “h”. This characteristic empirical relationship could be used to determine the discharge value for any future storm event by substituting the values in Equation 42. Using the empirical relationship for respective daily stage gauge height, a total volume of direct runoff per hour V_{DRH} is calculated from the total discharge of 20407 m³ using equation 43 (Doston, 2020; Scribd, 2023) and comes out to be 73465200 m³ ($V_{DRH} = 20407 \times 3600 = 73465200$ m³) in the river in four years as shown in Table 4.2A. This V_{DRH} is converted into equivalent rainfall depth in “mm” to compare with the actual rainfall figures and ascertain the catchment efficiency. The catchment efficiency explains how much water is absorbed/ stored by the total catchment area and how much water drains into the stream as surface runoff. This inflow of water is the actual water flow, which determines the required capacity of the channel and the strength of materials to be used for channel protection/ erosion control.

Equation 43: $V_{DRH} V_{DRH} = \int_t^0 Q_{DRH} (t) dt \cong \sum_i Q_{DRH} \Delta$

The graph in Figures 4.2 and 4.3 shows that rainfall and discharge/ total runoff have a proportional relationship. If the rainfall at a particular time increases in the catchment of River Swale, then discharge in the river also increases due to increased surface runoff. However, rainfall and total runoff vary each month but depend upon seasonal/ temporal variations. Figure 4.3 shows that the maximum total rainfall in a month has resulted in total runoff in mm on the whole catchment, and maximum rainfall was observed in May 2022, which resulted in maximum runoff from the river catchment and maximum discharge in the River Swale. However, it could be inferred from Figures 4.2 and 4.3 that a rainfall/ storm event did not result in the immediate runoff/ discharge event in the stream. Instead, a lag is observed in the creation of increased flow in the stream after rainfall, necessitating the conducting of a hydrograph analysis of the catchment to ascertain the time lag between a storm and a discharge. This time lag between

the conversion of rainfall into a flooding flow allows the designer to plan the storage ponds in the catchment, plan the placing of further obstructions to deter flash flooding and placement of flood prevention/ rescue/ relief mechanisms as per the creation of flash flood basing on catchment efficiency and hydrograph analysis. The exceedance probability of discharge is a statistical technique used to assess the occurrence of certain flooding levels, considering the streams' average flow levels over an extended duration of past data. It is used to plan preventive measures, protection against flooding, community hazards due to flash discharge events after a storm in a river catchment, surge in a base flow of a stream, replenishment of reservoirs through the storm events, regulation of storage water in the reservoirs to determine how much water is required to store and how much should be released on the occurrence of a storm so that existing water is gradually released. Fresh stormwater is stored in the reservoir instead of being converted into an accumulated flash flood (Doston, 2020). Figure 4.4 shows the exceedance probability of converting a storm event into a flash flood in the Swale River catchment. The flow duration curve showed less than a 1% chance that the base flow discharge would be more than $143 \text{ m}^3/\text{sec}$ as per the given discharge data. There is a chance that 90% of the time, it would be more than $1.7 \text{ m}^3/\text{sec}$, even if there is no rain. The river catchment could generate a maximum of $140 \text{ m}^3/\text{sec}$ base flow discharge. However, the flow range of $10\text{-}80 \text{ m}^3/\text{sec}$ is a normal range for the river in a regular storm event. Therefore, the designers must plan flood prevention infrastructure's capacity/ strength/ placement to cater to a flood event of $80\text{-}140 \text{ m}^3/\text{sec}$.

Table 4.1: River Swale Monthly Rainfall Data 2019-2022, Discharge, V_{DRH} and Catchment Efficiency.

Rainfall (mm)	2019	2020	2021	2022	Total
January	57.6	13	108.4	38.4	217.4
February	80.6	109.8	76.2	69	335.6
March	40.2	21	78.2	33	172.4
April	18.2	20.8	131.6	137.2	307.8
May	38	68.4	38.8	277.6	422.8
June	22	75.4	116.8	176	390.2
July	60.2	53.8	57.4	61.4	232.8
August	101.8	33.6	49.2	98.6	283.2
September	27.4	11.8	43.2	111.6	194
October	84	73	106.8	87.4	351.2
November	68.2	92.4	46	49.8	256.4
December	74.8	95.6	26.6	114.2	311.2
Total	673	668.6	879.2	1254.2	3475
Annual Discharge m ³ /sec	3951	3925	5161	7362	20407
Average V_{DRH} (m ³)	14227893	14134873	18587167	26515042	73465200
Equivalent Rainfall Depth (mm)	216.6	215.1	282.9	403.6	1118.2
Average Catchment Efficiency (%)	32.2	32.2	32.2	32.2	32.2

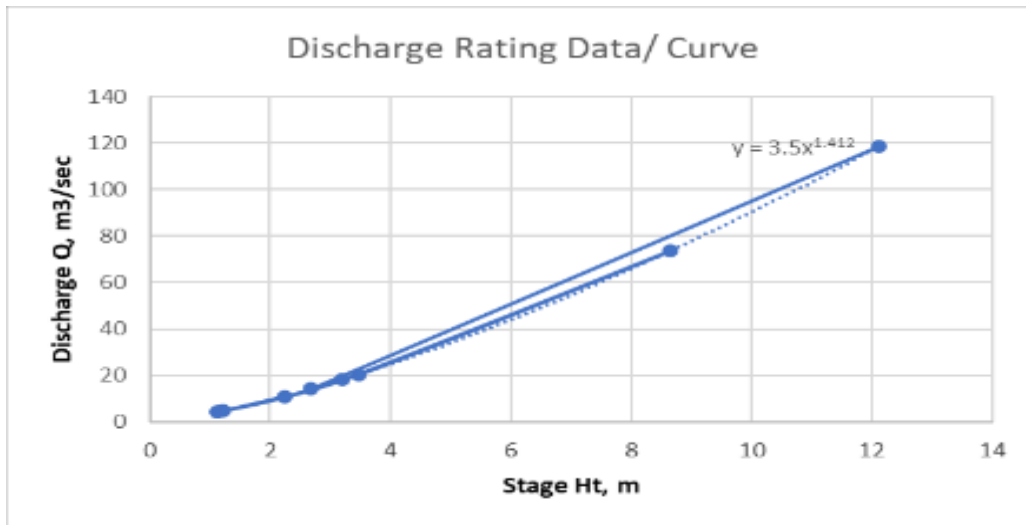
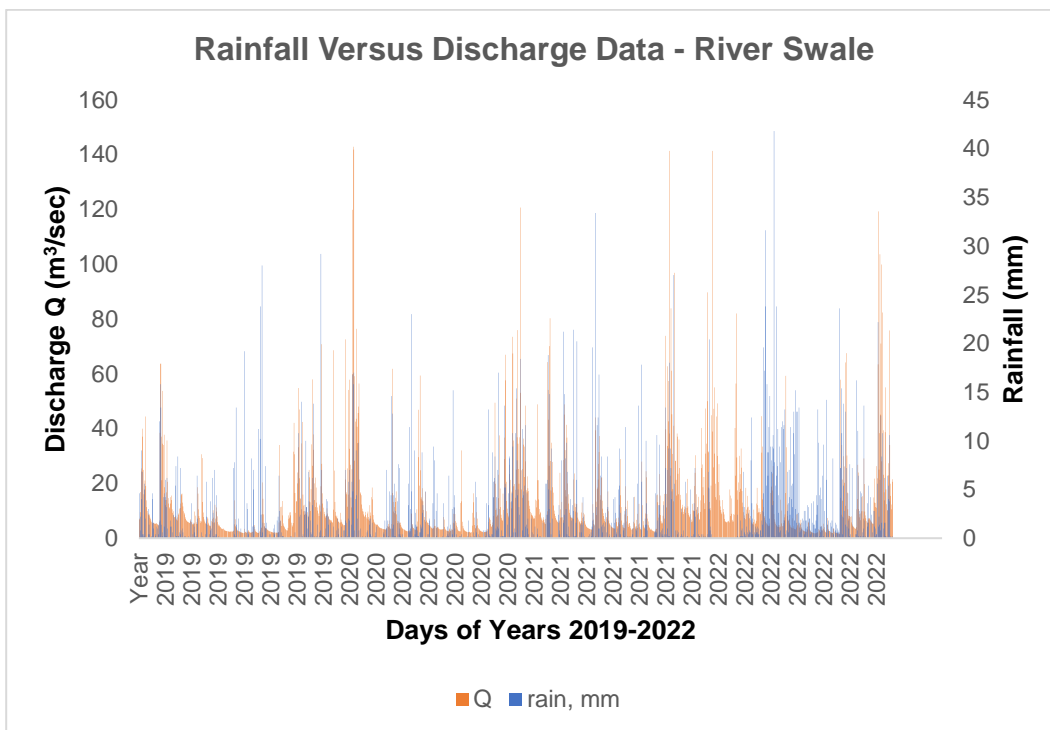


Figure 4.1: Empirical correlation between stream discharge and stage gauge reading



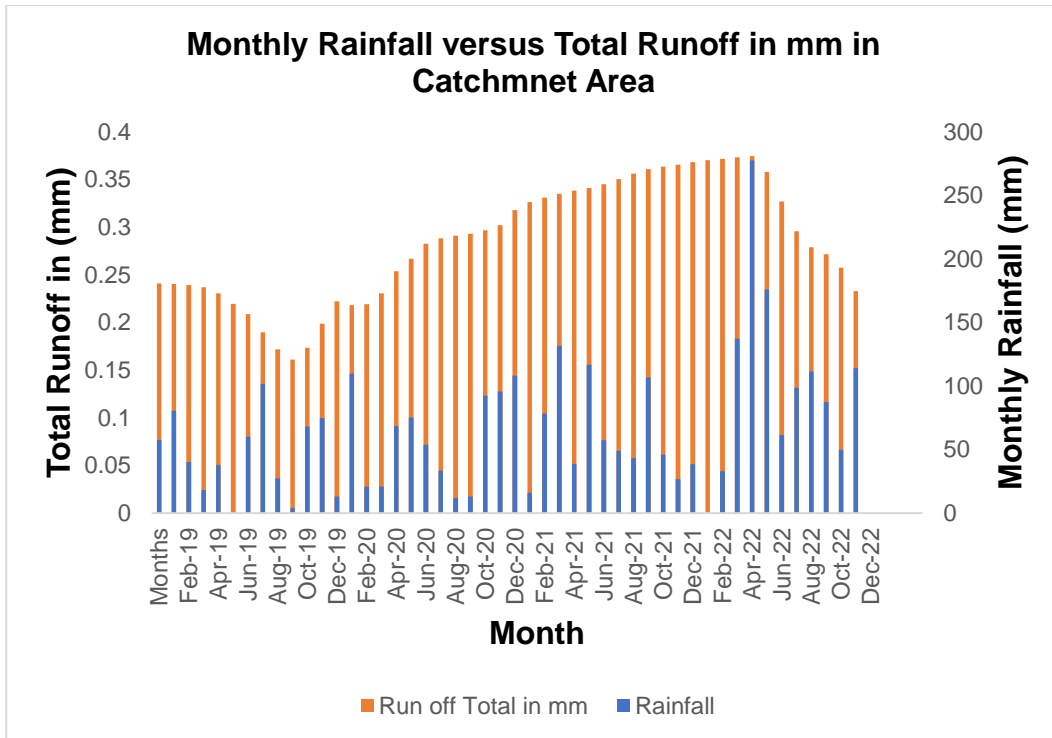


Figure 4.3: Comparison of Monthly rainfall versus total runoff (in mm) in the Swale River catchment area to ascertain a storm event and resultant discharge

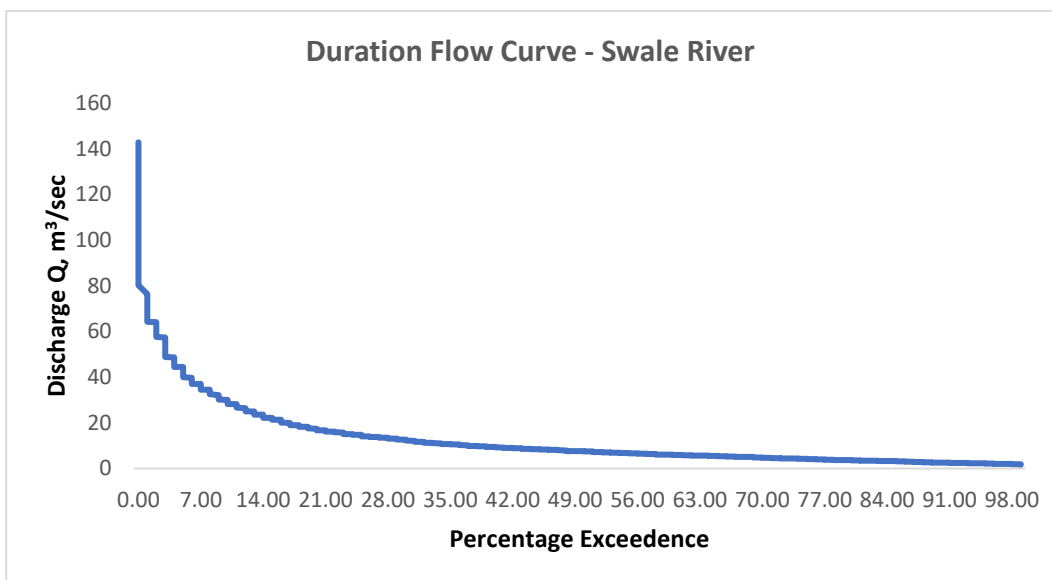


Figure 4.4: Duration flow curve to assess the probability of maximum base flow in River Swale

4.1.2 Hydrograph Analysis for Assumed/ Predicted 200 Years Return Period

Table 4.2A and Figure 4.5A illustrate a hydrograph analysis for a 200-year-return period storm of 2.75 cm/hr, generating a 200-year discharge event of 360 m³/sec in the portion of Swale River having a catchment area of 1446 km². Base flow (150 m³/sec) is subtracted from observed flow to obtain storm flow, and then, the total runoff volume is calculated using equation 43 or calculating the area under the curve in the hydrograph (Table 4.2A and Figure 4.3). The equivalent rainfall depth R_E of the adequate surface runoff volume is calculated by dividing V_{DRH} by the catchment area in meters (1446,000,000 m²) and multiplying it by 100 to get the equivalent rainfall depth in cm. The difference between R_T and R_E then calculates the rainfall loss. The infiltration index is calculated using R_i/R_E , and subsequently, adequate rainfall is obtained by subtracting the infiltration index from the hourly rainfall of the storm event (only positive values are considered, and negative values are taken as zero). The hydrograph calculations are shown below (Table 4.2A and Figure 4.5A). The unit hydrograph obtained by this calculation could now be used to calculate the storm hydrograph of any rainfall duration for the same section/ catchment.

$$\text{Total Discharge} = 14130000 \text{ m}^3$$

$$\text{Equivalent rainfall of total } V_{DRH} \text{ (in-depth cm)} = R_E = 14,130,000 / (1446 \times 1000 \times 1000) * 100 = 1.3 \text{ cm}$$

$$\text{Total rainfall during the storm event} = R_T = 0.25 + 2.75 + 2.75 + 0.25 = 6 \text{ cm}$$

$$\text{Total losses of rainfall volume in cm depth} = R_L = R_T \text{ (Total rainfall)} - R_E \text{ (Equivalent rainfall of total } V_{DRH}) = 6 - 1.3 = 4.7 \text{ cm}$$

$$\text{infiltration index } (\emptyset) = R_E / R_L = 1.3 / 4.7 = 30\%$$

$$\text{Effective Rainfall} = \text{Total rainfall} - \emptyset \text{ (no negative value to be considered)}$$

Table 4.2: **A:** Quantities of discharge and precipitation duration for a 200-year predicted hydrograph analysis and **B:** hydrographs for different storms.

A: Quantities of discharge and precipitation duration for a 200-year predicted hydrograph analysis

Rainfall Duration (h)	Total Rainfall (cm/hr)	R _z	Flow Time (h)	Observed Hydrograph m ³ /sec	storm Hydrograph m ³ /sec	Unit Hydrograph m ³ /sec	Runoff Volume m ³
			0	150	0	0	0
0 - 1	0.25	0	1	150	0	0	0
1 - 2	2.75	2.25	2	350	200	50	720000
2 - 3	2.75	2.25	3	800	650	162.5	2340000
3 - 4	0.25	0	4	1200	1050	262.5	3780000
			5	900	750	187.5	2700000
			6	750	600	150	2160000
			7	550	400	100	1440000
			8	350	200	50	720000
			9	225	75	18.75	270000
			10	150	0	0	0
			11	150	0	0	0
Total	6						14130000

B: Hydrographs for different storms

Time (h)	Unit Hydrograph (UH)	P1*UH	P2*UH	P3*UH	P4*UH	Storm Hydrograph (DRH)	Total Hydrograph (TH)
1	0	0				0	150
2	50	100				100	250
3	162.5	325	0			325	475
4	262.5	525	150			675	825
5	187.5	375	487.5	0		862.5	1012.5
6	150	300	787.5	75		1162.5	1312.5
7	100	200	582.5	243.75	0	1006.25	1156.25
8	50	100	450	393.75	25	968.75	1118.75
9	18.75	37.5	300	281.25	81.25	700	850
10	0	0	150	225	131.25	506.25	656.25
11	0	0	56.25	150	93.75	300	450
12			0	75	75	150	300
1			0	28.125	50	78.125	228.125
3				0	25	25	175
14				0	9.375	9.375	159.375
15					0	0	150
16					0	0	150

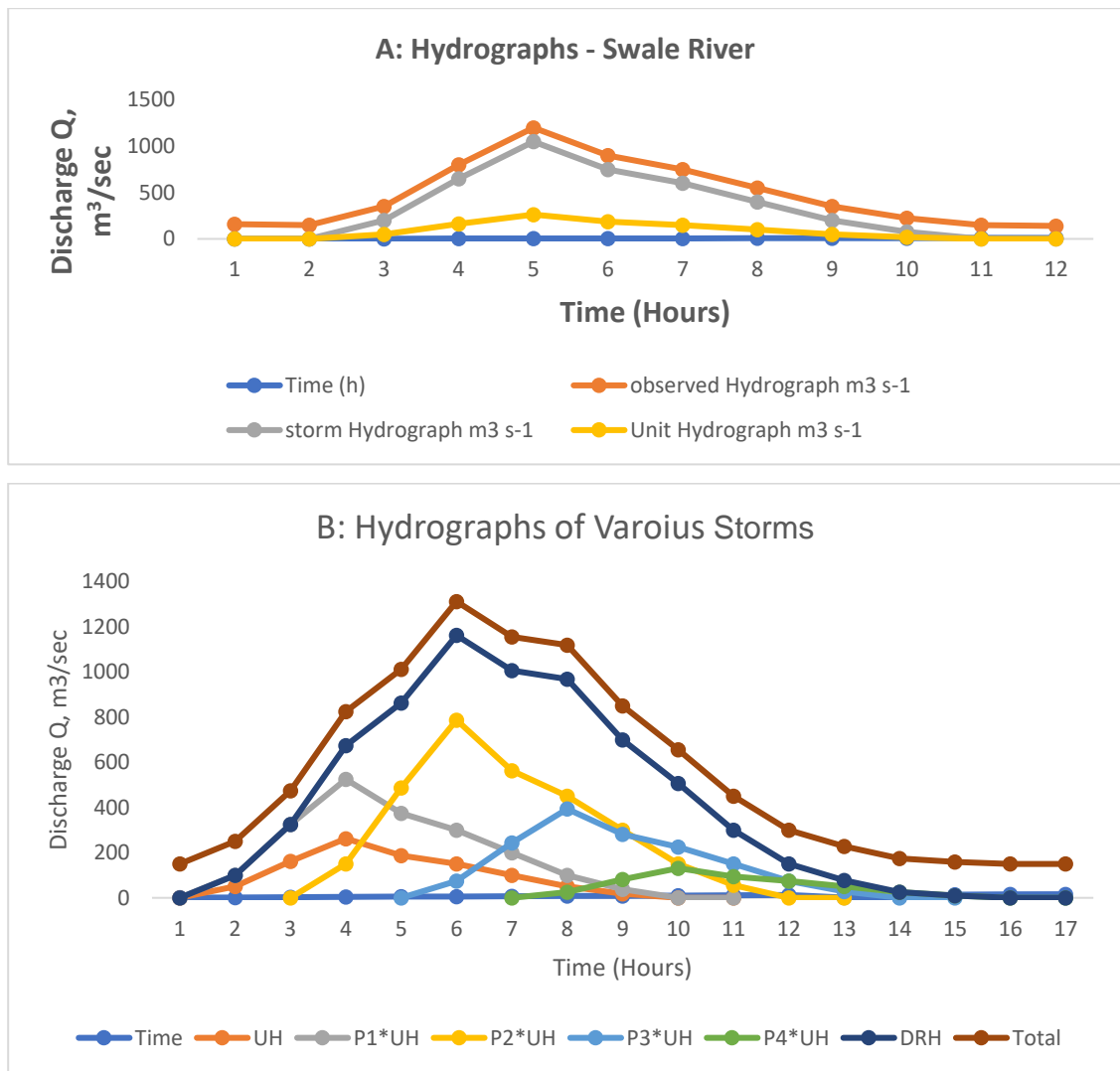


Figure 4.5: **A:** Hydrographs Analysis for 200 Years Predicted Storm Event - Swale River, **B:** Hydrographs of storms of different rainfall intensity/ intervals.

The hydrograph analysis elaborates that storm events generally resemble each other in particular catchment areas if they occur in the same season and with a frequency of rain. However, a storm event profile may be different for different areas based on spatial/ temporal variations as the catchment could be plain/ uneven, barren/ vegetated, smooth/ slopy, saturated/ unsaturated, clayey/ silty/ sandy/ rocky resulting in varying infiltration index. Flood event profile changes

due to the time of the season as saturated/ unsaturated soil conditions, the scale of vegetation, infiltration capacity of the soil, rate of evaporation and obstruction to flow of water from catchment to river due to vegetation may vary with the season/ weather. It is difficult to assess a precise flood event trend; however, a predicted storm event based on the historical flow pattern could demonstrate ideal conditions for flood/ storm forecasting. Generally, in the given catchment area of Swale River in the above data, flood events occurred after the peak rainfall with a 1 to 5-hour lag time and finished in 12 hours to return to the regular base flow. The probability of getting high discharge runoff in lesser lag time is higher in case of more rain in consecutive intervals of time, in wintery/ wet conditions, concluding that a prolonged spell of rain has more probability of a flash flood event.

4.1.3 Storm Hydrograph Calculations Using The Unit Hydrograph.

Once the hydrograph analysis was completed for a given section of a river catchment, the unit hydrograph value could be used to further calculate the hydrographs of different rainfall intensities in the same section of the river/ catchment. Table 4.2B and Figure 4.5B show the 2-hour storm hydrographs P1, P2, P3, and P4, obtained for the same section of the river using unit hydrograph (hydrograph of 1 cm rainfall in a river catchment), using 2 hours effective rainfall interval for a total storm event of 8 hours. The summation of all storm hydrographs (P1-P4) would be the accumulated storm hydrograph for the hourly direct runoff (DRH) in 8 hours. Adding the base flow of $150\text{m}^3/\text{sec}$ would give the total storm hydrograph likely to enter the river after the start of the storm. The storm event would take 17 hours to complete an entire cycle, starting from 0 hours (base flow) to reach the peak at the 8th hour and then return to the regular base flow after 17 hours, as shown in Figure 4.5B. The peak discharge is used to design the channel's capacity, and the hydrograph gives the time lag to plan flood prevention/ rescue infrastructure placement.

4.1.4 Channel Lining Designing Parameters

The channels are lined to protect the water losses due to infiltration in the soil during water transportation from head to tail in different reaches. The unlined canal raises the water table in the surrounding areas, causing saturated soil, water logging and salinity, and loss of precious water (especially if a channel is used for irrigation). The first and foremost design parameter is the impact of lining on the environment/ ecology/ natural habitat of the stream. The economic consideration comes next to deciding whether to construct a lined channel or let it be in the natural strata. The velocity of water, erosion control, structure/ alignment of channel (straight/ meandering), water inflow/ capacity, resistance to storm flow, type/ nature of soil strata of the channel catchment, area of the channel, shape of the cross-section and use/ type of materials are a few important considerations before finalising the decision of lining the channels and use of materials/ techniques. Due to ecological considerations, natural channels like River Swale in the UK are considered best in their natural profile/ strata. However, the sections causing frequent overflowing of the banks/ flooding, erosion, sediment/ gravel deposition, and safety to surrounding assets/ properties are considered to overrule the ecological factors. The necessity of incorporating engineering solutions to safeguard the channel embankments, structures (bridges, culverts, weirs, notches) and human beings/ assets is prioritised with minimal environmental impacts. Generally, the lining could be stone/brick pitching, wooden logs, gravel revetment or vegetation for a low discharge channel. Nevertheless, plain cement concrete with/ without fibres, canvas, meshes, polypropylene tubes/and reinforced earth/ panels are considered eco-friendly solutions for a high discharge channel. However, for very high discharge or in the case of poor bank strata, the use of reinforced cement concrete is considered the long-lasting lining solution (Gnilsen, 1987; www.ceh.ac.uk, 2022; www.directives.sc.egov.usda.gov, 2024; Leika et al., 2000; IFEH, (2008); Tahir et al., 2011; FEHWS, 2013; FEG, 2022; FDG, 2021; FSU, 2012; Scribd. 2023; NRFA, 2015; Kumar, 2020; USDA, 2020; Kim and Lee, 2021; Memon et al.,

2013; NHCP, 2022; Bakhshi and York, 2016; Chapter 5 Open Channels, 2016; Chapter 7 -Ditches and Channels, 2016; Section 44, 2016; The Constructor, 2018; CCLD, 2019; Engineering Toolbox, 2019; Waqas-Chaudhry, 2021; Synthetex, 2023;). The channel cross-section could be triangular for low discharge capacity or trapezoidal/ rectangular for higher discharge capacities. The trapezoidal cross-section is preferred for its better stability with a 2:1 horizontal to vertical slope in the form of 10-15 m panels with a proper jointing system. The preferable thickness of lining for plain concrete is a minimum of 10-20cm for PCC/ RCC and 20-50cm for bricks/ stone lining (IS: 3873- 19192, 1992; Thomason, 2019; Highway Design Manual chapter 860 -roadside channels topic 861 -general, 2020). After conducting the hydrograph analysis, the exact cross-section, discharge, area, wet perimeter, and thickness of lining could be calculated using the Manning equation (Equation 44), UK Flood Estimation Handbook (FEH), Rational method equation (for small catchments) and USGS handbooks (USGSWSS, 2016; Engineering Toolbox, 2019; www.chegg.com, 2023). However, in this research study, guidance is given in UK FEH (IFEH, 2008; FEHWS, 2013; FEG, 2022; FDG, 2021; FSU, 2012), USA design manual (Highway Design Manual chapter 860-roadside channels topic 861 -general, 2020) and Indian code of canal lining (IS: 3873- 19192, 1992) were used for assessment of the lining requirements without going into the details of all canal lining designing calculations as it is not in the scope of the present studies and the objective of the hydrology study is to ascertain the quantum of rainfall, discharge, lag time, infiltration index and channel dimensions to determine the material requirements and in turn assess the environmental impact of the use of concrete.

Equation 44: Manning Equation $Q = \frac{1}{n} AR^{2/3}S^{1/2} = \frac{1}{nP} A^{5/3}S^{1/2}$

Where Q is discharge in m³/sec, “n” is Manning N number from Manning Table, A is the area in m², R is the hydraulic radius in m, and S is the gradient in m/m.

Equation 45: Rational method equation $Q = \frac{1}{360} CiA$

Where Q is discharge in m³/sec, C is the runoff coefficient (ϕ) dimensionless, “i” is the mean rainfall intensity in mm/hr, and A is the catchment area in hectors.

Equation 46: Lag time $t_c = 0.01947 \cdot L^{0.77} / S^{0.385}$

Where L is the length of the catchment in feet, S is the slope of the catchment in foot/foot, and t_c is the lag time between storm and flood events in minutes.

After doing all the designing calculations, we could ascertain that a storm of accumulated rainfall of 6cm could generate a total discharge of 1200 m³/sec. With a 30% catchment efficiency/ infiltration index, only 360 m³/sec (30% of total discharge 1200 m³/se) would enter the stream in 4-5 hours. A trapezoidal channel (Figure 4.6) of 15m base width, 40 m top width, 1 m freeboard, 1 m side extensions, 13.4 m side length, 0.2 m thickness, 6 m depth, 2.6 m/sec flow velocity, area of cross-section 165 m², wetted area of cross-section 137.5 m², wetted perimeter 41m, total lined perimeter 44 m, hydraulic radius 4m, side slope 2:1, and longitudinal slope 0.045, manning n for concrete 0.013, was proposed to accommodate 360 m³/sec discharge, for a catchment area of 1446 km², and length of the river 118 km.

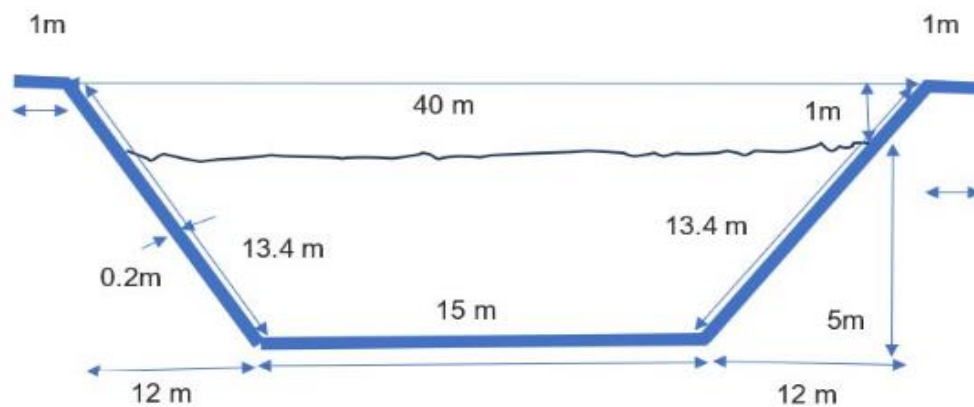


Figure 4.6: Proposed Channel Cross-Section for Swale River Channalisation.

4.1.5 Material Calculations and CO₂ Emissions by Concrete Channel Lining

The required strength of concrete was considered 30 MPa at 28 days of cube testing, the mix ratio is 1:2:3, and the reinforcement requirement was taken as 1% of the concrete (Team, 2018). So, the concrete and steel requirements were calculated as follows:

Total Concrete required = x-sec perimeter of channel x thickness of lining x length of channel

$$\text{Total concrete required} = 42 \times 0.2 \times 118000 = 991200 \text{ m}^3$$

$$\text{Concrete weight} = 991200 \times 2400 = 2,378,880,400 \text{ kg} = 2,378,880 \text{ tons}$$

$$\text{Cement required for } 991200 \text{ m}^3 \text{ of concrete in 1:2:3 ratio (@274 kg/ m}^3\text{)} = 274 \times 991200 = 271,588,800 \text{ kg} = 271.589 \text{ tons of cement}$$

$$\text{Steel reinforcement requirements (@1\% = 78 Kg/m}^3\text{)} = 78 \times 991200 = 77,313,600 = 77314 \text{ tons}$$

The GHG emissions from concrete and steel required lining of Swale River channels of the above-proposed cross-section were calculated using embodied CO₂ data from Table 2.5 with C25/30 concrete having 0.113 kgCO₂eq/ kg and steel having 0.198 kgCO₂eq/ kg (ICE Energy Briefing Sheet, 2011; Obinna, 2023):

$$\text{CO}_2 \text{ emission from concrete} = 0.113 \times 2,378,880,400 = 268,813,485 \text{ kgCO}_2\text{eq} = 5,159,568 \text{ tons}$$

$$\text{Cement required for } 991200 \text{ m}^3 \text{ of concrete in 1:2:3 ratio (@274 kg/ m}^3\text{)} = 274 \times 991200 = 271,588,800 \text{ kg} = 271.589 \text{ tons of cement}$$

$$\text{Cement CO}_2 \text{ emission} = 0.78 \times 271,588,800 = 211,839,264 \text{ kgCO}_2\text{eq} = 211839 \text{ tons}$$

$$\text{Steel CO}_2 \text{ emission} = 0.198 \times 77,313,600 = 15,308,093 \text{ kgCO}_2\text{eq} = 15308 \text{ tons}$$

$$\begin{aligned} \text{Total CO}_2 \text{ emissions from the proposed channel} &= 268,813,485 + 15,308,093 = \\ &= 284,121,578 \text{ kgCO}_2\text{eq} = 284.12 \text{ million kgCO}_2\text{eq} \text{ or } 5,159,568 + 15308 = \\ &= 5,174,876 \text{ tons } 5.12 \text{ million tons CO}_2. \end{aligned}$$

This small study on the designing/ application of channel lining explains that a 118 km long small channel cross-section construction with a 20 cm thick RCC lined channel would likely contribute around 284.12 million kgCO₂eq or 5.12 million tons in the atmosphere along with other ecological impacts on micro/ macro aqua life, biodiversity and natural habitat. It is, therefore, suggested that the use of alternative OPC/ PCR/ TCR in place of 100% cement concrete and fibre-based composites in place of RCC is essentially required to overcome this menace of GHG emissions from the construction industry/ water channel lining.

4.2 Density, Workability and Particle Size Distribution

4.2.1 Density

The density of concrete is a crucial engineering property which describes the compactness of the composite, porosity, air voids ratio and category of light (800-2000 kg/m³), standard (2000-2600 kg/m³) and heavy density concrete (>2600 kg/m³) (BS 12390-7, 2019). The compressive strength of a cube is affected by its density. The compressive strength reduces if the specimen's density falls in lightweight concrete compared to normal/high-density concrete. The density of all the materials under study was calculated using dry mass M_d of 100 mm cubes in the air on digital balance and then weighing the same cubes in water to find the wet mass M_w . The density was calculated using Equation 35:

Equation 35: Density “D” = $[M_d / (M_d - M_w)] \times 1000$

Table 4.3 describes the range of densities of different composites obtained at 7, 28, 90 and 270 days of curing of partial cement replacement (PCR), partial aggregate replacement (PAR), non-cement alternative lime-based fibre-reinforced innovative pozzolanic composites (NALFRIC), novel, alternative fibre-reinforced iron-based composites (NAFRIC). Generally, the densities remained the same at 7 and 28 days of testing. An improvement of up to 1 - 4% in the density of cubes cured for 270 days was observed compared to that of the cubes cured and tested after 28 days. However, some cubes, mainly containing 80%

lime and 20% MK with 2% wheat straw fibres, exhibited a reduction in density up to 2.5% and fell in the light density category, demonstrating less than 15 MPa strength, because of increased quantity of low weight lime, MK and WSF. However, 99% of mixes achieved a density range of 2220-2390 kg/m³ and fell in the standard concrete density range of 2000-2600 Kg/m³.

Table 4.3: Density Ranges - Composites Developed in the Research

Age of Curing (Days)	PCC Density (kg/m³)	PCR Density (kg/m³)	PAR Density (kg/m³)	NALFRIC Density (kg/m³)	NAFRIC Density (kg/m³)
7	2340	2325	2240	1840-2250	2220-2340
28	2340	2325	2240	1840-2250	2220-2340
90	2360	2340	2260	1870-2280	2250-2370
270	2390	2370	2300	1890-2300	2250-2390

4.2.2 Workability

The study aimed to formulate durable SCMs, especially against sulphate attack, so the bear minimum 0.35 w/c ratio was kept for all OPC-based SCMS/ PCRs/ TCRs and iron-based pozzolanic NAFRIC mixes along with a use of plasticiser equal to 0.20-0.25% of binder. A w/c ratio of 0.55 was kept for all hydrated-lime-based pozzolanic composites, including NALFRIC. Generally, all the specimens were observed to achieve a target S1 slump (10-40 mm) for persistently obtaining workable consistency, as specified for this study (BS, 12390-2:2019; Tuan et al., 2021).

4.2.3 Particle Size Distribution/ Gradation Curve / Sieve Analysis

Gradation testing was conducted to assess the particle size distribution and compare the strength parameters of different replacement materials. The particle size gradation is essential to assess the material's behaviour, intra-ingredients binding, strength, sulphate resistance, pore refinement, porosity, permeability and density (Alam and Ahmad, 2020). As discussed in section 3.5.3, the percentages of passing materials (on the Y-axis) were plotted versus the British Standards sieve sizes on the semi-logarithmic X-axis to incorporate all the minor/major sieve sizes' distribution befittingly. Generally, all the materials were observed to have a well-graded particle size distribution as these were pre-specified supplied materials from suppliers/ manufacturers on standards of BS 812-2:1995. All the coarse aggregates passed 100% from 28 number sieve, and 100 CT, 90% VCA, and 86% RCA passed through the 20 mm sieve. 89% CT passed from the 14 mm sieve, whereas 45% VCA and 26% RCA passed from the 10 mm sieve, showing almost identical size distribution for VCA and RCA, but CT exhibited slightly smaller particle size. Vey less coarse aggregates passed through 4.75 mm size as expected from a well-graded coarse aggregate. Almost all the fine aggregates passed through the 4.75 mm sieve as expected. More than 60% of RPB retained on the 2.36 mm sieve, showing lesser gradation, whereas 75% VFA, 84% CG and 73% CR passed through the 2.36 mm sieve. 4.8 – 27% of VFA passed up to 0.15 mm, 7-33% of CG passed up to 0.15 mm, 0.2 – 14 passed up to 0.15 mm, and 0.1 – 1.1% passed up to 0.15 mm, showing better fine particles grading in VFA, CG and RPB and slightly lesser fine aggregate distribution in CR. The results demonstrated identical well-graded particle size distribution by virgin and recycled coarse aggregates crushed tyres (CT), which was observed to be slightly less graded or gap-graded material. It could be predicted that VCA and RCA are likely to achieve identical engineering properties. Virgin fine aggregates, crushed glass (CG) and recycled plastic bottles (RPB) demonstrated well-graded particle size distribution and are expected to achieve identical engineering properties to a certain extent. However,

crumb rubber (CR) showed gap grading/ slightly less graded, as shown in Table 4.4 A and B and Figure 4.7 A and B.

Table 4.4: A and B: Sieve Analysis/ Particle Size Gradation.

A: Coarse Aggregate Sieve Analysis				
BS Sieve Size in (mm)	Virgin Coarse Aggregate (VCA) % Passing	Recycled Coarse Aggregate (RCA) % Passing	Crushed Tyres (CT) % Passing	
28	100.0	100.0	100	
20	90.7	86.8	100	
14	45.2	26.3	89.6	
10	9.6	7.6	55.2	
4.75	1.8	0.5	3.8	
2.36	1.5	0.4	0.5	
Pan	0.0	0.0	0.0	
B: Fine Aggregate Sieve Analysis				
BS Sieve Size in (mm)	Virgin Fina Aggregate (VFA) % Passing	Crushed Glass (CG) % Passing	Crumb Rubber (CR) % Passing	Recycled Plastic Bottles (RPB) % Passing
4.75	98.0	99.8	100.0	100.0
2.36	75.0	84.1	72.6	38.5
1.18	50.3	56.6	13.8	10.0
0.6	27.0	32.8	0.4	1.1
0.3	12.1	16.8	0.3	0.3
0.15	4.8	6.7	0.2	0.1
0.075	2.5	3.0	0.1	0.0
Pan	0.0	0.0	0.0	0.0

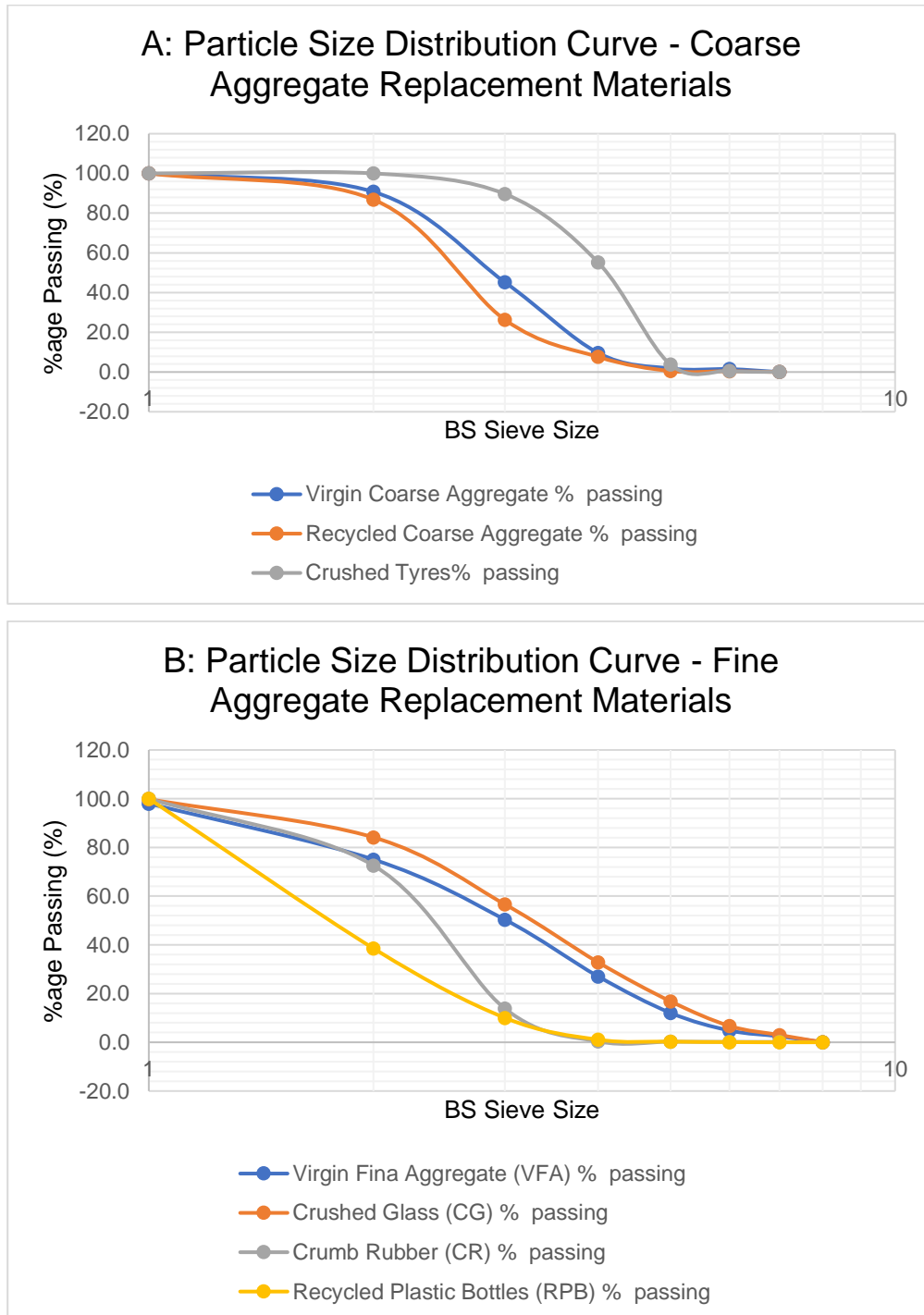


Figure 4.7: (A) and (B) Particle Size Gradation Curves - Virgin Coarse/ Fine Aggregates and Replacement Materials.

4.3 Evaluation of OPC-Based Pozzolanic SCMs (PCR Composites)

As discussed in section 3.4.1, two industrial waste materials, PFA and SF, one cement alternative waste industrial material, GGBS, one naturally occurring pozzolan MK (obtained from natural calcined kaolinite), and two agricultural ashes RHA and PA were used in this study. Their elemental composition was obtained through x-ray fluorescence spectrometry testing outsourced to UK Analytical (UKA) Laboratory Leeds and conducted with the methodology briefly discussed in section 3.7. Results are shown in Table 2.7 (data derived from existing literature and UKA lab testing). The XRF testing was outsourced by sending material samples to the UK Analytic Laboratory by Leeds Beckett University as no facility is available in the local material testing lab. The XRF/ XRD methods were discussed briefly in section 3.7. The samples are ground to powder ($<40\mu\text{m}$ particles) and pre-heated to 975°C for loss on ignition testing to check the pre-mature hydration on exposure to moisture before mixing of materials with water due to inadequate storage conditions (if LOI is more than 30% then pre-hydration is expected with a reduction of compressive strength). This process of grinding and pre-heating may result in a loss on the ignition but improved crystalline morphology, achieved perfect scattering by vibrating/agitating electrons from their shells to get better phases/ peaks of electron diffractions on colliding with x-rays, with more wavelength/diffraction distance “d” and to plot explicit identifiable materials’ peaks on XRF/ XRD spectrums to recognise the ingredients of specimens using AMCSD database (AMCSD, 2023). The job mix ratios of all these materials along with CEM1, virgin fine and coarse aggregate in 1:1:3 job mix formula using 0.35 w/c ratio and plasticiser at 0.20-0.25% of the binder to target S1 slump to obtain 45-60 MPa target characteristic compressive strength were explained in Figure 3.1 and Table 3.3. All the materials were evaluated through x-ray spectrometry to ensure they had more than 75% silicate/ alumina or other oxides of metals (Table 2.7) to accelerate the reaction with OH^- ions released from cement hydration to help form the calcium silica hydrate (C-S-H) gel ideally (Equation 15). The pozzolanic

materials provide silicates to cement concrete, which reacts with aquas portlandite Ca(OH)_2 to convert in the additional quantity of C-S-H gel, increasing the strength of the PCR composites, refining the pore structure/ surface, removing voids, and preventing the internal/ external chemical attack by checking ingress of hazardous salts and maximum utilisation of aquas Ca(OH)_2 (Sotiriadis, Nikolopoulou and Tsivilis, 2012; Divya, Rafat and Kunal, 2015; Kamau et al., 2016; Kavitha et al., 2016; Ahmed and Kamau, 2017; Nadir and Ahmed, 2021b).

Equation 15: $2\text{SiO}_2 + 3\text{Ca(OH)}_2 = 3\text{CaO} \cdot 2\text{SiO}_2 \cdot 3\text{H}_2\text{O}$

The control design mix contained 100% cement CEM1 52.5 as binder with fine river sand and crushed coarse aggregate in a 1:1:3 ratio. GGBS was replaced as 30%, 45% and 60% of the cement weight (kg) as it is considered a direct cement replacement material due to similar contents of SiO_2 and CaO to OPC, with a feasible optimum dosage of 40-80% of the binder (Nadir and Ahmed, 2021b, 2022a). PFA was replaced as 10, 20 and 40% of the OPC weight (kg) as the optimum dosage is up to 40% (Nadir and Ahmed, 2021b, 2022a). SF contained around 99% SiO_2 (Table 2.7) and was considered to react readily with Ca(OH)_2 to form C-S-H gel, but an extensive quantity of SiO_2 could cause the production of Si(OH)_4 gel, which has swelling properties (Equations 31-33).

Equation 26: $\text{SiO}_2 + 2\text{Ca(OH)}_2 = \text{Si(OH)}_4 \cdot 2\text{CaO}$

Equation 31: $\text{SiO}_2 + 2\text{H}_2\text{O} = \text{Si(OH)}_4$

Equation 32: $\text{Si(OH)}_4 + 2\text{Ca(OH)}_2 = \text{Si(OH)}_4 \cdot 2\text{CaO} + 2\text{H}_2\text{O}$

Equation 33: $\text{SiO}_2 (\text{Solid}) = \text{SiO}_2 (\text{Aqueous}) = \text{SiO}_2 (\text{Solution}) = \text{SiO}_2 (\text{gel})$

Swelling

Therefore, researchers suggested the optimum dosage of SF of up to 10%, so 2.5%, 5% and 10% SF were used to formulate the cement-based SF composites (Nadir and Ahmed, 2021b, 2022a). MK is the naturally occurring pozzolanic material derived from calcined kaolinite and contains SiO_2 and Al_2O_3 in abundance, making it less/slow-strength-inducing pozzolan. Studies are still underway to suggest the optimum dosages; therefore, 5, 10 and 20% of binder

weight were replaced with MK to ascertain cement-based MK composites' engineering properties/ benefits (Nadir and Ahmed, 2021b, 2022a). RHA and PA are agricultural waste-based ashes. RHA contains around 97% SiO_2 (Table 2.7), making it an excellent pozzolanic replacement material to produce sufficient C-S-H gel in reaction with $\text{Ca}(\text{OH})_2$. Still, the extensive presence of SiO_2 could produce swelling $\text{Si}(\text{OH})_4$ gel. PA has the least alumina/ silicate composition compared to MK, SF, RHA and PFA (Table 2.7). However, it still has around 55% $\text{SiO}_2 + \text{Al}_2\text{O}_3$ and 23% K_2O , making it a suitable alternative pozzolanic material to impart increased strength with the formation of additional C-S-H gel during the pozzolanic reaction phase of hydration. Although its optimum dosage is not yet determined and researchers use it carefully due to the increased presence of K_2O , which is considered a crack-inducing material (Hewlett, 2004; Neville, 2011; Premalatha et al., 2016; Jonida et al., 2018; Darweesh and Abo El-Suoud, 2019). Therefore, their testing dosages for the formulation of SCMs were kept at 2.5, 5 %, and 10% (Nadir and Ahmed, 2021b, 2022a), as shown in Figure 3.1 and Table 3.3. The compressive strength and split tensile strength results are shown in Figures 4.8 and 4.9.

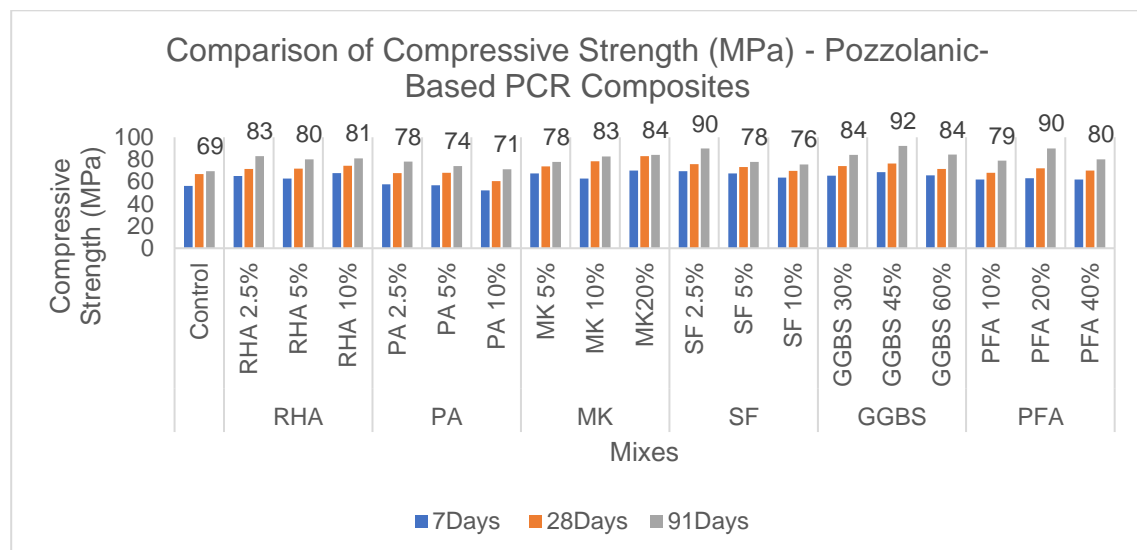


Figure 4.8: Comparison of Compressive Strength (MPa) - Pozzolanic-Based PCR Composites.

All the specimens demonstrated a normal concrete density range of 2250-2390 kg/m³ (Table 4.3). The workability was observed to be reduced with the increased dosages of pozzolanic materials, necessitating an increased quantity of plasticiser to maintain the consistency of the composites, keeping the w/c ratio of 0.35 constant. Figure 4.8 illustrates a massive increase in compressive strength of up to 23% in PCR composites compared to the control mix. The maximum compressive strength of 92 MPa was demonstrated by a PCR composite containing 45% GGBS, closely followed by 20% PFA and 2.5% SF-based composites exhibiting 90 MPa. All the composites achieved high-strength/ high-performance concrete strength, making them suitable for skyscrapers, bridges, dams, barrages and extremely high-strength concrete utilisations in all kinds of construction endeavours. The incorporation of pozzolanic materials as a partial replacement of cement led to an increase in the production of an additional quantity of C-S-H gel over a prolonged age of curing (90 days) (Kosmatka et al., 2002; Atis and Bilim, 2007; Ganesan et al., 2008; Bapat, 2012; Hannesson et al., 2012; Reddy et al., 2013). The optimum dosages of RHA, PA and SF were observed as 2.5%, beyond which the strength started to decrease but still achieved strength at par with the high-strength concrete. A partial replacement of cement by a meagre 2.5% quantity was expected to create a desirable impact on the carbon footprint of cement concrete by decreasing cement use by 100 million tons (2.5% of global use of 4400 million tons of cement) and resulting in a decrease of a hundred tons of embodied CO₂ emissions. However, in equivalent terms, to obtain a comparable high-strength cement-concrete, the job mix ratio would need improvement with increased cement quantity, thus supporting the beneficial use of pozzolans with cement as an improved/ greener PCR composite. Using 5-10% RHA, PA, and SF as pozzolanic cement replacements was suggested to be a better option for obtaining high-strength PCR concrete with a 1:1:3 ratio and promising environmental benefits. Use of 5-10% of RHA, PA and SF would likely result in reduced global annual consumption of 5-10% of 4.4 billion tons of cement, thus reducing 200-400 million tons of CO₂ emissions

(5-10% of 4400 million tons cement as an alternative, rounded off), still demonstrating 70-80 MPa strength. The optimum dosages for GGBS are 45% and 20% for PFA and MK as partial cement replacement, although all other dosages (60% GGBS and 40% PFA) equally performed beneficially in obtaining 80-90 MPa strength. GGBS is considered a direct cement replacement due to its inherent cement-like elemental composition (Table 2.7; Figure 2.46), but it is not available in abundance (makes up only 5% of total cement replacement) and depends basically on the steel industry from where it is obtained as a waste blast furnace slag incurring more transportation cost as compared to cement. However, its characteristic properties to impart additional C-S-H gel/ enhanced strength with reduced CO₂ emissions make it an established beneficial material for PCR composites. However, if it is available in abundance and resorted to as up to 60% cement replacement, then a considerable decrease in the GHG emissions of the construction industry could be observed, though it was not considered practically feasible. Therefore, using PFA up to 40% is another desirable option. However, it also presented the same availability/ transportation cost issue as it is obtained from coal-based power plants, which are increasingly getting obsoleted due to their inherent direct CO₂ emissions on burning of coal, and the world is transferring to alternative greener renewable fuels for power generations. PFA is only 3% of total cement replacement (Table 2.7; Figure 2.46; Scrivener, 2018) due to supply/ availability issues. However, if ideally used as PCR up to 40% feasible dosage, then it could result in a massive decrease in cement use/ CO₂ emissions but is not considered a very feasible future solution due to the disbanding of coal power plants (Malesev et al., 2010; Behbahani et al., 2011; Grzymiski et al., 2019; Pachideh and Gholhaki, 2019; Sowmya, 2020; Vu et al., 2020; Li et al., 2020; Ahmed et al., 2021; Lopez et al., 2022; Nadir and Ahmed, 2021b, 2022a). The best-suggested option is using MK, available in abundance as kaolinite calcined clay, which could be mixed with cement clinker in commercial manufacturing up to 20%, demonstrating up to 84 MPa compressive strength. Its extensive use of more than 20% is likely to reduce the

strength of PCR composites but still could be used in most construction stipulations/ infrastructures, achieving up to 20% reduction in cement usage/ CO₂ emissions by up to 800 million tons per year globally. However, its calcination process requires considerable energy, but it is still in the fraction of energy used to manufacture cement from limestone/ clinker. The split tensile strength of PCR composites improved by up to 17% compared to the control mix (plain cement concrete PCC 1:1:3), as illustrated in Figure 4.9, demonstrating a beneficial use of pozzolanic waste materials in PCR composites. However, split tensile strength is an important concrete property but is not taken as a dependable characteristic as concrete is considered weak in tension and requires reinforcement for improved tensile strength in structural utilisations so in structural design, the tensile strength of plain concrete is always ignored as per Eurocode 2 (Siddique, 2004; EN 1992-3, 2006; Akeem and Mitui, 2017; Scrivener, 2018; ASTM C 125, 2019; Selvapriya, 2019; Girts et al., 2020; Nadir and Ahmed, 2021b Appendix VII). This study suggests using the waste pozzolanic materials as PCR to formulate greener, eco-friendly composites with enhanced mechanical properties and reduced carbon footprints.

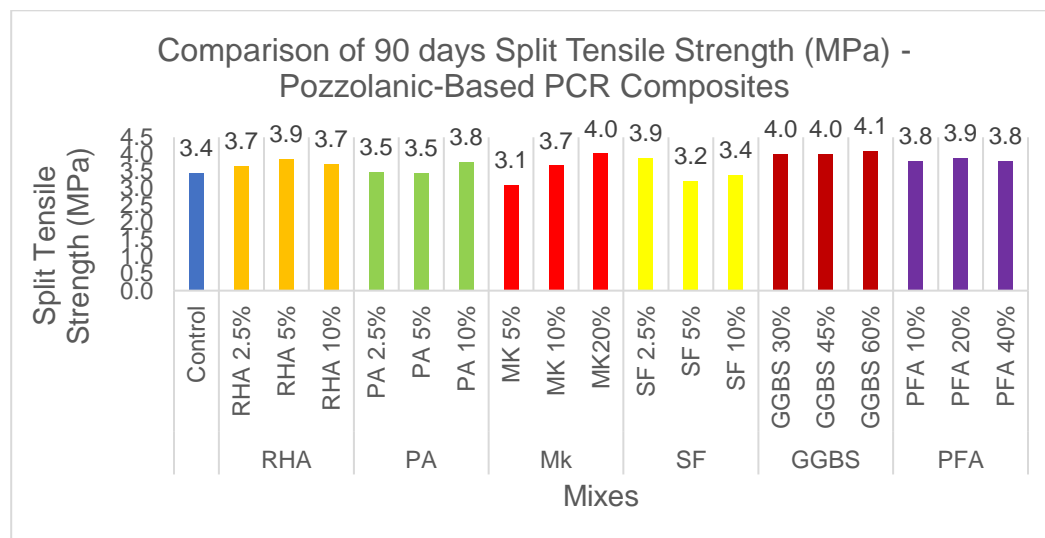


Figure 4.9: Comparison of Split Tensile Strength (MPa) - Pozzolanic-Based PCR Composites.

4.4 Fibre Reinforced Cement Concrete (FRC)

The concrete is considered weak in tension; therefore, steel reinforcement is an essential element of structural concrete for enhanced tensile/ flexural strength and to withstand tensile/ flexural failure (Cement Concrete, 2020; Nadir and Ahmed, 2021b, 2022a). However, the researchers found it uneconomical when there are lesser tensile/ flexural strength requirements, and steel is used as a reinforcement option. Therefore, endeavours were made to incorporate a variety of fibres in plain concrete to achieve improved tensile/ flexural strength compared to PCC. The incorporation of fibres was in use since pre-history times and was considered an economical, eco-friendly, global waste absorption and rewarding option for improvement in the engineering properties of concrete to certain specifications. However, when the tensile/ flexural strengths of the reinforced concrete members are the primary design consideration, the fibres cannot be used as a substitute for reinforcement in structural concrete. The incorporation of fibres is considered to improve the surface/ pore refinement, prevention of micro-structural cracks, prevention of ingress of moisture/ hazardous chemicals, alleviation of explosive spalling of concrete at high temperatures with polymer fibre and improvement in intra-ingredients binding in the internal structure of FRC if the fibres are used up to a specific optimum limit. However, the best results could be attributed to proper placement/ mixing of fibres, orientation, quantity, types of fibres/ concrete, the aspect ratio of fibres, w/c ratio, compaction, and relative toughness/ strength/ elasticity of fibres. The steel fibres are considered established fibres with 40-60 kg/m³ of PCC (10-17% of cement/ binder weight), and PPF is considered beneficial with an optimum dosage of 60-120 g/m³ (1-2% of cement/ binder weight). The understudy fibres like coir, PET bottles shredded fibres, and WSF are still under investigation for their optimum dosages; therefore, in line with the use of PPF, their dosages of 0.5% - 2% (Siddique, 2004; Akeem and Mitui, 2017; The Constructor, 2017; Scrivener, 2018; ASTM C 125, 2019; Selvapriya, 2019; Cement concrete, 2020; Girts et al., 2020; Nadir and Ahmed, 2021b Appendix VII; Admin, 2023) were considered for this study as discussed

in section 3.4.1.2 and shown in Figures 2.57 - 2.60, Figure 3.2 and Table 3.4. A job mix formula of 1:2:3 was used with white cement CEM1 52.5 as binder, virgin river sand and crushed aggregate as fine/ coarse aggregates, regular tap water with plasticiser of 0.2-0.25% of the binder was used to cast self-compacting workable 100 mm cubes for testing at 28, 90 and 270 days of water curing, cylinders and prisms at 90 days of air curing to analyse the compressive, split tensile and flexural strength of the FRC specimens. The fibres are not expected to improve the compressive strength of the composites considerably, but they could demonstrate a slight increase or sometimes even decrease in strength based on the quantity/ types of fibres used in the formulation of the composites. However, an enhancement in the flexural strength was observed using fibres, especially the absorption of energy with increased strain, withstanding increases. All the specimens demonstrated a normal concrete density range of 2250-2390 kg/m³ (Table 4.3). The workability was observed to be reduced with the increased dosages of fibres, especially the agricultural waste fibres of coir and wheat straw, necessitating an increased quantity of plasticiser to maintain the consistency of the composites, keeping the w/c ratio of 0.35 constant.

FRC composites are generally expected to improve flexural strength due to improved elasticity against the bending flexural forces, especially the ability of the materials to withstand the bending load, demonstrating the post-crack ductility before the failure/ rupture (Siddique, 2004; Akeem and Mitui, 2017; TheConstructor, 2017; Scrivener, 2018; ASTM C 618/ C125, 2019; Selvapriya, 2019; Cement concrete, 2020; Girts et al., 2020; Nadir and Ahmed, 2021b Appendix VII; Admin, 2023). Figure 4.10 illustrates the compressive strength of the control mix (without fibres) and FRC composites (with fibres). As expected, the established steel and polypropylene fibres (STF and PPF) exhibited improved compressive strength as compared to the control mix, with maximum strength obtained by PPF 2% composite (66 MPa) and STF 17% (62 MPa). The innovative fibres obtained from shredded PET bottles significantly performed at par with the PPF and STF fibres, elucidating their beneficial use for FRC composites

exhibiting up to 60 MPa strength. Disposal of PET bottles as fibre in FRC was evaluated as an exclusive option to absorb the global plastic waste, especially in the concrete lining of water channels, manufacturing of construction concrete blocks, coastal/ flood break walls, break stones along the sea shores, tunnel lining and embankments/ dams lining. The coconut coir extracted from coconut as agricultural waste and exhibited at par PPF results; however, wheat straw fibre WSF significantly reduced the compressive strength, restricting its use to up to 1%, but it would still be feasible for various structural applications as it still attained compressive strength of normal concrete category (40-50 MPa). Generally, fibre dosages up to 1% performed better in achieving compressive strength; however, increased dosages of fibres reduced compressive strength (Nadir and Ahmed, 2021b, 2022a), as shown in Figure 4.10.

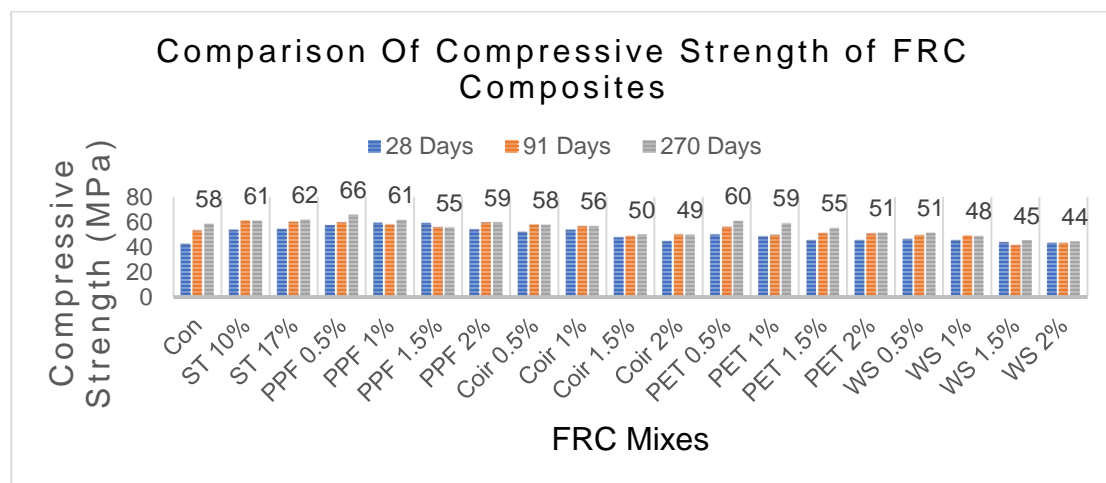


Figure 4.10: Comparison of Compressive Strength of FRC Composites

The split tensile strength of the FRC composites was determined by testing the cylinders at 90 days of air curing by testing as per the procedure outlined in section 3.5.5. Generally, the FRC composites slightly improved the split tensile strength. ST fibres, PET fibres and PPF exhibited the maximum tensile strength of 3.9 MPa, whereas a decreasing trend was observed in the FRC composites containing coir/ wheat straw fibres. The study suggested the beneficial use of PET fibres at par with the established fibres of steel (ST) and PPF; however,

careful use of coir fibres (COF) and wheat straw fibres (WSF) could also fulfil the pre-requisites for slightly lesser strength stipulations with improved tensile strength (Nadir and Ahmed, 2021b, 2022a) as shown in Figure 4.11.

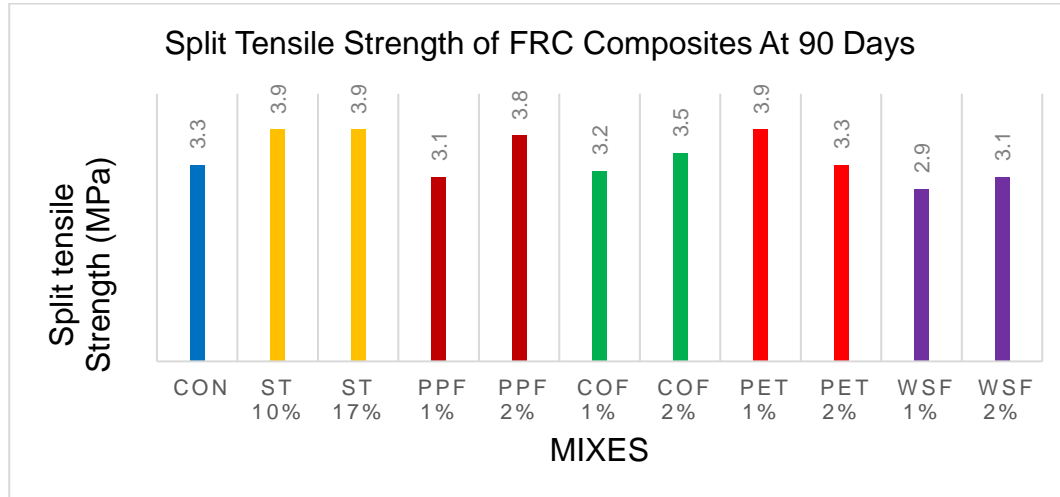


Figure 4.11: Split Tensile Strength of FRC Composites at 90 Days

Fibre-reinforced concrete was expected to perform considerably better than plain concrete in achieving flexural strength. The 500 x 100 x 100 mm air-cured prisms were tested per the procedure discussed in section 3.6 at 90 days. Figure 4.12 illustrates the flexural strengths of the FRC composites studied in this research. The FRC composites containing steel fibres (ST/ STF), PPF, PETF and COF demonstrated an increase of up to 90% in the flexural strength compared to the control mix (4.6 MPa). The maximum flexural strength was achieved by the STF 17% (8.7 MPa), coir 1% (8.3 MPa), PPF 2%, PET 1% (8 MPa) and WSF 2% (7.1 MPa). WSF composites demonstrated the least performance but still achieved around 20% improvement in the flexural strength, suggesting all the understudy fibres could be used with beneficial improvement in the flexural strength by 20-90% with increased/ optimum dosages up to 2%. However, taking into consideration the compressive strength (a vital concrete characteristic), it is suggested that 10-17% STF, 1-2% PPF and PETF and up to 1% coir/ WSF may be used as fibres in the formulation of FRC composites demonstrating enhanced

engineering properties in comparison to PCC with added benefits of prevention of cracks, external sulphate attack, improvement of internal structure, pore refinement and improved intra-ingredients binding along with global waste absorption from other industrial/ agricultural fields into the construction industry for greener/ eco-friendly materials (Nadir and Ahmed, 2021b, 2022a).

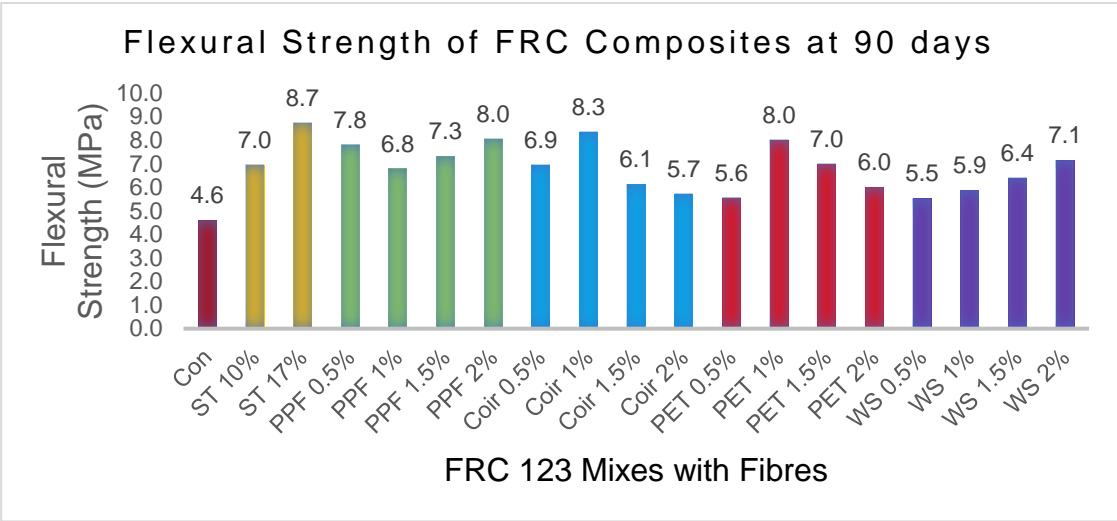


Figure 4.12: Flexural Strength of FRC Composites at 90 Days.

4.5 Investigation of OPC-Based Composites with Partial Replacement of Fine/ Coarse Aggregates

The total quantum of fine/coarse aggregate in the construction industry is estimated to be around 20 billion tons in Asia and around 60 billion tons globally (around 20 billion tons is used only for the production of concrete with 4.4 billion tons of cement), with an estimated net worth of around 500 billion USD, contributing around a billion tons of CO₂ (Mohammed and Najiim, 2020; GMI, 2023). Therefore, even partial replacement of virgin sand/ coarse aggregates with various waste materials like glass, rubber, plastic, tyres, recycled concrete and others would economise the cost of manufacturing the concrete with reduced CO₂ footprints as eco-friendly materials. The mining, excavation, and crushing industry for producing fine and coarse aggregates are experiencing a surge in demand and financial benefits. However, this trend has led to illegal and

uncontrolled production, resulting in a faster depletion of natural resources, non-conservation of these resources for future generations, and damaging environmental impacts. The ecology and biodiversity of natural habitats are also disturbed, and fauna and flora are adversely affected due to the loss of vegetation and reduced water levels after excavation (Kondolf, 1994; Boers, 2005; Stijns, 2005; Jia et al., 2007; Dugan et al., 2010; Freedman et al., 2013; Danielsen and Kuznetsova, 2014; Adu-Gymfi, 2016; Lousiagustin and Kusratmoko, 2016; Pitchaiah, 2017; Koehnken and Rintoul, 2018; Beiser, 2019; Haghnazar and Saneie, 2019; Jordan et al., 2019; Bendixen et al., 2021; Leal Filho et al., 2021; Liu et al., 2022). This study conducted a comparative analysis for investigation of the characteristic compressive and split tensile strength of concrete composites with partial replacement of virgin sand/coarse aggregate by 10-30% of crushed glass (CG), crumb rubber (CR), recycled PET bottles (RPB), recycled concrete aggregate (RCA) and 5-10% of shredded/ crushed tyres (CT) as discussed in section 3.4.1.3 and shown in Figures 3.3, 3.4, Tables 3.5 and 3.6. The job mix formula of 1:1:3 was used with cement CEM1 52.5, regular tap water/ 0.2 – 0.25% plasticiser, and various waste materials as fine/ coarse aggregate replacements to cast 100 mm cubes and prisms for testing at 7, 28 and 90 days of curing as per specified standards [(BS, 12350-1:2019; BS, 12390-2:2019; BS, 12390-3:2019) CEM1 52.5 (BS EN 197-1, 2015), lime (BS EN 459-1:2015), pozzolans, GGBS, iron powder (BS EN 450, 15167, 13263; ASTM C 618/ C125-19), fibres (STF, PPF, PET, COF, WSF) (BS EN 14889-1:2006) BS EN 12620/ 2013; BS EN 1008:2002; BS EN 13670:2009; BS EN 934-2:2009+A1:2012; BS EN 12390-1:2019; BS EN 12390-2:2019; BS EN 12390-3:2019; Kosmatka et al., 2002; Atis and Bilim, 2007; Ganesan et al., 2008; Bapat, 2012; Hannesson et al., 2012; Reddy et al., 2013)]. All the specimens demonstrated a normal concrete density range of 2250-2390 kg/m³ (Table 4.3). The workability was observed to be reduced with the increased dosages of replacement aggregates, especially the RCA, CR and CT composites exhibited reduced workability, necessitating an

increased quantity of plasticiser to maintain the consistency of the composites, keeping the w/c ratio of 0.35 constant.

All the composites containing fine aggregate replacements of 10-30% CG and RPB demonstrated up to 13% increase in compressive strength, whereas the composites containing 10-30% CR exhibited slightly reduced compressive strength but still achieved the C50 (50 MPa) strength suitable for all major structural concrete requirements in normal construction. The variation in the toughness, modulus of elasticity and density of CR are the main reasons for the reduction in the strength compared to the control mix and other replacement composites. The maximum strength was achieved by the RPB composites (73-78 MPa), closely followed by CG's composites, attaining (69-71 MPa) and reaching the high-strength threshold of cement-concrete with virgin aggregates, as shown in Figure 4.13. The primary reason for the comparative decrease in the compressive strength of CR-based fine aggregate replacement composites compared to that of the CG/ PET-based composites was attributed to the physical properties of the replacement materials like rigidity, toughness, density, strength and compactness. The glass is more formidable, denser, and more rigid/ compact than PET, and PET is better than CR, so CG and PET-based composites exhibited better strength than CR. Moreover, the increased volume of CR due to its low density is also a contributing factor which likely created vulnerable weaker zones/ lower intra-ingredients bonding in the CR composites than CG and PET composites. The coarse aggregate replacement composites also exhibited promising results, especially 10-30% RCA composites attaining a high-strength threshold of more than 70 MPa strength, exhibiting an overall enhancement in the strength by up to 12%. The composites with 5% CT performed at par with other high-strength attaining composites; however, a decreasing trend was observed with increased dosage of CT of more than 5% (Figure 4.14), nevertheless achieving more than C50 (50 MPa) strength sufficient for all prominent concrete utilisation in normal/ structural construction. All the mixes generally achieved the target compressive strength of C55/ 67 or M67 concrete

at 90 days of curing, exhibiting an increasing trend with the increased curing age. The composites with CR and CT exhibiting slightly lesser strength achieved the threshold C30/ 37 (37MPa) (required for most common concrete infrastructure/ structural applications). Generally, all the fine/ coarse aggregate composites attained marginally increased split tensile strength at 90 days of cylinder testing and exhibited up to 10% improvement compared to the control mix (3.9 MPa). The maximum split tensile strength was demonstrated by the replacement composites containing RPB (4.3 MPa), CG (4.2 MPa) and CR (4.1 MPa). A decreasing trend in tensile strength was observed in the composites containing CT (3.9 MPa), and the RCA composites exhibited the least strength (3.6 MPa), as shown in Figure 4.15. However, split tensile strength is not considered the primary characteristic of concrete utilisation as it is considered weak in tensile/ flexural strength and requires incorporating steel reinforcement for enhanced tensile/ flexural strength in structural concrete requirements. Therefore, the composites formulated in this study could be used broadly in all 50-80 MPa strength stipulations in the construction industry as greener, economical, and waste-absorbent materials with low CO₂ emissions. Suppose the construction industry adopts up to 30% replacement of fine/coarse aggregates. In that case, there would be a conclusive benefit in befitting disposal of 30% of waste from other industrial/ agricultural waste in the formulation of functional concrete composites, reducing the enormous global effort on waste disposal/ recycling. Using 30% replacement aggregates could reduce mining/ extraction of up to 30% virgin sand/ gravel and crushing rocks for manufacturing/ utilisation as fine/ coarse aggregate in the construction industry, amounting to around 6 billion tons per year (30% of 20 billion tons of aggregates used for concrete related construction). A 30% reduction could considerably reduce the cost of construction by using waste materials instead of precious natural resources and preserving them for the next generations. A reduced mining/ extraction of naturally occurring river/ marine sand and gravels/ crushed rocks would safeguard the ecology, geomorphology, natural habitats and stream channels from erosion/ disturbance.

Above all, a 30% decrease in the utilisation of virgin aggregates would save the planet from the embodied emission of 300 million tons of CO₂ per year from construction. This study has focussed on the formulation of medium to high-strength concrete composites using up to 30% aggregate replacements. However, added benefits could be obtained with the increased percentage of aggregate replacements for lower-strength concrete utilisation, fetching even better ecological/ environmental/economic benefits subject to further studies. The results are supported by contemporary research on using various fine/ coarse aggregate replacement materials, as already discussed (Brandit, 2008; Saikia, 2012; Onuaguluchi and Panesar, 2014; Rowhani and Rainey, 2016; Mohammed et al., 2021; Shahbaz and Tajara, 2021; Nadir and Ahmed, 2023c Appendix XIV).

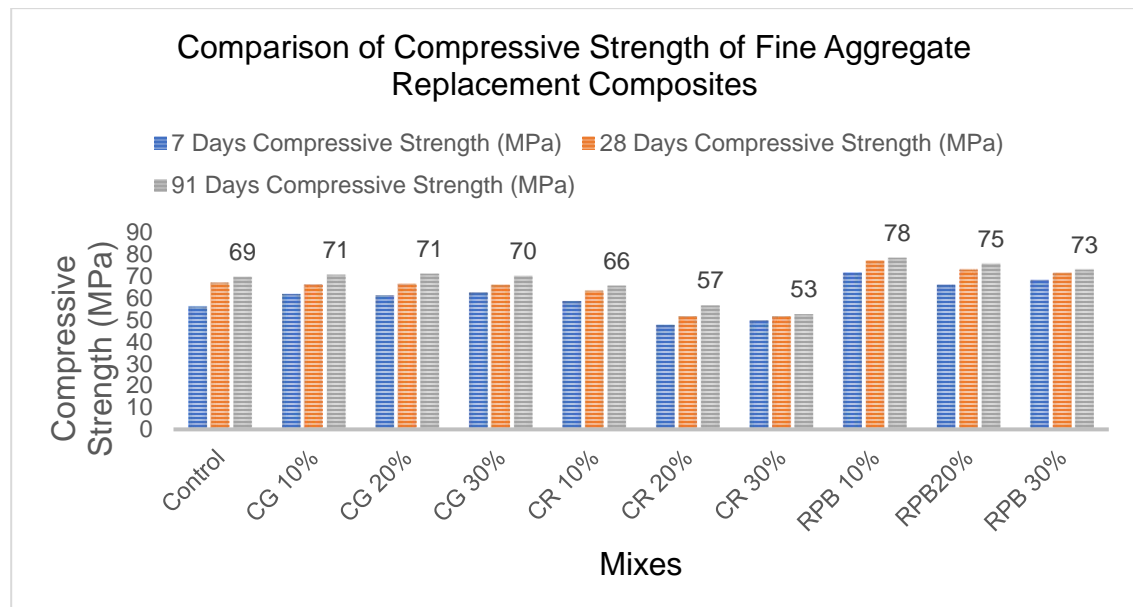


Figure 4.13: Comparison of Compressive Strengths of Fine Aggregate Replacement Composites

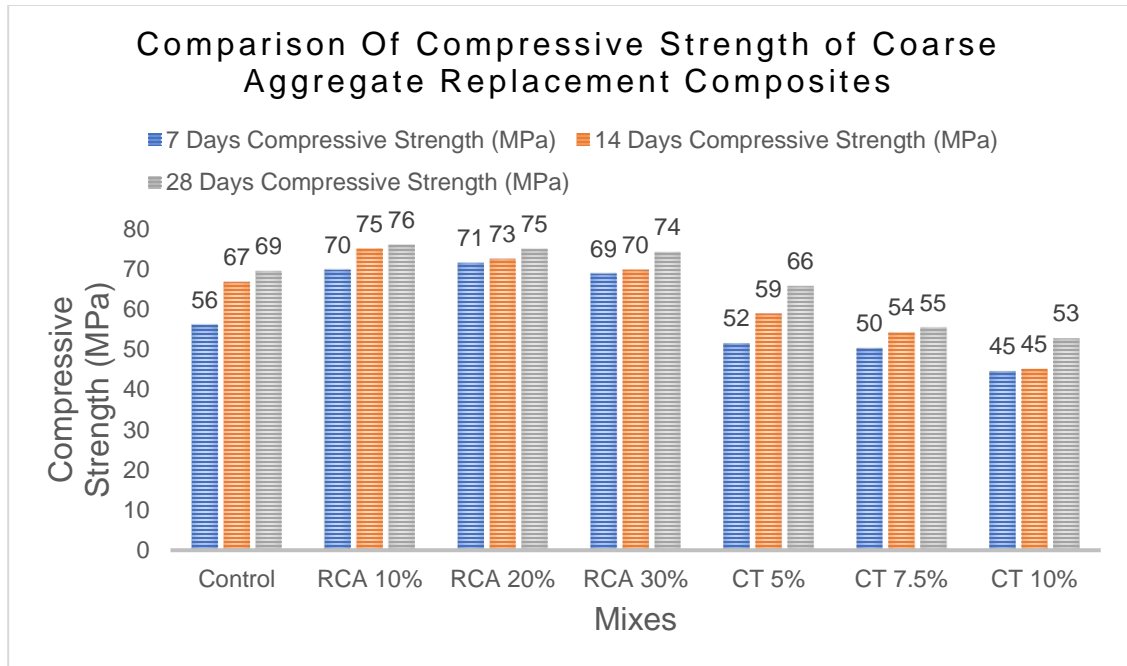


Figure 4.14: Comparison of Compressive Strength of Coarse Aggregate Replacement Composites

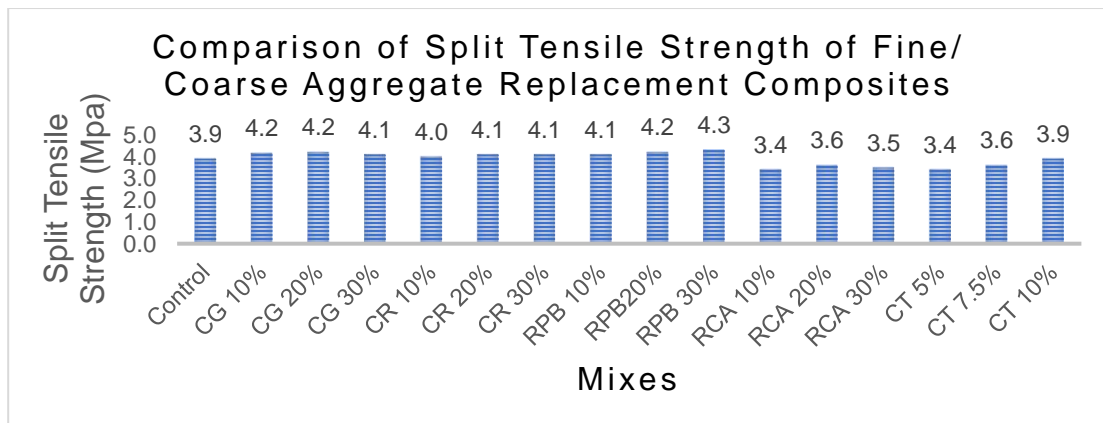


Figure 4.15: Comparison of Split Tensile Strength of Fine/ Coarse Aggregate Replacement Composites.

4.6 Elucidation of Cement-Free Hydrated Lime-Based Pozzolan Composites

In ancient civilisations, lime was used in historical buildings for thousands of years. However, its slow setting time and low strength make it less attractive for advanced structural construction in the modern era. Manufacturing Portland cement has revolutionised construction methods and enabled engineers to design/ construct master construction pieces involving skyscrapers and high-strength/ high-performance cement concrete structures. However, embodied CO₂ of the cement concrete (1 ton per ton of cement, the majority of which is emitted during cement manufacturing from limestone/ clinker) has compelled researchers and engineers to revert to lime-based construction materials, especially for low-strength construction requirements. Lime is still essential in cement manufacturing, constituting around 62% of lime (MIT, 2009; History of Concrete, 2012; EPA, 2015; Nadir et al., 2022b Appendix XII). The types of lime and its broad spectrum uses were discussed in sections 2.3.1 – 2.3.3. The large-scale environmental impact of extensive use of cement concrete influenced the research on forming cement-free lime-based composites in this research project. Therefore, the research was designed to use the hydrated lime Ca(OH)₂ as a binder with different cement alternative/ pozzolan materials having pozzolan characteristics/ oxides of metals up to 70% as per ASTM standards (ASTM C 618/ C125, 2019) as shown in Table 2.7. Lime (Sotiriadis, Nikolopoulou and Tsivilis, 2012), and SCMs like industrial/ agricultural pozzolan materials like pulverised fly ash (PFA), ground granulated blast furnace slag (GGBS) (Ahmed and Kamau, 2017), rice husk ash (RHA), palm ash (PA), corn cob ash (CCA) (Kamau et al., 2016), metakaolin (MK) (Kavitha et al., 2016), zeolite (Najimi et al., 2012) and silica fume (SF) (Divya, Rafat and Kunal, 2015) are good options of formulating cement-free limecrete.

In this study, ground granulated blast furnace slag (GGBS/ slag), pulverised fly ash (PFA) and silica fume (SF) were used as industrial waste materials having

pozzolanic qualities to blend with the hydrated lime. These materials are not available in abundance and have a limited supply (3-7% of global cement demand), which too is restricted by the production quantity of steel, the burning of coal in power plants and the silicon industry, which is likely to reduce in the future due to their extensive GHG emissions. Therefore, another naturally occurring pozzolanic material, metakaolin (MK), was added to this study. Metakaolin is extracted from the calcination of kaolinite (China clay) and is available in abundance as lime on Earth. Hydraulic lime and lime putty are common in the construction industry for mortars, facade work and binders for low-strength utilisation or mixing with cement/ pozzolans. However, a gap was observed when using hydrated lime with pozzolans to formulate cement-free lime-based composites. Therefore, 100% hydrated lime was used to prepare the control mixes, and 10-90% of the pozzolans (GGBS, PFA, SF and MK) were used in the job mix ratios of 1:1:2, 1:1:3, 1:2:3 and 2:1 as discussed in section 3.4.2 and Table 3.7 for the casting/ testing of these composites for compressive and flexural strength. Regular tap water was used in 0.55 water/ binder ratio with virgin sand/ aggregate to prepare the mixes for casting 100 mm cubes to test at 7, 28, 90 days of air curing (AC) and 90 days of water curing (WC) for compressive testing and 500 x 10 x 100 mm prisms for testing of flexural strength at 90 days of air curing. All the specimens demonstrated a normal concrete density range of 2000-2350 kg/m³ except MK-based 80% lime-containing composites, which exhibited reduced density and fell in the light concrete range of 1800-2000 kg/m³ (Table 4.3). The workability was observed to be reduced with the increased dosages of pozzolans, especially the MK, SF and PFA, necessitating an increased quantity of water to maintain the consistency of the composites, compelling to keeping an increased w/c ratio of 0.55 without adding any plasticiser (Nadir and Ahmed, 2020; Britannica, 2022; Rehan and Nehdi, 2020; Worrell et al., 2001; Rajkumar, 2017; Nadir and Ahmed, 2021b Appendix VII; Akca, Cakir and Pek, 2015; Yildirim, Sahmaran and Ahmed, 2015; Ahmed et al., 2020 Appendix IX).

4.6.1 Control Mixes

The control mixes for all the job mix ratios of 1:1:2, 1:1:3, 1:2:3 and 2:1 were formulated using 100% hydrated lime as a binder with sand and coarse aggregate. The cubes were cast and tested at 7, 28 and 90 days of air cured (AC) and 90 days of water curing (WC). The maximum compressive strength of 1.5 MPa (air-cured) and 1.6 MPa (water-cured) of the hydrated lime-based cement-free composites (limecrete) was exhibited by a 1:1:2 ratio, followed by 1:1:3, 1:2:3 and lastly, the 2:1 ratio as shown in Figure 4.16. Hydrated lime-based cement-free limecrete demonstrated a very meagre strength, limiting its use to meagre strength requirements rather than making it uneconomical to use costly materials for a meagre strength. The control mixes failed to reach the minimum target strength of 15 MPa for limecrete, suggesting formulating composites with pozzolanic materials to impart essential SiO_2 ingredients to the mixture during the hydration process to form strength-inducing C-S-H gel. Therefore, further research was conducted on the formulation/ testing of 10-90% pozzolanic-based limecrete. It is evident from the mix ratios that 1:2:3 contains 1 part of binder versus 6 parts of aggregates and is thus expected to be the weakest compared to other mixes having 1:1:2 (1 part binder with 3 part aggregate), 1:1:3 (1 part binder and 4 part aggregates) and 2:1 (1 part binder and 2 parts of total fine/coarse aggregates). The best performing ratio was observed to be the 1:1:2 having a balanced binder and aggregates ratio as compared to all others, either having more aggregates portions (1:2:3 or 1:1:3) or 2:1 ratio having a lesser portion of aggregates as compared to binder comparatively. As discussed in succeeding sections, the results supported using a 1:1:2 ratio as an optimum ratio for cement-free hydrated lime-based pozzolanic composites.

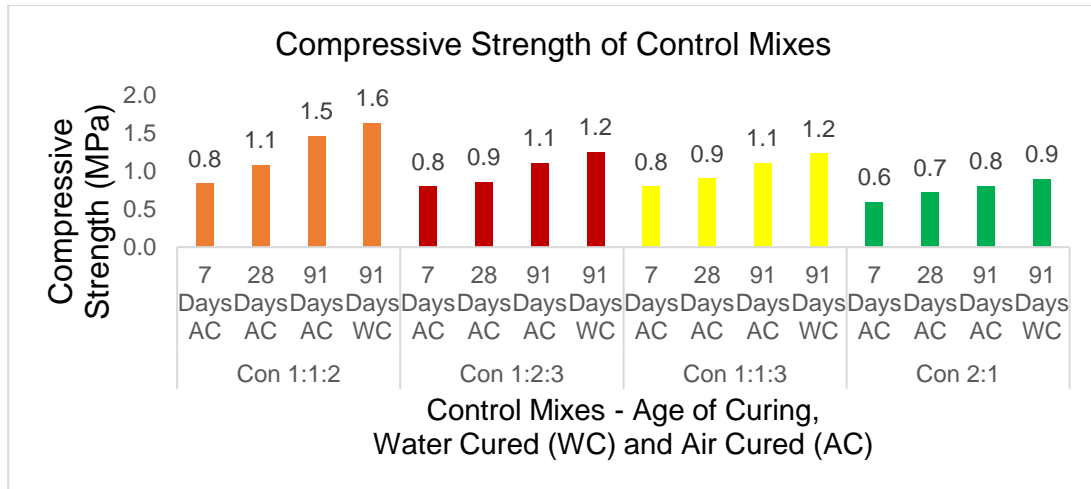


Figure 4.16: Compressive Strength of Cement Free Lime-Based Control Mixes.

4.6.2 Hydrated Lime (CL90)-Based Composites with 10-90% GGBS/ Slag (SL)

GGBS or slag (SL) is derived as waste material from the steel industry and is considered the direct cement replacement material, demonstrating the similar composition/ behaviour of OPC, as shown in Table 2.7. Slag is already used for the formulation of PCRs and geopolymers in the construction industry and is likely to impart considerable strength of composite if used with hydrated lime to induce pozzolanic reaction during the hydration process to form an adequate quantity of C-S-H gel. SL is considered a sustainable material which results in pore refinement, reduces voids, improves intra-ingredients binding, prevents creation/ propagation of cracks and stops ingress of hazardous chemicals (sulphates) from acting strongly against the sulphate attack/ formation of ettringite (Hewlett, 2004; Oner and Akyuz, 2007; Neville, 2011; Sakai, Nakamura, and Kishi, 2013; Samad and Shah, 2017; Prasanna, Srinivasu and Murthy, 2019; Cunliffe et al., 2021 Appendix III). The SL mixes for intended job mix ratios of 1:1:2, 1:1:3, 1:2:3 and 2:1 were formulated using 10-90% slag and 90-10% hydrated lime, respectively, as a binder with virgin river sand and coarse aggregate as shown in Table 3.7. A w/b ratio of 0.55 was used as a constant for all the mixes, although a few mixes

exhibited very wet (with fewer percentages of slag) and a few showed quite a dry mixture (with increased percentages of slag). Still, all the mixes demonstrated workable consistency for the casting of specimens. The cubes were cast and evaluated at 7, 28 and 90 days of air and 90 days of water curing. As expected, the best-performing job mix ratio was 1:1:2, demonstrating a maximum compressive strength of 21.8 MPa for air-cured cubes and 26.4 MPa for water-cured cubes. As expected, the age of curing affected the strength of the composites due to delayed chemical reactions for the formation of C-S-H gel during the hydration process. An increase of up to 21% strength was observed in water-cured specimens, suggesting achieving better results if cured in water or used in the water channels where composites could be exposed to water for a prolonged period. The best strength of 26.4 MPa was demonstrated by the SL80 (20% hydrated lime and 80% slag) in all the job mix ratios, closely followed by SL 60 to SL90 composites (Figure 4.17, 4.18). SL80 in the job mix ratio of 1:1:3 demonstrated 24 MPa (Figure 4.19), SL80 in the job mix ratio of 1:2:3 showed 23.2 MPa strength (Figure 4.20) and SL90 in the job mix ratio of 2:1 exhibited 23.2 MPa strength (Figure 4.21). Generally, the composites containing 20-50% lime and 50-90% slag achieved a target strength of 15-25 MPa. Figure 4.22 shows the flexural strength of CL90-based slag composites with inconsistent results. SL70 in the job mix ratio of 1:1:2 and SL60 in the 2:1 ratio demonstrated the best flexural strength of 2.6 MPa (at par with the PCC), SL90 in the job mix ratio of 1:1:3 and 1:2:3 achieved 2.5 and 2.5 MPa strengths. The results suggest a beneficial use of these composites for all standard concrete utilisations up to 15-25 MPa strength requirements (subgrades, foundations, flooring, walls, tiles, blocks, small channel lining, embankments, flood bunds, earthen embankment's stone pitching, standard building construction) with minimal embodied CO₂. However, the cost, supply, transportation and availability of slag in abundance are the issues restricting its large-scale use as cement replacement. Still, it is among the significant cement replacement materials and could successfully be employed in forming cement-free limecrete emitting a tiny quantity of CO₂. The

suggested use of this composite for low strength requirements is up to 30% and reduces the carbon footprints of the construction industry by up to 30% (around 1400 million tons of CO₂, i.e., 30% of 4400 million tons of global OPC use (Purnell, 2013; UNEP, 2020; Lupien, 2020; Obinna, 2023)).

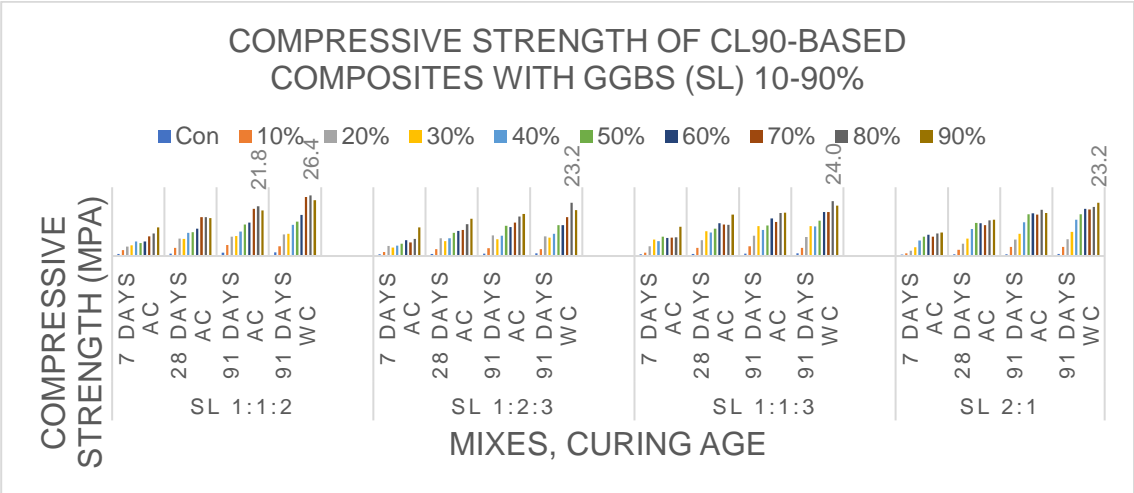


Figure 4.17: Compressive Strength of CL90-Based Composites With GGBS (SL) 10-90%.

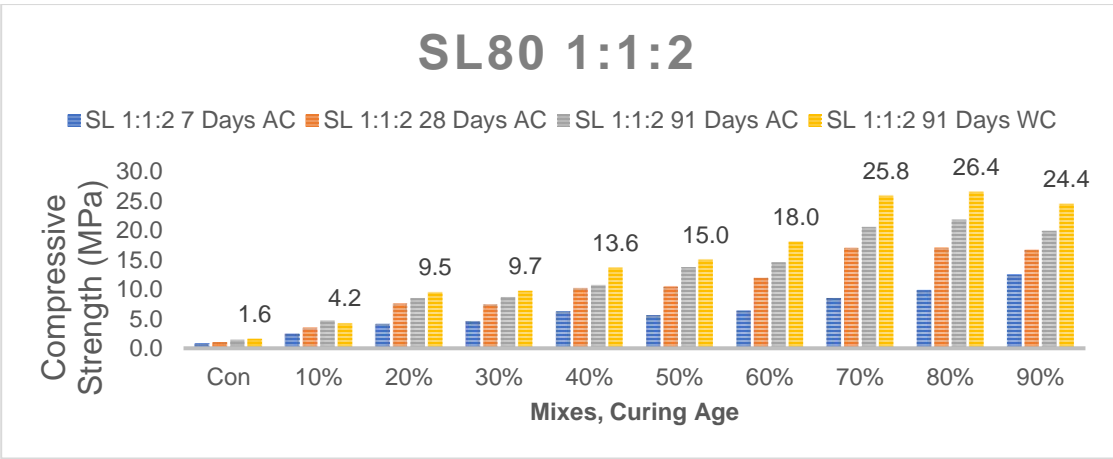


Figure 4.18: Compressive Strength of CL90-Based Composites With GGBS (SL) 10-90% 1:1:2 Job Mix Ratio

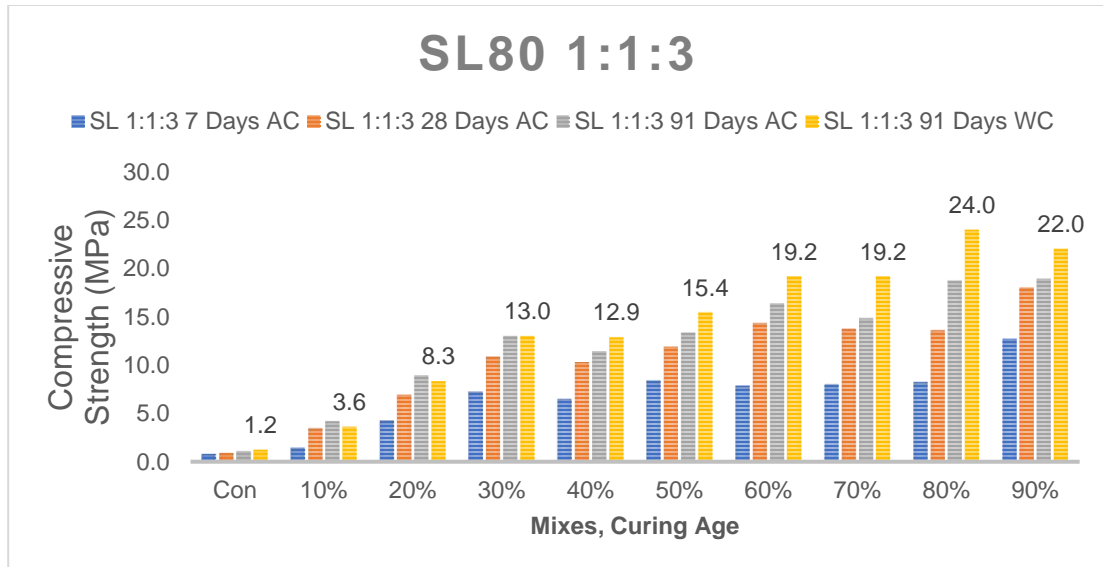


Figure 4.19: Compressive Strength of CL90-Based Composites With GGBS (SL) 10-90% 1:1:3 Job Mix Ratio

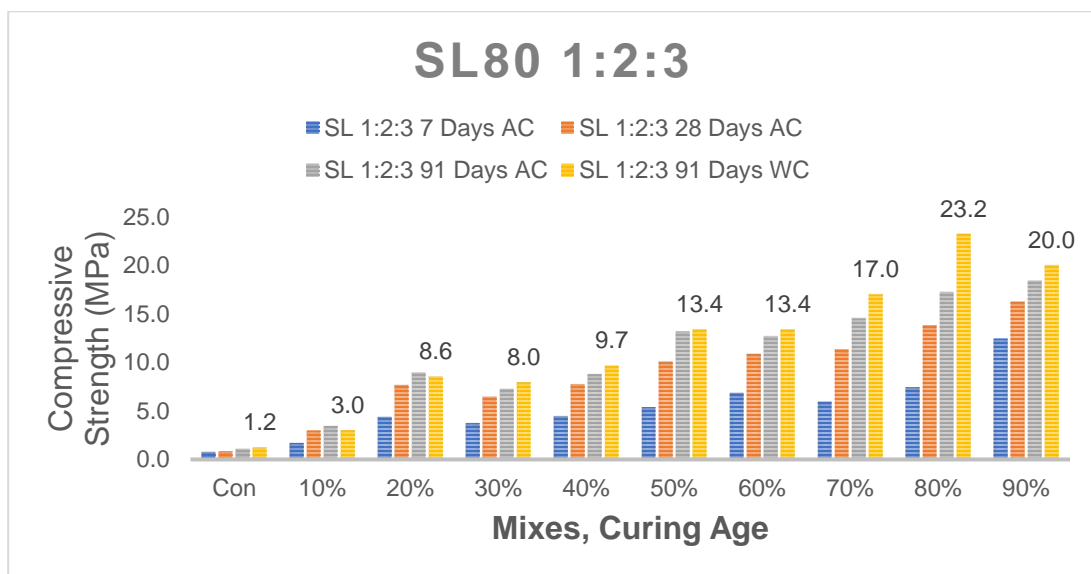


Figure 4.20: Compressive Strength of CL90-Based Composites With GGBS (SL) 10-90% 1:2:3 Job Mix Ratio

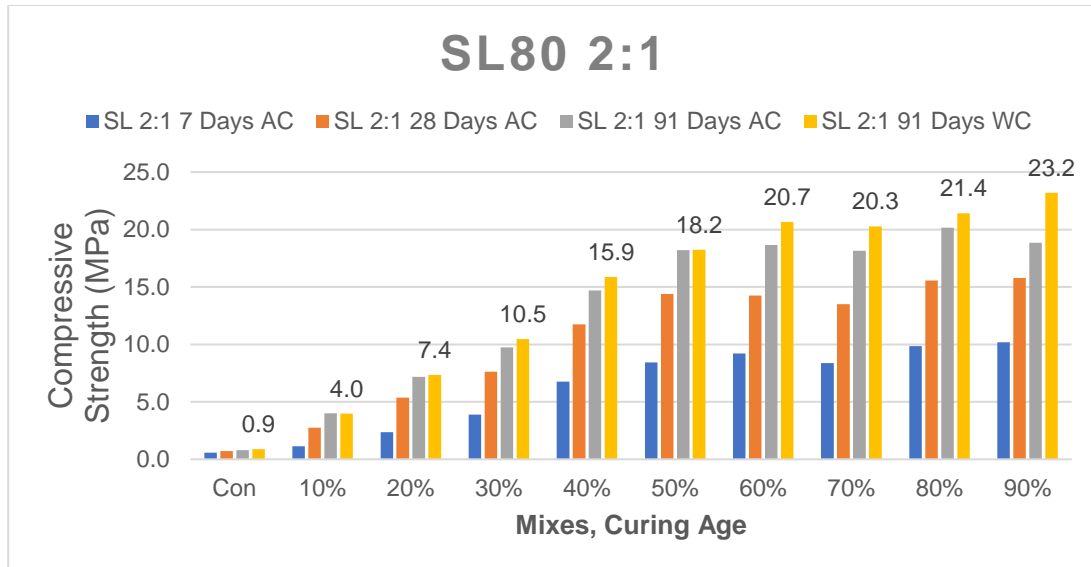


Figure 4.21: Compressive Strength of CL90-Based Composites With GGBS (SL) 10-90% 2:1 Job Mix Ratio

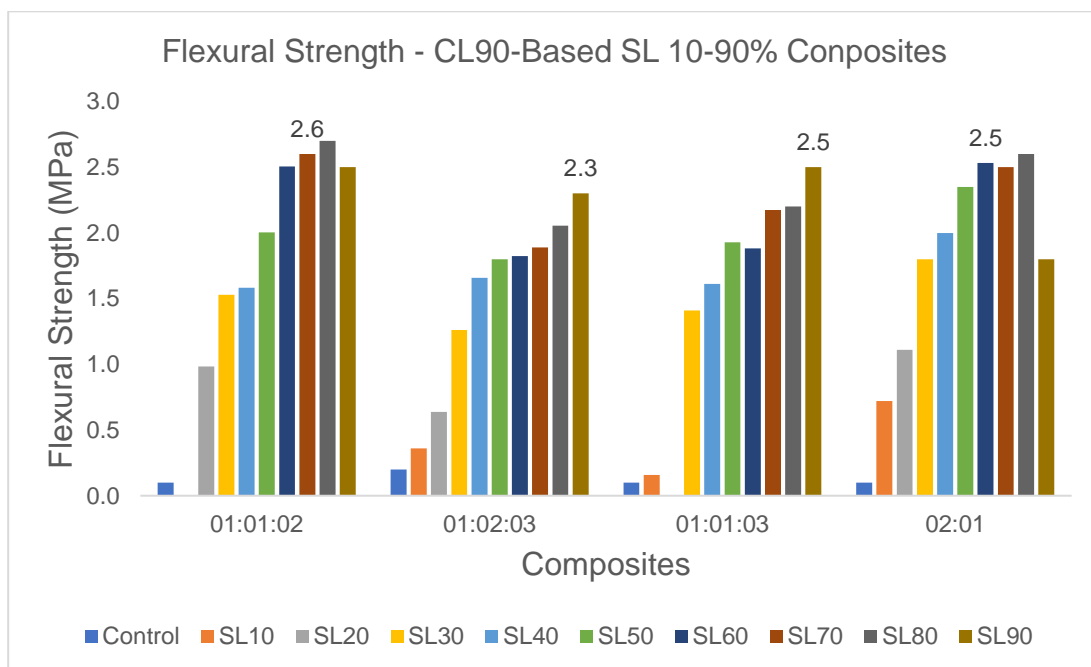


Figure 4.22: Flexural Strength - CL90-Based SL 10-90% Composites

4.6.3 Hydrated Lime (CL90)-Based Composites with 10 -90% Fly Ash (FA), Silica Fume (SF) and Metakaolin (MK)

The composites for all the job mix ratios of 1:1:2, 1:1:3, 1:2:3 and 2:1 were formulated using a mixture of 10-90% hydrated lime and 90-10% PFA or SF or MK (as a pozzolanic component) respectively, as a binder with sand and coarse aggregate (Table 3.7). The cubes were cast and tested at 7, 28 and 90 days of air and 90 days of water curing. All the composites/ mixes failed to reach the minimum target strength of 15 MPa for limecrete except MK50 composite, which was close to the target strength. All the composites demonstrated meagre flexural strength of less than 1 MPa. The possible cause of low strength production could be attributed to the increased pozzolanic reaction producing inadequate C-S-H gel and resulting in an extensive quantity of SiO_2 / production of $\text{Si}(\text{OH})_4$ gel, which has swelling properties and weakens the composites (Equations 31-33). All the composites with 50% lime and 50% pozzolanic replacement (MK, PFA, SF) performed better than others. MK50 exhibited the maximum compressive strength of 13.2 MPa (water-cured) with a 1:1:2 ratio of the 50% MK/ hydrated lime-based cement-free composites (limecrete) followed by 1:1:3, 1:2:3 and lastly, the 2:1 ratio as shown in Figure 4.23. PFA-50% exhibited the maximum compressive strength of 4.3 MPa (water-cured) with a 1:1:2 ratio of 50% PFA/ 50% CL90, followed by PFA-50% of 1:1:3, 1:2:3 and the 2:1 ratios as shown in Figure 4.24. SF50 exhibited the maximum compressive strength of 6.9 MPa (water-cured) with a 1:1:2 ratio of 50% SF/ 50% CL90, followed by SF-50% of 1:1:3, 1:2:3 and the 2:1 ratios as shown in Figure 4.25. Hydrated lime-based cement-free limecrete with PFA, SF and MK demonstrated low strengths, limiting its use to low strength requirements (subgrades, foundations, flooring, walls, MK could be used for single-story construction). However, these greener cement-free composites with a 50% use of lime plus 50% waste pozzolanic materials could help in the absorption of global waste, reduce the environmental impacts due to GHG and reduce CO_2 emissions by the construction industry by up to 20% (low strength construction requirements). Moreover, MK is abundant in naturally

occurring pozzolanic materials that could be used in vast construction applications. Figure 4.26 draws a comparison between the best-performing composites of job mix ratio 1:1:2. GGBS has performed the best in achieving the compressive strength target of 15-25 MPa strength, demonstrated at par flexural strength with OPC concrete and has out-performed all other composites/ materials formulated using CL90/ pozzolans (PFA, MK, SF). MK performed as the best material, with only MK50 1:1:2 reaching the minimum target of 15 MPa. SF50 1:1:2 performed the third best, exhibiting 6.9 MPa, and PFA50 reached up to 4.3 MPa. This study suggests the use of SL60-90 and MK 50-90 for medium and low strength construction as a substitute for cement concrete and PFA/ SF 50-70% for very low strength materials applications as a substitute for NHL2.5, NHL, 3.5, NHL5.5 mortars, and lime putty (Ahmed et al., 2022a, 2022b). The best-performing materials/ ratios, SL80 1:1:2 and MK50 1:1:2, were shortlisted for further study, incorporating fibres in the next section.

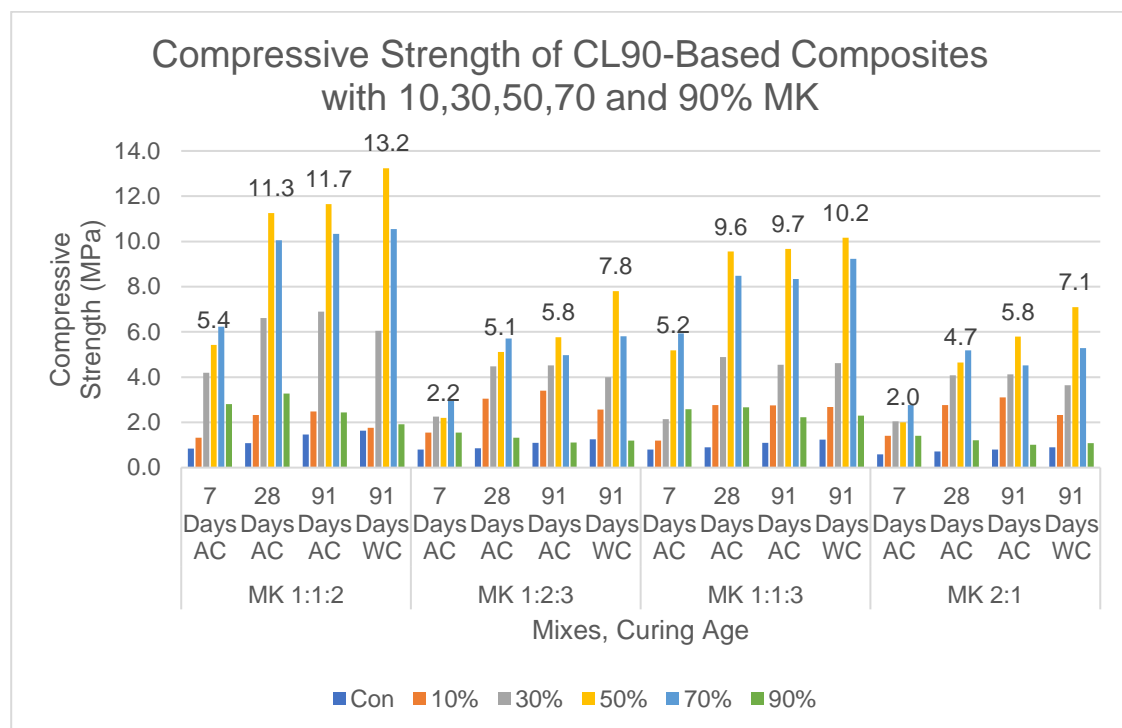


Figure 4.23: Compressive Strength of CL90-Based Composites with 10,30,50,70 and 90% MK.

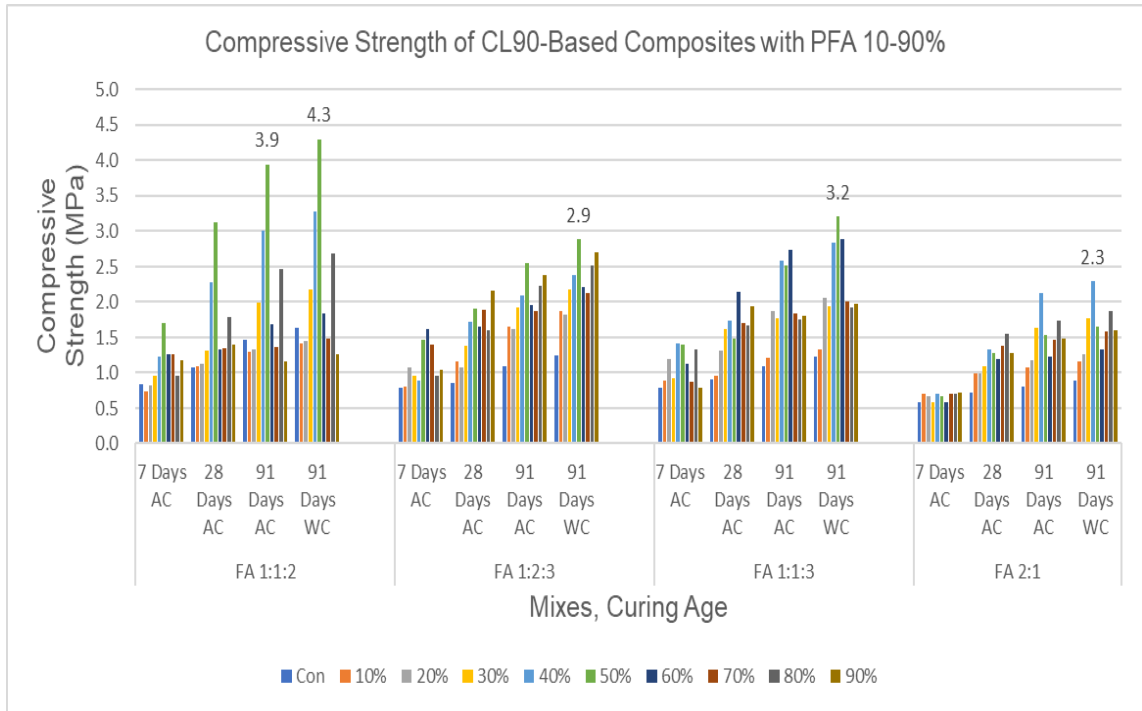


Figure 4.24: Compressive Strength of CL90-Based Composites with PFA 10-90%

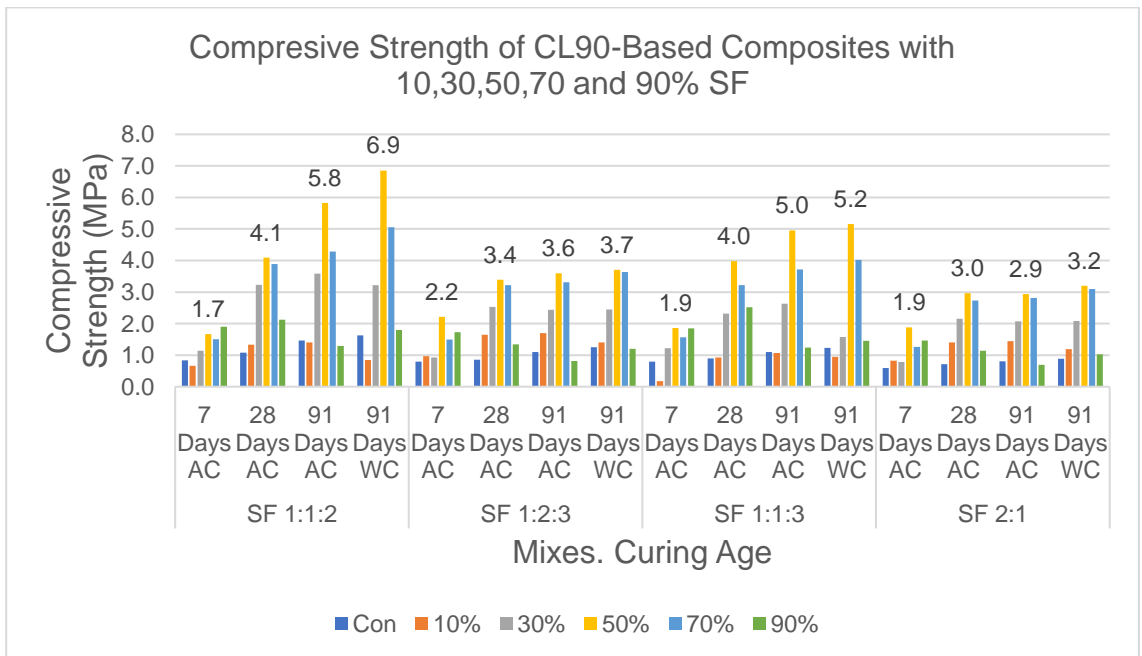


Figure 4.25: Compressive Strength of CL90-Based Composites with 10,30,50,70 and 90% SF

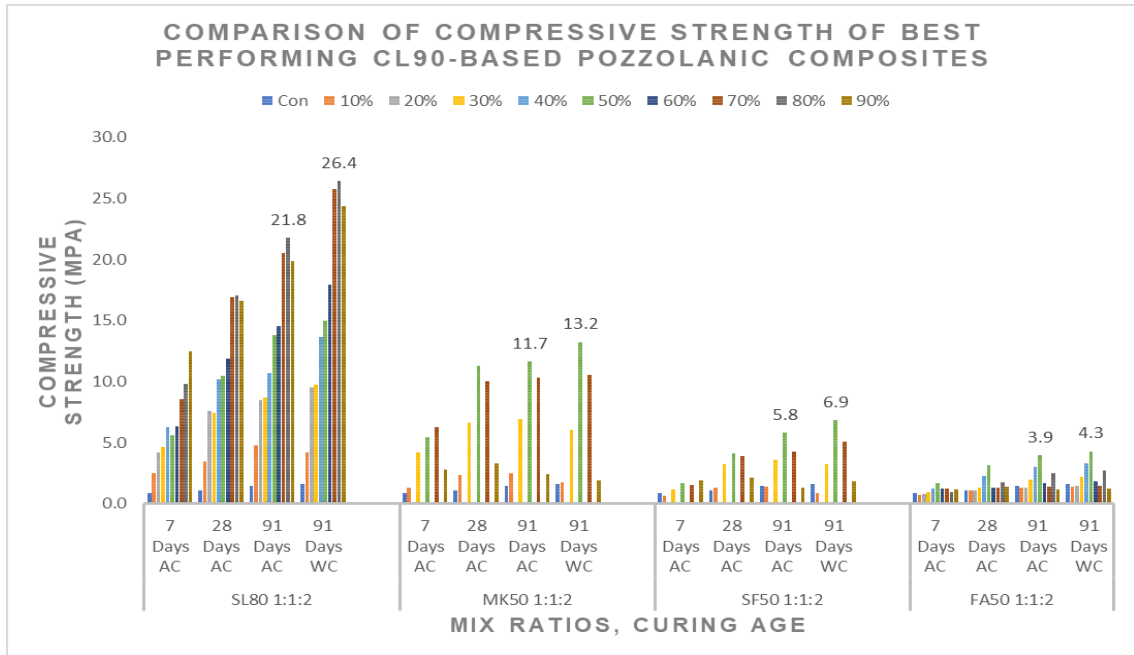


Figure 4.26: Comparison of Compressive Strengths of Best Performing CL90-Based Pozzolan Composites

4.7 Evaluation of Non-Cement, Alternative, Lime-Based Fibre-Reinforced Innovative Pozzolan Composites (NALFRIC)

The research in sections 4.6 and 4.7 has the primary objective of answering the research question framed in Chapter 1 if the cement-free composites containing hydrated lime and waste pozzolan materials along with the waste fibres could be used to make sustainable, greener construction materials exhibiting adequate compressive/ flexural strength for using in the diverse construction applications including water channel stabilisation/ hydromodifications. Section 4.6 conducted a detailed experimental study to formulate CL90-based cement-free pozzolan composites due to very little/ negligible research on using hydrated lime in such composites. As a conclusion to the previous study, the best-performing composites of SL80 (1:1:2 ratio) and MK50 (1:1:2 ratio) were shortlisted for further experimental research with the incorporation of industrial/ agricultural waste fibres to elucidate their engineering properties to develop as “Non-cement,

Alternative Lime-Based Fibre-Reinforced Innovative Pozzolan Composites (NALFRIC)". A target strength of 20-30 MPa was set for these medium-strength composites to be used as greener, environmentally friendly enhanced construction materials for versatile construction applications with a special focus on use along the small water channels. The incorporation of fibres from industrial/ agricultural waste has endeavoured to induce better flexural strength for use against the water thrust in streams, where RCC is deemed uneconomical, and PCRs/ TCRs with fibres could fulfil the strength requirements outperforming the use of cement concrete considering the cost-benefit analysis and environmental impacts. As already discussed in section 4.4, The incorporation of fibres is considered to improve the surface/ pore refinement, prevention of micro-structural cracks, prevention of ingress of moisture/ hazardous chemicals, and improvement in intra-ingredients binding in the internal structure of FRC if the fibres are used up to a specific optimum limit. However, the best results could be attributed to proper placement/ mixing of fibres, orientation, quantity, types of fibres/ concrete, the aspect ratio of fibres, w/c ratio, compaction, and relative toughness/ strength/ elasticity of fibres. STF was used with 10% and 17% dosages, and PPF, Coir, PET bottles shredded fibres, and WSF dosages of 0.5% - 2% were used as optimum dosages in line with the existing research/ technical instructions (Siddique, 2004; Akeem and Mitui, 2017; The Constructor, 2017; Scrivener, 2018; ASTM C 618/ C125, 2019; Selvapriya, 2019; Cement concrete, 2020; Girts et al., 2020; Nadir and Ahmed, 2021b Appendix VII; Admin, 2023). The 1:1:2 job mix ratio was used with a mixture of SL80 (20% CL90 + 80% Slag) and MK50 (50% CL90 + 50% MK) as binders with virgin river sand and crushed rock aggregates. A water/binder ratio of 0.55 was used consistently for a fair comparison of composites, as shown in Tables 3.8 and 3.9. The previous study observed that the longer curing period positively impacts the completion of the pozzolanic reaction, which is a very slow-paced reaction; therefore, curing some specimens in water for up to 270 days was implemented for this study. Long curing in water would also give comparable results for using the composites in

water channels/ hydromodifications and the resistance of the materials against external and internal sulphate attacks (would be studied separately). The incorporation of fibres in a composite would likely reduce the compressive strength if used beyond a specific percentage due to the weakening of intra-ingredients binding and the creation of weaker plains of failure due to the swift propagation of cracks along the fibres on experiencing extensive loading. However, incorporating fibres would likely improve flexural strength due to increased rupture modulus or the composites' post-crack ductility. Figure 4.27 and Table 4.5 compare the compressive strength of various NALFRIC composites. A strength improvement of up to 36% in the control mix was observed with a longer duration of curing from 90 days (19.8 MPa) to 270 days (27.1 MPa), elucidating a better performance of NALFRIC composites in water immersion compared to air exposure/ curing. Overall, a decreasing trend of up to 8% compressive strength (at 270 days) was observed between the control mix (27.1 MPa) and the best-performing NALFRIC composites of SL80 ST10% and SL80 PET2% (25 MPa). The composites with ST10% and ST17% have performed the best, exhibiting up to 25 MPa strength. The waste PET bottle fibres have performed at par with the STF and demonstrated 25 MPa strength at 270 days of curing, followed closely by the PPF 0.5-1.5% composites achieving up to 23 MPa strength. The last performance was demonstrated by the NALFRIC composites containing wheat straw fibres WSF and strength reduced to below target strength of 20 MPa, although still falling in the low strength range of construction materials (10-15 MPa) sufficient for a variety of low strength utilisation like subgrade, foundation, flooring, walls and single story construction. The study suggests using greener, innovative, enhanced NALFRIC composites with STF (10,17%), PET (0.5-2%), PPF (0.5-2%) and coir fibres for medium-strength applications in the construction industry with lower embodied CO₂ and minimised impact on the stream ecology. Figure 4.28 and Table 4.5 show an enhancement of 3.8 times in the flexural strength of the lime-based control mix (0.7 MPa) and an improvement of 36% from the plain SL80 composites (2.5 MPa)

to 3.4 MPa obtained by NALFRIC PPF1.5%. The best performance was demonstrated by PPF, STF, PET and coir-containing NALFRIC composites by achieving up to 2-3.4 MPa strength. However, WSF performed the least by achieving less than 2 MPa flexural strength.

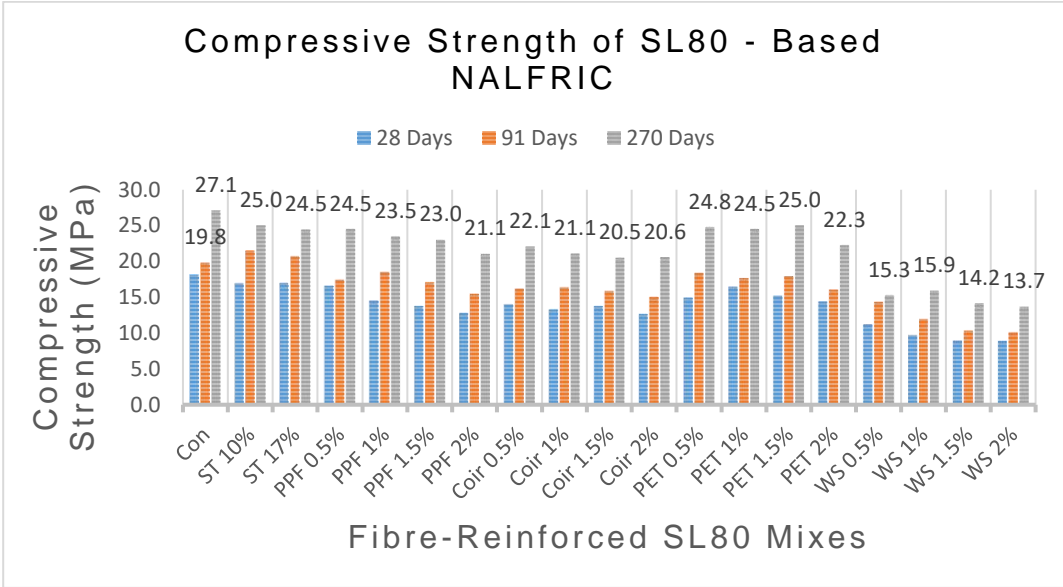


Figure 4.27: Compressive Strength of CL-90/ SL80-Based NALFRIC

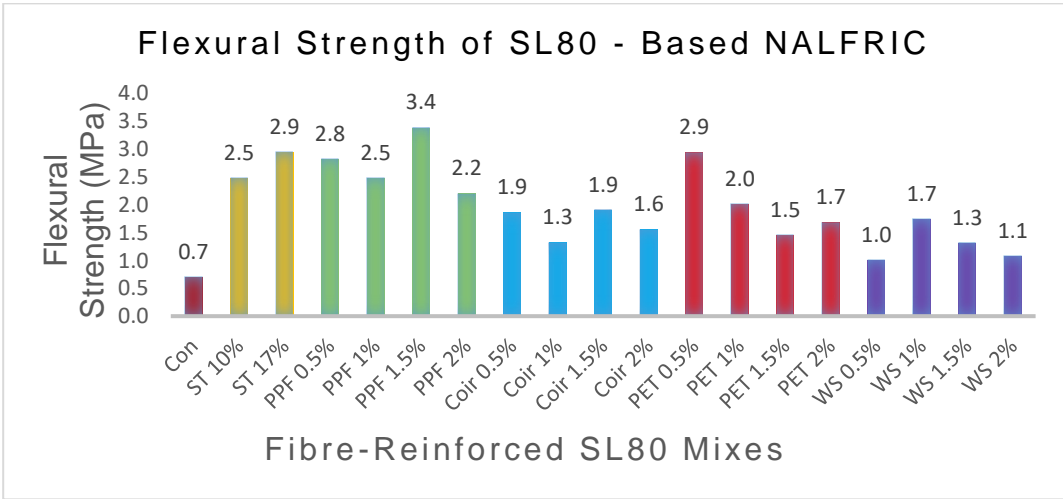


Figure 4.28: Flexural Strength of CL-90/ SL80-Based NALFRIC

Table 4.5: Compressive/ Flexural Strength of CL-90/ SL80-Based NALFRIC

Compressive/ Flexural Strength of CL-90+SL80-Based NALFRIC						
SL80 112	28 Days Compressive Strength (MPa)	90 Days Compressiv e Strength (MPa)	270 Days Compressiv e Strength (MPa)	90 Days Flexural Strengt h (MPa)	Water /Binde r (w/b) Ratio	Slum p (mm)
Con ST	18.2	19.8	27.1	0.7	0.55	S1
10% ST	16.9	21.5	25.0	2.5	0.55	S1
17% PPF	17.0	20.7	24.5	2.9	0.55	S1
0.5% PPF	16.6	17.4	24.5	2.8	0.55	S1
1% PPF	14.5	18.5	23.5	2.5	0.55	S1
1.5% PPF	13.8	17.1	23.0	3.4	0.55	S1
2% Coir	12.8	15.5	21.1	2.2	0.55	S1
0.5% Coir	14.0	16.2	22.1	1.9	0.55	S1
1% Coir	13.3	16.4	21.1	1.3	0.55	S1
1.5% Coir	13.8	15.9	20.5	1.9	0.55	S1
2% PET	12.7	15.0	20.6	1.6	0.55	S1
0.5% PET	14.9	18.4	24.8	2.9	0.55	S1
1% PET	16.5	17.7	24.5	2.0	0.55	S1
1.5% PET	15.2	17.9	25.0	1.5	0.55	S1
2% WS	14.4	16.1	22.3	1.7	0.55	S1
0.5% WS	11.2	14.4	15.3	1.0	0.55	S1
1% WS	9.7	12.0	15.9	1.7	0.55	S1
1.5% WS	9.0	10.3	14.2	1.3	0.55	S1
2%	8.9	10.1	13.7	1.1	0.55	S1

The second material selected for the formulation of the NALFRIC composite is MK. As discussed in section 4.6, only MK50 reached near 15 MPa strength. Still, due to its abundant occurrence and beneficial use of versatile construction applications, it was shortlisted as a second pozzolanic material to formulate NAFLRIC. All the established pozzolans are available up to 3-7% of the global cement demand, and only lime and MK are among the materials available in infinite abundance on the earth as natural materials. Therefore, substituting cement concrete could be a rewarding option with abundantly supplied materials for at least low-strength construction. Fibre dosages of STF 10% and 17 % and 0.5-2% PPF, PET, Coir, and WSF were used with 50% MK and 50% CL90 with virgin sand/ aggregates maintaining a water/ binder ratio of 0.55 as per Abrams law (Jain, 2020). Figure 4.29 and Table 4.6 show that the longer curing duration, from 90 days to 270 days, has enhanced the strength by 40% in the control mix. The incorporation of fibres has resulted in a decreasing trend in compressive strength. The composites with STF 10%, 17%, and PPF 0.5/1% have demonstrated the maximum compressive strength of 13.4, 11.8, 12.5, and 10.5 MPa, respectively. All other composites have exhibited a compressive strength of fewer than 10 MPa. The composites with STF, PPF and coir fibres have attained up to 3 times flexural strength (1.8 MPa) compared to the control mix (0.6 MPa), elucidating a beneficial use of fibre incorporation (Figure 4.30, Table 4.6). The use of MK-based NALFRIC is suggested for low-strength construction stipulation with a likely principal reduction in the carbon footprints of the construction industry. It could be used in lining small water distributaries and drains for lower water discharges, subgrade preparation, foundation, flooring, breaking stones, mortars, substitution of NHL2.5-NHL 5.5 and embankment/ façade improvements. However, its large-scale application in structural utilisation is not suggested. If the construction industry uses MK-based NALFRIC by 20%, it could significantly decrease around 800 million tons of CO₂ (20% of 4800 million tons emissions of OPC) economically.

Table 4.6: Compressive/ Flexural Strength of CL90 + MK50-Based NALFRIC

Compressive/ Flexural Strength of CL90 + MK50-Based NALFRIC

MK50 112	28 Days Compressive Strength (MPa)	90 Days Compressive Strength (MPa)	270 Days Compressive Strength (MPa)	90 Days Flexural Strength (MPa)	Water /Binder Ratio	Slump (mm)
Con	9.3	10.4	14.4	0.6	0.55	S1
ST						
10%	11.5	11.6	13.4	1.6	0.55	S1
ST						
17%	11.3	11.3	11.8	1.2	0.55	S1
PPF						
0.5%	9.6	11.6	12.5	1.3	0.55	S1
PPF						
1%	8.8	9.2	10.5	1.2	0.55	S1
PPF						
1.5%	6.3	7.9	8.7	1.2	0.55	S1
PPF						
2%	7.3	7.5	8.7	1.8	0.55	S1
Coir						
0.5%	8.2	8.2	8.7	0.5	0.55	S1
Coir						
1%	7.3	9.2	9.9	0.9	0.55	S1
Coir						
1.5%	7.1	8.7	8.8	1.2	0.55	S1
Coir						
2%	6.6	7.5	7.6	0.9	0.55	S1
PET						
0.5%	7.6	8.7	9.0	0.7	0.55	S1
PET						
1%	7.2	8.4	8.8	0.8	0.55	S1
PET						
1.5%	8.0	9.4	9.8	0.7	0.55	S1
PET						
2%	8.5	9.1	9.9	0.9	0.55	S1
WS						
0.5%	6.5	7.0	7.1	0.5	0.55	S1
WS 1%	6.2	8.6	8.7	0.8	0.55	S1
WS						
1.5%	7.1	8.2	8.4	0.7	0.55	S1
WS 2%	5.8	7.7	7.9	0.5	0.55	S1

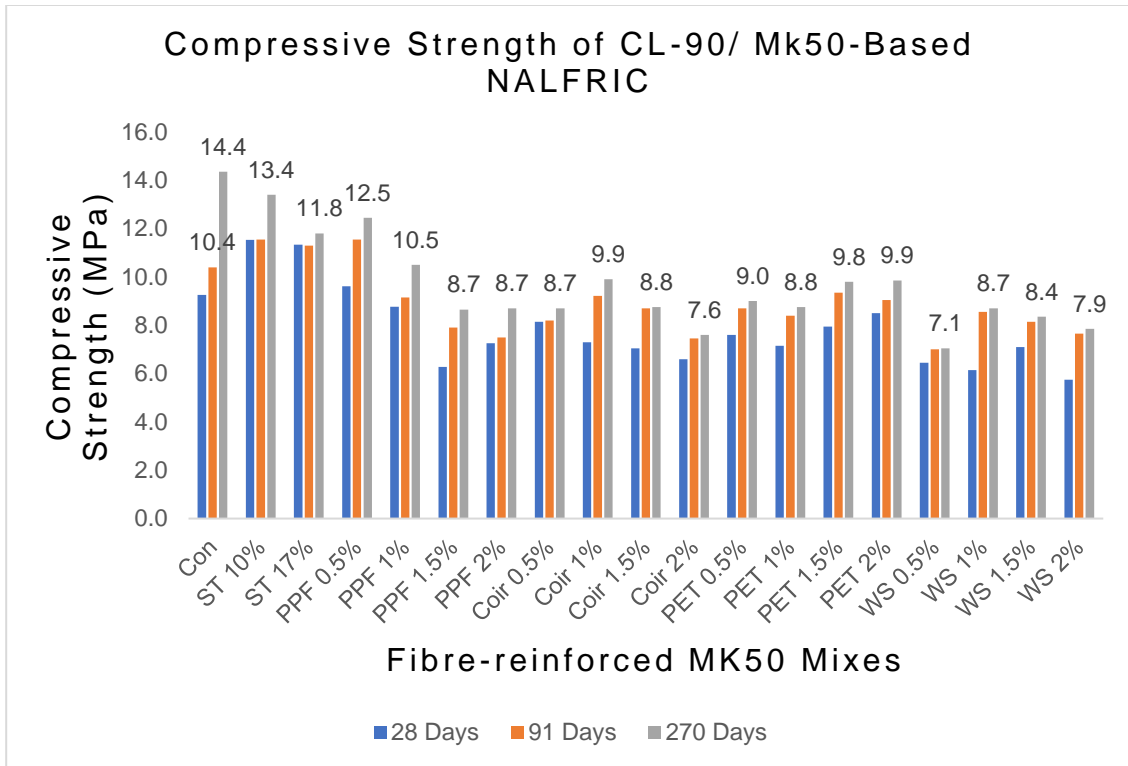


Figure 4.29: Compressive Strength of CL90 MK50-Based NALFRIC

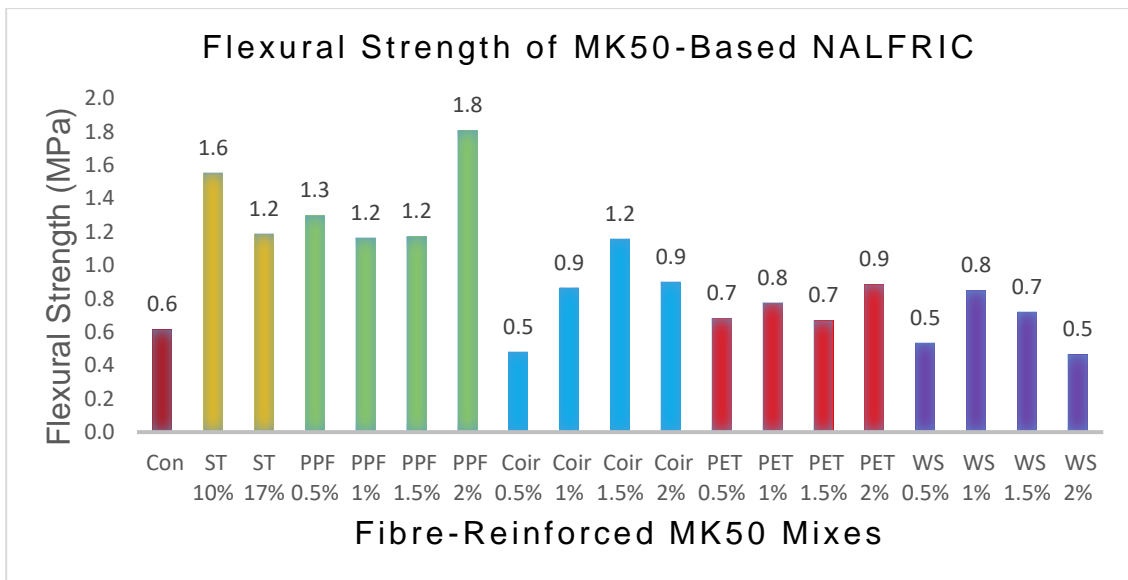


Figure 4.30: Flexural Strength of CL-90/ MK50-Based NALFRIC

4.8 Investigation of Iron-Based Binary/ Ternary Pozzolanic Composites

Section 4.8 deals with the research conducted to answer the research question framed in Chapter 1: could agricultural/ industrial waste be recycled into the formulation of high-strength fibre-reinforced carbon-neutral iron-based binary/ tertiary pozzolanic composites to minimise the environmental impacts by the construction industry? An endeavour was made to undertake extensive experimental research to formulate iron-based binary and ternary pozzolanic SCMs, as discussed in section 3.4.3. The composition of iron-based binary and ternary pozzolanic SCMs was outlined in Table 3.10. The existing research suggested that iron powder (**abbreviated as Fe/ F for simplification**) obtained as waste material from the steel industry could react with CO₂ to form siderite (ferrous carbonate FeCO₃), which forms rock-like material, exhibiting increased compressive strength and absorption of CO₂, making it a low-carbon material as shown in Equation 25 (Stone, 2010; Karuppasamy, Dinesh and Janardhan, 2011; Das, Souliman and Stone, 2014; USGS, 2014; Vijayan et al., 2019; Garcia et al., 2017; Iron Powder, 2023; Nadir, Ahmed and West, 2023 Appendix IV; Nadir, Ahmed and Moshi, 2024 Appendix VII).

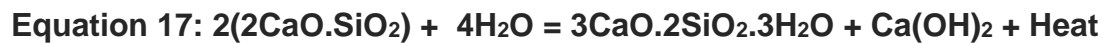
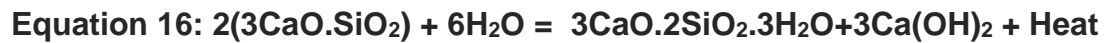
Equation 25: $\text{Fe} + \text{CO}_2 + \text{H}_2\text{O} = \text{FeCO}_3 + \text{H}_2$

Das et al. (2015) explored the sustainable use of Fe-composites as a full/ partially greener alternative to OPC as 100% Fe-composites or 10-50% conventional Fe-composites-based SCMs (Das et al., 2015). Vijayan et al. (2019) evaluated that 4-12% conventional Fe-composites replacement with OPC exhibited better engineering properties, with 8% as the optimum dosage. Karthika and Leema (2021) elucidated the impacts of using 5,10,15,20, and 25% conventional Fe-composites replacement with OPC. They suggested 10% as the optimum dosage, demonstrating the durability in sulphate attack and the best mechanical properties among all the mixes/ ratios of SCMs. This research endeavoured to

formulate a variety of binary/ternary pozzolanic modified Fe-composites by incorporating 20% PFA/ GGBS/ PA as the binary pozzolanic composites with 8% MK and using 10% PFA+10GGBS and 10%PFA +10% SF with 8% MK as ternary pozzolanic composites. 12% limestone and 2% oxalic acid were used as constant quantities to facilitate/ accelerate the carbonation of the iron reaction. 10-50% of these modified Fe-composites mixtures were used as 10-50% OPC replacement in a 1:2:3 ratio targeting C32/ 40 or M40 concrete (Table 2.4, Table 3.2). The iron-based OPC composites achieved better compressive strength than the standard cement concrete of the same job mix ratio due to the production of additional C-S-H gel by pozzolanic reaction and formation of FeCO_3 exhibiting/ incorporating rock-like characteristics. Therefore, the ratio of 1:2:3 was considered in this experimental research to expect an at-par strength of cement concrete, which was achieved with 1:1:2 or 1:1:3 ratios. The research was divided into two phases: formulating the plain binary/ternary iron-based pozzolanic composites and the then fibre-reinforced iron-based pozzolanic composites (NAFRIC). The materials were divided into two main categories: binary and ternary pozzolanic usage. These were further subdivided into five sets of materials, with set 1 using 20% PFA, set 2: 20% GGBS, set 3: 20% PA, set 4: 10% PFA+10%GGBS and set 5: 10% PFA+10%SF, along with 8% MK, 12 % CaCO_3 , 2% oxalic acid and then combining it with 10-50% of OPC. The composite materials were mixed using a 1:2:3 ratio with virgin sand/ crushed coarse aggregate using regular tap water with 0.35 w/c ration and 0.2-0.25% plasticiser to achieve an S1 slump and a workable consistency. 100 mm cubes and 500 x 100 x 100 mm prisms were cast to test at 7, 28, and 90 days for compressive strength and 90 days for flexural strength as per the related British standards for concrete testing (Kosmatka et al., 2002; Atis and Bilim, 2007; Ganesan et al., 2008; Bapat, 2012; Hannesson et al., 2012; Reddy et al., 2013).

The compressive and flexural strength results were tabulated in Table 4.7 and illustrated in Figures 4.31-4.37. The average density of all these composites fell in the standard concrete density range of 2240-2390 kg/m^3 (Table 4.3). The

increased dosage of modified Fe-composites decreased the workability, necessitating more plasticiser to achieve a workable S1 slump, consistently maintaining a w/c of 0.35 for a fair comparison as per Abram's law (Jain, 2020). The pozzolanic reaction between SiO_2 and Ca(OH)_2 to form C-S-H gel during the hydration process was delayed and started after the initial cement hydration of trisilicate and disilicate of OPC, as shown in Equation 15-17.



The reaction between Fe and CaCO_3 and CO_2 (released during hydration/ absorbed from the environment) also started after the initial cement hydration after a delayed period, resulting in the formation of C-S-H gel and FeCO_3 over a prolonged period. The delayed formation of C-S-H gel and FeCO_3 indicated that a longer curing time is required for achieving major strength up to 95% till 90 days of the curing (Shweta and Devender, 2020; Civil Giant, 2022; Johannes, 2021; Nadir and Ahmed 2021b Appendix VII; Nadir and Ahmed 2022b Appendix V; Nadir and Ahmed 2022c Appendix VI). The phenomenon of delayed strength gain could be observed with an increase of up to 53% in compressive strength of the control mix at 7 days (47 MPa) and the compressive strength of best performing set 2 (GGBS 20%) mix at 90 days (72 MPa). All the composites improved the compressive strength by up to 53% over a prolonged curing period of 90 days. The results showed that all the composites of all sets 1-5 with 10-30% OPC replacement by conventional/ modified Fe-composites materials improved the compressive strength up to 22% at 90 days of curing, whereas 40-50% replacement composites generally, demonstrated a decrease in the strength by 15%, suggesting optimum use of iron-based binary/ ternary pozzolanic mixture from 10-30% as partial replacement of OPC. The best-performing replacement dosage was observed at 10%; however, all the composites achieved a high

strength of 50-72 MPa with up to 10-50% replacement, elucidating these composites' productive/beneficial use. The best thing to conclude was that the iron-based pozzolanic composites formulated using a 1:2:3 job mix ratio achieved the same range of high-strength concrete, which is generally prepared using 1:1:2 or 1:1:3 job mix ratios with CEM1 52.5, saving on the cost/ quantity/ GHG emissions of cement concrete.

Table 4.7: Engineering Properties of Iron-Based Binary/ Ternary Pozzolanic Composites.

Engineering Properties of Iron-Based Pozzolanic Cement Concrete								
Set 1 - 5, 10%-50% Replacement of OPC with Conventional /Modified Fe-Composites								
Set	Mix Ratios	7 Days Compressive Strength (MPa)	28 Days Compressive Strength (MPa)	91 Days Compressive Strength (MPa)	91 Days Flexural Strength (MPa)	Water /cement Ratio	Slump (mm)	Plasticiser (ml)
Set 1 - 10%-50% Replacement of OPC with Conventional Fe-Composites with 20% PFA								
Set 1 (20%PFA)	Con	47	55	59	4.4	0.35	S1	0
	Fe-Mix10%	52	60	66	4.7	0.35	S1	10
	Fe-Mix20%	44	55	64	4.4	0.35	S1	10
	Fe-Mix30%	40	53	63	5.0	0.35	S1	10
	Fe-Mix40%	32	46	55	3.7	0.35	S1	15
	Fe-Mix50%	26	36	49	3.8	0.35	S1	15
Set 2 - 10%-50% Replacement of OPC with Modified Fe-Composites with 20% GGBS								
Set 2 (20%GGBS)	Con	47	55	59	4.4	0.35	S1	0
	Fe-Mix10%	51	60	72	5.2	0.35	S1	10
	Fe-Mix20%	46	57	71	5.8	0.35	S1	10
	Fe-Mix30%	45	56	67	5.5	0.35	S1	10
	Fe-Mix40%	35	51	63	5.0	0.35	S1	15
	Fe-Mix50%	28	43	61	4.9	0.35	S1	15
Set 3 - 10%-50% Replacement of OPC with Modified Fe-Composites with 20% PA								
Set 3 (20%PA)	Con	47	55	59	4.4	0.35	S1	0
	Fe-Mix10%	52	62	70	5.3	0.35	S1	10
	Fe-Mix20%	51	62	68	5.8	0.35	S1	10
	Fe-Mix30%	45	58	67	5.3	0.35	S1	10
	Fe-Mix40%	40	56	59	4.9	0.35	S1	15
	Fe-Mix50%	40	57	56	4.3	0.35	S1	15
Set 4 - 10%-50% Replacement of OPC with Modified Fe-Composites with 10%PFA+10% GGBS								
Set 4 (10%PFA+10%GGBS)	Con	47	55	59	4.4	0.35	S1	0
	Fe-Mix10%	51	62	67	5.3	0.35	S1	10
	Fe-Mix20%	52	62	65	5.5	0.35	S1	10
	Fe-Mix30%	50	62	62	5.3	0.35	S1	10
	Fe-Mix40%	40	56	56	4.9	0.35	S1	15
	Fe-Mix50%	38	50	50	4.8	0.35	S1	15
Set 5 - 10%-50% Replacement of OPC with Modified Fe-Composites with 10%PFA+10% SF								
Set 5 (10%PFA+10%SF)	Con	47	55	59	4.4	0.35	S1	0
	Fe-Mix10%	50	59	67	4.5	0.35	S1	10
	Fe-Mix20%	49	59	64	5.5	0.35	S1	10
	Fe-Mix30%	43	55	59	4.7	0.35	S1	10
	Fe-Mix40%	38	54	56	4.4	0.35	S1	15
	Fe-Mix50%	39	54	50	4.7	0.35	S1	15

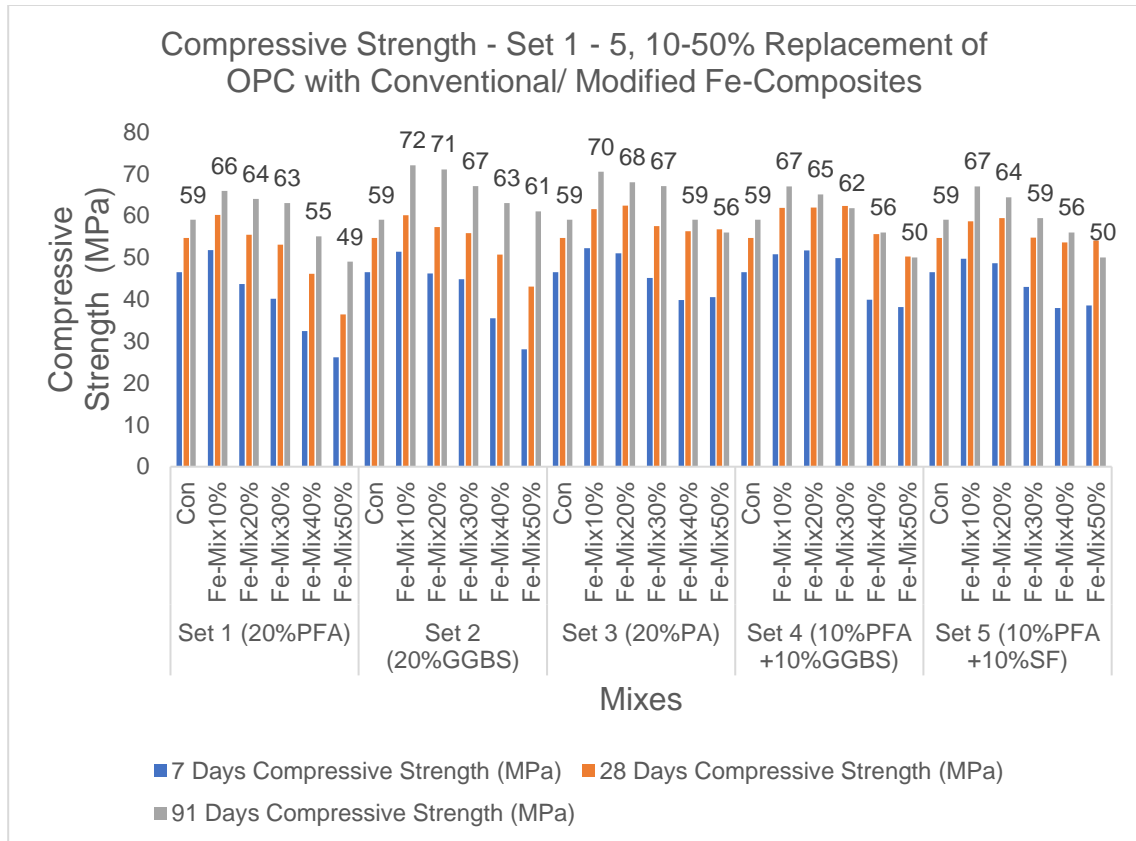


Figure 4.31: Compressive Strength - Set 1 - 5, 10-50% Replacement of OPC with Conventional/ Modified Fe-composites.

The best-performing materials belonged to set 2, containing 20% GGBS as binary pozzolanic material with 8% MK as expected due to intrinsic enhanced characteristics of GGBS. Fe/GGBS 10% demonstrated 72 MPa strength, Fe/GGBS 20% exhibited 71 MPa strength and the Fe/GGBS 30-50% composites obtained more than 60 MPa strength, making the best performing set as shown in Table 4.7, Figures 4.31 and 4.33. Set 3 composites containing a binary pozzolanic mix of 20% PA and 8% MK were the second best-performing replacement materials, achieving 70 MPa strength by Fe/PA 10%, 68 MPa by Fe/PA 20% and 67 MPa by Fe/PA 30%. Fe/PA 40 and 50 % also achieved 59 and 56 MPa, respectively, as shown in Table 4.7, Figures 4.31 and 4.34. The ternary pozzolanic replacement composites of set 4 (10%PFA+10%GGBS) and set 5 (10%PFA+10%GGBS) almost performed identically in gaining around 50-

67 MPa strength range by 10-50% replacement composites. The best strength of sets 4 and 5 was 67 MPa, achieved by 10% replacement of OPC. However, all their composites demonstrated more than 50 MPa strength, making them useful for utilisation in versatile high-strength concrete applications (60-70 MPa range), as shown in Table 4.7 and Figures 4.31, 4.35, 4.36. The conventional Fe-based composites containing 20% PFA and 8% MK as binary pozzolanic Fe-composite material demonstrated 49-64 MPa strength, the maximum strength achieved by Fe/PFA 10-30% composites, making them equally beneficial in use as PCR/ SCMs (Table 4.7 and Figures 4.31, 4.32) and these findings were found in line with the research conducted by Vijayan et al. (2019) and Shivani et al. (2022). The Fe-composites exhibited improved strength compared to the control mix and the set 1 conventional Fe-composites with a 1:2:3 ratio. FeCO_3 is considered an absorbent of CO_2 from the environment or produced during the hydration process within the cement concrete mixture, making it a low-carbon material (Stone and Widera, 2016). Suppose it is considered to be only a carbon-neutral material. In that case, it could absorb up to 30% of CO_2 if up to 30% iron-based binary/ ternary pozzolanic composites are substitutes for cement concrete in the construction industry (equal to around 1200 million tons of CO_2). Even composites with 40-50% replacement Fe-composites could be used for a broad spectrum of structural/ building applications, making it a better choice as sustainable, greener, waste-absorbent, eco-friendly SCMs. However, iron powder's cost/ availability/ transportation/ supply is an expected grey area, making it partially available for large-scale incorporation in broad-spectrum construction applications. However, its cost/ benefit analysis, especially its carbon absorbent characteristic, could propose a better preposition for its use over the omni-available cement but with massive embodied CO_2 . Karthika et al. (2021) and Das and Stone et al. (2015) proposed that the use of iron powder and pozzolans in the formulation of iron-based pozzolanic SCMs improves the pore structure, intra-ingredients bonding, prevention of micro-structural cracks, hardened impervious void free strata to prevent ingress of moisture and sulphate

attack. They observed that it improves the rupture modulus and increases the composites' flexural strength, thus increasing the post-crack ductility. Therefore, the iron-based pozzolanic composite's flexural strength is expected to increase compared to the control mix (PCC). However, increased dosages of the pozzolanic-based materials could produce swelling Si(OH)_4 gel instead of C-S-H gel and reduce compressive/ flexural strength. Generally, all the sets' composites demonstrated a 32% increase in flexural strength. 20% replacement composites of all the sets/ mixes exhibited the best flexural strength of 5.5-5.8 MPa, followed by 10%, 30% and 40-50% replacement composites, as shown in Figure 4.37 and Table 4.7. The least flexural strength of less than 4 MPa was demonstrated by 40-50% replacement composites of conventional Fe-composites containing 20% PFA in set 1, suggesting beneficial modification/ incorporation of alternative materials as binary/ ternary pozzolanic iron-based mixes. However, the flexural strength of plain concrete is not considered the primary designing parameter of structural concrete in construction, as it is strong in compression and weak in tension/ flexure. This study supports using 10-50% Fe-composites to demonstrate enhanced engineering properties. Therefore, the best-performing 10% composites would be used to study further the impact of the incorporation of fibres, durability, and micro-structural analysis for the chemical-mechanical synthesis of these innovative, sustainable, and greener SCMs in the succeeding sections.

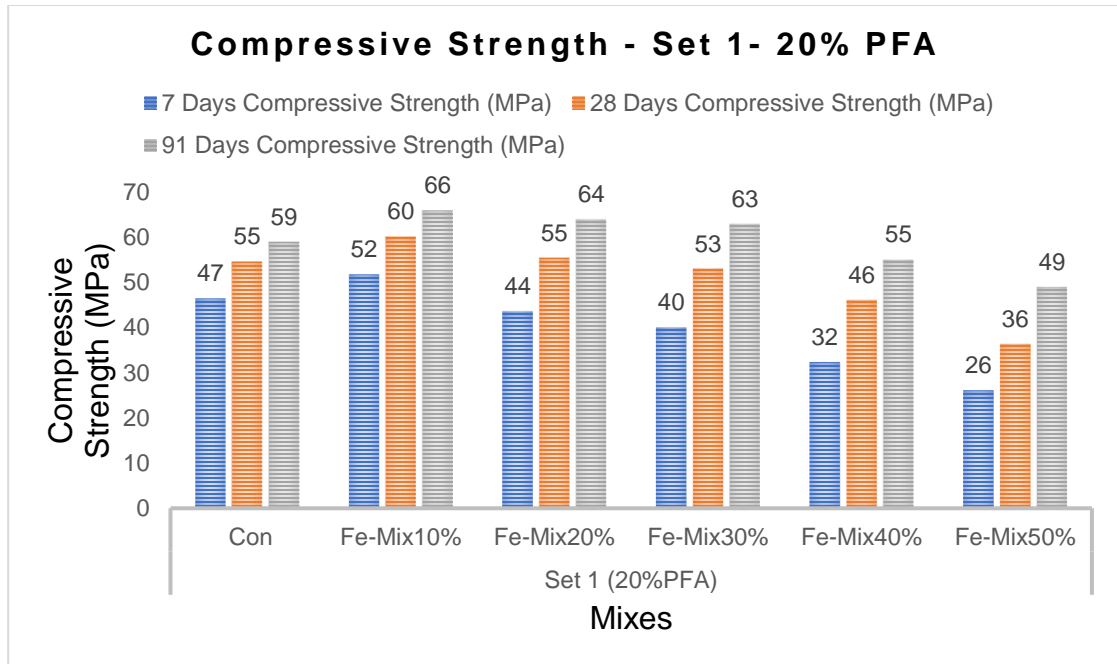


Figure 4.32: Compressive Strength - Set 1 20% PFA.

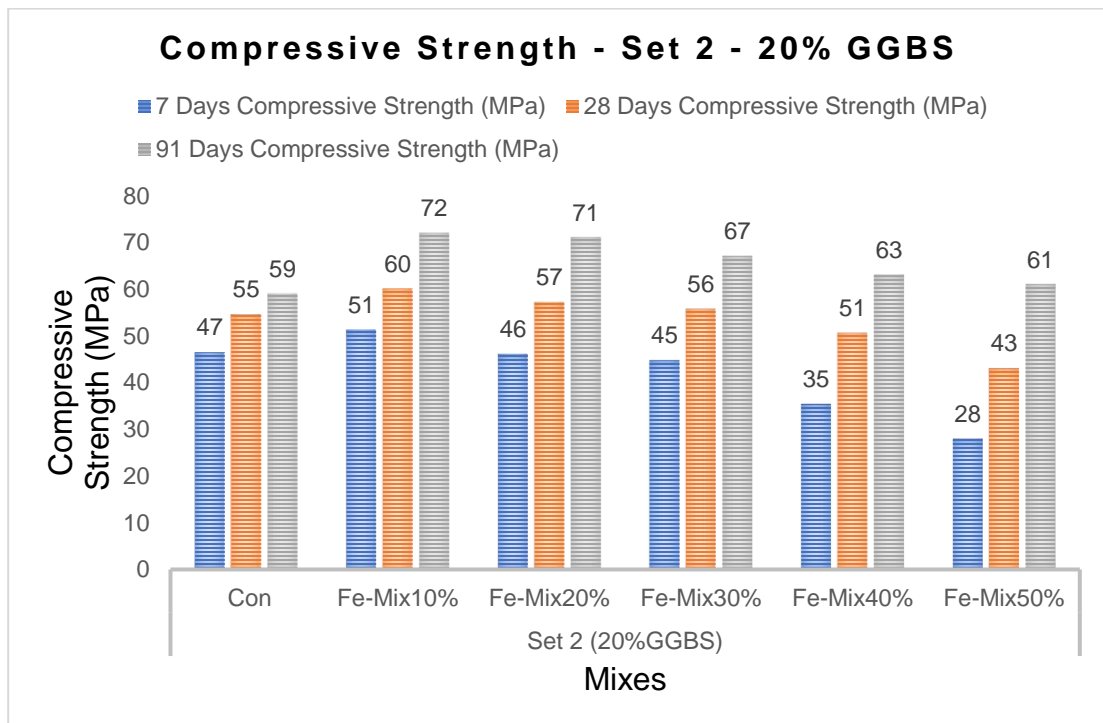


Figure 4.33: Compressive Strength - Set 2 20% GGBS

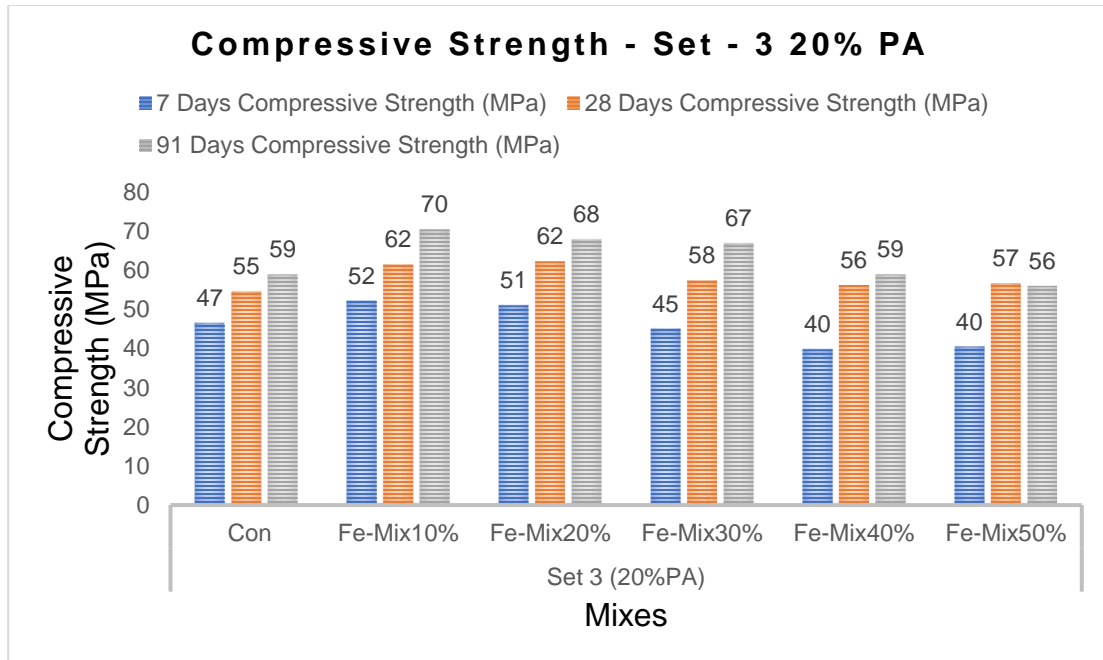


Figure 4.34: Compressive Strength - Set 3 20% PA.

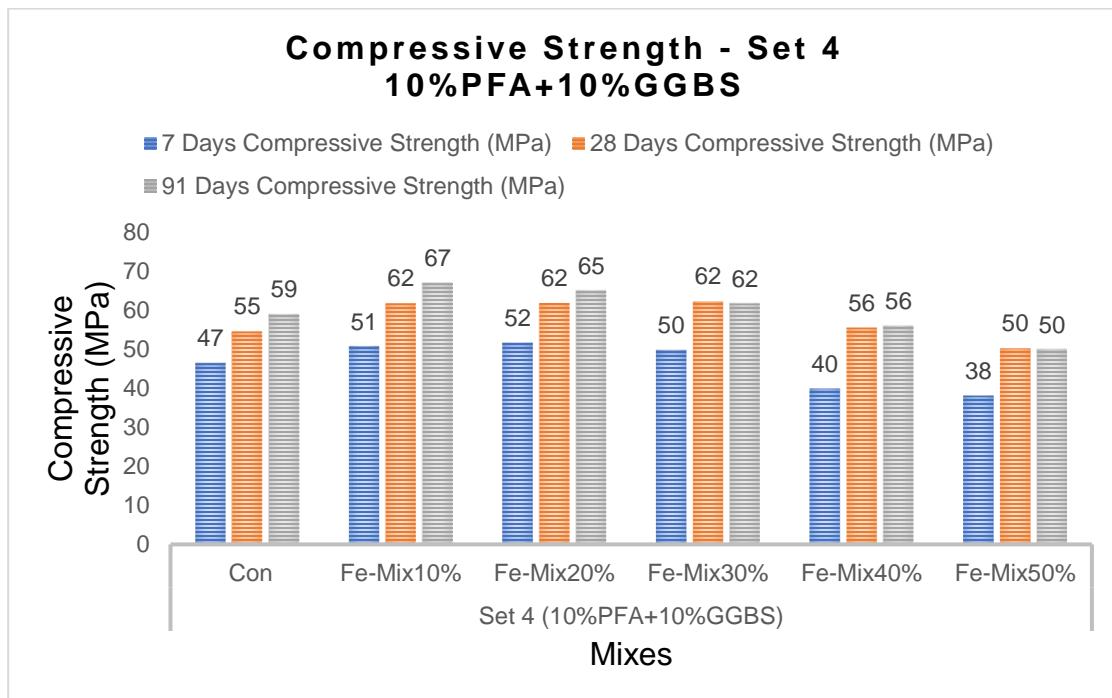


Figure 4.35: Compressive Strength - Set 4 10%PFA+GGBS.

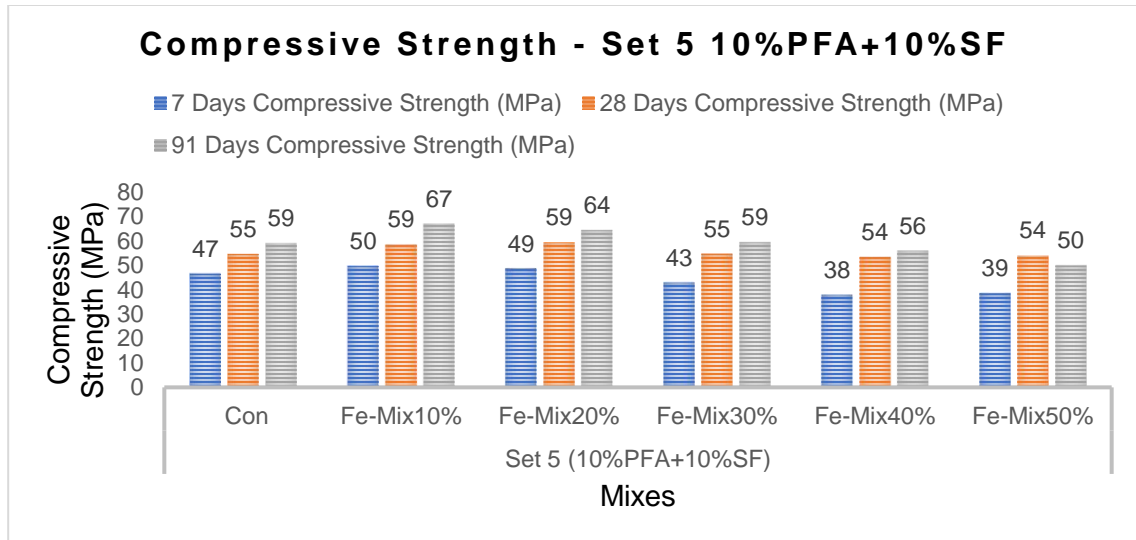


Figure 4.36: Compressive Strength - Set 5 10%PFA+10%SF.

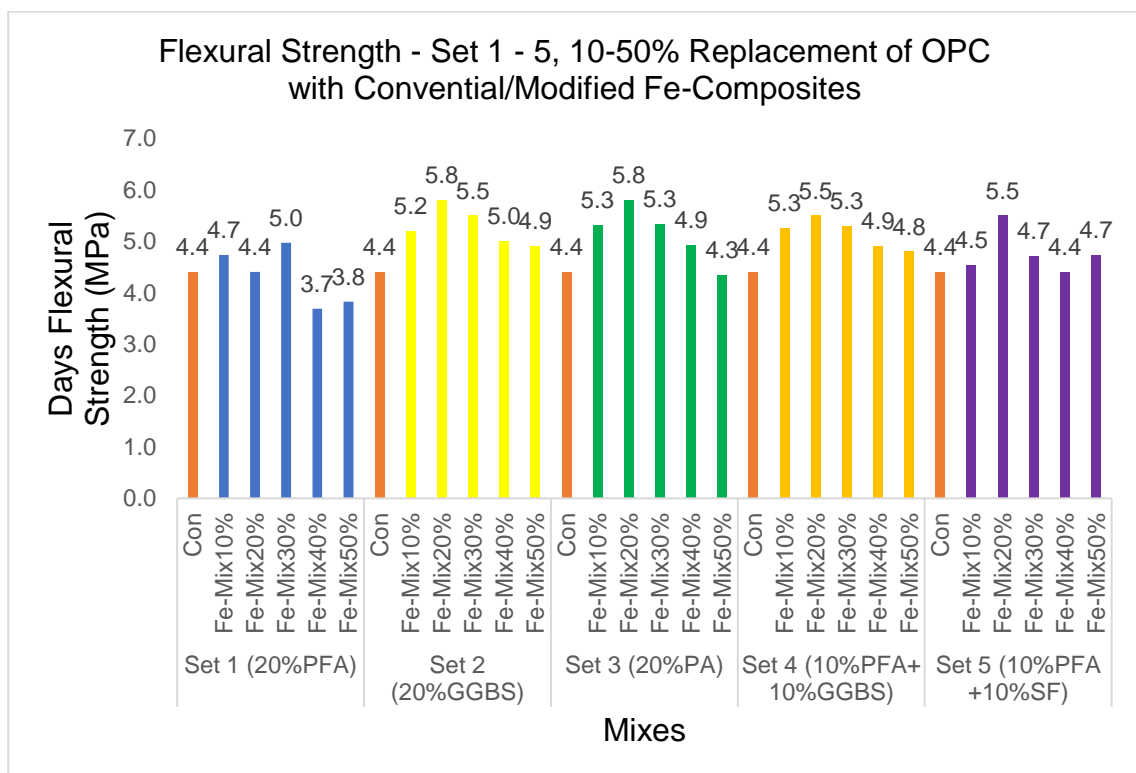


Figure 4.37: Flexural Strength - Set 1 - 5, 10-50% Replacement of OPC with Conventional/Modified Fe-composites.

4.9 Elucidation of Novel, Alternative, Fibre-Reinforced Iron-Based Binary/ Ternary Pozzolanic Composites (NAFRIC)

Cement concrete is considered the second most widely used material on earth after water, with its intrinsic characteristics of being a CO₂ emitter, strong in compression, and weak in tensile/ flexural strengths. The researchers pioneered the substantial disposal of waste materials exhibiting pozzolanic properties from diverse industrial/ agricultural fields to the construction industry to formulate greener supplementary cementitious composites (SCMs). These SCMs generate additional calcium silicate hydrate gel, inducing additional strength to the concrete by contributing silica during the cement hydration. The incorporation of fibres obtained from the shredding of scrap/ waste materials was envisaged as a rewarding/historically inexpensive solution to overcome the weak tensile/ flexural strength of binders for lower strength stipulations. The formulation of materials demonstrating comparable performance with cement concrete merely with negligible/ negative CO₂ balance has always been the aspiration of innovative construction. As a solution, iron-based pozzolanic composites (Fe-composites) were formulated using iron powder (Fe), metakaolin (MK), pulverised fly ash (PFA) and limestone, which is anticipated to accomplish a negative CO₂ equilibrium as it absorbs CO₂ from the environment to produce ferrous carbonate (FeCO₃) yielding a rock like (siderite) sustainable performance on drying/ setting. However, the cost/ availability of iron powder impedes the effective use of Fe-composites, necessitating consuming lower dosages in SCMs. A noticeable work was conducted exploring mechanical properties and chemical-mechanical synthesis of Fe-composites-based materials/ composites; however, more work has yet to be undertaken on formulating/ evaluating novel materials using fibres with Fe-composites-based OPC composites, indicating a research gap. Therefore, this study was conducted to elucidate the impacts of mixing 10% and 17% of steel fibres (STF), 1% and 2% of polypropylene fibres (PPF) as established materials and 1% and 2% of polyethene terephthalate plastic fibres (PET) and wheat straw fibres (WSF) as novel materials, to formulate better-

performing “Novel, Alternative, Fibre-Reinforced Iron-Based Binary/ Ternary Pozzolanic Composites (NAFRIC)”. 10% Fe-composites and 90% OPC-based SCMs containing the binary pozzolans (8% MK with 20% PFA or 20% GGBS or 20% palm ash PA) and the ternary pozzolans (8% MK+ 10%PFA+10%GGBS or 8% MK +10%PFA+10%SF) were evaluated setting a target characteristic compressive strength of C32/40 or M40 concrete. The mixes were formulated using CEM1 52.5 with coarse/ fine aggregates and 10% Fe-composites, 90% OPC, 0.2-0.25% plasticiser, tap water in 0.35 w/c ratio and 1-2% fibres mixing as FRC with a 1:2:3 mix ratio (Table 3.11). The 100 mm cubes were prepared/ tested for compressive strength at 28, 90 and 270 days in conformance with BS EN 12390-2:2019. The 500 x 100 x 100 mm prisms/ beams were prepared/ tested for flexural strengths at 90 days as per BS EN 12350-1 and were tested on a flexural testing machine with manual hydraulic three-point loading. The standard cone and rod apparatus were used to measure the slump to ascertain workability with the target S1 slump as per BS EN 8500. The target characteristic compressive strength of C32/40 or M40 concrete was set to be achieved by the mixes of this study. The compressive strengths at 28 days, 90 days and 270 days and flexural strengths at 90 days were compared with control mixes and NAFRIC composites of different mixes/ ratios, as shown in Table 4.8 and Figures 4.38-4.42.

All composites achieved a normal concrete density range of 2250-2390 kg/m³. Increased dosage of fibres, especially WSF, decreased the workability, necessitating an increased quantity of plasticiser to maintain the 0.35 w/c ratio consistently as per Abrams law. The increased curing age increased the strength to 4-10% as expected due to delayed pozzolanic/ carbonation reaction; however, maximum strength (up to 96%) was obtained in 90 days with a slightly increasing trend up to 270 days, as shown in Table 4.8.

Table 4.8: Compressive and Flexural Strength of NAFRIC Composites.

Compressive and Flexural Strength of NAFRIC Composites							
		28 Days Compressive Strength (MPa)	91 Days Compressive Strength (MPa)	270 Days Compressive Strength (MPa)	91 Days Flexural Strength (MPa)	Water /cement Ratio	Slump (mm)
PCC Control	Control	54	63	63	4.3	0.35	S1
Set1 F/PFA	F/Control	58	66	67	4.4	0.35	S1
	ST 10%	57	63	67	8.6	0.35	S1
	ST 17%	53	63	67	7.9	0.35	S1
	PPF 1%	52	58	65	7.2	0.35	S1
	PPF 2%	54	60	61	7.04	0.35	S1
	PET 1%	58	64	65	6.9	0.35	S1
	PET 2%	51	56	63	6.4	0.35	S1
	WS 1%	47	49	54	6	0.35	S1
Set2 F/GGBS	WS 2%	40	45	49	5.4	0.35	S1
	F/Control	58	66	66	4.8	0.35	S1
	ST 10%	56	63	66	8.1	0.35	S1
	ST 17%	58	64	68	7.5	0.35	S1
	PPF 1%	49	56	59	6.8	0.35	S1
	PPF 2%	51	54	61	6.9	0.35	S1
	PET 1%	54	60	65	6.8	0.35	S1
	PET 2%	57	57	66	6.2	0.35	S1
Set3 F/PA	WS 1%	50	54	56	6.8	0.35	S1
	WS 2%	39	45	50	5.7	0.35	S1
	F/Control	58	66	66	5.5	0.35	S1
	ST 10%	56	63	66	8	0.35	S1
	ST 17%	58	64	68	7.1	0.35	S1
	PPF 1%	49	56	59	6.8	0.35	S1
	PPF 2%	51	54	61	5.6	0.35	S1
	PET 1%	54	60	65	7.9	0.35	S1
Set4 F/PFA/GGBS	PET 2%	57	57	66	7.6	0.35	S1
	WS 1%	50	54	56	6	0.35	S1
	WS 2%	39	45	50	6	0.35	S1
	F/Control	56	67	70	5.2	0.35	S1
	ST 10%	58	62	69	8.9	0.35	S1
	ST 17%	56	62	67	8.3	0.35	S1
	PPF 1%	60	65	70	6.9	0.35	S1
	PPF 2%	55	62	62	5.6	0.35	S1
Set5 F/PFA/SF	PET 1%	58	62	66	7.3	0.35	S1
	PET 2%	52	55	61	6.3	0.35	S1
	WS 1%	49	59	55	6	0.35	S1
	WS 2%	42	49	51	6.1	0.35	S1
	F/Control	57	63	64	4.6	0.35	S1
	ST 10%	56	63	66	8.1	0.35	S1
	ST 17%	58	61	66	8	0.35	S1
	PPF 1%	56	66	68	6.8	0.35	S1
Set5 F/PFA/SF	PPF 2%	53	60	63	6	0.35	S1
	PET 1%	57	61	61	6.9	0.35	S1
	PET 2%	58	62	63	6.3	0.35	S1
	WS 1%	48	53	56	6.6	0.35	S1
	WS 2%	44	45	52	6.7	0.35	S1

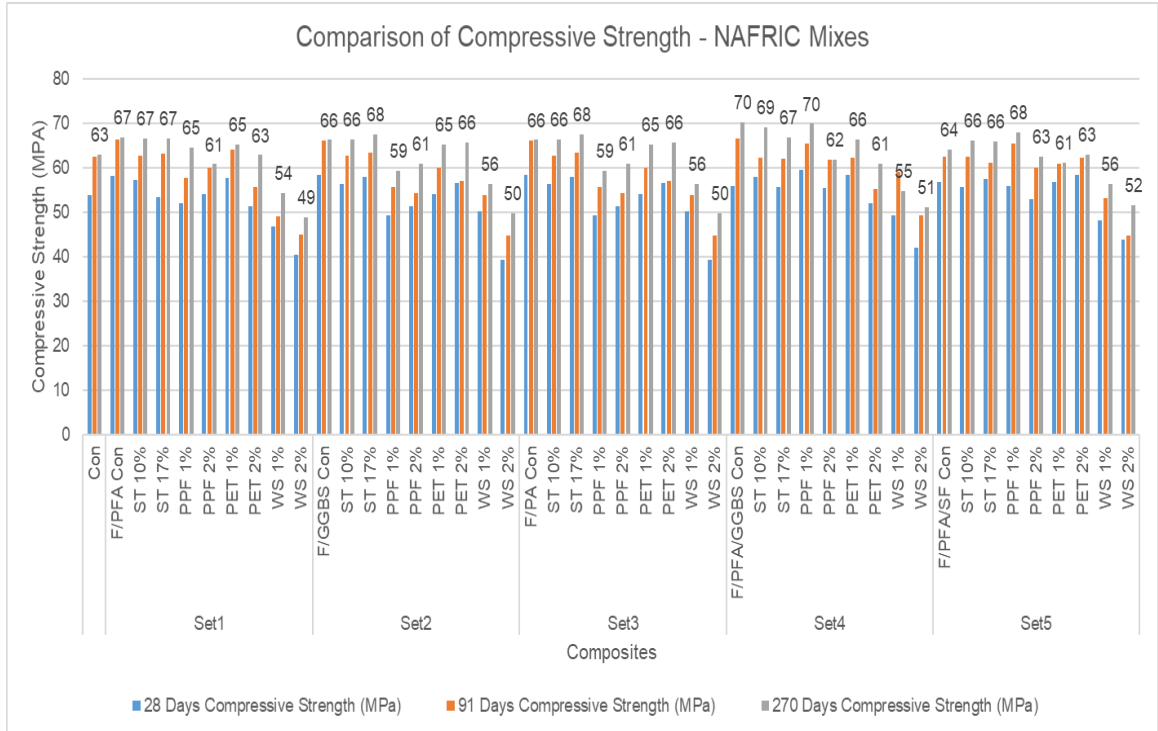


Figure 4.38: Comparison of Compressive Strength - NAFRIC Mixes.

4.9.1 Compressive Strength of NAFRIC Composites

The incorporation of fibres is likely to reduce the compressive strength beyond an optimum dosage due to the induction of weaker failure planes along the fibres compared to the aggregates due to the difference between their modulus of elasticity and toughness coefficient (Siddique, 2004; Akeem and Mitui, 2017; The Constructor, 2017; Scrivener, 2018; ASTM C 618/ C125, 2019; Selvapriya, 2019; Cement concrete, 2020; Girts et al., 2020; Nadir and Ahmed, 2021b Appendix VII; Admin, 2023). A slight decrease of around 2-5% was observed in compressive strength after incorporating fibres, but the high-strength concrete range of more than 60-70 MPa has still been achieved. The overall best-performing composites belonged to set 4 of ternary pozzolanic NAFRIC composites containing 10%PFA+10%GGBS with STF and PPF exhibiting up to 70 MPa strength, closely followed by the composites of NAFRIC with fibres (STF, PPF, PETF) and 20% GGBS and NAFRIC with 20%PA, 10%PFA+10%SF and lastly 20% PFA demonstrating more than 65 MPa strength by almost all NAFRIC

composites except the composites with 1-2% WSF although still obtaining a high strength of more than 50-56 MPa sufficient for all types of standard/ structural concrete applications as shown in Table 4.8 and Figure 4.38.

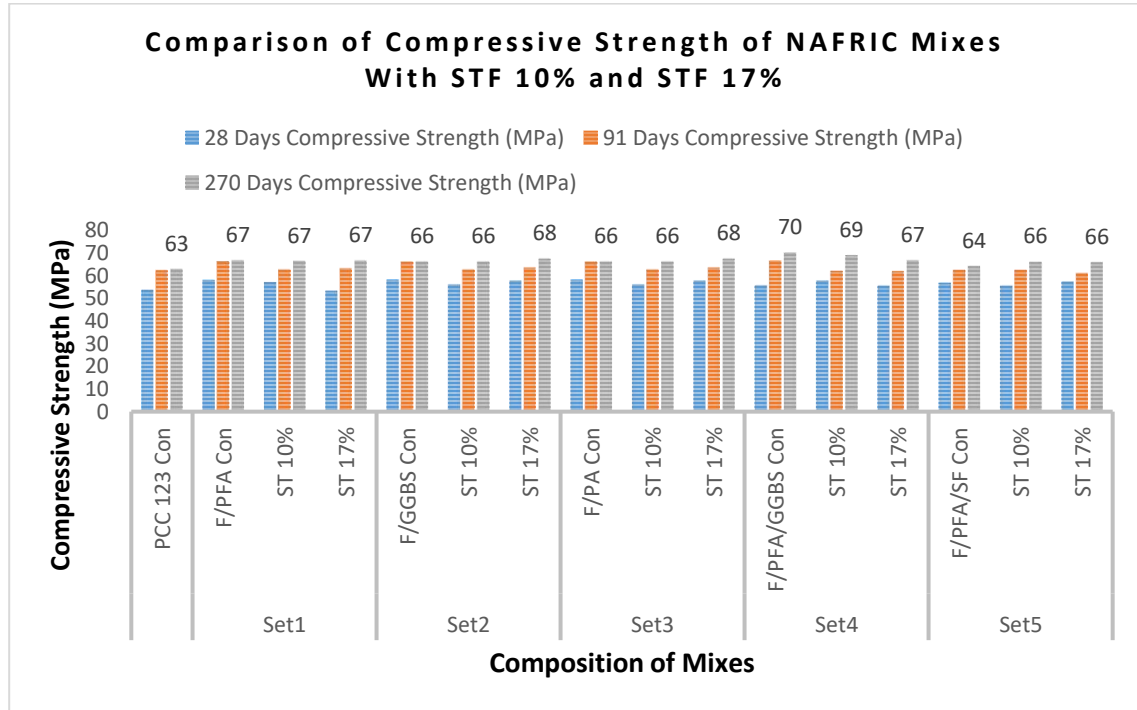


Figure 4.39: Comparison of Compressive Strength of NAFRIC Mixes With STF 10% and STF 17%.

The NAFRIC composites with STF 10% and STF 17% performed exceptionally well with iron powder and binary/ ternary pozzolans, achieving 66-69 MPa strength. STF is an established fibre expected to demonstrate mechanical properties at par with mildly reinforced concrete (Kim and Lee, 2021). NAFRIC with 10%PFA+10%GGBS has achieved 69 MPa strength with 10% STF and 67 MPa with 17% STF. NAFRIC with 20% GGBS and 20% PA have obtained 68 MPa with 17% STF and 66 MPa with 10% STF. NAFRIC with 20% PFA exhibited 67 MPa strength, and NAFRIC with 10%PFA+10%SF obtained 66 MPa strength (Figure 4.39). This study recommended the beneficial adoption of NAFRIC composites with STF for use in any structure applications as greener, waste

absorbent, low CO₂ embodied sustainable material which could save at least 10% of CO₂ emissions by the construction industry (equal to around 440 million tons of kgCO₂e equal to 10% of 4400 million tons of cement emissions).

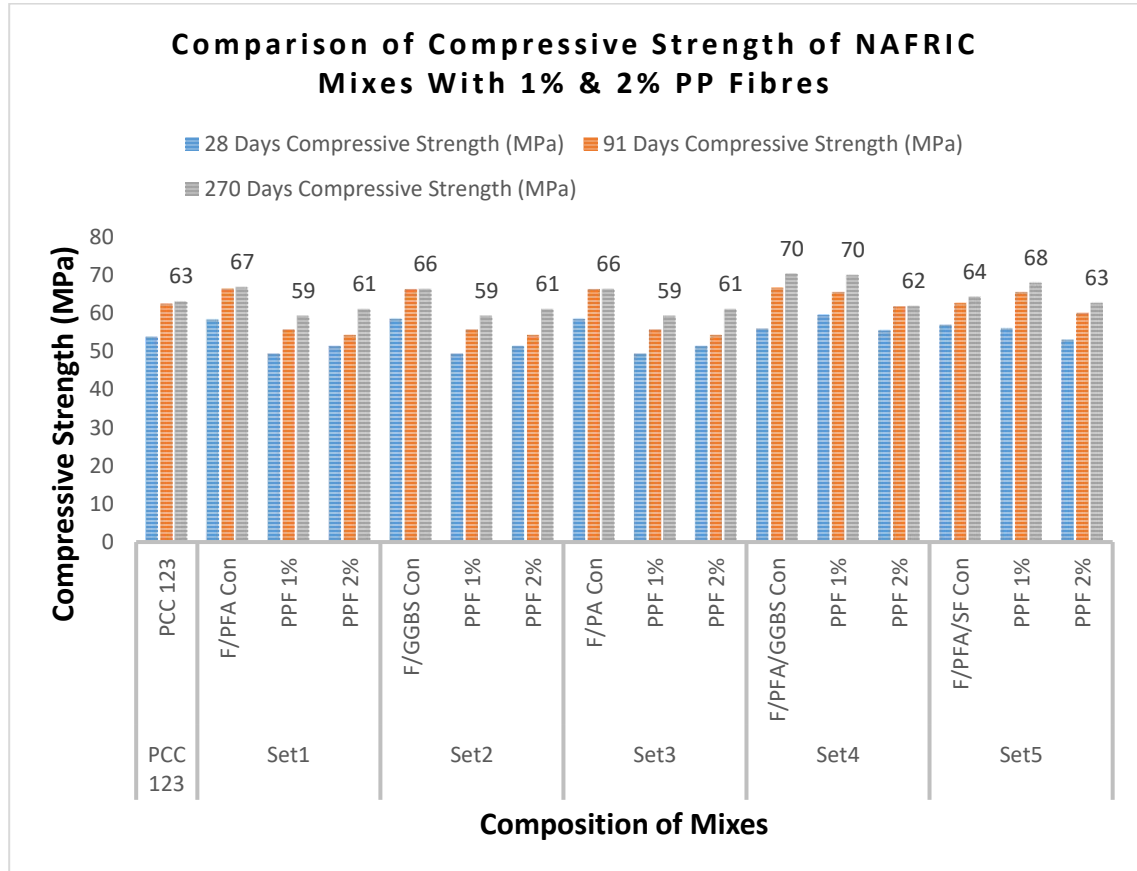


Figure 4.40: Comparison of Compressive Strength of NAFRIC Mixes With 1% & 2% PP Fibres.

PPF fibres are established fibres already in use in the construction industry on various linings, reinforced earth, façade safeguarding, anti-swelling, anti-sulphate attacks, and anti-crack formation/ propagation materials. Polypropylene is a stereognosis thermoplastic fibre transformed from 85% propylene. It has good properties and could be used as a concrete flexural/ tensile strength improvement material (Synthetic Fibres, 2020). The best-performing NAFRIC composite with 10%PFA+10%GGBS exhibited 70 MPa strength with PPF1%. All other

composites with NAFRIC binary/ ternary pozzolanic mixtures demonstrated 59-68 MPa strength with 1-2% fibres as the optimum dosage. The PPF 1-2% fibres induced 50-75% improvement in NAFRIC composites (Figure 4.40). The NAFRIC with 1-2% PPF could be used for all high-strength concrete applications with the added advantage of enhanced flexural strength properties as greener sustainable waste absorbent material safeguarding on carbon footprints of the construction industry up to 480 million tons of kgCO₂e annually (10% of CO₂ emissions of the construction industry).

Plastic, a very slowly degradable material, is always considered better to be recycled or reused instead of disposed of in landfills, sea or incinerators. 0.5-1-million-ton plastic waste is added daily, and 20,000 PET bottles are wasted every second worldwide. The shredding of PET bottles through a suitable shredder could produce plastic fibres with appropriate dimensions/ aspect ratios. These PET fibres are considered to perform at par with the PPF fibres in pore refinement, structural improvement, façade protection, RCC substitute of low reinforcement requirements for channels/ tunnels lining and other hydromodifications after uniformly embedding in the concrete for imparting better flexural strength (Hoornweg and Bhada (2012), (Hoornweg and Bhada,2012; Nadir et al., 2022a Appendix X). All the NAFRIC composites with 1-2% PET fibres demonstrated a high strength concrete range of 61-66 MPa, better than almost all the control mixes. NAFRIC with 20% GGBS and PA performed the best, achieving 66 MPa strength, closely followed by 20% PFA and ternary pozzolanic NAFRIC composites 61-65 MPa, as shown in Figure 4.41. The results support the beneficial use of 1-2% PET-incorporated NAFRIC composites for all types of structural concrete applications of 60-70 MPa with up to 60-70% improved flexural strength at par with the established fibres of STF and PPF. These composites could be suggested as low CO₂ embodied materials absorbing the global industrial waste and reducing the carbon footprints of the construction industry by around 10%.

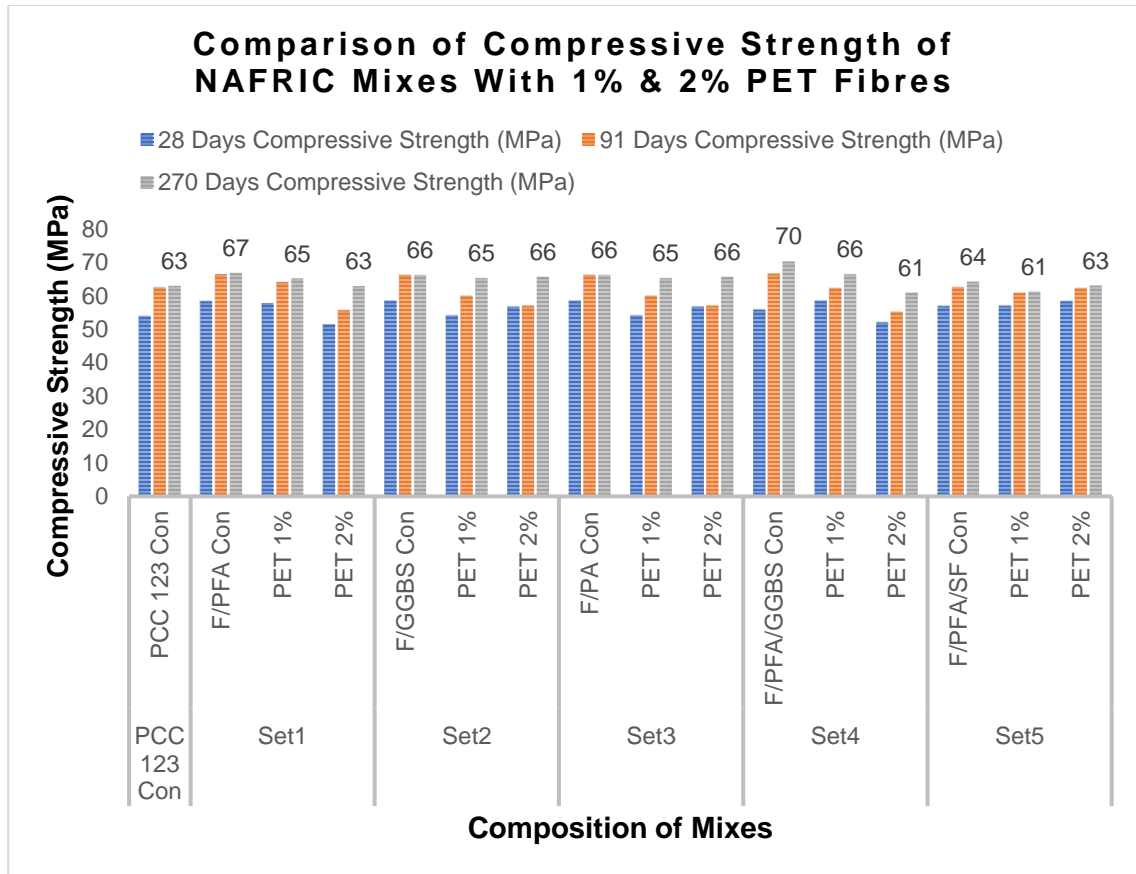


Figure 4.41: Comparison of Compressive Strength of NAFRIC Mixes With 1% & 2% PET Fibres.

Wheat straw is the residual byproduct of crops obtained as agricultural waste after harvesting wheat plants. Its modulus of elasticity and modulus of rupture makes it a good fibrous material which could be used for the improvement of tensile/ flexural strength of concrete to a certain extent as an innovative waste disposal option (Hector et al., 2011; Tufail et al., 2021; Nadir et al., 2022a Appendix X). In this study, WSF 1-2% was used as tensile/ flexural strength improvement material extracted from agricultural waste to improve the engineering properties of concrete and reduce the construction industry's carbon footprints. Although the NAFRIC composites containing WSF 1-2% obtained 50-56 MPa more than the target 40 MPa strength, up to 20% decrease in compressive strength was observed in all the composites compared to the control

mixes. In Binary pozzolanic NAFRIC composites, 20% GGBS and 20% PA achieved up to 56 MPa strength, followed closely by 20% PFA composites exhibiting 54 MPa strength. In ternary pozzolanic NAFRIC composites, 10%PFA+10%GGBS and 10%PFA+10%SF achieved 55-56 MPa strength, as shown in Figure 4.42 and Table 4.8. The density, workability and compressive strength of all the NAFRIC composites register a slight reduction in all the engineering properties with the increase in dosage of WSF from 1% to 2%, suggesting 1% as the optimum dosage. A slight decrease in compressive strength was observed. Still, all the NAFRIC composites with WSF 1-2% achieved more than 50 MPa strength, making them suitable for all everyday concrete applications in the construction industry.

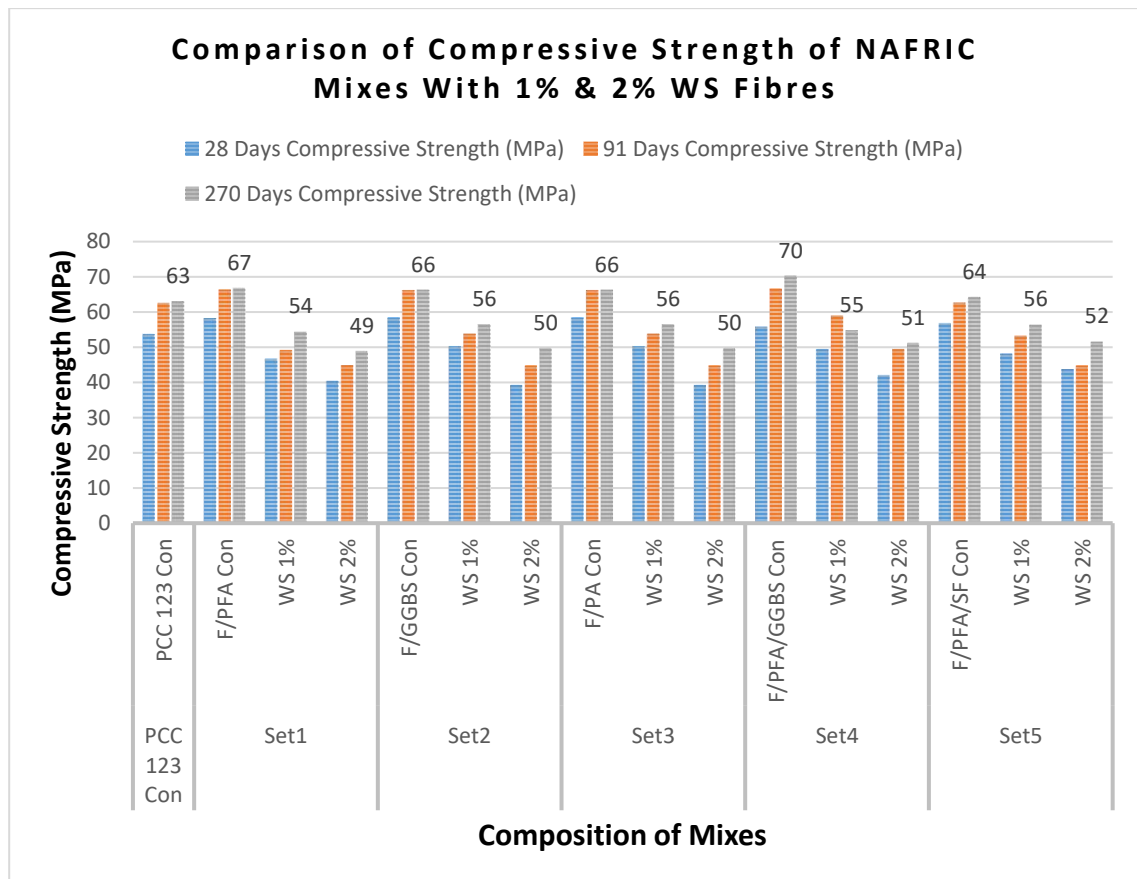


Figure 4.42: Comparison of Compressive Strength of NAFRIC Mixes With 1% & 2% WS Fibres.

4.9.2 Flexural Strength of NAFRIC Composites

The 10% and 17% STF composites demonstrated 100% improvement in flexural strength by exhibiting a strength of 8.1-8.9 MPa compared to the control mix (4.3 MPa), as shown in Figure 4.43. 20% PA-based NALFRIC was the best potent mix with 8.9 MPa flexural strength. The use of steel fibre reinforced concrete in tunnel shaft lining, water channel lining, in swelling strata, as anti-seismic mildly reinforced material, in marine sulphate attack environments, as an improved material against thawing, freezing, shrinkage, and failure resistant material was supported by the researchers due to their excellent elastic properties of 200 GPa modulus of elasticity and 1200-2600 MPa tensile strength. The established/suitable use of STF is designated at a rate of 10-17 % fibres to the cement weight (Koh, 2017; Lee, 2017; Tariq et al., 2017; USDT, 2020; Yasmin, Bitencourt and Osvaldo, 2020; Kim and Lee, 2021; Kwon and Yoo, 2021; Showkati, Salari-rad and Aghchai, 2021; Nadir et al., 2022a Appendix X; www.becaert.com/dosingdramix, 2024). The maximum flexural strength of 7-7.2 MPa was attained by 20% PFA-based NAFRIC. 20% GGBS-based composites obtained 6.8-6.9 MPa strength. NAFRIC with ternary pozzolans of 10%PFA+10%GGBS and 10%PFA+10%SF obtained 5.6-6.9 MPa strength, whereas 20% PA-based exhibited the least performance but still achieved flexural strength of 5.5-6.8 MPa (Figure 4.43). 20% PA with 1-2% PET fibres achieved the best flexural strength of 7.3-7.9 MPa (75% improvement). All other composites also demonstrated 6.3-6.9 MPa flexural strength, exhibiting 50-60% improvement (Figure 4.43). 20% PA and 20% GGBS NAFRIC composites demonstrated a maximum flexural strength of up to 6.7-6.8 MPa (up to 40% flexural strength improvement). All other composites containing 20% PFA, 10%PFA+10%GGBS and 10%PFA+10%SF exhibited flexural strength from 5.4-6.6 MPa (4.43).

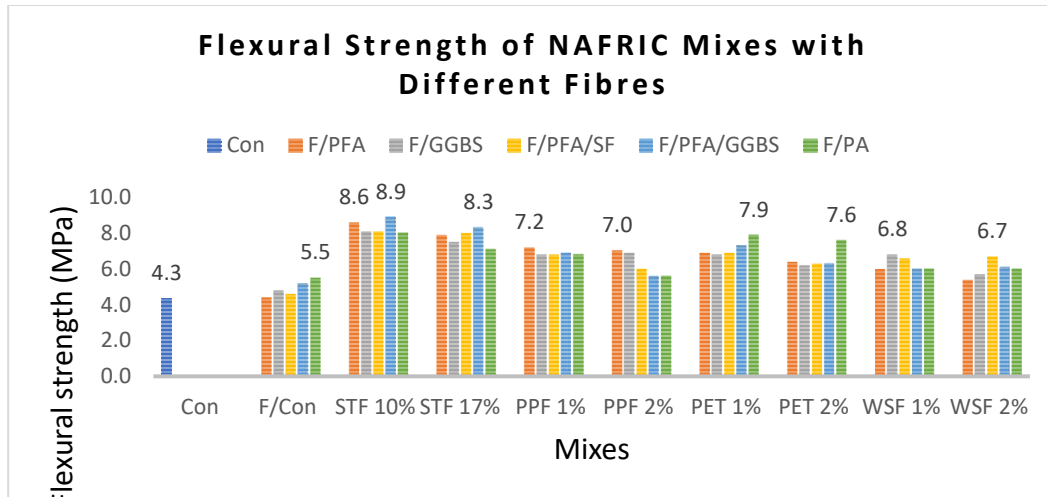


Figure 4.43: Flexural Strength of Fe-Based Composites with Different Fibres.

4.10 Analysis of Post-Crack Ductility of Fibre-Reinforced Composites

Concrete is universally considered strong in compression and weak in tension, necessitating reinforcement for enhanced tensile/ flexural strength. Flexural strength is the strength of a material to withstand a bending load and is a unique combination of tensile/ compressive strength experienced simultaneously across a neutral axis in a testing specimen. The tensile strength is induced at the lower portion of the specimen, where it tends to tear apart by the widening of the crack, whereas the upper portion is subject to compressive stress and tends to resist any crack formation due to compression. Assessing a material's elastic, plastic, ductility and toughness characteristics is essential. Elasticity shows a material's ability to revert to its original dimensions/ shape after removing the load, and plasticity is the ability to withstand the bending forces. However, the material experiences a permanent deformation and cannot be restored to its original position. Brittle materials do not exhibit elastic/ plastic behaviour but tend to rupture on exposure to a bending load after a crack generation. Ductility is the ability of a material to deform plastically before rupture/ failure. It could demonstrate a large quantity of strain/ crack width/ displacement of crack while absorbing the stress plastically, contrary to brittle materials, which rupture without absorbing the stress and exhibit more significant strain/ displacement of crack

width. Toughness is the ability of a material to absorb bending forces before fracture/ rupture. Generally, brittle materials like concrete exhibit high compression but deficient elasticity, plasticity, ductility, and toughness, necessitating reinforcement. However, not every concrete application warrants costly/ high CO₂ embodied steel reinforcement; instead, a slight improvement in the flexural strength could be achieved by incorporating fibres for enhanced ductility, like the lining of small water channels or façade protection of stone-pitched embankments.

The fibres in the specimens are considered to impart ductility in the material, and a large displacement/ crack width could be observed in flexural strength testing, keeping the specimen intact even after rupture, exhibiting a good post-crack ductility mechanism and more significant stress-strain displacement on the X-axis of the flexural strength versus displacement graphs (Figure 4.44) (Yap, Alengaram and Jumaat, 2013; Martinelli, Caggiano and Xargay, 2015; Younis, 2016; Sundar, 2017; Bahij et al., 2020; Saurav, 2021; Nadir et al., 2022a Appendix X). An increased quantity of fibres improved the tensile capability of fibre composites but simultaneously created weaker zones due to a lack of bonding in concrete ingredients, which resulted in lesser compressive strength, which ruptured the bottom layers of the prisms under bending load. However, the fibres and their natural elastic property hold the prism to rupture swiftly and continue to absorb energy even after the rupture (ductility and toughness), thus exhibiting good ductility (Yap, Alengaram and Jumaat, 2013; Martinelli, Caggiano and Xargay, 2015; Younis, 2016; Sundar, 2017; Bahij et al., 2020; Saurav, 2021; Nadir et al., 2022a Appendix X). All the samples with fibres have shown good ductility and energy absorption capability of fibre composites even after rupture. Samples with 10-17 % STF and 1-2% other fibres showed improved ductility. A qualitative analysis was carried out by visually observing the rupture pattern and ductile behaviour of all fibre mixes and plotting the flexural strength versus the displacement, which showed how long the sample absorbed energy after the development of crack/ rupture and remained intact due to the fibres (Figure 4.4).

Based on their post-rupture ductility behaviour and visual inspection, the composites were analysed qualitatively to be categorised as brittle (displacement less than 10mm), moderately ductile (displacement 20-30mm), highly ductile (displacement 30-40mm), and exceptionally high (displacement more than 40mm), while the control mix was categorised as brittle with no ductility (Tables 4.9-4.11). The student has chosen these qualitative references to segregate the specimens based on the crack width/ displacement observed after exposing the prisms to bending forces on a three-point loading machine. However, to make these results more meaningful, percentage increases of flexural strength/ displacements before rupture were introduced along with the qualitative analysis to support the finding quantitatively, as shown in Tables 4.9-4.11. The three-point loading machine for the flexural Testing has the maximum capacity of precisely giving around 54.5 mm displacement. After that, its base loading supports get displaced from the foundation of the machine and give more reading than 54 mm, but the load becomes zero, as is visible in Figures 4.44 and 4.45. Therefore, the materials exhibiting exceptional ductility have demonstrated a crack width of 54.5 mm, but if the machine had permitted/ was capable of doing so, then the displacement might be more than 54.5 mm.

4.10.1 Post-Crack Ductility of OPC-Based FRC

The load-displacement graph and visual pictures are shown in figures 4.44-4.51, which show that the control mix and mixes with fewer fibres ruptured abruptly without considerable displacement and energy absorption. In contrast, the composites with more fibres exhibited good energy absorption even after rupture and remained intact due to the fibres' ductility. The load-displacement graphs and post-rupture pictures of all samples are shown in Figures 4.44-4.51 and Table 4.9, categorising post-rupture ductility. The natural coir and wheat straw fibres gave better strengths but were outperformed by synthetic plastic/ polymer materials due to their inherent characteristics like elasticity, aspect ratio, coarseness, roughness, toughness and nature of materials. Steel fibre exhibited maximum elasticity, better energy absorption, and post-rupture ductility and

performed the best in absorbing bending forces and exhibiting ductility/ elasticity as expected, in line with the existing research/ material properties, followed by PPF. However, PET bottles' shredded fibres have exhibited equally high ductility and could be suggested as an alternative to STF and PPF. (Yap, Alengaram and Jumaat, 2013; Martinelli, Caggiano and Xargay, 2015; Younis, 2016; Sundar, 2017; Bahij et al., 2020; Saurav, 2021; Nadir et al., 2022a Appendix X).



Figure 4.44: Mechanism of Post-Crack Ductility in Fibre-Reinforced Prisms During Flexural Strength Testing.





	
FRC with PPF 2% (exceptionally ductile, remained intact after rupture)	SL80 PET 2% (exceptionally ductile but fully ruptured)
	
F/ GGBS with WSF 2% (moderately ductile, remained intact after rupture)	F/PFA/SF PET 2% (exceptionally ductile, remained intact after rupture)

Figure 4.45: Post-Crack Ductility of Various Prisms.

The control mix achieved a flexural strength of 3.4 MPa, and the crack width or displacement of the crack was observed as 3 mm. It was ruptured at a 2.5 mm crack and did not demonstrate any post-crack ductility by entirely breaking into two halves at a 3 mm crack width, suggesting it to be a brittle material, as shown in Figure 4.46 and Table 4.9.

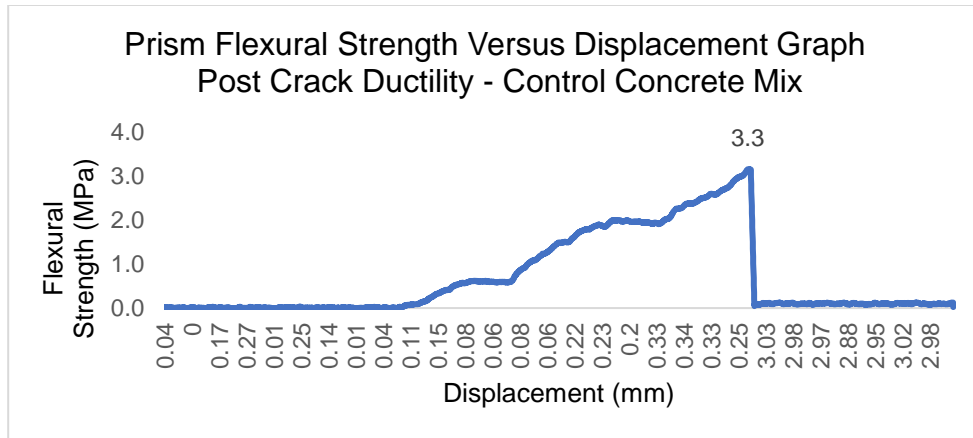


Figure 4.46: Prism Flexural Strength Versus Displacement Graph – FRC Control.

The FRC 1:2:3 composite with 17% STF achieved a maximum flexural strength of 8.7 MPa, extending the crack width or displacement of the crack while energy absorption was observed as 54 mm. It was ruptured at a 7.5 mm crack and demonstrated exceptionally high post-crack ductility by remaining intact even after extending to a crack width of 54 mm, suggesting it to be an exceptionally high ductile composite due to the established steel fibres, as shown in Figure 4.47 and Table 4.9.

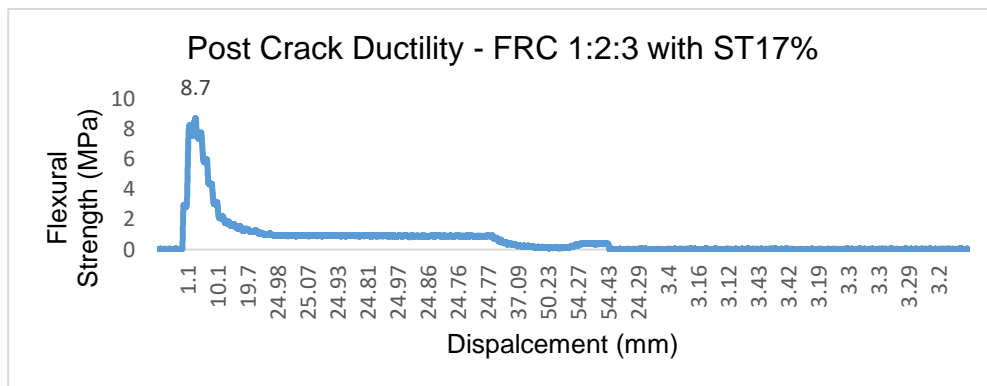


Figure 4.47: Post Crack Ductility - FRC 1:2:3 with ST17%.

The FRC 1:2:3 composite with PPF 2% achieved a maximum flexural strength of 5.7 MPa, extending the crack width or displacement of the crack during energy absorption up to 53 mm. It was cracked at a 0.7 mm crack and demonstrated

exceptionally high post-crack ductility by remaining intact even after extending to a crack width of 53mm, suggesting it to be an exceptionally high ductile composite due to the established PPF, as shown in Figure 4.48 and Table 4.9.

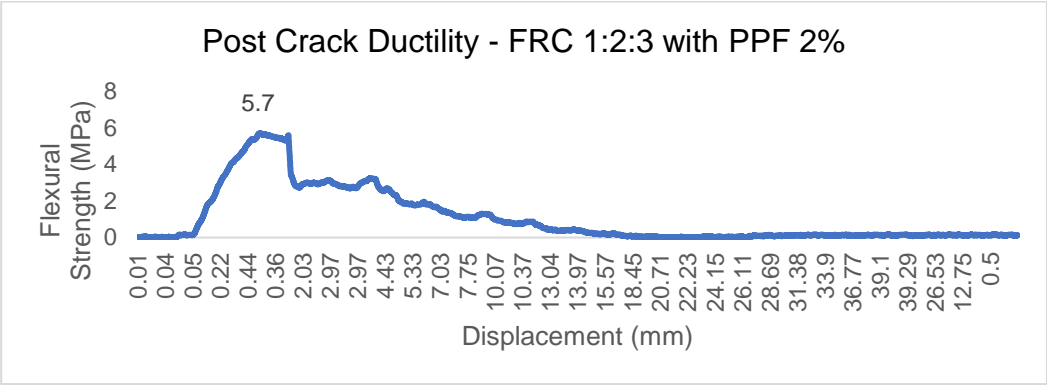


Figure 4.48: Post Crack Ductility - FRC 1:2:3 with PPF 2%.

The FRC 1:2:3 composite with coir 2% achieved a maximum flexural strength of 8.3 MPa, extending the crack width or displacement of the crack during energy absorption up to 34 mm. It was cracked at a 0.22 mm crack. It demonstrated exceptionally high post-crack ductility by remaining intact even after extending to a crack width of 34 mm, suggesting it to be a highly ductile composite even with the use of waste agricultural coconut coir fibre, suggesting a beneficial use at par with the STF and PPF, as shown in Figure 4.49 and Table 4.9.

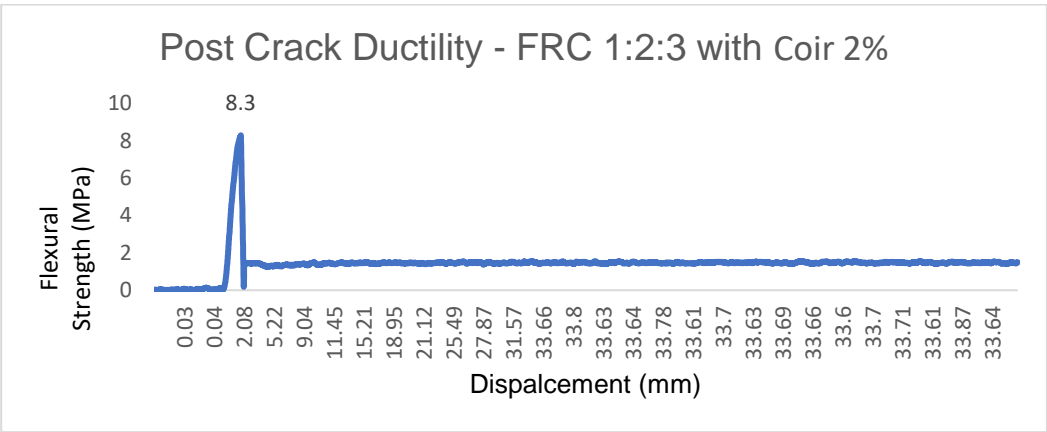


Figure 4.49: Post Crack Ductility - FRC 1:2:3 with Coir 2%.

The FRC 1:2:3 composite with PET 2% exhibited a maximum flexural strength of 8 MPa, extending the crack width or displacement of the crack during energy absorption up to 43 mm. It was cracked at a 3.7 mm crack width. It demonstrated exceptionally high post-crack ductility by remaining intact even after extending to a crack width of 43 mm, suggesting it to be an exceptionally ductile composite even with the use of waste PET bottle fibre, suggesting a beneficial use at par with the STF and PPF, as shown in Figure 4.50 and Table 4.9.

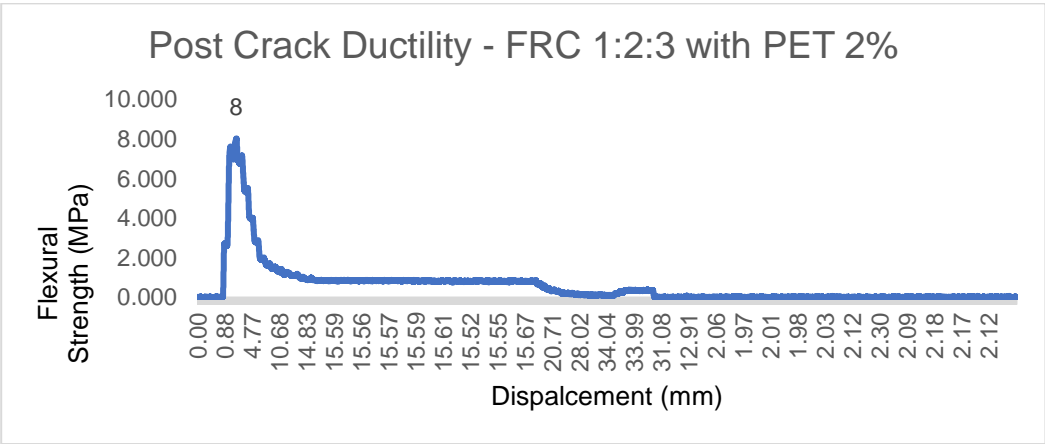


Figure 4.50: Post Crack Ductility - FRC 1:2:3 with PET 2%.

The FRC 1:2:3 composite with WSF 2% exhibited a maximum flexural strength of 7.1 MPa, extending the crack width or displacement of the crack during energy absorption up to 43 mm. It was cracked at a 0.81 mm crack width. It demonstrated exceptionally high post-crack ductility by remaining intact even after extending to a crack width of 32 mm, suggesting it to be an exceptionally ductile composite even with the use of waste agricultural wheat straw fibre, suggesting a beneficial use at par with the STF and PPF (although it under-performed in the compressive strength testing), as shown in Figure 4.51 and Table 4.9.

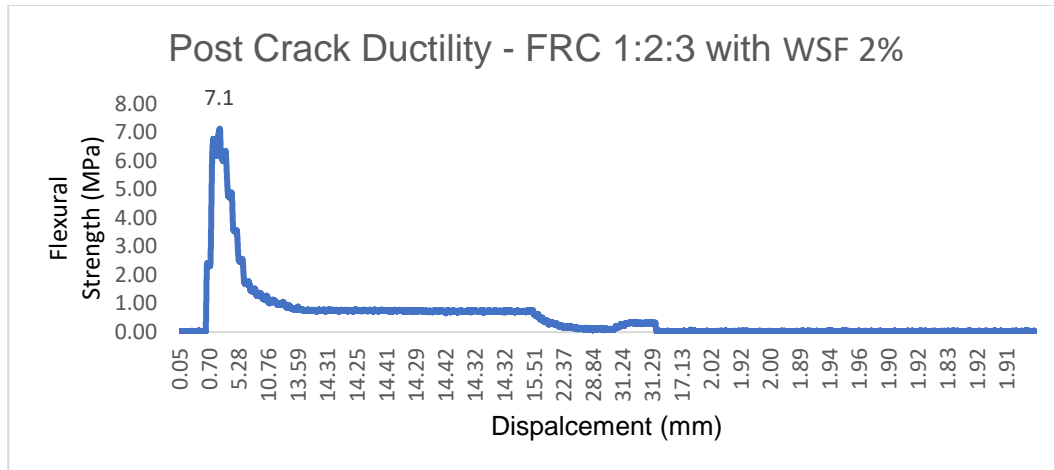


Figure 4.51: Post Crack Ductility - FRC 1:2:3 with WSF 2%.

Table 4.9: Qualitative/ Quantitative Analysis - Post-Crack Ductility - FRC 1:2:3.

Qualitative Analysis Post Crack Ductility - FRC 1:2:3					
Mixes	90 Days Flexural Strength (MPa)	Displacement (mm)	%age Increase in Flexural Strength Vs Control Mix (%)	%age Increase in Ductility Based on Displacement (%)	Ductility
Con	3.3	3			Brittle
ST 10%	7	54.6	112.1	680.0	Exceptionally Ductile
ST 17%	8.7	54.5	163.6	678.6	Exceptionally Ductile
PPF 0.5%	7.8	20.5	136.4	192.9	Moderately Ductile
PPF 1%	6.8	43.3	106.1	518.6	Exceptionally Ductile
PPF 1.5%	7.3	54.5	121.2	678.6	Exceptionally Ductile
PPF 2%	8	55.6	142.4	694.3	Exceptionally Ductile
Coir 0.5%	6.9	18.5	109.1	164.3	Brittle
Coir 1%	8.3	27.8	151.5	297.1	Moderately Ductile
Coir 1.5%	6.1	37.4	84.8	434.3	Highly Ductile
Coir 2%	5.7	34	72.7	385.7	Highly Ductile
PET 0.5%	5.6	5.4	69.7	-22.9	Brittle
PET 1%	8	30.9	142.4	341.4	Highly Ductile
PET 1.5%	5	35.7	51.5	410.0	Highly Ductile
PET 2%	5	42.3	51.5	504.3	Exceptionally Ductile
WS 0.5%	5.5	12.2	66.7	74.3	Brittle
WS 1%	5.9	23.3	78.8	232.9	Moderately Ductile
WS 1.5%	6.4	22	93.9	214.3	Moderately Ductile
WS 2%	7.1	31.7	115.2	352.9	Highly Ductile

4.10.2 Post-Crack Ductility of Hydrated Lime-Based Pozzolanic FRC NALFRIC.

The flexural strength of NALFRIC composites containing SL80 was almost one-third of the FRC composites, as shown in Figure 4.52. The flexural strength of NALFRIC composites containing MK50 was minimal, almost as one-seventh of the FRC composites, as shown in Figure 4.52. The results align with the existing findings that tensile and flexural strengths are around 10% and 0.7% of compressive strength. The NAFRIC composites demonstrated a low-medium range of compressive strength (10-25 MPa); therefore, the flexural strength of up to 10% of the compressive strength by fibre-reinforced lime-based pozzolanic composites is a good achievement of strength, making them beneficially useable for low strength construction applications. The post-crack ductility of NALFRIC composites was illustrated in Figures 4.51-4.54, and qualitative analysis was summarised in Table 4.10 for the composites exhibiting a range of ductility.

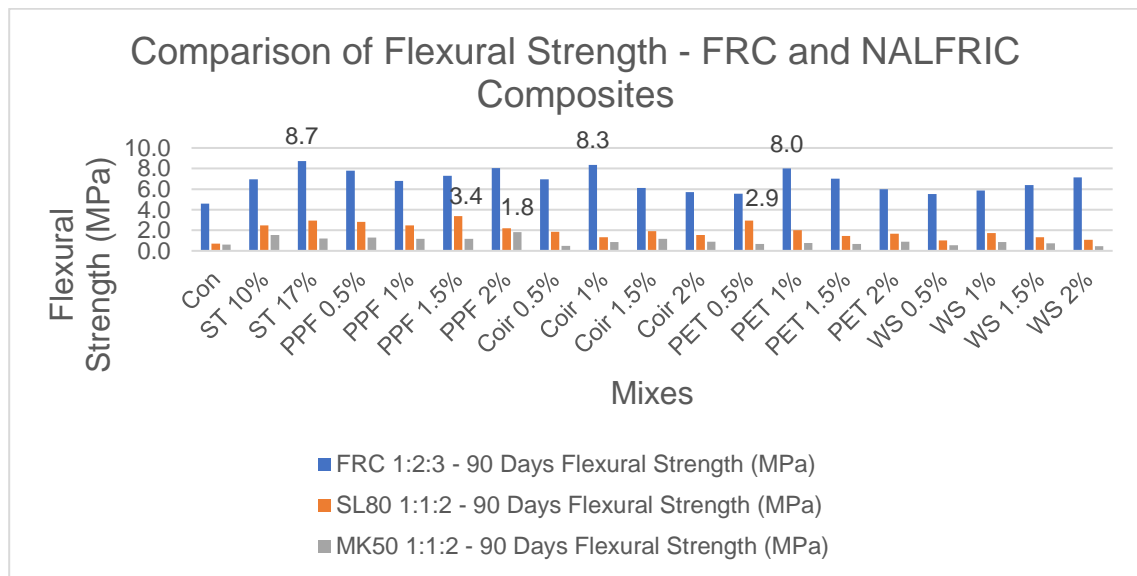


Figure 4.52: Comparison of Flexural Strength - FRC and NALFRIC Composites.

The NALFRIC SL80 1:2:3 composite with PET 2% exhibited a flexural strength of 2.9 MPa, extending the crack width or displacement of the crack during energy absorption up to 29 mm. It was ruptured at a 1 mm crack width and demonstrated

moderately high post-crack ductility by remaining intact even after extending to a crack width of 29 mm, suggesting it to be a good ductile composite even with the use of waste PET bottle fibre, suggesting a beneficial use at par with the STF and PPF, as shown in Figure 4.53 and Table 4.10.

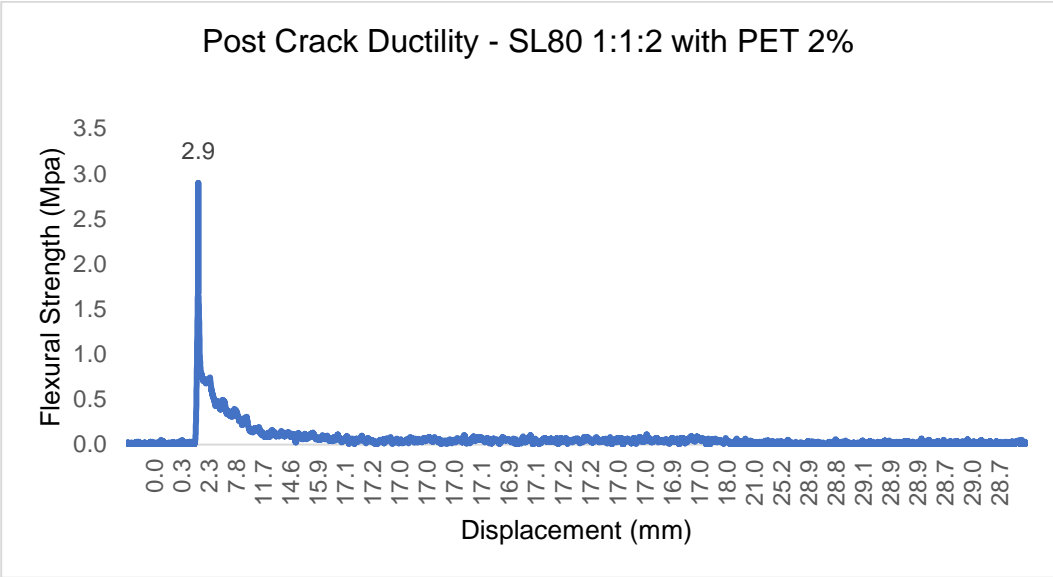


Figure 4.53: Post Crack Ductility - SL80 1:1:2 with PET 2%

The NALFRIC SL80 1:2:3 composite with STF 17% exhibited a flexural strength of 2.9 MPa, extending the crack width or displacement of the crack during energy absorption up to 50 mm. It was ruptured at a 1 mm crack width and demonstrated exceptionally high post-crack ductility by remaining intact even after extending to a crack width of 50mm, suggesting it to be an exceptionally ductile composite as expected for the established steel fibres, as shown in Figure 4.54 and Table 4.10. The NALFRIC SL80 1:2:3 composite with PPF 1.5% exhibited a maximum flexural strength of 3.4 MPa, extending the crack width or displacement of the crack during energy absorption up to 25 mm. It was ruptured at a 1 mm crack width and demonstrated moderately high post-crack ductility by remaining intact even after extending to a crack width of 25mm, suggesting it to be a considerably high ductile composite as expected for the established PPF, as shown in Figure 4.55 and Table 4.10.

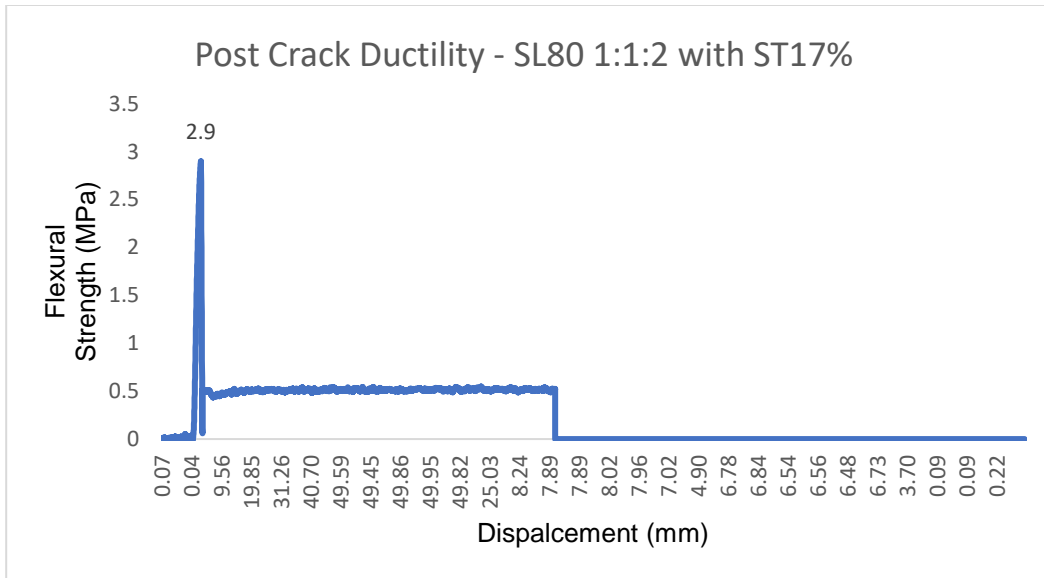


Figure 4.54: Post Crack Ductility - SL80 1:1:2 with ST17%

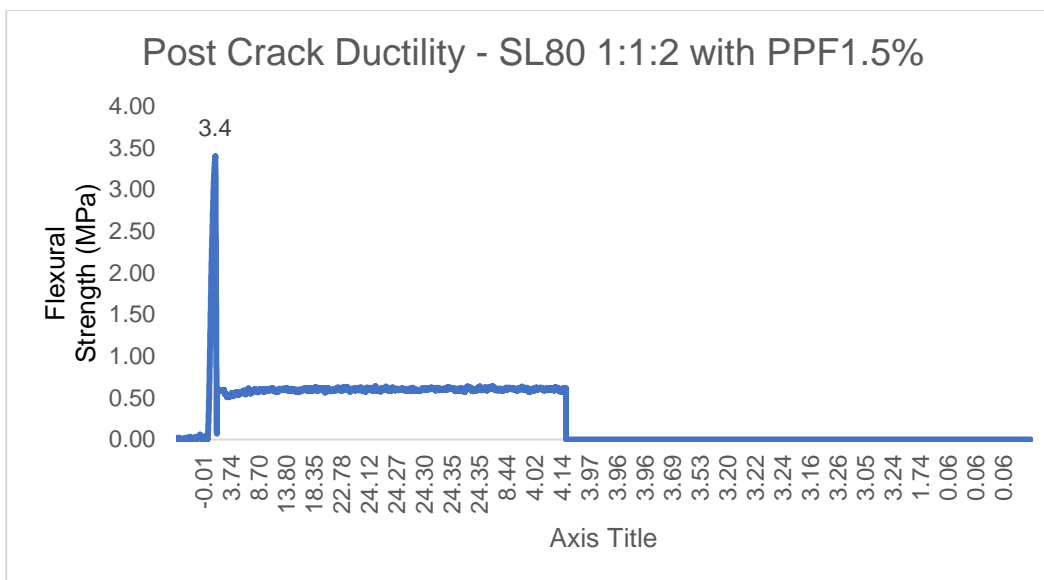


Figure 4.55: Post Crack Ductility - SL80 1:1:2 with PPF1.5%.

Table 4.10: Qualitative Analysis - Post-Crack Ductility of NALFRIC Composites (SL80 1:1:2 and MK50 1:1:2).

Qualitative Analysis - Post Crack Ductility on 91 Days Flexural Strength (MPa) Vs Displacement (mm)										
SL80 112						MK50 112				
Mixes	91 Days Flexural Strength (MPa)	Displacement (mm)	%age Increase in Flexural Strength Vs Control Mix (%)	%age Increase in Ductility Based on Displacement (%)	Qualitative Ductility Ranking	91 Days Flexural Strength (MPa)	Displacement (mm)	%age Increase in Flexural Strength Vs Control Mix (%)	%age Increase in Ductility Based on Displacement (%)	Qualitative Ductility Ranking
Con	0.7	5			Moderately Ductile	0.6	4			Moderately Ductile
ST 10%	2.5	23	255	353	Moderately Ductile	1.6	23	159	478	Moderately Ductile
ST 17%	2.9	50	321	891	Exceptionally Ductile	1.2	34	98	746	Highly Ductile
PPF 0.5%	2.8	18	303	263	Brittle	1.3	30	116	645	Moderately Ductile
PPF 1%	2.5	22	254	343	Moderately Ductile	1.2	21	94	413	Moderately Ductile
PPF 1.5%	3.4	24	383	387	Moderately Ductile	1.2	20	95	398	Brittle
PPF 2%	2.2	23	215	353	Moderately Ductile	1.8	24	201	511	Moderately Ductile
Coir 0.5%	1.9	21	166	329	Moderately Ductile	0.5	19	-20	367	Brittle
Coir 1%	1.3	26	89	427	Moderately Ductile	0.9	19	44	364	Brittle
Coir 1.5%	1.9	25	172	407	Moderately Ductile	1.2	20	93	406	Moderately Ductile
Coir 2%	1.6	29	122	473	Moderately Ductile	0.9	24	50	491	Moderately Ductile
PET 0.5%	2.9	24	320	374	Moderately Ductile	0.7	16	14	301	Brittle
PET 1%	2.0	23	188	370	Moderately Ductile	0.8	16	29	297	Brittle
PET 1.5%	1.5	24	108	381	Moderately Ductile	0.7	35	11	766	Highly Ductile
PET 2%	1.7	29	140	483	Moderately Ductile	0.9	26	48	546	Moderately Ductile
WS 0.5%	1.0	24	44	388	Moderately Ductile	0.5	12	-11	204	Brittle
WS 1%	1.7	28	149	464	Moderately Ductile	0.8	16	41	308	Brittle
WS 1.5%	1.3	21	88	320	Moderately Ductile	0.7	22	20	440	Moderately Ductile
WS 2%	1.1	29	54	480	Moderately Ductile	0.5	24	-23	500	Moderately Ductile

4.10.3 Post-Crack Ductility of Iron-Based Binary/ Ternary Pozzolanic FRC NAFRIC

The NAFRIC 1:2:3 composites performed better than FRC 1:2:3 at par with the high-strength concrete range of 1:1:2 or 1:1:3 job mix ratios and obtained up to 70-80 MPa strength due to expected pozzolanic reaction to produce additional C-S-H gel and rock-like strength due to formation of FeCO_3 (Section 4.8 and 4.9). The control mixes containing iron-based pozzolanic SCMs exhibited better flexural strength than the PCC control due to inherent ductility associated with iron compounds. The NAFRIC with 10-17% STF and 1-2% PPF performed better, demonstrating exceptionally high ductility with 6-8.6 MPa flexural strength and 30-50 mm displacement and remaining intact even after 40-50 mm of crack width

as expected being the established fibres; however, the innovative 2% PET fibres also performed at par with STF/ PPF achieving exceptionally high ductility by remaining intact even after extending to more than 40 mm crack width. WSF achieved 6-7 MPa flexural strength but performed slightly less in achieving a high ductile range due to the inherent lower toughness and flexibility of WSF compared to STF, PPF and PET fibres, as shown in Figures 4.45, 4.56-4.60 and Table 4.11.

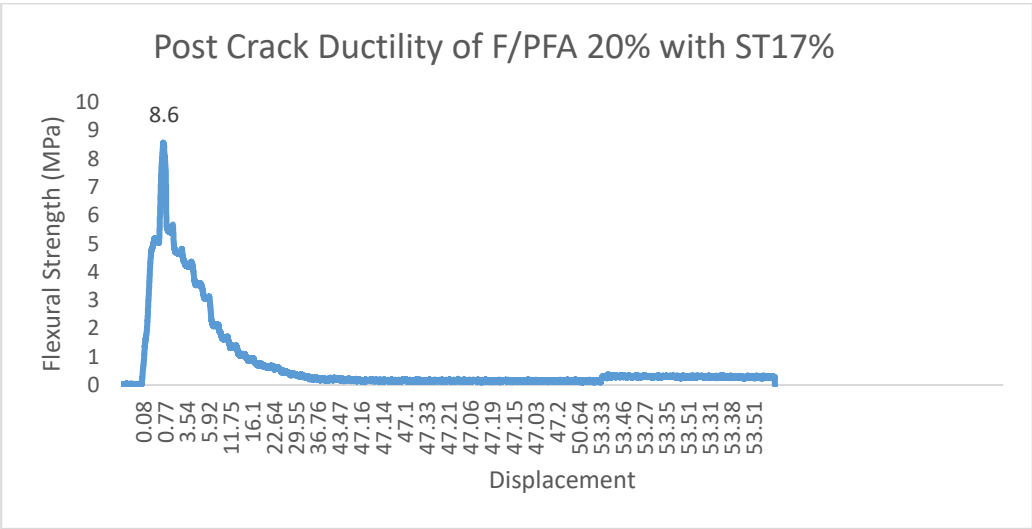


Figure 4.56: Post Crack Ductility of F/PFA 20% with ST17%

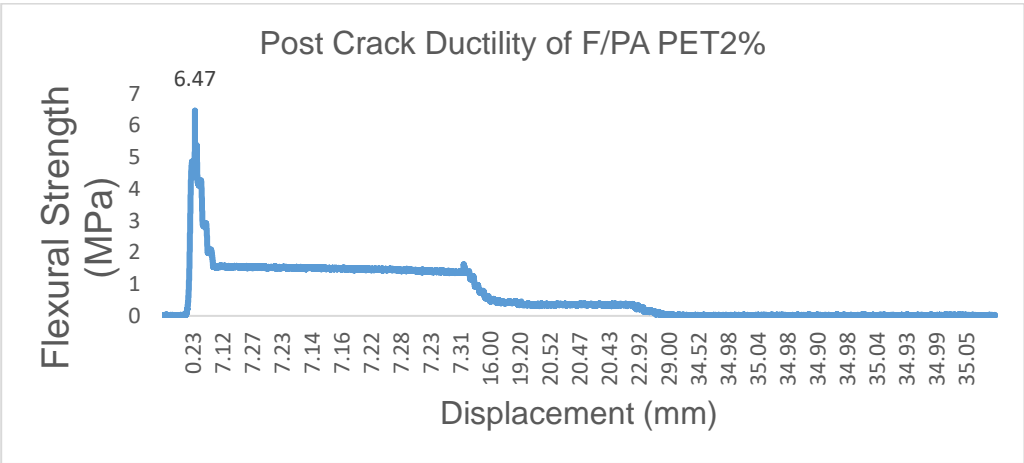


Figure 4.57: Post Crack Ductility of F/PA PET2%

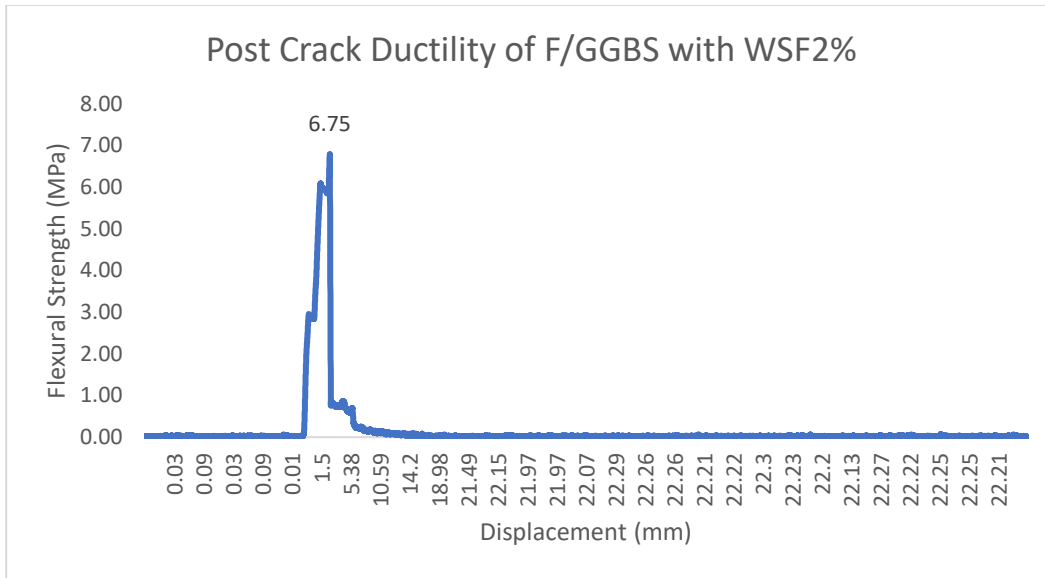


Figure 4.58: Post Crack Ductility of F/GGBS with WSF2%

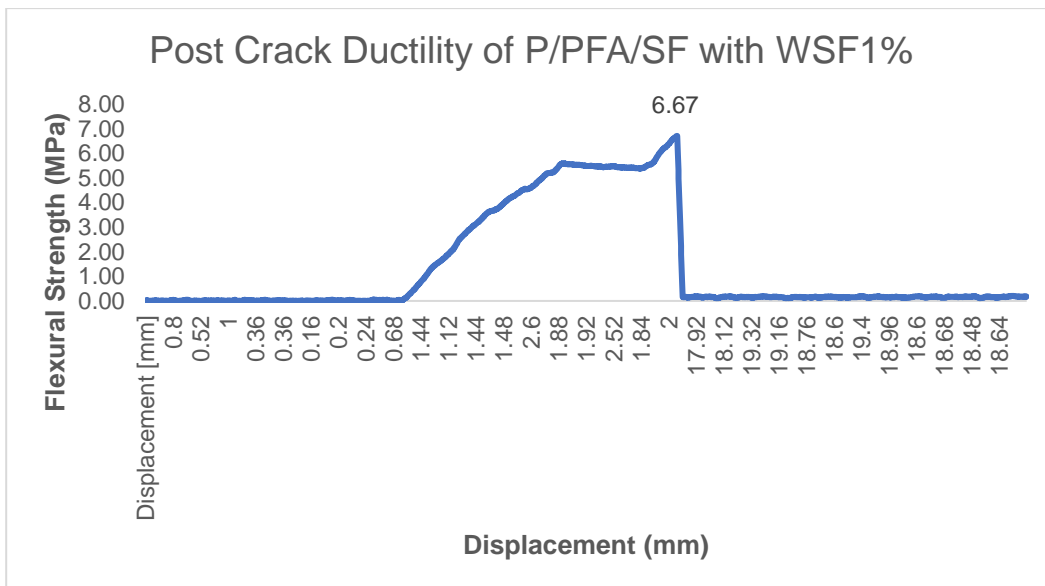


Figure 4.59: Post Crack Ductility of P/PFA/SF with WSF 1%.

Table 4.11: Qualitative/ Quantitative Analysis - Post-Crack Ductility of NAFRIC Composites.

Qualitative Analysis Post Crack Ductility of Binary Pozzolanic NAFRIC Composites (Fe/PFA, Fe/GGBS, Fe/PA 1:2:3)										
Fe/PFA						Fe/GGBS				
Mixes	91 Days Flexural Strength (MPa)	Displacement (mm)	%age Increase in Flexural Strength Vs Control Mix (%)	%age Increase in Ductility Based on Displacement (%)	Qualitative Ductility Ranking	91 Days Flexural Strength (MPa)	Displacement (mm)	%age Increase in Flexural Strength Vs Control Mix (%)	%age Increase in Ductility Based on Displacement (%)	Qualitative Ductility Ranking
Con	4.3	5.1			Brittle	4.3	5.1			Brittle
Fe/ Con	4.4	5.0	2.3	-2.0	Brittle	4.8	6.0	11.6	17.6	Brittle
ST 10%	8.6	54.6	100.0	971.0	Exceptionally Ductile	8.1	54.6	88.4	971.0	Exceptionally Ductile
ST 17%	7.9	54.5	83.7	969.4	Exceptionally Ductile	7.5	54.5	74.4	969.4	Exceptionally Ductile
PPF 1%	7.2	43.3	67.4	748.0	Exceptionally Ductile	6.8	43.3	58.1	748.0	Exceptionally Ductile
PPF 2%	7.04	55.6	63.7	990.0	Exceptionally Ductile	6.9	55.6	60.5	990.0	Exceptionally Ductile
PET 1%	6.9	30.9	60.5	505.9	Highly Ductile	6.8	30.9	58.1	505.9	Highly Ductile
PET 2%	6.4	42.3	48.8	730.2	Exceptionally Ductile	6.2	42.3	44.2	730.2	Exceptionally Ductile
WS 1%	6	23.3	39.5	357.1	Moderately Ductile	6.8	23.3	58.1	357.1	Moderately Ductile
WS 2%	5.4	31.7	25.6	520.8	Highly Ductile	5.7	31.7	32.6	520.8	Highly Ductile
Qualitative Analysis Post Crack Ductility of Ternary Pozzolanic NAFRIC Composites (F/10%PFA+10%GGBS, F/10%PFA+10%SF 1:2:3)										
Fe/PFA/GGBS						Fe/PFA/SF				
Mixes	91 Days Flexural Strength (MPa)	Displacement (mm)	%age Increase in Flexural Strength Vs Control Mix (%)	%age Increase in Ductility Based on Displacement (%)	Qualitative Ductility Ranking	91 Days Flexural Strength (MPa)	Displacement (mm)	%age Increase in Flexural Strength Vs Control Mix (%)	%age Increase in Ductility Based on Displacement (%)	Qualitative Ductility Ranking
Con	4.3	5.1			Brittle	4.3	5.1			Brittle
Fe/ Con	5.5	6.0	27.9	17.6	Brittle	4.6	7.0	7.0	37.3	Brittle
ST 10%	8	54.6	86.0	971.0	Exceptionally Ductile	8.1	54.6	88.4	971.0	Exceptionally Ductile
ST 17%	7.1	54.5	65.1	969.4	Exceptionally Ductile	8	54.5	86.0	969.4	Exceptionally Ductile
PPF 1%	6.8	43.3	58.1	748.0	Exceptionally Ductile	6.8	43.3	58.1	748.0	Exceptionally Ductile
PPF 2%	5.6	55.6	30.2	990.0	Exceptionally Ductile	6	55.6	39.5	990.0	Exceptionally Ductile
PET 1%	7.9	30.9	83.7	505.9	Highly Ductile	6.9	30.9	60.5	505.9	Highly Ductile
PET 2%	7.6	42.3	76.7	730.2	Exceptionally Ductile	6.3	42.3	46.5	730.2	Exceptionally Ductile
WS 1%	6	23.3	39.5	357.1	Moderately Ductile	6.6	23.3	53.5	357.1	Moderately Ductile
WS 2%	6	31.7	39.5	520.8	Highly Ductile	6.7	31.7	55.8	520.8	Highly Ductile

4.11 Carbonation Testing

The carbonation of the concrete can result in the corrosion of RCC (ISO 1920-12:2015; www.aeis.com, 2023). The 100 mm cubes were cut at a depth of 1 cm after 28, 90 and 270 days of curing, and the test was conducted at 18-25°C temperature, 60-75% relative humidity and under an average of 0.04% atmospheric CO₂ concentration to depict normal field carbonation process. Due to a lack of resources in the University laboratory, additional CO₂ exposure to the specimen using CO₂ tanks and the measurement of CO₂ absorption quantity were not included in the testing methodology. The main objective of conducting this test was to qualitatively assess the reaction of iron with absorbed CO₂ to form FeCO₃, depletion of Ca(OH)₂ to assess its conversion to C-S-H gel in pozzolanic phase with the reaction of SiO₂ and Ca(OH)₂. 1% Phenolphthalene solution was sprayed on the freshly cut surface of the cubes at a depth of 1 cm at 28, 90 and 270 days of age. The light pink colour or no colour showed the carbonation process completed, i.e., FeCO₃ was formed with the absorption of CO₂ by the iron powder or by Ca⁺⁺ ions derived from the aqueous Ca(OH)₂ to form CaCO₃. The dark pink colour showed Ca(OH)₂ and incomplete pozzolanic phase reaction but showed lesser concrete carbonation. No statistics were recorded from the carbonation testing as it was only aimed to demonstrate the alkaline condition of the specimen qualitatively (if the colour is pink, it means the solution is alkaline due to the presence of Ca(OH)₂ or no colour/ light pink colour means C-S-H gel/ CaCO₃/ FeCO₃ formed and alkalinity has decreased with depletion of Ca(OH)₂). However, the results obtained by microstructural analysis (section 4.13.1) exhibiting decreased Ca(OH)₂ and increased formation of C-S-H gel and FeCO₃ could predict the absorption of CO₂ quantitatively, thus predicting the decrease/ absorption of the CO₂ to reduce the emissions/ embodied CO₂ potential of composites (Ware, 2013; Prasad, 2019). In this study, a carbonation test was conducted to determine the consumption of CO₂ during the hydration process for

different specimens, especially NAFRIC mixes, to ascertain the production of FeCO_3 in iron-based binary/ ternary pozzolanic composites by total consumption of CO_2 . If the phenolphthalein spray turns light pink or remains colourless, then it means that iron powder has consumed all the CO_2 emitted during the hydration process and has even reacted with limestone CaCO_3 to convert itself into rock-like FeCO_3 , giving enhanced strength to the materials and fully converting CaO and SiO_2 into C-S-H gel. This phenomenon was supported by using Fe powder with pozzolans and CaCO_3 to produce high-strength SCMs with low-carbon, greener construction materials for better environmental impacts and to reduce the carbon footprints of the construction industry, as shown in Figure 4.60. The OPC-based composites demonstrated a dark pink colour at 28 days, exhibiting the presence of a large quantity of CO_2 , which gradually reduced to a lesser pink area at 90 days and even less at 270 days but still present significantly at deeper segments and areas showing containment of embodied CO_2 . SL80 exhibited negligible CO_2 presence at 270 days of curing due to the complete conversion of silica and lime into C-S-H gel, primarily due to the strong catalytic reaction of GGBS. MK50 also performed considerably better in forming C-S-H gel during MK pozzolanic reaction, and only a trace of pink colour is visible, showing very little presence of CO_2 . All the composites of NAFRIC absorbed almost all the CO_2 to convert to C-S-H gel and form FeCO_3 in the reaction of iron and CO_2 . Suggesting them to be carbon absorbent materials. Very few traces of pink colour were visible on the cubes after 270 days of curing, supporting the achievement of the increased strength, full completion of carbonation reaction and absorption of CO_2 , making them greener, eco-friendly, sustainable materials as compared to the cement-based concrete.

OPC
Concrete



28 Days



90 Days



270 Days

NALFRIC



SL80 270 Days



SL80 270 Days



MK50 270 Days

NAFRIC



F/PFA 270 Days



F/GGBS 270
Days



F/GGBS 270 Days

NAFRIC



F/PA 270 Days



F/PFA/GGBS 270
Days



F/PFA/SF 270 Days

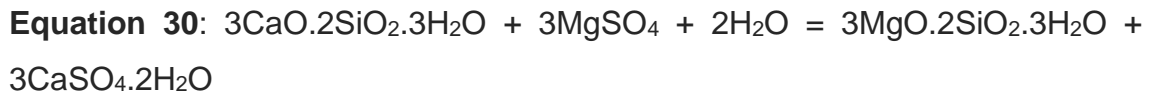
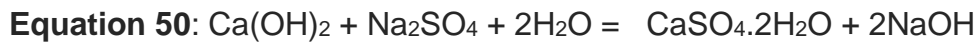
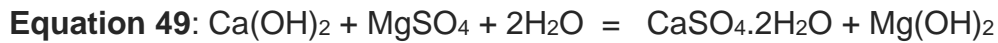
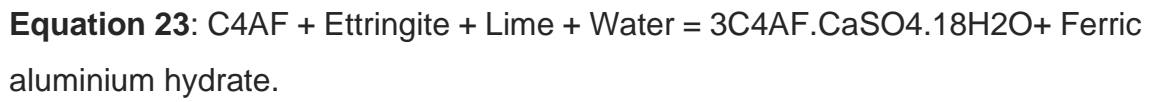
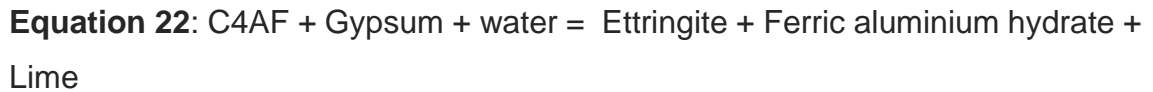
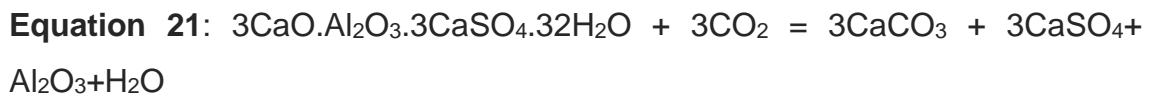
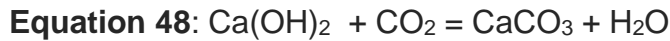
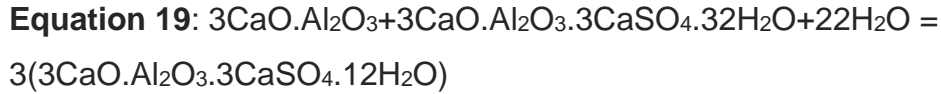
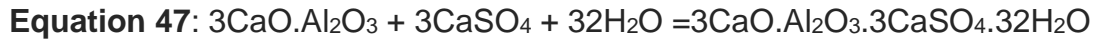
Figure 4.60: Carbonation Testing Using Phenolphthalein and Assessing Presence/ Absorption of CO₂ (Pink colour- CO₂ present, light pink or no colour – no or less CO₂ present)

4.12 Chemical-Mechanical Synthesis and Durability Testing Against Sulphate Attack

An essential characteristic of a material is its durability against chemical attacks like sulphate attacks by sodium and magnesium sulphate, especially in the marine environment or salt-rich soil/ strata. The methodology of durability testing was discussed in detail in sections 2.4 and 3.6. OPC contains tricalcium aluminates or celite (C_3A), which imparts early-setting properties to cement. Gypsum ($CaSO_4$) is added to the clinker during manufacturing to avoid the flash setting of cement paste. After the initial hydration reaction and strength gained by alite and blite with water, portlandite is produced in an aqueous form and remains in the pores (Bogues Compounds, 2022; Construction How, 2020; Prodyogi, 2018; Show, 2020; Nadir and Ahmed, 2022b; Nadir and Ahmed, 2022c Appendix V, VI). Meanwhile, gypsum reacts with celite and converts into an initial setting of ettringite (Equation 18) needles-like crystals, which propagate/ extend through the pores, resulting in material expansion and weakening of intra-ingredients bonding known as internal sulphate attack. During this reaction, gypsum is depleted, and ettringite is hydrated to form monosulphate aluminate hydrate ($3C_4ASH18$), which is 2.5 times smaller than ettringite, could only sustain in sulphates deficient solution and forms a membrane around C_3A to prevent the further flash setting and reformation of ettringite (Equation 19) (Shweta and Devender, 2020; Civil Giant, 2022; Johannes, 2021; Nadir and Ahmed 2021b Appendix VII; Nadir and Ahmed 2022b Appendix V; Nadir and Ahmed 2022c Appendix VI). Meanwhile, the absorption of CO_2 from the environment during hydration starts carbonating $Ca(OH)_2$ and ettringite to form $CaCO_3$ and monocarbonate calcium aluminate hydrates ($C_3A.CaCO_3.11H_2O$), as shown in Equations 20-21. These compounds resulted in pore refinement, prevention of further ettringite formation, hardening of cement/ lime paste and reduction in permeability (www.engr.psu.edu, 2023; Sidney and Francis, 1981; Steve and William, 1988; Michael and Zohn, 1999; Scribd, 2018). Nevertheless, increased carbonation starts the absorption of CO_2 and reduces the alkalinity of the

concrete paste, resulting in possible corrosion of steel reinforcement. Felite or ferrite (C_4AF tetracalcium alumina ferrite $4CaO.Al_2O_3.Fe_2O_3$) on hydration produces garnets (monosulphate ferric aluminium hydrates), which work as filler material for refined pore structure and does not contribute to strength (www.engr.psu.edu, 2023). Its reaction is completed in two phases. In the first phase, it reacted with gypsum and water to produce ettringite, ferric aluminium hydrates, and portlandite (equation 22). In the second phase, felite reacts with ettringite, water and portlandite to form garnets and ferric aluminium hydrates (equation 23) (Scribd, 2018; Civil Giant, 2022; www.engr.psu.edu, 2023). After complete hydration of Bogue's compounds, the cement paste contains 50-60% C-S-H gel, 20-25% ettringite, 20-25% portlandite and 5-6% voids/ entrapped air, as shown in Figure 2.35 (www.engr.psu.edu, 2023; Nadir and Ahmed 2022b). After considerable exposure to a sulphate environment, Na_2SO_4 or $MgSO_4$ could diffuse into the concrete and could react with monosulphate aluminate hydrate, supplying required sulphate ions to reconvert it to ettringite and react with the portlandite produced during early hydration to form ettringite, $CaSO_4$, $NaOH$ or $Mg(OH)_2$ known as the external sulphate attack (Worrell et al., 2001; Rehan and Nehdi, 2005; Rajkumar, 2017; Timperley, 2018; Britannica, 2020; Vashisht and Paliwal, 2020; Ahmed et al., 2020). $NaOH$ or $Mg(OH)_2$ produced after the anionic/cationic exchanges between Ca^{++} and Na^+ and Mg^{++} with OH^- and SO_4^{--} in the presence of portlandite and C-S-H gel, resulting in the formation of sodium-silicate-hydrate gel or magnesium-silicate-hydrate gel having no binding strength contrary to C-S-H gel (Marchand, Older and Skalny, 2003; Tixier and Mobasher, 2003; Idiat, Lopez and Carol, 2011; Ahmed and Kamau, 2017; Nadir and Ahmed, 2022b Appendix V). This exchange of ion reaction is considered the final impact of the sulphate attack, resulting in a weaker concrete composite having reduced C-S-H gel, as shown in Equations 27-30. Incorporating pozzolans is considered a solution to the second phase of sulphate attack by improving the pore refinement, working as a filler material and consuming the portlandite to convert to additional formation of C-S-H gel as the pozzolanic reaction

(www.engr.psu.edu, 2023; Eldidamony et al., 2012; Zhang, Vandeperre and Cheeseman, 2014; Akca, Kakar and Pek, 2015; Nadir and Ahmed, 2021b Appendix VII).



In this durability experimental study, three impacts of sulphate attack were analysed: impacting the elongation of specimens (specific to Na_2SO_4 reaction due to the formation of CaSO_4 and NaOH , and spalling/ expansion action), physical deterioration because of direct sulphate attack on the surface and resultant destruction/ deterioration of inner material on swelling/ ettringite formation (specific to MgSO_4 due to the formation of brucite layer initially and then production of CaSO_4 , magnesium silicate hydrates M-S-H gel, and ettringite) and

thirdly the reduction in the compressive strength of the specimens (specific to Na_2SO_4 and MgSO_4 both due to the formation of magnesium silicate hydrates M-S-H gel and ettringite) (Neville, 2004; Cefis and Claudia, 2017; Civil Giant, 2022b; Nadir and Ahmed 2022b; 2022c Appendix V, VI). A digital Vernier calliper with an accuracy of 0.02 mm was used to measure the elongation of cubes on pre-marked surfaces, as shown in Figure 4.68. The specimens were placed in water and 2.5% Na_2SO_4 +2.5% MgSO_4 concentrated solution to replicate 20 years of sulphate attack environment in the laboratory as per the specified ASTM standards (ASTM C1012M, 2015). Due to time/ resource constraints in this study, only the best performing fibre-reinforced OPC, NALFRIC and NAFRIC composites' cubes were selected and placed in a covered curing tank containing a combined, concentrated solution of 2.5% MgSO_4 +2.5% Na_2SO_4 after attaining more than 20 MPa strength (except low strength MK and lime-based specimens) for 270 days maintaining a temperature of $20 \pm 5^\circ\text{C}$. The objective of this sulphate resistance testing was to assess the durability/ behaviour of developed PCR/ SCMs/ lime and iron-based fibre-reinforced NALFRIC and NAFRIC composites after 270 days of exposure to the combined effect of elongation (by Na_2SO_4) and ettringite formation (by MgSO_4). (Bapat, 2012; Abdelalim et al., 2015; ASTM C 1012, 2015; Kamau et al., 2016; ASTM C 1012M, 2018; Babu et al., 2018; Nadir and Ahmed, 2021; Nadir and Ahmed 2022b; 2022c Appendix V, VI). Visual inspection was conducted to ascertain the physical deterioration qualitatively by scoring 0-5 (0, no damage to 5 maximum damage) of the conditions of specimens regarding total damage, partial damage, surface attack, pitting/ cracking and corner damage.

4.12.1 OPC-Based FRC Composites

OPC-based concrete is considered vulnerable to sulphate internal/ external attack due to its composition/ ingredients, mainly when used in marine environments and sulphate excess strata without pozzolans and high sulphate cement ingredients with more than 0.45 w/c ratio (BS 4027-1980 and BS 12-1996, IS 12330-1988 and BS EN 197-1/2000; www.engr.psu.edu, 2023;

Sotiriadis, Nikolopoulou and Tsivilis, 2012; Ideker and Thomas, 2015; Stutzman, Bullard and Feng 2016; Sara et al., 2020; Civil Giant, 2022b; Nadir and Ahmed 2022b; 2022c Appendix V, VI; SRC, 2022). However, sulphate testing for FRC composites was conducted to experimentally elucidate their performance for a fair comparison with the innovative NALFRIC and NAFRIC composites. The FRC cubes with 1:2:3 job mix ratio, 0.35 w/c ratio, 10-17% STF and 1-2% PPF, PETF, COF and WSF were kept for 270 days in a water curing tank and a closed tank having 2.5%MgSO₄+2.5%Na₂SO₄. The sulphate solution was renewed every three months, and cubes were taken out of the tank to give a field experience of wet/ drying in the laboratory environment. The cubes were then analysed for their physical appearance for qualitative analysis to classify the physical impact of the sulphate attack. Elongation in the specimen was measured/ analysed, and the deterioration in the compressive strength was analysed by conducting compressive testing on the cubes and comparing the results with the strength of water-cured cubes for 270 days. The cubes were marked/ measured on the faces, and the measurements were taken at the time of immersion (L_i), after the sulphate attack (L_s) and the inner dimensions of the mould (L_o =100mm). The change in length/ elongation was determined by using Equation 40 with the help of Vernier Calliper with 0.02 mm accuracy (Figure 4.68).

Equation 40: Length variation index (%) $\Delta L = [(L_s - L_i)/L_o] \times 100$

Where ΔL is the length variation index in %age, L_i is the initial length of the cube face on immersion. L_s is the length of the same cube surface after 270 days of immersion in a sulphate solution. L_o is the inner dimension of the original mould. A negative index shows reduction, and a positive index shows elongation in length.

The Strength deterioration index SDI (%) was calculated using Equation 41.

Equation 41: Strength Deterioration Index $SDI (\%) = [(f_w - f_s)/f_w] \times 100$

Where f_w is the compressive strength of water-cured cubes, f_s is the compressive strength of cubes' surface after 270 days of immersion in a sulphate solution. A negative strength variation index shows improved strength, and a positive index shows strength reduction.

4.12.1.1 *Physical Deterioration*

All the FRC composites demonstrated decolouration, mild pitting, mild corner damages and exposure of aggregates/ fibres on the uneven surface of the cubes. No cube was observed with total/ partial damage. FRC with 1-2% WSF was observed to get maximum physical deterioration. Nevertheless, cubes with STF, PPF, and COF exhibited lesser sulphate impact; however, an increased percentage of fibres demonstrated the increased impact of the sulphate attack, possibly due to lower intra-ingredients binding, production of weaker failure plains along the fibres, voids and permeability induced due to the fibres, as shown in Figure 4.61 and Table 4.12. The lesser w/c ratio with normal OPC CEM1 exhibited promising results and did not induce a more significant sulphate impact, suggesting the feasible use of FRC for all construction applications, even in sulphate-high strata. However, incorporating pozzolans or high sulphate-resistant cement is recommended in case of extreme sulphate attack possibilities in the marine environment. The formation of a $MgSO_4$ layer on the surface/ decolouring and mild pitting/ cracking were common impacts of the sulphate attack on almost all the cubes. The initial brucite layer formation protects the specimen from further sulphate attack for some time, but with consistent diffusion of sulphate ions, mono sulphates convert into ettringite, and the brucite layer results in cracking of the surface after extended exposure, especially with the use of STF, PPF, COF, PETF and WSF (Elsaid et al., 2011; Devi and Singh, 2013; Carnovale and Vecchio, 2014; Snoeck and Belie, 2015; Tian et al., 2016; Khan and Ali, 2018; Naaman, 2018; Wang and Han, 2018; Bheel et al., 2021).

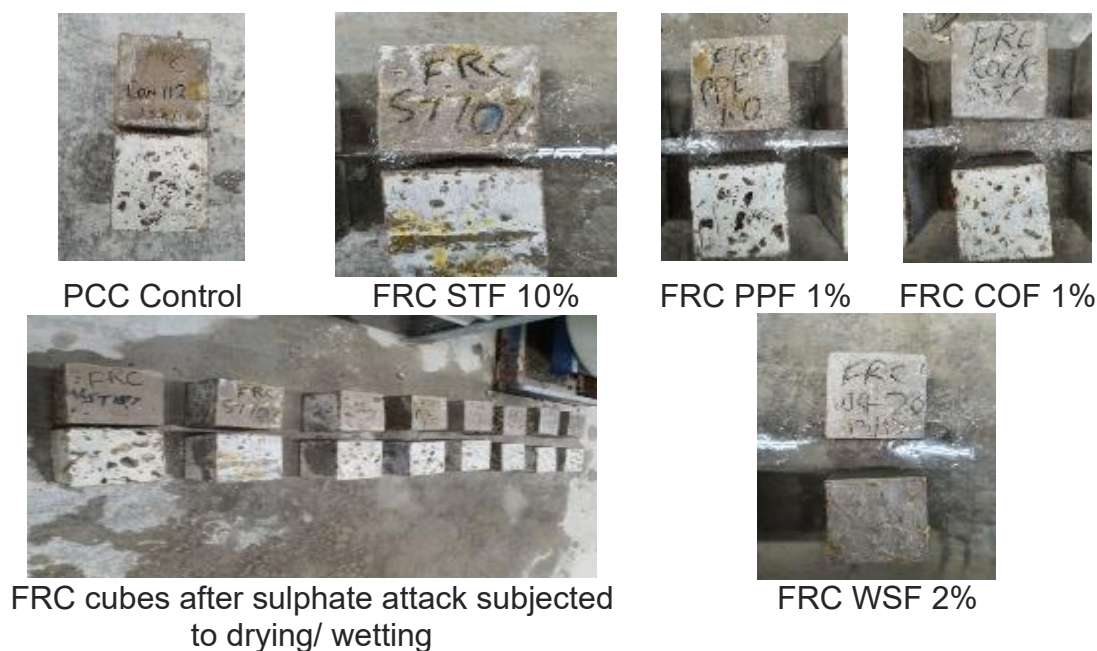


Figure 4.61: Decolouration, mild pitting, exposure of aggregates and corner damages in FRC Composites after Sulphate Attack.

4.12.1.2 *Elongation*

The elongation of the specimen characterises the sulphate attack by Na_2SO_4 . The control mix exhibited the maximum elongation of 0.11%, suggesting suitable use of the fibre incorporation as all the FRC composites demonstrated lesser elongation after the sulphate attack than the control mix. FRC composites with PETF performed the best with the least elongation of 0.06%, whereas STF, PPF and COF composites exhibited a nominally increased elongation from 0.07-0.08%. The composites with WSF, especially WSF2%, relatively underperformed by exhibiting 0.10% elongation close to the control mix, suggesting careful use of WSF optimally up to 1%, as shown in Table 4.13 and Figure 4.62. Table 4.13 and Figure 4.62 showed, generally, all the OPC-based FRC demonstrated up to 0.10% of elongation (increase in expansion, not reduction), which, although a negligible quantity bit in Comparison to other pozzolans-based NAFRIC mixes, showed greater vulnerability of OPC-based composites to external sulphate attack as expected.

Table 4.12: Physical Deterioration at 270 Days of Sulphate Attack - FRC 1:2:3.

Physical Deterioration at 270 Days of Sulphate Attack - FRC 1:2:3						
Qualitative Scoring 0-5	Total Damage	Partial Damage	Surface Attack	Pitting/ cracks	Corner Damage	Decolouration
Mixes						
Con	0	0	3	3	3	4
ST 10%	0	0	2	2	2	4
ST 17%	0	0	2	2	2	4
PPF 0.5%	0	0	2	2	2	4
PPF 1%	0	0	2	2	2	4
PPF 1.5%	0	0	2	2	2	4
PPF 2%	0	0	2	2	2	4
Coir 0.5%	0	0	2	2	2	4
Coir 1%	0	0	2	2	2	4
Coir 1.5%	0	0	2	2	2	4
Coir 2%	0	0	2	2	2	4
PET 0.5%	0	0	2	2	2	4
PET 1%	0	0	2	2	2	4
PET 1.5%	0	0	2	2	2	4
PET 2%	0	0	2	2	2	4
WS 0.5%	0	0	2	2	2	4
WS 1%	0	0	3	3	3	4
WS 1.5%	0	0	3	3	3	4
WS 2%	0	0	3	3	3	4

Table 4.13: Percentage Elongation after 270 Days Sulphate Attack – FRC 1:2:3.

Percentage Elongation of after 270 Days Sulphate Attack - FRC 123			
Mixes	%age Elongation	Mixes	%age Elongation
Con	0.11	Coir 2%	0.07
ST 10%	0.07	PET 0.5%	0.07
ST 17%	0.06	PET 1%	0.06
PPF 0.5%	0.07	PET 1.5%	0.06
PPF 1%	0.07	PET 2%	0.06
PPF 1.5%	0.07	WS 0.5%	0.08
PPF 2%	0.07	WS 1%	0.09
Coir 0.5%	0.08	WS 1.5%	0.09
Coir 1%	0.06	WS 2%	0.10
Coir 1.5%	0.07		

4.12.1.3 *Strength Deterioration Index (SDI)*

The most crucial factor of the sulphate attack testing was to assess the deterioration of the compressive strength of the cubes after 270 days of exposure to the concentrated sulphate solution. Figure 4.63 compares the compressive strength of FRC composites after 270 days of water curing and sulphate immersion. The control mix without fibres exhibited a loss of 8% strength and performed better than all the composites mixes except composites with STF 17% (7%) loss and coir 1.5% fibres, which anomalously demonstrated improvement of 6% compressive strength as against the findings of other researchers for PCC/FRC. All the FRC composites exhibited a loss in strength from 7-22%, as expected, due to the inherent induction of weaker failure plains along the fibres, increased porosity, permeability, and lower intra-ingredients binding by the incorporation of fibres as demonstrated by all the FRC results discussed earlier in section 4.4. The ingress of MgSO_4 through the porous/ weaker plains along the fibres resulted in increased sulphate attack and increased formation of ettringite, which caused expansion/ swelling in the internal pore structure of concrete by needle-like long crystals, which could propagate along with the cracking quickly to the longer dimensions causing the weakness of compressive strength. It could be suggested that fibres are responsible for increased ingress of sulphate solution, cement is responsible for the formation of ettringite, and MgSO_4 is responsible for the formation of strengthless magnesium silicate hydrate M-S-H gel in place of C-S-H gel. The FRC composite with 17% STF performed better than all the composites and the control mix (SDI 7%). PETF composites performed better than all the fibres, showing an SDI of 8-16%, coir fibres with an SDI of up to 17%, PPF with an SDI of up to 18% and the least performance was demonstrated by WSF by exhibiting maximum loss of strength and showing SDI of up to 22%, as shown in Figure 4.63 and Table 4.14.

Table 4.14: Compressive Strength and Strength Deterioration Index SDI (%) after 270 Days of Water Curing and Sulphate Exposure - FRC 1:2:3

Compressive Strength after 270 Days Water Curing and Sulphate Exposure - FRC 1:2:3			
FRC 123	270 Days Water Cured	270 Days Sulphate Cured	Strength Deterioration Index SDI (%)
Con	58	54	8
ST 10%	61	57	7
ST 17%	62	53	13
PPF 0.5%	66	55	17
PPF 1%	61	53	13
PPF 1.5%	55	50	10
PPF 2%	59	49	17
Coir 0.5%	58	49	14
Coir 1%	56	52	8
Coir 1.5%	50	53	-7
Coir 2%	49	41	17
PET 0.5%	60	51	16
PET 1%	59	52	12
PET 1.5%	55	50	8
PET 2%	51	45	12
WS 0.5%	51	40	21
WS 1%	48	44	9
WS 1.5%	45	39	13
WS 2%	44	34	22

Note: Positive SDI means strength decreased, and negative SDI means strength increased.

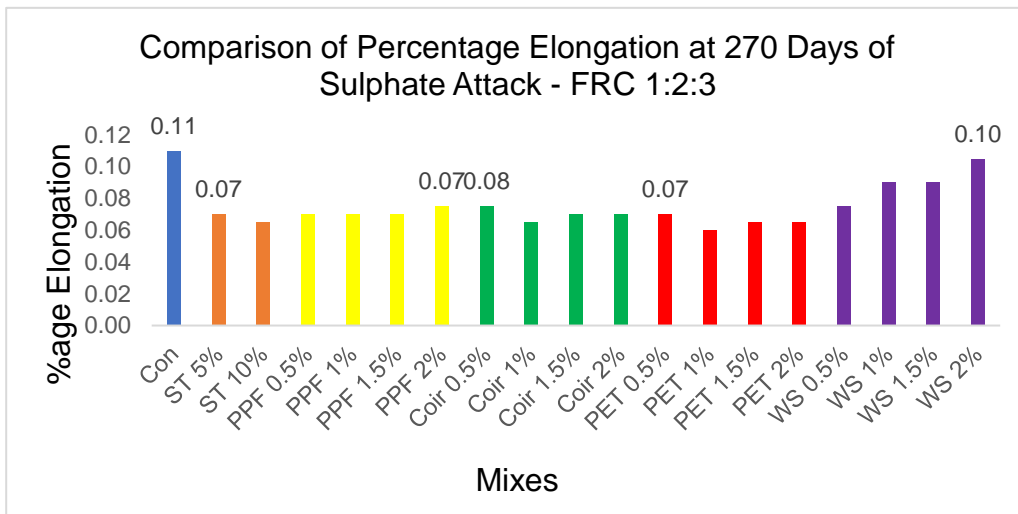


Figure 4.62: Comparison of Percentage Elongation at 270 Days of Sulphate Attack - FRC 1:2:3

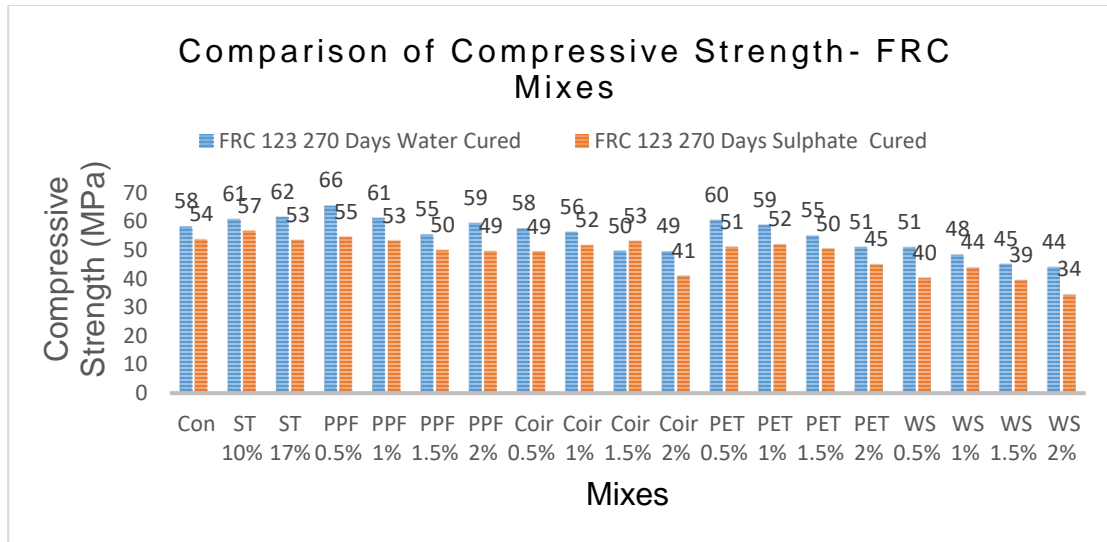


Figure 4.63: Comparison of Compressive Strengths after 270 Days of Water Curing and Sulphate Exposure.

4.12.2 NALFRIC Composites

The NALFRIC composites SL80 (containing 20% hydrated lime CL90 and 80% GGBS) and MK50 (containing 50% hydrated lime CL90 and 50% MK), with 10 and 17% STF, 1-2% PPF, PET, COF and WSF, formulated in 1:1:2 job mix ratio was immersed in water curing tanks and sulphate solution tank ($2.5\% \text{MgSO}_4 + 2.5\% \text{Na}_2\text{SO}_4$) for 270 days after reaching 20 MPa strength (except MK50 mixes which attained up to 15 MPa strength). MK50 composites were not eligible to be tested for durability testing due to achieving less than 20 MPa strength at 90 days of curing as per standard sulphate testing pre-requisites but were subjected to sulphate testing for a fair comparison with SL80-based NALFRIC composites (Bapat, 2012; Abdelalim et al., 2015; ASTM C1012, 2015; Kamau et al., 2016; ASTM C1012M, 2018; Babu et al., 2018; Nadir and Ahmed, 2021; Nadir and Ahmed 2022b; 2022c Appendix V, VI). GGBS-based cement composites performed better in the sulphate environment than the FRC composites and were observed to gain strength in the sulphate environment (Ecocem, 2023).

4.12.2.1 *Physical Deterioration*

The SL80-based NALFRIC composites performed the best in all the innovative/ traditional OPC/ PCR SCMs. No composite showed total/ partial damage and remained intact in a sulphate environment. Mild pitting/ cracking and decolouration of the external surface were observed in the majority of the specimens, but the overall physical condition of all the composites remained sustainable consistently, as shown in Figure 4.64 and Tab 4.15 in line with the existing research (Bapat,2012; Rughooputh and Rana, 2014; Kamau et al., 2016; Mukherjee et al., 2016; Robati et al., 2016; Ahmed et al., (2019); Nadir and Ahmed, 2021). The control mix and the composites with WSF were observed to perform slightly lower than all other composites but without any significant sign of damage/ destruction, suggesting the beneficial/ sustainable use of all the SL-80-based NALFRIC composites with/ without fibres in all types of construction applications including the marine environment, hydromodifications, channel lining and embankment/ flood defences stabilisation. The strong OPC-like behaviour/ composition of GGBS makes it an established alternative for cement concrete, and it was observed to have enhanced engineering properties and durability when used with CI90 as cement-free NALFRIC composites.

MK50-based NALFRIC was the most affected/ least sustainable composites in the sulphate environment. A few composites with increased dosages of fibres were observed to be damaged (MK50 with ST17%) or partially damaged (ST10%, PPF2%, COF 2% and WSF2%). Almost all the composites were highly impacted by surface deterioration and moderate pitting/ cracking, mostly were found with corners/ sides damaged and exposed the aggregates/ fibres after 270 days of sulphate attack (Figure 4.65), making them unsuitable to be used in marine environments and sulphate excess soil/ strata. The qualitative analysis to classify the physical deterioration of MK50-based NALFRIC composites demonstrated that almost all the composites suffered partial damage. Extensive side/corner damages, extensive pitting/ cracking and mild decolouration, are shown in Table 4.16.






			
SL80 Control Mix	SL80 with 10% STF	SL80 with PPF	SL80 with PET
			
SL80-based NALFRIC cubes after sulphate attack subjected to drying/wetting			

Figure 4.64: Decolouration, mild pitting, mild corner damages in SL80-based NALFRIC Composites after Sulphate Attack.









			
MK50 ST17%	MK50 ST10%	MK50 Control	MK50PET 0.5%
			
MK50 PPF 2%	MK50 PPF 2%	Side damage	Partial damage

Figure 4.65: Total/partial damage, pitting, and Corner damages in MK50-Based NALFRIC Composites after sulphate attack.

Table 4.15: Physical Deterioration after Sulphate Attack – NALFRIC (SL80).

Physical Deterioration at 270 Days of Sulphate Attack – NALFRIC (SL80)

Qualitative Scoring 0-5	Total Damage	Partial Damage	Surface Attack	Pitting/ cracking	Corner Damage	Decolouration
Con	0	0	1	2	1	3
ST 10%	0	0	1	2	1	3
ST 17%	0	0	1	2	1	3
PPF 0.5%	0	0	1	2	1	3
PPF 1%	0	0	1	2	1	3
PPF 1.5%	0	0	1	2	1	3
PPF 2%	0	0	1	2	1	3
Coir 0.5%	0	0	1	2	1	3
Coir 1%	0	0	1	2	1	3
Coir 1.5%	0	0	1	2	1	3
Coir 2%	0	0	1	2	1	3
PET 0.5%	0	0	1	2	1	3
PET 1%	0	0	1	2	1	3
PET 1.5%	0	0	1	2	1	3
PET 2%	0	0	1	2	1	3
WS 0.5%	0	0	1	2	1	3
WS 1%	0	0	1	3	1	3
WS 1.5%	0	0	1	3	1	3
WS 2%	0	0	1	3	1	3

Table 4.16: Physical Deterioration at 270 Days of Sulphate Attack – NALFRIC (MK50)

Physical Deterioration at 270 Days of Sulphate Attack – NALFRIC (MK50)

Qualitative Scoring 0-5	Total Damage	Partial Damage	Surface Attack	Pitting	Corner Damage	Decolouration
Con	0	5	4	4	3	3
ST 10%	0	5	4	4	3	3
ST 17%	5	4	4	4	4	3
PPF 0.5%	0	3	4	4	3	3
PPF 1%	0	3	4	4	3	3
PPF 1.5%	0	3	4	4	3	3
PPF 2%	0	3	4	4	3	3
Coir 0.5%	0	3	4	4	3	3
Coir 1%	0	3	4	4	3	3
Coir 1.5%	0	3	4	4	3	3
Coir 2%	0	3	4	4	3	3
PET 0.5%	0	3	4	4	3	3
PET 1%	0	3	4	4	3	3
PET 1.5%	0	3	4	4	3	3
PET 2%	0	3	4	4	3	3
WS 0.5%	0	3	4	4	3	3
WS 1%	0	5	4	4	3	3
WS 1.5%	0	5	4	4	3	3
WS 2%	5	4	4	4	4	3

4.12.2.2 Elongation

SI-80-based NALFRIC composites performed at par with the FRC composites in elongation under the sulphate attack. The control mix without fibres exhibited an elongation of 0.13%. The composites with increased dosages generally demonstrated more impact of Na₂SO₄ sulphate attack by showing slightly more elongation. However, all the composites except WSF performed strong/sustainable and exhibited a minor elongation of 0.05-0.09% at 270 days of accelerated sulphate attack, which depicted 20 years of field conditions, as shown in Table 4.17. The deterioration of WSF-based composites was expected as they demonstrated lesser compressive strength as compared to other SCMs/

fibres due to their inherent lower elastic modulus/ tensile strength/ organic nature of material exhibiting lesser elongation, more water absorption, deterioration on the chemical attack, lower aspect ratio, presence of lignin/ pith/ cellulose and is not generally recommended as high strength concrete application, especially in high sulphate environment. Secondly, its use with lime-based MK50 composites (Table 4.17) is not recommended for any application in a sulphate-rich environment as they achieved less than 20 MPa strength and could not be used in a sulphate-rich environment as per ASTM C1012M:2015 (A composite should achieve a minimum of 20 MPA strength before it is subject to sulphate attack). The SL80-based NALFRIC composites with STF, PPF and COF attained an elongation of 0.07-0.09%, whereas the best strength against the sulphate attack was exhibited by the composites containing PET fibres showing a minor elongation of 0.05-0.07%. The composites with WSF demonstrated the lowest performance by showing the sulphate impact of elongation exhibiting a marginally high elongation of 0.11-0.14%. However, all the composites could be regarded as performing sustainably well for Na₂SO₄-specific sulphate attack, making them suitable/ sustainable materials for any construction application in any environment.

As expected, MK50-based NALFRIC composites demonstrated gross impact by the sulphate elongation due to lower strength. All the composites performed with attaining a marginally higher elongation of 0.12-0.24%, as shown in Table 4.17. Generally, all the composites with all the fibres and the control mix exhibited a slightly larger elongation, showing a gross spalling/ expansion effect by the Na₂SO₄ specific sulphate attack. The composites with larger dosages of the fibres and WSF 1-2% performed as the most impacted composites by exhibiting up to 0.24% elongation after 270 days of exposure in the concentrated sulphate environment, suggesting them unsuitable to employ in marine environments and sulphate-rich soils.

Table 4.17: Percentage Elongation at 270 Days of Sulphate Attack - NALFRIC Composites.

Percentage Elongation at 270 Days of Sulphate Attack - NALFRIC Composites		
Mixes	SL80 1:1:2	MK50 1:1:2
	%age Elongation	%age Elongation
Con	0.13	0.16
ST 10%	0.07	0.15
ST 17%	0.09	0.17
PPF 0.5%	0.07	0.13
PPF 1%	0.08	0.15
PPF 1.5%	0.09	0.17
PPF 2%	0.09	0.18
Coir 0.5%	0.08	0.13
Coir 1%	0.09	0.13
Coir 1.5%	0.09	0.16
Coir 2%	0.08	0.16
PET 0.5%	0.05	0.12
PET 1%	0.07	0.14
PET 1.5%	0.07	0.12
PET 2%	0.07	0.13
WS 0.5%	0.11	0.23
WS 1%	0.13	0.24
WS 1.5%	0.14	0.26
WS 2%	0.12	0.23

4.12.2.3 *Strength Deterioration Index SDI (%)*

The chemical attack's impact on a material's strength is the primary factor in considering its sustainability for employment in sulphate-rich environments. SL80-based NALFRIC consistently performed exceptionally well, and all the composites demonstrated increased compressive strength withstanding the sulphate attack specific to $MgSO_4$. The SL80 composites with all the fibres improved the strength of cubes after 270 days of curing in a sulphate environment by 4-40%, as shown in Figure 4.46 and Table 4.18. The inherent characteristic

of GGBS to withstand chemical attacks is an established characteristic. The formation of the brucite layer at the outer surface prevented the ingress of sulphate solution in the specimens, and resultantly, the formation of no or very little ettringite/ M-S-H gel was observed in all the composites, including WSF mixes. The effective pozzolanic reaction and addition of lime with GGBS up to 20% suggested a sustainable formulation of greener, cement-free, environmentally friendly composites which could be used from low-medium strength applications (15-30 MPa) in any environment, in line with the existing research (Bapat,2012; Rughooputh and Rana, 2014; Kamau et al., 2016; Mukherjee et al., 2016; Robati et al., 2016; Ahmed et al., (2019); Nadir and Ahmed, 2021).

However, as expected, all the MK50-based NALFRIC composites were observed to reduce the compressive strength up to 50% after 270 days of MgSO_4 -specific sulphate attack (Figure 4.47 and Table 4.18) and could be suggested as unsuitable for utilisation in a sulphate-rich environment. MK50 composites with STF 10-17% performed better in water curing and reached up to 13 MPa strength. However, no composite could withstand the sulphate attack and exhibited a considerable reduction after the sulphate attack, with COF and WSF composites performing the least in withstanding the chemical attack. STF, PPF, and PETF composites performed comparatively better in reducing lesser strength than agricultural fibres, but still, none could be suggested for utilisation in standard construction in a sulphate-rich environment. However, their low-strength utilisation in low-strength construction where no imminent sulphate attack could make them a cost-effective, greener solution like flooring, walls, and subgrade preparation façade tiles.

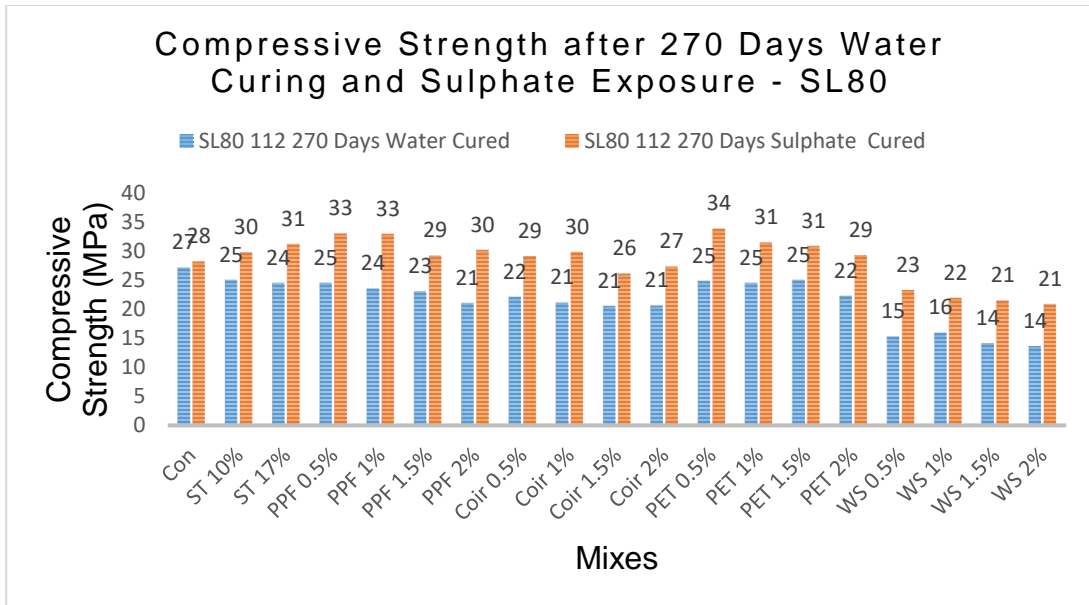


Figure 4.66: Compressive Strength of SL80-Based NALFRIC Composites after 270 Days of Water Curing and Sulphate Exposure.

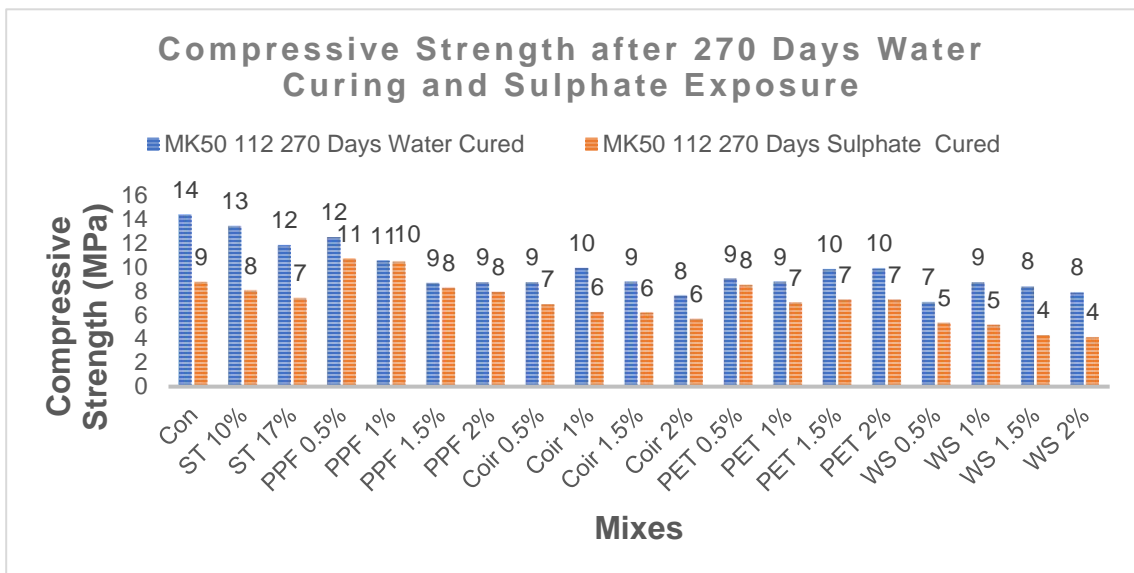


Figure 4.67: Compressive Strength of MK50-Based NALFRIC Composites after 270 Days of Water Curing and Sulphate Exposure.

Table 4.18: Compressive Strength and Strength Deterioration Index of NALFRIC Composites after 270 Days of Water Curing and Sulphate Exposure.

Compressive Strength and Strength Deterioration Index of NALFRIC Composites after 270 Days of Water Curing and Sulphate Exposure						
	SL80 112			MK50 112		
Mixes	270 Days Water Cured	270 Days Sulphate Cured	Strength Deterioration Index SDI (%)	270 Days Water Cured	270 Days Sulphate Cured	Strength Deterioration Index SDI (%)
Con	27	28	-4	14.4	8.7	39
ST 10%	25	30	-19	13.4	8	40
ST 17%	24	31	-27	11.8	7.4	38
PPF						
0.5%	25	33	-34	12.5	10.7	14
PPF 1%	24	33	-40	10.5	10.4	1
PPF						
1.5%	23	29	-27	8.7	8.2	5
PPF 2%	21	30	-43	8.7	7.9	9
Coir						
0.5%	22	29	-32	8.7	6.9	21
Coir 1%	21	30	-41	9.9	6.2	37
Coir						
1.5%	21	26	-27	8.8	6.2	30
Coir 2%	21	27	-33	7.6	5.7	26
PET						
0.5%	25	34	-36	9	8.5	6
PET 1%	25	31	-28	8.8	7	20
PET						
1.5%	25	31	-23	9.8	7.3	26
PET 2%	22	29	-31	9.9	7.3	26
WS						
0.5%	15	23	-52	7.1	5.3	25
WS 1%	16	22	-38	8.7	5.2	41
WS						
1.5%	14	21	-52	8.4	4.3	49
WS 2%	14	21	-53	7.9	4.1	48

Note: Positive SDI means strength decreased, and negative SDI means strength increased.

4.12.3 NAFRIC Composites

The NAFRIC composites containing 10% modified iron-based binary/ ternary pozzolanic SCMs were prepared using a 1:2:3 job mix ratio. The iron reacts with

CO₂ and forms rock-like FeCO₃, making it a carbon-neutral/ absorbent material. FeCO₃ improves pore structure and surface protection to prevent chemical ingress and improve strength. The mixing of pozzolans with OPC is considered beneficial as a filler material, which results in pore refinement, reduced voids, formation of the additional quantity of C-S-H gel during the pozzolanic reaction, consumption of portlandite to convert to C-S-H gel and reduction of ettringite formation and M-S-H gel at the later stage. However, using fibres incorporates weaker failure plains and reduced intra-ingredient binding and could help produce/ propagate the ettringite crystal cracks along the fibres. Excess use of pozzolans could result in the swelling of SCMs due to the formation of Si(OH)₄, and MgSO₄ could exchange cations with C-S-H gel to form ettringite and mushy M-S-H gel after the sulphate attack. The hard rock-like characteristics of FeCO₃ prevent the Na₂SO₄ specific sulphate attack, resulting in increased elongation. The iron-based pozzolanic binary composites with PFA and MK were considered to withstand the sulphate attack with minimum elongation, surface deterioration and loss of strength. The cubes were immersed in a water tank and a sulphate solution in a combined 2.5%Na₂SO₄+2.5MgSO₄ solution for 270 days. The solution was refreshed every three months, along with cubes exposed to dry/ wetting field-like conditions. The cubes were analysed for surface deterioration, and qualitative classification was used for total/ partial damage, pitting/ cracking, surface attack, side/ corner damage, and discolouration. The elongation/ length variation index and strength deterioration index were calculated using length/ strength in water cured versus the length/ strength in the sulphate exposure of 270 days to determine the durability of the specimens considering the Na₂SO₄ triggered elongation and MgSO₄ triggered strength loss/ ettringite formation (Siddique, 2004; Stone, 2010; Karuppasamy, Dinesh and Janardhan, 2011; Das, Souliman and Stone, 2014; USGS, 2014; Akeem and Mitui, 2017; Garcia et al., 2017; TheConstructor, 2017; Scrivener, 2018; ASTM C125/ C619, 2019; Selvapriya, 2019; Vijayan et al., 2019; Cement concrete, 2020; Girts et al., 2020;

Nadir and Ahmed, 2021b; Admin, 2023; Iron Powder, 2023; Nadir, Ahmed and West, 2023; Nadir, Ahmed and Moshi, 2024).

4.12.3.1 *Physical Deterioration*

Generally, all the NAFRIC composites remained intact and composed in the 270 days of sulphate attack and demonstrated very mild discolouration and mild pitting/ cracking; no sides or corner damages were observed, no specimen exhibited total/ partial damage, and the surface of all the specimens remained intact. The salt deposition was observed on a few points in a few specimens, and the control mixes and a few mixes with WSF and composites with increased dosages of 2% fibres showed very mild surface deterioration, as shown in Figure 4.68 and Table 4.19.

			
Fe/GGBS WSF1%	Fe/ PFA ST10%	Fe/PFA/GGBS	Fe/PFA/SF
			
Fe/PFA PPF 2%	Fe/ GGBS PET1%	Fe/ PFA CON	Fe/ PA PPF 1%

Figure 4.68: Qualitative Analysis and Physical Deterioration in NAFRIC Composites after 270 Days of Sulphate Attack.

4.12.3.2 Elongation

Elongation results from Na_2SO_4 attack due to spalling/ expansion caused by cationic/ anionic exchange of Ca^{++} , Na^+ and SO_4^{--} and OH^- . All the NAFRIC composites exhibited mild elongation due to the Na_2SO_4 attack ranging from 0.04-0.09%. The maximum elongation was observed in PCC control of 0.11%, followed by F/PFA control of 0.09%. All other control mixes of NAFRIC composites exhibited 0.07-0.08% elongation. The maximum elongation of 0.09% was exhibited by a few specimens of WSF with GGBS and PFA-based NAFRIC composites. PA-based NAFRIC composites elongated 0.05-0.07% with all the fibres, suggesting they were the best iron-based binary pozzolanic NAFRIC composite material. The traditional PFA+MK-based binary pozzolanic NAFRIC exhibited the maximum elongation in a few mixes of 0.09%, suggesting it to be comparatively more impacted but still under 0.09%. The composites containing ternary pozzolans with iron (PFA/ GGBS/ SF with MK and lime) equally performed at par with the binary composites and showed an elongation of 0.06-0.08%, as shown in Table 4.20.

Table 4.19: Deterioration at 270 Days of Sulphate Attack - NAFRIC

Deterioration at 270 Days of Sulphate Attack - NAFRIC						
Qualitative Scoring 0-5	Total Damage	Partial Damage	Surface Attack	Pitting/ Cracking	Corner Damage	Decolouration
Con	0	0	2	2	1	2
ST 10%	0	0	2	2	1	2
ST 17%	0	0	2	2	1	2
PPF 0.5%	0	0	2	2	1	2
PPF 1%	0	0	2	2	1	2
PPF 1.5%	0	0	2	2	1	2
PPF 2%	0	0	2	2	1	2
Coir 0.5%	0	0	2	2	1	2
Coir 1%	0	0	2	2	1	2
Coir 1.5%	0	0	2	2	1	2
Coir 2%	0	0	2	2	1	2
PET 0.5%	0	0	2	2	1	2
PET 1%	0	0	2	2	1	2
PET 1.5%	0	0	2	2	1	2
PET 2%	0	0	2	2	1	2
WS 0.5%	0	0	2	2	1	2
WS 1%	0	0	2	2	1	2
WS 1.5%	0	0	2	2	1	2
WS 2%	0	0	2	2	1	2

Table 4.20: Percentage Elongation at 270 Days of Sulphate Attack - NAFRIC Composites.

Percentage Elongation at 270 Days of Sulphate Attack - NAFRIC Composites						
Mixes	PCC 123	Fe/PFA	Fe/GGBS	Fe/PA 20%	Fe/10%PF A + 10%GGBS	Fe/10%PFA+10 % SF
	Con %age Elongatio n	20% %age Elongatio n	20% %age Elongatio n	20% %age Elongatio n	%age Elongation	%age Elongation
PCC Con	0.11					
F/Con		0.09	0.08	0.07	0.08	0.08
ST 10%		0.04	0.05	0.07	0.06	0.05
ST 17%		0.05	0.04	0.07	0.04	0.03
PPF 1%		0.04	0.05	0.06	0.05	0.05
PPF 2%		0.05	0.05	0.06	0.05	0.05
PET 1%		0.05	0.07	0.06	0.09	0.08
PET 2%		0.06	0.06	0.07	0.07	0.07
WS 1%		0.09	0.09	0.05	0.05	0.08
WS 2%		0.09	0.09	0.06	0.05	0.07

4.12.3.3 *Strength Deterioration Index (SDI)*

The sulphate attack by MgSO_4 is characterised by the loss of compressive strength due to ettringite formation and, finally, the conversion of C-S-H gel into strengthless mushy M-S-H gel. The complex rock-like properties of FeCO_3 and pozzolanic reaction by the pozzolans in the SCMs consume Ca(OH)_2 to form additional C-S-H gel, increasing the strength. The sulphate attack specific to MgSO_4 reduces the compressive strength of fibre-reinforced composites due to weaker plains/ random distribution/ pore disturbance. As a net result, some NAFRIC composites exhibited a gain in strength, and some showed a loss. Generally, all the NAFRIC composites except a few remained compact and intact in the 270 days of accelerated sulphate attack depicting 20 years of field conditions. The best-performing NAFRIC composites are shown in Table 4.21. The SDI was observed up to 2-11% in control mixes without fibres (Table 4.22). The least performing composites belong to the traditional NAFRIC, with 20% PFA exhibiting a 3-12% SDI. The best performing binary NAFRIC composites

belonged to the 20% PA-based SCMs, exhibiting an SDI of -2-12% (negative value means strength gain in sulphate solution), followed by 20% GGBS-based composites showing an SDI of 2-11%. The best performing ternary pozzolanic NAFRIC composites belonged to 10%PFA+10%SF, exhibiting an SDI of 6-11%, followed by 10%PFA+10%GGBS composites showing -2-12% SDI. Overall, most NAFRIC composites demonstrated an SDI of less than 10%, which is well within the 10% strength variation and could be considered as maintaining their strength in a 20-year field depicted sulphate attack. The results suggested the ideal durability of NAFRIC composites and suggest all the NAFRIC composites with 10-17%STF, 1-2% PPF, PETF and even WSF (though WSF composites should be used for up to 50 MPa strength requirements with care/ optimum 1% dosage) are sustainable, greener, eco-friendly materials which could be used as cement alternative for high-strength (50-70 MPa) construction applications in all type of structural/ hydraulic/ hydromodifications/ marine construction in sulphate rich environments/ strata without the use of high-sulphate resistant cement contents.

Table 4.21: Best-Performing Composites Selected for Microstructural Analysis.

Mixes	28 Days Compressive Strength (MPa)	90 Days Compressive Strength (MPa)	270 Days Compressive Strength in water (MPa)	270 Days Compressive Strength in Sulphate (MPa)	Recommended for SEM and XRD
SL80 Coir 1% SL80 PET	13.3	16.4	21.1	29.8	Recommended
0.5% Fe/PFA/SF PET	14.9	18.4	24.8	33.8	Recommended
1%	56.9	60.9	61.2	64.8	Recommended
Fe/PA PET 1%	55.1	61.1	64.7	63.4	Recommended

Table 4.22: Comparison of Compressive Strength and Strength Deterioration Index (SDI%) - NAFRIC Composites after 270 days of Sulphate Attack.

Qualitative Analysis Post Crack Ductility of Binary Pozzolanic NAFRIC Composites (Fe/PFA, Fe/GGBS, Fe/PA 1:2:3)										
Fe/PFA						Fe/GGBS				
Mixes	91 Days Flexural Strength (MPa)	Displacement (mm)	%age Increase in Flexural Strength Vs Control Mix (%)	%age Increase in Ductility Based on Displacement (%)	Qualitative Ductility Ranking	91 Days Flexural Strength (MPa)	Displacement (mm)	%age Increase in Flexural Strength Vs Control Mix (%)	%age Increase in Ductility Based on Displacement (%)	Qualitative Ductility Ranking
Con	4.3	5.1			Brittle	4.3	5.1			Brittle
Fe/ Con	4.4	5.0	2.3	-2.0	Brittle	4.8	6.0	11.6	17.6	Brittle
ST 10%	8.6	54.6	100.0	971.0	Exceptionally Ductile	8.1	54.6	88.4	971.0	Exceptionally Ductile
ST 17%	7.9	54.5	83.7	969.4	Exceptionally Ductile	7.5	54.5	74.4	969.4	Exceptionally Ductile
PPF 1%	7.2	43.3	67.4	748.0	Exceptionally Ductile	6.8	43.3	58.1	748.0	Exceptionally Ductile
PPF 2%	7.04	55.6	63.7	990.0	Exceptionally Ductile	6.9	55.6	60.5	990.0	Exceptionally Ductile
PET 1%	6.9	30.9	60.5	505.9	Highly Ductile	6.8	30.9	58.1	505.9	Highly Ductile
PET 2%	6.4	42.3	48.8	730.2	Exceptionally Ductile	6.2	42.3	44.2	730.2	Exceptionally Ductile
WS 1%	6	23.3	39.5	357.1	Moderately Ductile	6.8	23.3	58.1	357.1	Moderately Ductile
WS 2%	5.4	31.7	25.6	520.8	Highly Ductile	5.7	31.7	32.6	520.8	Highly Ductile
Qualitative Analysis Post Crack Ductility of Ternary Pozzolanic NAFRIC Composites (F/10%PFA+10%GGBS, F/10%PFA+10%SF 1:2:3)										
Fe/PFA						Fe/PFA/SF				
Mixes	91 Days Flexural Strength (MPa)	Displacement (mm)	%age Increase in Flexural Strength Vs Control Mix (%)	%age Increase in Ductility Based on Displacement (%)	Qualitative Ductility Ranking	91 Days Flexural Strength (MPa)	Displacement (mm)	%age Increase in Flexural Strength Vs Control Mix (%)	%age Increase in Ductility Based on Displacement (%)	Qualitative Ductility Ranking
Con	4.3	5.1			Brittle	4.3	5.1			Brittle
Fe/ Con	5.5	6.0	27.9	17.6	Brittle	4.6	7.0	7.0	37.3	Brittle
ST 10%	8	54.6	86.0	971.0	Exceptionally Ductile	8.1	54.6	88.4	971.0	Exceptionally Ductile
ST 17%	7.1	54.5	65.1	969.4	Exceptionally Ductile	8	54.5	86.0	969.4	Exceptionally Ductile
PPF 1%	6.8	43.3	58.1	748.0	Exceptionally Ductile	6.8	43.3	58.1	748.0	Exceptionally Ductile
PPF 2%	5.6	55.6	30.2	990.0	Exceptionally Ductile	6	55.6	39.5	990.0	Exceptionally Ductile
PET 1%	7.9	30.9	83.7	505.9	Highly Ductile	6.9	30.9	60.5	505.9	Highly Ductile
PET 2%	7.6	42.3	76.7	730.2	Exceptionally Ductile	6.3	42.3	46.5	730.2	Exceptionally Ductile
WS 1%	6	23.3	39.5	357.1	Moderately Ductile	6.6	23.3	53.5	357.1	Moderately Ductile
WS 2%	6	31.7	39.5	520.8	Highly Ductile	6.7	31.7	55.8	520.8	Highly Ductile

Note: Positive SDI means strength decreased, and negative SDI means strength increased.

4.13 Microstructural Analysis Using XRD/ XRF and SEM/ EDM.

4.13.1 Microstructural Analysis Using XRD/ XRF.

Microstructural study of materials is an essential/ advanced method of investigating the morphology, shape, pattern, type alignment, elemental composition and quantity assessment/ mapping of various chemicals identified using x-ray and electron beams. The x-ray/ electrons are made to strike with the

target testing material specimen to scatter the electrons from the K, L, and M electron orbits with specific intensity and scattering angles θ , releasing specific energy photons characteristically identical for each element/ compound/ chemical matching it to the AMCSD database (AMCSD, 2023), and then creating a 2D, 3D image and 2D spectrum exhibiting peaks and phases of various electronic diffractions as discussed in section 3.7. X-ray fluorescence analysis was conducted to ascertain the elemental composition of various pozzolanic materials and OPC in oxides, as shown in Table 2.7. The crushed specimens of the four selected NALFRIC (SL80 Coir1% and SL80 PET0.5%) and NAFRIC (F/PFA/SF PET1% and F/PA PET1%) composites, after 270 days of sulphate exposure, were ground to particles of size less than 150 μ m using a ball mill, heated up to 975°C, tested for loss of ignition and then analysed for several elements using a Philips Minipal 4 EDXRF machine (Figure 3.14) to assess the elemental configuration through XRF as oxides of metals as shown in Table 4.23. For XRD analysis and identification of the presence of compounds, these samples were ground to particle size less than 150 μ m using a ball mill, heated up to 975°C, assessed for loss of ignition and then analysed for compounds using powder diffractometry techniques employing a Bruker D500 XRD machine. The traces were identified for crystalline compounds using EVA software to create a spectrum showing different peaks/ phases of the compounds Table 4.24. The XRF in Table 4.23 shows that the specimens contained 33-38% SiO₂ due to pozzolans and 50-56% CaO due to using lime and cement as the significant components identical to cement concrete and demonstrating the formation of up to 80-90% of C-S-H gel inducing a good compressive strength. Fe elements were observed as 1.45 to 3.7%, as expected due to GGBS and iron powder mixing in iron-based pozzolanic composites showing the formation of FeCO₃ and ferrites. The composites with palm ash PA contained slightly more potassium, which could cause swelling/ loss of strength in the mixtures. SL80 composites were found to have 3% alumina, compared to NAFRIC composites with OPC as 90% binder with around 4% alumina showing celite reaction (calcium aluminosilicate-

hydrates). The presence of a few traces of Na₂O showed a minimum impact of Na₂SO₄ during sulphate attack, whereas the presence of magnesium oxide (1.1-2.26%) and SO₃⁻ (0.4-0.9%) exhibits a very mild sulphate attack due to MgSO₄. Table 4.24 and Figure 4.69 show the elemental compound composition determined by XRD/ Eva software using an X-ray diffraction technique. The specimens contained rich quantities of 44-60% quartz and 48-58% lime, predicting an excellent formation of C-S-H gel. Dolomite and pigeonite with Fe and Mg show the formation of ferrous carbonate and brucite after the sulphate attack. Less than 0.9% ettringite shows the durability of the material and its strength to withstand the sulphate attack with maintained/ improved strength. The presence of portlandite was observed as minimal in NAFRIC composites, and almost no/ negligible quantity was observed in NALFRIC composites, indicating the complete formation of C-S-H gel by utilising a maximum quantity of CaO, SiO₂ and Ca(OH)₂ and leaving very less aqueous portlandite to initiate cationic/ anionic exchange of Ca⁺⁺, Na⁺ and Mg⁺⁺ with OH⁻ and SO₄⁻ essential for the sulphate attack by Na₂SO₄ and MgSO₄. The XRF and XRD results support the findings about the durability/ strength of the innovative NALFRIC and NAFRIC composites by chemical-mechanical synthesis/ laboratory testing and identify these as sulphate-resistant strong composites with the complete formation of strength-inducing C-S-H gel.

Table 4.23: Elemental Composition of Composites Using X-RAY Spectrometry.

Elemental Composition of Composites Using XRF				
Elemental Composition	SL80 Coir 1.0	SL80 PET 0.5	Fe/PFA/SF PET 1.0	Fe/PA PET 1.0
Fe ₂ O ₃ %	1.45	1.85	2.46	3.73
SiO ₂ %	37.7	43.5	33	33.7
TiO ₂ %	0.44	0.4	0.27	0.3
CaO %	51.4	51.4	56.5	54.2
K ₂ O %	0.42	0.44	0.37	0.48
Al ₂ O ₃ %	3.21	3.5	3.62	3.81
MgO %	1.22	1.01	2.26	1.7
Na ₂ O %	0.15	0.2	0.27	0.2
P ₂ O ₅ %	<0.1	<0.1	<0.1	<0.1
SO ₃ %	0.43	0.39	0.52	0.95
Cl %	<0.1	<0.1	0.12	0.41
Cr ₂ O ₃ %	<0.1	<0.1	<0.1	<0.1
MnO %	0.16	0.12	<0.1	<0.1
SrO %	0.1	<0.1	0.12	0.11

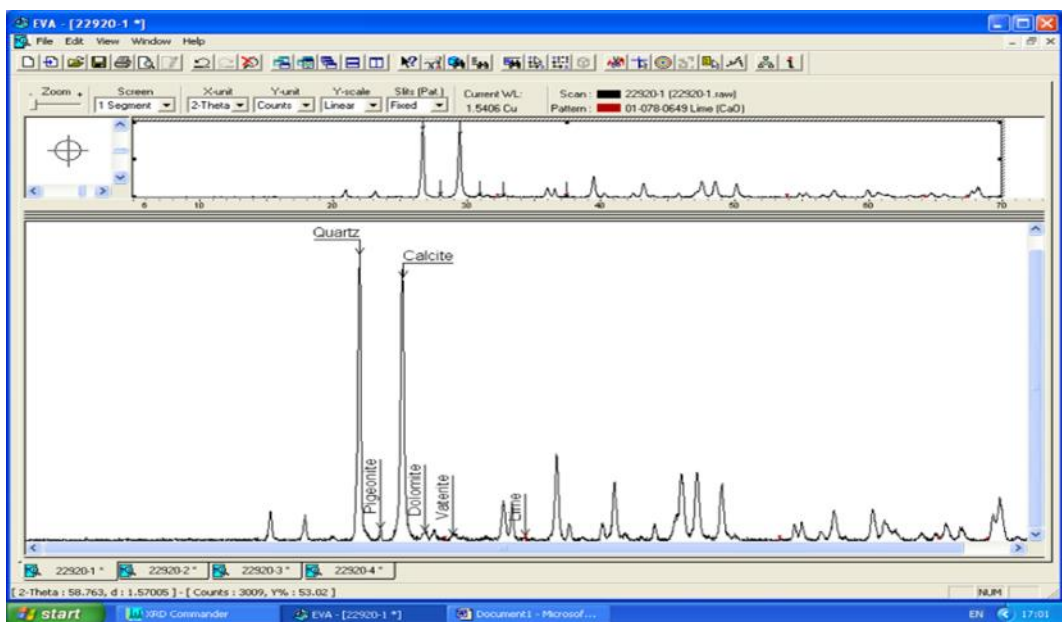


Figure 4.69: XRD Spectrometry - Compound Composition, Phases/ Peaks of SL80 COF1%.

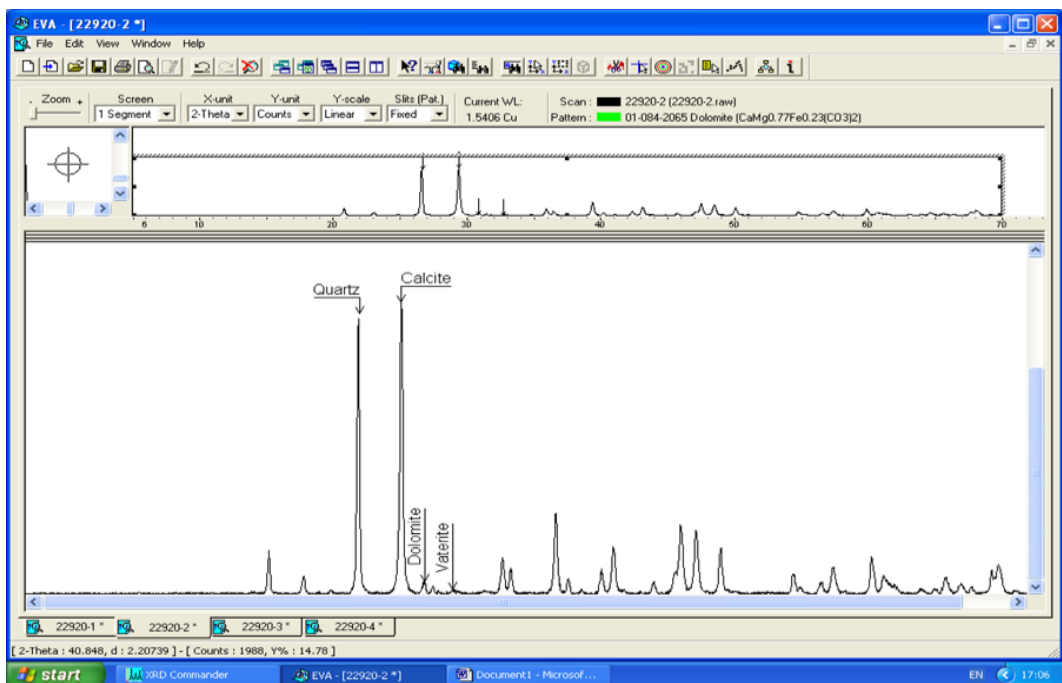


Figure 4.70: XRD Spectrometry - Compound Composition, Phases/ Peaks of SL80 PET0.5%.

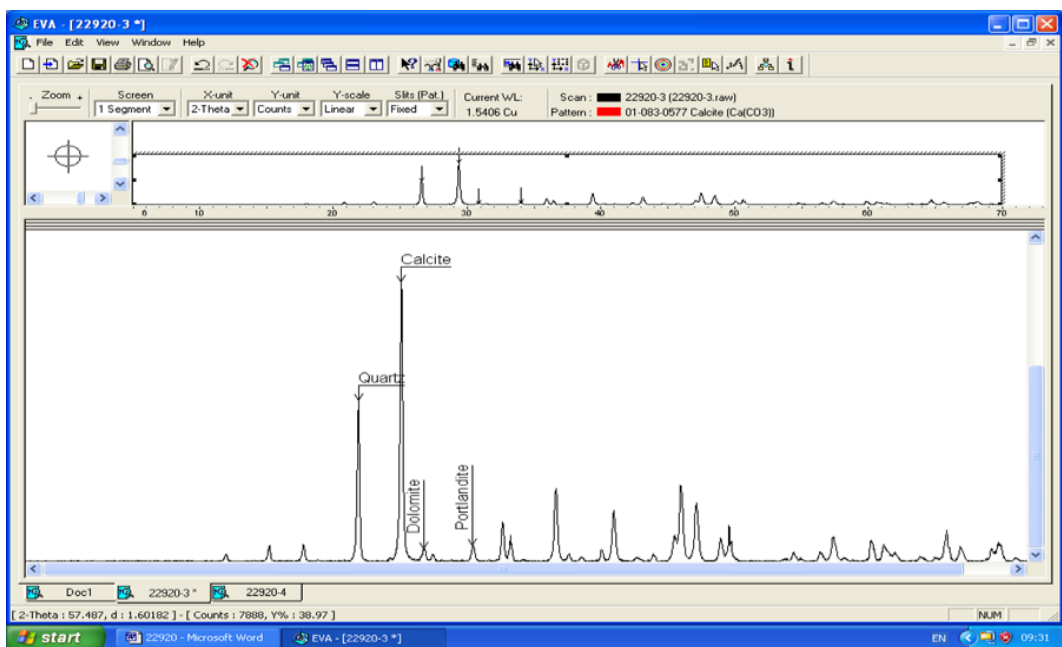


Figure 4.71: XRD Spectrometry - Compound Composition, Phases/ Peaks of F/PFA/SF PET1%.

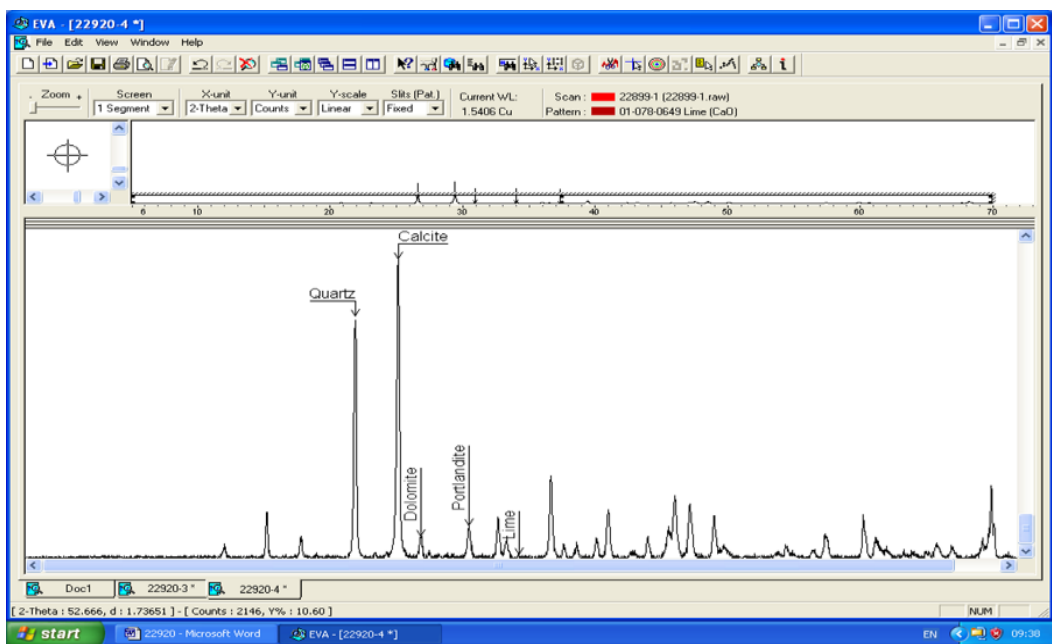


Figure 4.72: XRD Spectrometry - Compound Composition, Phases/ Peaks of F/PA PET1%.

Table 4.24: Elemental Compound Composition of Composites Using X-RAY Spectrometry/ Eva Software.

Elemental Compound Composition		Quartz SiO ₂	Calcium Carbonate CaCO ₃	Vaterite CaCO ₃	Dolomite CaMg0.77Fe0.23(CO ₃) ₂	Lime CaO	Pigeonite (Mg1.05Ca.16Fe0.72Al.04TiO ₃)(Si1.98Al.0 ₂)O ₆	Portlandite, syn Ca(OH) ₂	Ettringite (3CaO.Al ₂ O ₃ .32H ₂ O)
SL80 COIR 1.0	Eva	49.80%	40.30%	5.90%	3.40%	0.60%	0.01%		<0.01%
	Y-axis	91.05	100	2.49	3.42	1.36	6.5		<0.9
	Normalised	44.45	48.82	1.22	1.67	0.66	3.17		<0.7
SL80 PET 0.5%	Eva	47.40%	48.40%	2.40%	1.80%				<0.01%
	Y-axis	95.59	100	1.82	2.49				<0.7
	Normalised	47.82	50.03	0.91	1.25				<0.5
Fe/PFA/SF PET 1.0	Eva	59.90%	35.10%		2.40%			2.60%	<0.01%
	Y-axis	100	56.92		4.65			4.88	<0.4
	Normalised	60.08	34.2		2.79			2.93	<0.3
Fe/PA PET 1.0	Eva	37.10%	55.10%		2.70%	0.30%		4.70%	<0.01%
	Y-axis	79.5	100		7.51	0.12		10.5	<1.1
	Normalised	40.23	50.6		3.8	0.06		5.31	<0.9

4.13.2 Microstructural Analysis Using Energy Dispersive X-ray Spectroscopy (EDS)

SEM produces 2D/ 3D images of 20 - 30000 times magnification with 50-100 µm resolution, showing spatial variation in the sample size from 5 microns to 1 cm. EDS could determine the chemical composition of the crystalline structure/ orientation and perform the SEM. In this study, a section from each of the specimen's slices was mounted, coated and examined by SEM and EDS under various magnifications using an SEM machine (Figure 3.15) and getting microfabric/ crystallographic results in the attached visual display monitor as images and EDS spectrum (Carleton.edu, 2023; JEOL Ltd., 2023). The images and EDS spectrum could be used to analyse the crystalline/ amorphous morphology of the specimen with up to 25000 times magnification, showing the presence of different compounds which could be identified by matching these to an AMCSD-like database by SEM experts, augmented by EDS-spectrum quantifying the exact percentage presence of various compounds in the given specimen.

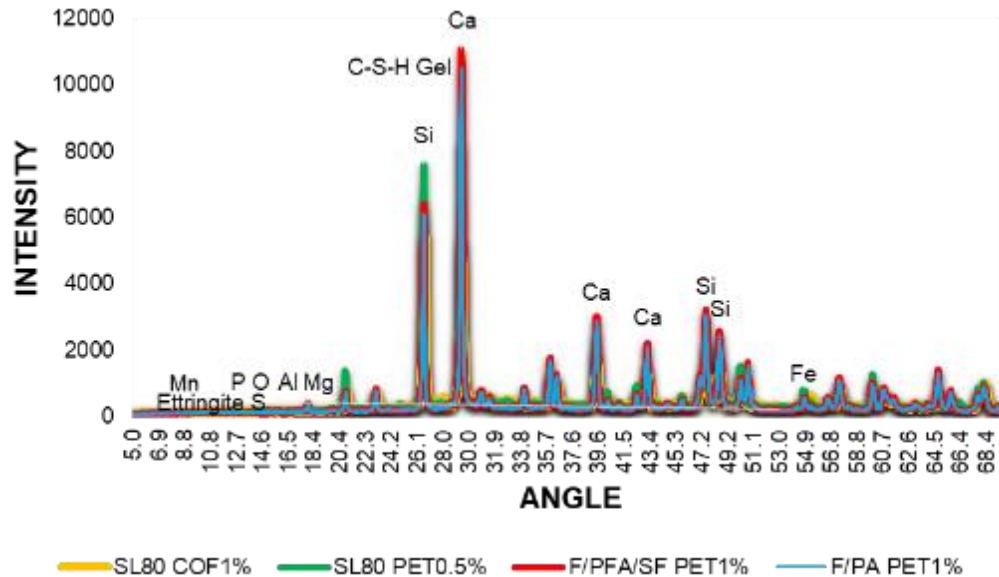


Figure 4.73: Combined Spectrum of NALFRIC/ NAFRIC Composites after Sulphate Attack Using EDS.

Figure 4.73 shows a combined EDS spectrum of the four specimens showing multiple pointed peaks at different phases of electron diffractions at different intensities/ angles. The pointed peaks showed that the specimens contained crystalline materials. The smaller peaks showed the phases of minor compound reactions, and larger peaks with different phases showed the formation of dense C-S-H gel by the highest peaks, followed by the hydration phases, portlandite phase, polymerisation/ pozzolanic phases, brucite and ettringite formation phases. All four specimens' peaks coincided with different optimum quantities at the same peak configuration. However, it could be inferred that the maximum peaks were achieved by Ca and Si, elucidating the presence of C-S-H gel in maximum quantity. Ca and Si were observed in several phases configuring multiple peaks, suggesting the spread of C-S-H gel all over the specimen. The uniform spread of C-S-H gel exhibited the completion of the hydration process, completing the formation of strength-inducing calcium silicate hydrates. The formation of monosulphate aluminate hydrates was determined by the presence of aluminium, and brucite is characterised by very small peaks of Mg, P, Mn, and

S, which are also present as minor peaks in negligible quantities. The presence of sulphur and Mg showed the sulphate attack and formation of brucite and ettringite, but the size of peaks identified their minimal quantities, suggesting the materials were not affected by the sulphate attack. The individual EDS spectrums are shown in Figures 4.74-4.77. Figures 4.74 and 4.75. They showed two high peaks of Ca and Si, indicating up to 90% formation of C-S-H gel, which was responsible for inducing around 30 MPa strength to SL80 COF1% and SL80 PET0.5 NALFRIC composite even after the sulphate attack. Minor peaks of S, Fe, Mg, Al, and other elements showed that negligible impact of MgSO_4 was observed/ induced in the specimen, showing no impact on the strength as per experimental findings of this research and in line with the findings of other researchers that GGBS performs better in sulphate environment and even gain strength (Bapat, 2012; Rughooputh and Rana, 2014; Abdelalim et al., 2015; ASTM C1012/C1012M-15, 2015; Kamau et al., 2016; Mukherjee et al., 2016; Robati et al., 2016; ASTM C1012/C1012M-18, 2018; Babu et al., 2018; Ahmed et al., 2019; Nadir and Ahmed, 2021; Nadir and Ahmed 2022b; 2022c Appendix V, VI, Ecocem, 2023). Figures 4.76 and 4.77 also showed two significant peaks and several others of Ca and Si.

The “Ca” peak was more extensive than Si, showing more composition of C-S-H gel and $\text{Ca}(\text{OH})_2$. Fe peak showed the formation of FeCO_3 . The minor Mg and S peaks showed the presence of brucite and ettringite but in very small quantities, elucidating the sustainable use of strong NAFRIC composites as durable sulphate-resistant materials. The NAFRIC composites were found to contain some portlandite due to the significant binding ingredients of OPC. Si quantity was observed to be lesser than the SL80 NALFRIC composites because only 2.8% of the total binder was incorporated as the ternary pozzolanic component. Increasing pozzolanic material would likely increase strength as the quantity of Si and some portlandite was still available and could be converted into additional C-S-H gel on further pozzolanic reaction to a specific optimum dosage. However, the findings of this research that iron-based binary and ternary pozzolanic

composites are stronger and more durable than OPC-based concrete/ SCMs is supported by the microstructural analysis in line with the findings of research about Fe-composites (Siddique, 2004; Stone, 2010; Karuppasamy, Dinesh and Janardhan, 2011; Das, Souliman and Stone, 2014).

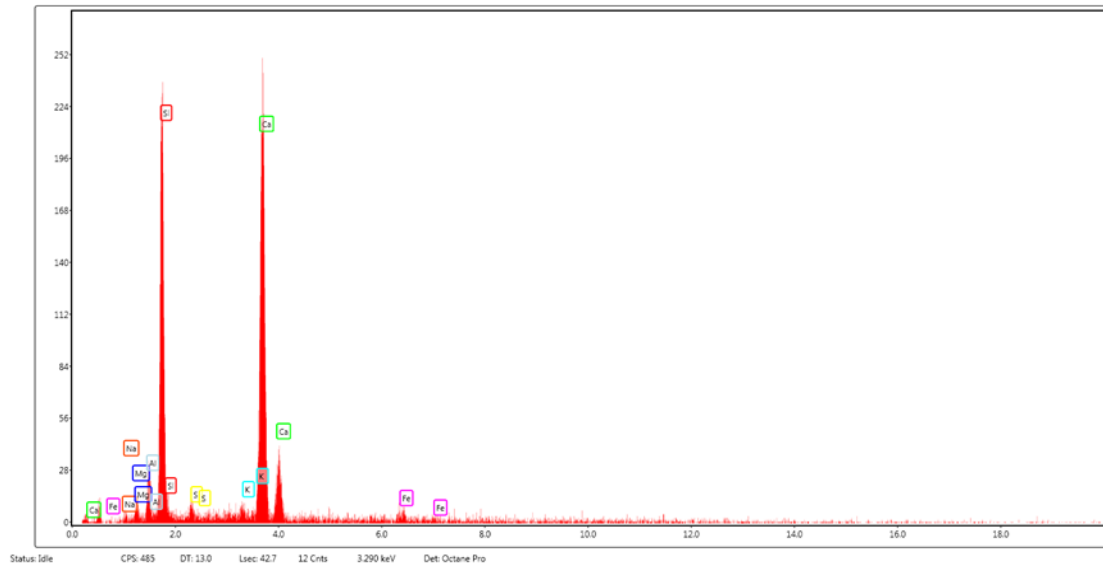


Figure 4.74: Spectrum of NALFRIC SL80 COF1% Composites after Sulphate Attack Using EDS.

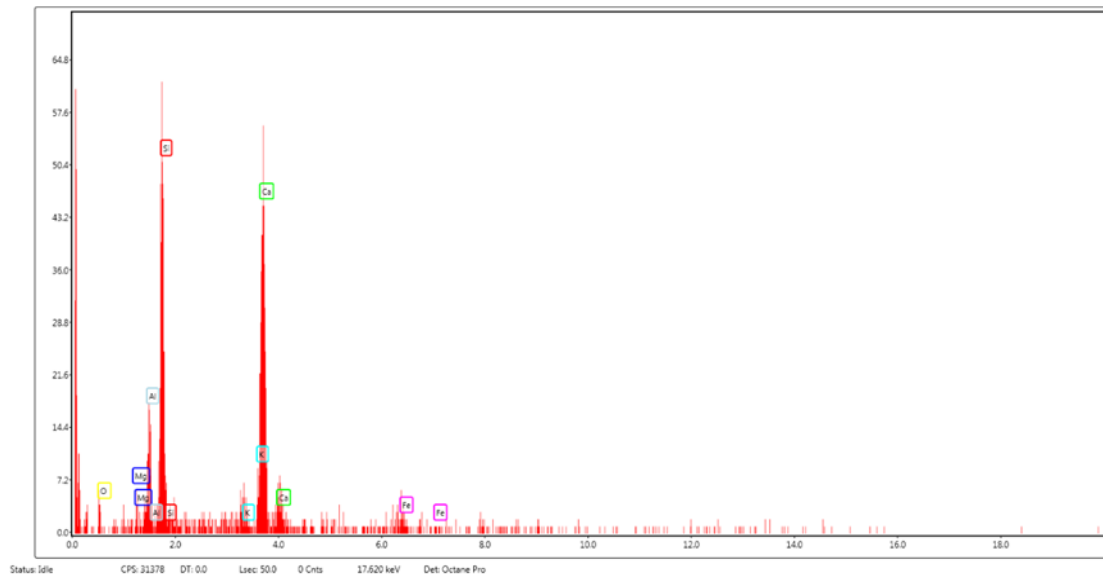


Figure 4.75: Spectrum of NALFRIC SL80 PET0.5% Composites after Sulphate Attack Using EDS.

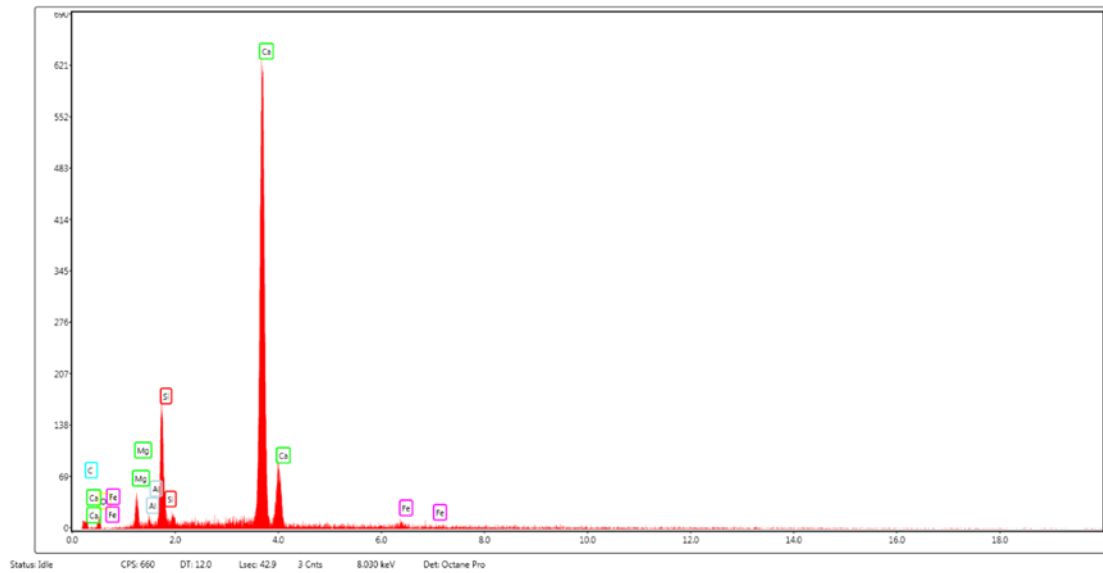


Figure 4.76: Spectrum of NAFRIC F/PFA/SF PET1% Composites after Sulphate Attack Using EDS.

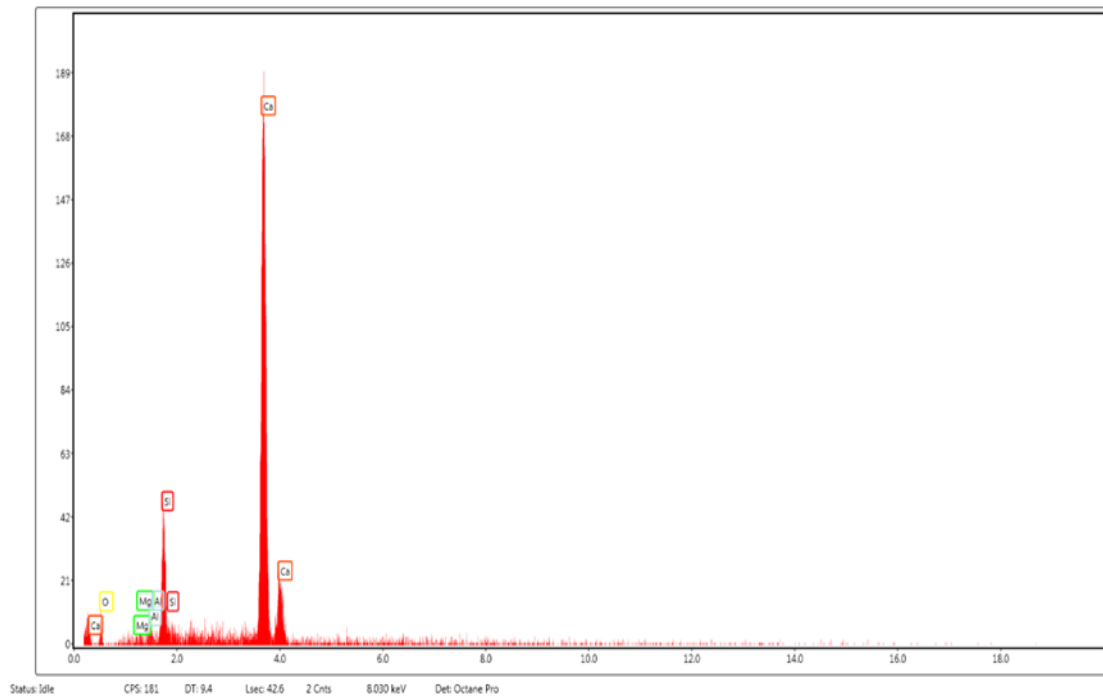


Figure 4.77: Spectrum of NAFRIC F/FA PET1% Composites after Sulphate Attack Using EDS.

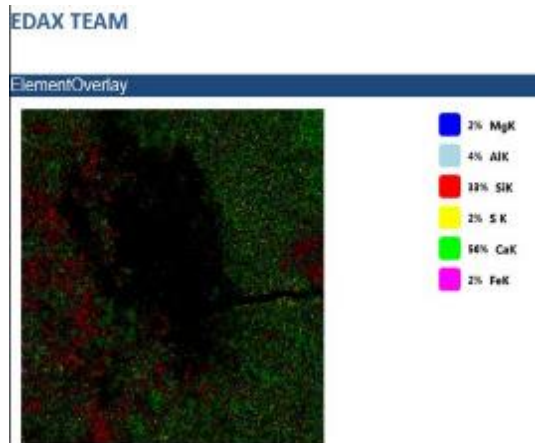


Figure 4.78: Elemental Mapping Using EDAX-TEM for SL80 COF1%

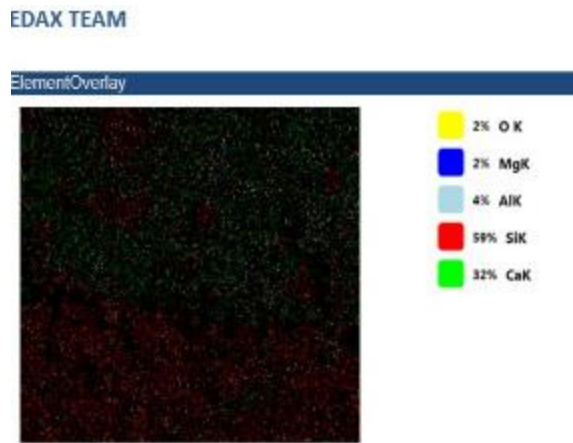


Figure 4.79: Elemental Mapping Using EDAX-TEM for SL80 PET 0.5%

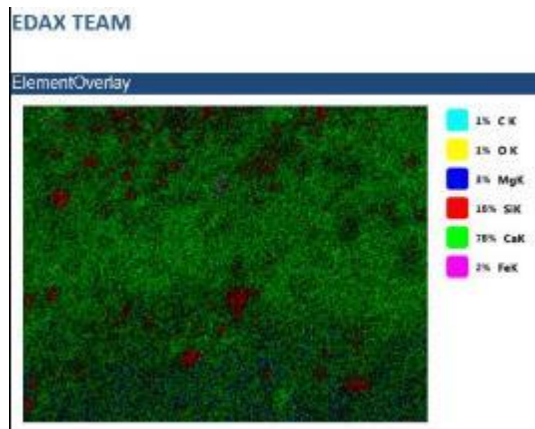


Figure 4.80: Elemental Mapping Using EDAX-TEM for F/PFA/SF PET1%

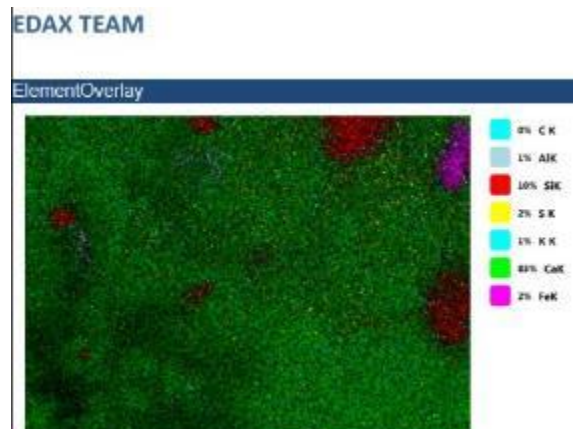


Figure 4.81: Elemental Mapping Using EDAX-TEM for F/PA PET1%

4.13.3 Microstructural Analysis Using Energy Dispersive Analysis with X-ray Spectroscopy (EDAX) and Transmission Electron Microscopy (TEM) with TEAM Software

The microstructural analysis conducted using XRF, XRD and EDS was further supported by the study of specimens using Energy Dispersive Analysis using X-ray and Transmission Electron Microscopy using TEAM software on an SEM machine, another advanced feature. They provided a colourful dispersal mapping of elements present on the specimen with different colour coding and phase

identification. Figures 4.78 to 4.81 show the elemental mapping with colour coding for the electrons scattered from the K orbit phase. All the specimens were mapped with up to 90% calcium and silica, showing a uniform spread all over the specimen, indicating a large-scale formation of C-S-H gel with full hydration, formation of negligible Mg and “S” showed minor impact of sulphate attack with less than 2% production of ettringite and brucite. The presence of Fe showed the formation of FeCO_3 , which was another strength and rock-like formation provider. These results were finally analysed with SEM images of the crystals' real-time morphology and orientation. All the above analyses using XRF, XRD, EDAX, and TEM supported the strength/ durability characteristics of the innovative NALFRIC and NAFRIC composites with up to 90% of strength-inducing C-S-H gel and negligible quantity of ettringite/ sulphate attack.

4.13.4 Microstructural Analysis Using Scanning Electron Microscopy (SEM)

The SEM provide real-time imaging of the specimen generated by scattered/ diffracted electron beams, with 10-25000 magnification, 2-5 μm , using SE mode, HV of 5kV, angles θ -5 θ on Nova Nano SEM machine. Figures 4.82 and 4.83 show the SEM images of NALFRIC composites of SL80 COF1% and SL80 PET0.5%. The images show the crystalline morphology of the material. The dense formation of C-S-H gel was visible, with bigger grey crystals uniformly spread all over the specimen, elucidating the composite's excellent completion of the hydration process and strength attainment. Very few ettringite needles-like crystals could be observed. The black holes showed the voids and the white cloudy matter showed the untreated lime/ slag particles. The vast spread of C-S-H gel was responsible for the strength of a material. The formation of calcite CaCO_3 was also observed with calcium sulfoaluminate hydrates and brucite, making an external membrane on the outer surface. The formation of a good quantity of C-S-H gel and pozzolanic reaction systematically improved the pore structure, making an ingredient bonding more pronounced with the nanomaterial

crystalline formation. The impervious crystalline structures, refined pores, pozzolanic filler action, and calcite/ mono-sulphate-aluminate hydrate membrane on the outer surface prevented ingress of the hazardous sulphate chemicals and improved the resistance against the chemical attack, thus resulting in increased strength and durability even during the exposure to the sulphate environment. Full utilisation of $\text{Ca}(\text{OH})_2$ made it impossible for the external sulphate attack to occur as MgSO_4 needed aqueous portlandite to ingress/ react to exchange cations and formation of brucite and ettringite.

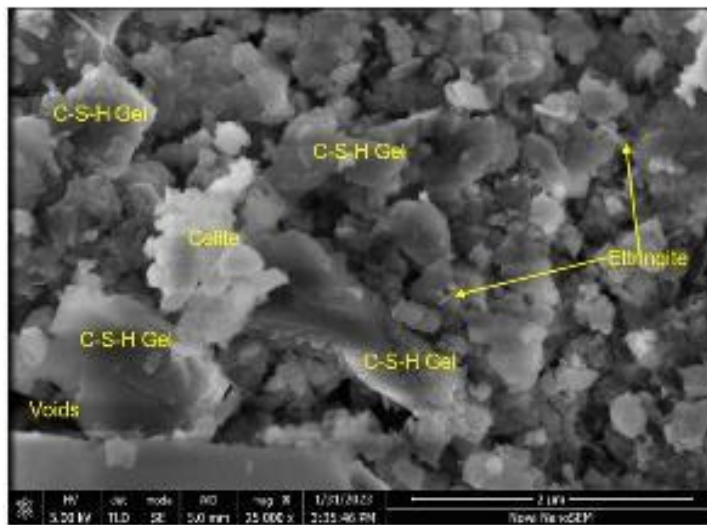


Figure 4.82: SEM Image- SL8- COF1%

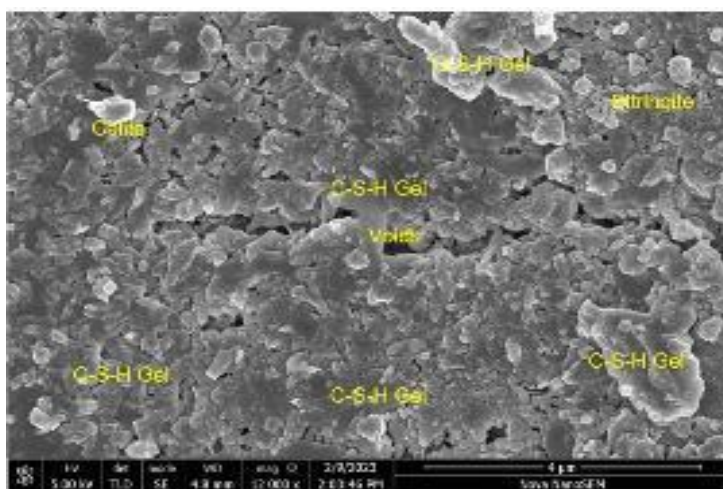


Figure 4.83: SEM Image SL80 PET0.5%.

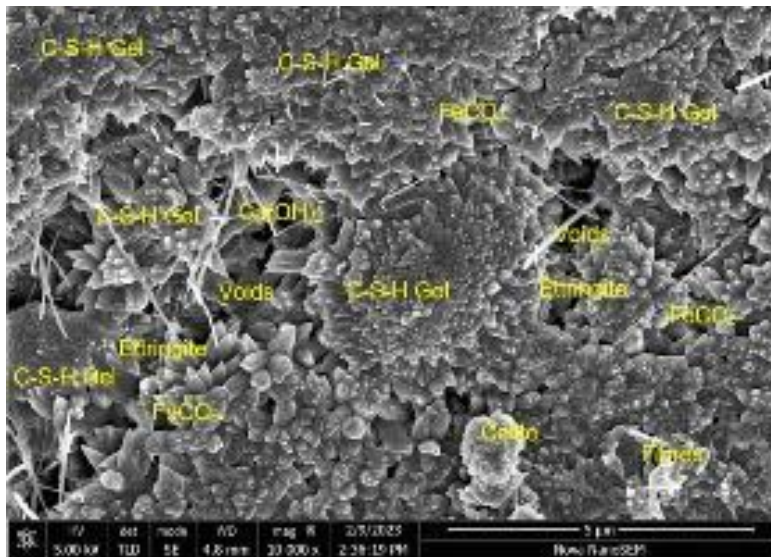


Figure 4.84: SEM Image - F/PFA/SF PET1%.

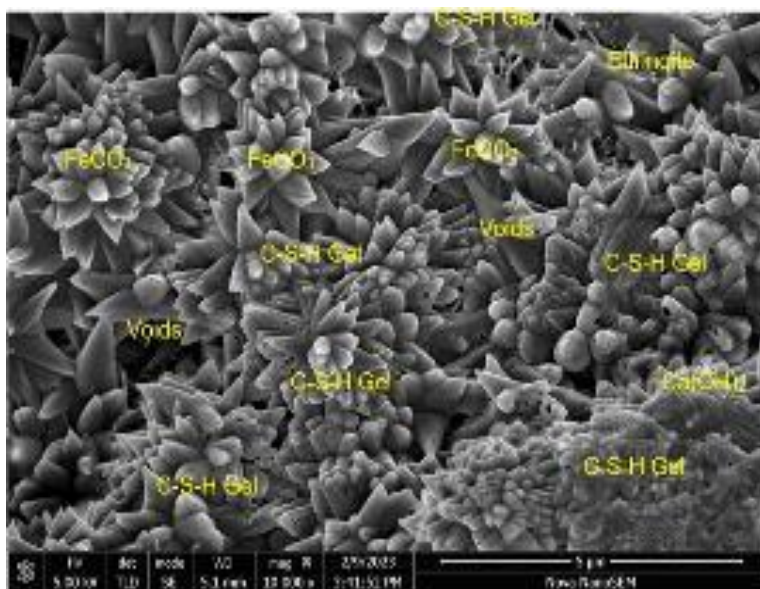


Figure 4.85: SEM Image F/PA PET1%.

Figures 4.84 and 4.85 show the SEM images of NAFRIC composites of iron-based binary and Ternary pozzolanic mixes of F/PFA/SF PET1% and F/PA PET1%. The images showed that the materials had crystalline morphology. The dense formation of C-S-H gel was visible, with bigger dark grey crystals uniformly spread all over the specimen, supporting the composite's full hydration process,

and the formation of additional C-S-H gel due to swift hydration of alite, belite, celite, CaO , SiO_2 and pozzolanic reaction (SiO_2) with Ca(OH)_2 . Some Ca(OH)_2 was observed as an untreated quantity in the mix, which identified a further formation of C-S-H gel if an additional amount of pozzolans is made available, giving room to increase the pozzolanic percentage for an increase in strength. The formation of an appropriate quantity of C-S-H gel and its spread all over the specimen exhibited enhanced compressive strength. Very few ettringite needles-like crystals could be observed. The black holes showed the voids and the white cloudy matter showed the untreated lime/ slag particles. The vast spread of C-S-H gel was responsible for the strength of the NAFRIC material. The prominent flowery petals-like protruding crystals and the formation of C-S-H gel show the presence of FeCO_3 formed with a reaction of iron powder and CO_2 released during the hydration process or absorbed from the environment. The untreated particles of Fe predicted the room to use an additional quantity of CO_2 from the environment or may be injected into the specimen and cured in a saturated CO_2 tank for the additional formation of FeCO_3 . The increased quantity of FeCO_3 produced would likely increase the strength of the composites and would increase the capability of NAFRIC composites further to absorb the CO_2 from the environment or CO_2 tank, making it a suitable carbon absorbent material by capturing more CO_2 . Calcite (CaCO_3) was also observed with calcium monosulphate aluminate hydrate and brucite, making an external membrane on the outer surface. A few crystals of ettringite were observed, elucidating the material's enhanced durability and capacity to withstand sulphate attack in a better way. The formation of a good quantity of C-S-H gel and pozzolanic reaction systematically improved the pore structure, making an ingredient bonding more pronounced with the nanomaterial crystalline formation. The impervious crystalline structures, refined pores, pozzolanic filler action, and calcite/mono sulphate aluminate hydrates membrane on the outer surface prevented the ingress of the hazardous sulphate chemicals and improved the resistance against the chemical attack, thus resulting in increased strength and durability even after

the exposure to the concentrated sulphate environment. Full utilisation of Ca(OH)_2 made it impossible for the external sulphate attack to occur as MgSO_4 needed aqueous portlandite to ingress/ react to exchange cations and formation of brucite and ettringite. All the advanced XRF, XRD, SEM, EDAX, and TEAM testing fully supported innovative composites' strength gains capabilities, durability characteristics, and sustainability parameters in accelerated sulphate exposure of 270 days, depicting a field sulphate attack of 20 years. The advanced testing provided scientific evidence that all the NALFRIC and NAFRIC composites are adequate in forming the required C-S-H gel due to the complete reaction of hydration, pozzolanic, and iron carbonation (FeCO_3) to induce befitting compressive strength. The composites were observed to develop unique sulphate resistance due to the formation of brucite/sulfoaluminate membrane on the outer surface, development of rock-like FeCO_3 , pore refinement with pozzolanic fillers, improved intra-ingredients bonding, full depletion of gypsum and portlandite and removal of voids to prevent ingress of chemicals a crack/ sulphates propagation. Therefore, the research could be successfully evaluated as fulfilling the primary objectives of the research, i.e., the development/ elucidation of sustainable waste-absorbent low-carbon materials for greener infrastructure construction and hydromodifications/ water channel stabilisation with enhanced engineering properties.

4.14 Significance of PhD Research and the Developed Composites.

This PhD research endeavoured to integrate hydrological studies with material science by collaborating on the issues faced due to anthropogenic activities like hydromodifications and stream morphology/ ecology changes. The unplanned modifications without proper hydrological/ hydraulics studies lead to flood disasters by overflowing the rivers from the natural flood plains/ banks. The unplanned urbanisation and irrational use of advanced construction technology without considering a catchment level trans-borders holistic river management strategy results in climatic variations, cloud bursts, flash flooding and glaciers

bursting, damaging every asset coming in their course of flow. The increased waste production by the vast world population, non-disposal of waste properly, uncontrolled use of fossil fuels, manufacturing of modern polymer materials/ alloys, relentless depletion of natural resources, manufacturing of non-biodegradable construction materials and disposal of demolition waste were observed as the major issues being faced by the world with technological advancements. Ideally, natural flood management is the best option to avoid catastrophic natural flooding disasters, but their limited scope and enormous anthropogenic activities entail augmentation by the structural measures to control any such event along the water streams. The choice of materials and type of construction for any hydromodification in the form of channelisation, barrages, dams, embankments, gabions, weir/ notches, flood defences, sluice gates, break walls, break stones and marine structures was observed as essential planning/ execution element for any hydraulic structure, as it directly impacts the climate, ecology, environment and natural habitats. The construction of megastructures and masterpieces of civil engineering infrastructures are considered the basics of modern metropolitans, requiring advanced high-strength materials, including cement concrete, resulting in increased CO₂ emissions by the construction industry. Section 2.1 – 2.2. elucidated the hydrological studies/ implications for flood risk assessments/ mitigations. Natural flood management measures were investigated for their efficacy and extent of use, and it was observed that NFM could be applicable for a limited extent of a stream stretch in the case of small water channels, proposing the use of structural measures for sufficient strength and feasible applicability to harness the forces of the nature. Section 2.2.5 discussed the efficacy of employing environmental impact assessment to prevent the environmental damage caused by uncontrolled construction. However, it was observed to partially succeed in its implementation due to political/ personal benefits over environmental protection. EIA remained partially successful in controlling the carbon footprints of the construction industry as it did not prevent the use of modern high-carbon emission materials. Therefore, manufacturing

greener, more sustainable, low-carbon, economical materials is the option to go alongside low emissions and modern construction. Section 2.3 evaluated the literature on available options of existing/ proposed low carbon emissions construction materials, followed by section 2.4 to introduce the testing mechanisms for evaluation of the strength/ durability parameters of the construction materials. Chapter 3 elucidated the use of different methods/composition of materials to formulate innovative composites and investigate their engineering properties to support their befitting use in the construction industry. This research has endeavoured to investigate, evaluate, compare, and formulate existing and new composite materials as alternatives to cement concrete to introduce greener, low-carbon materials. As discussed in sections 4.6-4.14, the partial cement/ aggregate replacement composites, cement-free lime-based pozzolanic composites and iron-based pozzolanic composites are beneficial to use in all types of low, medium and high-strength applications in all types of construction with added advantages of 3-90% cost benefits and 5%-2800% low emissions benefits resulting in 2.5-80% disposal/ recycling of waste agricultural/ industrial materials, 2.5-30% preservation of natural resources from depletion and above all likely reduction of 2.5%-30% GWP of construction industry. The use of cement alternatives/ partial replacement composites is the foremost applicable solution to reduce the carbon footprints of the construction industry by 30-50%, as stipulated in COP28 for 2030 and 2050 targets.

4.15 Calculation of Embodied CO₂ and Cost-Benefits Analysis of Developed Composites.

Cement is the leading cause of the carbon footprint of concrete in the construction industry. It is classified as third in the GHG emissions after the iron and steel industries, but its large-scale manufacturing/ utilisation of around 4.4 billion tons annually makes it the most CO₂ embodied material in the world. Cement emits 10% of GHG and 30% of global energy consumers (Purnell, 2013; UNEP, 2020;

Lupien, 2020; Obinna, 2023). The conversion of limestone CaCO_3 into slaked lime CaO after burning at 1450°C is the most energy-intensive and CO_2 emitting process of cement manufacturing, accounting for around 80% of GHG emissions of cement concrete (0.8-0.9 tons of CO_2 per ton of cement manufacturing). Concrete main ingredients are binder (cement responsible for up to 80% of GHG emissions), fine/ coarse aggregate (responsible for up to 5% GHG emissions), admixtures (responsible for up to 2% GHG emissions) and water (zero emissions) (Brander and Davis, 2012; Gagg, 2014; www.grandviewresearch.com, 2020; Nadir and Ahmed, 2021a; Garside, 2022a; Garside, 2022b; MPA, 2007; Nadir et al., 2022b Appendix XII). The GHG emissions from cement concrete manufacturing could be divided into five phases. The mining, extraction, and calcination of cement raw materials, fine and coarse aggregates and manufacturing of admixtures (including air entrainers, plasticisers, accelerators, retarders, and curing compounds) are the significant CO_2 emitting processes (up to 75-80%). The second phase accounts for up to 6% of emissions, including national/international transportation of cement/ other ingredients. The third phase is mixing concrete ingredients in the insitu/ onsite or at the concrete plants away from the construction sites. The fourth phase is transporting fresh concrete from the plants to the construction sites using transit mixers. The fourth and fifth/ final stages are responsible for up to 10-15% of CO_2 emissions and include the transportation, placement of concrete for construction using formwork, concrete pumps, vibrators, curing, hydration, ultimately demolition, recycling as recycled aggregates/ waste disposal as shown in Figure 4.86 (Spencer et al., 2023). Figure 4.87 shows that a project emits almost 50% of its total lifecycle GHG emissions during the extraction, procurement, transportation, and manufacturing of raw materials in the cradle-to-gate phase of the product module. The on-site construction phase is responsible for around 5% of emissions, whereas whole-life operation/ use is responsible for up to 25% of emissions till the end of life, followed by around 2% in the final phase of demolition or recycling as the circular economy (Victor, 2023).

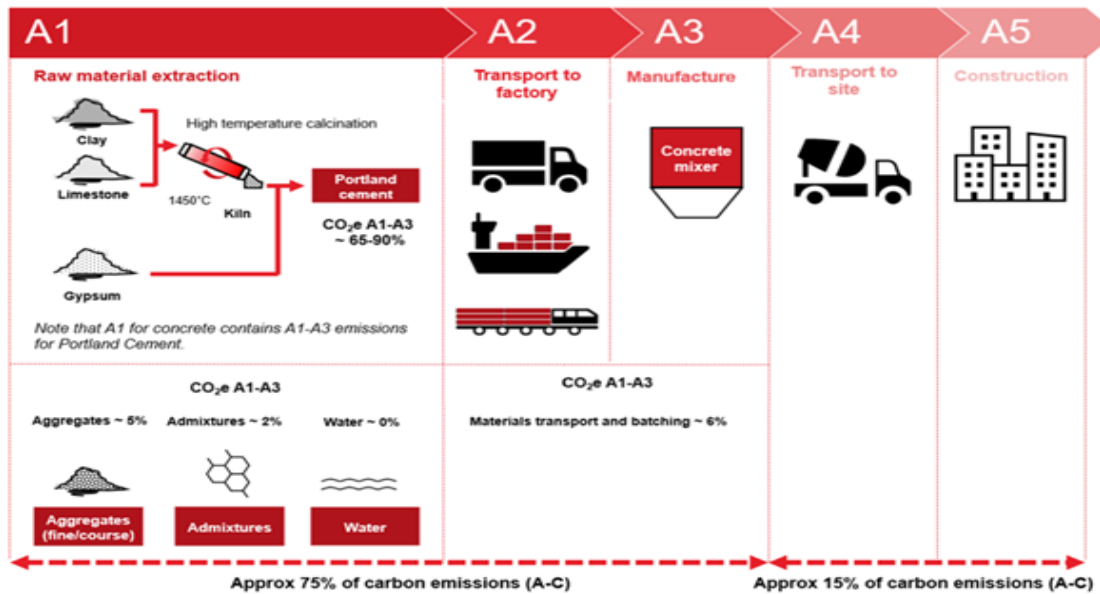


Figure 4.86: GHG Emissions Phases of Cement Concrete Manufacturing (Spencer et al., 2023).

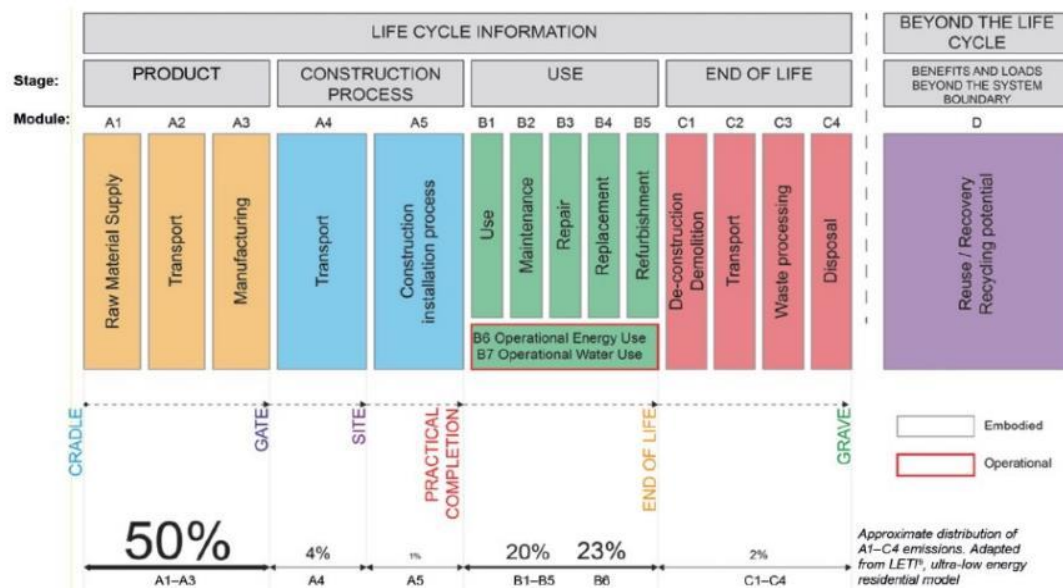


Figure 4.87: Lifecycle Stages of GHG Emissions of a Project - Cradle to Grave (Victor, 2023).

Figure 4.88 illustrates the contribution of different sectors/ processes to achieving a net zero CO₂ balance. The maximum 6% CO₂ absorption could be achieved by

efficiently absorbing/ capturing the CO₂ produced during any manufacturing process in the CO₂ sink for re-carbonation/ other uses, and 36% CO₂ could be captured/ recirculated using carbon capture/ utilisation and storage (CCUS). 36% of CO₂ is being absorbed/ recycled commercially by recycling for the industrial reformation of fossil fuels-related products, deceiving the disposal of hazardous gases but getting the commercial benefits in producing more GHG-emitting products (GCCA, 2021). Oxford's university research by Smith's School of Enterprise and Environment observed CCUS as the most uneconomical method of tackling GHG and reducing the quantity of CO₂ from the environment/manufacturing facilities as it could cost around a trillion dollars per year to decrease it by 2050 as per COP28 goal set for 30% reduction in CO₂ emissions as compared to exercising control on the use of fossil fuels and GHG emitting activities/ processes globally (Way, 2023). The world is currently focussing on renewable energy resources as alternatives to coal and fossil fuels, but all the targets set to achieve even a small reduction in GHG emissions/ rising global temperature and climatic variations are deemed futile (Way, 2023). The burden of reduction of CO₂ comes on the construction industry as the projected control on clinker production (11% reduction), curtailing CO₂ emissions from cement/ binders (9%), efficiency in concrete production (11%) and finally, efficiency in design and construction in the form of sustainable building and construction materials (22%), all add up to a saving of 53% GHG emissions from the construction industry (Figure 4.88) (GCCA, 2021). The world leaders' so-called focus on the reduction of GHG emissions and climate control could well be perceived by not diverting the attention on the adoption of alternative fuels, production of fossil fuels manifold as compared to a few decades ago, avoidance of agreement by the developed nations to implement climate emergency, allocation of funds and adoption of agreed principles of prevention/ cure for at least 1.5°C reduction of temperature and reduction of CO₂ emissions by 30% by 2030 and net zero by 2050. The Conference of Parties-28 was held in Dubai in December 2023 (COP28). Holding a UN climate action conference in a country

that comes tenth on the oil-producing list and constructing a huge new infrastructure full of emissions proves the leaders' lack of interest in coping with the climate emergency. Therefore, the construction industry must adopt low-CO₂ embodied construction materials and designs to shoulder the responsibility of reducing carbon footprints. The total discontinuation of cement concrete is not considered an immediate solution. It would likely continue in construction like using fossil fuels for at least a considerable future time, necessitating formulation of greener/ sustainable eco-friendly materials by controlling/ reducing the use of clinker (calcination of lime), lowering of cement contents as PCR/ SCMs, use of naturally sourced fine/ coarse aggregates, incorporation of waste from other industries having any pozzolanic/ cementing properties, use of alternative materials for steel, aluminium and plastic. The total quantum of fine/ coarse aggregate is estimated to be around 20 billion tons, contributing around a billion tons of CO₂. The quarrying, transportation and crushing/ extraction of approximately 20 billion tons of sand, gravel and aggregates for the construction industry emit one billion tons of additional CO₂ per year; still, the main GHG emissions are caused by the use of cement, steel, aluminium and polymers. (Nazari and Sanjayan, 2016; ICCS, 2017; John, 2018; Karen et al., 2018a; Karen et al., 2018b; Millward-Hopkins, 2018; Scrivener et al., 2018; GCCA, 2019; ICE V3 Database Circular Ecology, 2019; Maria et al., 2019; Moynihan, 2019; Burridge, 2020; Jannie et al., 2020; Orr, Gibbons and Arnold, 2020; Vashisht and Paliwal, 2020; Astle, 2021; Nadir and Ahmed, 2021b; Sentucq and Clayton, 2021; The Concrete Centre, 2021; Arch Daily, 2022; ICE, 2022 ; OCO Technology, 2022; ITC. 2023; Fragkoulis and Karen, 2023; GCCA, 2023a; GCCA, 2023b; Harvey, 2023; Sky News, 2023; Spencer et al., 2023; UKGBS, 2023; Venkat, 2023; Victor, 2023; WBCSD, 2023; www.lowcarbonmaterials.com, 2024; www.cis.ihs.cm, 2024; www.constructionnational.co.uk, 2024). The waste materials from different industries/ agriculture contribute to 90% of waste disposal/ recycling efforts worldwide. Increased use of OPC and concrete poses a severe environmental sustainability threat because of its large-scale

contribution to greenhouse gas emissions. Therefore, this study suggests the use of alternative pozzolanic-based PCRs/ SCMS, pozzolanic-based limecrete (NALFRIC) and iron-based pozzolanic composites (NAFRIC) with/ without fibres as formulated in this study.

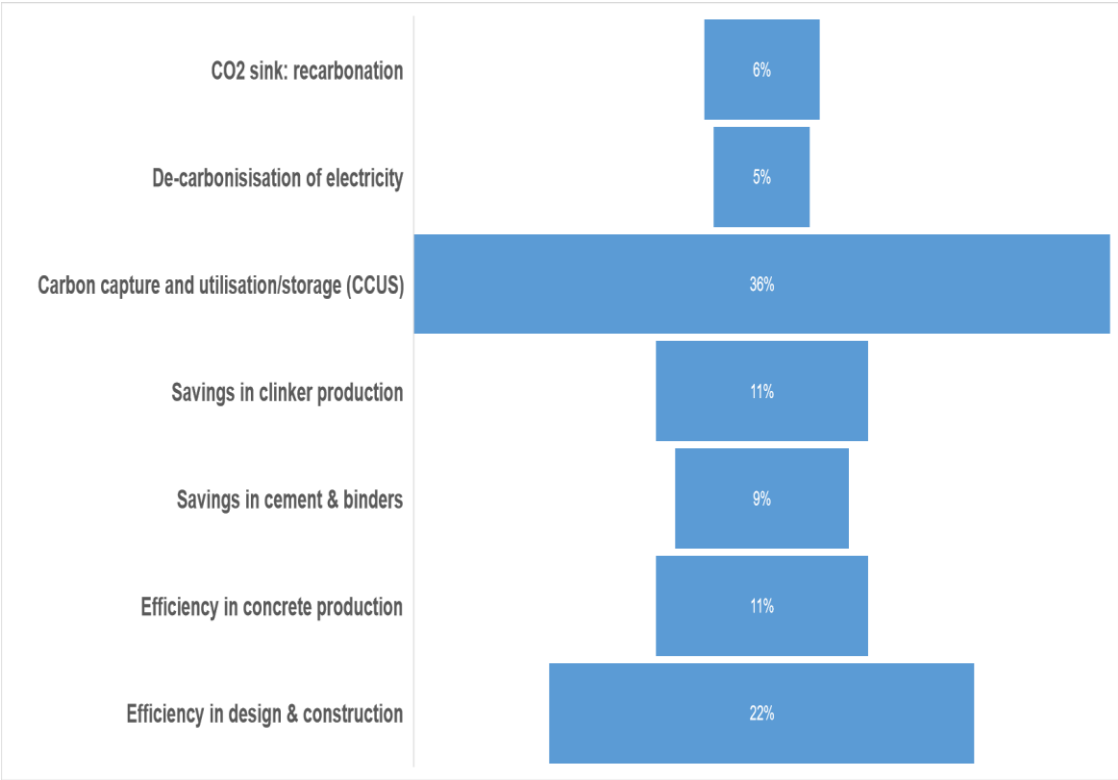


Figure 4.88: %age Contributing Sectors to Achieve Net Zero CO₂ Emissions (GCCA, 2021).

Table 4.25 shows the established/ calculated embodied CO₂ of different construction materials used in this study to formulate PCRs/ SCMs/ TCRs composites, including NALFRIC and NAFRIC. The transportation cost and minor ingredients like additives, accelerators, plasticisers and curing compounds are responsible for a very meagre amount of CO₂ emissions as compared to the main cement contents; therefore, attention was concentrated on the assessment of binders/ aggregates related embodied CO₂ emissions and impact of savings in the total quantity of CO₂ emissions per m³ or per ton of traditional cement concrete and innovative composites discussed/ formulated in this research. The

ICE database version 3 of circular ecology for the assessed values of embodied CO₂ by the construction materials was used to calculate the composites of 1 m³ concrete with standard 1:2:3 mix ratio with cement as 340 kg/m³, fine aggregate as 680 kg/m³ and coarse aggregate as 1020 kg/m³ (ICE V3 Database Circular Ecology, 2019) and Table 2.5 and 3.1 were used to calculate the cost benefits. The embodied CO₂ was calculated for each PCR's/SCM's/TCR's constituent material as per their dosages/ ratios. The use of 1-2% fibres from other industries as waste material is likely to reduce GHG emissions by up to 1%, so it has not been considered while purely calculating for the binders/ aggregates. The results of the assessment of embodied CO₂, along with percentage savings in the quantity of kgCO₂e/m³, kgCO₂e/ton and cost benefits, are summarised in Table 4.26 for partial cement/aggregate replacement composites and Tables 4.27 and 4.28 for NALFRIC and NAFRIC composites.

Table 4.26 shows that a 27-53% reduction of GHG emission is possible with the use of 30%- 60% of GGBS as a partial replacement of cement with a 5-10% cost-benefit. 10-40% use of PFA as partial cement replacement could reduce 10-39% of embodied CO₂ of cement concrete with 3-12% cost-benefit. Partial cement replacement of 2.5-10% with SF is helpful for the reduction in the concrete's emissions by up to 2-9%; however, due to less availability/ transportation cost, it is more expensive than cement concrete by up to 2%. 5-20% use of MK as partial cement replacement is beneficial in the reduction of emissions up to 4-16% with 1-3% cost benefit in cost of construction as MK is available in abundance in different countries as kaolinite and calcination of kaolinite is, although, an energy-intensive process produces lesser CO₂ emissions as compared to calcination of lime for cement clinker. 2.5-10% of RHA and PA were observed reducing emissions by 2-9% with a 1-3% cost-benefits, along with up to 10% agricultural waste absorption. An example of calculation control mix and for 60% GGBS use as cement replacement is as follows:

Control Mix of 1 m³ concrete 1:2:3 ratio = cement 340 kg + Aggregates 1875 kg

Embodied CO₂ of 1kg cement is 0.78/kg, and fine/ coarse aggregate is 0.005/kg (Table 2.5).

Embodied CO₂ 1 m³ cement concrete Control Mix 1:2:3 ratio = cement 340 x 0.78 kg + Aggregates 1700 x 0.005 kg

Embodied CO₂ 1 m³ cement concrete Control Mix 1:2:3 ratio = Total kgCO₂e/m³
= **274** kgCO₂e/m³

Total kgCO₂e/m³ of 60% GGBS replacement composite in 1 m³ of Mix 1:2:3 ratio:

60% GGBS composite contains = 40% of 340 kg OPC + 60% of 340 kg of GGBS
+ 1700 kg of fine/ coarse Aggregates

Embodied CO₂ of GGBS = 0.067/ kg

Total kgCO₂e/m³ of 60% GGBS replacement composite = 40% x 340 x 0.78 + 60%
x 340 x 0.067 + 1875 x 0.005 = **128** kgCO₂e/m³

%age Savings in emissions if 60% GGBS replacement is made with OPC in concrete = 100 x (**274** – **128**)/ **274** = **53%**

%age saving in cost = 100 x (cost of 1 m³ of cement concrete – cost of 1 m³ of 60% GGBS SCM)/ cost of 1 m³ of cement concrete (cost from Table 3.1)

%age saving in cost = 100 x [(340 x 0.64 + 680 x 0.06 + 1020 x 0.06) – (0.4 x 340 x 0.64 + 0.6 x 340 x 0.48)] / (340 x 0.64 + 680 x 0.06 + 1020 x 0.06)]

= 100 x (323 – 290)/323 = **10%**

The percentage savings in kgCO₂e/kg and cost per cubic material of every composite were calculated using the same analogy, using data from Tables 2.5 and 4.25, and were tabulated in Tables 4.26-4.28. Detailed calculations in the Micro Soft Excel sheets are attached in Appendix XVIII.

Table 4.25: Embodied CO₂ (kgCO_{2e}/kg) of Cement, aggregate and SCMs.

Embodied CO₂ kgCO_{2e}/ kg of Cement, aggregate and SCMs	
Material/ constituent	Embodied CO₂ (kgCO_{2e}/ kg)
CEM I	0.78
Sand	0.005
Coarse Aggregate	0.005
GGBS	0.067
Fly ash	0.004
Silica fume	0.028
Metakaolin	0.15
Natural Pozzolans (e.g., volcanic ashes, trass)	0.05
Calcined Natural Pozzolans (e.g., calcined clay, LC3)	0.2
Limestone fines	0.075
Alkali-activated materials / "Geopolymers."	0.15-0.4
Steel	2.89
RCC 32/37 (110 kg/m ₃ of steel)	0.2
Aluminium	8.5
Fe/PFA (60% iron+20% PFA+10%LIME+8%MK)	0.028
Fe/GGBS (60% iron+20% PFA+10%LIME+8%MK)	0.041
Fe/PA (60% iron+20% PFA+10%LIME+8%MK)	0.047
Fe/PFA/GGBS (60% iron+20% PFA+10%LIME+8%MK)	0.038
Fe/PFA/SF (60% iron+20% PFA+10%LIME+8%MK)	0.034

Note: Embodied CO₂ of all Fe-composites have been calculated using kgCO_{2e}/kg of each material from Table 2.5 (ICE Energy Briefing Sheet, 2011; Obinna, 2023).

Table 4.26: Embodied CO₂ and Cost-Benefits of PCRs/ SCMs Composites.

Partial Replacement of Cement with Pozzolanic Materials					Partial Replacement of Aggregate with Alternative Materials				
Mix Material	Total kgCO ₂ e/m ³	%age Saving of kgCO ₂ e m ³	Cost/m ³ GBP	%age Saving in Cost/m ³	Mix Material	Total kgCO ₂ e/m ³	%age Saving of kgCO ₂ e m ³	Cost/m ³ GBP	%age Saving in Cost/m ³
Control	274	0	323	0	Control	274	0	323	3
GGBS 30%	201	27	307	5	CG 10%	266	3	321	4
GGBS 45%	165	40	299	8	CG 20%	266	3	319	5
GGBS 60%	128	53	290	10	CG 30%	266	3	316	5
PFA 10%	247	10	313	3	CR 10%	266	3	351	-5
PFA 20%	221	19	304	6	CR 20%	266	3	380	-14
PFA 40%	168	39	285	12	CR 30%	266	3	408	-23
SF 2.5%	267	2	324	0	RPB 10%	266	3	323	3
SF 5%	261	5	326	-1	RPB20%	266	3	323	3
SF 10%	248	9	328	-2	RPB 30%	266	3	323	4
MK5%	263	4	321	1	RCA 10%	266	3	321	4
MK 10%	252	8	318	1	RCA 20%	266	3	319	5
MK 20%	231	16	313	3	RCA 30%	267	3	316	5
RHA 2.5%	268	2	321	1	CT 5%	265	3	348	-4
RHA 5%	262	4	318	1	CT 7.5%	266	3	360	-8
RHA 10%	251	9	313	3	CT 10%	266	3	373	-12
PA 2.5%	268	2	321	1					
PA 5%	262	4	319	1					
PA 10%	251	9	315	3					
Positive values of %age show savings and negative values show increase in values compared to PCC 1:2:3 mix.									
All the mixes have been considered using 1:2:3 job mix ratio for a fair comparison purpose.									

Partly replacing fine/coarse aggregate with virgin cement concrete is another option to control GHG emissions. However, the net effect of partial replacement of fine aggregate with 10%-30 % CG, CR, and 10-30 replacement of coarse aggregate with RCA was observed to be up to 3%, with up to 5% cost benefit. Whereas the replacement of 10-30% fine aggregate with CR and coarse aggregate with 5-10% CT demonstrated a reduction of up to 3% emissions, but the cost increased to 4-23% compared to cement concrete, making it eco-friendly waste absorbent composites but the uneconomical cost of construction with lesser compressive strength.

Tables 4.27 and 4.28 summarise the assessment of embodied CO₂ and cost benefits of using NALFRIC and NAFRIC composites formulated in this study as innovative, greener, sustainable construction materials as alternatives to low-medium and high-strength/ high-performance cement concrete. The cement-free

hydrated lime-based pozzolanic composites have significantly decreased GHG emissions compared to cement concrete, as shown in Table 4.27. A standard PCC 1:2:3 mix demonstrates 274 kgCO₂e/m³ or 805 kgCO₂e/ton global warming potential (GWP). The NALFRIC composites have exhibited a negligible quantity of 9-54 kgCO₂e/m³ or 25-160 kgCO₂e/ton GWP, 5 times less than cement concrete. 100% CL90-based mix gives a meagre strength of around 5MPa, but its embodied CO₂ is 28 times lesser than cement concrete with 28% lesser cost, making it the best-suited material for low-strength requirements of mortars, sub-grades, flooring and walls façade. 10-90% GGBS-based limecrete demonstrated up to 89-96% saving/ reduction in GHG emissions with 20-27% cost benefits compared to cement concrete, making it the best suitable material for medium-strength construction applications (15-25 MPa). GGBS-based CL90 composites exhibited remarkable durability in concentrated sulphate attack against elongation and reduction of strength, rather than resulting in improvement of strength due to inherent characteristics of GGBS, making the most suitable alternative materials in all aspects. PFA-based CL90 limecrete composites exhibited 96-97% lesser CO₂ emissions with a 6-29% cheaper construction cost. However, it attained significantly less strength, up to 5MPa, making it suitable only for low-strength requirements. Cost-benefit analysis regarding the strength/ cost of cement concrete makes it uneconomical, although it has the best eco-friendly potential. SF-based CL90 limecrete demonstrated a 94-97% reduction in GWP, but it incurred up to 12% more construction cost than cement concrete. Its low strength attainment (up to 5 MPa) makes it a good choice for very low-strength applications, but strength/ cost-benefit analysis compared to cement concrete makes it uneconomical. MK-based NALFRIC composites exhibited 80-90% times lesser emissions and 1-13% reduced cost of construction than cement concrete; its calcination process is energy extensive, low strength attainment of 10 MPa restricts its use for low strength applications as an alternative to concrete but could be employed with many construction applications and is the second best cement-free limecrete option based on its abundance in different countries.

Table 4.27: Embodied CO₂ and Cost-Benefits of NALFRIC Composites.

NALFRIC Composites				
Mix Material	Total kgCO ₂ e/m ³	%age Saving of kgCO ₂ e m ³	Cost/m ³ GBP	%age Saving in Cost/m ³
PCC Control	274	0	334	0
CL90 Control	9	97	241	28
GGBS 10%	11	96	244	27
GGBS 20%	13	95	247	26
GGBS 30%	15	94	250	25
GGBS 40%	18	94	252	24
GGBS 50%	20	93	255	24
GGBS 60%	22	92	258	23
GGBS 70%	24	91	260	22
GGBS 80%	27	90	263	21
GGBS 90%	29	89	266	20
PFA 10%	9	97	313	6
PFA 20%	9	97	304	9
PFA 30%	9	97	294	12
PFA 40%	9	97	285	15
PFA 50%	9	97	275	18
PFA 60%	9	97	266	20
PFA 70%	9	97	256	23
PFA 80%	10	97	247	26
PFA 90%	10	96	237	29
SF 10%	9	97	328	2
SF 30%	11	96	339	-2
SF 50%	13	95	350	-5
SF 70%	15	94	361	-8
SF 90%	17	94	372	-11
MK10%	14	95	318	5
MK 30%	24	91	309	8
MK 50%	34	88	299	10
MK 70%	44	84	290	13
MK 90%	54	80	280	16
Positive values of %age show savings and negative values show increase in values compared to PCC 1:2:3 mix.				
All the mixes have been considered using 1:2:3 job mix ratio for a fair comparison purpose.				

The NAFRIC are the high-strength concrete alternatives considered low-carbon materials due to the absorption of CO₂ by Fe to form FeCO₃. Apart from this carbonation process, 10-50% iron-based pozzolanic NAFRIC composites exhibited a reduced embodied CO₂ by 6-48% but with up to 14-83% increased construction cost, as shown in Table 4.28. Iron powder is available in limited supply and involves transportation costs from the steel industry to construction industries/ sites, making it costly. Its high-strength achievement and 6-48% reduced GWP make it an ideal construction material as a 1:2:3 job mix ratio gives at a par high strength of more than 60-70 MPa of 1:1:3 cement concrete job mix ratio saving on the quantity of cement, reducing the emissions and gaining the high strength with even 10-50% more absorption of CO₂ as carbonation reaction. 10-50% NAFRIC with 20% GGBS-based composites exhibited 9-46% reduced

emissions with 14-83% increased construction cost. 10-50% NAFRIC with 20% PFA and PA-based composites demonstrated an 8-48% reduction in embodied CO₂ but increased the cost by 14-83%. The iron-based ternary pozzolanic NAFRIC composites with 10%PFA and 10%GGBS/ 10%SF reduced CO₂ emissions by 6-48% but increased the cost by 14-83%. The high-strength performance, up to 46% reduction in GWP, durability in sulphate attack and utilisation in all types of construction applications make it an ideal, greener and sustainable material if its increased cost and low availability could be compromised on its environmental benefits and lower carbon footprints to attain lower CO₂ emissions' targets.

Table 4.28: Embodied CO₂ and Cost-Benefits of NAFRIC Composites.

NAFRIC Composites				
Mix Material	Total kgCO ₂ e/m ³	%age Saving of kgCO ₂ e m ³	Cost/m ³ GBP	%age Saving in Cost/m ³
PCC Control	274	0	334	0
NAFRIC 10% with GGBS 20%	249	9	380	-14
NAFRIC 20% with GGBS 20%	223	18	438	-31
NAFRIC 30% with GGBS 20%	198	28	495	-48
NAFRIC 40% with GGBS 20%	173	37	553	-66
NAFRIC 50% with GGBS 20%	148	46	610	-83
NAFRIC 10% with PFA 20%	253	8	380	-14
NAFRIC 20% with PFA 20%	227	17	438	-31
NAFRIC 30% with PFA 20%	202	26	495	-48
NAFRIC 40% with PFA 20%	176	36	553	-66
NAFRIC 50% with PFA 20%	142	48	610	-83
NAFRIC 10% with PA 20%	250	9	380	-14
NAFRIC 20% with PA 20%	225	18	438	-31
NAFRIC 30% with PA 20%	201	27	495	-48
NAFRIC 40% with PA 20%	176	36	553	-66
NAFRIC 50% with PA 20%	151	45	610	-83
NAFRIC 10% with PFA 10%+GGBS10%	256	6	380	-14
NAFRIC 20% with PFA 10%+GGBS10%	231	16	438	-31
NAFRIC 30% with PFA 10%+GGBS10%	206	25	495	-48
NAFRIC 40% with PFA 10%+GGBS10%	169	38	553	-66
NAFRIC 50% with PFA 10%+GGBS10%	144	48	610	-83
NAFRIC 10% with PFA 10%+SF10%	251	9	380	-14
NAFRIC 20% with PFA 10%+SF10%	225	18	438	-31
NAFRIC 30% with PFA 10%+SF10%	200	27	495	-48
NAFRIC 40% with PFA 10%+SF10%	175	36	553	-66
NAFRIC 50% with PFA 10%+SF10%	149	46	610	-83
Positive values of %age show savings and negative values show increase in values compared to PCC 1:2:3 mix.				
All the mixes have been considered using 1:2:3 job mix ratio for a fair comparison purpose.				

4.16 Applications of NALFRIC and NAFRIC in Channel Stabilisation, Hydromodifications and Infrastructure Construction.

4.16.1 Channel Stabilisation with Lining

Channel stabilisation with the lining of bed/ banks using cement-concrete (with/ without steel reinforcement as per the size, depth, and capacity), geomembrane, polymers, canvas, ramped earth, vegetation, gravel/ stone pitching, and brick blast is a common practice worldwide to save the adjacent flood plain areas from bank overflowing., seepage, water logging/ salinity, loss of water in irrigation channels, maintaining required water levels and strengthening of channels to be used as transportation means. Section 4.1 elaborates on the hydrological studies required to assess the capacity and size of water channels for stabilisation using cement-concrete lining. Section 4.1.5 evaluated that channelising a small section of around 118 km with 20 cm lining thickness with 1% steel reinforcement (20 mm c/c 300 mm) resulted in 284.12 million kgCO₂eq or 5.12 million tons, with around 279 million kgCO₂eq, contributed by 1:2:3 PCC (3000 psi or 21 MPa strength) alone, as shown below.

CO₂ emission from concrete = $0.113 \times 2,378,880,400 = 268,813,485 \text{ kgCO}_2\text{eq} = 5,159,568 \text{ tons}$

Steel CO₂ emission = $0.198 \times 77,313,600 = 15,308,093 \text{ kgCO}_2\text{eq} = 15308 \text{ tons}$

Total CO₂ emissions from the proposed channel = $268,813,485 + 15,308,093 = 284,121,578 \text{ kgCO}_2\text{eq} = 284.12 \text{ million kgCO}_2\text{eq}$ or $5,159,568 + 15308 = 5,174,876 \text{ tons (5.17) million tons CO}_2$.

Replacement of cement-concrete with SL80-based NALFRIC giving 3000 psi (21 MPa) would reduce the emissions by 9 times to 30 million kgCO₂eq, reducing cost by 18% (Table 4.27). Replacement of cement-concrete for this lining project with MK50-based NALFRIC (2500 psi or 18 MPa strength) would reduce the CO₂ emissions by 7 times and the cost by 7%. This project uses partial cement/ aggregate composites with 1:2:3 cement-concrete would provide up to 60 MPa strength (three times the strength requirements) with 10-110% reduced

emissions and 5-90% reduced cost (Table 4.26). The use of NAFRIC composites instead of cement-concrete in this lining project would give more than 60 MPa strength (three times the strength requirements), with a 90% reduction in CO₂ emissions, but the cost could increase up to 7% with a definite benefit of absorption of waste from other industries. The use of NALFRIC and NAFRIC as greener/ economical materials as bricks, breakstones, break walls, readymade/ insitu concrete canvas, gabions, flood protection walls, weirs, notches, dams, docks, scour protection for bridges, embankments, erosion control for industrial sites, mines, water storage/ waste water treatment plants/ storage, landfills, locks/ dykes, marine/ coastal erosion control, harbours, ports, river and canal erosion and roads/ highways/ airports erosion control and stabilisation is suggested as helpful application of this research output (Figures 4.89, 4.90). The use of 1-2% (2-4 kg/m³) PPF, PETF and COF are also recommended for small channels/ tunnel lining with up to 300% improved tensile strength as compared to PCC and controlling/ stopping creation of cracks due to plastic shrinkage/ settlement, thawing/ freezing, long-term drying shrinkage, crazing, improved pore refinement, enhanced impermeability/ post-crack ductility, resistance to spalling/ reinforcement corrosion, reduced alkali-aggregate reaction and further reduction of up to 56% in embodied CO₂ and absorption of 1-2% global waste (Yin et al., 2016; Bonar, 2019; Chaturvedi, Singh and Sharma, 2021; Nadir et al., 2022a; Adfil, 2023). Suppose 10-17% (40-60 kg/m³) steel fibres (0.75-1 mm, 50 mm long, aspect ratio of 50-67) are used as it is considered a suitable alternative to 1% steel reinforcement with the same shear force resistance and up to 60% bending moment resistance (subject to the structural design considerations, size/ capacity of the channel). In that case, it could further result in the reduction of CO₂ emissions by 50% by not using the steel bars for the reinforcement and could reduce the cost by up to 150%, as investigated by Kim and Lee (2021) for designing the steel fibres reinforced concrete for tunnel lining (Figure 4.92). Therefore, the eco-friendly composites formulated in this study could be used

with different options of channel lining, less embodied CO₂, and increased strength/ durability.



Concrete Lining (The Constructor, 2018)



Side Drains (Team, 2023)



Brick Lining (Fakhri, 2023)



Paver Tiles Lining (Boson, 2023)

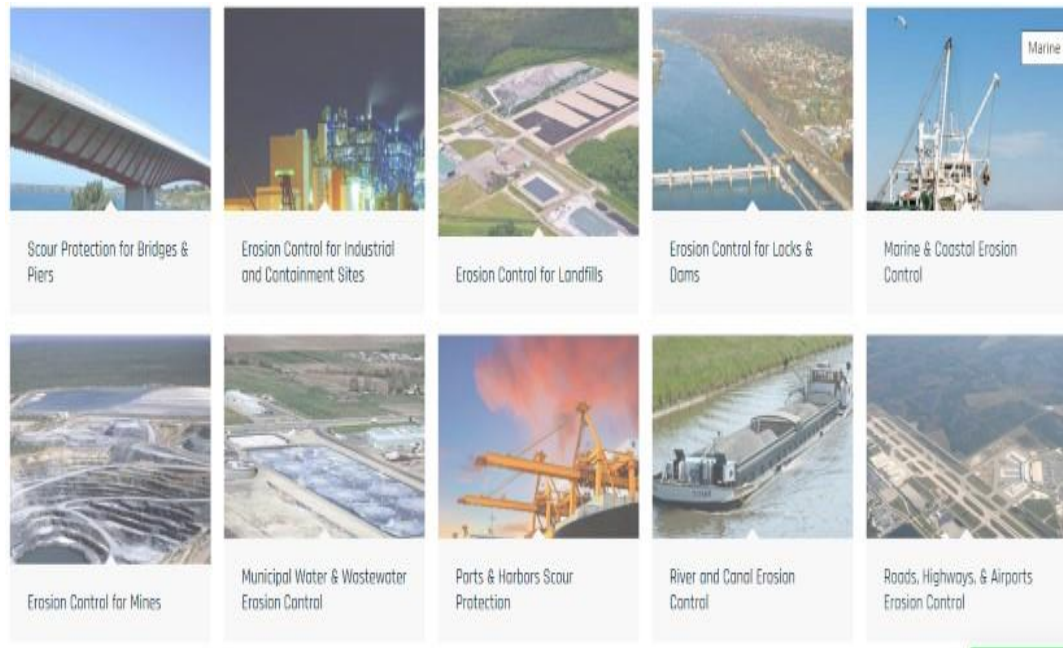


Readymade Concrete Canvas (www.concretecanvas.com, 2023)



Concrete Canvas (Synthetics, 2023)

Figure 4.89: Recommended uses of NALFRIC and NAFRIC as Alternative Materials



Recommended uses of NALFRIC and NAFRIC (Synthetics, 2023)



Flood protection concrete wall Flood Protection Bunds and Gabions (www.pixshark.com, 2023; Admin, 2012)



Pyramid breakwater stones with Raised berms/ walls and edges, River Wharfe Weir at Tadcaster (www.geograph.org.uk, 2023; Glazzard, 2007)

Figure 4.90: Recommended uses of NALFRIC and NAFRIC as Alternative Erosion Control Materials.

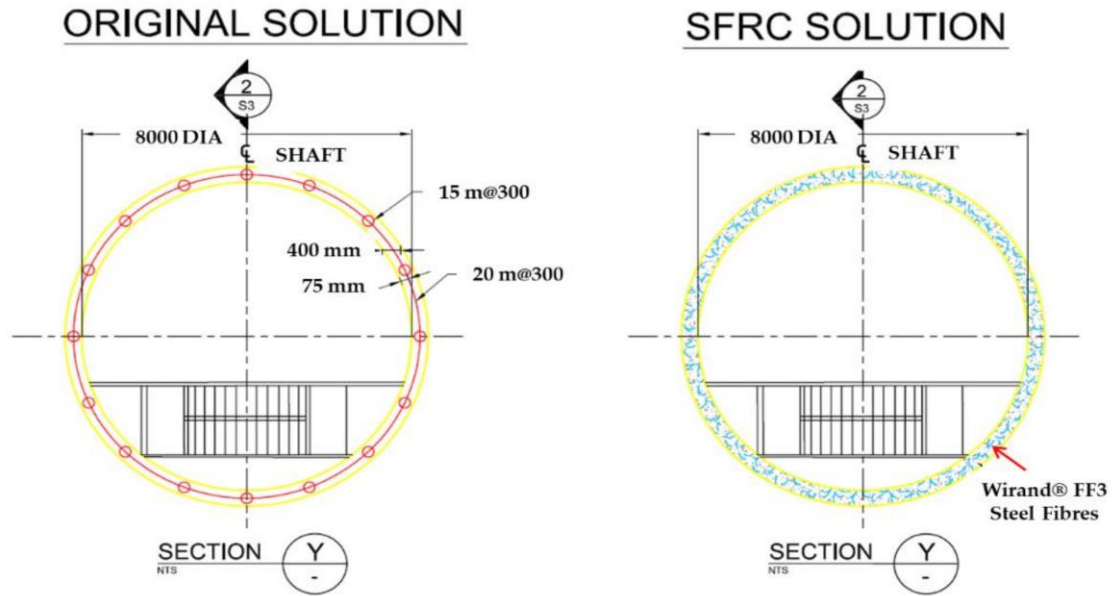


Figure 4.91: Use STF-Based SCMs in Tunnel Lining (Kim and Lee, 2021).

4.16.2 Use of NALFRIC and NAFRIC in Infrastructure/ Building Construction

The use of greener NALFRIC (Non-Cement Alternative, Lime-Based Fibre-Reinforced Pozzolanic, Innovative Composites) and NAFRIC (Novel, Alternative Fibre-Reinforced Iron-Based Composites) materials could be recommended for low, medium and high-strength construction as alternatives to cement concrete. PFA, MK and SF-based NALFRIC composites could be used for low-strength requirements like flooring, shotcreting, walls, blocks, cement-free brick/ stone mortars, and façade works for up to 5-15 MPa strength applications (Ahmed et al., 2022a; 2022b) as per Table 2.2 and 2.4, as shown in Figure 4.92-4.93. GGBS-based NALFRIC could be used in all types of construction applications in buildings, infrastructure, highways, and marine/ coastal construction for up to 30 MPa (4500 psi), covering all the standard concrete applications in the construction industry with up to 30 times lesser CO₂ emissions and up to 90% lesser cost. The shotcreting, tiles, blocks, stones and gabions manufactured using NALFRIC composites could be a good option for stabilisation of tunnels, channels (laminar/turbulent flow), embankments, earth filling, buttresses,

groynes, cascades, and mountains stabilisation against rock falling, scouring/ coastal erosion and strengthening/ facade of bricks/ stone pitched surfaces and floors. NAFRIC composites are high-strength, flexible and crack-resistant alternatives (compared to concrete) exhibiting 60-70 MPa strength. They could be used in all types of high-strength construction applications with enhanced engineering properties, up to 90% reduced emissions and up to 80% reduced cost (with GGBS, PFA and MK) (Widera and Stone, 2016); Koh, 2017; Lee, 2017; USDT, 2020; Yasmin, Bitencourt and Osvaldo, 2020; Han et al., 2020; Kim and Lee, 2021; Kwon and Yoo, 2021; Showkati, Salari-rad and Aghchai, 2021).



www.cemex.co.uk, 2023



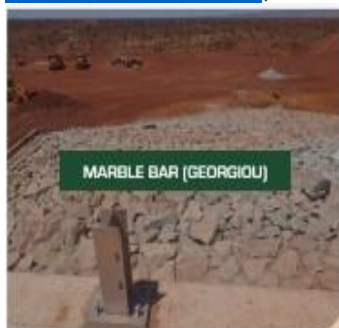
Geotechnical Engineering, (2023)



www.cemex.co.uk, 2023



www.wikimedia.org, 2024



ABM Landscaping, (2023)

Figure 4.92: Recommended Uses of NALFRIC and NAFRIC Composites.



Building Construction (Team, 2018)



Fe-concrete with CO₂ injection (Bonnefin, 2017)



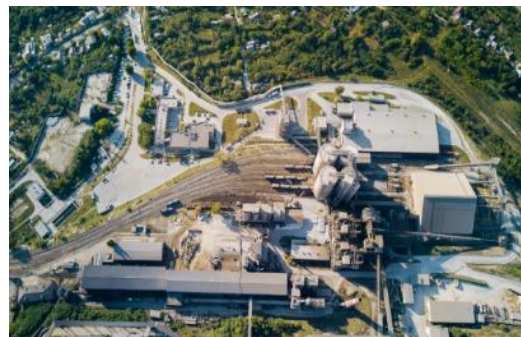
Flooring (Stone, 2017)



Building Construction (Singh,, 2016)



Paving Tiles (Stone, 2017)



Plant Construction (www.Mainpac.com, 2024)

Figure 4.93: Recommended Uses of NAFRIC Composites.

4.16.3 Preservation/ Reducing the Depletion of Natural Resources and Waste Recycling

The mining, excavation, and crushing industry for producing cement, fine and coarse aggregates is experiencing a surge in demand and financial benefits. However, this trend has led to illegal and uncontrolled production (Leal Filho et al., 2021, GCCA, 2023), resulting in a faster depletion of natural resources like calcareous rock, lime, gypsum, sand and gravel/ shingles/ rocks (Pitchaiah, 2017 Ahmed and Nadir, 2023c), non-conservation of these resources for future generations (Koehnken and Rintoul, 2018), and damaging impacts on the environment (Adu-Gyamfi, 2016; Dugan et al., 2010). The researchers have identified significant repercussions of uncontrolled extraction/ mining/ quarrying/ crushing of sand and coarse aggregate on human health/ wellbeing, disturbed eco-system and depletion of natural resources (Bendixen et al., 2021). The extensive mining/ extraction of sand/ gravel from rivers impacts the geological/ hydrological profile of rivers and may result in increased flooding, weaker channel structure, localised impact on the water table and may impact on the water quality/ sediment transportation (Kondolf, 1994; Boers, 2005; Freedman et al., 2013; Danielsen and Kuznetsova, 2014; Lousiagustin and Kusratmoko, 2016; Beiser, 2019; Haghazadeh and Saneie, 2019; Jordan et al., 2019; Liu et al., 2022). The worst impact of uncontrolled mining/ extraction of cement raw materials, river sand as fine aggregate and gravel/ crushed rocks as coarse aggregate is also depleting the gravel deposits/ mountain ranges at a faster rate than their reproduction, thus resulting in the obliteration/ extinction/ depletion of natural resources, especially in low-income developing countries where these activities are not adequately regulated (Stijns, 2005). The desert sand, being very fine in particle size, cannot fulfil the purpose of fine aggregate usage in concrete; therefore, river sand extraction is depleting at a rapid rate as it takes millions of years to produce the alluvial/ fluvial deposits on the river delta, which is being extracted in a matter of years only badly impacting the flood plains and river deltas. Therefore, the use of 2.5-60% industrial/ agricultural waste materials

having required pozzolanic properties as SCMs and 5-30% of waste materials alternatives to fine/ coarse aggregate in this research proposes an applicable solution to control rapid depletion/ extinction of the natural resources to preserve them for future generations along with economising the efforts and reducing the GWP of the construction industry.

This research used 2.5-60% industrial/ agricultural waste pozzolanic ashes produced during the manufacturing process of other materials or as burning of agricultural waste, thus economising on the energy potential of the construction materials and contributing to reducing CO₂ emissions as per COP28 targets for 2030 (30% reduction) and 2050 to become net zero construction industry. The research showed a reduction of up to 2.5-60% in the use of cement for PCRs/ SCMs/ NAFRIC and 100% cement replacement with lime/ waste pozzolans in NALFRIC, thereby reducing the demand for OPC by up to at least 20-25% as per the availability of alternative materials. Use of 2.5-30% of concrete demolition, PET/ HDPE bottles, crumb rubber, crushed glass, crushed/ shredded tyres, rice husk ash, palm ash, silica fume, metakaolin, GGBS, PFA, iron powder, and fibres of waste materials help absorb around 2 billion tons of waste annually going into sea/ landfill otherwise (Guerrero et al., 2013; Hoornweg and Bhada-Tata, 2021; Nadir et al., 2022; Thomas and Gupta, 2013; Shahbaz and Faraj, 2020).

4.17 Summary

Chapter 4 commenced analysing the established/ innovative OPC-based pozzolanic SCMs (PCR with PFA, GGBS, MK, SF, RHA and PA) in a 1:1:3 ratio demonstrating high-strength/ high-performance concrete strength of 70-90 MPa. Composites with partial replacement of fine/ coarse aggregate (CG, CR, PET, RCA and ST) in a 1:1:3 ratio were analysed, achieving a high strength of more than 70 MPa. OPC-based FRC composites in a 1:2:3 ratio exhibited a high strength of more than 60 MPa (except composites with WSF). Cement-free hydrated lime-based composites with CL90 and PFA, GGBS, SF and MK were analysed as innovative, greener materials. NALFRIC composites formulated

using best-performing ratios of SL80% and MK50% with fibres (STF, PPF, PETF, COF, WSF) were observed demonstrating a low to medium strength range of 10-25 MPa as sustainable alternatives to lower strength concrete applications with the least embodied CO₂. As a step forward, experimental results were elucidated to evaluate carbon-neutral/ carbon absorbent high-strength iron-based pozzolanic SCMs in a 1:2:3 ratio exhibiting strength of 60-70 MPa, at par with high-strength cement concrete formulated in a 1:1:3 ratio. NAFRIC composites formulated using iron-based binary/ ternary pozzolanic composites with fibres were investigated and found to exhibit more than 60 MPa compressive strength and up to double the flexural strength of standard OPC-based FRC/ concrete. The analysis was conducted using the laboratory results exhibiting the engineering properties of composites with a particular focus on the strength parameters. The strength-specific chemical-mechanical analysis outlined the best-performing innovative NALFRIC and NAFRIC composites compared to the OPC-based composites. The microstructural analysis of these innovative NALFRIC and NAFRIC composites was conducted to ascertain scientific evidence for strength, reliability, durability and sustainability to understand the underlying chemical composition. The best-performing composites were shortlisted for micro-structural analysis using advanced XRF, XRD, SEM, EDS and TEM testing. The objective was to ascertain the elemental composition, formation of hydration compounds and C-S-H gel, and presence of ettringite to scientifically suggest that these innovative composites are sustainable and demonstrate the required compressive strength and sulphate attack resistance. The embodied CO₂ and cost-benefit analysis supported the use of most of these materials, with 7-97% reduced emissions and cost-effectiveness.

5 Chapter 5: Conclusions and Recommendations

This chapter concisely concludes the research outcome in light of research questions, aims, and objectives set out in Chapter One and findings from the results discussed in Chapter Four, followed by recommendations for future research in this field. The research was conducted to develop/ elucidate sustainable materials for greener infrastructure construction and hydromodifications/ water channel stabilisation. The research questions were framed to investigate whether or not industrial/ agricultural waste creates a global nuisance through enormous disposal efforts and whether it could be recycled into the construction industry as partial/ complete construction materials in place of OPC, aggregates and fibres with enhanced engineering properties of SCMs. The detailed investigation/ results concluded that the majority of the composites fulfilled the target strengths, cost benefits and lower GWP of the formulated materials except for a few composites which either could not achieve the strength targets or were observed uneconomical with cost-benefit analysis and quantum of embodied CO₂, as expected in any research projects.

5.1 Conclusions

5.1.1 Impacts of Technical Advancement, Urbanisation, Anthropogenic Activities and Hydromodifications.

5.1.1.1 The construction of hydraulic structures without proper catchment studies results in climatic variations and flooding disasters. To overcome previous hydromodifications/proposed construction, they entail the integration of hydrology/ structural engineering and material sciences.

5.1.1.2 Natural flood management is the best environmental strategy, but its limited scope necessitates augmentation by structural interventions and hydromodifications.

5.1.2 Global Impacts of Waste Materials and CO₂ Emissions

5.1.2.1 The World is facing an enormous issue of around 2 billion tons of waste production annually, which would likely reach 12 billion tons annually by 2050.

5.1.2.2 The construction industry's carbon footprint is mainly due to the annual manufacturing of around 4.4 billion tons of cement, which produces around one ton of CO₂ per ton of cement.

5.1.2.3 The world has committed to decreasing global emissions by 30% by 2030 with a net-zero aim in 2050 (though both seem unachievable), and so does the cement industry, as committed by GCCA during COP28 in Dubai in December 2023.

5.1.2.4 A considerable reduction of up to 25% was envisaged by partially replacing raw cement materials with alternative/ recycled materials to reduce 25% of emissions by 2030. Therefore, this study focused on the formulation of alternative materials.

5.1.3 Selection of Waste Materials as SCMs/ PCRs

5.1.3.1 The research suggested a beneficial option to absorb global waste by recycling up to 2.5%- 80% of industrial waste materials/ ashes having pozzolanic characteristics/a cumulative quantity of metal oxides, including SiO₂, Al₂O₃, and CaO, more than 70%.

5.1.3.2 Silica fume SF, pulverised fly ash PFA, metakaolin MK, ground granulated blast furnace slag GGBS, rice husk ash RHA, and palm ash PA with hydrated lime and iron powder were used as alternative pozzolanic material for cement replacement.

5.1.3.3 5-30% crushed glass, recycled plastic bottles, crumb rubber, recycled concrete aggregate and crushed tyres were replaced with 5-30% fine/ coarse aggregate.

5.1.3.4 10-17% steel fibres, 0.5-2% coconut coir, shredded plastic fibres, polymer fibres, and wheat straw fibres were incorporated in this project as enhancers of the engineering properties of concrete.

5.1.4 PCC and Partial Cement Replacement (PCRs) / Supplementary Cementitious Materials (SCMs).

5.1.4.1 OPC-based pozzolanic SCMs (PCR with 20-45% PFA, 30-60% GGBS, 5-20% MK, 2.5-10% SF/ RHA and PA) in a 1:1:3 ratio demonstrating a normal concrete density of 2200-2600kg/m³, decreased workability and high-strength/ high-performance concrete strength of 60-90 MPa except composites with wheat straw exhibiting up to 50 MPa strength, still sufficient to use in the standard construction applications (up to 40-50 MPa).

5.1.4.2 The incorporation of fibres increased the flexural strength by 2.5 times compared to PCC with STF, PPF, and PETF, demonstrating a high to exceptional post-crack ductility, suggesting a beneficial use of fibres with PCC.

5.1.4.3 The durability testing showed a decrease of up to 10-30% in compressive strength of the PCC specimen, whereas the pozzolanic-based composites performed better by reducing up to 15% strength under concentrated sulphate attack of 270 days in a 5% sulphate concentrated solution.

5.1.4.4 A 27-53% reduction of GHG emission was observed using 30%-60% of GGBS as a partial replacement of cement with 5-10% cost-benefit. 10-40% use of PFA as partial cement replacement could reduce 10-39% of embodied CO₂ of cement concrete with 3-12% cost-benefit. The cost-benefit of MK was observed to be reduced because of increased cost and CO₂ emissions due to the consumption of energy in calcination of kaolinite to prepare MK; however, the least cost-benefit and embodied CO₂ was observed in 2.5%-10% SF use followed by RHA and PA with obvious reasons of lesser dosage and increased cost of these materials in the UK.

5.1.4.5 This study concluded a beneficial use of 30-60% GGBS, 10-30% PFA, 5-20% MK-based, 2.5-10% RHA, PA, and SF-based pozzolanic partial

cement composites for high-strength, greener, sustainable applications. FRC with 1-2% PETF, PPF, COF and STF 10-17% are supported for enhanced flexural strength applications.

5.1.5 Fine/ Coarse Aggregate Replacement Composites.

5.1.5.1 Composites with partial replacement of fine/ coarse aggregate (10-30% CG, CR, PET, RCA and 5-10% ST) in a 1:1:3 ratio were observed to achieve the target of this research of high compressive strength of more than 60-70 MPa.

5.1.5.2 The composites exhibited the same density of normal concrete range of 2200-2300 kg/m³, except 30% PET and CR, showing a slight decrease comparatively but still falling in the average density range.

5.1.5.3 The workability of all the composites was observed to decrease with increased dosages/ percentage of replacement fine/ coarse aggregate, necessitating more use of plasticiser as the w/c ratio was kept constant as per Abrams's law.

5.1.5.4 The composites with 10-30% crumb rubber (CR) and 2.5-10% crushed tyres (CT) exhibited a reduction in strength due to hydrophobic characteristics and lesser toughness of rubber/tyre aggregates. An increased dosage of recycled aggregates (RCA) by more than 20% also reduced the strength, but all these composites still achieved more than 50 MPa strength, sufficient for major construction applications.

5.1.5.5 A slight decrease of up to 3% was observed in the embodied CO₂ and cost effect due to lesser CO₂ emissions attributed to the fine/ coarse aggregates than cement.

5.1.5.6 10-30% use of replacement aggregate derived from industrial/ polymer and demolition waste was suggested as beneficial utilisation and successful recycling of 10-30% global waste in the constitution of strong concrete at par with virgin aggregate concrete, economising waste disposal efforts.

5.1.6 NALFRIC Materials

5.1.6.1 NALFRIC composites were formulated as non-cement hydrated lime-based pozzolanic composites. 10-90% GGBS, PFA, SF and MK were used with an alternate 90-10% quantity of CL90 with a 1:2:3 ratio using virgin fine/coarse aggregate.

5.1.6.2 A typical 2000-2250 kg/m³ density was observed except for a few MK-based composites showing less than 2000 kg/m³ density.

5.1.6.3 A delayed setting time of 3-7 times less than PCC was observed, with a slow rate of strength achievement.

5.1.6.4 Workability was observed to reduce with increased dosages of pozzolans, and an increased water/ binder ratio of 0.55 (constant as per Abram's law) was used without plasticiser (plasticiser not recommended for lime).

5.1.6.5 GGBS-based limecrete composites exhibited up to 25 MPa strength with water curing of 90 days, followed by MK-based composites attaining up to 12 MPa strength, whereas PFA and SF-based composites attained less than 8 MPa strength, not reaching the target strength of 10-18 MPa set for this research for low strength composites.

5.1.6.6 The best-performing materials/ ratios of SL80% and MK50% were used to make fibre-reinforced limecrete with fibres (10-17 % STF and 0.5-2% PPF, PETF, COF, WSF) and named NALFRIC.

5.1.6.7 SL80 and MK50-based NALFRIC demonstrated a low to medium strength range of 10-25 MPa as sustainable alternatives to lower-strength concrete applications with the most economical and the least embodied CO₂ options.

5.1.6.8 The fibre-reinforced composites with STF, PETF, and PPF improved up to 2.5 times in flexural strength and demonstrated high post-crack ductility.

5.1.6.9 MK50-based composites were observed to be the most impacted by the sulphate attack due to their inherent weakness of material and lesser compressive strength (less than 20 MPa strength composites are not suitable to use in sulphate environment as per ASTM C1012M:2019). They are not

recommended for utilisation in water/ marine construction and could only be used for very low-strength applications with the lowest embodied CO₂ (up to 95% reduction) and 16% lesser cost than cement concrete.

5.1.6.10 SL80-based NALFRIC performed as the best material in the sulphate environment and improved strength by up to 10-25%, and no deterioration was observed due to inherent characteristics of GGBS to perform better against sulphate attack by consuming the maximum quantity of Ca(OH)₂ to convert to C-S-H gel (MgSO₄ requires Ca(OH)₂ to ingress in the specimen).

5.1.6.11 The microstructural analysis using SEM/ TEM/ XRD EDS supported these results by giving evidence of the full-scale formation of C-S-H gel by completion of the pozzolanic reaction, almost complete depletion of Ca(OH)₂ and negligible/ no formation of ettringite.

5.1.6.12 The GGBS-based composites demonstrated 96% lesser embodied CO₂ and up to 27% less cost, suggesting they should be used in all low-medium strength applications in infrastructural construction and hydromodifications with maximum environmental and economic benefits.

5.1.7 NAFRIC Materials

5.1.7.1 As a step forward, an experimental study was conducted to evaluate low carbon high-strength iron-based pozzolanic SCMs in a 1:2:3 ratio exhibiting strength of 60-70 MPa, at par with high-strength cement concrete formulated in a 1:1:3 ratio, named NAFRIC.

5.1.7.2 NAFRIC composites formulated using iron-based binary/ ternary pozzolanic composites with fibres were found to exhibit 60-70 MPa compressive strength and up to double the flexural strength/ exceptional post-crack ductility of standard OPC-based FRC/ concrete.

5.1.7.3 All the composites achieved a normal density range of 2250-2350 kg/m³. The workability decreased with increased dosages of iron powder and pozzolans, requiring more plasticiser while keeping the w/c ratio constant at 0.35, as per Abrams's law for a fair comparison of the components.

5.1.7.4 The use of ternary pozzolans as a combination of 10%GGBS+10% PFA with 8% MK in making the iron composites using 60% iron powder demonstrated the best performance when used as a partial replacement of 10-30% OPC, followed by 10%PFA+10%SF and binary pozzolans of 8% MK with 20% GGBS, 20% PA and finally 20% PFA. However, using iron-based pozzolanic composites more than 30% as PCR reduced the compressive strength of the SCMs.

5.1.7.5 The NAFRIC composites remained composed and intact with excellent resistance to the 5% concentrated $\text{Na}_2\text{SO}_4 + \text{MgSO}_4$ solution, immersed for 270 days. Less than 8% strength reduction was observed after the sulphate attack; instead, a few composites improved strength by up to 7% (much better performance compared to PCC, which reduced strength up to 30% in sulphate attack), suggesting a beneficial use of NAFRIC composites in water structures/ marine environment without incorporation of costly sulphate resistant cement. The pozzolanic reaction absorbed the $\text{Ca}(\text{OH})_2$, and iron absorbed CO_2 from the environment to form a siderite-like rock formation on the outer surface, thus not letting the ingress of MgSO_4 to the inner structure form ettringite.

5.1.7.6 The microstructural analysis of these innovative NAFRIC composites was conducted to ascertain scientific evidence for strength, reliability, durability and sustainability to understand the underlying chemical composition using advanced XRF, XRD, SEM, EDS and TEM testing. They supported the chemical/ mechanical properties ascertained during laboratory testing by giving numerical evidence of the production of up to 90% C-S-H gel, FeCO_3 and less than 0.1% ettringite formation, making these materials extremely strong, sulphate resistant, durable, flexible, waste absorbent, and CO_2 absorbent greener composites.

5.1.7.7 The carbonation test using phenolphthalein suggested the absorption of CO_2 by iron powder to form FeCO_3 , exhibiting a lower embodied CO_2 .

5.1.7.8 GGBS-based NAFRIC composites demonstrated up to 46% less embodied CO₂, followed by PA, PFA and SF-based iron composites with up to 48% less embodied CO₂. However, their cost was observed to be more than the PCC by 14-83% based on the dosages/ mixing ratios of iron powder and pozzolans.

5.1.7.9 The increased dosage of iron composites decreases the embodied CO₂ but increases the cost, necessitating using an economical option of using 10-30% iron-based pozzolanic composites with OPC to get the same strength with 1:2:3 ratio as is achieved by PCC 1:1:3.

5.1.7.10 The enhanced engineering properties, lower embodied CO₂ and cost-benefit analysis supported using most of these NAFRIC materials with up to 48% reduced emissions in various greener infrastructure construction or hydromodifications in marine environments as waste-absorbent sustainable materials.

5.1.7.11 It could be concluded that the research project has satisfactorily attained its target aims/ objectives within the stipulated research questions/ framework in the formulation of waste absorbent, low CO₂ embodied, low, medium, high-strength cement/ aggregate replacement composites, cement-free lime-based pozzolanic composites and iron-based pozzolanic composites (except a few composites) with waste fibres for utilisation in a variety of greener infrastructure construction/ channel stabilisation/ hydromodifications resulting in reduced carbon footprints and global waste.

5.2 Recommendations for Future Research.

The research mainly focussed on the formulation of waste absorbent, low CO₂ embodied, low, medium, high-strength cement/ aggregate replacement composites, cement-free lime-based pozzolanic composites and iron-based pozzolanic composites with waste fibres as PCRs/ TCRs/ SCMs. Further study is recommended to investigate more aspects of such materials with different combinations as follows:

- The partial cement replacement composites were formulated using industrial/ agricultural waste pozzolanic materials. A further study on using naturally occurring pozzolans, like volcanic ash and zeolite, etc, is recommended as PCR material with better results for reduced embodied CO₂.
- The pozzolanic-based PCR composites require further study with the incorporation of waste fibres to improve flexural strength and disposal of waste by up to 2%.
- The replacement aggregates derived from different waste materials were used only with PCC to investigate their engineering properties, cost-benefit analysis and embodied CO₂. Future studies are recommended to use replacement aggregates with NAFRIC and NALFRIC, along with the incorporation of fibres to make the composites more cost-effective and waste-absorbent.
- Pozzolans with hydrated lime did not perform well and remained under-strength compared to the target. Further studies may be conducted to use more pozzolans as per the w/w% ratio instead of the w/v% ratio to see if they could improve strength.
- NAFRIC iron-based pozzolanic composites were formulated as partial cement replacement composites. Further studies are required to investigate the impact of using iron-based composites with pozzolans without cement, as iron-based composites are likely to provide less embodied CO₂ than PCC/ NAFRIC composites if the cost/ availability of iron powder supports the study.
- The durability testing to ascertain the resistance of composites against sulphate attack was determined by immersing them in 2.5%Na₂SO₄+2.5%MgSO₄ solution due to lack of time/ resources. Further studies may investigate the sulphate attack by immersing the composites separately in 5% Na₂SO₄ and 5% MgSO₄ solution to see separate elongation and strength deterioration impacts.
- Iron-based composites were considered to absorb CO₂ from the environment, but due to lack of time/ resources, it was not gauged as to how

much it could gain strength if cured in CO₂ concentrated environment and how much CO₂ it could absorb during the hydration process. Further studies are recommended to investigate the impact of curing NAFRIC composites in enclosed CO₂ tanks with proper gauging of how much CO₂ was absorbed by iron to form FeCO₃.

6 References.

- Abbas et al., (2018). Abbass K, Qasim MZ, Song H, Murshed M, Mahmood H, Younis I. A review of the global climate change impacts, adaptation, and sustainable mitigation measures. *Environ Sci Pollut Res Int.* 2022 Jun;29(28):42539-42559. doi 10.1007/s11356-022-19718-6. Epub 2022 4 April. PMID: 35378646; PMCID: PMC8978769. Retrieved 23 March 2023.
- Abbasi, S., Jannaty, M.H., Faraj, R.H., Shahbaz, P.S., Mosavi, A., (2020) The effect of incorporating silica stone waste on the mechanical properties of sustainable concrete. *Materials* 13(17): 3832.
- Abdalla, T.A. and Salih, N.B. (2020). Hydrated Lime Effects on Geotechnical Properties of Clayey Soil. *Journal of Engineering*, 26(11), pp.150–169. doi:10.31026/j.eng.2020.11.10.
- Abdelalim A.M.K, Abdelaziz G.E., Fawzy A. and Zahran R. (2015) Role of pozzolanic materials on the degradation processes of reinforced concrete in severe. 9th Arab Structural Engineering Conference, Emerging Technologies in Structural Engineering, Abu Dhabi, UAE, pp. 1141-1148, Nov. 29-Dec. 1, 2033. Cairo, Egypt: ResearchGate. Available from: https://www.researchgate.net/publication/271767628_role_of_pozzolanic_materials_on_the_degradation_processes_of_reinforced_concrete_in_severe_conditions. [Accessed 10 June 2022].
- ABM Landscaping, (2023). Rock Pitching Perth. [online] Available at: <https://abmlandscaping.com.au/services/rock-pitching/> [Accessed 11 Dec. 2023].
- ACI Committee 318 (2008). ACI 318-08: Building Code Requirements for Structural Concrete and Commentary. American Concrete Institute. ISBN 0-87031-264-2.
- Adeoye, N. O., Ayanlade. A., and Babatimehin. O., 2009. Climate change and menace of floods in Nigerian Cities: Socio-economic implications. *Advances in Natural and Applied Sciences*.2009;3(3):369-77.

- Adfil, (2023). Adfil construction fibres. Properties of Poly-propylene by Synthetic Fibres, available at <https://adfil.com/gb-en/>.
- Adithya A. and Magudeswaran P., (2017). SEM Analysis on Sustainable High-Performance Concrete. 6. 10.15680/IJIRSET.2017.0606016.
- Admin (2012). Hospital Featured in FEMA Floodproofing Publication. [online] Flood Break Automatic Flood Barriers. Available at: <https://floodbreak.com/hello-world/>. [Accessed 2 Oct. 2023].
- Admin (2023). Fiber Reinforced Concrete: A Sustainable Building Material for the Future. [online] Construction Placements. Available at: <https://www.constructionplacements.com/fiber-reinforced-concrete-frc/>. [Accessed 20 November 2023].
- Adnan S.H., Rahman I.A., Loon L.Y (2010) Performance of recycled aggregate concrete containing micronised biomass silica. Int J Sustain Construct Eng Technol 1(2).
- Adu-Gyamfi, F. (2016). The Environmental Degradation Resulting from Illegal Sand Mining in Port St. Johns East. Cape. The Portfolio Research Proposal (HMENV80 –773080). 2016. Available online: https://www.researchgate.net/publication/291335557_ENVIRONMENTAL_DEGRADATION_RESULTING_FROM_ILLEGAL_SAND_MINING. (accessed on 13 June 2023).
- Aeyates. 2018. Tadcaster flood-damaged bridge construction. [Online]. [Accessed 2 October 2023]. Available from: <https://www.aeyates.co.uk/spi-piling/roads-and-highways-projects/tadcaster-flood-damaged-bridge-reconstruction-c21101>.
- Agopyan V (1998) Vegetable fibre-reinforced building materials development in Brazil and other Latin American countries. Concrete Technology and Design Natural Fibre Reinforced Cement and Concrete,
- Agopyan, V, (1998). Vegetable fibre reinforced building materials- development in Brazil and other Latin American countries. Concrete Technology and

- Design Natural Fibre Reinforced Cement and Concrete, 5, 1998, pp. 208-240.
- Ahmaran M, Özkan N, Keskin SB, Uzal B, Yaman I_Ö, Erdem TK. Evaluation of natural zeolite as a viscosity-modifying agent for cement-based grouts. *Cem Concr Res* 2008;38(7):930–7.
- Ahmed A, Hyndman F, Kamau J, Fitriani H (2020) Rice Husk Ash as a Cement Replacement in High Strength Sustainable Concrete, *Materials Science Forum*, ISSN: 1662-9752, 1007: 90-98.
- Ahmed A, Kamau J, Pone J, Hyndman F, Fitriani H (2019) Chemical reactions in pozzolanic concrete. *Modern Approaches on Material Science* 1(4): 128-133.
- Ahmed A., Nadir H., Colin Y., and Lee Y. (2020). Use of Coconut Coir in Fibre Reinforced Concrete, Soil and Lime, Page 391-399, Volume 3 - Issue 4, Intl Journal of Modern Approaches on Material Science, published by Lupine publishers ISSN: 2641-6921 on 02 December 2020, <http://dx.doi.org/10.32474/MAMS.2020.03.000166>,
<https://lupinepublishers.com/material-science-journal/fulltext/use-of-coconut-coir-in-fiber-reinforced-concrete-soil-and-lime.ID.000166.php>.
- Ahmed D., Elwahab, A. & Awad, M., Elyamany, Hafez, & Elmoty, M. (2008). Magnesium sulfate resistance of silica fume concrete specimens and RC columns.
- Ahmed et al., (2022a). Ahmed, A., Haslam, G., Sutherland, C., Yates, C., Yates, L., & Nadir, H. M. (2022a). Compressive And Flexural Strength of Non-Hydraulic Lime Mortar with Metakaolin Pozzolan. *Modern Approaches on Material Science*, 5(1), 627-634. doi:[10.32474/MAMS.2022.05.000202](https://doi.org/10.32474/MAMS.2022.05.000202).
- Ahmed HU, Faraj RH, Hilal N, Mohammed AA, Sherwani AFH (2021) Use of recycled fibres in concrete composites: A systematic, comprehensive review. *Composites Part B* 215: 108769.
- Ahmed, A. & Kamau, J. (2017). Performance of Ternary Class F Pulverised Fuel Ash and Ground Granulated Blast Furnace Slag Concrete in Sulfate

- Solutions. European Journal of Engineering Research and Science. 2. 8. 10.24018/ejers.2017.2.7.401.
- Ahmed, A., Sutherland, C., Yates, C., Yates, L. and Nadir, H. (2022). Compressive and Flexural Strength of Non-Hydraulic Lime Mortar with Slag (GGBS). Journal of Material Sciences & Manufacturing Research, pp.1–6. doi:10.47363/jmsmr/2022(3)137.
- Ahmed, Ash & Kamau, John. (2017). Performance of Ternary Class F Pulverised Fuel Ash and Ground Granulated Blast Furnace Slag Concrete in Sulfate Solutions. European Journal of Engineering Research and Science. 2. 8. 10.24018/ejers.2017.2.7.401.
- Aiswarya S, Prince A.G., Dilip C, (2013). A review on the use of metakaolin in concrete, IRACST – Engineering Science and Technology: An International Journal (ESTIJ), ISSN: 2250-3498, Vol.3, No.3, June 2013
- Ajileye, E.V. (2012). Investigations on Microsilica (Silica Fume) As Partial Cement Replacement in Concrete. Global Journal of Researches in Engineering Civil and Structural Engineering 12 (1), 17-23.
- Akca, K.R., Çakir, O., Ipek, M., (2015) Properties of polypropylene fibre reinforced concrete using recycled aggregates. Construct Build Mater 98: 620-630.
- Akeem A. R., Mutiu A. K., (2017). Chemical Composition and Physical Characteristics of Rice Husk Ash Blended Cement. International Journal of Engineering Research in Africa, ISSN: 1663-4144, Vol. 32, pp 25-35, doi:10.4028/www.scientific.net/JERA.32.25, 2017 Trans Tech Publications, Switzerland.
- Akula, P., Hariharan, N., Little, D.N., Lesueur, D. and Herrier, G. (2020). Evaluating the Long-Term Durability of Lime Treatment in Hydraulic Structures: Case Study on the Friant-Kern Canal. Transportation Research Record: Journal of the Transportation Research Board, 2674(6), pp.431–443. doi:10.1177/0361198120919404.

- Alam F., (2014). An Overview of Coconut or Coir Fibre
Dept of Textile Engineering Southeast University, Dhaka,
<https://textilelearner.blogspot.com/2014>.
- Alamy Limited (2019). Alamy – Stock Photos, Stock Images & Vectors. [online]
Alamy.com. Available at: <https://www.alamy.com>.
- Alam, M.D. and Ahmad, S.I., (2020). Sieve Analysis and Gradation of Coarse and
Fine Aggregates. 10.13140/RG.2.2.34247.11680 available at:
https://www.researchgate.net/publication/343584873_Sieve_Analysis_and_Gradation_of_Coarse_and_Fine_Aggregates.
- Albaniainia.A. (2008). Empires of the Indus, The story of a river. First USA Edition
20101 published by WW Norton& Company, New York. ISBN 978-0-393-
33860-7
- Ali A., (2013). Indus Basin Floods, Mechanism, Impacts and Management,
Mandoline City Philippines Asian Development Bank 2013, ISBN 978-92-
9254-284-9 (Print), 978-92-9254-285-6
- Almeshal, I., Tayeh, B.A., Alyousef, R., Alabduljabbar, H., Mustafa Mohamed, A.
and Alaskar, A. (2020). Use of recycled plastic as fine aggregate in
cementitious composites: A review. Construction and Building Materials,
[online] 253, p.119146. doi
<https://doi.org/10.1016/j.conbuildmat.2020.119146>.
- Al-Salem SM, Lettieri P, Baeyens J. Recycling and recovery routes of plastic solid
waste (PSW): a review. Waste Manag 2009;29(10):2625–43.
- AMCSD, (2023). rruff.geo.arizona.edu. (n.d.). American Mineralogist Crystal
Structure Database. [online] Available at:
<http://rruff.geo.arizona.edu/AMS/amcsd.php>.
- Anderson N.P., Hart J.M., Sullivan D.M., Christensen N.W., Horneck D.A., and
Pirelli G.J., (2013). Applying Lime to Raise Soil pH for Crop Production
(Western Oregon), OSU Extension Catalog, May 2013.

- Anderson, G. and Bell, R. (2019). Wheat grain-yield response to lime application: relationships with soil pH and aluminium in Western Australia. *Crop and Pasture Science*, 70(4), p.295. doi:10.1071/cp19033.
- Anggraini V., Afshin A. and Haslinda N. (2014), Effect of coir fiber and lime on geotechnical properties of marine clay soil, 7th International Congress on Environmental Geotechnics: 7icg2014, Australia, Volume: 2014: 1430-1437. ISBN:9781922107237, Availability: <<http://search.informit.com.au/document>.
- Anon, (2022). Sulphate Attack On Concrete | How To Prevent Sulphate Attack On Concrete? - Civil Giant. [online] Available at: <https://www.civilgiant.com/sulphate-attack-on-concrete/> [Accessed 20 Jun. 2022].
- Anon, (2022). What Is Hydration Of Cement? Know Heat Of Hydration & Products Of Cement Hydration Here - Civil Giant. [online] Available at: <https://www.civilgiant.com/hydration-of-cement/#hydration-process-of-cement> [Accessed 19 Jun. 2022].
- AON, (2023). Global Insured Losses From Natural Disasters Exceeded \$130 Billion In 2022, Driven By Second-Costliest Event On Record, available online at <https://aon.mediaroom.com/2023-01-25-Aon-Global-Insured-Losses-from-Natural-Disasters-Exceeded-130-Billion-in-2022,-Driven-by-Second-Costliest-Event-on-Record>.
- apps.engipedia.com. (1992). engipedia.com. [online] Available at: <https://apps.engipedia.com/articles/strength-and-deformation-characteristics-for-concrete-according-to-eurocode-2-1992-1-1> [Accessed 22 Jun. 2023].
- Apuke, O.D. (2017). Quantitative Research Methods: A Synopsis Approach. Kuwait Chapter of Arabian Journal of Business and Management Review, 6(10), pp.40–47.
- Arabani, M. and Mirabdolazimi, S.M. (2011). Experimental investigation of the fatigue behaviour of asphalt concrete mixtures containing waste iron powder.

- Materials Science and Engineering: A, 528(10-11), pp.3866–3870.
doi:10.1016/j.msea.2011.01.099.
- ArchDaily. (2022). Concrete Jungles: 6 Cement Alternatives that Could Reduce its Impact in Cities. [online] Available at: <https://www.archdaily.com/985952/concrete-jungles-6-cement-alternatives-that-can-reduce-its-impact-in-cities>.
- Arioz, E., Arioz, Ö. and Koçkar, Ö.M. (2013). Mechanical and Microstructural Properties of Fly Ash Based Geopolymers. International Journal of Chemical Engineering and Applications, pp.397–400. Doi <https://doi.org/10.7763/ijcea.2013.v4.333>.
- Arup, "Low Carbon Concrete: Practical guidance for Arup engineers," 2019.
- Arya, C. (2009). Design of structural elements: concrete, steelwork, masonry and timber designs to British standards and Eurocodes, Spon Press, London and New York, Taylor & Francis.
- Astle P., (2021). "How could we reduce the embodied carbon of structural concrete? " The Institute of Structural Engineers, 2021.
- ASTM C125-19 (2019). C09.91, ASTM C125-19 Standard Terminology Relating to Concrete and Concrete Aggregates, Annu. B. ASTM Stand, vol. 04.02(2019), doi <http://dx.doi.org/10.1520/C0125-15A>.
- ASTM C1012/C1012M–15, (2015). American Society for Testing And Materials C1012/C1012M–15. Standard Test Method for Length Change of Hydraulic-Cement Mortars Exposed to a Sulfate Solution¹. 100 Barr Harbor Drive, PO Box C700, West Conshohocken, PA 19428-2959. United States.
- ASTM C1012/C1012M-15, (2018). ASTM C1012/C1012M-15: 2018 (updated) Standard Test Method for Length Change of Hydraulic-Cement Mortars Exposed to a Sulphate Solution. [online] Available at: https://www.astm.org/c1012_c1012m-15.html [Accessed 29 Oct. 2023].
- ASTM C150/ 150M, (2022). Standard specifications of OPC, available at: <https://cdn.standards.iteh.ai/samples/112915/067fa9aaab0a4971b5d0db060b563eb4/ASTM-C150-C150M-22.pdf>.

- Atis, D. and Bilim, C. (2007). Wet and dry cured compressive strength of concrete containing ground granulated blast-furnace slag. *Building and Environment*, 42, 3060-3065.
- Babu G.R., Reddy B.M. and Ramana NV (2018) Quality of mixing water in cement concrete “a review”. *Materials Today: PROCEEDINGS*. [Online]. 5 (1) (1), pp. 1313-1320. Available from: <https://doi.org/10.1016/j.matpr.2017.11.216>. Accessed 16 November 2022].
- Bahij S, Omary S, Feugeas F, Faqiri A., (2020). Fresh and hardened properties of concrete containing different forms of plastic waste—A review. *Waste Manag* 2020;113: 157–75.
- Bai, J. (2016). The durability of sustainable construction materials. *Sustainability of Construction Materials*, pp.397–414. doi:10.1016/b978-0-08-100370-1.00016-0.
- Bakhshi, M. and York, N. (2016). Resilient infrastructure design of fibre-reinforced tunnel segmental lining according to new aci report. [online] Available at: <https://core.ac.uk/download/pdf/61694293.pdf> [Accessed 5 Nov. 2023].
- Bangash F., (2018). Demolished buildings and sewage multiply public problems published by The News on 17 February 2018, available on TheNews.com. <https://www.thenews.com.pk/print/98845-Demolished-buildings-sewage-multiply-public-problems>. Retrieved 3 March 2023.
- Bapat J. D., (2012). Mineral admixtures in cement and concrete: CRC Press, 2012. Available at <https://www.taylorfrancis.com/books/mono/10.1201/b12673/mineral-admixtures-cement-concrete-jayant-bapat>.
- Barros, J.A.O. (2011). Steel fibre reinforced concrete: Material properties and structural applications, Editor(s): R. Figueiro, In *Woodhead Publishing Series in Textiles, Fibrous and Composite Materials for Civil Engineering Applications*, Woodhead Publishing, 2011, Pages 95-155, ISBN 9781845695583, <https://doi.org/10.1533/9780857095583.2.95>. Accessed on 1 May 2021, available at <https://www.sciencedirect.com/science/article/pii/>.

- Base Concrete, (2018). Base Concrete. [online] Baseconcrete.co.uk. Available at: <https://www.baseconcrete.co.uk/different-types-of-concrete-grades-and-their-uses/>.
- Beddoe, R.E. and Dorner, H.W. (2005). Modelling acid attack on concrete: Part I. The essential mechanisms. *Cement and Concrete Research*, 35(12), pp.2333–2339. doi:10.1016/j.cemconres.2005.04.002.
- Behbahani H.P., Nematollahi B. and Farasatpour M. (2011) Steel fibre reinforced concrete: A review. In: ICSECM, Volume: Proceedings of the International Conference on Structural Engineering Construction and Management, Kandy, Sri Lanka. Kandy, Sri Lanka: ICSECM. Available from: https://www.researchgate.net/publication/266174465_Steel_Fiber_Reinforced_Concrete_A_Review. [Accessed 20 June 2022].
- Beiser, V. (2019). Why is the world running out of sand? [online] Bbc.com. Available at: <https://www.bbc.com/future/article/20191108-why-the-world-is-running-out-of-sand>.
- Benameur S, Benkhaled A, Meraghni D, Chebana F, Necir A (2017) Complete flood frequency analysis in Abiod watershed, Biskra (Algeria). *Nat Hazards* 86(2):519–534
- Bendixen, M., Iversen, L.L., Best, J., Franks, D.M., Hackney, C.R., Latrubesse, E.M. and Tusting, L.S. (2021). Sand, gravel, and UN Sustainable Development Goals: Conflicts, synergies, and pathways forward. *One Earth*, 4(8), pp.1095–1111. doi <https://doi.org/10.1016/j.oneear.2021.07.008>.
- Bezak N, Brilly M, Sraj M (2014). Comparison between the peaks-over threshold method and the annual maximum method for flood frequency analysis. *Hydrol Sci J* 59(5):959–977
- Bheel, N., Sohu, S., Awoyera, P., Kumar, A., Abbasi, S.A. and Olalusi, O.B. (2021). Effect of Wheat Straw Ash on Fresh and Hardened Concrete Reinforced with Jute Fiber. *Advances in Civil Engineering*, 2021, pp.1–11. doi:10.1155/2021/6659125.

- Bibi T, Nawaz F, Rahman AA, Razak KA, Latif A, (2018) Flood Risk Assessment of River Kabul and Swat Catchment Area, District Charsada, Pakistan. The International Archives of the Photogrammetry, Remote Sensing and Spatial Information Sciences, Volume XLII-4/W9, 2018 International Conference on Geomatics and Geospatial Technology (GGT 2018), 3–5 September 2018, Kuala Lumpur, Malaysia.
- Blitzitzco. (n.d.). [online] Available at: <https://blitzco.de/wp-content/uploads/2020/Calcium%20carbonate%2CApplication.pdf>. [Accessed 20 Jul. 2022].
- Boers, M. Effects of a Deep Sand Extraction Pit. Final Report of the PUTMOR Measurements at the Lowered Dump Site, Rijkswaterstaat 2005. Available online: <https://repository.tudelft.nl/islandora/object/uuid%3A3e60f497-ced3-4dab-8d90-8f8c549e11e1>. (accessed on 3 June 2023).
- Bogues Compounds, (2022). Know 4 Types Of Major Components Of Cement Quickly - Civil Giant. [online] Available at: <https://www.civilgiant.com/bogues-compound/>, [Accessed 19 Jun. 2022].
- Bond, A., Fischer, T.B. and Fothergill, J. (2017). "Progressing quality control in environmental impact assessment beyond legislative compliance: An evaluation of the IEMA EIA Quality Mark certification scheme." Environmental Impact Assessment Review, [online] 63, pp.160–171. Available at: <https://www.sciencedirect.com/science/article/pii/S0195925516303900>. [Accessed 11 March 2023].
- Bonnefin, I., (2017). Emerging Materials: Ferrock. [online] Certifiedenergy.com.au. Available at: <https://www.certifiedenergy.com.au/emerging-materials/emerging-materials-ferrock>.
- Bosun. (2023). Bosun Precast Water Channel Linings and V-Drain Channels - Learn More. [online] Available at: <https://www.bosun.co.za/products/erosion->

control/bosun-precast-water-channel-linings-and-v-drain-channels/
[Accessed 11 Dec. 2023].

- Bramley, M.E. and Bowker, P.M., 2002, May. Improving local flood protection to the property. In Proceedings of the Institution of Civil Engineers-Civil Engineering (Vol. 150, No. 5, pp. 49-55). Thomas Telford Ltd.
- Brander, M., & Davis, G. (2012). Greenhouse Gases, CO₂, CO₂e, and Carbon: What Do All These Terms Mean? Econometrica, White Papers. Available at <https://scirp.org/reference/referencespapers.aspx?referenceid=3174668>, accessed on 14 January 2023.
- Brandt, A.M., (2008) Fibre-reinforced cement-based (FRC) composites after over 40 years of development in building and civil engineering. Com- pos Struct 86(1-3): 3-9.
- Breyse, D. (2010). Deterioration processes in reinforced concrete: an overview. Non-Destructive Evaluation of Reinforced Concrete Structures, pp.28–56. doi:10.1533/9781845699536.1.28.
- Britannica, (2018). The Editors of Encyclopaedia. "Concrete". Encyclopaedia Britannica, 1 Jun. 2020, <https://www.britannica.com/technology/concrete-building-material>. Accessed 5 May 2022.
- Britannica, (2020). The Editors of Encyclopedia. "Concrete". Encyclopedia Britannica, 1 Jun. 2020, <https://www.britannica.com/technology/concrete-building-material>. Accessed 5 May 2022.
- Brookes, A., Gregory, K.J. & Dawson, F.H. (1983). An Assessment of River Channelisation in England and Wales. The Science of the Total Environment. 27, pp.97–111.
- Bruhn-Tysk S. and Eklund M. 2002. A case study of biofuel energy plants in Sweden: EIA a tool for sustainable development, published by Environmental Impact Assessment Review 22 (2002) 129–144.
- BS 8500-2:2019, (2019). Concrete - Complementary British Standard to BS EN 206. [online] Available at: <https://www.BSgroup.com/en-GB/industries-and->

[sectors/construction-and-building/bs-8500-concrete-complementary-british-standard-to-bs-en-206/](https://www.BSgroup.com/en-GB/industries-and-sectors/construction-and-building/bs-8500-concrete-complementary-british-standard-to-bs-en-206/).

- BS EN 12350-1:2019 (2019). Testing fresh concrete. Sampling and common apparatus for flexural strength, available at <https://www.thenbs.com/PublicationIndex/documents/details?DocID=326929>, assessed on 7 January 2023.
- BS EN 12620:2013 (2013). Aggregates for concrete. Published 31-May-2013. ISBN: 9780580697142, Material Number: 3021256, available at <https://www.standardsuk.com/products/BS-EN-12620-2013>, accessed on 26 January 2023.
- BS EN 197-1:2011 (2011). Cement. Composition, specifications and conformity criteria for common cement. Published 30-Sep-2011. ISBN: 9780580919640, Material Number: 30331489, available at <https://www.standardsuk.com/products/BS-EN-197-1-2011>, accessed on 6 January 2023.
- BS EN 206:2013+A2:2021 (2021). Concrete. Specification, performance, production and conformity, available at <https://knowledge.BSgroup.com/products/concrete-specification-performance-production-and-conformity-2/standard>, assessed on 27 January 2023.
- BS EN 8500-1:2019 (2019a). BS 8500 Improve testing procedures and ingredients of Concrete <https://www.BSgroup.com/en-GB/industries-and-sectors/construction-and-building/bs-8500-concrete-complementary-british-standard-to-bs-en-206/>. [Accessed 7 June 2023].
- BS - BS EN 1008:2002 (2002). Mixing Water for Concrete - Specification for Sampling, Testing and Assessing the Suitability of Water, Including Water Recovered from Processes in the Concrete Industry, as Mixing Water for Concrete. Published 24-Jul-2002, ISBN: 0580401413, Material Number: 19990036. Available at: <https://www.standardsuk.com/products/BS-EN-1008-2002>, [Accessed 7 January 2023].

- BS - BS EN 12390-2 (2019). Testing hardened concrete Part 2: Making and curing specimens for compressive strength tests, available at <https://standards.globalspec.com/std/13376847/BS%20EN%2012390-2>, assessed on 7 January 2023.
- BS - BS EN 12390-2 (2019). Testing hardened concrete Part 2: Making and curing specimens for compressive strength tests, available at <https://standards.globalspec.com/std/13376847/BS%20EN%2012390-2>, assessed on 27 January 2023.
- BS - BS EN 12390-6:2009 Testing hardened concrete - Tensile splitting strength of test specimens Published on: 30 Jun 2010, available at <https://knowledge.BSgroup.com/products/testing-hardened-concrete-tensile-splitting-strength-of-test-specimens/standard>, accessed on 7 June 2023.
- BS (2015). BS EN 459-1:2015. Building lime - Definitions, specifications and conformity Available at: <https://knowledge.BSgroup.com/products/building-lime-definitions-specifications-and-conformity-criteria?version=tracked>. [Accessed 24 Oct. 2023].
- BS, (12390-7:2019). BS EN 12390-7:2019 Testing hardened concrete. The density of hardened concrete is available at <https://landingpage.BSgroup.com/LandingPage/Standard?UPI=0000000000030360097>.
- BS, (1990a). BS 5328: 1990 Part 2: 1990. Concrete. Part 2. Methods for specifying concrete mixes. BS, London: UK. BSOL.
- BS, (1990b). BS 5328: Part 1: 1990. Concrete. Part 1 Guide to specifying concrete. BS, London: UK. BSOL.
- BS, (1999). BS 3762-4.2:1986 ISO 697:1981. Analysis of formulated detergents —Part 4: Physical test methods —Section 4.2 Method for determination of apparent bulk density. BS, London, UK. BSOL.

- BS, (2000a). BS 410-1:2000. ISO 3310-1:2000. Incorporating Corrigendum No. 1. Test sieves — Technical requirements and testing —Part 1: Test sieves of metal wire cloth. BS. London, UK.
- BS, (2000b). BS EN 197-1:2000. Part 1. Cement composition, specifications and conformity criteria for common cement. British Standards Institution (BS), London, UK. BSOL.
- BS, (2000c). BS EN 12390-4:2000. Testing hardened concrete. Compressive strength. Specification for testing machines. BS, London, UK.
- BS, (2001). BS EN 206-1:2000. Concrete —Part 1:Specification, performance, production and conformity. Incorporating Corrigenda Nos. 1 and 2 and Amendments Nos. 1, 2 and 3. BS, London, UK. BS Standards Publication.
- BS, (2002). BS EN 1008:2002. Mixing water for concrete. Specification for sampling, Testing and assessing the suitability of water, including water recovered from processes in the concrete industry, as mixing water for concrete, available at: <https://knowledge.BSgroup.com/products/mixing-water-for-concrete-specification-for-sampling-testing-and-assessing-the-suitability-of-water-including-water-recovered-from-processes-in-the-concrete-industry-as-mixing-water-for-concrete?version=standard>.
- BS, (2004). BS EN 1992-1-1:2000. Eurocode 2:Design of Concrete Structures, Part 1-1: General Rules and Rules for Buildings. BS, London, UK.
- BS, (2005). BS EN 196-1:2005. Methods of testing cement: Determination of strength. BS, London, UK.
- BS, (2006). BS EN 14889-1:2006 Fibres for concrete. Steel fibres - Definitions, specifications, and conformity are available at <https://www.thenbs.com/PublicationIndex/documents/details?DocId=285227>.
- BS, (2006). BS EN 15167-1:2006. Incorporating Corrigendum No. 1Ground granulated blast furnace slag for use in concrete, mortar and grout. Part 1: Definitions, specifications and conformity criteria. BS, London, UK.

- BS, (2009a). BS EN 12350-2:2002. Testing fresh concrete Part 2: Slump-test. BS, London, UK.
- BS, (2009b). BS EN 12390-2:2009. Making and curing specimens for strength tests. BS, London, UK.
- BS, (2010a). BS EN 196-8:2010. Methods of testing cement. Heat of hydration - solution method. BS, London, UK.
- BS, (2010b). BS EN 196-9:2010. Methods of testing cement - semi-adiabatic method. BS, London, UK.
- BS, (2010c). BS EN 316:2009. Wood fibre boards —Definition, classification and symbols. BS, London, UK.
- BS, (2010d). BS EN 13263-1 :2005+A1: 2009. Silica fume for concrete. Part 1: Definitions, requirements and conformity criteria. BS, London, UK.
- BS, (2010e). BS EN 12390-6:2009. Testing hardened concrete Part 6: Tensile splitting strength of test specimens. BS, London, UK.
- BS, (2011a). BS EN 772-11:2011. Methods of test for masonry units Part 11: Determination of water absorption of aggregate concrete, autoclaved aerated concrete, manufactured stone and natural stone masonry units due to capillary action and the initial rate of water absorption of clay masonry units. BS, London, UK.
- BS, (2011b). BS EN 772-16:2011. Methods of test for masonry units Part 16: Determination of dimensions. BS, London, UK.
- BS, (2011c). BS EN 1097-1:2011. Tests for mechanical and physical properties of aggregates Part 1: Determination of the resistance to wear (micro-Deval). BS, London, UK.
- BS, (2011d). BS EN 12390-3:2009. Testing of Hardened Concrete, Part 3: Compressive strength of test specimens. BS, London, UK.
- BS, (2012). BS EN 934-2:2009+A1:2012 Admixtures for concrete, mortar and grout Concrete admixtures. Definitions, requirements, conformity, marking and labelling. Available at <https://www.en-standard.eu/bs-en-934-2-2009-a1->

[2012-admixtures-for-concrete-mortar-and-grout-concrete-admixtures-definitions-requirements-conformity-marking-andlabelling/#:~:text=](#)

- BS, (2012a). BS EN 450-1:2012. Fly ash for concrete: Part 1: Definition, specifications and conformity criteria. BS, London, UK.
- BS, (2012b). BS EN 12390-1:2012. Testing hardened concrete. Part 1: Shape, dimensions and other requirements for specimens and moulds. BS, London, UK.
- BS, (2013a). BS EN 196-2:2013. Methods of Testing Cement: Part 2. Chemical Analysis of Cement. BS, London, UK.
- BS, (2013b). BS EN 206:2013. Concrete-Specification, performance, production and conformity. BS, London, UK. BS Standards Publication.
- BS, (2013c). BS EN 12620:2013. Aggregates for concrete. BS, London, UK.
- BS, (2013d). BS EN 13369:2013. Common rules for
- BS, (2015). BS 8500-1:2015. Concrete –Complementary British Standard to BS EN 206. Part 1: Method of specifying and guidance for the specifier. BS, London, UK.
- BS, (2009). BS EN 13670:2009 Execution of concrete structures available at: <https://knowledge.BSgroup.com/products/execution-of-concrete-structures?version=standard>.
- BS, (2016). BS, "BS EN 196-1:2016, Part 1: Methods of testing cement. Determination of strength. " BS Standards Publication, 2016.
- BS, (2019). BS EN 12390-3:2019. Testing hardened concrete. Compressive strength of test specimens
- BS, (2021). BS EN 206:2013+A2:2021 Concrete. Specification, performance, production and conformity, <https://doi.org/10.3403/30257890>, available at <https://landingpage.BSgroup.com/LandingPage/Standard?UPI=0000000000030407978>.
- Buisson, L., Thuiller, W., Lek, S., Limp, P. & Grenouillet, G., (2008). Climate change hastens the turnover of stream fish assemblages. *Global Change Biol.* 14, 2232–2248. doi:10.1111/j.1365-2486.2008.01657.

- Bülbül, A. and Kaçar, R. (2016). Factors Affecting Kinetics of Strain Aging in S275JRC Steel. *Materials Research*, [online] 20(1), pp.210–217. Doi <https://doi.org/10.1590/1980-5373-mr-2016-0496>.
- Business Dictionary (2018): Environmental Impact Assessment (EIA). BusinessDictionary.com. Retrieved 28 February 2019, from BusinessDictionary.com website: <http://www.businessdictionary.com/definition/environmental-impact-assessment-EIA.html>.
- Cai, Y., Shi, B., Ng, C. W. W. & Tang, C. S. (2006). Effect of polypropylene fibre and lime admixture on engineering properties of clayey soil. *Engineering Geology*, 87, No. 3–4, 230–240.
- Carleton.edu. (2023). Available at: https://cdn.serc.carleton.edu/images/research_education/geochemsheets/techniques/UWSEM.jpg [Accessed 30 Oct. 2023].
- Carmeuse. (2020). HYDRATED LIME | Civil Eng. & Construction. [online] Available at: <https://www.carmeuse.com/na-en/products-services/product/hydrated-lime-civil-eng-construction>, [Accessed 20 Jul. 2022].
- Carre A., (2011): A Comparative Life Cycle Assessment of Alternative Constructions of a Typical Australian House Design, Final Report, Project No: PNA147-0809 Forest & Wood Products Australia, Melbourne, Victoria, 2011.
- Cassagnabère, F., Mouret, M., Escadeillas, G., Broilliard, P. and Bertrand, A. (2010). Metakaolin, a solution for the precast industry to limit the clinker content in concrete: Mechanical aspects. *Construction and Building Materials*, 24(7), pp.1109–1118. doi:10.1016/j.conbuildmat.2009.12.032.
- CCLD, (2019). CONCRETE CHANNEL LINING DETAILS N/A. (2019). Available at: <https://www.fusedind.com/wp-content/uploads/2019/11/Concrete-Channel-Lining-Details.pdf> [Accessed 5 Nov. 2023].
- (<https://www.sciencedirect.com/science/article/pii/S0008884616307578>)

- Cefis, Claudia, C., (2017). Chemo-mechanical modelling of the external sulfate attack in concrete, *Cement and Concrete Research*, Volume 93, 2017, Pages 57-70, ISSN 0008-8846, <https://doi.org/10.1016/j.cemconres.2016.12.003>. (<https://www.sciencedirect.com/science/article/pii/S0008884616307578>).
- CementConcrete (2020). Properties of Fiber Reinforced Concrete (FRC) – Types, Uses, and Advantage. [online] Cement Concrete. Available at: <https://cementconcrete.org/concrete/fiber-reinforced-concrete-frc/2524/>.
- Cement's basic molecular structure was finally decoded (MIT, 2009) and Archived on 21 February 2013 at the Wayback Machine.
- Cemex.co.uk. (2023). Available at: <https://www.cemex.co.uk/sprayed-concrete-shotcrete-solutions> [Accessed 11 Dec. 2023].
- Chapter 5, (2016). Open Channels County of Roanoke Chapter 5 -Open Channels. (2016). Available at: <https://www.roanokecountyva.gov/DocumentCenter/View/7709/Ch-5-Open-Channels---2016-Design-Manual>.
- Chapter 7 -Ditches and Channels. (2016). Available at: <https://www.virginiadot.org/business/resources/LocDes/DrainageManual/chapter7.pdf>.
- Chatham House (2021) Making concrete change: Innovation in low-carbon cement and concrete.
- Chaturvedi, R., Singh, P.K. and Sharma, V.K. (2021). Analysis and the impact of polypropylene fibre and steel on reinforced concrete. *Materials Today: Proceedings*, 45, pp.2755–2758. doi:<https://doi.org/10.1016/j.matpr.2020.11.606>.
- Chi, M.C. and Huang, R. (2014). Durability Performance of Concrete Containing CFBC Fly Ash and Coal-Fired Fly Ash. *Applied Mechanics and Materials*, 627, pp.283–287. doi:10.4028/www.scientific.net/amm.627.283.
- Chick. D. 2018. Flood Risk Management in Practice, Mott MacDonald UK.
- Chisholm, Hugh, ed. (1911). "[Coir](#)" *Encyclopaedia Britannica*. 6(11th ed.). Cambridge University Press. p. 654.

- Chrest, A.P., 1994. Guide to Using Silica Fume in Precast/Prestressed Concrete Products.
- Civil Concept, (2020). Characteristic strength of concrete- Formula, Uses, and calculation. [online] Civil Concept. Available at: <https://www.civilconcept.com/characteristic-strength-of-concrete/>.
- Civil Giant, (2021). Chemical Composition Of Cement And Functions Of Ingredients Present In Cement - Civil Giant. [online] Available at: <https://www.civilgiant.com/chemical-composition-of-cement/#functions-of-chemical-compounds-present-in-cement>. [Accessed 22 Jun. 2022].
- Civil Giant, (2022a). What Is Hydration Of Cement? Know Heat Of Hydration & Products Of Cement Hydration Here - Civil Giant. [online] Available at: <https://www.civilgiant.com/hydration-of-cement/#hydration-process-of-cement>. [Accessed 19 Jun. 2022].
- Civil Giant, (2022b). Sulphate Attack On Concrete | How To Prevent Sulphate Attack On Concrete? - Civil Giant. [online] Available at: <https://www.civilgiant.com/sulphate-attack-on-concrete/>, [Accessed 20 Jun. 2022].
- Civil Sir. (2021). Types of concrete grade and their ratio as per British Standard (BS). [online] Available at: <https://civilsir.com/types-of-concrete-grade-and-their-ratio-as-per-british-standard-bs/>. Assessed on 6 February 2023.
- Clean Technica. (2018). CleanTechnica. [online] Available at: <https://www.cleantechnica.com>. [Accessed 2 Oct. 2023].
- Cleveland, C.J. & Morris, C.G. (2009) – Dictionary of Energy: Expanded Edition; Elsevier
- Cohen SP, (2004). The Idea of Pakistan. Brookings Institution Press. ISBN 0815797613.
- Colella C. In: C̣ejka J, van Bakkum H, Corma A, Schueth F, editors. Introduction to zeolite science and practice. Amsterdam: Elsevier; 2007. p. 999–1035.

- Colleparidi, M. (2003). A state-of-the-art review on delayed ettringite attack on concrete. *Cement and Concrete Composites*, 25(4-5), pp.401–407. doi:10.1016/s0958-9465(02)00080-x.
- Concrete Question (2022). How do you clean absolutely any stain off concrete? Available at <https://concretequestions.com/how-to-clean-absolutely-any-stain-off-concrete/>. Accessed on 3 January 2023.
- concrete.org.uk. (2023). High-strength concrete. [online] Available at: <https://concrete.org.uk/fingertips-nuggets.asp?cmd=display&id=528> [Accessed 8 Oct. 2023].
- Condit, Carl W (1968). "The First Reinforced-Concrete Skyscraper: The Ingalls Building in Cincinnati and Its Place in Structural History". *Technology and Culture*. 9 (1): 1–33. doi:10.2307/3102041. JSTOR 3102041.
- Conserv, (2020) STONE TECH (Cleveland) Ltd. t/a Conserv available at <https://www.lime-mortars.co.uk/>.
- constructionhow.com. (2020). Chemical Composition Of Cement - Construction How. [online] Available at: <https://constructionhow.com/chemical-composition-of-cement/> [Accessed 19 Jun. 2022].
- Courland, Robert (2011). [Concrete planet: The strange and fascinating story of the world's most common man-made material](#). Amherst, N.Y.: Prometheus Books. ISBN 978-1616144814. Retrieved 28 August 2015.
- Creasey R., Andrews, J.P. Ekelu, S.O. Kruger, D., (2017). Long-term 20-year performance of surface coating repairs applied to façades of reinforced concrete buildings, *Case Studies in Construction Materials*, Volume 7, 2017, Pages 348-360, ISSN 2214-5095, <https://doi.org/10.1016/j.cscm.2017.11.001>.
- Cunliffe, J. Nadir, H, Ahmed, A, Yates, C, Yates, L, Abdelwahab, O, Aljahed, A, Limbu, N and Patel, N (2021) Potential Sustainable Cement Free Limecrete Based on GGBS & Hydrated Lime as an Alternative for Standardised Prescribed Concrete Applications. *Research & Development in Material*

- Science, 15 (5). pp. 1753-1763. ISSN 2576-8840 DOI: <https://doi.org/10.31031/RDMS.2021.15.000874>.
- Cunnane C (2010) Statistical distributions for flood frequency analysis. J Hydraul Res 5(650):28.
- Cunningham, S.C, Mac Nally, R., Baker, P.J, Cavagnaro, T.R, Beringer, J. Thomson, J., Thompson, R.M., (2015). Balancing the environmental benefits of reforestation in agricultural regions. Perspectives in Plant Ecology, Evolution and Systematics 17 (2015) pp. 301–317.
- Dadson, S.J., Hall, J.W., Murgatroyd, A., Acreman, M., Bates, P., Beven, K., Heathwaite, L., Holden, J., Holman, I.P., Lane, S.N., O'Connell, E., Penning-Roswell, E., Reynard, N., Sear, D., Thorne, C. and Wilby, R. (2017). A restatement of the natural science evidence concerning catchment-based 'natural' flood management in the UK. Proceedings of the Dales to Vale Rivers Network. (2018). River Wharfe Catchment Management Plan – Dales to Vale River Network. [Online]. [Accessed 1 October 2023]. Available at: <http://dvrn.co.uk/upper-wharfe-catchment/>.
- Dams and Locks on Mississippi River (2015). By US Army Corps of Engineers, Emergency Flood Management Plan 2015, www.mvr.usace.army.mil. (n.d.). Flood. [online] Available at: <https://www.mvr.usace.army.mil/About/Offices/Emergency-Management/Flood/Locks-Dams/>. [Accessed 25 March 2023].
- Damtoft JS, Lukasik J, Herfort D, Sorrentino D, Gartner EM., (2018). Sustainable development and climate change initiatives. Cem Concr Res 2008;38(2):115–27.
- Danielsen, S.W. and Kuznetsova, E. (2014). Environmental Impact and Sustainability in Aggregate Production and Use. Engineering Geology for Society and Territory - Volume 5, pp.41–44. doi https://doi.org/10.1007/978-3-319-09048-1_7.

- Darweesh H.H.M. Abo El-Suoud M.R., (2019). Palm Ash as a Pozzolanic Material for Portland Cement Pastes, Chemistry Journal Vol 4 (2019) ISSN: 2581-7507, <http://purkh.com/index.php/tochem>.
- Das S., Souliman B., Stone D., Neithalath N., (2014) Synthesis and Properties of a Novel Structural Binder Utilizing the Chemistry of Iron Carbonation. Applied Materials. ASC (1)2014, pp 1-19.
- Das, S., Hendrix, A., Stone, D. and Neithalath, N., 2015. Flexural fracture response of a novel iron carbonate matrix – Glass fibre composite and its comparison to Portland cement-based composites. Construction & Building Materials, 93, 360-370.
- DEFRA (2008) – Development of an embedded carbon emissions indicator; Department for Environment, Food and Rural Affairs
- DEFRA (2012) – Embedded Carbon Emissions Indicator; Department for Environment, Food and Rural Affairs
- Deng X, Ren W, Feng P (2016) Design flood recalculation under land surface change. Nat Hazards 80:1153–1169
- Densley Tingley, D. & Davison, B. (2011). Design for deconstruction and material reuse Proceedings of the Institution of Civil Engineers - Energy 2011 164:4, 195-204. ICE Virtual Library. [online] Available at: <https://www.icevirtuallibrary.com/action/showCitFormats?doi=10.1680%2Fener.2011.164.4.195>. [Accessed 9 Oct. 2023].
- Department of Civil Engineering (2015). "[History of Concrete Building Construction](#)". CIVL 1101 – History of Concrete. University of Memphis. Retrieved 25 April 2015.
- Desta, E. and Jun, Z. (2018). A Review on Ground Granulated Blast Slag GGBS in Concrete. Eighth International Conference On Advances in Civil and Structural Engineering - CSE 2018. doi:10.15224/978-1-63248-145-0-14.
- Dezhampanah, S., Nikbin, ImanM., Charkhtab, S., Fakhimi, F., Bazkiaei, S.M. and Mohebbi, R. (2020). Environmental performance and durability of concrete incorporating waste tyre rubber and steel fibre subjected to acid

- attack. Journal of Cleaner Production, 268, p.122216.
doi:10.1016/j.jclepro.2020.122216.
- Didier L., Franck M., Hermann O., Ulrike P., Christopher P., Frederik V., (2011).
Impact of quicklime reactivity and origin on Autoclaved Aerated Concrete
production, Cement, Wapno, Beton · January 2011.
- directives.sc.egov.usda.gov.(2007). Available at:
<https://directives.sc.egov.usda.gov/OpenNonWebContent.aspx?content=17784.wba>
- DiStasio Cat, (2015). Seventeen million under a flood warning as Mississippi
River expected to reach highest crest since 1993 published by Inhabitat -
Green Design, Innovation and Architecture on 30 December 2015 available
at <https://inhabitat.com/wp-content/blogs.dir/1/files/2015/12/NOAA-Mississippi-River-at-St-Louis.jpg>. [Accessed 25 March 2023].
- Divya C., Rafat S., Kunal., (2015). Strength, permeability and microstructure of
self-compacting concrete containing rice husk ash, Biosystems Engineering,
Volume 130, 2015, Pages 72-80, ISSN 1537-5110,
<https://doi.org/10.1016/j.biosystemseng.2014.12.005>.
(<https://www.sciencedirect.com/science/article/pii/S1537511014002207>).
- Dojkov I, Stoyanov S, Ninov J, Petrov B, “On the consumption of lime by
metakaolin, fly ash and kaoline in model systems”, Journal of Chemical
Technology and Metallurgy, 48, 2013, pp. 54-60.
- Dongre, Archanaa, Reddy, Ragavendra S., (2017). Fibre Reinforced Concrete-
A Case Study, [online] Available at:
https://www.researchgate.net/publication/321937230_Fibre_Reinforced_Concrete-_A_Case_Study.
- Doston, J., (2020). Published by Sciencing. How to Calculate Exceedance
Probability. [online] Available at: <https://sciencing.com/calculate-exceedance-probability-5365868.html>.
- Dramix, (2023). Dramix steel fibre concrete reinforcement solutions. [online]
Bekaert. Available at:

<https://www.bekaert.com/en/products/construction/concrete-reinforcement/dramix-steel-fiber-concrete-reinforcement-solutions>.

- Duan, Z., Singh, A., Xiao, J. and Hou, S. (2020). Combined use of recycled powder and recycled coarse aggregate derived from construction and demolition waste in self-compacting concrete. *Construction and Building Materials*, 254, p.119323. doi <https://doi.org/10.1016/j.conbuildmat.2020.119323>.
- Dudgeon, D. et al. (2006). Freshwater biodiversity: importance, threats, status and conservation challenges. *Biol. Rev.* 81, 163–182. (doi:10.1017/S1464793105006950).
- Dugan, P.J.; Barlow, C.; Agostinho, A.A.; Baran, E.; Cada, G.F.; Chen, D.; Cowx, I.G.; Ferguson, J.W.; Jutagate, T.; Mallen-Cooper, M.; et al. Fish Migration, Dams, and Loss of Ecosystem Services in the Mekong Basin. *Ambio* 2010, 39, 344–348.
- Dutrow, B. and Clark, C. (2019). X-ray Powder Diffraction (XRD). [online] Techniques. Available at: https://serc.carleton.edu/research_education/geochemsheets/techniques/XRD.html.
- Ekolu, S.O., Tchadjié, L.N. and Abdolhossein Naghizadeh (2022). Alkali-silica reaction resistance versus susceptibility of geopolymer binders. *MATEC web of conferences*, 361, pp.06003–06003. doi:<https://doi.org/10.1051/mateconf/202236106003>.
- Edodzigi M., Cropped-Area and Yield Survey (CAYS), Report 2000 Wet Season, Agric. Development Project (A.D.P), Niger State, Nigeria, 2001, 2.
- EIA-GOV.UK, (2019). Environmental Impact, Assessment Regulation available at <https://www.gov.uk/guidance/environmental-impact-assessment>, Retrieved 3 March 2023.
- [ElAshkar N.H.](#), [Mohr B.](#), [Nanko. H](#) and [Kurtis K.E.](#) (2002). The durability of pulp fibre-cement composites to wet/dry cycling, International Conference on Advances in Building Technology 4–6 December 2002, Hong Kong, China,

[Volume I](https://doi.org/10.1016/B978-008044100-9/50029-2), 2002, Pages 233-237 <https://doi.org/10.1016/B978-008044100-9/50029-2>

Eldidamony, Hamdy & El-Sokkari, T. & Khalil, Kh & Heikal, Mohamed & Ahmed, Inas. (2012). Hydration Mechanisms Of Calcium Sulphoaluminate C(4)A(3)(S)over-bar, C(4)A(S) over-bar Phase And Active Belite beta-C2S. *Ceramics Silikaty*. 56. 389-395.

Emery, S. B. and Hannah, D. M. (2014), Managing and researching floods: sustainability, policy responses and the place of rural communities. *Hydro. Process.*, 28: 4984–4988. , DOI: <http://dx.doi.org/10.1002/hyp.10258>.

Encyclopedia Britannica ["Building construction: The invention of reinforced concrete"](#). 2020.

Endale, S.A., Taffese, W.Z., Vo, D.-H. and Yehualaw, M.D. (2022). Rice Husk Ash in Concrete. *Sustainability*, 15(1), p.137. doi <https://doi.org/10.3390/su15010137>.

Engineering Toolbox (2019). Manning's Roughness Coefficients. [online] Engineeringtoolbox.com. Available at: https://www.engineeringtoolbox.com/mannings-roughness-d_799.html.

English Heritage Information Pack 2011/12 Resources Contents. (n.d.). Available at: <https://historicengland.org.uk/images-books/publications/eh-info-pack-2011-12/eh-info-pack-2011-12/>. [Accessed 2 Oct. 2023].

Environment Agency. 1999. Upper Wharfedale “Best Practice” Project - Information Series No 4: Where have all the gravels gone? The behaviour of an upland gravel-bed river. Environment Agency Report.

Environment Agency. 2014. A Summary of information about the Water Environment in the Wharfe and Lower Ouse management catchment. [Online]. [Accessed 19 November 2018].

Environment Agency. 2016. Humber River Basin District Management Plan 2015-2021. [Online]. [Accessed 25 September 2023]. Available from. https://circabc.europa.eu/webdav/CircaBC/env/wfd/Library/framework_directive/implementation_documents_1/2012-

[2014%20WFD%20public%20information%20and%20c
onsultation%20documents/UK/UK04%20Humber/Wharfe%20and%20Lowe
r%20Ouse.pdf.](#)

Environment Agency. 2018a. Environment Agency - Catchment Data Explorer. [Online]. [Accessed 21 November 2018]. Available at: <https://environment.data.gov.uk/catchment-planning/OperationalCatchment/3507/Summary>.

Environment Agency. 2018b. Working with Natural Processes - Evidence Directory. Bristol: Environment Agency.

Environment.ec.europa.eu. (2021.). Floods. [online] Available at: https://www.ec.europa.eu/environment/water/flood_risk/pdf/flooding. [Accessed 2 Oct. 2023].

Environmental Agency, 2010. Ouse catchment flood management plan. [Online]. [Accessed 25 September 2023]. Available from: https://assets.publishing.service.gov.uk/government/uploads/system/uploads/attachment_data/file/289228/River_Ouse_Catchment_Flood_Management_Plan.pdf

EPA, (2023). United States Environmental Protection Agency (2023). Overview of Greenhouse Gases. [online] US EPA. Available at: <https://www.epa.gov/ghgemissions/overview-greenhouse-gases>. 3
December 2023.

Ephraim M. E., Akeke G. A., Ukpata J.O., Compressive strength of concrete with rice husk ash as Partial Replacement of Ordinary Portland Cement, Eng Res J., 2 (2012), 22-26.

Erhan Guneyisi, Mehmet Gesoglu, Seda Karaoglu, Kasım Mermerdas “Strength, permeability and shrinkage cracking of silica fume and metakaolin concretes” Construction and Building Materials 34, (2012) 120–130.

Estokov, A., Harbuláková, V.O., Luptáková, A. and Števílová, N. (2012). Study of the Deterioration of Concrete Influenced by Biogenic Sulphate Attack.

- Procedia Engineering, 42, pp.1731–1738.
doi:10.1016/j.proeng.2012.07.566.
- EU EIA (2016, 2017, 2019, 2022). https://environment.ec.europa.eu/law-and-governance/environmental-assessments/environmental-impact-assessment_en. [Accessed 25 March 2023].
- Europe Economics. (2017). The economic benefits of woodland - A report for the Woodland Trust prepared by Europe Economics. [Online]. [Accessed 19 November. 2018]. Available from: <https://www.woodlandtrust.org.uk/mediafile/100821354/economic-benefits-of-woodland-report-jan-2017.pdf?cb=f6c0d8f471e44643b3106138076beeb7>.
- Euro Code 2 EN 1992-3, (2006). Eurocode 2: Design of concrete structures, available online at: <https://eurocodes.jrc.ec.europa.eu/EN-Eurocodes/eurocode-2-design-concrete-structures>.
- Eurocode Applied (2017). Table of concrete design properties (fcd, fctm, Ecm, fctd) - Eurocode 2. [online] EurocodeApplied.com. Available at: <https://eurocodeapplied.com/design/en1992/concrete-design-properties>.
- Eva Vejmelkova, Milena Pavlikova, Martin Keppert, Zbynek Keršner, Pavla Rovnanikova, Michal Ondracek, Martin Sedlmajer, Robert Cerny “High-performance concrete with Czech metakaolin: Experimental analysis of strength, toughness and durability characteristics” Construction and Building Materials 24 (2010), pp. 1404–1411.
- Ewemoje TA., Ewemooje OS. (2011). Best distribution and plotting positions of daily maximum flood estimation at Ona River in Ogun Oshun River Basin, Nigeria Agriculture Engineering International: CIGR Journal, 13(3).
- Fakhris, (2023). Fakhris || Erosion-Control-or-River-Slope-Control-Blocks. [online] www.fakhris.com. Available at: <https://www.fakhris.com/view-product/5#gallery-2>. [Accessed 12 Dec. 2023].
- Fakouri H.M. (2017). Re: Is anyone familiar with XRD at high temperatures? Retrieved from:

- [https://www.researchgate.net/post/Is anyone familiar with XRD at high temperature/59f41f6fb0366def2d4e8207/citation/download](https://www.researchgate.net/post/Is_anyone_familiar_with_XRD_at_high_temperature/59f41f6fb0366def2d4e8207/citation/download). Accessed on 12 June 2024.
- Fan, H., Dhir, R.K. and Hewlett, P.C. (2021). GGBS Use in Concrete as Cement Constituent: Strength Development and Sustainability Effects – Part 1. Magazine of Concrete Research, pp.1–41. Doi <https://doi.org/10.1680/jmacr.21.00009>.
- FAO Rice Market Monitor. Records retrieved August 8, 2014, from <http://fao.org/3/a-i4294e.pdf>.
- FAO Statistical Database, (2013). Records, Retrieved September 3, 2013, from <http://appsfaostat.org/default.html>.
- Farooq M., Safique M., Khattak SM., (2018). Flood Frequency Analysis of River Swat, Arabian Journal of Geosciences, 2018 11:216
- Farzadkia, M. and Bazrafshan, E. (2014). Lime Stabilization of Waste Activated Sludge. Health Scope, 3(3). doi:10.17795/Healthscope-16035.
- FDG, (2021). GOV.UK. (2021). Fluvial design guide. [online] Available at: <https://www.gov.uk/flood-and-coastal-erosion-risk-management-research-reports/fluvial-design-guide>.
- FEG, (2022). Flood estimation guidelines Version 09. Estimation of flood flows following Environment Agency best practice, published by Environment Agency, December 2022. GOV.UK. [online] Available at: <https://www.gov.uk/government/publications/flood-estimation-guidelines> [Accessed 8 Nov. 2023].
- FEHWS, (2013). Home Page - Ceh.ac.uk.FEH Web Service. [online] Available at: <https://fehweb.ceh.ac.uk/>.
- FEMA (1993). Mississippi River Flood by Federal Emergency Management Agency (1993).
- Ferroglobe, 2020. Silicon Metal [online]. Available at: <https://www.ferroglobe.com/products/silicon-metal/>. [Accessed 26 January 2023].

- Figiel B., Simonova H. and Korniejenko K. (2022) State of the art, challenges, and emerging trends: Geopolymer composite reinforced by dispersed steel fibres. *Reviews on Advanced Materials Science*. [Online]. 61 (1), pp. 1-15. Doi/10.1515/rams-2021-0067/HTML.
- Fischer, T.B., Fothergill, J., (2015). Das IEMA UVP Gütezeichen (EIA Quality Mark) Im Vereinigten Königreich: Ein Beispiel Freiwilliger Akkreditierung (UVP Report). ("Environmental Impact Assessment And Strategic Environmental Assessment"). Available at <https://www.worldscientific.com/doi/abs/10.1142/S1464333215500167>. Assessed on 3 March 2023.
- Flood Protection Bunds and Gabions [Online]. [Accessed 1 October 2023]. Available from: (www.pixshark.com, 2023).
- Flood site, 2009. Flood risk assessment and flood risk management, an introduction and guidance based on experiences and findings of Flood site, Delft, the Netherlands: Deltares, Delft Hydraulics.
- Fly Ash (2018). Fly Ash by Wikipedia, available at https://en.wikipedia.org/wiki/Fly_ash#:~:text=Fly%20ash%20material%20. Accessed on 26 January 2023.
- FOE (2014). Briefing on EIA April 2014, Friends of the Earth England, Wales and Northern Ireland. Friends of the Earth, UK. (n.d.). Friends of the Earth | Home. [online] Available at: <https://www.foe.co.uk>. [Accessed 25 March 2023].
- Forest Research, (2018). Riparian woodland and water protection. [Online]. [Accessed 17 September 2023]. Available from: https://assets.publishing.service.gov.uk/government/uploads/system/uploads/attachment_data/file/507117/LIT_10206_HUMBER_FRMP_PART_B.pdf
- Fragkouli K and Karen S., (2023), "The confused world of low-carbon concrete," *Concrete Magazine*, vol. 57, no. 3, pp. 36-39, 2023. Published by (Arup), EPFL. (2023). The confused world of low-carbon concrete. [online] Available at: <https://www.epfl.ch/labs/lmc/the-confused-world-of-low-carbon-concrete/> [Accessed 4 December 2023].

- Freedman, J.A.; Carline, R.F.; Stauffer, J.R., Jr. Gravel dredging alters diversity and structure of riverine fish assemblages. *Freshwater Biol.* 2013, 58, 261–274.
- FSU, (2012). Flood studies and update programme. Available online at https://opw.hydronet.com/data/files/FSU%20Work%20Package%204_2.pdf.
- FWO (2019). Project Brief to Director-General on Construction of Swat Expressway BOT Project 2019, Frontier Works Organization Pakistan.
- Gagg CR (2014) Cement and concrete as an engineering material, historical appraisal and case study analysis. *Engineering Failure Analysis* 40: 114-140.
- Galloway G., (2004). USA: Flood Management - Mississippi River Integrated Flood Management Case Study published by WMO/GWP Associated Programme on Flood Management (APFM) in January 2004.
- Galvao J.C.A., Portella K.F., Joukoski A., Mendes R. and Ferreira E.S. (2011) Use of waste polymers in concrete for repair of dam hydraulic surfaces. *Construction and Building Materials*. pp. 1049-1055. doi.org/10.1016/j.conbuildmat.2010.06.073.
- Ganesan, K., Rajagopal, K. and Thangavel, K. (2008). Rice husk ash blended cement: Assessment of optimal level of replacement for strength and permeability properties of concrete. *Construction and Building Materials*, 22, 1675-1683.
- García, Alejandro, Ashik T A, Bello J and Donovan T. "A Life Cycle Comparison to Ordinary Portland Cement." (2017). Available at <https://www.semanticscholar.org/paper/A-Life-Cycle-Comparison-to-Ordinary-Portland-Cement-Garc%C3%ADa-Achaiah/b2929c7c6aa5e2395e8ad23746d48be281145d0c>, accessed on 14 January 2023.
- Garg, N. and Shrivastava, S. (2022). A review on the utilization of recycled concrete aggregates (RCA) and ceramic fines in mortar application. *Materials Today: Proceedings*. Doi:<https://doi.org/10.1016/j.matpr.2022.09.226>.

- Garside, M. (2022a). Global cement industry – statistics and facts, published by Statista 22 October 2022, available online at <https://www.statista.com/topics/8700/cement-industry-worldwide/#topicOverview>.
- Garside, M. (2022b). Cement production worldwide from 1995 to 2022, published by Statista 6 April 2023, available online at <https://www.statista.com/statistics/1087115/global-cement-production-volume/>.
- Gaw, B. G., & Zamora-Palacios, S. A. (2010). Soil Reinforcement with Natural Fibres for Low-Income Housing Communities. Retrieved from <https://digitalcommons.wpi.edu/mqp-all/2622>.
- GCCA, (2019). Global Cement and Concrete Association, "Availability: Abundant, Local and Cost-effective," [Online]. Available: <https://gccassociation.org/sustainability-benefits-of-concrete/availability/>.
- GCCA, (2021). Global Cement and Concrete Association, "Concrete future: The GCCA 2050 Cement and Concrete Industry Roadmap for Net Zero Concrete," October 2021. [Online].
- GCCA, (2023). Global Cement and Concrete Association publishes Cement Industry Net Progress Report 2023. [online] www.globalcement.com. Available at: <https://www.globalcement.com/news/item/16655-global-cement-and-concrete-association-publishes-cement-industry-net-progress-report-2023>. [Accessed 4 December 2023].
- GCCA, (2023b). Global Cement and Concrete Association, "Circular Economy," 2023. [Online]. Available: <https://gccassociation.org/sustainability-benefits-of-concrete/circular-economy/>.
- GCCA. (2021). 2050 Net Zero Roadmap - One Year On. [online] Available at: <https://gccassociation.org/2050-net-zero-roadmap-one-year-on/>.
- Geotechnical Engineering, (2023). Shotcreting. [online] Available at: <https://www.geotech.net.au/capabilities/slope-stabilisation/shotcreting.html>. [Accessed 11 Dec. 2023].

- Geyer R., Jambeck J.R., Law K.L, Production. Use. and the fate of all plastics ever made. *Sci. Adv.* 3 (7) (2017) e1700782.
- Ghutke, V. S. & Bhandari, P.S. (2014). Influence of silica fume on concrete. *IOSR Journal of Mechanical and Civil Engineering*, 44-47.
- Girts B, Laura V, Liga S, Janis L, Aleksandrs K, Diana B., (2020). Evaluation of Industrial by-products as pozzolans: A road map for use in concrete production, *Case Studies in Construction Materials* 13 (2020) e00424, www.elsevier.com/locate/cscm.
- Glasson, J., (1999). The first ten years of the UK EIA system: strengths, weaknesses, opportunities and threats. *Plan. Pract. Res.* 14, 363–375.
- Glazzard, P. (2007). River Wharfe Weir at Tadcaster, available online at: (<https://www.northyorks.gov.uk/sites/default/files/fileroot/Environment.pdf>).
- Global Cement and Concrete Association, (2023). "Cement and concrete around the world," [Online]. Available: <https://gccassociation.org/concretefuture/cement-concrete-around-the-world/>. [Accessed 06 June 2023].
- GMI, (2023). Construction Aggregates Market Size & Share Report, 2023-2032 by Global Market Insights Inc. available at <https://www.gminsights.com/industry-analysis/construction-aggregates-market>. Assessed on 12 June 2024.
- Gnilsen, R. (1987). Plain Concrete Tunnel Lining-Design Concepts. [online] Available at: <https://onlinepubs.trb.org/Onlinepubs/trr/1987/1150/1150-003.pdf>. [Accessed 5 Nov. 2023].
- Goulding, K.W.T. (2016). Soil acidification and the importance of liming agricultural soils with particular reference to the United Kingdom. *Soil Use and Management*, [online] 32(3), pp.390–399. doi:10.1111/sum.12270.
- GOV. UK (2014, 2017, 2019). Environmental Impact Assessment. [online] GOV.UK. Available at: <https://www.gov.uk/guidance/environmental-impact-assessment>. Retrieved 3 March 2023.

- Gravina, R.J., S.T. de Silva, Law, D.W. and Sujeeva Setunge (2016). Micro- and nano-engineered high-volume ultrafine fly-ash cement composite with and without additives. 10(1), pp.113–124. doi <https://doi.org/10.1007/s40069-015-0122-7>.
- Grist, E., Paine, K. and Heath, A. (2016). Hydraulic lime – pozzolan concretes: Properties, uses and research needs. The 9th International Concrete Conference 2016, [online] pp.314–326. Available at: <https://researchportal.bath.ac.uk/en/publications/hydraulic-lime-pozzolan-concretes-properties-uses-and-research-ne>. [Accessed 8 Dec. 2023].
- Grzymiski F., Musial M. and Trapko T. (2019) Mechanical properties of fibre-reinforced concrete with recycled fibres. Construction and Building Materials. [Online]. 198 February, pp. 323-331. Available from: <https://doi.org/10.1016/j.conbuildmat.2018.11.183>. [Accessed 7 June 2022].
- Gu L, Ozbakkaloglu T., Use of recycled plastics in concrete: a critical review, Waste Manag. 51 (2016) 19-42.
- Guerrero LA, Maas G, Hogland W., (2013c). Solid waste management challenges for cities in developing countries. Waste Manag 2013;33(1):220–32.
- Haan CT, (1977). Statistical Methods in Hydrology, Table 7.7 page 142, Published by Iowa State University Press 1977 ISBN 081381510X, 9780813815107
- Haghnazar, H.; Saneie, M. Impacts of pit distance and location on river sand mining management. Model. Earth Syst. Environ. 2019, 5, 1463–1472.
- Han, X., Wang, X., Zhu, Y., Huang, J.-S., Yang, L., Chang, Z. and Fu, F. (2020). An Experimental Study on Concrete and Geomembrane Lining Effects on Canal Seepage in Arid Agricultural Areas. 12(9), pp.2343–2343. doi <https://doi.org/10.3390/w12092343>. (Han et al., 2020)
- Hannesson, G., Kuder, K., Shogren, R. and Lehman, D. (2012). The influence of high volume of fly ash and slag on the compressive strength of self-consolidating concrete. Construction and Building Materials, 30, 161-168.

- Harvey, F. and editor, F.H.E. (2023). What is Cop28, and why does it matter? The Guardian. [online] 29 Nov. Available at: <https://www.theguardian.com/environment/2023/nov/29/what-is-cop28-and-why-does-it-matter>.
- Harman, J., Bramley, M.E. and Funnell, M., 2002, May. Sustainable flood defence in England and Wales. In Proceedings of the Institution of Civil Engineers-Civil Engineering (Vol. 150, No. 5, pp. 3-9). Thomas Telford Ltd.
- Haseeb B. (2017). The Supreme Court (SC) sets aside the Lahore High Court (LHC) decision against the Orange Line train and orders the Punjab govt to complete the project published on 8 December 2017 by DAWN Pakistan, available at <https://www.dawn.com/news/1375327/sc-sets-aside-lhc-decision-against-orange-line-train-orders-punjab-govt-to-complete-project>, retrieved on 10 March 2023.
- Hasik, V., Ororbia, M., Warn, G.P. and Bilec, M.M. (2019). Whole building life cycle environmental impacts and costs: A sensitivity study of design and service decisions. Building and Environment, 163, p.106316. doi <https://doi.org/10.1016/j.buildenv.2019.106316>.
- Health and safety executive (2022). Risk Assessment - HSE. [online] Hse.gov.uk. Available at: <https://www.hse.gov.uk/simple-health-safety/risk/index.htm>.
- Héctor A. RuizHéctor A. RuizDenise S. RuzeneDaniel P. SilvaShow all 6 authorsJosé A TeixeiraJosé A, (2011). Teixeira Evaluation of a hydrothermal process for pretreatment of wheat straw—effect of particle size and process conditions. January 2011Journal of Chemical Technology & Biotechnology 86(1):88 - 94 Follow journal DOI: 10.1002/jctb.2518
- Helsel DR, Hirsch RM, (2010) Statistical Methods in Water Resources.Available at <http://water.usgs.gov/pubs/twri/twri4a3>.
- Hemant, C., (2011). “Effect of Activated Fly ash in Metakaolin based Cement” National Conference on Recent Trends in Engineering & Technology 13-14 May 2011, BVM Engineering College, Gujarat, India.

- Hemn U, Rabar H. Faraj, Nahla Hilal, Azad A. Mohammed, Aryan Far H. Sherwani, (2021). Use of recycled fibers in concrete composites: A systematic, comprehensive review, *Composites Part B* 215 (2021) 108769, available at www.elsevier.com/locate/compositesb, accessed on 25 April 2021 on ScienceDirect.
- Hemn U. A., Rabar H. F., Nahla H., Azad A. Mohammed, Aryan F. Sherwani, H. (2021). Use of recycled fibres in concrete composites: A systematic, comprehensive review, *Composites Part B* 215 (2021) 108769, available at www.elsevier.com/locate/compositesb, accessed on 25 April 2021 on ScienceDirect.
- Hemsath, T., (2021). Evaluating Environmental Impacts of Our Buildings Using Whole Building Life Cycle Assessment (WBLCA) Aids. [online] BVH Architecture. Available at: <https://bvh.com/blog/evaluating-environmental-impacts-of-our-buildings-using-whole-building-life-cycle-assessment-wblca-aids-in-designing-purposeful-environmentally-consciencious-architecture/> [Accessed 9 Oct. 2023].
- Herath C., Gunasekara C., Law D.W. and Setunge S. (2020) Performance of high volume fly ash concrete incorporating additives: A systematic literature review. *Construction and Building Materials*. [Online]. 258 October, pp. 1-13. Available at: <https://doi.org/10.1016/j.conbuildmat.2020.120606>, accessed on 30 January 2023.
- Hewlett PC (2004) *Lea's chemistry of cement and concrete*, 5th ed, Oxford: Elsevier Science & Technology Books. ISBN: 0470 24416 X (Wiley).
- Higgins, D.D. (2003). Increased sulfate resistance of ggbs concrete in the presence of carbonate. *Cement and Concrete Composites*, 25(8), pp.913–919. doi:10.1016/s0958-9465(03)00148-3.
- Higgins, D.D. (2003). Increased sulfate resistance of GGBS concrete in the presence of carbonate. *Cement and Concrete Composites*, 25(8), pp.913–919. doi:10.1016/s0958-9465(03)00148-3.

- High Calcium Hydrated Lime - Graymont - SDS US 4.12 Safety Data Sheet (2020). https://www.graymont.com/2022/sites/default/files/pdf/msds/HIGH%20CALCIUM%20HYDRATED%20LIME_Graymont%20-%20SDS%20US%204.12English%20%28US%29.pdf.
- High Strength Concrete Design by the Concrete Society, available at <https://concrete.org.uk/fingertips-nuggets.asp?cmd=display&id=528>, accessed on 16 January 2023.
- Highway Design Manual CHAPTER 860 -ROADSIDE CHANNELS Topic 861 - General. (2020). Available at: <https://dot.ca.gov/-/media/dot-media/programs/design/documents/chp0860-a11y.pdf>.
- Highway pavements using machine learning models, Struct. Infrastruct. Eng. Hobbs D.W., The tensile strength of rocks. Int. J. Rock Mech. Mining Science 1963, 1, pp 385-396.
- Hoerbinger Li, J., Weissteiner S., Peng C. , L., & RauchH. P. (2020). River restoration challenges with a specific view on hydromorphology. Frontiers of Structural and Civil Engineering, 14(5), 1033–1038. <https://doi.org/10.1007/s11709-020-0665-9>.
- Holt, R.D., Barfield, M. and Peniston, J.H. (2022). Temporal variation may have diverse impacts on range limits. Philosophical Transactions of the Royal Society B: Biological Sciences, 377(1848). Doi: <https://doi.org/10.1098/rstb.2021.0016>. (Holt, Barfield and Peniston, 2022)
- Hoornweg D, Bhada-Tata P. What a waste: a global review of solid waste management. World Bank 2012, Environment_Waste_production_must_peak_this_century accessed on 29 April 2021, available at <https://www.researchgate.net/publication/258216813> .
- Hoornweg, D., Bhada-Tata, P., (2021) What a waste: a global review of solid waste management. World Bank 2012, Environment_Waste_production_must_peak_this_century.

- Hoxha E., Habert G., Lasvaux S., Chevalier J. and Le Roy R. (2017): Influence of construction material uncertainties on residential building LCA reliability, J. Clean. Prod. 144 (2017):33-47.
<https://doi.org/10.3403/30360097>, (published 16/07/2019), available at <https://landingpage.BSgroup.com/LandingPage/Standard?UPI=000000000030360097>.
- Hu, C., Liu, P. and Liu, Y. (2011). High-Temperature X-Ray Diffraction Studies Of The Sample Heating Units. Procedia Engineering, 24, pp.404–411. doi:<https://doi.org/10.1016/j.proeng.2011.11.2666>. Accessed on 12 June 2024.
- Hwidi, R.S., Tengku Izhar, T.N., Mohd Saad, F.N. and Adam, T. (2018). Hydrogen Sulphide Emissions Reduction Using Hydrated Lime. IOP Conference Series: Materials Science and Engineering, 429, p.012082. doi:10.1088/1757-899x/429/1/012082.
- Hydrated Lime Treatment (Emerging Technology) www.emersan-compendium.org. (n.d.). Compendium of Sanitation Technologies in Emergencies. [online] Available at: <https://www.emersan-compendium.org/en/technologies/technology/hydrated-lime-treatment-emerging-technology#:~:text=Hydrated%20Lime%20Treatment%20is%20a%20cost-effective%20chemical%20treatment>, [Accessed 27 Jul. 2022].
- Hy-Tex Coir Mesh Erosion Control Products UK available at <https://www.hy-tex.co.uk/surface-erosion-control/>
- IAIA (2019). IAIA eNews January 2019 available at <https://www.iaia.org/news.php>, Retrieved 3 March 2023,
- ICCS, (2017). The Institute of Chartered Surveyors, "Whole life carbon assessment for the built environment," 2017.
- ICE V3 Database Circular Ecology. (2019). Embodied Carbon Training Course. [online] Available at: <https://circularecology.com/embodied-carbon-training.html>. [Accessed 4 December 2023].

- ICE Energy Briefing Sheet, (2011). Embodied Energy and Carbon Institution of Civil Engineers. (2011). Available at: https://www.ice.org.uk/media/w4kjruf/embodied_energy_and_carbon.pdf.
- Ideker C. and Thomas J.H, M.D.A. (2015). Alkali–silica reaction: Current understanding of the reaction mechanisms and the knowledge gaps. Cement and Concrete Research, [online] 76, pp.130–146. doi:10.1016/j.cemconres.2015.05.024.
- Idiart A.E., Lopez C.M., Carol I., (2011). Chemo-mechanical analysis of concrete cracking and degradation due to external sulfate attack: a mesoscale model., Cem. Concr. Compos. 33 (2011) 411–423.
- IEMA (2017). Institute of Environmental Management & Assessment Report 2017 UK.
- IFEH, (2008). Joint Defra / Environment Agency Flood and Coastal Erosion Risk Management R&D Programme Improving the FEH statistical procedures for flood frequency estimation Science Report: SC050050. Available at: https://assets.publishing.service.gov.uk/media/602e5c0f8fa8f54331b080e6/Improving_the_FEH_Statistical_Procedures_for_Flood_Frequency_Estimation_Technical_Report.pdf [Accessed 8 Nov. 2023].
- Inkoom, S. Sobanjo J., Barbu A., Niu, X., (2019) Prediction of the crack condition of highway pavements using machine learning models, Struct. Infrastruct. Eng.
- Institution of Civil Engineers (ICE). (2022). Low Carbon Concrete Routemap. [online] Available at: <https://www.ice.org.uk/engineering-resources/briefing-sheets/low-carbon-concrete-routemap>.
- Iron Powder (2023). The manufacturing facts of Iron powder by MB Glass Manufacturer, available at <https://www.mbfmg.co.uk/ironpowder.html>, accessed on 30 January 2023.
- IS: 3873- 19192, (1992). Laying cement concrete/ stone slab Lining on canals – Indian code of practice, IS 3873- 19192:1992, available online at

<https://ia600403.us.archive.org/26/items/gov.in.is.3873.1993/is.3873.1993.pdf>.

ISE, (2020). The Institute of Structural Engineers, "How to Calculate Embodied Carbon," 2020.

Islam, M.M.U., Li, J., Wu, Y.-F., Roychand, R. and Saberian, M. (2022). Design and strength optimisation method for the production of structural lightweight concrete: An experimental investigation for the complete replacement of conventional coarse aggregates by waste rubber particles. Resources, Conservation and Recycling, [online] 184, p.106390. doi <https://doi.org/10.1016/j.resconrec.2022.106390>.

Ismail, Z.Z., Al-Hashmi, E.A., (2008) Use of waste plastic in concrete mixture as aggregate replacement. Waste Manag 28(11): 2041-2047.

Issues of Orange Train (2018). Available at www.TheNews.com, 2018. Retrieved 3 March 2023.

ITC. (2023). International Trade Centre Trade Map - Trade Statistics for International Business Development. [online] Trademap.org. Available at: <https://www.trademap.org/Index.aspx>.

ISO 1920-12:2015. 14:00-17:00 (2015). [online] ISO. Available at: <https://www.iso.org/standard/57932.html#:~:text=This%20procedure%20specified%20in%20ISO%201920-12%3A2015%20is%20a>. [Accessed 9 Dec. 2023].

Jain, D.B.C.P.K.J.K. (2020). Reinforced Concrete Structures: Volume I [1 July 2012] Punmia, Dr. B. C.; Jain, Ashok Kr. and Jain, Arun Kr. [online] The Open Library. Laxmi Publication. Available at: https://openlibrary.org/books/OL32179913M/Reinforced_Concrete_Structures. [Accessed 22 November 2023].

Jamal H, (2017). Munda Headworks Reconstruction on River Swat available at www.aboutcivil.org

- Jannie S. J. van Deventer, Claire E. White, Rupert J. Myers (2020) 'A Roadmap for Production of Cement and Concrete with Low-CO₂ Emissions', Waste and Biomass Valorization (2020)
- Jawahar, J. & Lavanya, D & Sashidhar, Chundpalle. (2016). Performance of Fly Ash and GGBS-Based Geopolymer Concrete in Acid Environment. International Journal of Research and Scientific Innovation. 3. 101-104.
- Jawahar, J. & Lavanya, D & Sashidhar, Chundpalle. (2016). Performance of Fly Ash and GGBS-Based Geopolymer Concrete in Acid Environment. International Journal of Research and Scientific Innovation. 3. 101-104.
- JBA Consulting, (2013). Restoring the River Wharfe SSSI A River Restoration Plan. [Online]. [Accessed 25 September 2023]. Available from: <http://www.yorkshiredalesrivertrust.com/wp-content/uploads/2014/08/51213-Restoring-the-River-Wharfe-SSSI-Restoration-Plan-WeBSte.pdf>.
- JBA Consulting, (2018). Natural Flood Management. [Online]. [Accessed 21 Nov. 2018]. Available from: <https://www.jbaconsulting.com/what-we-do/environmental-services/natural-flood-management/nfm-for-web/>. Accessed 25 September 2023
- JEOL Ltd., 2023. Scanning Electron Microscope (SEM) Products JEOL Ltd. (n.d.). Scanning Electron Microscope (SEM) | Products | JEOL Ltd. [online] Available at: <https://www.jeol.com/products/scientific/sem/>.
- Jia, L.; Luo, Z.; Yang, Q.; Ou, S.; Lei, Y. Impacts of the large amount of sand mining on riverbed morphology and tidal dynamics in lower reaches and delta of the Dongjiang River. J. Geogr. Sci. 2007, 17, 197–211.
- Jiricka, A., Formayer, H., Schmidt, A., Völler, S., Leitner, M., Fischer, T.B. and Wachter, T.F. (2016). Consideration of climate change impacts and adaptation in EIA practice — Perspectives of actors in Austria and Germany. Environmental Impact Assessment Review, 57, pp.78–88.
- Johannes F., (2021). Chemistry of Setting Chapter 10.2.3 in Petroleum Engineer's Guide to Oil Field Chemicals and Fluids (Third Edition), 2021,

available at <https://www.sciencedirect.com/topics/engineering/tricalcium-silicate#:~:text=When%20the%20maximum%20degree%20of%20supersaturation%20is%20reached%2C,of%20the%20CSH%20formed%20and%20C%2FS%20%3C%202.>

- John L. P., (2018) 'Alkali-activated materials', Cement and Concrete Research, 114, pp40-48
- Johnson, B. and Christensen, L.B. (2020). Educational research: quantitative, qualitative, and mixed approaches. Los Angeles: Sage Publications, Inc.
- Jones, M., Newlands, M., Halliday, J., Csetenyi, L., Zheng, L., McCarthy, M. and Dyer, T. (2016). The 9th International Concrete Conference 2016: Environment, Efficiency and Economic Challenges for Concrete, pp. 314-326. [online] Discovery - the University of Dundee Research Portal. Dundee: University of Dundee. Available at: <https://discovery.dundee.ac.uk/en/publications/the-9th-international-concrete-conference-2016-environment-effici>, [Accessed 8 Dec. 2023]
- Jonida P., Ahmed A., Kamau J. Hyndman F., (2018). Palm Oil Fuel Ash as A Cement Replacement in Concrete, Modern Approaches on Material Science, published by Luprin Publishers 2018, DOI: 10.32474/MAMS.2018.01.000102, ISSN: 2641-6921.
- Jordan, C.; Tiede, J.; Lojek, O.; Visscher, J.; Apel, H.; Nguyen, H.Q.; Quang, C.N.X.; Schlurmann, T. Sand mining in the Mekong Delta revisited—Current scales of local sediment deficits. Sci. Rep. 2019, 9, 1–14.
- Kaladarshan, (2006). An overview map of the Gandhara region, from the Kabul River valley in the west to Taxila, east of the Indus, available at <http://www.livius.org/ga-gh/gandara/gandara.html>, and <http://www.columbia.edu/itc/mealac/pritchett/00maplinks/early/gandhara/gandhara.html>,
- Kamal V, Mukherjee S, Singh P, Sen R, Vishwakarma CA, Sajadi P, Asthana H, Kamau, J, Ahmed, A, Hirst, P and Kangwa, J (2016). Suitability of Corncob Ash as a supplementary Cementitious Material. International Journal of Materials

- Science and Engineering. 4 (4), pp. 215-228.
<https://doi.org/10.17706/ijmse.2016.4.4.215-228>.
- Kamau, J, Ahmed, A, Hirst, P and Kangwa, J (2016). Suitability of Corncob Ash as a supplementary Cementitious Material. International Journal of Materials Science and Engineering. 4 (4), pp. 215-228.
<https://doi.org/10.17706/ijmse.2016.4.4.215-228>
- Karen et al., (2018a). Karen L. Scrivener, Vanderley M. John, Ellis M. Gartner (2018) 'Eco-efficient cement: Potential economically viable solutions for a low-CO2 cement-based materials industry', UN Environment
- Karen et al., (2018b). Karen Scrivener, Fernando Martirena, Shashank Bishnoi, Soumen Maity (2018) 'Calcined clay limestone cement (LC3)', Cement and Concrete Research, 114, pp49-56
- Karthika S., Leema A.R, and Priyadarshini¹ G (2021). Sustainable Development on Ferrock Mortar Cubes Published under licence by IOP Publishing Ltd Journal of Physics: Conference Series, Volume 2040, International Conference on Physics and Energy 2021 (ICPAE 2021) 24 March 2021, Kancheepuram, India. DOI 10.1088/1742-6596/2040/1/012020.
- Karuppasamy, S., Dinesh Kumar, K. and Janardhan, K., 2011. Experimental Study on Ferrock: A Life-Cycle Compression to Ordinary Portland Cement. Thiruvallur, India.
- Kavitha O.R., Shanthi V.M., Arulraj G. Prince., Sivakumar V.R., (2016). Microstructural studies on eco-friendly and durable Self-compacting concrete blended with metakaolin, Applied Clay Science, Volumes 124–125, 2016, Pages 143-149, ISSN 0169-1317,
<https://doi.org/10.1016/j.clay.2016.02.011>.
- Keep, H. 2017. Natural Flood Management Measures – a practical guide for farmers. [Online]. [Accessed 25 September 2023]. Available from:
http://www.yorkshiredales.org.uk/data/assets/pdf_file/0003/1010991/11301_flood_management_guide_WEBx.pdf.

- Keerthi G.B.S, Easwara G. L.P, Velmurgan R, (2015). Probabilistic Study of Tensile Properties of Coir Fibre Reinforced Polymer Matrix Composite. International Journal of Advanced Materials Science ISSN 2231-1211 Volume 6, Number 1 (2015), pp. 7-17, Research India Publications <http://www.ripublication.com>.
- Khaliq F., (2018). "Tourists throng Swat to explore its natural beauty". DAWN.com.
- Kim, M.S. and Lee, S.S. (2021). Design Study of Steel Fibre Reinforced Concrete Shaft Lining for Swelling Ground in Toronto, Canada. Applied Sciences, 11(8), p.3490. doi:<https://doi.org/10.3390/app11083490>.
- Koehnken, L.; Rintoul, M. Impacts of Sand Mining on Ecosystem Structure, Process and Biodiversity in Rivers, WWF Review. 2018. Available online: https://d2ouvy59p0dg6k.cloudfront.net/downloads/sand_mining_impacts_on_world_rivers. (accessed on 20 June 2023).
- Koh, S.I., (2017). The mechanical characteristics of the shield TBM segment are reinforced with steel fibre and their application to tunnelling. PhD. Thesis, Dongguk University, Seoul, Korea, 2017.
- Koks, EE., Jongman. 2015. Combining hazard, exposure and social vulnerability to provide lessons for flood risk management. Environmental Science and Policy. 47. pp. 42-52.
- Kondolf, G.M. Geomorphic and environmental effects of instream gravel mining. Landsc. Urban Plan. 1994, 28, 225–243.
- Kosmatka, H., Panarese, C., Allen, G. E. & Cumming, S. (2002). Design and control of concrete mixtures, Portland Cement Association Skokie, IL.
- Kothari, C.R. (2004). Research Methodology: Methods and Techniques. 2nd ed. New Delhi: New Age International (P) Limited, Publishers.
- KPK Irrigation Department, (2019). Discharge Data of Swat River, <http://irrigation.gkp.pk/>.
- Krishnan, M. (2021). M50 concrete mix design -Steps|IS-10262:2009 |IS-456:2000 available at <https://www.eigenplus.com/detailed-calculation-of->

[m50-concrete-mix-design-is-102622009-is-4562000/](https://doi.org/10.1063/5.0100361), assessed on 6 February 2023.

- Krygier, A., Wehrenberg, C.E., Bernier, J.V., Clarke, S., Coleman, A.L., F. Coppari, Duffy, T.S., Gorman, M.G., Hohenberger, M., D. Kalantar, Kemp, G.E., Khan, S.F., C. Krauland, Kraus, R.G., Lazicki, A., MacDonald, M.J., MacPhee, A.G., Marley, E., Marshall, M.C. and May, M. (2022). X-ray source characterization and sample heating on x-ray diffraction experiments at the National Ignition Facility. *Physics of plasmas*, [online] 29(10). doi:<https://doi.org/10.1063/5.0100361>. Available at: <https://pubs.aip.org/aip/pop/article/29/10/103302/2848056/X-ray-source-characterization-and-sample-heating>. Accessed on 12 June 2024.
- Kumar V., (2017). 15 Biggest and Worst Floods Ever in History, published by Rank Red Science & Technology on 16 March 2017, available at <https://www.rankred.com/top-10-biggest-and-worst-floods-ever-in-history/>.
- Kumar, A. (2020). Department of Civil Engineering B.TECH -6 The SEM Water Resources and Irrigation Engineering (WRE) CE-603(A) LNCT Group of Colleges, Bhopal. [online] Available at: <https://lnct.ac.in/wp-content/uploads/2020/03/UNIT-IV-CANALS-AND-STUCTURE-WORD-PDF.pdf>. [Accessed 5 Nov. 2023].
- Kumar, R., Dhaka, J. (2016). Review paper on partial replacement of cement with silica fume and its effect on concrete properties. *International Journal for Technological Research in Engineering*. 4,(1).
- Kumar, K. and Kumar, M. (2023). Experimental investigation of construction and demolition waste in bituminous concrete. *Materials Today: Proceedings*. [online] doi:<https://doi.org/10.1016/j.matpr.2023.04.303>.
- Kundzewicz, Z. W. (2002). Non-structural Flood Protection and Sustainability. *Water International*, 27(1), 3–13. <https://doi.org/10.1080/02508060208686972>.

- Kwon, S.Y.; Yoo, M.T., (2021). A study on the dynamic behaviour of a vertical tunnel shaft embedded in liquefiable ground during earthquakes. *Appl. Sci.* 2021, 11, 1560.
- Landwehr, K., & Rhoads, B. L. (2003). Depositional response of a headwater stream to channelisation, East Central Illinois, USA. *River Research and Applications*, 19(1), 77-100. <https://doi.org/10.1002/rra.699>.
- Lane, S.N., Tayefi, V., Reid, S.C., Yu, D. and Hardy, R.J., 2007. Interactions between sediment delivery, channel change, climate change and flood risk in a temperate upland environment. *Earth Surface Processes and Landforms: The Journal of the British Geomorphological Research Group*, 32(3), pp.429-446.
- Laville S., (2019). Single-use plastics a serious climate change hazard, study warns, article published by The Guardian on 15 May 2019, accessed on 1 May 2021, available at <https://www.theguardian.com/environment/2019/may/15/single-use-plastics-a-serious-climate-change-hazard-study-warns>.
- LawTeacher (2013). The main problems of Environmental Impact Assessment (EIA). [online]. Available from: <https://www.lawteacher.net/free-law-essays/international-law/the-main-problems-of-environmental-impact-assessment-international-law-essay.php?vref=1>. [Accessed 5 March 2023].
- Leal Filho, W., Hunt, J., Lingos, A., Platje, J., Vieira, L.W., Will, M. and Gavrilitea, M.D. (2021). The Unsustainable Use of Sand: Reporting on a Global Problem. *Sustainability*, [online] 13(6), p.3356. doi <https://doi.org/10.3390/su13063356>.
- Lee, J.H., (2017). Influence of concrete strength combined with fibre content in the residual flexural strengths of fibre-reinforced concrete. *Compos. Struct.* 2017, 168, 216–225.
- Leeds County Council. 2015. Strategic Flood Investigation Report under Section 19 of the Flood and Water Management Act 2010, Storm Eva flood event, 25-29 December 2015. [Online]. [Accessed 21 September 2023]. Available

from:

<http://opendata.leeds.gov.uk/downloads/flooding/S19InvestigationReport2015.pdf>.

- Leedsbeckett.ac.uk. (2021). Risk Register Documents. [online] Available at: <https://www.leedsbeckett.ac.uk/our-university/public-information/regulatory-compliance-and-assurance/risk-management/> [Accessed 30 Oct. 2023].
- Lei, M., Peng, L., Shi, C. and Wang, S. (2013). Experimental study on the damage mechanism of tunnel structure suffering from sulfate attack. *Tunnelling and Underground Space Technology*, 36, pp.5–13. doi:10.1016/j.tust.2013.01.007.
- Leika et al., 2000. DESIGN OF SPRAYED CONCRETE FOR UNDERGROUND SUPPORT 2. (n.d.). Available at: <https://tunnel.ita-aites.org/media/k2/attachments/public/recommendations%20AFTES%20sprayed%20concrete.pdf> [Accessed 5 Nov. 2023].
- Li, T., Li, J. and Zhang, D.D. (2020). Yellow River flooding during the past two millennia from historical documents. *Progress in Physical Geography: Earth and Environment*, 44(5), pp.661–678. doi:<https://doi.org/10.1177/0309133319899821>.
- Liu, K., Mo, L., Deng, M. and Tang, J. (2015). Deterioration mechanism of Portland cement paste subjected to sodium sulfate attack. *Advances in Cement Research*, 27(8), pp.477–486. doi:10.1680/adcr.14.00051.
- Liu, Y., Liu, H., Chen, Y., Gang, C. and Shen, Y. (2022). Quantifying the contributions of climate change and human activities to vegetation dynamics in China based on multiple indices. *Science of The Total Environment*, 838, pp.156553–156553. doi <https://doi.org/10.1016/j.scitotenv.2022.156553>.
- Inkoom S, Sobanjo J, Barbu A, Niu X (2019) Prediction of the crack condition of highway pavements using machine learning models, *Struct. Infrastruct. Eng* 15: 940-953,

- Lupien, J.R. (2020). Executive Summary. Asia Pacific Journal of Clinical Nutrition, 11(1), pp.S97–S97. doi <https://doi.org/10.1046/j.1440-6047.11.s.6.6.x>.
- Lusiagustin, V.; Kusratmoko, E. Impact of Sand Mining Activities on the Environmental Condition of the Komerling River, South Sumatera. Int. Symp. Curr. Prog. Math. Sci. 2016, 1862, 30–198.
- Mahajan, B. (2020). Water-Cement Ratio And Concrete Strength: Formula & Calculation. [online] Available at: <https://civiconcepts.com/blog/water-cement-ratio#:~:text=Water%20cement%20ratio%20is%20a%20measure%20of%20the>. [Accessed 13 Jun. 2024].
- Mahajan, B. (2021). Concrete Mix Ratio | Concrete Ratio | Concrete Proportions | Concrete Mix Ratio Table | Concrete Grade Ratio | Concrete Mix Design Ratio - Civiconcepts. [online] civiconcepts.com. Available at: <https://civiconcepts.com/blog/concrete-mix-ratio>.
- Malik MI, Ahmad F (2014) Flood Inundation Mapping and Risk Zoning of the Swat River Pakistan using HEC-RAS Model. Lasbela Univ J Sci Technol 13:45–52.
- Malesev M., Radonjanin V. and Marinkovic S. (2010) Recycled concrete as aggregate for structural concrete production. Sustainability, 2, pp. 1204-1225.
- Mainpac.com, (2023). Available at: https://mainpac.com/wp-content/uploads/2019/06/108365355_I-e1560503798667.jpg. [Accessed 11 Dec. 2023].
- Mansour, M.A.; Ismail, M.H.B.; Imran Latif, Q.B.a.; Alshalif, A.F.; Milad, A.; Bargi, W.A.A. A Systematic Review of the Concrete Durability Incorporating Recycled Glass. Sustainability 2023, 15, 3568. <https://doi.org/10.3390/su15043568>.
- Maria et al., (2019). C.G. Juenger, Ruben Snellings, Susan A. Bernal 'Supplementary cementitious materials: New sources, characterisation, and performance insights', Cement and Concrete Research, 122, pp257-273.

- Marchand, J., Skalny, J.P. and Odler, I. (2019). Sulfate Attack on Concrete. [online] Google Books. CRC Press. Available at: https://books.google.co.uk/books/about/Sulfate_Attack_on_Concrete.html?id=kIByygEACAAJ&redir_esc=y [Accessed 9 Dec. 2023].
- Marinković SB, Malešev M, Ignjatović I (2014) 11 Life cycle assessment (LCA) of concrete made using recycled concrete or natural aggregates. In: Eco-Efficient construction and building materials, pp 239–266.
- Martinelli E, Caggiano A, Xargay H. An experimental study on the post-cracking behaviour of hybrid industrial/recycled steel fibre-reinforced concrete. *Construct Build Mater* 2015;94:290–8.
- Martinelli E, Caggiano A, Xargay H., (2015). An experimental study on the post-cracking behaviour of hybrid industrial/recycled steel fibre-reinforced concrete. *Construct Build Mater* 2015;94:290–8.
- Mather, A.S. & Chapman, K. (1995). *Environmental Resources*. ISBN 9780582101685
- Mathwave EasyFit 5.6 Pro (2019): 1-month Trial version provided by www.mathwave.com, downloaded on 6 July 2019
- McCarthy, M.J. and Dyer, T.D. (2019). Pozzolanas and Pozzolanic Materials. *Lea's Chemistry of Cement and Concrete*, pp.363–467. doi:10.1016/b978-0-08-100773-0.00009-5.
- McDonald, A., Lane, S.N., Haycock, N.E. and Chalk, E.A. (2004). Rivers of Dreams: on the gulf between theoretical and practical aspects of an upland river restoration. *Transactions of the Institute of British Geographers*, 29(3), pp.257–281. DOI: <https://doi.org/10.1111/j.0020-2754.2004.00314.x>. [Accessed 22 September 2023]. Available at: <https://www.dec.ny.gov/lands/92418.html>.
- Megacity - Wikipedia (2023). Available at <https://en.wikipedia.org/wiki/Megacity>. Retrieved 23 March 2023.
- Mehta PK. Concrete technology for sustainable development. *Concr Int* 1999;21(11):47–52.

- Memon, A.A., Leghari, K.Q., Agha, Khatri, K.L., Syed Attique Shah, Pinjani, K.K., Soomro, R. and Ansari, K. (2013). Design and Evaluation of Dadu Canal Lining for Sustainable Water Saving. *Journal of Water Resource and Protection*, 05(07), pp.689–698.
doi:<https://doi.org/10.4236/jwarp.2013.57069>.
- MFDP (2004). Mississippi Flood Design Project (2004). Public Domain by Wikimedia is available at <https://commons.wikimedia.org/w/index.php?curid=35245766>. [Accessed 25 March 2023].
- Michael M. & John Z (1999): *Materials for Civil and Construction Engineers*, Addison Wesley Longman, Inc., Jeremy P. Ingham, 5 - Concrete, Editor(s): Jeremy P. Ingham, *Geomaterials Under the Microscope*, Academic Press, 2013, Pages 75-120, ISBN 9780124072305, <https://doi.org/10.1016/B978-0-12-407230-5.50013>
(<https://www.sciencedirect.com/science/article/pii/B9780124072305500133>)
- Michael M. & John Z (1999): *Materials for Civil and Construction Engineers*, Addison Wesley Longman, Inc., Jeremy P. Ingham, 5 - Concrete, Editor(s): Jeremy P. Ingham, *Geomaterials Under the Microscope*, Academic Press, 2013, Pages 75-120, ISBN 9780124072305, <https://doi.org/10.1016/B978-0-12-407230-5.50013>
(<https://www.sciencedirect.com/science/article/pii/B9780124072305500133>)
- Miller, N. (2021). The industry creates a third of the world's waste. [online] [www.bbc.com](https://www.bbc.com/future/article/20211215-the-buildings-made-from-rubbish). Available at: <https://www.bbc.com/future/article/20211215-the-buildings-made-from-rubbish>.
- Millington N, Das S, Simonovic SP (2011) The Comparison of GEV, Log-Pearson Type 3 and Gumbel Distributions in the Upper Thames River Watershed under Global Climate Models. Available at <http://ir.lib.uwo.ca/wrrr/40/>.

- Millward-Hopkins, J., Zwirner, O., Purnell, P., Velis, C.A., Iacovidou, E. and Brown, A. (2018). Resource recovery and low carbon transitions: The hidden impacts of substituting cement with imported 'waste' materials from coal and steel production. *Global Environmental Change*, 53, pp.146–156. doi <https://doi.org/10.1016/j.gloenvcha.2018.09.003>. Ecocem GGBS. [online] Available at: <https://www.ecocemglobal.com/en-gb/products-projects/ecocem-ggbs/>. [Accessed 29 November 2023].
- Mineral Processing & Metallurgy. (2015). Difference Between XRF and XRD. [online] Available at: <https://www.911metallurgist.com/blog/difference-between-xrf-and-xrd>.
- Mineral Products Association (2007) Embodied CO₂ of UK Cement, additions and cementitious material fact Sheet 18 [Part 1], p. 8.
- Ministry of MSME India, 63rd Annual Report Coir Board, New Delhi, 2017. How coir is made - material, making, history, used, processing, product, industry, machine, History Archived 2006-07-14 at the Wayback Machine available at <http://www.madehow.com, 2019/Volume-6/Coir.html>.
- Mississippi River | Map, Length, History, Location (2023). Available at: <https://www.mississippiriverinfo.com/wp-content/uploads/2013/07/Large-Map-Of-The-Mississippi-River.jpg>. [Accessed 15 March 2023].
- Mississippi River drainage basin (2023). Available at: https://upload.wikimedia.org/wikipedia/commons/3/39/Mississippi_River_lee_ma. [Accessed 15 March 2023].
- Mississippi River Historical Pictures are available at www.mshistorynow.mdah.ms.gov/images/214.jpg. [Accessed 15 March 2023].
- Mississippi River improvement (2004), published in Military History Brief 2004 by US Army Corps of Engineers, available at Public Domain <http://www.hq.usace.army.mil/history/Brief/05-growing-nation/River-improvement-lq.jpg>,

and

<https://en.wikipedia.org/w/index.php?curid=17524944>, retrieved 3 March 2023.

- Mohammadi Y, Carkon-AR, Singh SP, Kaushik SK (2009) Impact re-resistance of steel fibrous concrete containing fibres of mixed aspect ratio. *Construct Build Mater* 23(1): 183-189.
- Mohammadi, Y., Carkon-Azad, R., Singh, S.P., Kaushik, S.K., (2009) Impact resistance of steel fibrous concrete containing fibres of mixed aspect ratio. *Construct Build Mater* 23(1): 183-189.
- Mohammed BH, Sherwani AFH, Faraj RH, Qadir HH, Younis KH. Mechanical properties and ductility behaviour of ultra-high performance fibre reinforced concrete effect of low water-to-binder ratios and micro glass fibres. *Ain Shams Engineering Journal* 2021. In press, <https://www.sciencedirect.com/science/article/pii/S2090447921000046>.
- Mohammed, S.I. and Najim, K.B. (2020). Mechanical strength, flexural behaviour and fracture energy of Recycled Concrete Aggregate self-compacting concrete. *Structures*, 23, pp.34–43. doi:<https://doi.org/10.1016/j.istruc.2019.09.010>.
- Mohsin RU, (2016). Water Resource Potential of Pakistan – Challenges and Opportunities, Country Water Assessment workshop Beijing, China 21-25 June 2016.
- Molina N.E, Trolle D, Martínez-P.S., Sastre M.A., Jeppesen E. Hydrological and water quality impact assessment of a Mediterranean limo-reservoir under climate change and land use management scenarios. *J Hydrol.* 2014;509:354–66.
- Moon, H.-Y., Lee, S.-T. and Kim, S.-S. (2003). Sulphate resistance of silica fume blended mortars exposed to various sulphate solutions. *Canadian Journal of Civil Engineering*, 30(4), pp.625–636. doi:<https://doi.org/10.1139/I03-024>.
- Mulongu, P.L. and Ekolu, S.O. (2013a). Kinetic model to predict cement susceptibility to delayed ettringite formation. Part 1: Theoretical concept.

- Magazine of Concrete Research, 65(10), pp.629–639. doi: <https://doi.org/10.1680/mac.12.00184>. (Mulongo and Ekoru, 2013)
- Mulongo, P.L. and Ekoru, S.O. (2013b). Kinetic model to predict cement susceptibility to delayed ettringite formation. Part 2: Model validation and application. Magazine of Concrete Research, 65(10), pp.640–646. doi:<https://doi.org/10.1680/mac.12.00183>.
- Moon H.Y., Lee S.T., and Kim S.S., "Sulphate resistance of silica fume blended mortars exposed to various sulphate solutions," Canadian Journal of Civil Engineering, vol. 30, pp. 625-636, 2003.
- Morgan W. (1995). "[Reinforced Concrete](#)". The Elements of Structure. Retrieved 25 April 2021 – via John F. Claydon's website.
- Moynihan, M. (2019). Steel, concrete and climate change - The Institution of Structural Engineers. [online] www.istructe.org. Available at: <https://www.istructe.org/resources/blog/steel-concrete-and-climate-change/>.
- [27] Burridge J., (2020). "How to specify lower carbon concrete," The Institution of Structural Engineers, 2020.
- MPA (2007). Embodied CO₂ of UK Cement, additions and cementitious material. Fact Sheet 18 [Part 1], p. 8, by Mineral Products Association, UK.
- Nadir et al., (2022a). Nadir, H., Ahmed, A., Paul, P., & Mitchell, M. (2022a). Potential of Utilizing Coir, Straw, and Recycled PET Fibres as Sustainable & Economical Alternative in Fibre Reinforced Concrete. *Research and Developments in Materials Science*, 16(5), 1885-1897. doi:[10.31031/RDMS.2022.16.000899](https://doi.org/10.31031/RDMS.2022.16.000899).
- Nadir et al., (2022b). Nadir, H. M., Ahmed, A., Yates, C., & yates, L. (2022b). A Review of the Utilisation of Hydrated Lime (CL-90) in Engineering Applications and its Sustainability Implications. *Journal of Materials and Polymer Science*, 2(3), 1-7.
- Nadir, H. and Ahmed, A & West, J., (2023.). Experimental Investigation of Engineering Properties of Iron-Based Binary and Ternary Pozzolanic

- Supplementary Cementitious Materials. *Journal of Materials and Polymer Science*, 3(1), 1-13. DOI: doi.org/10.47485/2832-9384.1024.
- Nadir, H. and Ahmed, A. (2021). Comparative Evaluation of Potential Impacts of Agricultural and Industrial Waste Pozzolanic Binders on Strengths of Concrete. *Journal of Material Sciences & Manufacturing Research*, pp.1–8. doi:10.47363/jmsmr/2021(2)119.
- Nadir, H. M., & Ahmed, A. (2020). Causes and Monitoring of Delays and Cost Overrun in Construction Projects in Pakistan. *International Journal of Engineering Inventions*, 9(8), 20-33. Retrieved from <http://www.ijejournal.com/papers/Vol9-Issue8/D09082033.pdf>.
- Nadir, H. M., & Ahmed, A. (2021a). Impact of Nitrate Vulnerable Zones and Catchment Sensitive Farming on Water Quality in the UK: Case Study of Ingbrichworth and Scout Dyke Reservoirs. *Research & Development in Material Science*, 14(5), 1610-1619. doi:[10.31031/RDMS.2021.14.000848](https://doi.org/10.31031/RDMS.2021.14.000848).
- Nadir, H. M., & Ahmed, A. (2022a). Hydrological Analysis and Statistical Modelling of Swat River Basin for Flood Risk Assessment. *Advances in Earth & Environmental Science*, 3(4), 1-13.
- Nadir, H. M., & Ahmed, A. (2022b). The Mechanisms of Sulphate Attack in Concrete – A Review. *Modern Approaches on Material Science*, 5(2), 658-670. doi:[10.32474/MAMS.2022.05.000206](https://doi.org/10.32474/MAMS.2022.05.000206).
- Nadir, H. M., & Ahmed, A. (2022c). Elucidating Chemo-Mechanical Synthesis and Microstructural Study on the Performance of Partial Cement-Based Concrete Composites Against Sulphate Attack – A Review. *Research & Development in Material Science*, 18(2), 2065-2078. doi:[10.31031/RDMS.2022.18.000935](https://doi.org/10.31031/RDMS.2022.18.000935).
- Nadir, H. M., & Ahmed, A. (2023a). The Critical Review of the Performance of the EU Water Framework Directive in Improving the Rivers' Water Quality and the Impediments in its Implementation. *Novel Research in Science*, 14(4), 1-7. doi:[10.31031/NRS.2023.14.000843](https://doi.org/10.31031/NRS.2023.14.000843).

- Nadir, H. M., & Carrvick, J. (2019). Impact of Adjacent Land Use, Infrastructure and Urbanization on Water Quality in a River from Headwater to Downstream. *International Journal of Advances in Science Engineering and Technology*, 7(3), 16-23.
- Nadir, H. M., Ahmed, A & West, J., (2023). Experimental Investigation of Engineering Properties of Iron-Based Binary and Ternary Pozzolanic Supplementary Cementitious Materials. *Journal of Materials and Polymer Science*, 3(1), 1-13. DOI: doi.org/10.47485/2832-9384.1024
- Nadir, H. M., Ahmed, A. (2023b). The Critical Review of the Efficacy of the Environmental Impact Assessment (EIA) Process As a Tool Intended to Protect the Environment from Construction Development's Hazards. *Journal of Civil Engineering Research & Technology*, 5(2), 1-7. doi:[10.47363/JCERT/2023\(5\)143](https://doi.org/10.47363/JCERT/2023(5)143).
- Nadir, H., Ahmed, A., Paul, P., & Mitchell, M. (2022). Potential of Utilizing Coir, Straw, and Recycled PET Fibres as Sustainable & Economical Alternative in Fibre Reinforced Concrete. *Research and Developments in Materials Science*, 16(5), 1885-1897. doi:[10.31031/RDMS.2022.16.000899](https://doi.org/10.31031/RDMS.2022.16.000899)
- Nadir, H.M. (2023). Analytic Evaluation of the Case Studies of Rivers and Reservoirs to Review Relative Impacts of Different Pollution Sources on Catchment Level Stream Ecosystems. *Adv Civil Eng Tech*. 5(5). ACET.000622. 2023. DOI: [10.31031/ACET.2023.05.000622](https://doi.org/10.31031/ACET.2023.05.000622).
- Nadir, H.M. (2023). Comparative Assessment of Environmental Distributive Impact of Air Pollution on Least/ Most Deprived Areas of Leeds and London, UK. *Tr Civil Eng & Arch* 4(4)- 2022. TCEIA.MS.ID.000193. DOI: [10.32474/TCEIA.2023.04.000193](https://doi.org/10.32474/TCEIA.2023.04.000193).
- Nadir, H.M., Ahmed, A. and Moshly, I., (2023). Experimental Investigation of Engineering Properties of Iron-Based Binary and Ternary Pozzolanic Supplementary Cementitious Materials.
- Nadir, H. M., et al., (2024). Strategic Integration of Catchment Level Natural and Structural Methods of Sustainable Flood Management: A Case Study of River

- Wharfe Catchment Area. Adv Earth & Env Sci; 5(2):1-11. DOI: <https://doi.org/10.47485/2766-2624.1043>.
- Naghizadeh, A. and Ekolu, S.O., (2017). Pozzolanic Materials and Waste Products for Formulation of Geopolymer Cements in Developing Countries: a Review. Available online at https://www.researchgate.net/publication/321168666_Pozzolanic_Materials_and_Waste_Products_for_Formulation_of_Geopolymer_Cements_in_Developing_Countries_a_Review.
- Najim K.B., Hall M.R., (2013). Crumb rubber aggregate coatings/pre-treatments and their effects on interfacial bonding, air entrapment and fracture toughness in self-compacting rubberised concrete (SCRC), Mater. Struct. 46 (12) (2013) 2029–2043.
- Najimi M., Sobhani J., Ahmadi B., Shekarch M., (2012). An experimental study on durability properties of concrete containing zeolite as a highly reactive natural pozzolan, Construction and Building Materials, Volume 35, 2012, Pages 1023-1033, ISSN 0950-0618, <https://doi.org/10.1016/j.conbuildmat.2012.04.038>. (<https://www.sciencedirect.com/science/article/pii/S0950061812002401>).
- Nanoscience Instruments (2018). Scanning electron microscopy - nanoscience instruments. [online] Nanoscience Instruments. Available at: <https://www.nanoscience.com/techniques/scanning-electron-microscopy/>.
- NASA (1993) Mississippi River flood 1993. available at: <https://earthobservatory.nasa.gov/images/5422/great-flood-of-the-mississippi-river-1993>. [Accessed 15 March 2023].
- Natarajan, S., Ravichandran, N., Basha, N.A.S. and Ponnusamy, N. (2020). Partial Replacement of Fine Aggregate by Using Glass Powder. IOP Conference Series: Materials Science and Engineering, 955, p.012050. doi <https://doi.org/10.1088/1757-899x/955/1/012050>.

- National Center for Biotechnology Information (2023). PubChem Compound Summary for CID 971, Oxalic Acid. Retrieved January 7, 2023, from <https://pubchem.ncbi.nlm.nih.gov/compound/Oxalic-Acid>.
- Nazari, A. and Sanjayan, J.G. (2016). Handbook of Low Carbon Concrete. [online] Google Books. Butterworth-Heinemann. Available at: https://books.google.co.uk/books/about/Handbook_of_Low_Carbon_Concrete.html?id=3m1_CwAAQBAJ&redir_esc=y. [Accessed 4 December 2023].
- NDMA., 2010. NDMA Annual Report. The Natural Disaster Management Authority. Government of Pakistan; 2010. Available at: www.ndma.gov.pk.
- Nehdi M., Pardhan M., and Koshowski S., (2004). "Durability of self-consolidating concrete incorporating high-volume replacement composite cement," Cement and Concrete Research, vol. 34, pp. 2103-2112, 2004.
- NEPA, (1970). United States. National Environmental Policy Act of 1969. Pub.L. 91–190, Approved 1 January 1970. Available at: <https://www.energy.gov/nepa/articles/national-environmental-policy-act-1969>. [Accessed 5 March 2023].
- Neville AM (2011) Properties of Concrete, 5th Edn, Longman Essex (UK), ISBN: 978-0-273-75580-7 (pbk.). <http://www.pearsoned.co.uk>.
- Neville, A. (2004). The confused world of sulfate attack on concrete. Cement and Concrete Research, 34(8), pp.1275–1296. doi:10.1016/j.cemconres.2004.04.004.
- Neville, A.M. and Brooks, J.J. (2010). Concrete Technology. [online] Google Books. Prentice Hall. Available at: https://books.google.co.uk/books/about/Concrete_Technology.html?id=iVr8QQAACAAJ&redir_esc=y. [Accessed 8 Dec. 2023].
- NFPP IV, (2018). National Flood Protection Plan-IV Final, 2018 by Federal Flood Commission Government of Pakistan, available at <https://www.mowr.gov.pk/wp-content/uploads/2018/05/National-Flood-Protection-Plan-IV-NFPP-IV-1.pdf>.

- NHCP, (2022). Notice of Proposed Changes to the National Handbook of Conservation Practices for the Natural Resources Conservation Service] proposed full text for practice standard code 468. (2022). Available at: <https://www.nrcs.usda.gov/sites/default/files/2022-12/468-NHCP-CPS-Lined-Waterway-or-Conveyance-Channel.pdf> [Accessed 5 Nov. 2023].
- Nitin T., Neelima S. (2020) An experimental study on the behaviour of lime and silica fume treated coir geotextile reinforced expansive soil subgrade International Journal Engineering Science and Technology Journal 23 (2020) P:1214-1222 available at: <https://www.researchgate.net/publication/338495052>,
- Nkomo N.Z., Masu L.M. and Nziu P.K. (2022) Effects of polyethylene terephthalate fibre reinforcement on mechanical properties of concrete. Advances in Materials Science and Engineering. <https://www.hindawi.com/journals/amse/2022/4899298/>.
- Nkomo N.Z., Masu L.M. and Nziu P.K. (2022) Effects of polyethylene terephthalate fibre reinforcement on mechanical properties of concrete. Advances in Materials Science and Engineering. <https://www.hindawi.com/journals/amse/2022/4899298/>.
- NMRM (2018). National Mississippi River Museum, 2018, available at http://www.shootforthemoon.com/our_work/river-museum-expansion/. Retrieved 3 March 2023.
- North Yorkshire County Council 2017. Flood Investigation Report, Tadcaster. [Online]. [Accessed 18 September 2023]. Available from: <https://www.northyorks.gov.uk/sites/default/files/fileroot/Environment%20and%20waste/Flooding/Tadcaster%20S19%20Version%204%20final%20for%20public%20ation.pdf>.
- Northern Sheet Piles Ltd. (n.d.). Home. [online] Available at: <https://www.northernsheetpiles.co.uk, 2021>. [Accessed 2 Oct. 2023].

- NP&EIA, (2016). EU Commission on Environment available at http://ec.europa.eu/environment/legal/law/2/module_3, Retrieved 3 March 2023.
- NRFA, (2015). National River Flow Archive. (2015). How are Flows Measured? [online] Available at: <https://nrfa.ceh.ac.uk/how-are-flows-measured>. (National River Flow Archive, 2015)
- O'Dogherty MJ, Huber JA, Dyson J, Marshall CJ (1995) A study of wheat straw's physical and mechanical properties. Journal of Agricultural Engineering Research 62(2): 133-142.
- Oates J.A.H., Projet de., (1998). Lime and Limestone – Chemistry and Technology, Production and Uses. Wiley-VCH, [ISBN 3-527-29527-5](#) (1998)
- Oates, T., (2010). "Lime and Limestone". Kirk-Othmer Encyclopedia of Chemical Technology:doi:10.1002/0471238961.1209130507212019.a01.pub3. ISBN 978-0471238966.
- Obinna, U. (2023). Carbon Footprint of Reinforced Concrete Structures - Structville. [online] Available at: <https://structville.com/carbon-footprint-of-reinforced-concrete-structures>.
- OCO Technology, (2022). "Sustainable Construction Products," 2023. [Online]. Available: <https://oco.co.uk/sustainable-construction-products/>. [Accessed 3 December 2023].
- O'Dogherty M.J., Huber J.A., Dyson J., Marshall C.J., (1995). A Study of the Physical and Mechanical Properties of Wheat Straw, Journal of Agricultural Engineering Research, Volume 62, Issue 2, 1995, Pages 133-142, ISSN 0021-8634, <https://doi.org/10.1006/jaer.1995.1072>. Accessed on 1 May 2021, available at (<https://www.sciencedirect.com/science/article/pii/S0021863485710724>).
- Ogbonna, O.S., Akinlabi, S.A., Nkosinathi Madushele, Adedeji, P.A. and Ekolu, S.O. (2020). Image Segmentation and Particle Size Analysis of Vibratory Disc Milled Titanium Alloy Powder. Lecture notes in mechanical engineering, pp.367–374. doi https://doi.org/10.1007/978-981-15-5753-8_34.

- Ohemeng, EA., and Ekolu, S.O., (2020). Comparative analysis on costs and benefits of producing natural and recycled concrete aggregates: A South African case study. *Case Studies in Construction Materials*. 13. 1 - 13. 10.1016/j.cscm.2020.e00450.
- Oke MO, Aiyelokun OA, (2014). Statistical Approach to Flood Disaster Management and Risk Reduction in Ibu River Basin available at www.researchgate.com assessed in July 2019.
- Ologunorisa TE, Abawua MJ (2005) Flood risk assessment: a review. *App Sci Environ Mgt J* 9(1):57–63
- Oner, A., and Akyuz, S., 2007. An experimental study on optimum usage of GGBS for the compressive strength of concrete. *Cement and Concrete Composites*, 29 (6), 505-514.
- Onuaguluchi, O., Panesar, D.K., (2014) Hardened properties of concrete mixtures containing pre-coated crumb rubber and silica fume. *J Clean Prod* 82: 125-131.
- Orr, J., Gibbons, O. and Arnold, W. (2020). A brief guide to calculating embodied carbon. [online] Available at: <https://www.istructe.org/IStructE/media/Public/TSE-Archive/2020/A-brief-guide-to-calculating-embodied-carbon.pdf>.
- Oscrite Alphaflow 420 Plasticise fact sheet (2014). By Oscrite manufacturer, available at https://www.oscrete.com/uploads/datasheets/2014/01/Alphaflow_420.pdf, Accessed 7 January 2023.
- Oscrite Alphaflow 420 Plasticise fact sheet (2014). By Oscrite manufacturer, available at https://www.oscrete.com/uploads/datasheets/2014/01/Alphaflow_420.pdf, Accessed 7 April 2023.
- Oyetola B.E., Abdulahi M., The use of rice husk ash in low-cost concrete block production. *Leonardo electronic J. Practices and Technol.*, 8 (2006), 58-70.

- Pachideh G. and Gholhaki M. (2019) Effect of pozzolanic materials on mechanical properties and water absorption of autoclaved aerated concrete. Journal of Building Engineering. [Online]. 26 November, pp. 1-7. Available from: <https://doi.org/10.1016/j.jobbe.2019.100856>. Accessed 15 June 2022].
- Paiva H, Velosa.A Cachim. P, Ferreira. V.M. “ Effect of metakaolin dispersion on the fresh and hardened state properties of concrete” Cement and Concrete Research 42 (2012) 607–612.
- Pakistan Bureau of Statistics (2018): KPK regional breakup and population Summary 2018.
- Panda, B., Imran, N.T. and Samal, K. (2020). A Study on Replacement of Coarse Aggregate with Recycled Concrete Aggregate (RCA) in Road Construction. Recent Developments in Sustainable Infrastructure, pp.1097–1106. Doi https://doi.org/10.1007/978-981-15-4577-1_91.
- Panesar, D.K. (2019). Supplementary cementing materials. Developments in the Formulation and Reinforcement of Concrete, pp.55–85. doi:10.1016/b978-0-08-102616-8.00003-4.
- Parashar, A.K., Sharma, P. and Sharma, N. (2022). Effect on the strength of GGBS and fly ash-based geopolymer concrete. Materials Today: Proceedings. doi:10.1016/j.matpr.2022.04.662.
- Parrett (1993). The areal extent of flooding in the Upper Mississippi River Basin during the Great Midwest Flood of 1993.
- Prasad (2019). Non Destructive Testing of Concrete - Structural Guide. [online] Structural Guide. Available at: <https://www.structuralguide.com/non-destructive-testing-of-concrete/>.
- Perlman, H. (2002). pH: Water properties, from the USGS Water-Science School. [online] Usgs.gov. Available at: <https://water.usgs.gov/edu/ph.html>. (2017) 1008–1017, <https://doi.org/10.4236/eng.2017.912060>.
- Perri E.B.L, (1998). Innovative Methods for Levee Rehabilitation published vide USACE Technical Report REMR-GT-26, September 1998.

- Peter B.,(2013), The lime cycle for high-calcium lime available at [https://en.wikipedia.org/wiki/Lime_\(material\)#/media/File:The_lime_cycle.jpg](https://en.wikipedia.org/wiki/Lime_(material)#/media/File:The_lime_cycle.jpg).
- Phoenix Technologies materials properties of PET fibres, (2020). <https://phoenixtechnologies.net/media/371/PET%20Properties%202008.pdf>.
- Pierce, Y., Kumar, S. and B. Niteen (2021). Experimental Studies on Concrete Using the Partial Replacement of Cement by Glass Powder and Fine Aggregate as Manufactured Sand. Lecture notes in civil engineering, pp.545–555. Doi https://doi.org/10.1007/978-981-15-8293-6_45.
- Piringer, H. (2017). Lime Shaft Kilns. Energy Procedia. 120. 75-95. 10.1016/j.egypro.2017.07.156, available at https://www.researchgate.net/publication/319916223_Lime_Shaft_Kilns, [Accessed 20 Jul. 2022].
- Pitchaiah, P.S. Impacts of Sand Mining on Environment—A Review. SSRG Int. J. Geoinform. Geol. Sci. 2017, 4, 1–5.
- Plate, E.J., 2000, September. Flood management as part of sustainable development. In Proc. International Symposium on Flood Defence. Universität–Gesamthochschule Kassel. pp. 20-23.
- Plate, E.J., 2002. Flood risk and flood management. Journal of Hydrology, 267(1-2), pp. 2-11.
- PMD, (2019). Historical Annual Rainfall and Discharge Data was collected and compiled from the Flood Forecasting Division of the Pakistan Meteorological Department in Lahore in 2019.
- Powers, T.C. & Steinour, H.H. 1955, "An interpretation of some published researches on the alkali-aggregate reaction. Part 1 - The chemical reactions and mechanism of expansion", J.Am.Concr.Inst., no. 6, pp. 497-516.
- Prabakar, J. & Sridhar, R. (2002). Effect of random inclusion of sisal fibre on strength behaviour of soil. Construction and Building Materials, 16, No. 2, 123–131.

- Pradhan, D. & Dutta, D. (2013). Effects of Silica Fume in Conventional Concrete. International Journal of Engineering Research and Applications. 3(5).
- Prasanna, P.K., Srinivasu, K. and Murthy, A.R., 2019. Compressive Strength Assessment using GGBS and Randomly Distributed Fibers in Concrete. International Journal of Innovative Technology and Exploring Engineering, 9 (2), 1078-1086.
- Prashanth, M., Gokul, V., and Shanmugasundaram, M. (2019). Investigation on Ferrock-Based Mortar an Environment-Friendly Concrete. SSRN Electronic Journal. doi:10.2139/ssrn.3461209.
- Premalatha, P., Vinodh, K., Anto, L. and Nithiya, R. (2016). Properties of Palm Ash Concrete. [online] Available at: [https://www.ijesi.org/papers/Vol\(5\)8/version-2/D0508022932.pdf#:~:text=Replacement%20of%20cement%20by%20palm%20ash%20in%20concrete](https://www.ijesi.org/papers/Vol(5)8/version-2/D0508022932.pdf#:~:text=Replacement%20of%20cement%20by%20palm%20ash%20in%20concrete). [Accessed 13 Jun. 2024].
- Prevention Web, 2008. Europe - disaster statistics. Accessed on 10th January 2015 at http://www.preventionweb.net/english/countries/statistics/index_region.php?rid
- Price C. (2018). US Army Corps of Engineers Plan to Deepen the Mississippi River to 50 Feet, published by Biz The Magazine Neo Orleans February 2018.
- PRODYOGI. (2018). Bogue Compounds- Hydration Reactions. [online] Available at: <https://www.prodyogi.com/2018/03/bogue-compounds-hydration-reactions.html>. [Accessed 19 Jun. 2022].
- Properties of Polypropylene by Synthetic Fibres, (2020) available at <http://syntechfibres.com/polypropylene/properties-of-polypropylen-fibres/>.
- Published 3 August 1995, by Routledge.
- Purnell, P. (2013). The carbon footprint of reinforced concrete. Advances in Cement Research, 25(6), pp.362–368. doi:https://doi.org/10.1680/adcr.13.00013.

- Qadir, H.H., Faraj, R.H., Sherwani, A.F.H., Mohammed, B.H., Younis, K.H. (2020) Mechanical properties and fracture parameters of ultra-high performance steel fibre reinforced concrete composites made with extremely low water per binder ratios. *SN Applied Sciences* 2(9): 1-12.
- Qi, H., and Altinaker, MS. 2011. A GIS-based decision support system for integrated flood management under uncertainty with two-dimensional numerical simulations. *Environmental Modelling and Software*. 26. Pp. 817-821.
- Ragab, A.M., Elgammal, M.A., Hodhod, O.A. and Ahmed, T.E. (2016). Evaluation of field concrete deterioration under real conditions of seawater attack. *Construction and Building Materials*, 119, pp.130–144. doi:10.1016/j.conbuildmat.2016.05.014.
- Rahman AS, Rahman A, Zaman MA, Haddad K, Ahsan A, Imtiaz M (2013) A study on selection of probability distributions for at-site flood frequency analysis in Australia. *Nat Hazards* 69:1803–1813.
- Rajesh V, Patel M, Hardik J Solanki on “Development of Carbon Negative Concrete by using Ferrock”, *IJSRSET* (2018).
- Rajkumar. M.R., (2017) Recent Advances in Materials, Mechanics and Management, in 3rd Int. Conf. Mater. Mech. Manag., Trivandrum (India), 2017: p. 450.
- Ramujee, K., (2018). ‘Strength Properties of Polypropylene Fibre Reinforced Concrete.’ (2018). *International Journal of Engineering Research and Advanced Technology*. doi:10.7324/ijerat.2018.3199.
- Rao DK, Raju GP, Sowjanya C, Rao JP (2009) Laboratory studies on the properties of stabilised marine clay from Kakinada Sea Coast, India. *International Journal of Engineering Science and Technology* 3(1): 422- 428.
- Rashid H., Ali K.M, Ahmed U.T., Durability of mortar in the presence of rice husk ash, *World Academy Sci. Eng. and Technol.*, 43 (2010), 736-739.

- Raven, E.K., Lane, S.N., Ferguson, R.I. and Bracken, L.J., 2009. The spatial and temporal patterns of aggradation in a temperate, upland, gravel-bed river. *Earth Surface Processes and Landforms*, 34(9), pp.1181-1197.
- Rehan R., Nehdi M. (2005). Carbon dioxide emissions and climate change: policy implications for the cement industry, doi:10.1016/j.envsci.2004.12.006, *Environmental Science & Policy* 8 (2005) 105–114, available at www.elsevier.com/locate/envsci.
- Reid, S.C., Lane, S.N., Berney, J.M. and Holden, J., 2007. The timing and magnitude of coarse sediment transport events within an upland, temperate gravel-bed river. *Geomorphology*, 83(1-2). pp.152-182.
- Relief Web, (2015). Accumulated Rainfall Map Pakistan is available at <https://reliefweb.int/sites/reliefweb.int/files/resources/ACCUMULATED%20RAINFALL>.
- Ren, F., Mo, J., Wang, Q. and Ho, J.C.M. (2022). Crumb rubber as a partial replacement for fine aggregate in concrete: An overview. *Construction and Building Materials*, [online] 343, p.128049. doi <https://doi.org/10.1016/j.conbuildmat.2022.128049>.
- Renard B, Kochanek K, Lang M, Garavaglia F, Paquet E, Neppel L, Najib K, Carreau J, Arnaud P, Aubert Y (2013) Data-based comparison of frequency analysis methods: a general framework. *Water Resour Res* 49(2):825–843.
- Riaz S, (2012). Flood Hazard Assessment during Monsoon Floods of 2010: Case Study of Charsadda and Nowshera districts. *International Poster Journal of Science and Technology*. 2012;1(1):7.
- Richard W. S (1995). ["History of Concrete"](#) (PDF). The Aberdeen Group. Archived from [the original](#) (PDF) on 28 May 2015. Retrieved 25 April 2021.
- River flooding – Geography for 2018 and beyond available at www.geographypod.com, 2018.
- Robert R.B., (2008). History Repeats: The Great Flood of 1993. [online] livescience.com. Available at: <https://www.livescience.com/7508-history-repeats-great-flood-1993.html>.

- Rohit, P & Sk, Alisha & Varma, P. (2021). Partial Replacement of Fine Aggregate with Crumb Rubber in Concrete. *The International Journal of Analytical and Experimental Modal Analysis*, ISSN NO:0886-9367, page 3161-3163, vol 12, issue 7, published July 2021.
- Rosenbalm, D. and Zapata, C.E. (2017). Effect of Wetting and Drying Cycles on the Behavior of Compacted Expansive Soils. *Journal of Materials in Civil Engineering*, 29(1). doi:[https://doi.org/10.1061/\(asce\)mt.1943-5533.0001689](https://doi.org/10.1061/(asce)mt.1943-5533.0001689).
- Rossi B., Marique A.-F., Reiter S. (2012): Life-cycle assessment of residential buildings in three different European locations, case study, *Build. Environ.* 51 (2012):402-407.
- Rowhani A., Rainey T., Scrap tyre management pathways and their use as a fuel—a review, *Energies* 9 (11) (2016) 888.
- Rowinski PM, Strupczewski WG, Singh VP (2002) A note on the applicability of log-Gumbel and log-logistic probability distributions in hydrological analyses: I. Available pdf. *Hydrol Sci J* 47(1):107–122.
- Rowland, C.S.; Morton, R.D.; Carrasco, L.; McShane, G.; O'Neil, A.W.; Wood, C.M. (2007) Land Cover Map. 2015 (vector, GB). NERC Environmental Information Data Centre.[Online]. [Accessed 25 September 2023]. Available from: <https://digimap.edina.ac.uk/os>.
- Roy, D. K. (2012). Effect of Partial Replacement of Cement by Silica Fume on Hardened Concrete. *International Journal of Emerging Technology and Advanced Engineering*, 2(8), 472-475.
- Royal Society A: Mathematical, Physical and Engineering Sciences, [online] 473(2199), p.20160706. doi:<https://doi.org/10.1098/rspa.2016.0706>.
- Ruiz HA, Ruzene DS, Silva DP, Teixeira JA (2011) Evaluation of a hydrothermal process for pretreatment of wheat straw-effect of particle size and process conditions. *Journal of Chemical Technology & Biotechnology* 86(1): 88-94.

- Rukzon S., Chindaprasirt P., Mahachai R., Effect of grinding on chemical and physical properties of rice husk ash, *Int. J. of Minerals, Metallurgy and Mater.*, 16, 2 (2009), 242-247.
- Rulfova Z, Buishand A, Roth M, Kysely J (2016). A two-component generalised extreme value distribution for precipitation frequency analysis. *J Hydrol* 534:659–668.
- Sabir B.B, Wild S, Bai J, “Metakaolin and calcined clay as pozzolans for concrete :a review” *Cement and concrete composite* 23,(2001),pp.441-454.
- Sagastume Gutiérrez, A., Van Caneghem, J., Cogollos Martínez, J.B. and Vandecasteele, C. (2012). Evaluation of the environmental performance of lime production in Cuba. *Journal of Cleaner Production*, 31, pp.126–136. doi:10.1016/j.jclepro.2012.02.035.
- Saghafian B, Golian S, Ghasemi A (2014) Flood frequency analysis based on simulated peak discharges. *Nat Hazards* 71:403–417.
- Saikia, N., De-Brito, J., (2012) Use of plastic waste as aggregate in cement mortar and concrete preparation: a review. *Construct Build Mater* 34: 385-401.
- Sakai, Y., Nakamura, C. and Kishi, T., 2013. Correlation between Permeability of Concrete and Threshold Pore Size obtained with Epoxy-Coated Sample. *Journal of Advanced Concrete Technology*, 11 (8), 189-195.
- Saleh AA, (2011). Developing an empirical formula to estimate rainfall intensity in Riyadh region, published by *Journal of Engineering Sciences King Saud University* 2011 Volume 23 Page 81-88 ISSN 1018-3639.
- Samad, S., Shah, A. and Limbachiya, M.C., 2017. Strength development characteristics of concrete produced with blended cement using ground granulated blast furnace slag (GGBS) under various curing conditions. Springer Science and Business Media LLC.
- Santhanam M, Cohen M.D., Olek J., (2002). Mechanism of sulfate attack: a fresh look: part 1: summary of experimental results, *Cem. Concr. Res.* 32.6 (2002) 915–921.

- Santhanam, M. and Otieno, M. (2016). Deterioration of concrete in the marine environment. *Marine Concrete Structures*, [online] pp.137–149. doi:10.1016/b978-0-08-100081-6.00005-2.
- Sarah S., Barbara L., Tilo P., Andreas B., Frank W., (2020), Effect of relative humidity on the carbonation rate of portlandite, calcium silicate hydrates and ettringite, *Cement and Concrete Research*, Volume 135, 2020, 106116, ISSN 0008-8846, <https://doi.org/10.1016/j.cemconres.2020.106116>. (<https://www.sciencedirect.com/science/article/pii/S0008884620301204>)
- Satyanarayana K.G., Kulkarni A.G. and Rohatgi P.K. 1981; Structure and properties of coir fibres, Regional Research Laboratory, Trivandrum, Proc. Indian Acad. Sci. (Engg. Sci.) Vol. 4, Pt. 4, December 1981, pp. 419-436.
- Saurav, C. (2021). Stress-Strain Curve: Definition, Formula, Relation, Hooke's Law. Embibe Exams. [online] Available at: <https://www.embibe.com/exams/stress-strain-curve/>.
- Schleifstein M, (2011). The Times-Picayune. Mississippi River flooding in the New Orleans area could be massive if the Morganza spillway stays closed; available at <https://www.nola.com/news/weather/>.
- Science
- Scottish Gov (2016). Scottish Environmental Impact Assessment regulations: consultation, Published by Energy and Climate Change Directorate 9 August 2016 ISBN: 9781786523778.
- Scribd. (2018.). Hydration of Cement | PDF. [online] Available at: <https://www.scribd.com/presentation/436064664/Hydration-of-Cement>, [Accessed 19 Jun. 2022].
- Scribd. (2023). Application of Unit Hydrograph To Derive Runoff Hydrograph | PDF | Microsoft Excel | Hydrology. [online] Available at: <https://www.scribd.com/document/394224482/Application-of-Unit-Hydrograph-to-Derive-Runoff-Hydrograph> [Accessed 6 Nov. 2023].

- Scrivener et al., (2018). Scrivener K., Martirena F., Bishnoi S. and Maity S., (2018) "Calcined clay limestone cement," in Cement and Concrete Research, 2018.
- Scrivener, K., (2018). Lectures on Lowering Environmental Impact – Cement chemistry and sustainable cementitious materials are available online at <https://www.youtube.com/watch?v=HN-EyRPW65s>.
- Sebastiaan N. Jonkman, Hessel G. Voortman, Wouter Jan Klerk & Saskia van Vuren (2018). Developments in the management of flood defences and hydraulic infrastructure in the Netherlands, Structure and Infrastructure Engineering, 14:7, 895-910, DOI:10.1080/15732479.2018.1441317.
- Section 44. (2016). Online [Accessed 5 Nov. 2023]. Available at: <https://saccountyspecs.saccounty.gov/Documents/PDF%20Documents%202016/Specifications/Section%2044.pdf>.
- Selvapriya1 R., (2019). Silica fume as Partial Replacement of Cement in Concrete, International Research Journal of Multidisciplinary Technovation (IRJMT), ISSN 2582-1040.
- Sentucq, E. and Clayton, M. (2021). "Beyond Portland cement: Low-carbon alternatives," The Institution of Structural Engineers. Beyond Portland cement: Low-carbon alternatives - The Institution of Structural Engineers. [online] Available at: <https://www.istructe.org/resources/guidance/beyond-portland-cement-low-carbon-alternatives/>.
- Shah, M.C., Gupta, K.K., Nainwal, A., Negi, A. and Kumar, V. (2021). Investigation of mechanical properties of concrete with natural aggregates partially replaced by recycled coarse aggregate (RCA). Materials Today: Proceedings. Doi:<https://doi.org/10.1016/j.matpr.2020.12.456>.
- Shahbaz, P.S., Faraj, R.H., (2020) Feasibility study on the use of shell sunflower ash and shell pumpkin ash as supplementary cementitious materials in concrete. Journal of Building Engineering 30: 101271.

- Shahbaz, P.S., Tajara, M.K., Faraj, R.H., Mosavi, A., (2021) Studying the C-H crystals and mechanical properties of sustainable concrete containing recycled coarse aggregate with used nano-silica. *Crystals* 11(2): 122.
- Shahbazpanahi S, Faraj RH., (2020). Feasibility study on the use of shell sunflower ash and shell pumpkin ash as supplementary cementitious materials in concrete. *Journal of Building Engineering* 2020;30:101271.
- Shahbazpanahi S, Tajara MK, Faraj RH, Mosavi A (2021) Studying the C–H crystals and mechanical properties of sustainable concrete containing recycled coarse aggregate with used nano-silica, *Crystals* 11: 122.
- Shandana M., 2012. The Copenhagen Post: Half fear home flooding available at <http://cphpost.dk/news/half-fear-home-flooding.2106.html>.
- Shanmugapriya, T. & Uma R. N.(2013) Experimental Investigation on Silica Fume as partial Replacement of Cement in High-Performance Concrete, *The International Journal of Engineering And Science (IJES)* .2 (5), 40-45.
- Shannag, M.J. and Shaia, H.A. (2003). Sulfate resistance of high-performance concrete. *Cement and Concrete Composites*, 25(3), pp.363–369. doi:10.1016/s0958-9465(02)00049-5.
- Sharma R., Bansal P.P., Use of different forms of waste plastic in concrete-a review, *J. Cleaner. Prod.* 112 (2016) 473-482.
- Sheikh K., F., Natasya M., P., Halim A.G., Bazilah A., N., Juki, M., Shahidan, S. and Haziman, M. (2018). A Utilization of Palm Fuel Ash (POFA) and Ceramic Waste as Cement Materials Replacement in Concrete Production. *International Journal of Engineering & Technology*, 7(3.9), p.89. doi <https://doi.org/10.14419/ijet.v7i3.9.15284>.
- Shirleyana.S & Anindya.S.A. (2012). The emergence of informal riverside settlements and challenges for planning: the case of Kali Mas in Surabaya, Indonesia available at: <https://www.researchgate.net/publication/281765440>.
- Shivani A.B., Nihana N., Gowri A.S. Hasna Jalal , Arjun R., Jinudarsh M.S. P., (2022). Experimental investigation of ferrock by complete and partial replacement of cement in concrete. *International Research Journal of*

Engineering and Technology (IRJET) e-ISSN: 2395-0056 Volume: 09 Issue: 09 | Sep 2022 www.irjet.net. P-ISSN: 2395-0072.

Show D. (2020). Cement || Definition, Introduction, Types, Composition and Tests. [online] Mechanical Notes. Available at: <https://mechanicalnotes.com/cement-definition-introduction-types-composition-and-tests/>, [Accessed 19 Jun. 2022].

Showkati, A.; Salari-rad, H.; Aghchai, M.H., (2021). Predicting long-term stability of tunnels considering rock mass weathering and deterioration of primary support. Tunn. Undergr. Sp. Tech. 2021, 107, 1–15.

Shreeshail B.H, Jaydeep C., Dhanraj P., Amar K. (2014). Effects of coconut fibres on the properties of concrete, IJRET: International Journal of Research in Engineering and Technology, Volume: 03 Issue: 12 | Dec-2014, Available @ <http://www.ijret.org>

Shumuye, Eskinder & JUN, ZHAO. (2018). A Review on Ground Granulated Blast Slag GGBS in Concrete. 5-10. 10.15224/978-1-63248-145-0-14.

Shweta G., Devender S. (2020)., CO2 Sequestration on cement Chapter 6.2.1.1 in Start-Up Creation (Second Edition), 2020, available at <https://www.sciencedirect.com/topics/engineering/tricalcium-silicate#:~:text=When%20the%20maximum%20degree%20of%20supersaturation%20is%20reached%2C,of%20the%20CSH%20formed%20and%20C%2FS%20%3C%202.>

Siddique R. and Klaus J. (2009) Influence of metakaolin on the properties of mortar and concrete: A review. Applied Clay Science. [Online]. 43 (3-4) March, pp. 392-400. Available at: <https://www.sciencedirect.com/science/article/pii/S0169131708002706>. Accessed 26 January 2023.

Siddique R., (2004). Performance characteristics of high-volume class F fly ash concrete. Cem. Concr. Res., 34, 3 (2004), 487-93.

- Sidney M & Francis Y (1981): Concrete, Prentice-Hall, Inc., Englewood Cliffs, NJ, pp. 671.
- Singh, M., Singh, J. and Siddique, R. (2022). Bagasse ash. Sustainable Concrete Made with Ashes and Dust from Different Sources, pp.177–233. doi:10.1016/b978-0-12-824050-2.00001-2.
- Singh, S. K., 2016. Polypropylene Fibre Reinforced Concrete: An Overview. Retrieved from Structural Engineering Division, Central Building Research Institute.
- Singh, R. (2016). ferrock cement. [online] Slideshare.net. Available at: <https://www.slideshare.net/RajbirSingh58/ferrock-cement>.
- Singo LR, Kundu PM, Odiyo JO, Mathivha FI, Nkunan TR (2013) Flood frequency analysis of annual maximum streamflow for Luvuvhu River catchment, Limpopo Province, South Africa. [https:// www.researchgate.net](https://www.researchgate.net).
- Singgu, F., Ekolu, S.O., Naghizadeh, A. and Quainoo, H.A. (2023). Evaluation of metakaolin pozzolan for cement in South Africa. Developments in the Built Environment, [online] 14, p.100154. doi:<https://doi.org/10.1016/j.dibe.2023.100154>.
- Singgu F., Ekolu, S.O., Naghizadeh A and Quainoo, H.A. (2022). Experimental study and classification of natural zeolite pozzolan for cement in South Africa. Journal of The South African Institution of Civil Engineering, 64(4), pp.1–14. doi:<https://doi.org/10.17159/2309-8775/2022/v64n4a1>.
- Sir, B. (2021). Types of concrete grade and their ratio as per British Standard (BS). [online] Civil Sir. Available at: <https://civilsir.com/types-of-concrete-grade-and-their-ratio-as-per-british-standard-bs/#:~:text=According%20to%20British%20standard%2C%20concrete%20grade%20is%20categorised>. [Accessed 8 Oct. 2023].
- Sivakumar Babu, G., Vasudevan, A. & Sayida, M. (2008). Use of coir fibres for improving the engineering properties of expansive soils. Journal of Natural Fibres, 5, No. 1, 61–75.

- Skariah T, B., Yang, J., Bahurudeen, A., Chinnu, S.N., Abdalla, J.A., Hawileh, R.A. and Hamada, H.M. (2022). Geopolymer concrete incorporating recycled aggregates: A comprehensive review—Cleaner Materials, [online] 3, p.100056. doi:10.1016/j.clema.2022.100056.
- Skullestad J.L., Bohne R.A., Lohne J. (2016): High-rise timber buildings as a climate change Mitigation measure - a comparative LCA of structural system alternatives, Energy Procedia 96 (2016):112-123.
- Sky News. (2023). UK's first air capture plant is turned on to remove CO2 from the atmosphere and turn it into jet fuel. [online] Available at: <https://news.sky.com/story/amp/uks-first-air-capture-plant-is-turned-on-to-remove-co2-from-the-atmosphere-and-turn-it-into-jet-fuel-13025531>. [Accessed 9 Dec. 2023].
- Smith, M. & Bentley, S.J. (2015). Sediment capture in flood plains of the Mississippi River: A case study in Cat Island National Wildlife Refuge, Louisiana. Proceedings of the International Association of Hydrological Sciences, 367, pp.442–446.
- Snellings, R.; Mertens G.; Elsen J. (2012). "Supplementary cementitious materials". Reviews in Mineralogy and Geochemistry. 74 (1): 211–278. Bibcode:2012RvMG.74.211S. doi:10.2138/rmg.2012.74.6.
- Soares D, Brito J, de Ferreira J, Pacheco J (2014) Use of coarse recycled aggregates from precast concrete rejects: Mechanical and durability performance. Construct Build Mater 71:263–272.
- Solin, L., and Skubinčan, P. (2013). Flood risk assessment and management: a review of concepts definitions and methods. Geographical Journal. 65. pp.23-44.
- Sotiriadis K., Nikolopoulou E., Tsvilis S., (2012). Sulfate resistance of limestone cement concrete exposed to combined chloride and sulfate environment at low temperature, Cement and Concrete Composites, Volume 34, Issue 8, 2012, Pages 903-910, ISSN 0958-9465,

<https://doi.org/10.1016/j.cemconcomp.2012.05.006>.

(<https://www.sciencedirect.com/science/article/pii/S0958946512001163>)

Sowmya C. (2020). Flexural Strength of Concrete. [online] EngineeringCivil.org.

Available at: <https://engineeringcivil.org/articles/structural-engineering/flexural-strength-of-concrete/>.

Spencer et al., (2023). Spencer Jo, Leonora Pilakoutas (Skanska), Fragkoulis Kanavaris, Magdalena Janota, Orlando Gibbons, Liu Chang, Beth Lockhart, Conor Hayes, George Dalkin, Cameron Creamer, Rogier van Reen. Buildings & Infrastructure Priority Actions for Sustainability Embodied Carbon Concrete. (2023) published by ARUP Reference: 07762000-RP-SUS-0003, 1 June 2023. Available at:

https://www.istructe.org/IStructE/media/Public/Resources/ARUP-Embodied-carbon-concrete_1.pdf.

SRC, (2022). Sulphate Resistant Cement | Standards and Specifications | SRC Grade 42.5. [online] Available at: <http://www.tigercement.com/cement-products/sulphate-resistant-cement/> [Accessed 22 Jun. 2022].

Stefanidou. M, Papachristoforou. M and Kesikidou. F, (2016), Fibre-reinforced lime mortars, Conference paper Historic Mortars Conference held in Greece November 2016

Stelmakh, S.A., Shcherban', E.M., Beskopylny, A., Mailyan, L.R., Meskhi, B., Beskopylny, N. and Zhrebtssov, Y. (2022). Development of High-Tech Self-Compacting Concrete Mixtures Based on Nano-Modifiers of Various Types. Materials, 15(8), p.2739. doi <https://doi.org/10.3390/ma15082739>.

Steve K & William P (1988): Design and Control of Concrete Mixes, Portland Cement Association, Skokie, Ill. pp. 205.

Stewart E.J., Reed D.W., Faulkner D.S., Reynard N.S., 1999. The FOREX method of rainfall growth estimation I: a review of requirement. Hydrol. Earth Syst. Sci. 3 (2), 187–195.

- Stijns, J.-P.C. (2005). Natural resource abundance and economic growth revisited. *Resources Policy*, 30(2), pp.107–130. doi <https://doi.org/10.1016/j.resourpol.2005.05.001>.
- Stone D.,(2010). First Demonstration Structures Using a New, Carbon-negative Building Material. The University of Arizona, pp 1-3, 2010.
- Stone, D., (2017). David Stone's Ferro Rock Rocks! – ArgonPath.com. [online] Available at: <https://argonpath.com/?p=741> [Accessed 11 Dec. 2023].
- Stutzman, P.E., Bullard, J.W. and Feng, P. (2016). Phase Analysis of Portland Cement by Combined Quantitative X-Ray Powder Diffraction and Scanning Electron Microscopy. *Journal of Research of the National Institute of Standards and Technology*, 121, p.47. doi:10.6028/jres.121.004.
- Sudhira, H.S., and Ann Jacob.; Reuse of By-Products in Coir Industry: A Case Study." Internet Conference on Material Flow Analysis of Integrated Bio-Systems (March-October,2000) available at <http://www.ias.unu.edu/proceedings/icibs/ic>.
- Sukontasukkul P., Tiamlom K., Expansion under water and drying shrinkage of rubberised concrete mixed with crumb rubber with different sizes, *Constr. Build. Mater.* 29 (2012) 520–526.
- Sulphate Resistant Cement | Standards and Specifications | SRC Grade 42.5. [online] Available at: <http://www.tigercement.com/cement-products/sulphate-resistant-cement/>, [Accessed 22 Jun. 2022].
- Sundar (2017). Stress-Strain Curve | Stress Strain diagram. [online] Extrudesign. Available at: https://extrudesign.com/stress-strain-curve/?expand_article=1. [Accessed 26 November 2023].
- Suresh, D. and Nagaraju, K. (2015). Ground Granulated Blast Slag (GGBS) in Concrete: A review, *IOSR Journal of Mechanical and Civil Engineering (IOSR-JMCE)* e-ISSN: 2278-1684,p-ISSN: 2320-334X, Volume 12, Issue 4 Ver. VI (Jul. - Aug. 2015), PP 76-82 www.iosrjournals.org.
- Sutton K & Rayan W. 2020, Erosion Control and Slope Stabilization using Coir, Washington University Publications and research available at

- <https://depts.washington.edu/propplnt/Chapters/erosioncontrolchapter%5B1%5D.pdf>. Accessed in September 2020.
- Swain S., Therival R., (2014). "Environmental impacts of civil emergency plans and their exemption from SEA". Journal of Environmental Assessment Policy and Management 16,1450027".
- Swapp S., (2023). By Scribd 2023.Scanning Electron Microscopy (SEM) PDF Scanning Electron Microscope Electron Microscope. [online] Available at: <https://www.scribd.com/document/168386089/Scanning-Electron-Microscopy-SEM> [Accessed 31 Oct. 2023].
- Swider, J.R., (2017). X-ray Diffraction–Solving Problems with Phase Analysis. [online] McCrone. Available at: <https://www.mccrone.com/mm/xray-diffraction-phase-analysis-solutions/>. Accessed on 12 June 2024.
- Synhetex. (2023). Concrete Channel Lining Solutions. [online] Available at: <https://synhetex.com/erosion-and-scour-solutions/channel-lining/> [Accessed 5 Nov. 2023].
- Tahir et al., (2011). Abdu, Tahir & Ibrahim, Tarig & Abdel-Magid, Isam. (2011). Design Considerations of Concrete Lined Channels: Experience of Rawakeeb Research Station. Sudan Academy of Sciences Journal. 4. 1-16.
- Tajima et al., (2016). Tajima R., Gore, T., Fischer, T.B., 2014. Policy integration between environmental assessment and disaster management. Journal of Environmental Assessment Policy and Management 16, 450028.
- Tanveer R., (2016). Orange Line 'not at the cost of heritage sites' Published: 1 February 2016, The Express Tribune Pakistan available at <https://tribune.com.pk/story/1037840/orange-line-not-at-the-cost-of-heritage-sites/>. Retrieved on 10 March 2023.
- Tariq, N. Al-Shafi, Huda, T, Ridha, Maha, Abduljalel, S. (2017). An experimental investigation on the pullout strength of straight steel bars in high-performance concrete. 10.13140/RG.2.2.25316.4288.
- Tarmac. (2023). Snowcrete. [online] Available at: <https://www.en-standard.eu/bs-en-12350-2-2019-testing-fresh-concrete-slump>

- [test/#:~:text=This%20standard%20BS%20EN%2012350-2%3A2019%20Testing%20fresh%20concrete,consistence%20of%20fresh%20concrete%20by%20the%20slump%20test.](#) [Accessed 17 Oct. 2023].
- Tchadjie, L.N. and Ekolu, S.O. (2017). Enhancing the reactivity of aluminosilicate materials toward geopolymer synthesis. *Journal of Materials Science*, 53(7), pp.4709–4733. doi <https://doi.org/10.1007/s10853-017-1907-7>.
- Team, D. (2018). Steel Requirements For RCC Beam, Column, Slab, Foundation, & Lintel. [online] DAILY CIVIL. Available at: <https://dailycivil.com/steel-requirements-rcc-beam-column-slab-foundation-lintel-1/>. [Accessed 9 Nov. 2023].
- Team, E. (2018). Green Building Materials in Ultra-Modern Offices. [online] TerraMai. Available at: <https://www.terramai.com/blog/green-building-materials-ultra-modern-offices/>. [Accessed 11 Dec. 2023].
- Team, G. (2023). Channel Lining: Material dan Perencanaannya - Geosinindo. [online] Tetrasa Geosinindo. Available at: <https://www.geosinindo.co.id/post/channel-lining-fungsi-jenis-material-dan-perencanaannya>. [Accessed 5 Nov. 2023]. (Team, 2023)
- Technology, P. in C., (2010). Types of Sulphate Attack in Concrete- Influences and Sources. [online] The Constructor. Available at: <https://theconstructor.org/concrete/types-sulphate-attack-concrete/5266/>.
- Tenenbaum D.J. (2010). River Health: Finding Fixes published in The Why files: The Science Behind the News by the University Of Wisconsin Board Of Regents in 2010, available at <https://whyfiles.org/2010/river-health-finding-tonics/>.
- Teng S., Afroughsabet V. and Ostertag C.P. (2018) Flexural behaviour and durability properties of high-performance hybrid-fibre-reinforced concrete. *Construction and Building Materials*. [Online]. 182 September, pp. 504-515. Available from: <https://doi.org/10.1016/j.conbuildmat.2018.06.158>. [Accessed 7 June 2022].

- Thakur J., Fischer T.B. (2016). Twenty-five years of the UK EIA System: Strengths, weaknesses, opportunities and threats the UK. *Journal of Environmental Impact Assessment Review* 61 (2016) 19–26.
- The Blue Register (2018). Effects Of Orange Line Metro Train On The Environment Of Lahore published by The Blue Register on 26 July 2018, available at <https://theblueregister.com/effects-of-orange-line-metro-train-on-the-environment-of-lahore/>, retrieved on 3 March 2023.
- The cement's basic molecular structure was finally decoded (MIT, 2009) and Archived on 21 February 2013 at the Wayback Machine.
- The Concrete Centre, (2021). "Specifying Sustainable Concrete - Understanding the Role of Constituent Materials," www.concretecentre.com/publications, 2021.
- The Constructor, (2016). <https://www.facebook.com/TheConstructor> (2016). Sulphate Attack on Concrete - Process and Control of Sulphate Attack. [online] The Constructor. Available at: <https://theconstructor.org/concrete/sulphate-attack-on-concrete-prevention/2162/>.
- The Constructor. (2018). Canal Linings - Types and Advantages. [online] Available at: <https://theconstructor.org/water-resources/canal-linings-types-advantages/11052/>.
- The Flow Partnership. (2021). The Flow Partnership. [online] Available at: <https://www.theflowpartnership.org> [Accessed 2 Oct. 2023].
- The History of Concrete, (2012). Dept. of Materials Science and Engineering, University of Illinois, Urbana-Champaign. Archived from the original on 27 November 2012, retrieved 8 December 2023.
- The Nation, (2016). Restoration work of Munda Headworks Inaugurated, a staff report on 7 January 2016 available at www.nation.com.pk.
- The Upside (2021). Ferrock: A Carbon-Negative Building Material? Available at <https://www.theuptide.com/ferrock-building-material/>. Accessed on 3 January 2023.

- TheConstructor (2017). Fiber Reinforced Concrete - Types, Properties and Advantages. [online] The Constructor. Available at: <https://theconstructor.org/concrete/fiber-reinforced-concrete/150/>.
- Thiel C., Campion N., Landis A., Jones A., Schaefer L., Bilec M., (2013): A materials life cycle assessment of a net-zero energy building, *Energies* 6 (2):1125-1141.
- Thirumalai R., Babu S.S., Naveennayak V., Nirmal, R. Lokesh. G., (2017) A review on stabilisation of expansive soil using industrial solid wastes, *Engineering* 09 (2017) 1008–1017, <https://doi.org/10.4236/eng.2017.912060>.
- Thirumalai, R. Babu, S.S. Naveennayak, V. Nirmal, R. Lokesh, G. A review on stabilisation of expansive soil using industrial solid wastes, *Engineering* 09
- Thomas B.S., Gupta R.C., Kalla P., Cseteneyi L., (2014). Strength, abrasion, and permeation characteristics of cement concrete containing discarded fine rubber aggregates, *Constr. Build. Mater.* 59 (2014) 204–212.
- Thomas Bjorkan. (2011), The limestone quarry at Akselberget, Bronnøy, Norway available at https://commons.wikimedia.org/wiki/File:Limestone_quarry.jpg.
- Thomas BS, Gupta RC. Mechanical properties and durability characteristics of concrete containing solid waste materials. *J Clean Prod* 2013:1–6.
- Thomas M., (2007). Optimising the use of PFA in cement concrete, published by Portland Cement Association USA in 2007, available at https://www.cement.org/docs/default-source/fc_concrete_technology/is548-optimizing-the-use-of-fly-ash-concrete.pdf, (accessed on 1 October 2022).
- Thomason, C. (2019). Hydraulic Design Manual Manual: Hydraulic Design Manual. [online] Available at: <http://onlinemanuals.txdot.gov/TxDOTOnlineManuals/TxDOTManuals/hyd/hyd.pdf> [Accessed 5 Nov. 2023].
- Thorne, C.R, and Warburton, J. (2010). Applied fluvial geomorphology for sustainable flood risk management. [online]. Available from: https://www.researchgate.net/publication/311672979_Applied_fluvial_geom

- orphology_for_sustainable_flood_risk_management. Accessed 19th Nov 18.
Accessed 25 September 2023
- Tian, Z., Ramsbottom, D., Sun, L., Huang, Y., Zou, H. and Liu, J. (2023). Dynamic adaptive engineering pathways for mitigating flood risks in Shanghai with regret theory. *Nature Water*, [online] 1(2), pp.198–208. doi: <https://doi.org/10.1038/s44221-022-00017-w>.
- Timperley, J. (2018). Q&A: Why cement emissions matter for climate change. [online] Carbon Brief. Available at: <https://www.carbonbrief.org/qa-why-cement-emissions-matter-for-climate-change/>.
- Tiseo, I. (2023a). Global CO2 emissions by sector. [online] Statista. Available at: <https://www.statista.com/statistics/276480/world-carbon-dioxide-emissions-by-sector/>.
- Tiseo, I. (2023b). Key figures on glass recycling worldwide from 2018 to 2022, published by Statista on 6 February 2023, are available online at <https://www.statista.com/statistics/1055604/key-figures-glass-recycling-globally/>.
- Tixier R., Mobasher B., Modeling of damage in cement-based materials subjected to external sulfate attack, I: Formulation., *ASCE J. Mater. Civ. Eng* 15 (2003) 305–322.
- Tofiq, F. and Guven, A. (2015). Optimal design of trapezoidal lined channel with least cost: Semi-theoretical approach powered by genetic programming. *Water SA*, 41(4), p.483. doi:<https://doi.org/10.4314/wsa.v41i4.07>. (Tofiq and Guven, 2015)
- Torichigai, T., Seki, K., Watanabe, K. and Sakai, G. (2021). Development and Future of Carbon Negative Concrete that Absorbed CO₂ by Carbonation Curing. *Concrete Journal*, 59(9), pp.813–818. doi:10.3151/coj.59.9_813.
- Torii, K., Taniguchi, K. and Kawamura, M. (1995). Sulfate resistance of high fly ash content concrete. *Cement and Concrete Research*, 25(4), pp.759–768. doi:10.1016/0008-8846(95)00066-I.

- Tuan N.M., Hau Q.V., Chin S. and Park S. (2021) In-situ concrete slump test incorporating deep learning and stereo vision. *Automation in Construction*. [Online]. 121 January, pp. 1-19. Available from: <https://doi.org/10.1016/j.autcon.2020.103432>. [Accessed 3 July 2022].
- Tufail T, Saeed F, Afzaal M (2021) Wheat straw: A natural remedy against different maladies. *Food Science & Nutrition* 9(4): 2335-2344.
- Tufail T, Saeed F, Afzaal M, et al. Wheat straw: A natural remedy against different maladies. *Food Science & Nutrition*. 2021 Apr;9(4):2335-2344. DOI: 10.1002/fsn3.2030.
- Ty-Mawr Lime Industries Ltd (2019), Sustainable building materials for healthier homes, available at <https://www.lime.org.uk/products/lime.html>
- Uday V.S. & Ajitha B. (2017). Concrete Reinforced with Coconut Fibres, Volume 7 Issue No.4 *International Journal of Engineering Science and Computing*, April 2017 <http://ijesc.org/>.
- UKA, (2023). The XRF testing of cement and alternative pozzolanic materials was conducted by UK Analytics and held by Material Science Lab, Leeds Beckett University.
- UKEssays. November 2018. Soil stabilisation with lime in road construction. [online]. Available from: <https://www.ukessays.com/essays/engineering/soil-stabilization-with-lime-in-road-construction-engineering-essay.php?vref=1>. [Accessed 14 July 2022].
- UKGBC. (2023). Embodied Carbon Modelling and Reporting. [online] Available at: <https://ukgbc.org/resources/embodied-carbon-modelling-and-reporting/>. [Accessed 9 Dec. 2023].
- UNCED (1992). The United Nations conference on environment and development (UNCED Report A/CONF151/5/Rev.1, United Nations, New York, 13 June 1992).
- UNEP (2020). Building sector emissions hit record high, but low-carbon pandemic recovery could help transform sector – UN report. [online] UN

- Environment. Available at: <https://www.unep.org/news-and-stories/press-release/building-sector-emissions-hit-record-high-low-carbon-pandemic>.
- UNEP. Single-use plastics: A roadmap for sustainability. United Nations Environment Programme, (2018).
- USACE History (2016). by US Army Corps of Engineers, <https://www.usace.army.mil/About/History/Brief-History-of-the-Corps/The-Growing-Nation/>.
- University of Alberta, (2023). Sample Preparation – EAS X-Ray Diffraction Laboratory – University of Alberta. [online] Available at: <https://cms.eas.ualberta.ca/xrd/sample-preparation/#:~:text=Ideally%2C%20you%20need%20to%20achieve>. Accessed on 12 June 2024.
- USACE, (2008). US Army Corps of Engineers Mississippi River Restoration Report 2008.
- USDA, (2020). Irrigation ditch lining by United States Department of Agriculture. Available at: https://www.nrcs.usda.gov/sites/default/files/2022-09/Irrigation_Ditch_Lining_428_NHCP_CPS_2020.pdf. [Accessed 5 Nov. 2023].
- USDT, (2020). US Department of Transportation. Precast Concrete Segmental Liners for Large Diameter Road Tunnels-Literature Survey and Synthesis; US Department of Transportation: Washington, DC, USA, 2020.
- USGSWSS, (2016). The United States Geological Survey's Water Science School.
- Vashisth, A. (2018). Determination of fineness modulus of coarse aggregates and fine aggregate. 10.13140/RG.2.2.18131.68648, available at: https://www.researchgate.net/publication/323748312_determination_of_fineness_modulus_of_coarse_aggregates_and_fine_aggregate.
- Vashisht P., Paliwal M. C., (2020). Partial Replacement of Cement with Rice Husk Ash in Cement Concrete, International Journal of Engineering

- Research & Technology (IJERT), ISSN: 2278-0181, Vol. 9 Issue 12, December-2020, Published by: <http://www.ijert.org>.
- Vashisht P., Paliwal M. C., (2020). Partial Replacement of Cement with Rice Husk Ash in Cement Concrete, International Journal of Engineering Research & Technology (IJERT), ISSN: 2278-0181, Vol. 9 Issue 12, December-2020, Published by: <http://www.ijert.org>.
- Venkat. k., (2023). Decarbonization Endeavours of The Global Cement Industry. [online] World Construction Today. Available at: <https://www.worldconstructiontoday.com/news/decarbonization-endeavours-of-the-global-cement-industry/>. [Accessed 8 December 2023].
- Victor, O. (2023). Estimating the Embodied Carbon in Structures. [online] STRUCTURES CENTRE. Available at: <https://structurescentre.com/estimating-the-embodied-carbon-in-structures/>. [Accessed 4 December 2023].
- Vijayan, D.S., Dineshkumar, Arvindan, S. and Shreelakshmi J T. (2019). Evaluation of ferrock: A greener substitute to cement. Materials Today: Proceedings. doi:10.1016/j.matpr.2019.10.147.
- Vikas S, Rakesh K, Agarwal V.C, Mehta P.K., (2012). "Effect of Silica Fume and Metakaolin Combination on Concrete", International Journal of Civil and Structural Engineering, Volume 2, No 3, 2012, ISSN 0976 – 4399, pp. 893-900.
- Vrijling, J.K., (1989). Developments in the Probabilistic Design of Flood Defences in the Netherlands, Seminar on the reliability of hydraulic structures. In Proceedings, XXIII Congress, International Association for Hydraulic Research, Ottawa, Canada (pp. 88-138).
- Vu C., Ple O., Weiss J. and Amitrano D. (2020) Revisiting the concept of characteristic compressive strength of concrete. Construction and Building Materials. [Online]. 263 December, pp. 120-126. Available from: <https://doi.org/10.1016/j.conbuildmat.2020.120126>. [Accessed 6 June 2022].

- Wang R., Kalin L., Kuang W., Tian H., (2014). Individual and combined effects of land use/cover and climate change on Wolf Bay watershed streamflow in southern Alabama. *Hydrol Process*. 2014;28(22):5530–46.
- Wang, J., Cai, G. and Wu, Q. (2018). Basic mechanical behaviours and deterioration mechanism of RC beams under chloride-sulphate environment. *Construction and Building Materials*, 160, pp.450–461. doi:10.1016/j.conbuildmat.2017.11.092.
- Ware, T. (2013). Diagnosing and repairing carbonation in concrete structures. *Journal of Building Survey, Appraisal & Valuation*, [online] 1(4), pp.338–344. Available at: <https://www.henrystewartpublications.com/sites/default/files/Ware.pdf>.
- Waqas-C. (2021). What Is Channel Lining? Which types of lining are mostly used? [online] Civil Rack. Available at: <https://civilrack.com/construction/channel-lining/> [Accessed 5 Nov. 2023]. ()
- Waterhouse, E.K., (2008). Interactions between coarse sediment transfer, channel change, river engineering and flood risk in an upland gravel-bed river (Doctoral dissertation, Durham University), available at <http://etheses.dur.ac.uk/2056/>.
- Way.R., (2023). Heavy dependence on carbon capture and storage is 'highly economically damaging', says the Oxford report | Smith School of Enterprise and the Environment. [online] Available at: <https://www.smithschool.ox.ac.uk/news/heavy-dependence-carbon-capture-and-storage-highly-economically-damaging-says-oxford-report>. [Accessed 5 December 2023].
- WBCSD, (2023).World Business Council for Sustainable Development (WBCSD). (n.d.). Net-zero buildings: Halving construction emissions today. [online] Available at: <https://www.wbcsd.org/Pathways/Built-Environment/Resources/Net-zero-buildings-Halving-construction-emissions-today>.

- WCR, (2020). World Cement Report,2020 by EU Cement Beauró International, available at <https://cembureau.eu/media/m2ugw54y/cembureau-2020-activity-report.pdf>.
- Weller, A., (2023). WHAT ARE FLOOD DEFENCES? By JBA UK, available online at <https://www.jbarisk.com/news-blogs/what-are-flood-defences/>.
- Wen H, McLean DI, Willoughby K (2015) Evaluation of recycled concrete as aggregates in new concrete pavements. Transp Res Rec J Transp Res Board 2508, 73–78.
- Werrity, A. 2006. Sustainable flood management: oxymoron or new paradigm. Area. 38(1). pp. 16-23.
- Wesche, K., 2014. Fly Ash in Concrete: Properties and Performance. CRC Press.
- What is GGBS by CSMA? Available at <https://ukcsma.co.uk/what-is-ggbs/>, accessed on 6 January 2023.
- WHO, (2011). Government of Pakistan, World Health Organization. Weekly Epidemiological Bulletin: Flood Response in Pakistan: Volume 2, Issue 4, Monday 25 July 2011. 2011.
- Widera, B. & Stone, D. (2016). Analysis of Possible Application of Iron-Based Substitute for Portland Cement in Building and its Influence on Carbon Emissions. The Examples of Jizera Mountains Region and Tohono O'odham Indian Reservation.
- WIKI2, (2019). The 2011 Flood in Mississippi River is available at https://wiki2.org/en/2011_Mississippi_River_floods.
- Wikimedia.org, (2023). Available at: https://upload.wikimedia.org/wikipedia/commons/thumb/d/dd/NYTimes_Building_under_construction.jpg/256px-NYTimes_Building_under_construction.jpg. [Accessed 11 Dec. 2023].
- Wilkinson, M.E., Quinn, P.F. and Hewett, C.J.M. 2013. The Floods and Agriculture Risk Matrix: a decision support tool for effectively communicating flood risk from farmed landscapes. International Journal of River Basin Management. 11(3), pp.237–252.

- Wikipedia Contributors (2019). Energy-dispersive X-ray spectroscopy. [online] Wikipedia. Available at: https://en.wikipedia.org/wiki/Energy-dispersive_X-ray_spectroscopy. Accessed on 12 June 2024.
- Williams, J. (2017). What could the world do with 1.5 billion waste tyres? [online] The Earthbound Report. Available at: <https://earthbound.report/2017/06/29/what-can-the-world-do-with-1-5-billion-waste-tyres/>.
- Woodward, G., Perkins, D.M. and Brown, L.E. (2010). Climate change and freshwater ecosystems: impacts across multiple levels of an organisation. Philosophical Transactions of the Royal Society B: Biological Sciences, 365(1549), pp.2093–2106.
- World Bank Report 2005: Hydrology Appraisal Report of Munda Dam Pakistan Appendix C, Staff Appraisal Report 2005.
- Worrell, E., Price, L., Martin, N., Hendriks, C., Meida, L.O., 2001. Carbon dioxide emissions from the global cement industry. Annu. Rev. Energy Environ. 26, 303–329.
- WWF (Worldwide Fund for Nature), (2012). Living Planet Report 2012: Biodiversity, biocapacity and better choices. Worldwide
- WWF Scotland, 2010. Flood planner, A manual for the natural management of river floods. [Online]. [Accessed 25 September 2023]. Available from: <http://www.scotlink.org/pdf/WWFFloodPlannerManual.pdf>.
- www.aeis.com, 2023, (2023). Carbonation Test. [online] Available at: <https://www.aeis.com, 2023/what-we-do/specialty-field-testing/carbonation-test>.
- www.ceh.ac.uk, 2022. (2022). Flood Estimation Handbook and Flood Studies Report | UK Centre for Ecology & Hydrology. [online] Available at: <https://www.ceh.ac.uk, 2022/services/flood-estimation-handbook>.
- www.chegg.com. (2023). 1. Using the Rational formula $Q = (CIA) / 3.6$, and | Chegg.com. [online] Available at: <https://www.chegg.com/homework-help/questions-and-answers/1-using-rational-formula-q-cia-36-reference->

- drainage-reference-data-appendices-calculate-p-q51245994 [Accessed 8 Nov. 2023].
- www.cis.ihs.com. (2023). Cementitious materials: the effect of ggbs, fly ash, silica fume and limestone fines on the properties of concrete - The Construction Information Service. [online] Available at: <https://cis.ihs.com/cis/document/299663>. [Accessed 4 December 2023].
- www.concretcanvas.com, (2023). <https://www.concretcanvas.com/uploads/CC-Channel-Lining-HS2-Compound-0-UK-1.pdf>
- www.concrete.org.uk. (2023). Recycled glass aggregate. [online] Available at: <https://www.concrete.org.uk/fingertips-nuggets.asp?cmd=display&id=783>.
- www.constructionnational.co.uk. (2023). Publications update from The Concrete Centre. [online] Available at: <https://www.constructionnational.co.uk/news-topmenu-19/3001-publications-update-from-the-concrete-centre>. [Accessed 4 December 2023].
- www.drawellanalytical.com. (2022). What Is The Difference Between XRD And XRF? - Drawell. [online] Available at: <https://www.drawellanalytical.com/what-is-the-difference-between-xrd-and-xrf/#:~:text=XRD%20is%20X-ray%20diffraction%20spectrum%2C%20%28X-ray%20diffraction%20analysis%29> [Accessed 29 Oct. 2023].
- www.drawellanalytical.com. (2024). XRD Sample Preparation: Best Practices for Different Sample Forms - Drawell. [online] Available at: <https://www.drawellanalytical.com/xrd-sample-preparation-best-practices-for-different-sample-forms/>. [Accessed 12 Jun. 2024].
- www.engr.psu.edu, 2023. (2023). Hydration. [online] Available at: <https://www.engr.psu.edu/2023/ce/courses/ce584/concrete/library/construction/curing/Hydration.htm#:~:text=Once%20all%20the%20gypsum%20is%20used%20up%20as> [Accessed 19 Jun. 2022].

www.geograph.org.uk, 2023. (2023). Geograph: Coastal protection © Graham Horn cc-by-sa/2.0. [online] Available at: <https://www.geograph.org.uk/2023/photo/1897792>, [Accessed 2 Oct. 2023]. Pyramid breakwater stones with Raised berms/ walls and edges (<https://www.geograph.org.uk/2023/photo/1897792>).

www.geography.org.uk, 2021. (2023). Geographical Association - For Geography Teachers. [online] Available at: <https://www.geography.org.uk>, 2021.

www.grandviewresearch.com. (2020). Aggregates Market Growth | Industry Report, 2020-2027. [online] Available at: <https://www.grandviewresearch.com/industry-analysis/aggregates-market>.

www.graymont.com, 2022. (2022). High-Calcium Hydrated Lime | Graymont. [online] Available at: <https://www.graymont.com/2022/en/products/hydrated-lime/high-calcium-hydrated-lime>.

www.graymont.com, 2022. (2022). Lime in the Steel Industry | Graymont. [online] Available at: <https://www.graymont.com/2022/en/markets/steel>.

www.lowcarbonmaterials.com. (2022). Low Carbon Materials - Helping the Construction Sector Reach Net Zero. [online] Available at: <https://www.lowcarbonmaterials.com/>. [Accessed 3 December 2023].

www.madehow.com, 2019. (2019). How coir is made - material, making, history, used, processing, product, industry, machine, History. [online] Available at: <http://www.madehow.com/2019/Volume-6/Coir.html>.

www.sustainableconcrete.org.uk (2023). "Sustainable concrete: Admixtures," The Concrete Centre, [Online]. Available: <https://www.sustainableconcrete.org.uk/Sustainable-Concrete/What-is-Concrete/Admixtures.aspx>.

www.sustainableconcrete.org.uk., (2023). Cementitious Materials. [online] Available at: <https://sustainableconcrete.org.uk/Sustainable-Concrete/What-is-Concrete/Cementitious-Materials.aspx>.

- www.usgs.gov, 2023. (2023). Lime Statistics and Information | U.S. Geological Survey. [online] Available at: <https://www.usgs.gov, 2023/centers/national-minerals-information-center/lime-statistics-and-information>.
- Xie, J., Zhao, J., Wang, J., Wang, C., Huang, P. and Fang, C. (2019). Sulfate Resistance of Recycled Aggregate Concrete with GGBS and Fly Ash-Based Geopolymer. *Materials*, 12(8), p.1247. doi:10.3390/ma12081247.
- Yalley, P.P., & Kwan, A. (2012). Coconut Fibre as enhancement of concrete. School of Civil Engineering Cardiff University UK available at <https://orca.cf.ac.uk/43403/1/Yalley%20Kwan%20KNUST%20paper%20.%201.pdf>.
- Yap SP, Alengaram UJ, Jumaat MZ., (2013) Enhancement of mechanical properties in polypropylene–and nylon–fibre reinforced oil palm shell concrete. *Mater Des* 2013;49:1034–41.
- Yasmin, T.; Bitencourt, L.A.G., Jr.; Osvaldo, L.M., (2020). Design of SFRC members aided by a multiscale model: Part II–Predicting the behaviour of RC-SFRC beams. *Compos. Struct.* 2020, 241, 1–13.
- Yi Y., Zhu D., Guo S., Zhang Z. and Shi C. (2020) A review on the deterioration and approaches to enhance the durability of concrete in the marine environment. *Cement and Concrete Composites*. [Online]. 113 October, pp. 1-14. Available at: <https://doi.org/10.1016/j.cemconcomp.2020.103695>. Accessed 4 June 2022].
- Yildirim G, Saharan M, Ahmed HU (2015). Influence of hydrated lime addition on the self-healing capability of high-volume fly ash incorporated cementitious composites. *J Mater Civ Eng* 27(6): 04014187. <https://ascelibrary.org/doi/pdf/10.1061/%28ASCE%29MT.1943-5533.0001145>.
- Yin, S., Tuladhar, R., Riella, J., Chung, D., Collister, T., Combe, M. and Sivakugan, N. (2016). Comparative evaluation of virgin and recycled polypropylene fibre reinforced concrete. *Construction and Building Materials*,

- 114, pp.134–141. doi:<https://doi.org/10.1016/j.conbuildmat.2016.03.162>.the const
- Yorkshire Dales River Trust. 2017. Oughtershaw Demonstration. [Facebook]. 7 August 2017. [Accessed 25 September 2023]. Available from: https://www.facebook.com/pg/yorkshiredalesrivertrust/photos/?tab=album&album_id=1385838591536961.
- Yorkshire Dales River Trust. 2018. NFM Gallery. [Online]. [Accessed 20 November 2018]. Available from: <http://www.yorkshiredalesrivertrust.com/natural-flood-management/gallery/>.
- Younis KH., (2016). Mechanical performance of concrete reinforced with steel fibres extracted from post-consumer tyres. In: In the second international engineering conference on developments in civil and computer applications. IEC; 2016. 2016.
- Youssef O., Hassanli R., Mills J.E., Retrofitting square columns using FRP-confined. Crumb rubber concrete to improve confinement efficiency, Constr. Build. Mater.153 (2017) 146–156.
- Yuan, Q., Liu, Z., Zheng, K. and Ma, C. (2021). Inorganic cementing materials. Civil Engineering Materials, pp.17–57. doi:10.1016/b978-0-12-822865-4.00002-7.
- Zeybek, Ö., Özkılıç, Y.O., Karalar, M., Çelik, A.İ., Qaidi, S., Ahmad, J., Burduhos-Nergis, D.D. and Burduhos-Nergis, D.P. (2022). Influence of Replacing Cement with Waste Glass on Mechanical Properties of Concrete. Materials, [online] 15(21), p.7513. doi <https://doi.org/10.3390/ma15217513>.
- Zhan et al. (2020). Zhan, P., He, Z., Ma, Z., Liang, C., Zhang, X., Annulo Addisayehu Abraham and Shi, J. (2020). Utilisation of nano-metakaolin in concrete: A review. 30, pp.101259–101259. Doi <https://doi.org/10.1016/j.jobbe.2020.101259>.

- Zhang, L., Dawes, W.R., and Walker, G.R. 2001. Response of mean annual evapotranspiration to vegetation changes at catchment scale. *Water Resources Research*, Vol. 37, No. 3, Pages 701–708, March 2001.
- Zhang, L., Nan, Z., Xu, Y. & Li, S. (2016). Hydrological Impacts of Land Use Change and Climate Variability in the Headwater Region of the Heihe River Basin, Northwest China. *PLOS ONE*, [online] 11(6), p.e0158394. Available at:
<https://journals.plos.org/plosone/article?id=10.1371/journal.pone.0158394>.
[Accessed 5 March 2023].
- Zhang, T., Vandeperre, L.J. and Cheeseman, C.R. (2014). Formation of magnesium silicate hydrate (M-S-H) cement pastes using sodium hexametaphosphate. *Cement and Concrete Research*, 65, pp.8–14. doi:10.1016/j.cemconres.2014.07.001.
- Zhu et al. (2018). Zhu H., Liang J., Xu J., Bo M., Li J., Tang B., Research on anti-chloride ion penetration property of crumb rubber concrete at different ambient temperatures, *Constr. Build. Mater.* 189 (2018) 42–53.

7 Appendices

Appendix I

Risk Assessment, Health and Safety, Ethical Approval and Permission of DoS to Reuse Published Research Papers in Dissertation

Health and Safety and Risk Assessment of Laboratory Working	
What are the hazards?	Falling and flying objects, punctures, cutting hazards, and burn hazards from wet concrete, including fatigue and Slips, trips and falls
Who might be harmed and how?	Researcher and helpers; Crushing, punctures,
Further action	None
Action by whom?	Researcher, helpers and Laboratory staff
Action by when?	Before each laboratory experiment
What are the hazards?	Dust inhalation
Who might be harmed and how?	Researcher and helpers: Respiratory complications
Mitigation	Use dust masks
Further action	Cover the mixer during mixing
Action by whom?	Researcher and helpers
Action by when?	When carrying out work
What are the hazards?	Cube moulds falling from vibrating table
Who might be harmed and how?	Researcher and helpers: Crushing by cube moulds
Mitigation	Ensure that the surface of the vibrating table is always clean and dry
Further action	Always secure two sides of the cube moulds firmly on the vibrating table before pressing the start button
Action by whom?	Researcher, helpers and laboratory staff
Action by when?	When carrying out work
What are the hazards?	Electricity hazards
Who might be harmed and how?	Researcher and helpers: Electrocution
Mitigation	Researcher and helpers to know how to switch off the electricity in an emergency and have access to fuse box
Further action	Laboratory manager to ensure that qualified electricians carry out safety checks and also carry out visual checks of plugs, sockets, cables and on/off switches
Action by whom?	Researchers, helpers and laboratory manager
Action by when?	Before and when carrying out work
What are the hazards?	Fire
Who might be harmed and how?	If trapped, researcher and helpers could suffer smoke inhalation and burns
Mitigation	A comprehensive fire risk assessment
Further action	All actions necessary set out in the fire risk assessment and communicated to the researcher and helpers
Action by whom?	Laboratory manager
Action by when?	Before accessing the lab for the first time, followed by regular reminders
What are the hazards?	Trapping fingers in crushing machines
Who might be harmed and how?	Researcher and helpers: Trapping and crushing
Mitigation	Secure guard before commencing tests
Further action	Do not remove the specimens until the machine has stopped
Action by whom?	Researcher and helpers
Action by when?	During tests
What are the hazards?	Flying particles
Who might be harmed and how?	Researcher and helpers: Particles entering eyes
Mitigation	Use eye protection
Further action	None
Action by whom?	Researcher and helpers
Action by when?	During experiments



My Applications

New Application

If you wish to submit a new application, click on 'New Applications' above.



Existing applications

If you wish to edit an existing application prior to submission, click on the Application Title or select the 'Edit/Continue'  button.

If you have submitted an application and now need to make changes to it, click on the 'Make Revision/Copy'  button. Please add to the title the version number (for example, v2).

10 records per page

Search:

Title	Risk Category	Status	Date Created	Action
Use of Novel Materials for Channel Stabilization and Catchment Defenses in Flood Prone Areas of Developing Countries	Risk Category 1	Approved by supervisor	13-MAY-20	 

Showing 1 to 1 of 1 entries

← Previous 1 Next →



Form B- Risk Assessment

Location/Campus:	CC	Building:	NT G15 & Unit 3
Role:	School Technical Manager		
Date Completed:	21 August 2023		
Author of Assessment:	Kev Smith	Signed:	
		Review Date:	21 August 2024
Brief Description of the activity			
Use of the laboratories NT G13, G14, G15 and Unit 3			
Method Statement (Detailing the activity from the start to finish)			
METHOD STATEMENT			
STEP			
1.	Covid-19 revised procedures.		
2.	i) Disposable gloves are available in the lab.		
3.	ii) Students should wipe down equipment they use, before and after use, either with an alcohol wipe (70% by content) or a cloth with suitable cleaner on it.		
4.	iii) Extra housekeeping will be required by both local staff and from CARES staff as appropriate.		
5.	iv) Anybody experiencing any of the known symptoms of Covid-19 should not enter the lab, they should go home and contact NHS 111 for further guidance.		
6.			
7.			
8.			
9.			
10.			
11.			
12.			

Risk Assessment Form B

What are the hazards? (use the table above to help)	Who might be harmed and how	What are you doing already	Risk Level H/M/L	Do you need to do anything else to manage the risk?	Action by whom	Action by when (priority)?	Completed Yes/No
Various hazards associated when working within a practical lab environment.	Students. Cuts, burns, lacerations, broken limbs, head injury, substance absorption, chest infection, eye injury.	Students are provided with H&S briefing every time a piece of equipment is used. Authorised students are only allowed in the areas. Pin code access into the lab. Unit 3 - Key staff members only have the key to open the building. H&S Code of Practice is provided to students. Students are limited to what they can use. Any equipment used must be used with permission.	L	Supervision of students	Staff	Continuously monitored	Yes
Students misusing machinery, equipment and processes.	Students. Cuts, burns, lacerations, broken limbs, head injury, substance absorption, chest infection, eye injury.	Effective and constant supervision of student activities whilst lab is operational. If certain machines/equipment are not in use, they will be isolated thus operation on equipment and machines is limited. Ideally minimum of 1 academic and 1 learning officer for each session.	L	Quantity and quality of supervision in relation to physical student numbers and the hazardous nature of work has to be in balance. Recognising the lab can accommodate up to a maximum of 30 students at any one time.	Staff	Continuously monitored	Yes
Various hazards associated when working within a lab environment when internal or external maintenance is being undertaken.	Staff, students and contractors. Personal injury and or injury to students and staff working within the area, damage to property	All maintenance is to be carried out under supervision by learning officer staff, where machinery is locally isolated and sufficient space is made available to undertake such maintenance.	L	Where possible such maintenance must not be allowed to affect the safety of other staff and students working within this area. It is preferable that maintenance is performed when there is no student work happening in the area.	Staff	Continuously monitored	Yes

PPE required - Yes ☒ No ☐ NA ☐

COSHH Considerations? Yes ☒ No ☐ NA ☐

	<input checked="" type="checkbox"/>		<input checked="" type="checkbox"/>		<input type="checkbox"/>		<input checked="" type="checkbox"/>
	<input checked="" type="checkbox"/>		<input checked="" type="checkbox"/>		<input checked="" type="checkbox"/>		<input type="checkbox"/>
	<input type="checkbox"/>	If Personal Protective Equipment is required please tick all that apply from the pictograms above.					

	<input checked="" type="checkbox"/>		<input checked="" type="checkbox"/>		<input checked="" type="checkbox"/>		<input checked="" type="checkbox"/>
	<input checked="" type="checkbox"/>		<input checked="" type="checkbox"/>		<input checked="" type="checkbox"/>		<input checked="" type="checkbox"/>

* Safety footwear is compulsory in NT Q15 and the workshop area of Unit 3 other PPE is available for use as/when required

EQUIPMENT TO BE USED - YES NO						
Item	Trained to Use	yes	no	NA	Checked Inspected	and
Step Ladders	N/A					
Barriers	N/A					
Safety Signage	N/A					
Power Tools	N/A					
Battery Tools	N/A					
Hand Tools	N/A					
Temporary power	N/A					
Scaffolding	N/A					
Access power equipment	N/A					

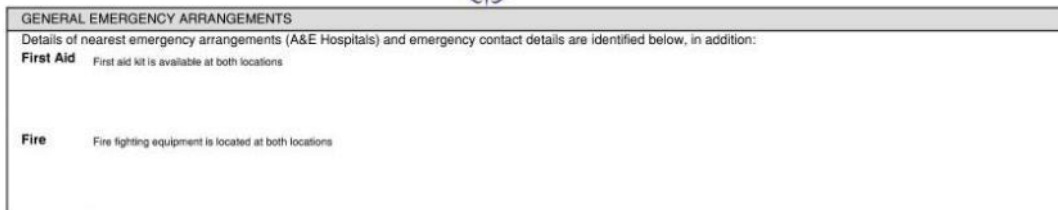
Permissions received for activity - YES/NO/NA			
Area	yes	no	NA
Health and Safety Team			<input checked="" type="checkbox"/>
Security (HC/CC)			<input checked="" type="checkbox"/>
Conferencing Team			<input checked="" type="checkbox"/>
Grounds			<input checked="" type="checkbox"/>
Estates Services			<input checked="" type="checkbox"/>
Estates Helpdesk			<input checked="" type="checkbox"/>
CARES Helpdesk			<input checked="" type="checkbox"/>
Local SHW Coordinator			<input checked="" type="checkbox"/>

Risk Assessment Form B

What are the hazards? (use the table above to help)	Who might be harmed and how	What are you doing already	Risk Level H/M/L	Do you need to do anything else to manage the risk?	Action by whom	Action by when (priority)?	Completed Yes/No
Particle inhalation due to build-up of dust on floor.	Staff students and contractors. Substance absorption, chest infection, eye injury.	Clean up after every lab session.	L		Staff	Continuously monitored	Yes
Various hazards associated with the Fork lift truck use.	Staff and students. Fatality. Musculoskeletal injuries.	Only authorised, trained staff can use the fork lift. Pre use checklist in place. No students in area whilst fork lift truck in use. Safety test conducted on fork lift truck – (LOLER & PUWER regulations)	L	The key must be removed from the machine when not in use.	Staff	Continuously monitored	Yes
Possible exposure to the Covid-19 virus.	All users of the area. Infection by Covid-19, which in extreme cases may lead to death.	As the guidelines and advice changes, all changes to be communicated with students via the usual channels, i.e. emails from academic/admin staff, and from technical staff in the form of verbal instructions and where relevant the installation of guidance notices.	M	Increase hand washing. Ensure that sinks are well stocked with soap and paper towel. (this should already be the case, but maybe have CARES check it more frequently or provide some spare) Install handwashing infographics at all sinks Hand sanitizer to be used when entering/leaving the lab. Restrict the use of multi use/person PPE, i.e. encourage students to wear suitable old clothes in the lab rather than wearing a lab coat to protect clothes. Provision of 70% alcohol wipes to wipe down control panels, handles, etc on equipment before and after use. Disposable gloves should be worn by all those actively participating in laboratory sessions, to minimise the risk of cross contamination from the use of tools and equipment.	Staff	Continuously monitored	Yes
Possible exposure to the Covid-19 virus.	Clinically vulnerable persons	Individual risk assessments on clinically vulnerable persons to be undertaken, for members of staff this is to be performed by the relevant manager, for students it should be done by the supervising academic.	M	Implement the recommendations of the individual risk assessments.	Staff	Continuously monitored	Ongoing

Risk Assessment Form B

What are the hazards? (use the table above to help)	Who might be harmed and how	What are you doing already	Risk Level H/M/L	Do you need to do anything else to manage the risk?	Action by whom	Action by when (priority)?	Completed Yes/No
Dropping heavy items whilst carrying / moving	Staff and students. Crushed toes	All persons working in the labs to be instructed in the correct manual handling techniques, where possible all lifting/moving of heavy objects to be done by staff. All persons to wear safety footwear.	L	Students are required to provide their own safety footwear	Staff	Continuously monitored	Yes
Unloading vehicle deliveries	Staff. Injury to persons back, hands and feet.	All staff associated in the area have up to date manual handling training	L	Training arranged through generic university training scheme and checked at PDR stages. Persons must request assistance from colleagues to reduce risk of possible injury.	Staff	Continuously monitored	Yes
Electrical machinery and equipment.	Staff and students. Shock, fire or electrocution.	The school arranges electrical contractors to carry out electrical testing of all associated machinery and power tools.	L	Electro Test Services carry out electrical tests annually for portable appliances and every 5 year for fixed items.	SHW co-ordinator	Continuously monitored	Yes
Particle inhalation when operating machinery or undertaking processes.	Staff and students. Substance absorption, chest infection, eye injury.	Use of LEV and ensuring adequate ventilation where LEV is not available. Staff and students reminded to use correct PPE.	L		Staff	Continuously monitored	Yes



Re: Permission for Using Published/ unpublished Research Papers in PhD Dissertation - Message (HT... Search

File **Message** Insert Options Format Text Review Help Grammarly

Recipients receive: Flag for follow up.

To Nadir, Hafiz Muhammad (Student)

Cc

Send Subject Re: Permission for Using Published/ unpublished Research Papers in PhD Dissertation

Sure Nadir,

Best Wishes and Kind Regards :

Ash

Dr Ash Ahmed MBSC
Reader in Materials Science
School of the Built Environment & Engineering
Leeds Beckett University
Formerly Leeds Metropolitan University
Civic Quarter
Northern Terrace
Leeds
LS2 9AG

E: 19 sept 2025, at 16:25, Nadir, Hafiz Muhammad (Student) <[H.Nadir@leedsbeckett.ac.uk](#)>

Publication of Research Basing the PhD Project – 13 x Journal Research Papers (Appendices II – XIV)

Research Article

ISSN 2766-2624

Advances in Earth and Environmental Science

Hydrological Analysis and Statistical Modelling of Swat River Basin for Flood Risk Assessment

Hafiz Muhammad Nadir¹, Ash Ahmed^{2*}

¹PhD Researcher, Civil Engineering Group, School of Built Environment & Engineering, Leeds Beckett University, Civic Quarter Northern Terrace Leeds, LS2 8AG, UK.

²Reader/ Associate Professor, Civil Engineering Group, School of Built Environment & Engineering, Leeds Beckett University, Civic Quarter Northern Terrace Leeds, LS2 8AG, UK.

*Correspondence author

Ash Ahmed

Reader/ Associate Professor,
Civil Engineering Group,
School of Built Environment & Engineering,
Leeds Beckett University,
Civic Quarter Northern Terrace Leeds,
LS2 8AG, UK.

Submitted : 15 Sept 2022 ; Published : 1 Oct 2022

Citation: Nadir, H. M. & Ahmed, A. Hydrological Analysis and Statistical Modelling of Swat River Basin for Flood Risk Assessment. *Adv Earth & Env Sci*; 2022; 3(4): 1-13.

Abstract

The climatic variations and anthropogenic activities in the river catchments worldwide are causing severe weather events and flooding. The narrowing down of natural floodplains/ channels, land-use changes, deforestation and mushroom urbanisation with unplanned infrastructure development are aggravating causes of severe storms and floods, especially in developing countries. Hydrological studies, flood modelling and statistical flood frequency analysis are considered imperative to assess the hazards/ risks of flooding and their mitigation measures. Estimating predicted storms/ floods for different return periods can give a reasonable idea about the frequency of storm events. This study analysed the Swat river basin to determine the predicted return periods with expected storm/ flood in its catchment and Swat river. The weather and rainfall in the Swat river basin remain unpredictable. Historically, it has seen peak precipitation of 150mm – 274mm and a super flood of 10050 m³/sec in 2010, more than its 200 years return period. Flood frequency and statistical analysis using Log Pearson 3 (LP3), Generalized Extreme Value (GEV) and Gumbel Maximum (Gumb-Max) on Easy Fit software and Log Pearson 3 equations have predicted weather instability in the Swat basin with the prediction of super flood like 2010 happening in 40 years return period. Construction of Swat expressway on elevated embankment will disturb the natural drainage pattern and likely result in inundation in flood plains due to inadequate capacity of cross drainage structures to withstand the spontaneous flash flooding. However, these have been designed on 100 years return period. However, probability density and hazard functions show a lesser probability of any mega hazard; therefore, cross drainage structures and crisscrossing channels in the river catchments may be planned on a minimum 100 years return period as an economic/ reasonable safe limit. Still, additional structural/ non-structural measures should augment these for efficient flood-fighting like plantation and maintenance of drainage structures, construction of small dams/ reservoirs for swift water management in case of a flash flood and placement of rescue/ relief resources at accessible points as per flood zoning.

Keywords : Historical flooding, Swat river basin, flood frequency analysis, statistical analysis, predicted return periods.

Introduction

Historical preview, climate changes and impact of flood and storm events

Water has a special place in the life of human beings as a necessity (Shirleyana & Anindya, 2012), and all civilisations were developed along the waterfront, which resulted in ecological modifications/ pollution, glaciers melting, extraordinary precipitation events, flooding, and damage to aqua life and wildlife (Worldwide Fund for Nature (WWF), 2012). Yangtze River in China has a history of devastating floods periodically, especially the floods in 1911, 1935 and 1954 were the worst floods which resulted in the deaths

of millions of people and swapping of properties/ land in 6300 KM stretch, Yellow River in China, Indus in Pakistan, Ganges, Jumna and Brahma Putra in India and Bangladesh are the major flood causing rivers mainly arising from climatic changes and urbanisation/ modifications along natural rivers stretches (Kumar, 2017). The surge in 2011 in the Mississippi River was the worst of its kind in the USA, which impacted 31 states, including hundreds of casualties and destruction/ evacuation of millions of populations (HEITMEYER, 2008; Schleifstein, 2011; National Mississippi River Museum (NMRM), 2018; WIKI2, 2019). In the last few decades, there have been numerous casualties and loss of property because of heavy rain/ flood events due to climatic changes and human

Adv Earth & Env Sci; 2022

www.unisciencepub.com

Volume 3 | Issue 4 | 1 of 13


Potential Sustainable Cement Free Limecrete Based on GGBS & Hydrated Lime as an Alternative for Standardised Prescribed Concrete Applications

ISSN: 2576-8840



*Corresponding author: Ash Ahmed, Associate Professor, Civil Engineering Group, School of Built Environment & Engineering, Leeds Beckett University, UK

Submission:  October 01, 2021

Published:  October 14, 2021

Volume 15 - Issue 5

How to cite this article: Joshua Cunliffe, Hafiz Muhammad Nadir, Ash Ahmed, Colin Yates, Lee Yates, et al. Potential Sustainable Cement Free Limecrete Based on GGBS & Hydrated Lime as an Alternative for Standardised Prescribed Concrete Applications. Res Dev Material Sci. 15(5). RDMS.000874. 2021.
 DOI: 10.31031/RDMS.2021.15.000874

Copyright© Ash Ahmed. This article is distributed under the terms of the Creative Commons Attribution 4.0 International License, which permits unrestricted use and redistribution provided that the original author and source are credited.

Joshua Cunliffe¹, Hafiz Muhammad Nadir¹, Ash Ahmed^{2*}, Colin Yates³, Lee Yates¹, Neshe Limbu¹, Osama Abdelwahab¹, Abdu Aljahed¹ and Nayan Patel¹

¹Researcher, Civil Engineering Group, School of Built Environment & Engineering, Leeds Beckett University, UK

²Associate Professor, Civil Engineering Group, School of Built Environment & Engineering, Leeds Beckett University, UK

³Conserv Lime Products, UK

Abstract

A fundamental issue with the active ingredient of concrete, Portland cement, is its energy-intensive manufacturing process, which has led to the cement industry emitting up to 10% of global CO₂ levels. To facilitate the reduction in the embodied CO₂ of concrete, the Portland Cement (PC) content has been entirely replaced volumetrically with Hydrated Lime (HL) and ground granulated blast furnace slag (GGBS or SL). GGBS was used to replace hydrated lime content in 10% increments up to 100% GGBS. Analysis of compressive and flexural strength and density testing was performed on samples to investigate the mechanical and physical properties at 7, 28 and 91-day curing ages, whilst flexural testing was conducted at 91 days curing age. Four standard mix ratios, 1:1:3, 1:2:3, 1:1:2 and 2:1 was made for comparison. Two curing conditions were tested at 91-day curing age, these being air-cured and water curing. Results have shown the optimum mix ratio to be 1:1:2 for all mixes. The optimum mix being HL 1:1:2 SL80%, water cured exceeding 25MPa. Throughout the different ratios, it can be concluded that the optimum replacement of GGBS lies between 80-90%; it can also be noted that 100% GGBS content sees a significant drop in compressive and flexural strength, indicating the presence of hydrated lime to be a catalyst for strength gain.

Introduction and Background

Portland Cement (PC) is the key ingredient used in concrete; mixed with its other constituents, aggregates and water, a chemical reaction occurs, resulting in calcium silicate hydrate (C-S-H) gel production, which strongly binds the constituents through a chemical process known as hydration. This hydration process continues with time, and at the 28-day point, concrete produced with PC has reached approximately 99% of its mechanical properties, mainly compressive and tensile strength [1].

PC can be manufactured in various forms. A range of raw materials are used in PC production; these are typically calcareous materials such as limestone and shale and clays are normally used. The chemical compounds contained in the raw materials are crucial to the quality of the cement. The chemical composition of the PC is dependent on the raw materials used; predominantly, compounds of lime (CaO) are present along with silicon dioxide (SiO₂) and alumina (Al₂O₃). The lime content is sourced from the use of limestone, whilst the silica and alumina content are obtained from the use of argillaceous materials such as clay [2]. PC

Experimental Investigation of Engineering Properties of Iron-Based Binary and Ternary Pozzolanic Supplementary Cementitious Materials

Hafiz Muhammad Nadir¹, Ash Ahmed^{2*} and James West³

¹PhD Researcher, Civil Engineering Group, School of Built Environment & Engineering, Leeds Beckett University, Civic Quarter Northern Terrace Leeds, LS2 8AG, UK.

²Reader/ Associate Professor, Civil Engineering Group, School of Built Environment & Engineering, Leeds Beckett University, Civic Quarter Northern Terrace Leeds, LS2 8AG, UK.

³MSc Student, Civil Engineering Group, School of Built Environment & Engineering, Leeds Beckett University, Civic Quarter Northern Terrace Leeds, LS2 8AG, UK.

*Correspondence author

Ash Ahmed,
Reader/ Associate Professor,
Civil Engineering Group,
School of Built Environment & Engineering,
Leeds Beckett University,
Civic Quarter Northern Terrace Leeds,
LS2 8AG, UK.

Submitted : 24 Jan 2023 ; Published : 13 Feb 2023

Citation : Nadir, H.M. et al. Experimental Investigation of Engineering Properties of Iron-Based Binary and Ternary Pozzolanic Supplementary Cementitious Materials. *J mate poly sci*, 2023; 3(1): 1-13.

Abstract

The characteristic global warming potential of ordinary Portland cement (OPC) makes it a huge challenge for researchers to weigh its enormous use with potentially feasible engineering properties versus the environmental impacts. The formulation of sustainable, economical, and greener supplementary cementitious materials (SCMs) is an ongoing phenomenon, attracting the large-scale attention of industry/ academia. The formulation of ferrock by David Stone with low embodied energy, lower consumption of natural resources and minimal global warming potential has paved the way for the use of novel material comprising iron powder, pozzolans (pulverised fly ash (PFA) and metakaolin (MK) and lime exhibiting at par performance with OPC. However, a gap has been identified in its formulation, raising a further research question on how it will perform if PFA and MK are replaced by ground granulated blast furnace slag (GGBS) or other pozzolans like silica fume (SF) etc., with different mix ratios. Therefore, an endeavour has been made in this study to identify the engineering properties with sustainable use of modified binary and ternary pozzolans/ GGBS in place of 20% PFA in conventional ferrock.

The conventional ferrock contains 8% MK and 20% PFA (as binary pozzolans), 60% iron powder, 12% lime and 2% oxalic acid (set 1). An effort has been made to formulate the different mixes of 10, 20, 30, 40 and 50% by keeping 60% iron powder, 12% lime, 8% MK and 2% oxalic acid constant but replacing 20% PFA with 20% GGBS (set 2), with 10%PFA+10%GGBS (set 3) and with 10%PFA+10%SF (set 4). A target compressive strength of C32/40 or M40 concrete was selected for this study to achieve and compare results with the control mix (0% ferrock) and conventional ferrock during the experimental investigation of modified novel materials. 10-20% ratios of modified mixes exhibited the best performance and achieved the threshold strength of 60 MPa of high-strength cement concrete. Maximum compressive strength of 65 MPa was achieved by the 10% mix of set 2 (20% GGBS), followed by 20% mix ratios of set 3 (10%PFA+10%GGBS) and set 4 (10%PFA+10%SF), achieving 64 MPa. Whereas the 10% mix of the conventional ferrock (set1) reached 63 MPa strength, and the control mix with no ferrock gained 57 MPa strength at 56 days of curing. Overall, an increase of 2-13% compressive strength was observed with 10-30% mixes of all the SCMs; however, a decrease of 3-27% was observed with 40-50% use of SCMs. The use of iron powder increased the ductility of ferrock-based SCMs mixes and exhibited more flexural strength. Set 3 performed the best in exhibiting up to 5.8 MPa flexural strength, followed by set 4, set 2 and lastly, set 1 of conventional ferrock. 20% and 30% mix ratios exhibited flexural strength of more than 5% MPa, better than 10% and 40/ 50% mixes. The study supports the use of 10-20% ferrock-based SCMs for high-strength concrete and 10-50% for concrete mixes with a target strength of C32/40 or M40 to decrease the CO₂ footprints of the construction industry significantly.

Keywords : Conventional ferrock, modified ferrock, pozzolans, engineering properties, global warming potential.

Introduction

The invention of ordinary Portland cement (OPC) has paved the way for the modern construction industry due to its sound engineering properties and method of delivery employing insitu casting, precast or modular construction (Nadir & Ahmed,

2021). Concrete is considered the second most widely used material on earth after water; however, embodied CO₂ emitted during manufacturing and use of cement concrete is estimated to be one ton of CO₂ per ton of OPC, ranging to around 10% of global emissions, making it the second highest emitter in




The Mechanisms of Sulphate Attack in Concrete – A Review

Hafiz Muhammad Nadir and Ash Ahmad*

Civil Engineering Group, School of Built Environment & Engineering, Leeds Beckett University, Civic Quarter, Northern Terrace Leeds, UK

*Corresponding author: Ash Ahmed, Civil Engineering Group, School of Built Environment & Engineering, Leeds Beckett University, Civic Quarter, Northern Terrace Leeds, UK

Received:  October 14, 2022

Published:  October 21, 2022

Abstract

The exposure of engineering structures to complex chemical hazards in omnifarious geographical/ environmental locations and emission of greenhouse gases from manufacturing and usage of cement have encouraged researchers to explore the chemical synthesis taking place in the blending of different raw materials, formation of complex compounds, hydration of cement concrete and reactions taking place during internal/ external sulphate attacks. This study has carried out an in-depth elucidation of the contemporary research to understand better the raw material composition of cement-like calcareous and argillaceous minerals, hydration process, the reaction of complex compounds to create cement paste, kinetics associated with the formation of ettringite, monosulphate aluminate ferrate hydrates, exchange of cations and anions between reactive metals hydroxide, hydrates, sulphates and their impacts on long term sustainability properties of concrete. An endeavour has been made to explore the use of lime and pozzolans derived from industrial, agricultural and natural resources. The microstructural studies were examined, which augmented the research findings that the development of cracks/ failure in concrete is attributed to the formation of ettringite, gypsum, brucite, M-S-H gel, thaumasite, portlandite, expansive silica hydroxide gel and carbonation of metal hydroxides due to internal/ external sulphate attacks on samples having more water-cement ratio and exposed to more concentrated magnesium/ sodium sulphate solutions.

Keywords: Cement; hydration; sulphate attack; supplementary cementitious materials; microstructural studies

Introduction

The human's desire to conquer oceans, rivers, plains, mountains and deserts has led to the construction of diverse infrastructure in different environments, thus giving rise not only to disturbance to the natural environment but equally causing hazards to infrastructure from the environment too in the form of deterioration/ depletion due to ageing, spalling, thawing, corrosion, erosion, temperature variation, chemicals attacks, ingress of moisture/ acidic/ alkaline solutions and different atmospheric conditions [1]. Historically, the building materials, like stone, clay, lime, pozzolanic binders, and modern-day cement-based ingredients, have been on the construction inventory for various construction requirements. One of the most widely used materials in modern construction is concrete which is preferred due to its mechanical properties and ease of use [2,3]. The variation in the performance of cement concrete in different climatic conditions is its vulnerability against ex

ternal/ internal chemical attacks, especially sulphate attacks, over an extended exposure period [2-8]. These phenomenal concrete vulnerabilities have encouraged researchers to study the chemical synthesis igniting the sulphate attack and to formulate composite sustainable materials [9,10]. This paper reviews contemporary research conducted on cement composition, chemical reactions, hydration process, chemo-mechanical kinetics and microstructural synthesis during sulphate attack.

Literature Review on the use of cement, lime and SCMs

Lime

The quicklime CaO and slaked lime Ca(OH)₂ are considered among the oldest construction materials which have been in use for thousands of years in construction since the inception of great

Elucidating Chemo-Mechanical Synthesis and Microstructural Study on the Performance of Partial Cement-Based Concrete Composites Against Sulphate Attack – A Review

ISSN: 2576-8840



***Corresponding author:** Ash Ahmed, Associate Professor, Civil Engineering Group, School of Built Environment & Engineering, Leeds Beckett University, Civic Quarter Northern Terrace Leeds, LS2 8AG, UK

Submission:  December 12, 2022
Published:  December 22, 2022

Volume 18 - Issue 2

How to cite this article: Hafiz Muhammad Nadir and Ash Ahmed*. Elucidating Chemo-Mechanical Synthesis and Microstructural Study on the Performance of Partial Cement-Based Concrete Composites Against Sulphate Attack – A Review. Res Dev Material Sci. 18(2). RDMS. 000935. 2022.
 DOI: 10.31031/RDMS.2022.18.000935

Copyright © Ash Ahmed. This article is distributed under the terms of the Creative Commons Attribution 4.0 International License, which permits unrestricted use and redistribution provided that the original author and source are credited.

Hafiz Muhammad Nadir¹ and Ash Ahmed^{2*}

¹PhD Researcher, Civil Engineering Group, School of Built Environment & Engineering, Leeds Beckett University, UK

²Associate Professor, Civil Engineering Group, School of Built Environment & Engineering, Leeds Beckett University, UK

Abstract

The well-known weakness of cement concrete against external/internal sulphate attack and an estimated 7-10% global greenhouse gas emission by the construction industry (mainly contributed by cement manufacturing and supply) have encouraged researchers to elucidate the chemical synthesis taking place in the preparation and hydration of cement concrete along with the factors affecting the sustainability of hardened concrete. In this review study, an endeavour has been made to explore the use of Supplementary Cementitious Materials (SCMs) of different hydrocarbon compositions, including organic/ inorganic compounds like pozzolans derived from natural (zeolite/ metakaolin derived from kaolinite), agricultural (rice husk ash, corn cob ash) and industrial fields Pulverised Fly Ash (PFA), Silica Fume (SF) and a renowned cement replacement material, i.e., Ground Granulated Blast Furnace Slag (GGBS). The partial replacement of 0-30% pozzolans with cement as a binder has been reviewed objectively to achieve economic/ environmental benefits by enhancing strength and durability against dangerous sulphate attacks. The chemo-mechanical synthesis involving SCMs has been explored to understand the formation of additional calcium silicate hydrate C-S-H gel by blending various pozzolans. The research elucidates an improvement in strength up to optimum ratios of 1-15% for different SCMs. However, the strength was observed to reduce beyond a certain % ratio of SCMs blending due to the formation of expansive alkaline silica hydroxide gel, which causes cracking and weak structure. The aviation industry is considered the top emitter of CO₂ (3% of total global emissions), however, the construction industry emits 7-10% of global greenhouse gases, which is nearly three times greater. Therefore, the supportive use of up to 90% SCMs can result in a significant reduction of CO₂ by the construction industry based on the type/ratio of blending SCMs. Microstructural studies using scanning electron microscopy SEM and X-ray Diffraction (XRD) have also been explored. These microstructural studies have further clarified the development of ettringite in concrete after sulphate attack and the beneficial use of pozzolans to a certain extent to prevent the formation/ propagation of ettringite-specific cracks in the micro/ nano-pores of concrete structures. In general, research has shown that the addition of SCMs in concrete results in an increase in strength and superior resistance to sulphate attack.

Keywords: Chemical synthesis; Sulphate attack; Pozzolans-based SCMs; Mechanical properties; Micro-structural scanning

Introduction

Technological advancement has enabled engineers to produce masterpieces of construction in diverse geographical/ ecological locations by harnessing nature's power, enabling a comfortable human life but subjecting the environment and infrastructure to different chemical / pollution hazards [1]. The use of lime and natural volcanic pozzolans has been in use since ancient civilisations [2]. The invention of ordinary Portland cement in the 1860s suppresses the use of lime/ pozzolans due to its swift setting time and easy insitu handling [2,3]. Still, it resulted in up to 10% of global CO₂ emissions [4]. The cement concrete was found to be highly vulnerable to the ingress of sulphates and chlorides in marine environments [2-8].

Comparative Evaluation of Potential Impacts of Agricultural and Industrial Waste Pozzolanic Binders on Strengths of Concrete

Hafiz Muhammad Nadir¹ and Ash Ahmed^{2*}

¹PhD Researcher, Civil Engineering Group, School of Built Environment & Engineering, Leeds Beckett University, Civic Quarter Northern Terrace Leeds, LS2 8AG, UK

²Reader (Associate Professor), Civil Engineering Group, School of Built Environment & Engineering, Leeds Beckett University, Civic Quarter Northern Terrace Leeds, LS2 8AG, UK

ABSTRACT

Concrete is one of the most widely used construction material in the world which uses aggregates and cement as a binder. Use of cement concrete and mining/transportation of raw materials makes the construction industry the biggest emitter of CO₂ by contributing up to 7-10% of global emissions. The waste materials from different industries and agriculture contribute to 90% of waste disposal/ recycling effort in the world. This research has focused to use a selection of waste materials as supplementary cementitious materials (SCM) to minimize the emission of CO₂ and recycling/ absorption of waste from other industries to construction industry to make it more sustainable. The contemporary research has established use of pulverized fly ash (PFA), silica fume (SF), metakaolin (MK) and granulated ground blast furnace slag (GGBS) as suitable SCMs. This study has focused on using two established industrial waste SF and MK and two agricultural wastes, rice husk ash (RHA) and palm ash (PA), to determine and compare their potential use as pozzolanic SCMs and to expand the family of alternative pozzolanic binders in addition to PFA and GGBS. The w/c (w/b) ratio was 0.4 with an intended design mix strength classification of C50/60. The chemical composition of all the materials was determined through x-ray spectrometry/ diffraction test to ascertain the chemistry. All four materials satisfied the ASTM constituent criteria for pozzolans. In comparison to the control mix (100% cement content), all these materials improved the compressive strength from 2.5% to 30% and enhanced tensile strength from up to 17%, indeed all the SCM mixes had a higher compressive strength than the control. RHA exhibited the best performance in agricultural waste with 10% optimum quantity to give maximum compressive strength of 83 MPa and PA exhibited the optimum performance with 2.5% content and gave maximum compressive strength of 78 MPa. The addition of MK progressively increased the compressive strength with 20% content mix giving a strength of 84 MPa. The SF performed the best at optimum quantity of 2.5% and exhibited the highest compressive strength of 90 MPa. The results suggest that these SCM based concrete are recommended for formulation of high-strength concrete applications, i.e., 60+ MPa. Furthermore, all the SCMs had at least one mix which satisfied the C60/75 classification without reducing the w/b ratio below 0.4; this has significant positive ramifications for the development of sustainable high-performance concrete. The absorption of waste materials from industrial and agricultural fields can substantially reduce waste disposal and more pertinently facilitate in reducing the CO₂ emission associated with the construction industry.

*Corresponding author

Ash Ahmed, Reader (Associate Professor), Civil Engineering Group, School of Built Environment & Engineering, Leeds Beckett University, Civic Quarter Northern Terrace Leeds, LS2 8AG, UK. E-mail: a.ahmed@leedsbeckett.ac.uk

Received: September 07, 2021; Accepted: September 14, 2021; Published: September 21, 2021

Keywords: Pozzolanic Materials, Cement Replacement, Comparative Analysis, High-Performance Concrete, Sustainability

Introduction

The ordinary Portland cement (OPC) concrete has revolutionized the construction industry due to its intrinsic mechanical properties, quick setting and ease of use and has become the most widely used construction material [1-10]. The shift of use from naturally occurring lime as construction material in ancient time to present use of cement concrete has successfully enabled the construction of mega infrastructure but has also posed a serious sustainability threat to the environment because of its large-scale contribution to greenhouse gas's emission. The cement industry is considered to be one of the biggest CO₂ emitters in the world. It is estimated that around 4 billion tons of CO₂ is contributed annually that

makes 7-10% of global CO₂ emissions [11]. The mining of raw materials, transportation, cement production, delivery, concrete preparation and fuel usage by the industry all are considered hazardous to the environment and raising serious questions on sustainability and environment protection [2]. The researchers are in quest of formulating SCMs to produce improved cement composites with partial/ full cement replacement using sustainable pozzolanic industrial and agricultural waste materials. The faster growth, urbanization, increased population and technological advancement in the world are resulting into invention of new materials/ resources and production of more waste especially in developing African and Asian countries. World's waste production is estimated to be 2.2 billion tons per year by 2025 including 50% agricultural waste, 40% industrial waste and 10% domestic or miscellaneous waste [3]. If this enormous waste is recycled



Elucidation of novel, alternative, fiber-reinforced iron-based pozzolanic composites as SCMs

Hafiz Muhammad Nadir^{1,*}, Ash Ahmed¹, Ikram Moshir¹

Academic Editor: Raul D.S.G. Campilho

Abstract

The researchers pioneered incorporating waste materials exhibiting pozzolanic properties and waste fibers from diverse industrial/agricultural fields into the construction industry to formulate enhanced, greener supplementary cementitious composites (SCMs). This research focused objectively on the formulation/evaluation of low-CO₂-embodied greener construction materials known as "novel, alternative, fiber-reinforced iron-based binary/ternary pozzolanic composites (abbreviated as NAFRIC)". The composites incorporated iron powder (Fe), metakaolin (MK), pulverized fly ash (PFA), ground granulated blastfurnace slag (GGBS), palm ash, silica fume, and limestone, which are anticipated to absorb CO₂ while producing siderite (ferrous carbonate FeCO₃). All the NAFRIC mixes formulated in this study demonstrated up to 4–13% improvement in compressive strength and 70–130% in flexural strength with an enhanced rupture modulus/post-crack ductility. The ternary pozzolanic iron-based fiber-reinforced concrete (FRC) composites containing 8% MK + 10% PFA + 10% GGBS and steel/polypropylene/polyethylene terephthalate (PET) fibers performed the best with attaining up to 70 MPa compressive and up to 8.9 MPa flexural strengths. The sulfate testing evaluated the durability of NAFRIC SCMs formulated in a 1:2:3 ratio better than cement concrete control mix with a 1:1:3 ratio. NAFRIC specimens demonstrated minimal surface deterioration/elongation and negligible/no strength reduction after 270 days of concentrated sulfate attack. The microstructural analysis using X-ray diffraction/fluorescence, scanning electron microscopy/energy-dispersive analysis with X-ray spectroscopy supported the strength and durability parameters by showing minimal/no ettringite formation and increased calcium silicate hydrates gel formation due to the use of FeCO₃ and pozzolans. The study demonstrated the sustainable use of these better-performing NAFRIC SCMs with 10–12% reduced embodied CO₂ as eco-friendly high-strength SCMs with enhanced engineering/environmental benefits.

Keywords: iron, pozzolans, FRC, NAFRIC SCMs, durability, embodied CO₂.

Citation: Nadir HM, Ahmed A, Moshir I. Elucidation of novel, alternative, fiber-reinforced iron-based pozzolanic composites as SCMs. *Academia Materials Science* 2024;1. <https://doi.org/10.20935/AcadMatSci7277>

1. Introduction

1.1. Background

The CO₂ emission from ordinary portland cement (OPC) manufacturing, raw materials quarrying, and transportation is estimated to be around 10% of global emissions (0.8–0.9 tons of CO₂ per ton of cement manufacturing), making the construction industry the second most significant contributor to global warming and depleting natural resources. The earth is facing another challenge of increased production/disposal of waste materials from industries, agricultural, and domestic fields. Waste production has intensified manifold in the last few decades due to technological advancements, increased world population, and inventions of new materials and is estimated to reach more than 2.2 billion metric tons annually by 2025 [1–9]. The global greenhouse gas (GHG) emissions from cement concrete manufacturing can be divided into five phases. In the first phase, the mining, extraction, and calcination of cement raw materials, fine and coarse aggregates, and manufacturing of admixtures (including air entrainers, plasticizers, accelerators, retarders, and

curing compounds) are the significant CO₂ emitting processes (up to 75–85%). The second phase accounts for up to 6% of emissions, including national/international transportation of cement/other ingredients. The third phase is mixing concrete ingredients in the in situ/onsite or at the concrete plants away from the construction sites. The fourth phase is transporting fresh concrete from the plants to the construction sites using transit mixers. The fourth and fifth/final phases are responsible for up to 10–15% of CO₂ emissions and include the transportation, placement of concrete for construction using formwork, concrete pumps, vibrators, curing, hydration, ultimately demolition, and then recycling it to use as recycled aggregates as useful waste disposal [10]. Concrete main ingredients are binder (cement responsible for up to 80% of GHG emissions), fine/coarse aggregate (responsible for up to 5% GHG emissions), admixtures (responsible for up to 2% GHG emissions), and water (zero emissions) [4, 3, 7, 10–12]. The use of cement alternatives/partial replacement composites is the foremost applicable solution to reduce the carbon footprints of the construction

¹Civil Engineering Group, School of Built Environment & Engineering, Leeds Beckett University, Leeds LS2 8AG, UK.
*email: hafiznadir786@gmail.com

Use of Coconut COIR in Fiber Reinforced Concrete, Soil and Lime


Ash Ahmed^{1*}, Hafiz Nadir², Colin Yates³ and Lee Yates³

¹Associate Professor, Civil Engineering Group, Leeds Beckett University, UK

²Doctoral Researcher, Civil Engineering Group, Leeds Beckett University, UK

³Conserv Lime Products, UK

*Corresponding author: Ash Ahmed, Associate Professor, Civil Engineering Group, Leeds Beckett University, UK

Received:  October 30, 2020

Published:  December 02, 2020

Abstract

The use of lime as a binder and natural fibers as reinforcements have been in use since ancient human history. However, ordinary Portland cement and concrete have substituted these comparatively cheaper eco-friendlier materials due to their quick setting and strength parameters since the 19th century. However, their large-scale impact on the environment due to greenhouse gases emission has encouraged further research to develop novel composite materials comprising natural fibers like coconut coir and lime as partial cement substitute. In this review study, contemporary research studies conducted by different researchers were explored and has found this field quite encouraging and progressive for modern trends in construction materials. Coir is a material with great potential due to its high strength and ductility comparable to steel; the use of lime or saline treated coir in cement by 1% as optimum quantity and in some cases up to 2% quantity, enhanced the compressive, tensile and flexural strengths up to 5%-20%. Ductility and flexibility of concrete improved with more energy absorption capacity. However, more use of coir did not improve engineering properties of concrete rather deteriorated after 2% use by weight of cement. 1% to 2% coir use in expensive marine soil augmented by 5% use of lime revealed considerable increase in engineering properties of soil especially increase of compressive strength by 1.5 times, increase of compaction factor and plasticity and reduction in shrinkage and liquid limit thus supporting a fruitful use of coir and lime mixture in its properties enhancement. Coir being a natural fiber has a limitation of lesser degradation life so needs to be treated with some suitable natural coating material to enhance its life from 3 to 20 years and needs to be cleaned properly by soaking in lime or saline water to remove lignin, pith, cellulose and silicate crystals. The overall use of coir and lime as substituent of cement binders is highly recommended though further research is required to maximize usage for this economical and eco-friendly material.

Introduction

Cement, concrete, and mortar are considered as the basic materials in the world construction industry. The construction sector contributes one tenth of global GDP up to 15 Trillion USD and causes up to 10% of greenhouse emission mainly due to production of cement, use of fossil fuel, machinery/ equipment, and other petroleum products/ materials [1]. It is estimated that at least 0.9 metric ton CO₂ is produced during manufacturing of 1 metric ton of ordinary Portland cement (OPC) [2,3]. Research has focused on preparation of various composite materials which are environmentally friendly, cost effective and consumes the waste products/materials from other industrial sectors [4]. A composite is generally developed by mixing of binding materials like cement,

lime and pozzolanic materials with fine or coarse aggregate [5,6]. Such cementitious composite materials are generally characterized by their good compressive strength but weak tensile/ flexural/ torsional strength [5]. Researchers have been endeavoring to introduce new composite materials using lime and pozzolanic binders like volcanic ash (Tuff) as substitute for cement to minimize the pollution and incorporation of natural fibers to improve the strength of novel materials [7].

Use of Lime

Lime has been in use for centuries for stone masonry, facade work even in Egyptian, Romans, Greek and Iranians empires in

Potential of Utilizing Coir, Straw, and Recycled PET Fibres as Sustainable & Economical Alternative in Fibre Reinforced Concrete

Hafiz Muhammad Nadir¹, Ash Ahmed^{2*}, Parneet Paul³ and Mark Mitchell⁴

¹Researcher, Civil Engineering Group, Leeds Beckett University, UK

²Associate Professor (Reader), Civil Engineering Group, Leeds Beckett University, UK

³Professor and Head of Engineering, Department of Engineering, School of Built Environment, Engineering and Computing, Leeds Beckett University, UK

⁴Technical Director, Adfil Construction Fibres, Hull, UK

ISSN: 2576-8840



*Corresponding author: Ash Ahmed, Associate Professor (Reader), Civil Engineering Group, Leeds Beckett University, UK

Submission:  March 21, 2022

Published:  April 13, 2022

Volume 16 - Issue 5

How to cite this article: Hafiz Muhammad Nadir, Ash Ahmed², Parneet Paul and Mark Mitchell. Potential of Utilizing Coir, Straw, and Recycled PET Fibres as Sustainable & Economical Alternative in Fibre Reinforced Concrete. Res Dev Material Sci. 16(5). RDMS.000899. 2022.
DOI: 10.31031/RDMS.2022.16.000899

Copyright © Ash Ahmed. This article is distributed under the terms of the Creative Commons Attribution 4.0 International License, which permits unrestricted use and redistribution provided that the original author and source are credited.

Abstract

Researchers have been working on formulating Fibre Reinforced Concrete (FRC) composites that are economical, eco-friendly, and waste absorbent. Incorporating agricultural/ industrial waste into the construction industry as fibre-reinforced composites is a novel research field that can recycle and convert waste into valuable supplementary materials. In this study, concrete composites with fibres of coconut coir (COF), wheat straw (WSF), and shredded fibres from waste plastic bottles (PETF) were evaluated and compared against the established use of polypropylene fibres (PPF) and steel fibres (SF). The study's objectives were set to attain the strength of 32-40MPa (C32/40 European grade) for using these waste fibres as alternatives in FRC. A concrete mix ratio of 1:2:3 with 1-2% waste fibres (COF & PETF), 1-2% PPF and 10% & 17% steel fibres were used to produce cubes, cylinders, and prisms for testing on 7 and 28 days for evaluation of compressive, split tensile and flexural strengths. Generally, all FRC mixes with 1% fibre dosage exhibited an increase of compressive strength by 9-44% at 28 days of curing. All fibre composites gave characteristic compressive strength of 40-60MPa. The split tensile strength of all-fibre composites was improved up to 48% with 1-2% fibres. The flexural strength of all-fibre composites improved by 11-42% with 1% fibre and 10% steel fibre but increased fibre's quantity to 2% and steel fibre to 17% reduced the flexural strength suggesting that fibre content should not exceed more than 2% of cement weight in composites. Shredded fibres of PET plastic bottles outperformed the established micro/macro PPF as PETF exhibited better flexural strength than PPF with both 1 and 2% dosages. The natural fibres of coir/ wheat straw gave better/ at par flexural strength (7.3MPa) compared to steel fibres (6.9MPa). In conclusion, it is suggested that the optimum quantity of 1-2% of these novel alternative fibres after necessary treatment is feasible for the formulation of environmentally friendly fibre concrete composite with enhanced mechanical properties.

Keywords: Fibre-reinforced concrete; Waste fibres materials; Mechanical properties; Post crack ductility; Empirical modelling

Introduction

Concrete is an internationally recognised primary construction material used at a large scale for all types of modern construction due to its favourable mechanical properties, ease of use, economy, and sustainability. The fundamental binding ingredient of concrete is the cement which has replaced all old pozzolanic binders and lime with commercially produced grey/ white ordinary Portland cement. This cement was derived from hydrated lime, given the name of Ordinary Portland Cement (OPC) by Joseph Aspdin in 1824 due to its resemblance to Portland stone found in Isle of Portland, Dorset, UK. The enhanced version of commercial cement was introduced by his son William Aspdin in 1840 and is mainly in use in present manufacturing industries with some improvements/modifications/additions [1]. Concrete is among the most widely used materials due to its compressive strength, durability, early setting time, and in situ usability. Still, it exhibits lower tensile/ flexural strength and

Advances in Earth and Environmental Science

Strategic Integration of Catchment Level Natural and Structural Methods of Sustainable Flood Management: A Case Study of River Wharfe Catchment Area

Hafiz Muhammad Nadir¹, Ash Ahmed², Molly Asher³, Chris Goodwin³, Oliver Kenyon³, Luke Rogers³ and Craig Routledge¹¹PhD Researcher, Civil Engineering Group, School of Built Environment & Engineering, Leeds Beckett University, Civic Quarter Northern Terrace Leeds, LS2 8AG, UK.²Reader/ Associate Professor, Civil Engineering Group, School of Built Environment & Engineering, Leeds Beckett University, Civic Quarter Northern Terrace Leeds, LS2 8AG, UK.³MS Students School of Geography, University of Leeds, Woodhouse, Leeds, LS2 9JT, UK.***Corresponding author****Hafiz Muhammad Nadir,**
PhD Researcher, Civil Engineering Group,
School of Built Environment & Engineering,
Leeds Beckett University,
Civic Quarter Northern Terrace Leeds,
LS2 8AG, UK.

Submitted : 8 Apr 2024 ; Published : 17 May 2024

Citation: Nadir, H. M. et al. (2024). Strategic Integration of Catchment Level Natural and Structural Methods of Sustainable Flood Management: A Case Study of River Wharfe Catchment Area. *Adv Earth & Env Sci*; 5(2):1-11. DOI : <https://doi.org/10.47485/2766-2624.1043>**Abstract**

Water has a crucial place in the advent of humankind the flourishing of mega population centres, and is an essential source of food, water transportation, and irrigation. The anthropogenic activities in taming the natural water streams to the optimum benefit of human beings disturb natural flood plains, ecology and habitat. The channelisation of streams and hydromodifications in dams, barrages or reservoirs result in climatic variations locally/ regionally and impact transborder stream flow. Researchers have been endeavouring to restore the flood plains to their natural conditions. Still, huge hydromodifications and the development of megacities right in the flood plains or adjacent to the streams have resulted in irreversible disturbances to the natural lay of ground/ landscape. Therefore, to avoid flooding disasters, further structural interventions are undertaken to augment the natural flood prevention methods using advanced materials like cement concrete, steel, and polymers rather than increasing the emissions of greenhouse gases. Considering the strategic necessity of engineering structures as an integrated catchment level solution to augment the natural methods, the researchers/ engineers are now focussing on the use of sustainable, eco-friendly materials and demountable/ hydraulic structures to minimise the carbon footprints of hydromodifications and to decrease the obstruction to the natural flow of streams by using the flood prevention structures/ gates/ walls/ reservoirs only in case of disastrous flooding and otherwise keeping them unemployed during normal stream discharges. This study has been used to review sustainable flood management using natural and structural techniques in the Wharf River catchment in the UK, reviewing the existing research/ flood management schemes giving the pictorial coverage. The study suggests that natural flood management techniques have restricted application parameters and must be augmented by engineering structures to achieve effective flood management against heavy flooding. Low CO₂ embodied greener infrastructure structural materials containing supplementary cementitious materials (SCMs) can be a beneficial option for an environmentally friendly flood management strategy.

Keywords: Catchment level integration, sustainable flood management, natural methods, engineering structures, eco-friendly alternative materials.**Introduction**

Flood management is about managing flood risk to minimise loss of life, damage to property and economic disruption (Solin & Skubincan, 2013). Flood management measures can have unintended adverse social or environmental impacts downstream, e.g., on river ecology (Keep, 2017). Sustainable flood management aims to provide maximum physical, social and economic resilience to flooding and its impacts (Wernity, 2006). It is susceptible to various interpretations according to the causes/ effects of flooding, intended objectives, and the quantum/ capacity of flood protection management

(Kundzewicz, 2002). Sustainability depends on local context, drivers of flooding and flood risk (Qi & Altinaker, 2011) and incorporates the requisite balancing of environmental goals by amicably addressing the social and economic consequences of any anthropogenic activities/ hydromodifications (Emery & Hannah, 2014). It includes natural flood management and resilience measures employed using structural solutions (Qi & Altinaker, 2011). Sustainable flood management includes several techniques which can be employed alone or as a combination based on required protection, the geology of the

A Review of the Utilisation of Hydrated Lime (CL-90) in Engineering Applications and it's Sustainability Implications

Hafiz Muhammad Nadir¹, Ash Ahmed^{2*}, Colin Yates³ and Lee Yates³

¹PhD Researcher, Civil Engineering Group, School of Built Environment & Engineering, Leeds Beckett University, Civic Quarter Northern Terrace Leeds, LS2 8AG, UK.

²Reader/Associate Professor, Civil Engineering Group, School of Built Environment & Engineering, Leeds Beckett University, Civic Quarter Northern Terrace Leeds, LS2 8AG, UK.

³Conserv Lime Products, UK.

*Correspondence author

Ash Ahmed,
Reader/ Associate Professor
Civil Engineering Group
School of Built Environment & Engineering
Leeds Beckett University
Civic Quarter Northern Terrace Leeds
LS2 8AG
UK.

Submitted : 17 Aug 2022 ; Published : 9 Sept 2022

Citation: Ahmed, A. et al. A Review of Worldwide Applications of Hydrated Lime and Its Implications on Environmental Protection and Engineering Benefits in Different Industries. J mate poly sci, 2022; 2(3): 1-7.

Abstract

Lime is one of the widely used materials in several industries, with an estimated production of 430 million tons worldwide, with the iron, steel and metal industries as the leader, using 250 million tons, followed by the construction industry using around 75 million tons and the chemical industry with 55 million tons usage per annum worldwide. The broadly used types of lime are quick lime CaO (CL90 Q), hydrated lime Ca(OH)_2 (CL90 S), hydraulic lime and lime putty. The primary purpose of hydrated lime is to induce alkalinity and use it as filler material to control porosity. Hydrated lime, unlike hydraulic lime, does not exhibit much-cementing properties on mixing with water. Therefore, it requires blending with suitable binders like cement, pozzolans, and bitumen to acquire better binding characteristics. Hydrated lime is widely used in the iron and steel industry as a cheap, sustainable material for converting iron into pig iron and steel and improving the durability of refractories in the blast furnace. The agriculture and food industry also relies heavily on hydrated lime to be used as a purifying flocculating coagulating agent, especially in the sugar industry. The hydrated lime acts as an alkali activator, deodorizing and anti-bacterial chemical in treating wastewater/sludge, agricultural fields and environmental protection. The hydrated lime is used to treat wet, marine and cohesive expansive clayey soils as it absorbs moisture and improves engineering properties like compressibility, strength, plasticity, bearing capacity, consistency, shear strength and shrinkage etc. One of the main usages of hydrated lime in civil engineering applications is in cement-based mortars as a plasticiser. Therefore, the hydrated lime can be recommended for use in diverse industries and multi-purpose roles.

Keywords: Hydrated lime, CL-90, worldwide usage, applications, chemical reaction, benefits.

Introduction

There are different types of lime products including hydrated lime, quick lime, hydraulic lime and lime putty. Most of these products originate from limestone and have differing mechanical & chemical properties and hence applications. In this paper, the emphasis will be on hydrated lime. It is well known that hydrated lime is produced by carefully mixing quick lime CaO with water to make Ca(OH)_2 containing 25% water and 75% lime (Graymont, (n.d.)). Quick and hydrated lime are among the topmost used lime types in different industries, including construction, manufacturing, agriculture and food industries. Worldwide use of lime is estimated to be 430 million tons per year (USGS, (n.d.)). The construction

industry had been a significant lime user in ancient times. Still, with the advancement of chemical and manufacturing industries after the industrial revolutions in the 1900s, these industries have become prominent users of lime (USGS, (n.d.); Carmeuse, (n.d.) Carmeuse, (n.d.)). Fig 1 shows iron and steel industry has now become the leading user of 51% lime, followed by the construction industry, chemical industry and environmental protection/ waste disposal and treatment (USGS, (n.d.); Piringer, (2017)).

The Critical Review of the Efficacy of the Environmental Impact Assessment (EIA) Process as A Tool Intended to Protect the Environment from Construction/ Development's Hazards

Hafiz Muhammad Nadir^{1*} and Ash Ahmed²

¹PhD Researcher, Reader/ Associate Professor

²Civil Engineering Group, School of Built Environment & Engineering, Leeds Beckett University, Civic Quarter Northern Terrace Leeds, LS2 8AG, UK

ABSTRACT

The developed countries have been doing extraordinary marvels in science, technology and construction with a desire to tame nature coherently. This domination desire has negatively/ irreversibly impacted the environment. However, after generating enormous challenges to nature through uncontrolled developments, the developed countries started endeavouring to save the environment from the devastating impacts of construction projects at the end of the 20th century by incorporating the environmental impact assessment (EIA). EIA is the process of identifying, evaluating, and mitigating development projects' damaging environmental and social effects. In the last 25 years, EIA has developed into a mature system and is an effective tool for assessing, minimising and mitigating severe impacts of development projects on the environment. EIA is only an assessment tool to ascertain the damaging effects of projects on the environment and alternative proposals for their mitigation; however, the final decision rests with political authorities who may consider the EIA report or turn it down in the name of better interests of society/country. Unfortunately, EIA has not proved to be a fully effective process as the developed countries are still undertaking unobstructed/ unopposed mega development projects best conforming to their better interests, and developing countries are still far behind in the apprehension of the necessity of EIA. However, with the UN, USA and EU efforts, more than 120 countries have pledged to exercise EIA to assess development projects before their commencement. In this study, an endeavour has been made to review the necessity/ objectives of EIA, its historical evolutionary process, internationally recognised legal obligations, the stages of the EIA process based on the nature of projects, constraints/ pros and cons of the implementation of EIA process and efficacy of EIA as an intended tool to save the environment from the hazards of mega projects duly supported by three case studies of international projects in USA, Sweden and Pakistan.

*Corresponding author

Hafiz Muhammad Nadir PhD Researcher, Civil Engineering Group, School of Built Environment & Engineering, Leeds Beckett University, Civic Quarter Northern Terrace Leeds, LS2 8AG, UK.

Received: April 19, 2023; Accepted: April 25, 2023; Published: April 30, 2023

Keywords: EIA Process, Objectives, Pros and Cons, Constraints, Efficacy Case Studies

Introduction

International Establishment of EIA

The USA pioneered the spearhead lead in 1969 by officially promulgating the "National Environmental Policy Act". It incorporated environmental protection as the government's responsibility, incorporating the legal authority for the regulators to repudiate a project if considered an anthropogenic environmental hazard [1]. The Stockholm conference in 1972 enlightened/ commenced the world's attention to the environmental consequences of inadvertent development [2]. The UN summit on environment and development (UNCED), also termed the 1992's Rio de Janeiro convention, took the leading initiative in developing the binding concept of sustainable development by considering EIA paraphernalia as a pre-planning requisite [3]. The major countries in the world are signatories to implementing

the EIA as a process to identify the effects of anthropogenic activities on nature/ environment by any large project. The planning authorities widely accept EIA as an assessment tool to anticipate, identify, and mitigate mega projects' environmental impacts/ paradigms to ensure sustained development with minimum environmental repercussions [4]. "The International Association for Impact Assessment (IAIA)" was established in 1980 as a leading global policy-making forum on EIA. It has over 1,600 members representing all countries [5]. EU also followed the USA and proposed the first agreed regulations in 1985, which have been amended several times till the present-day form of the 2017 directive [6].

EU EIA Directive and EIA in the UK

EU EIA directive comprises eight principles, i.e., participation, transparency, certainty, accountability, credibility, cost-effectiveness, flexibility and practicality. These principles give complete discretion to experts to assess and evaluate the projects'

A Comparative Study Investigating the Feasibility and Potential of Utilising Polymer, Demolition & Glass Waste as a Partial Replacement for Fine and Coarse Aggregate in Concrete

Ash Ahmed^{1*} and Hafiz Muhammad Nadir²

¹Associate Professor, Civil Engineering Group, School of Built Environment & Engineering, Leeds Beckett University, Civic Quarter Northern Terrace Leeds, UK

²PhD Researcher, Civil Engineering Group, School of Built Environment & Engineering, Leeds Beckett University, Civic Quarter Northern Terrace Leeds, UK

ABSTRACT

The construction industry is a key CO₂ contributor. Contemporary research focuses on formulating cement replacement composites; however, less attention is deliberated to formulating fine/coarse aggregate replacement composites. The waste from different fields contributes enormously to adverse environmental effects, thus necessitating reuse/recycling. The demolition/reconstruction of old buildings/infrastructure is adding further to the waste contribution by the construction industry. The total quantum of fine/coarse aggregate in the construction industry is estimated to be around 20 billion tons, contributing around a billion tons of CO₂. Therefore, even partial replacement of virgin sand/coarse aggregates with various waste materials like glass, rubber, plastic, tyres, recycled concrete and others will economise the cost of manufacturing the concrete with reduced CO₂ footprints as eco-friendly materials. This study conducted a comparative analysis for investigation of the characteristic compressive and split tensile strength of concrete composites with partial replacement of virgin sand/coarse aggregate by 10-30% of Crushed Glass (CG), Crumb Rubber (CR), Recycled PET Bottles (RPB), Recycled Concrete Aggregate (RCA) and 5-10% of Shredded Tyres (ST). Generally, all the composites demonstrated par/ better strength with the control mix, achieving the target strength of C35/67 concrete. The composites with CG, RPB and RCA exhibited an improvement in compressive strength, attaining more than 70 MPa (high-performance concrete strength) and up to 10% improvement in split tensile, attaining 4.3 MPa. CR and 5-10% ST exhibited a slight decrease in compressive strength. All the composites formulated in this study explicate their diverse uses for multipurpose infrastructural applications in the construction industry as improved, economical, eco-friendly waste absorbent composites.

*Corresponding authors

Ash Ahmed, Associate Professor, Civil Engineering Group, School of Built Environment & Engineering, Leeds Beckett University, Civic Quarter Northern Terrace Leeds, UK.

Received: November 13, 2022; Accepted: November 25, 2023; Published: December 28, 2023

Keywords: Eco-Friendly Composites, Fine/ Coarse Aggregate Replacement, Compressive Strength, Split Tensile Strength, Preservation of Natural Resources

Introduction

The construction industry is envisaged among the top global waste and carbon dioxide (CO₂) contributors. 80% of the construction sector's share is contributed by manufacturing/ transportation/ formulation of cement concrete alone. Fine and coarse aggregate are the essential ingredients of concrete and account for around 15-20% share of the construction industry's waste/ greenhouse gas emissions. Moreover, mining/extracting gravel/ sand or crushing rocks to get fine/ coarse aggregate depletes these naturally occurring resources faster, resulting in a scarcity of resources and environmental/ ecological impacts. The construction industry is estimated to produce around 5 billion tons of CO₂ globally, mainly contributed by cement concrete. Global cement production is approximately 4.1 billion tons per year; therefore, cement production alone accounts for more than 4 billion tons of CO₂, with around one ton of CO₂ emission per ton of cement. The quarrying, transportation and crushing/ extraction of around 20 billion tons

of sand, gravel and aggregates for the formulation of cement concrete/ road construction account for about one billion tons of additional CO₂ emission per year. The global aggregate market size is estimated at around 500 billion USD. Concrete manufacturing makes up 70% of the global aggregate market share, highways/ airfield construction 18%, and 12% is the market share of all other industries/ uses, as illustrated in Figure 1. The USA, Canada and Mexico in North America, Brazil in South America, Germany and the UK in Europe, Gulf countries in the Middle East, and China and India in Pacific Asia are the major consumers of the aggregates due to significant ongoing construction/development works in these countries.

The mining, excavation, and crushing industry for producing fine and coarse aggregates is experiencing a surge in demand and financial benefits. However, this trend has led to illegal and uncontrolled production, resulting in a faster depletion of natural resources, non-conservation of these resources for future generations and damaging impacts on the environment [1-5]. The ecology and biodiversity of natural habitats are also disturbed and fauna and flora are adversely affected due to the loss of vegetation

A Projected Hydrological Study and Catchment-Level Hydrograph Modelling for Channel Stabilisation

Hafiz Muhammad Nadir*

Civil Engineering Group, School of Built Environment & Engineering, Leeds Beckett University, Leeds, UK

ABSTRACT

The environmental impacts and anthropogenic activities in the name of the development of water streams, like the construction of bridges, roads, and built-up areas across water drainage paths, disturb the natural flow pattern and give rise to inundation and flood disasters in low-lying areas. These phenomena are incredibly pronounced in the absence of concerted hydrological modelling and environmentally friendly construction materials while planning for construction in a river basin for flood prevention, hydromodifications or hydraulic structures. This study has endeavoured to conduct the hydrological study of one of the fastest-flowing rivers in the UK, 'The Swale River', as a projected case study to assess a projected 200-year rainfall/storm event, statistical modelling for catchment level efficiency, discharge quantum, lag time, projected hydrograph analysis for extracted rainfall, runoff, discharge flow data and exceedance from existing 48 months rainfall/runoff data. The potential impact of these findings on future construction projects is significant, as they can guide the development of more sustainable and environmentally friendly construction practices. The statistical modelling proposed a heavy 200-year flood of 360 m³/sec discharge for a catchment area of 1446 km² and 118 km length, using a projected heavy flood event of 6 cm precipitation in 8 hours for Swale River to ascertain the formation of discharge in the river after a 6-8 hours lag time with 30% catchment efficiency. This hydrograph modelling gives detailed working for the requirement of flood protection and placement of rescue and relief operations in case of flooding caused by the overflowing of the river to stretch of 1-2 km along the channel having a water depth of 2-10 feet, likely to impact the life and properties.

*Corresponding author

Hafiz Muhammad Nadir, Civil Engineering Group, School of Built Environment & Engineering, Leeds Beckett University, Leeds, UK.

Received: September 16, 2024; Accepted: September 23, 2024; Published: October 05, 2024

Keywords: Hydrology, Statistical Modelling, Hydrograph Analysis, Rainfall/ Discharge Forecasting, Lag Time, Flooding Extent

deployment of suitable flood protection techniques/rescue/ relief equipment as per the lag time are imperative for the catchment-level safe management of river discharge.

Introduction

Water is crucial in humankind's advent and mega population centres' establishment. However, the powerful human desire to tame natural water resources for their benefit grossly impacts the ecology and natural inhabitants, the local/ regional climatic variations and disturbed transborder stream flow. The reclamation of land for agricultural purposes, deforestation, peatland modification, the convergence of vast flood plains to narrow streams, heavy hydro-structural modifications, surface runoff obstructions, disturbed water cycle, lesser sub-soil absorption and increased runoff velocity are among the significant anthropogenic activities in river basins. The cloud bursts due to global warming/ climatic variations cause heavy precipitation in short intervals, thus decreasing the lag time between a storm event and a peak discharge, resulting in flash flooding/ disasters. Researchers endeavoured to restore the floodplains using natural and structural methods separately or in combination. The natural methods of floodplain restoration are short-lived, limited and less efficient, especially for the extensive stretches of more significant streams. This necessitates the incorporation of structural methods of flood protection in the form of dams, reservoirs, barrages, channels, the lining of rivers and the erection of artificial means/ hydraulic structures, which are considered robust, strong, efficient and resilient but likely to cause environmental/ ecological disorder [1-3]. Therefore, deliberate hydrological/ statistical studies and

Historical Flood Events

Water has a special place in the life of human beings as a basic necessity, and all civilisations developed along the waterfront which resulted in ecological modifications/ climate changes, glaciers melting, extraordinary precipitation events, flooding and damage to aqua life and wildlife [4,5]. The disturbance in transborder water streams results in demand-supply gaps and international conflicts to establish control over land/ water resources. In the South Asian sub-continent, Kashmir is the originating point of many significant rivers of Pakistan and India. Both countries fought three major wars in the last around 75 years, and the region is still considered a nuclear war flash point. Moreover, these rival countries' construction of dams and unannounced water storage/ release in upstream/ downstream of the transborder rivers resulted in floods and drought events even in the recent past [6]. Yangtze River in China has a history of devastating floods periodically, especially the worst floods in 1911, 1935 and 1954, which resulted in the deaths of millions of people and the swapping of properties/ land in a 6300 km stretch, Yellow River in China, Indus in Pakistan, Ganges, Jumna and Brahma Putra in India and Bangladesh are the major flood causing rivers mainly arising from climatic changes and urbanisation/ modifications along natural rivers flood plains [7,8]. The flood in 2011 in the Mississippi River was the worst of its kind, impacting 31 American states, causing hundreds of casualties and destruction/evacuation of millions of

**A Comparative Evaluation of Embodied Environmental Impacts of Channel
Stabilisation Using Concrete Lining and Alternative Pozzolanic Materials**

Hafiz Muhammad Nadir

PhD, Research Associate,

Civil Engineering Group, School of Built Environment & Engineering,
Leeds Beckett University, Leeds, UK.

|

Abstract:

Channel stabilisation with the lining of bed/ banks using cement-concrete (with/ without steel reinforcement as per the size, depth, and capacity), geomembrane, polymers, canvas, ramped earth, vegetation, gravel/ stone pitching, and brick blast is a common practice worldwide to save the adjacent flood plain areas from bank overflowing, seepage, water logging/ salinity, loss of water in irrigation channels, maintaining required water levels and strengthening of channels to be used as transportation means. A trapezoidal channel of cross-section 165 m^2 and a lined perimeter of 42m was proposed to accommodate a super flood of $360 \text{ m}^3/\text{sec}$ discharge for a catchment area of 1446 km^2 and 118 km length, using a projected heavy flood event of 6 cm precipitation in 8 hours for Swale River to ascertain the material calculation and its environmental impact. This concrete lining would likely produce an equivalent global warming potential/ embodied carbon dioxide (CO_2) of 284 million $\text{kgCO}_2\text{-eq}$ (kilogram CO_2 equivalent) with the projected use of around 271 million kg of cement concrete and 78 million kg of steel. The enormous amount of embodied CO_2 emissions from this projected lining project suggested using natural means of flood/ channel protection if feasible, or alternative supplementary cementitious materials with fibres should be used to minimise the environmental impacts.

Keywords: Hydrology, materials science, channel stabilisation with lining, cement concrete, embodied CO_2 , environmental impacts.

Introduction

The natural methods of floodplain restoration are short-lived, limited and less efficient, especially for the extensive stretches of more significant streams. This necessitates the incorporation of structural methods of flood protection in the form of dams, reservoirs, barrages, channels, the concrete lining of rivers and the erection of artificial means/ hydraulic structures, which are considered robust, strong, efficient and

resilient but likely to cause environmental/ ecological disorder due to use of cement as a basic material (Nadir and Ahmed, 2022b; Nadir, 2024a; 2024b; 2024c). Cement is the leading cause of the carbon footprint of concrete in the construction industry. As professionals in the field, the audience plays a crucial role in finding and implementing sustainable solutions to this issue. Cement is classified as third in the greenhouse gas (GHG) emissions after the iron and steel industries, but its large-scale

Summary of Results (Other results could be provided on request)

Compressive Strength of FRC and NALFRIC

28 Days and 91 Days Compressive Strength															
FRC 123					SL80 112					MK50 112					
	28 Days Compressive Strength (MPa)	91 Days Compressive Strength (MPa)	270 Days Compressive Strength (MPa)	270 Days Compressive Strength (MPa) in Sulphate		28 Days Compressive Strength (MPa)	91 Days Compressive Strength (MPa)	270 Days Compressive Strength (MPa)	270 Days Compressive Strength (MPa) in Sulphate			28 Days Compressive Strength (MPa)	91 Days Compressive Strength (MPa)	270 Days Compressive Strength (MPa)	270 Days Compressive Strength (MPa) in Sulphate
FRC 123					SL80 112							MK50 112			
Con	42.3	53.0	58.2	53.7	Con	18.2	19.8	27.1	28.2	Con		9.3	10.4	14.4	8.7
ST 5%	53.5	60.8	60.8	56.7	ST 5%	16.9	21.5	25.0	29.7	ST 5%		11.5	11.6	13.4	8.0
ST 10%	54.1	60.1	61.5	53.4	ST 10%	17.0	20.7	24.5	31.2	ST 10%		11.3	11.3	11.8	7.4
PPF 0.5%	57.2	59.5	65.5	54.5	PPF 0.5%	16.6	17.4	24.5	33.0	PPF 0.5%		9.6	11.6	12.5	10.7
PPF 1%	59.2	57.6	61.2	53.1	PPF 1%	14.5	18.5	23.5	32.9	PPF 1%		8.8	9.2	10.5	10.4
PPF 1.5%	58.9	55.5	55.4	49.9	PPF 1.5%	13.8	17.1	23.0	29.2	PPF 1.5%		6.3	7.9	8.7	8.2
PPF 2%	53.8	59.6	59.5	49.4	PPF 2%	12.8	15.5	21.1	30.2	PPF 2%		7.3	7.5	8.7	7.9
Coir 0.5%	51.8	57.6	57.5	49.3	Coir 0.5%	14.0	16.2	22.1	29.1	Coir 0.5%		8.2	8.2	8.7	6.9
Coir 1%	53.5	56.5	56.3	51.6	Coir 1%	13.3	16.4	21.1	29.8	Coir 1%		7.3	9.2	9.9	6.2
Coir 1.5%	47.4	48.5	49.7	53.0	Coir 1.5%	13.8	15.9	20.5	26.1	Coir 1.5%		7.1	8.7	8.8	6.2
Coir 2%	44.5	49.7	49.5	40.8	Coir 2%	12.7	15.0	20.6	27.3	Coir 2%		6.6	7.5	7.6	5.7
PET 0.5%	49.8	55.9	60.5	51.1	PET 0.5%	14.9	18.4	24.8	33.8	PET 0.5%		7.6	8.7	9.0	8.5
PET 1%	48.3	49.4	58.7	51.8	PET 1%	16.5	17.7	24.5	31.5	PET 1%		7.2	8.4	8.8	7.0
PET 1.5%	45.2	50.7	55.0	50.3	PET 1.5%	15.2	17.9	25.0	30.8	PET 1.5%		8.0	9.4	9.8	7.3
PET 2%	45.1	50.6	51.0	44.9	PET 2%	14.4	16.1	22.3	29.3	PET 2%		8.5	9.1	9.9	7.3
WS 0.5%	46.2	49.3	51.0	40.2	WS 0.5%	11.2	14.4	15.3	23.3	WS 0.5%		6.5	7.0	7.1	5.3
WS 1%	45.1	48.7	48.4	43.8	WS 1%	9.7	12.0	15.9	21.9	WS 1%		6.2	8.6	8.7	5.2
WS 1.5%	43.6	41.4	45.1	39.4	WS 1.5%	9.0	10.3	14.2	21.5	WS 1.5%		7.1	8.2	8.4	4.3
WS 2%	43.1	43.2	44.0	34.4	WS 2%	8.9	10.1	13.7	20.9	WS 2%		5.8	7.7	7.9	4.1

Flexural Strength of FRC and NALFRIC

91 Days Flexural Strength										
FRC 123				SL80 112				MK50 112		
3	Flexural Strength (MPa)	Displacement (mm)		SL80 112	Flexural Strength (MPa)	Displacement (mm)		MK50 112	Flexural Strength (MPa)	Displacement (mm)
Con	6.2	5		Con	2.3	22		Con	0.8	21
ST 5%	7.0	55		ST 5%	3.5	23		ST 5%	1.6	23
ST 10%	8.7	55		ST 10%	4.9	50		ST 10%	2.0	34
PPF 0.5%	7.8	21		PPF 0.5%	3.4	18		PPF 0.5%	1.3	30
PPF 1%	6.8	43		PPF 1%	4.1	22		PPF 1%	1.8	21
PPF 1.5%	7.3	54		PPF 1.5%	3.4	24		PPF 1.5%	1.8	20
PPF 2%	8.0	56		PPF 2%	3.2	23		PPF 2%	1.7	24
Coir 0.5%	6.9	19		Coir 0.5%	3.7	21		Coir 0.5%	1.1	19
Coir 1%	8.3	28		Coir 1%	3.1	26		Coir 1%	1.8	19
Coir 1.5%	6.1	37		Coir 1.5%	3.9	25		Coir 1.5%	2.0	20
Coir 2%	5.7	34		Coir 2%	3.6	29		Coir 2%	1.9	24
PET 0.5%	5.6	5		PET 0.5%	3.8	24		PET 0.5%	1.2	16
PET 1%	5.4	31		PET 1%	4.0	23		PET 1%	1.7	16
PET 1.5%	5.0	36		PET 1.5%	2.7	24		PET 1.5%	1.6	35
PET 2%	5.0	42		PET 2%	2.6	29		PET 2%	1.2	26
WS 0.5%	5.5	12		WS 0.5%	2.7	24		WS 0.5%	1.5	12
WS 1%	5.9	23		WS 1%	2.0	28		WS 1%	1.8	16
WS 1.5%	6.4	35		WS 1.5%	2.7	21		WS 1.5%	1.7	22
WS 2%	7.1	32		WS 2%	2.3	34		WS 2%	1.5	51

Flexural Strength Vs Displacement Data FRC and NALFRIC						
	FRC 123	Displacement (mm)	SL80 112	Displacement (mm)	MK50 112	Displacement (mm)
Con	6.2	5.1	0.7	21.8	0.6	20.8
ST 10%	7.0	54.6	2.5	22.6	1.6	23.1
ST 17%	8.7	54.5	2.9	49.6	1.2	33.9
PPF 0.5%	7.8	20.5	2.8	18.2	1.3	29.8
PPF 1%	6.8	43.3	2.5	22.2	1.2	20.5
PPF 1.5%	7.3	54.5	3.4	24.3	1.2	19.9
PPF 2%	8.0	55.6	2.2	22.7	1.8	24.4
Coir 0.5%	6.9	18.5	1.9	21.4	0.5	18.7
Coir 1%	8.3	27.8	1.3	26.4	0.9	18.6
Coir 1.5%	6.1	37.4	1.9	25.4	1.2	20.3
Coir 2%	5.7	34.0	1.6	28.7	0.9	23.6
PET 0.5%	5.6	5.4	2.9	23.7	0.7	16.0
PET 1%	8.0	30.9	2.0	23.5	0.8	15.9
PET 1.5%	5.0	35.7	1.5	24.1	0.7	34.7
PET 2%	5.0	42.3	1.7	29.2	0.9	25.8
WS 0.5%	5.5	12.2	1.0	24.4	0.5	12.2
WS 1%	5.9	23.3	1.7	28.2	0.8	16.3
WS 1.5%	6.4	22.0	1.3	21.0	0.7	21.6
WS 2%	7.1	31.7	1.1	29.0	0.5	24.0

**Compressive and Tensile Strength of Composites with Partial Cement
Replacement by Pozzolanic Materials**

Material	Mix Ratio	Compressive Strength(Mpa)			Tensile Strength Mpa
		7Days	28Days	91Days	91 Days
	Control	56	67	69	3.4
RHA	RHA 2.5%	65	71	83	3.7
	RHA 5%	63	72	80	3.9
	RHA 10%	68	74	81	3.7
PA	PA 2.5%	58	68	78	3.5
	PA 5%	57	68	74	3.5
	PA 10%	52	61	71	3.8
MK	MK 5%	67	74	78	3.1
	MK 10%	63	78	83	3.7
	MK20%	70	83	84	4.0
SF	SF 2.5%	70	76	90	3.9
	SF 5%	67	73	78	3.2
	SF 10%	64	70	76	3.4
GGBS	GGBS 30%	65	74	84	4.0
	GGBS 45%	68	76	92	4.0
	GGBS 60%	66	71	84	4.1
PFA	PFA 10%	62	68	79	3.8
	PFA 20%	63	72	90	3.9
	PFA 40%	62	70	80	3.8

Density and Compressive Strength of PFA-Based Pozzolanic PCRs

Mix:	10% PFA								Mix:	20% PFA								Mix:	40% PFA								
Cube No.	Mass Dry	Mass Wet	Density	Max Load	Strength	Age			Cube No.	Mass Dry	Mass Wet	Density	Max Load	Strength	Age			Cube No.	Mass Dry	Mass Wet	Density	Max Load	Strength	Age			
	(kg)	(kg)	(kg/m ³)	(kN)	(N/mm ²)	(days)				(kg)	(kg)	(kg/m ³)	(kN)	(N/mm ²)	(days)				(kg)	(kg)	(kg/m ³)	(kN)	(N/mm ²)	(days)			
1	2.3573	1.3365	2309.267	597.5	59.75	7	59.87		1	2.3991	1.3592	2307.049	540	54	7	54.505		1	2.3678	1.3395	2302.635	599.4	59.94	7	58.975		
2	2.3455	1.329	2307.427	599.9	59.99	7			2	2.2612	1.2832	2312.065	550.1	55.01	7			2	2.4266	1.3663	2288.598	580.1	58.01	7			
3	2.3388	1.3338	2327.164	620.6	62.06	14	63.1		3	2.302	1.2873	2268.651	643.3	64.33	14	65.805		3	2.3547	1.3272	2291.679	613.7	61.37	14	62.49		
4	2.3796	1.3585	2330.428	641.4	64.14	14			4	2.2815	1.2884	2297.352	672.8	67.28	14			4	2.4095	1.3757	2330.722	636.1	63.61	14			
5	2.3899	1.3654	2332.748	722.1	72.21	28	72.315		5	2.3001	1.3003	2300.56	766.1	76.61	28	77.22		5	2.3915	1.3576	2313.086	684.7	68.47	28	68.31		
6	2.4222	1.3892	2344.821	724.2	72.42	28			6	2.3447	1.3345	2321.026	778.3	77.83	28			6	2.3582	1.3405	2317.186	681.5	68.15	28			

Results Non-Cement Hydrated Lime-Based Pozzolan Composites

7-day							
Ratio	Mass in air (g)	Mass in water (g)	Maximum Load (Kn)	Density (Kg/m ²)	Average Density (Kg/m ³)	Strength (N/mm ²)	Average Strength (N/mm ²)
1 1 2	2101.40	1086.00	8.40	2069.53	2073.17	0.84	0.84
	2098.40	1088.00	8.30	2076.80		0.83	
1 2 3	2159.20	1160.00	8.20	2160.93	2147.95	0.82	0.80
	2167.00	1152.00	7.70	2134.98		0.77	
1 1 3	2104.80	1120.00	7.90	2137.29	2150.65	0.79	0.80
	2154.70	1159.00	8.00	2164.01		0.80	
2 1	2007.40	985.00	6.00	1963.42	1963.44	0.60	0.59
	1923.80	944.00	5.80	1963.46		0.58	
28-day							
Ratio	Mass in air (g)	Mass in water (g)	Maximum Load (Kn)	Density (Kg/m ²)	Average Density (Kg/m ²)	Strength (N/mm ²)	Average Strength (N/mm ²)
1 1 2	2089.20	1097.00	8.90	2105.62	2089.12	0.89	0.90
	2057.90	1065.00	9.00	2072.62		0.90	
1 2 3	2084.30	1105.00	9.10	2128.36	2114.41	0.91	0.86
	2036.60	1067.00	8.00	2100.45		0.80	
1 1 3	2051.90	1127.00	11.00	2218.51	2194.42	1.10	1.08
	2077.00	1120.00	10.50	2170.32		1.05	
2 1	1808.40	823.00	6.90	1835.19	1814.72	0.69	0.72
	1710.10	757.00	7.40	1794.25		0.74	
91-day							
Ratio	Mass in air (g)	Mass in water (g)	Maximum Load (Kn)	Density (Kg/m ²)	Average Density (Kg/m ²)	Strength (N/mm ²)	Average Strength (N/mm ²)
1 1 2	1955.80	958.00	9.20	1960.11	1965.47	0.92	0.90
	1912.30	942.00	8.80	1970.83		0.88	
1 2 3	2048.00	1050.00	10.30	2052.10	2058.62	1.03	1.12
	2086.20	1076.00	12.00	2065.14		1.20	
1 1 3	1881.40	976.00	11.30	2077.98	2101.43	1.13	1.46
	2074.10	1098.00	17.80	2124.88		1.78	
2 1	1758.00	820.00	8.20	1874.20	1846.34	0.82	0.80
	1713.00	771.00	7.70	1818.47		0.77	

GGBS-Based NALFRIC (without fibres)

GGBS-Based Non-Cement CL90 Composites											
		Con	10%	20%	30%	40%	50%	60%	70%	80%	90%
SL 1:1:2	7 days	0.8	2.5	4.2	4.6	6.3	5.6	6.4	8.6	9.8	12.5
	28 Days	1.1	3.5	7.6	7.5	10.2	10.5	11.9	16.9	17.0	16.6
	91 Days	1.5	4.8	8.5	8.7	10.7	13.8	14.6	20.5	21.8	19.9
	91 Days W	1.6	4.2	9.5	9.7	13.6	15.0	18.0	25.8	26.4	24.4
SL 1:2:3	7 days	0.8	1.7	4.4	3.8	4.5	5.4	6.9	6.0	7.4	12.5
	28 Days	0.9	3.0	7.7	6.5	7.8	10.1	10.9	11.4	13.8	16.3
	91 Days	1.1	3.4	9.0	7.3	8.8	13.2	12.7	14.5	17.2	18.4
	91 Days W	1.2	3.0	8.6	8.0	9.7	13.4	13.4	17.0	23.2	20.0
SL 1:1:3	7 days	0.8	1.5	4.3	7.2	6.5	8.4	7.9	8.0	8.2	12.7
	28 Days	0.9	3.5	6.9	10.9	10.3	11.9	14.4	13.8	13.6	18.0
	91 Days	1.1	4.2	8.9	13.0	11.4	13.3	16.4	14.8	18.7	18.9
	91 Days W	1.2	3.6	8.3	13.0	12.9	15.4	19.2	19.2	24.0	22.0
SL 2:1	7 days	0.6	1.1	2.4	3.9	6.8	8.4	9.2	8.4	9.9	10.2
	28 Days	0.7	2.8	5.4	7.6	11.8	14.4	14.2	13.5	15.6	15.8
	91 Days	0.8	4.0	7.2	9.7	14.7	18.2	18.6	18.1	20.2	18.8
	91 Days W	0.9	4.0	7.4	10.5	15.9	18.2	20.7	20.3	21.4	23.2

MK-Based NALFRIC (without fibres)

MK-Based Non-Cement CL90 Composites							
		Con	10%	30%	50%	70%	90%
MK 1:1:2	7 days	0.8	1.3	4.2	5.4	6.2	2.8
	28 Days	1.1	2.3	6.6	11.3	10.0	3.3
	91 Days	1.5	2.5	6.9	11.7	10.3	2.4
	91 Days W	1.6	1.8	6.0	13.2	10.5	1.9
MK 1:2:3	7 days	0.8	1.6	2.3	2.2	3.0	1.6
	28 Days	0.9	3.0	4.5	5.1	5.7	1.3
	91 Days	1.1	3.4	4.5	5.8	5.0	1.1
	91 Days W	1.2	2.6	4.0	7.8	5.8	1.2
MK 1:1:3	7 days	0.8	1.2	2.1	5.2	5.9	2.6
	28 Days	0.9	2.8	4.9	9.6	8.5	2.7
	91 Days	1.1	2.8	4.5	9.7	8.3	2.2
	91 Days W	1.2	2.7	4.6	10.2	9.2	2.3
MK 2:1	7 days	0.6	1.4	2.0	2.0	2.8	1.4
	28 Days	0.7	2.8	4.1	4.7	5.2	1.2
	91 Days	0.8	3.1	4.1	5.8	4.5	1.0
	91 Days W	0.9	2.3	3.6	7.1	5.3	1.1

PFA-Based NALFRIC (without fibres)

		Con	10%	20%	30%	40%	50%	60%	70%	80%	90%
FA 1:1:2	7 days	0.8	0.7	0.8	1.0	1.2	1.7	1.3	1.3	1.0	1.2
	28 Days	1.1	1.1	1.1	1.3	2.3	3.1	1.3	1.3	1.8	1.4
	91 Days	1.5	1.3	1.3	2.0	3.0	3.9	1.7	1.4	2.5	1.2
	91 Days W/C	1.6	1.4	1.5	2.2	3.3	4.3	1.8	1.5	2.7	1.3
FA 1:2:3	7 days	0.8	0.8	1.1	1.0	0.9	1.5	1.6	1.4	1.0	1.0
	28 Days	0.9	1.2	1.1	1.4	1.7	1.9	1.7	1.9	1.6	2.2
	91 Days	1.1	1.7	1.6	1.9	2.1	2.6	2.0	1.9	2.2	2.4
	91 Days W/C	1.2	1.9	1.8	2.2	2.4	2.9	2.2	2.1	2.5	2.7
FA 1:1:3	7 days	0.8	0.9	1.2	0.9	1.4	1.4	1.1	0.9	1.3	0.8
	28 Days	0.9	1.0	1.3	1.6	1.7	1.5	2.1	1.7	1.7	1.9
	91 Days	1.1	1.2	1.9	1.8	2.6	2.5	2.7	1.8	1.8	1.8
	91 Days W/C	1.2	1.3	2.1	1.9	2.8	3.2	2.9	2.0	1.9	2.0
FA 2:1	7 days	0.6	0.7	0.7	0.6	0.7	0.7	0.6	0.7	0.7	0.7
	28 Days	0.7	1.0	1.0	1.1	1.3	1.3	1.2	1.4	1.5	1.3
	91 Days	0.8	1.1	1.2	1.6	2.1	1.5	1.2	1.5	1.7	1.5
	91 Days W/C	0.9	1.2	1.3	1.8	2.3	1.7	1.3	1.6	1.9	1.6

PFA-Based NALFRIC (without fibres)

SF-Based Non-Cement CL90 Composites							
		Con	10%	30%	50%	70%	90%
SF 1:1:2	7 days	0.8	0.7	1.1	1.7	1.5	1.9
	28 Days	1.1	1.3	3.2	4.1	3.9	2.1
	91 Days	1.5	1.4	3.6	5.8	4.3	1.3
	91 Days W	1.6	0.9	3.2	6.9	5.1	1.8
SF 1:2:3	7 days	0.8	1.0	0.9	2.2	1.5	1.7
	28 Days	0.9	1.7	2.5	3.4	3.2	1.3
	91 Days	1.1	1.7	2.4	3.6	3.3	0.8
	91 Days W	1.2	1.4	2.5	3.7	3.6	1.2
SF 1:1:3	7 days	0.8	0.2	1.2	1.9	1.6	1.9
	28 Days	0.9	0.9	2.3	4.0	3.2	2.5
	91 Days	1.1	1.1	2.6	5.0	3.7	1.2
	91 Days W	1.2	1.0	1.6	5.2	4.0	1.5
SF 2:1	7 days	0.6	0.8	0.8	1.9	1.3	1.5
	28 Days	0.7	1.4	2.2	3.0	2.7	1.1
	91 Days	0.8	1.4	2.1	2.9	2.8	0.7
	91 Days W	0.9	1.2	2.1	3.2	3.1	1.0

Results - Iron-Based Fe-Composites (without fibres)

Engineering Properties of Iron-Based Pozzolanic Cement Concrete								
Set 1 - 5, 10%-50% Replacement of OPC with Conventional /Modified Fe-Composites								
Set	Mix Ratios	7 Days Compressive Strength (MPa)	28 Days Compressive Strength (MPa)	91 Days Compressive Strength (MPa)	91 Days Flexural Strength (MPa)	Water /cement Ratio	Slump (mm)	Plasticiser (ml)
Set 1 (20%PFA)	Con	47	55	59	4.4	0.35	S1	0
	Fe-Mix10%	52	60	66	4.7	0.35	S1	10
	Fe-Mix20%	44	55	64	4.4	0.35	S1	10
	Fe-Mix30%	40	53	63	5.0	0.35	S1	10
	Fe-Mix40%	32	46	55	3.7	0.35	S1	15
Set 2 (20%GGBS)	Fe-Mix50%	26	36	49	3.8	0.35	S1	15
	Con	47	55	59	4.4	0.35	S1	0
	Fe-Mix10%	51	60	72	5.2	0.35	S1	10
	Fe-Mix20%	46	57	71	5.8	0.35	S1	10
	Fe-Mix30%	45	56	67	5.5	0.35	S1	10
Set 3 (20%PA)	Fe-Mix40%	35	51	63	5.0	0.35	S1	15
	Fe-Mix50%	28	43	61	4.9	0.35	S1	15
	Con	47	55	59	4.4	0.35	S1	0
	Fe-Mix10%	52	62	70	5.3	0.35	S1	10
	Fe-Mix20%	51	62	68	5.8	0.35	S1	10
Set 4 (10%PFA +10%GGBS)	Fe-Mix30%	45	58	67	5.3	0.35	S1	10
	Fe-Mix40%	40	56	59	4.9	0.35	S1	15
	Fe-Mix50%	40	57	56	4.3	0.35	S1	15
	Con	47	55	59	4.4	0.35	S1	0
	Fe-Mix10%	51	62	67	5.3	0.35	S1	10
Set 5 (10%PFA +10%SF)	Fe-Mix20%	52	62	65	5.5	0.35	S1	10
	Fe-Mix30%	50	62	62	5.3	0.35	S1	10
	Fe-Mix40%	40	56	56	4.9	0.35	S1	15
	Fe-Mix50%	38	50	50	4.8	0.35	S1	15
	Con	47	55	59	4.4	0.35	S1	0
Set 5 (10%PFA +10%SF)	Fe-Mix10%	50	59	67	4.5	0.35	S1	10
	Fe-Mix20%	49	59	64	5.5	0.35	S1	10
	Fe-Mix30%	43	55	59	4.7	0.35	S1	10
	Fe-Mix40%	38	54	56	4.4	0.35	S1	15
	Fe-Mix50%	39	54	50	4.7	0.35	S1	15

NAFRIC Results - Iron-Based Fe-Composites (with fibres)

Density

	Fe/PFA		Fe/GGBS		Fe/PFA/SF		Fe/PFA/GGBS		Fe/PA	
	28 Days Average Density (Kg/m ³)	91 Days Average Density (Kg/m ³)	28 Days Average Density (Kg/m ³)	91 Days Average Density (Kg/m ³)	28 Days Average Density (Kg/m ³)	91 Days Average Density (Kg/m ³)	28 Days Average Density (Kg/m ³)	91 Days Average Density (Kg/m ³)	28 Days Average Density (Kg/m ³)	91 Days Average Density (Kg/m ³)
	2347	2353								
F/Con	2318	2350	2344	2345	2308	2334	2320	2349	2328	2338
ST 10%	2342	2352	2330	2335	2334	2408	2338	2341	2361	2367
ST 17%	2340	2366	2348	2361	2345	2359	2340	2367	2372	2374
PPF 1%	2298	2315	2309	2341	2307	2325	2335	2345	2303	2305
PPF 2%	2296	2314	2338	2357	2314	2324	2326	2335	2314	2320
PET 1%	2339	2341	2344	2368	2342	2336	2333	2343	2327	2332
PET 2%	2311	2327	2330	2338	2339	2348	2320	2324	2334	2334
WS 1%	2223	2307	2303	2300	2324	2357	2316	2341	2288	2299
WS 2%	2274	2277	2304	2299	2289	2277	2398	2339	2285	2288

Compressive Strength NAFRIC Binary Pozzolanic Composites

	Fe 10% 123 F/PFA				Fe 10% 123 F/GGBS				Fe 10% 123 F/PA			
Mix	28 Days Compressive Strength (MPa)	91 Days Compressive Strength (MPa)	270 Days Compressive Strength (MPa)	270 Days Compressive Strength (MPa) in Sulphate	28 Days Compressive Strength (MPa)	91 Days Compressive Strength (MPa)	270 Days Compressive Strength (MPa)	270 Days Compressive Strength (MPa) in Sulphate	28 Days Compressive Strength (MPa)	91 Days Compressive Strength (MPa)	270 Days Compressive Strength (MPa)	270 Days Compressive Strength (MPa) in Sulphate
Con	58.3	66.4	66.8	60.1	58.4	66.2	66.3	65.2	56.7	69.4	69.4	61.5
ST 10%	57.3	62.7	66.5	63.4	56.3	62.7	66.3	63.9	54.8	67.0	71.1	69.0
ST 17%	53.4	63.3	66.7	62.8	57.9	63.5	67.5	58.2	61.8	67.1	72.5	68.3
PPF 1%	52.0	57.8	64.5	58.4	49.3	55.7	59.3	59.3	56.8	65.4	69.5	65.6
PPF 2%	54.1	60.0	60.8	59.3	51.3	54.3	61.0	61.0	54.7	61.5	67.5	62.2
PET 1%	57.6	64.1	65.2	57.5	54.0	60.0	65.3	56.7	55.1	61.1	64.7	63.4
PET 2%	51.3	55.7	62.9	53.8	56.6	57.1	65.6	55.4	51.1	55.9	62.1	63.0
WS 1%	46.7	49.2	54.4	51.3	50.3	53.8	56.4	54.3	43.1	51.8	53.4	48.5
WS 2%	40.5	44.9	48.9	39.6	39.3	44.8	49.8	45.9	36.8	38.8	47.1	41.5

Compressive Strength NAFRIC Control and Ternary Pozzolanic Composites

	Fe 10% 123 Con					Fe 10% 123 F/PFA/GGBS					Fe 10% 123 F/PFA/SF				
	28 Days Compressive Strength (MPa)	91 Days Compressive Strength (MPa)	270 Days Compressive Strength (MPa)	270 Days Compressive Strength (MPa) in Sulphate	Mix	28 Days Compressive Strength (MPa)	91 Days Compressive Strength (MPa)	270 Days Compressive Strength (MPa)	270 Days Compressive Strength (MPa) in Sulphate	28 Days Compressive Strength (MPa)	91 Days Compressive Strength (MPa)	270 Days Compressive Strength (MPa)	270 Days Compressive Strength (MPa) in Sulphate		
Con															
PCC 123 Con	58.8	65.5	66.0	60.1	Con	55.8	66.7	67.3	61.6	53.9	59.6	64.2	61.3		
F/PFA Con	58.3	66.4	66.8	60.1	ST 10%	57.9	62.2	69.1	64.8	55.6	62.6	66.1	64.1		
F/GGBS Con	58.4	66.2	66.3	65.2	ST 17%	55.7	62.0	66.8	60.8	57.5	61.1	66.0	64.3		
F/PFA/SF Con	53.9	59.6	64.2	61.3	PPF 1%	59.5	65.5	69.9	64.0	55.9	65.5	68.0	60.2		
F/PFA/GGBS Con	55.8	66.7	70.3	61.6	PPF 2%	55.4	61.7	61.8	62.6	53.0	60.0	62.6	58.2		
F/PA Con	56.7	69.4	69.4	61.5	PET 1%	58.4	62.3	66.5	61.8	56.9	60.9	61.2	64.8		
					PET 2%	52.0	55.3	61.0	62.0	58.3	62.3	63.1	61.7		
					WS 1%	49.4	59.0	54.9	51.8	48.2	53.3	56.4	55.5		
					WS 2%	42.1	49.4	51.2	48.1	43.8	44.8	51.6	48.6		

Compressive Strength NAFRIC Control and Binary Ternary Pozzolanic Composites after Sulphate Attack

Mixes	PCC 123 Con		F/PFA 20%		F/GGBS 20%		F/PA 20%		F/10%PFA + 10%GGBS		F/10%PFA+10% SF	
	270 Days Water Cured	270 Days Sulphate Cured	270 Days Water Cured	270 Days Sulphate Cured	270 Days Water Cured	270 Days Sulphate Cured	270 Days Water Cured	270 Days Sulphate Cured	270 Days Water Cured	270 Days Sulphate Cured	270 Days Water Cured	270 Days Sulphate Cured
Con	66	60	67	60	66	65	69	62	70	62	64	61
ST 10%			67	63	66	64	71	69	69	65	66	64
ST 17%			67	63	68	62	72	68	67	61	66	64
PPF 1%			65	58	59	59	70	66	70	64	68	60
PPF 2%			61	59	61	61	68	62	62	63	63	58
PET 1%			65	58	65	60	65	63	66	62	61	65
PET 2%			63	57	66	58	62	63	61	62	63	62
WS 1%			54	51	56	54	53	48	55	52	56	55
WS 2%			49	44	50	46	47	42	51	48	52	49

Flexural Strength - NAFRIC Control and Binary Ternary Pozzolanic Composites

Mixes	91 Days Flexural Strength (MPa)	Displacement (mm)	Ductility	91 Days Flexural Strength (MPa)	Displacement (mm)	Ductility	91 Days Flexural Strength (MPa)	Displacement (mm)	Ductility	Mixes	91 Days Flexural Strength (MPa)	Displacement (mm)	Ductility	91 Days Flexural Strength (MPa)	Displacement (mm)	Ductility
Con	4.3	5.1	Brittle	4.3	5.1	Brittle	4.3	5.1	Brittle	Con	4.3	5.1	Brittle	4.3	5.1	Brittle
ST 10%	7.0	54.6	Exceptionally Ductile	7.0	54.6	Exceptionally Ductile	7.0	54.6	Exceptionally Ductile	ST 10%	7.0	54.6	Exceptionally Ductile	7.0	54.6	Exceptionally Ductile
ST 17%	8.7	54.5	Exceptionally Ductile	8.7	54.5	Exceptionally Ductile	8.7	54.5	Exceptionally Ductile	ST 17%	8.7	54.5	Exceptionally Ductile	8.7	54.5	Exceptionally Ductile
PPF 1%	6.8	43.3	Exceptionally Ductile	6.8	43.3	Exceptionally Ductile	6.8	43.3	Exceptionally Ductile	PPF 1%	6.8	43.3	Exceptionally Ductile	6.8	43.3	Exceptionally Ductile
PPF 2%	8.0	55.6	Exceptionally Ductile	8.0	55.6	Exceptionally Ductile	8.0	55.6	Exceptionally Ductile	PPF 2%	8.0	55.6	Exceptionally Ductile	8.0	55.6	Exceptionally Ductile
PET 1%	8.0	30.9	Highly Ductile	8.0	30.9	Highly Ductile	8.0	30.9	Highly Ductile	PET 1%	8.0	30.9	Highly Ductile	8.0	30.9	Highly Ductile
PET 2%	5.0	42.3	Exceptionally Ductile	5.0	42.3	Exceptionally Ductile	5.0	42.3	Exceptionally Ductile	PET 2%	5.0	42.3	Exceptionally Ductile	5.0	42.3	Exceptionally Ductile
WS 1%	5.9	23.3	Moderately Ductile	5.9	23.3	Moderately Ductile	5.9	23.3	Moderately Ductile	WS 1%	5.9	23.3	Moderately Ductile	5.9	23.3	Moderately Ductile
WS 2%	7.1	31.7	Highly Ductile	7.1	31.7	Highly Ductile	7.1	31.7	Highly Ductile	WS 2%	7.1	31.7	Highly Ductile	7.1	31.7	Highly Ductile

Results of Embodied CO₂ and Cost-Benefit Analysis

Embodied CO ₂ and Cost-Benefit Analysis - Partial Replacement of Cement with Pozzolanic Materials													
Mix Material	Cement (kg)	Replacement Material (Kg)	Aggregate (kg)	Cement kgCO ₂ /kg	Aggregate kgCO ₂ /kg	Pozzolans kgCO ₂ /kg	Total kgCO ₂ /m ³	kgCO ₂ /ton	Saving of kgCO ₂ /m ³	Saving of kgCO ₂ /ton	%age Saving of kgCO ₂ / ton or m ³	Cost/m ³ GBP	%age Saving in Cost/m ³
Control	340	0	1700	0.78	0.005	0	274	805	0	0	0	323	0.0
GGBS 30%	238	102	1700	0.78	0.005	0.067	201	591	73	214	27	307	5.1
GGBS 45%	187	153	1700	0.78	0.005	0.067	165	484	109	321	40	299	7.6
GGBS 60%	136	204	1700	0.78	0.005	0.067	128	377	146	428	53	290	10.1
PFA 10%	306	34	1700	0.78	0.005	0.004	247	727	27	78	10	313	2.9
PFA 20%	272	68	1700	0.78	0.005	0.004	221	650	53	155	19	304	5.9
PFA 40%	204	136	1700	0.78	0.005	0.004	168	494	106	311	39	285	11.8
SF 2.5%	331.5	8.5	1700	0.78	0.005	0.028	267	786	7	19	2	324	-0.4
SF 5%	323	17	1700	0.78	0.005	0.028	261	767	13	38	5	326	-0.8
SF 10%	306	34	1700	0.78	0.005	0.028	248	730	26	75	9	328	-1.7
MK5%	323	17	1700	0.78	0.005	0.15	263	773	11	32	4	321	0.7
MK 10%	306	34	1700	0.78	0.005	0.15	252	742	22	63	8	318	1.5
MK 20%	272	68	1700	0.78	0.005	0.15	231	679	43	126	16	313	2.9
RHA 2.5%	331.5	8.5	1700	0.78	0.005	0.1	268	788	6	17	2	321	0.7
RHA 5%	323	17	1700	0.78	0.005	0.1	262	771	12	34	4	318	1.5
RHA 10%	306	34	1700	0.78	0.005	0.1	251	737	23	68	9	313	2.9
PA 2.5%	331.5	8.5	1700	0.78	0.005	0.1	268	788	6	17	2	321	0.6
PA 5%	323	17	1700	0.78	0.005	0.1	262	771	12	34	4	319	1.3
PA 10%	306	34	1700	0.78	0.005	0.1	251	737	23	68	9	315	2.5

Positive values of %age show savings and negative values show increase in values compared to PCC 1:2:3 mix.
All the mixes have been considered using 1:2:3 job mix ratio for a fair comparison purpose.

Embodied CO ₂ and Cost-Benefit Analysis - Partial Replacement of Aggregate with Alternative Materials														
Mix Material	Cement (kg)	Sand	Coarse Aggregate	Replacement Material (Kg)	Cement kgCO ₂ e/kg	Aggregate kgCO ₂ e	Replacement Aggregates kgCO ₂ e/kg	Total kgCO ₂ e/m ³	kgCO ₂ e/ton	Saving of kgCO ₂ e/m ³	Saving of kgCO ₂ e/ton	%age Saving of kgCO ₂ e/ton or m ³	Cost/m ³ GBP	%age Saving in Cost/m ³
Control	340	680	1020	1700	0.78	0.005	0	274	805	0	0	0	323	3.3
CG 10%	340	612	1020	68	0.78	0.005	0	266	781	8	24	3	321	4.1
CG 20%	340	544	1020	136	0.78	0.005	0	266	782	8	23	3	319	4.8
CG 30%	340	476	1020	204	0.78	0.005	0	266	783	8	22	3	316	5.4
CR 10%	340	612	1020	68	0.78	0.005	0	266	781	8	24	3	351	-5.4
CR 20%	340	544	1020	136	0.78	0.005	0	266	782	8	23	3	380	-14.2
CR 30%	340	476	1020	204	0.78	0.005	0	266	783	8	22	3	408	-23.0
RPB 10%	340	612	1020	68	0.78	0.005	0	266	781	8	24	3	323	3.4
RPB20%	340	544	1020	136	0.78	0.005	0	266	782	8	23	3	323	3.5
RPB 30%	340	476	1020	204	0.78	0.005	0	266	783	8	22	3	323	3.5
RCA 10%	340	680	918	102	0.78	0.005	0	266	781	8	24	3	321	4.1
RCA 20%	340	680	816	204	0.78	0.005	0	266	783	8	22	3	319	4.8
RCA 30%	340	680	714	306	0.78	0.005	0	267	784	7	21	3	316	5.5
CT 5%	340	680	969	51	0.78	0.005	0	265	780	9	25	3	348	-4.3
CT 7.5%	340	680	943.5	76.5	0.78	0.005	0	266	781	8	24	3	360	-8.2
CT 10%	340	680	918	102	0.78	0.005	0	266	781	8	24	3	373	-12.0
Positive values of %age show savings and negative values show increase in values compared to PCC 1:2:3 mix.														
All the mixes have been considered using 1:2:3 job mix ratio for a fair comparison purpose.														

Embodied CO ₂ and Cost-Benefit Analysis - NALFRIC Composites														
Mix Material	Cement (kg)	Lime (CL90)	Replacement Material (Kg)	Aggregate (kg)	Cement kgCO ₂ e/kg	Aggregate kgCO ₂ e	Pozzolans kgCO ₂ e/kg	Total kgCO ₂ e/m ³	kgCO ₂ e/ton	Saving of kgCO ₂ e/m ³	Saving of kgCO ₂ e/ton	%age Saving of kgCO ₂ e/ton or m ³	Cost/m ³ GBP	%age Saving in Cost/m ³
PCC Control	340	0	0	1700	0.78	0.005	0	274	805	0	0	0	334	0.0
CL90 Control	0	340	0	1700	0.78	0.005	0.075	9	25	266	780	97	241	27.7
GGBS 10%	0	306	34	1700	0.78	0.005	0.067	11	32	263	773	96	244	26.9
GGBS 20%	0	272	68	1700	0.78	0.005	0.067	13	38	261	767	95	247	26.1
GGBS 30%	0	238	102	1700	0.78	0.005	0.067	15	45	259	760	94	250	25.3
GGBS 40%	0	204	136	1700	0.78	0.005	0.067	18	52	256	753	94	252	24.5
GGBS 50%	0	170	170	1700	0.78	0.005	0.067	20	58	254	747	93	255	23.7
GGBS 60%	0	136	204	1700	0.78	0.005	0.067	22	65	252	740	92	258	22.8
GGBS 70%	0	102	238	1700	0.78	0.005	0.067	24	72	250	733	91	260	22.0
GGBS 80%	0	68	272	1700	0.78	0.005	0.067	27	79	247	726	90	263	21.2
GGBS 90%	0	34	306	1700	0.78	0.005	0.067	29	85	245	720	89	266	20.4
PFA 10%	0	306	34	1700	0.78	0.005	0.004	9	25	265	780	97	313	6.1
PFA 20%	0	272	68	1700	0.78	0.005	0.004	9	26	265	779	97	304	9.0
PFA 30%	0	238	102	1700	0.78	0.005	0.004	9	26	265	779	97	294	11.8
PFA 40%	0	204	136	1700	0.78	0.005	0.004	9	27	265	778	97	285	14.7
PFA 50%	0	170	170	1700	0.78	0.005	0.004	9	27	265	778	97	275	17.5
PFA 60%	0	136	204	1700	0.78	0.005	0.004	9	27	265	778	97	266	20.4
PFA 70%	0	102	238	1700	0.78	0.005	0.004	9	28	265	777	97	256	23.2
PFA 80%	0	68	272	1700	0.78	0.005	0.004	10	28	264	777	97	247	26.1
PFA 90%	0	34	306	1700	0.78	0.005	0.004	10	29	264	776	96	237	28.9
SF 10%	0	306	34	1700	0.78	0.005	0.028	9	28	265	777	97	328	1.7
SF 30%	0	238	102	1700	0.78	0.005	0.028	11	33	263	772	96	339	-1.6
SF 50%	0	170	170	1700	0.78	0.005	0.028	13	39	261	766	95	350	-4.9
SF 70%	0	102	238	1700	0.78	0.005	0.028	15	45	259	760	94	361	-8.1
SF 90%	0	34	306	1700	0.78	0.005	0.028	17	50	257	755	94	372	-11.4
MK10%	0	306	34	1700	0.78	0.005	0.15	14	40	260	765	95	318	4.7
MK 30%	0	238	102	1700	0.78	0.005	0.15	24	70	250	735	91	309	7.6
MK 50%	0	170	170	1700	0.78	0.005	0.15	34	100	240	705	88	299	10.4
MK 70%	0	102	238	1700	0.78	0.005	0.15	44	130	230	675	84	290	13.3
MK 90%	0	34	306	1700	0.78	0.005	0.15	54	160	220	645	80	280	16.1
Positive values of %age show savings and negative values show increase in values compared to PCC 1:2:3 mix.														
All the mixes have been considered using 1:2:3 job mix ratio for a fair comparison purpose.														

Embodied CO ₂ and Cost-Benefit Analysis - NAFRIC Composites														
Mix Material	Cement (kg)	Iron+Pozzolan (kg)	Replacement Material (Kg)	Aggregate (kg)	Cement kgCO ₂ e/kg	Aggregate kgCO ₂ e	Iron+Pozzolan s kgCO ₂ e/kg	Total kgCO ₂ e/m ³	kgCO ₂ e/ton	Saving of kgCO ₂ e/m ³	Saving of kgCO ₂ e/ton	%age Saving of kgCO ₂ e/ton or m ³	Cost/m ³ GBP	%age Saving in Cost/m ³
PCC Control	340	0	0	1700	0.78	0.005	0	274	805	0	0	0	334	0.0
NAFRIC 10% with GGBS 20%	306	34	34	1700	0.78	0.005	0.041	249	731	25	74	9	380	-13.9
NAFRIC 20% with GGBS 20%	272	68	68	1700	0.78	0.005	0.041	223	657	51	148	18	438	-31.1
NAFRIC 30% with GGBS 20%	238	102	102	1700	0.78	0.005	0.041	198	583	76	222	28	495	-48.3
NAFRIC 40% with GGBS 20%	204	136	136	1700	0.78	0.005	0.041	173	509	101	296	37	553	-65.5
NAFRIC 50% with GGBS 20%	170	170	170	1700	0.78	0.005	0.041	148	435	126	370	46	610	-82.7
NAFRIC 10% with PFA 20%	306	34	204	1700	0.78	0.005	0.028	253	744	21	61	8	380	-13.9
NAFRIC 20% with PFA 20%	272	68	238	1700	0.78	0.005	0.028	227	668	47	137	17	438	-31.1
NAFRIC 30% with PFA 20%	238	102	272	1700	0.78	0.005	0.028	202	593	72	212	26	495	-48.3
NAFRIC 40% with PFA 20%	204	136	306	1700	0.78	0.005	0.028	176	518	98	287	36	553	-65.5
NAFRIC 50% with PFA 20%	170	170	34	1700	0.78	0.005	0.028	142	418	132	387	48	610	-82.7
NAFRIC 10% with PA 20%	306	34	68	1700	0.78	0.005	0.047	250	736	24	69	9	380	-13.9
NAFRIC 20% with PA 20%	272	68	102	1700	0.78	0.005	0.047	225	663	49	142	18	438	-31.1
NAFRIC 30% with PA 20%	238	102	136	1700	0.78	0.005	0.047	201	590	73	215	27	495	-48.3
NAFRIC 40% with PA 20%	204	136	170	1700	0.78	0.005	0.047	176	516	98	289	36	553	-65.5
NAFRIC 50% with PA 20%	170	170	204	1700	0.78	0.005	0.047	151	443	123	362	45	610	-82.7
NAFRIC 10% with PFA 10%+GGBS10%	306	34	238	1700	0.78	0.005	0.038	256	753	18	52	6	380	-13.9
NAFRIC 20% with PFA 10%+GGBS10%	272	68	272	1700	0.78	0.005	0.038	231	679	43	126	16	438	-31.1
NAFRIC 30% with PFA 10%+GGBS10%	238	102	306	1700	0.78	0.005	0.038	206	605	68	200	25	495	-48.3
NAFRIC 40% with PFA 10%+GGBS10%	204	136	34	1700	0.78	0.005	0.038	169	497	105	308	38	553	-65.5
NAFRIC 50% with PFA 10%+GGBS10%	170	170	68	1700	0.78	0.005	0.038	144	422	130	383	48	610	-82.7
NAFRIC 10% with PFA 10%+SF10%	306	34	102	1700	0.78	0.005	0.034	251	737	23	68	9	380	-13.9
NAFRIC 20% with PFA 10%+SF10%	272	68	136	1700	0.78	0.005	0.034	225	662	49	143	18	438	-31.1
NAFRIC 30% with PFA 10%+SF10%	238	102	170	1700	0.78	0.005	0.034	200	588	74	217	27	495	-48.3
NAFRIC 40% with PFA 10%+SF10%	204	136	204	1700	0.78	0.005	0.034	175	513	99	292	36	553	-65.5
NAFRIC 50% with PFA 10%+SF10%	170	170	238	1700	0.78	0.005	0.034	149	439	125	366	46	610	-82.7
Positive values of %age show savings and negative values show increase in values compared to PCC 1:2:3 mix. All the mixes have been considered using 1:2:3 job mix ratio for a fair comparison purpose.														

Embodied CO₂ of Different Materials (ICE Energy Briefing Sheet, 2011; Obinna, 2023)

Embodied CO ₂ kgCO ₂ e/kg of Cement, aggregate and SCMs	
Material / constituent	Embodied CO ₂ kgCO ₂ e/kg
CEM I	0.78
Sand	0.005
Coarse Aggregate	0.005
GGBS	0.067
Fly ash	0.004
Silica fume	0.028
Metakaolin	0.15
Natural Pozzolans (e.g., volcanic ashes, trass)	0.05
Calcined Natural Pozzolans (e.g., calcined clay, LC3)	0.2
Limestone fines	0.075
Alkali activated materials / "Geopolymers"	0.15-0.4
Steel	2.89
RCC 32/37 (110 kg/m ₃ of seel)	0.2
Aluminium	
F/PFA (60% iron+20% PFA+10%LIME+8%MK)	0.028
F/GGBS (60% iron+20% PFA+10%LIME+8%MK)	0.041
F/PA (60% iron+20% PFA+10%LIME+8%MK)	0.047
F/PFA/GGBS (60% iron+20% PFA+10%LIME+8%MK)	0.038
F/PFA/SF (60% iron+20% PFA+10%LIME+8%MK)	0.034

Unreinforced, C30/37, UK average	0.103
ready-mixed concrete EPD[1] (35% cement replacement)	0.12
Unreinforced, C32/40, 25% GGBS cement replacement[3]	0.089
Unreinforced, C32/40, 50% GGBS cement replacement	0.063
Unreinforced, C32/40, 75% GGBS cement replacement	0.138
Unreinforced, C40/50, 25% GGBS cement replacement	0.102
Unreinforced, C40/50, 50% GGBS cement replacement	0.072
Unreinforced, C40/50, 75% GGBS cement replacement	0.178
Unreinforced, C40/50 with average UK cement mix	
Reinforced, 150mm prestressed hollow core slab: British Precast Concrete Federation average EPD	50.2kgCO ₂ e/m ²
UK: BRC EPD	0.684
Worldwide: Worldsteel LCI study data, 2018, world average	1.99
Assume the same as reinforcement bars	Assume the same as reinforcement bars
UK open sections: British Steel EPD	2.45
Europe (excl. UK): Bauforumstahl[8] average EPD	1.13
Worldwide: Worldsteel LCI study data, 2018, world average	1.55
UK: TATA Comflor EPD	2.74
Lightweight blocks	0.28
Generic, UK	0.213
CLT, 100% FSC/PEFC	0.437
Glulam, 100% FSC/PEFC	0.512
Softwood, 100% FSC/PEFC	0.263
Plywood, 100% FSC/PEFC	0.681
Minimum 60% recycled content	0.39
Specific EPD: Amotherm steel WB, Amonn	2.31

Matetrial	Source/ Brand Name	Est Price (GBP/ unit)	Est Price (GBP/ kg)
White cement CEM1 52.5	Snowcrete	16/ 25kg bag	0.64
Plasticiser	Oscrite - AlphaFlow 420	1/ litre	1.00
Fine aggregate (sand)	Huws Gray	53/ 850kg	0.06
Coarse aggregate	Huws Gray	55/ 850kg	0.06
Hydrated lime CL90	Conserv	10/ 25kg bag	0.40
Hydraulic lime NH2, NH3.5, NH5	Conserv	11/ 25kg bag	0.44
Lime putty	Conserv	7/ 10 kg tub	0.70
Limestone CaCO3	Tarmac	8/ 25kg bag	0.32
Crushed glass	EcoSand - Mone brothers	27.60/ ton	0.03
Crumb rubber	Murfitt Industries	12/ 25kg bag	0.48
Recycled PET bottles (crushed)	Plasgran	60/ ton	0.06
Recycled concrete aggregate	Yarrows Aggregates	38/ 850kg	0.04
Shredded tyres	Rebound (Adamast)	277.20/ 500 kg	0.55
PFA	J&J Sharpe	9/ 25 kg bag	0.36
Rice husk ash RHA	e-Coco	9/ 25 kg bag	0.36
Palm ash (PA)	e-Coco	10.00/ 25kg bag	0.40
Metakaolin	Conserv	10/ 20kg bag	0.50
SF	Carbon Enterprises	16/ 20kg bag	0.80
GGBS	J&J Sharpe	12/ 25kg bag	0.48
Iron powder	MB Fibreglass	90/ 25kg tub	3.60
Oxalic acid	AG Woodcare	38/ 5kg	7.60
Steel fibres	Dramix 45/50 B	12/ 25kg bag	0.48
PP fibres (micro/ macro)	Adfil/ Bonar	10/ 25kg bag	0.40
Coconut coir	e-Coco	100/ ton	0.10
Wheat straw	farm	80/ ton	0.08

River Swale 4 years Rainfall Data

Sum of rain, mm	Year	2019												2020												2021												2022																
		Total												Total												Total												Total																
		Month	1	2	3	4	5	6	7	8	9	10	11	12	1	2	3	4	5	6	7	8	9	10	11	12	1	2	3	4	5	6	7	8	9	10	11	12	1	2	3	4	5	6	7	8	9	10	11	12				
Day	1	4.6	0.4	1.2	0	0.6	0	0	0	7.4	2	0	6.2	22.2	2.2	0.8	10	0	0	0	1	0	0	0	0.8	0	14.6	15.4	0	2.4	1.6	0	1.4	0.4	0	3.8	1.8	0	0	28.8	0	0	0	12	16	0	3	1.4	1.6	13	4.6	5.6	57	
	2	0	0.2	1.8	0	0.2	0	7.2	0	1	0	0	3.4	13.8	1.4	0	1	0.2	0	0	9	0	3.2	0	0.2	0	14.6	8	0	0	6.1	0.26	33	0	0	27	0	99.2	0	0	0	3.6	8.8	11	13	1	0	7.2	0.6	22	68			
	3	0.8	1.2	1.2	0	0	0.2	7.8	0	1.6	1	0	14	27.2	0	7	0	0.6	4.4	0	3	0	4.4	0	0	0	0.8	19.8	4.4	0.4	19	2.4	0	0.2	0.2	0.2	34	5.6	0	35.6	0.2	0	0	2	6.4	12	2	1	1.2	1.2	0.2	12	26.6	
	4	2.2	0	0	0	0	0	0.4	0	0	0	0	2.8	0	1.8	0	0	15	0	3	0	1	0	3.6	0.2	24.6	5	0	5	15	0	0	1.6	0	0	9.6	0.8	5	41.8	0	0	0	0.4	8.8	1.8	1	1.8	1.8	0	1	2.2	18.4		
	5	4	0	0	0	0	0	0	0	0	0	11	0.2	15.2	1.6	0	1	1.2	13	6	0	0	0	0	0.8	0.2	23.4	0	0	3	0	1.4	3.2	0	0	0	3.4	0	0.2	11.2	0.4	0	2.4	0	11	13	1	4.4	0	4.6	14	14	52.8	
	6	9	1	0.6	0.2	0	0	0.2	8.2	0	0	2.2	0	21.4	0	1.6	0	1	3	0	0	0.4	0	0	0.2	6.6	3.2	1.2	15	8.2	0.6	12	0	0	0.2	0	0	0	39.8	0	0	0.2	1.4	2	0.4	1	24	8.2	1.8	0	6	23.2		
	7	0.4	0.4	0	0	0	0	13.4	0	0	0	0	0	14.4	0	0	0	0	1.4	1	0	0	0	0	13	0.2	15.4	2.4	0.16	3.6	16	0	0.2	2	0.6	0	0.2	11.6	5.2	0	0	0.6	15	0	2	3.4	0.4	1	1.8	0.8	29.4			
	8	6.8	1.4	2.4	0	0.4	0	1.4	1.2	0	0	2.4	0	16	0	0.2	0	0	4.4	11	0	0	0	0	3.4	5.2	24.6	18.4	0	0	9.8	1.4	12	4	0	1.4	0	0.8	0	48.2	6.8	0	0	1.2	9.4	0.8	1	13	1	0.2	0.2	13	46.4	
	9	0.4	12	0	0	0	0	0	7	0	0	0	0	19.4	0	2	0	0	0.2	1	5	0	0	0	0.4	14	22.2	0	0	0.4	0.4	0	1	0.2	0	10	0.8	0.4	0	13.2	3	0	0	0.4	8	2.8	2	9.8	0	7.6	0	1.8	35.2	
	10	0.2	1.8	0	1.8	5.8	0	0	5	0.4	0	0	0.2	15.2	0	5.8	0	0	5.6	3	0	0	0	1	0.2	5.2	20.4	0	1	9.2	6.8	4.2	17	1.6	0	3.6	0.4	0	0.4	44	20.4	0	0.2	1	6.8	6.8	0	0.2	0.8	0.4	0	8.4	45	
	11	5.6	15.8	5.4	3.6	2.2	0	2	1.2	0.4	0	14	0	50.2	1.2	7	0	0	28	23	0	0.2	0	0	0.2	5.6	40	0	0.4	0	12	2.2	1	4.2	0.2	1.4	1	0.6	3.6	15.8	0.8	1.8	0.6	9.4	0.6	2	4.4	1.6	0	1.2	11	33		
	12	5	13.4	7.4	0	1.4	0	0	0	0	0	0.2	1.4	28.8	0	1.8	0	0	0.2	5	0	0	0	0	0	0	7	0.8	0	2	0.2	0.2	0	2.6	0	0.8	0.2	0	2.8	9.6	1.2	0	0.2	0.6	3.4	3.6	3	1.2	1.4	0	3.6	1	19	
	13	2	1.4	0.2	0	0	0	0	0	0	0	0.4	0	4	0	0	0	0	0	1	0	3.6	0.2	0	0	5.6	11.2	0	0	0	0	6.4	0.4	1	0	3.4	0	7.2	29.6	0	0	0.8	1.2	11	7	0	5.2	0.72	1.6	0	34			
	14	0	0	0.2	0.4	0	0	0	0	0	0	0	0	0	0	0	0	0	0	0	0	0	0	6.4	0	6.4	4.4	0	0.02	0.8	6.4	0.6	0.4	0	0	0	2.2	16.2	0.4	0	1	0.4	9.2	4.2	3	4.6	0	5.4	1.6	29.6				
	15	0	0.6	0	0	0	0	0	0	0	0	0.6	1.2	0	1.4	0	0	0	0	0	0	0.2	4	0.4	1.4	8.2	4.8	0.2	0	0	1.2	0	0	0	0.4	0.2	0	6.8	0	0	0.2	1	4.2	2.4	2	1.2	1	0	0	6.2	55.6			
	16	0	0.2	8.4	1.6	0.4	0	1	0	0	0	2.4	0.2	14.2	0.2	5.8	0	0	3.8	0	2	0	0.4	1.8	0	21.6	0.2	0.2	0	4	1	1.4	1	4.2	0	13	3	0	27.4	0	0	0.2	0.4	7.8	11	1	0.8	0.8	0	0.16	24			
	17	0	4.2	0.2	0.6	0	0	0	0	0	0	2.8	0.8	8.6	0.8	1.7	1	0	7.6	9	2	0	0	0	5.8	4.6	47	5.4	0	0	1.8	0	0.6	5	0	0	7.2	0.4	3.2	23.6	0	0	6.8	0	0.2	4	2	6.4	0.6	0	0	0.2	20	
	18	0.4	1.2	0.2	1.2	3.8	0	0	0	1	0	0	29	37	0	4.8	1	0.6	0.4	0	0	0.2	0	0	4.2	8.2	19.6	11.6	0	0	0	0	1.6	0	0	0	0	0	13.2	0	0	0.6	0.8	5.4	5.4	1	9.6	0.4	0.4	0.2	27.8			
	19	3	4.6	0.6	0.2	0.8	0	0	0	1.4	0	10	7	27.6	2	16	0	0.4	7.2	3	0	0	0	0	6.2	8.4	43	1.2	0	0	3.4	0	0	5.4	0	0	0.4	0.2	0	10.6	0	0	3.2	0.8	24	3.2	3	0.2	24	0.4	2.4	0	0	61
	20	1.4	4.2	0.4	0.2	1	0	0	11.2	0.4	0	3.2	0	22.2	0	17	0	0	1	1	0	1.2	0	0	8.4	0	29	1.4	0	0	0	0.2	1.2	9.2	1.2	0	7	0.8	0.4	21.4	0	0	0.4	0.2	6.4	5.6	3	2.8	7.2	0	0	25.8		
	21	0.4	6	7.2	0	0	0	0	0	0	0.32	0	16.8	0.4	0	0	1.8	0.2	1	0	0	0.4	0	0	0	0.2	4.2	4.6	1.6	0	2.8	0	0	0.4	0.8	0	1	0	0.2	11.4	0	0	0.2	1.8	7.4	11	0	0	7.2	16	0.6	6.4	50.6	
	22	0	0.2	0.8	6.4	6.2	0	0	10.2	0	0	1	0.2	25.2	1	0.8	1	0	0.4	1	0	0.2	0	0	1	3.8	10	1	0	0	21	0	2.6	2.6	1	0	9.2	0	0.2	3.8	0	0	2.8	11	13	2	0	15	0.4	0	4	48.8		
	23	0	3.2	0	2	2.6	0	19.2	23.8	0	0	2.2	0	53	0	4	2	0	0	1	4	6.4	0	0	4.2	4.6	25.6	2	0	2.4	0.2	0.4	0	0	5.6	0	0.2	0	0	10.8	0	0	1.2	1.4	2.6	1.8	2	0	11	0.8	0	5.4	26	
	24	0	6.2	0	0	0.2	0	0	2.4	1.8	0	6.8	0.2	17.6	0	9	2	7	0	0	9	0.6	0	0.8	11	39.8	0.4	0	3.4	0.2	0	0.6	0	0	0	18.58	0	28.4	0	0	0.6	4.6	4.4	8.6	0	6	0.4	11	2.8	11	49.4			
	25	0.2	1	1	0	0	0	0	0.2	0	0	3.8	0.2	6.4	0	4.4	0	1	0.4	0	0	0	0	0	12	9.4	17	0	0	0.8	0.2	0.6	0	0	14	0.6	0.2	0	0.4	16.4	0	0	0	20	0.6	3	1	14	22	0.2	1.2	3.8	45.6	
	26	4	0	0.6	0	7	0	0	28	2.2	0	0	0	41.8	0.2	0	0	1.8	0	0	8	0	0	0	7	17	0.4	0	0	0.4	1.6	0.2	8.4	1.4	0	0.6	9.2	0	0	21.8	0	0	0.4	0	9.4	15	1	0	5.4	6.4	2.8	0.2	40.4	
	27	4.6	0	0	0	0.2	0	0	0.6	0.6	0	0	1	7	1.2	2	2	1.2	0	1	0	1.8	0	0	0	1	0.6	9.6	0	5.6	0	6	12	3.2	0.8	0	4.6	7.2	0.2	0	28.8	0	0	2.6	17	7.8	1.6	4	1.4	1.4	0	0.2	0	48.2
	28	1.6	0	0.2	0	0.4	0	3.6	1.6	6.4	0	1.8	0	15.6	0	0	0	0.2	0	1	0	0.8	0.2	0	17	1	19.8	0	5.6	0	20	20	0	1.6	0	0.8	4	0.2	0.4	5.4	0	0	0.6	2.4	0.8	13	0	0.8	2.8	2.8	1	0	45.6	
	29	1	0	0	0	4.4	0	3	0	2.8	1	0.6	4	16.4	0	0	0	0	1	3	3	0	1	3	0	1	3.6	11.6	0	8	0	1.8	0	0.2	0.6	4.8	0	0	15.4	0	0	0.8	32	11	0	2	1.8	0	0.2	0.4	0	47.8		
	30	0	0	0.2	0	0.4	0	0.6	1.2	0	0	0.4	2.4	5.2	0	0	4.8	0	1	0	0.4	1.8	0	0.2	11	19.4	2	0	0	2.6	0.2	2.8	0	11	0	0	0.2	18.4	0	0	0.6	5.4	0	13	4	0	1.4	4.8	0.4	0.2	29.6			
	31	0	0	0	0	0	0.4	0	0	0	0	3.8	4.2	0.8	0	0	0	0	5	15	0	0	0	0	20.6	0.6	0	0	0	0	0	11	18	0	0	0	29.8	0	0	8	12	1	0	0	0	0	0	0	21.4					
	Grand Total	57.6	80.6	40.2	18.2	38	0.2	60.2	101.8	27	4	68	75	571	13	110	21	21	68	75	54	34	12	13	92	96	609	108	16	78	132	39	117	57	49	43	107	46	27	819	38.4	0	33	137	278	176	61	99	112	87	50	114	1185	

An Example of use of Use of Log Pearson3 (LP3) Equations for Forecasting of Rain/ Flood Forecasting (Nadir and Ahmed, 2022a)

Raw Calculation of Storm Frequency Analysis using LP3 Equations – River Swat at Munda Headworks

Rank (m)	Year	Munda Headworks Peak Annual Discharge (Q) m ³ /sec	Log (Q)	Avg Log (Q), Mean M	(Log(Q)- Avg(Log Q)) ²	(\sum (Log(Q)- Avg(Log Q)) ² /(n- 1)) ^{1/2} S _d	(Log(Q)- Avg(Log Q)) ³ skewness Coefficient G	skewness Coefficient \sum (Log(Q)- Avg(Log Q)) ³ /(n- 1)*(n-2)*S _d	Return Period (T _r) =2n/(2m- 1), m=Rank, n=No of years	Exceeden ce Probabili ty (1/Tr)
1	2010	10052	4.002252	3.042074	0.921943	0.29415	0.88523	0.248756	38	0.026316
2	2003	2548	3.406199	3.042074	0.132587		0.048278		12.66667	0.078947
3	2011	2548	3.406199	3.042074	0.132587		0.048278		7.6	0.131579
4	2004	1388	3.142389	3.042074	0.010063		0.001009		5.428571	0.184211
5	2006	1133	3.05423	3.042074	0.000148		1.8E-06		4.222222	0.236842
6	2002	1019	3.008174	3.042074	0.001149		-3.9E-05		3.454545	0.289474
7	2005	1019	3.008174	3.042074	0.001149		-3.9E-05		2.923077	0.342105
8	2001	991	2.996074	3.042074	0.002116		-9.7E-05		2.533333	0.394737
9	2009	991	2.996074	3.042074	0.002116		-9.7E-05		2.235294	0.447368
10	2014	991	2.996074	3.042074	0.002116		-9.7E-05		2	0.5
11	2007	954	2.979548	3.042074	0.003909		-0.00024		1.809524	0.552632
12	2008	951	2.978181	3.042074	0.004082		-0.00026		1.652174	0.605263
13	2000	878	2.943495	3.042074	0.009718		-0.00096		1.52	0.657895
14	2012	821	2.914343	3.042074	0.016315		-0.00208		1.407407	0.710526
15	2015	708	2.850033	3.042074	0.03688		-0.00708		1.310345	0.763158
16	2016	651	2.813581	3.042074	0.052209		-0.01193		1.225806	0.815789
17	2018	651	2.813581	3.042074	0.052209		-0.01193		1.151515	0.868421
18	2013	566	2.752816	3.042074	0.08367		-0.0242		1.085714	0.921053
19	2017	547	2.737987	3.042074	0.092469		-0.02812		1.027027	0.973684
			3.042074		1.557436		0.895619			

Q _T =M+K _T * S _d 2 year	Q _T =Anti Log (Q _T) 2 year	Q _T =M+K _T * S _d 5 year	Q _T =Anti Log (R _T) 5 year	Q _T =M+K _T * S _d 10 year	Q _T =Anti Log (Q _T) 10 year	Q _T =M+K _T * S _d 25 year	Q _T =Anti Log (Q _T) 25 year	Q _T =M+K _T * S _d 50 year	Q _T =Anti Log (Q _T) 50 year	Q _T =M+K _T * S _d 100 year	Q _T =Anti Log (Q _T) 100 year	Q _T =M+K _T * S _d 200 year	Q _T =Anti Log (Q _T) 200 year
3.037073	1089.114	3.287983	1940.812	3.422116	2643.114	3.576839	3774.32	3.677144	4754.927	3.769213	5877.773	3.85481	7158.31
	1089	3	1941	3	2643	4	3774	4	4755	4	5878	4	7158
3.042074	1101.727	3.289748	1948.715	3.419174	2625.272	3.557131	3606.872	3.646258	4428.515	3.726267	5324.354	3.799804	6306.733